

Patterns and Relations in Gila River Chemistry and Thermodynamic Process: Database  
Description and Evolution

(Draft)

Pierre-Charles Bierly



## Preface

The Gila is well known as a most resilient river, famous for occasionally vanishing into the sand only to resurface further on downstream. But the basic processes that govern the river's behavior have never been thoroughly explored. This study focuses on a single event at a single site, drawing on a large dataset of the physical characteristics of the Gila. Bringing together information from a number of different sources, it provides a comprehensive view of the river's flow and density regimes at the site. With a few key assumptions and numerous calculations, the dataset is expanded to investigate the main chemistry and thermodynamic processes. Throughout, the interrelations between the various processes are analyzed and evaluated to create a dynamic picture of a river's response to its environment.

It all began with the chance observation of a singular phenomenon in the chemistry of the Gila. Normally a high sodium-chloride water in Arizona, occasionally the concentration of bicarbonate temporarily exceeds that of chloride. Put that way, it does not sound like a particularly momentous event but changes in two of the major ions are bound to be significant. The distinctive pattern of occurrence of this phenomenon is first placed in its environmental context by comparison with patterns of flow and density. Then the ramifications within chemistry and thermodynamic processes are examined to determine the significance for the system as a whole.

The material is technical and in high detail but should present no difficulty for the general reader familiar with basic chemistry and algebra. Indeed, some may find the topics too elementary, the methods too unsophisticated. But a simple, broad strokes study of patterns and relations can sometimes give a better understanding of general system function than can narrowly quantitative work. The precision of the analysis is appropriate to the subject, not exceeding the state of the art of environmental science. In particular, researchers in the applied sciences, often faced with coming to conclusions in spite of large data gaps and having to use together numbers of widely varying sensitivity, precision, and accuracy, should find the detailed data analysis useful.

The analytical methods used are limited to equilibrium chemistry and descriptive statistics with a focus on fundamental quantities, especially volume, entropy, and time. The source of information is public records water quality, climate, and river flow data available on the internet or by request. The source data, though generally of very high quality, was originally compiled to answer questions quite different from those being asked here. The analytical approach developed, highly detailed in places to highly general in others, is an attempt to find the best 'views' of available information to answer questions about fundamental system functions. There are descriptive passages, graphs, and tables of values for those primarily seeking information.

The study is presented as the narrative of a search for patterns and relations, a blow-by-blow presentation of an investigative process. The goal was to generate as many views of the system as possible and use the essence of as many of these as possible to create the final picture. Arguments take as little as possible for granted and explicit procedural detail helps the reader in the critical evaluation of conclusions. A number of false starts and dead-ends, inevitable in any investigation, are included. Deducing why these 'don't work' is as important as finding any and all evidence that supports the final picture. This study is not, however, a textbook in logic or

anything else for that matter. It is, instead, a rather long and involved 'essay,' an opportunity to look at a fascinating river in a new and different way.

In fact, readers should be aware that parts of this work are 'experimental.' The use of statistical process and laboratory analytical control terms and methods with systems not under 'control' is open to question. But the assumption here is that a normal distribution of data means 'reproducibility' in either context; only the nature and meaning of 'outliers' differs. The search for patterns is primarily done with graphs some of which manipulate and juxtapose data curves of quite different derivations and/or magnitudes. Particularly aggressive examples are labelled "Assay" to clearly distinguish them from more straightforward depictions. Several novel analytical approaches are also used to bridge data gaps and extract as much useful information as possible. These examples of modelling sometimes test how far readily available data can be pushed to yield information. Supporting argument and evidence is presented but it is ultimately up to the reader to decide to what degree to accept modelling results.

More than ten years were spent finding new and interesting subjects of inquiry in this dataset. Following each new path to see what might develop became a bit of an obsession which may explain why the organization is sometimes chaotic and/or repetitive. Most of the text was written while the discovery process was still going on and the final product thrown together rather hastily. But, whatever the quality of the writing, this work is entirely a product of enjoyment. It was done on the author's own, with no funding and no publications list in mind. It exists because, once started, the process of analysis, one thing leading to another, created ever new vistas beckoning with promise. It is hoped that the thrill of discovery experienced in the creation of this work will somehow, in spite of all the work's faults, be passed on to the reader.

One fault, in particular, may have a beneficial aspect. The occasional rapid alternation of nitty-gritty detail followed by sweeping generality, the latter often starting at a rather elementary level, may be disconcerting to some readers. But the wide scope of the work means that the terms and patterns investigated come to resonate with one another across very different time and spatial frames and at different levels. Making connections over such wide ranges can be dangerous but inevitably stimulates, in the discerning reader, the need for corroboration. The reader who perseveres is given not a limited set of static perspectives but rather a procedure to continue on his own the exploration into the river's patterns and relations and their meaning.

As a repository of information on the Gila River, the study is finished. The original and derived data, included in an appendix, serve both as checks on the work done and as potential sources for further research. Much more information was generated than could possibly be fully evaluated by a single person and many areas need quantification. It is hoped that the picture of basic processes and their interrelations presented here will stimulate further investigation. As to how the Gila River has been so successful in its struggle to survive in the arid southwest for so long, this study is just a beginning and there remains much to be learned.

Dedicated to Dr. G.K.Vemulapalli

Table of Content (pagination is for full size font text (12))

<a href="#"><u>What is a major ion ‘inversion’?</u></a>	6
<a href="#"><u>Inversion analysis, average behavior</u></a>	32
<a href="#"><u>Flow patterns</u></a>	35
<a href="#"><u>Patterns of material transport</u></a>	82
<a href="#"><u>Volume relations</u></a>	106
<a href="#"><u>Density patterns</u></a>	116
<a href="#"><u>External energy</u></a>	145
<a href="#"><u>Molar functions, general</u></a>	147
<a href="#"><u>Temperature patterns</u></a>	164
<a href="#"><u>Molar functions, Safford specific</u></a>	166
<a href="#"><u>Constant amount control reservoir</u></a>	193
<a href="#"><u>Dynamic control reservoir</u></a>	207
<a href="#"><u>Ionic strength relations</u></a>	217
<a href="#"><u>Ion pair dissociation/formation</u></a>	229
<a href="#"><u>Total thermodynamic function patterns</u></a>	248
<a href="#"><u>Graphical Synthesis</u></a>	312
<a href="#"><u>Patterns of Resilience</u></a>	329
<a href="#"><u>Afterword</u></a>	335
<a href="#"><u>Footnotes</u></a>	341

(Appendix - original & study data, programs, notes on methods - available as separate Excel files – ‘Dataset Physical Characteristics Gila River at Safford’ and ‘Study Notes’ at website [www.gilariverdata.info](http://www.gilariverdata.info))



## The Journey of the Gila



Map of the Gila River – Wikimedia (bordered labels and shapes added)

The Gila River of the southwestern United States, nearly midway on its journey from New Mexico across the Sonoran desert of central Arizona to join the Colorado at Yuma, flows into the Safford Valley -- a new river, completely transformed. The change is so sudden and dramatic that it captured the attention of USGS researchers in the mid-1900s. They noted the rise in levels of sodium (Na) and chloride ion (Cl) and were able to pinpoint the source as one of the major tributaries of the Gila, the San Francisco after it has passed Clifton Hot Springs.<sup>1</sup>

What has not been noted previously is that this dramatic event at this particular point in the river, or rather its inverse, has an echo in time. Once or twice a year on the Gila at Safford, the concentration of chloride (Cl) falls and is temporarily exceeded by that of bicarbonate ion (HCO<sub>3</sub>) with sodium (Na) and calcium (Ca) following their lead respectively. There is, for a while anyway, a more or less complete inversion of the usual positions of four of the six major ions. This event may be seen as a reversion to an earlier time in the river's history. More significantly, it creates a situation to which the river responds in an orchestrated series of events that determine its changing characteristics for the immediate, short term future.

The term inversion is used here in a new sense and has nothing to do with its traditional use in thermodynamics.<sup>2</sup> They are only related in sharing the basic meaning of the word 'inversion': a turning-upside-down or, more generally, a change of order, position, or direction to its opposite. But the inversion is more than just a random change in direction of a system process. It is the signal of a radical transformation of the system, one that pushes the river's fundamental pattern of response to its environment to a new level. Only when put into the context of the river's everyday patterns of behavior is it possible to understand the full significance of the inversion on the system.

While the effects of the inversion are far reaching and profound, inversion analysis is operationally very simple. It consists of labeling samples by whether the sample date shows an inversion ('inv' (HCO<sub>3</sub>>Cl)) or not ('non-inv' (Cl>HCO<sub>3</sub>)) or, for sample differences, by the difference in inversion status from the previous sample (e.g. non-inv to inv, inv to inv, etc). The labeled samples are analyzed, then sorted and averaged by inversion status. This simple procedure was used over and over again for everything from characterizing general flow and density processes to investigating the intricacies of a matrix shift. The fact that the patterns produced so often 'make sense' suggests that there is a link between the inversion process and some very fundamental system function(s).

In terms of amounts, the inversion is a change in a tiny portion of the river water. The six major ions represent about 93% of the dissolved solids but the dissolved solids as a whole represent only about 0.03% of river water. The river water 'solution', consisting of dissolved solids, dissolved gases, and solvent, is roughly 99.9% solvent, i.e. H<sub>2</sub>O. (There is also a variable amount of suspended solids and organic matter which are not considered part of but rather are added to the (dissolved) 'solution' to make the 'whole water' or 'total solution').

The dissolved solids portion is, however, a 'complete' system in itself within the larger river (whole) water system. Its makeup can be deduced in a parts and the whole differentiation scheme

(speciation). And it has an inordinate effect, far out of proportion to the amount of material it represents, on the properties of the river water solution as a whole. Water itself (i.e. H<sub>2</sub>O) is a neutral molecule with a conductance near zero but ‘water,’ (i.e. H<sub>2</sub>O with ‘things’ in it), can have a conductance of 1 or 2 to several thousand uS/cm. The property of conductance is entirely a result of a subgroup of the dissolved solids group being charged species. Indeed, it is the fact that the charged species are a complete subsystem, exactly balanced 50% plus-50% minus to maintain electro-neutrality, which makes speciation possible.

The inversion can initially be described in terms of the number and pattern of incidents in time. Of the 161 samples from the Arizona Department of Environmental Quality (ADEQ) Surface Water Quality Database used in this study, 53 or 33% showed inversion. Typically a one ‘grab’ (‘instantaneous’) sample affair, extended periods of inversion can be from two to five grab samples or 28 to 208 days long. It is not certain, however, that the inversion actually lasts over the duration of these extended periods.

Over the entire thirty seven year span of the study, of which twenty nine had data, five years had inversion twice per year, one in winter, one in summer, and seventeen had one inversion per year (11 winter and 6 summer). Looked at on a yearly basis, then, three quarters of the years (22/29) had one or more inversions. These results are obtained by converting extended periods into single events and adjusting seasons to years where there was overlap. While fairly common on a sample by sample basis, the year to year grouping suggests that inversion is a regular part of the seasonal cycle of events.

It is of fundamental importance to be able to recognize an inversion when it occurs and fortunately that is not difficult. The following discussion shows what an inversion ‘looks like’ as well as introducing the different analytical methods used. This is the ‘experimental’ data for the study. Major ion concentration inversion immediately stands out as something ‘different’ in river water quality charts. It represents a break in the steady position of the ions before and after. The following time-series graph shows the summer 1977 inversion of ‘grab’ (‘instantaneous’) samples in terms of a surrogate for concentration, the major ion charge % (50% cation, 50% anion).

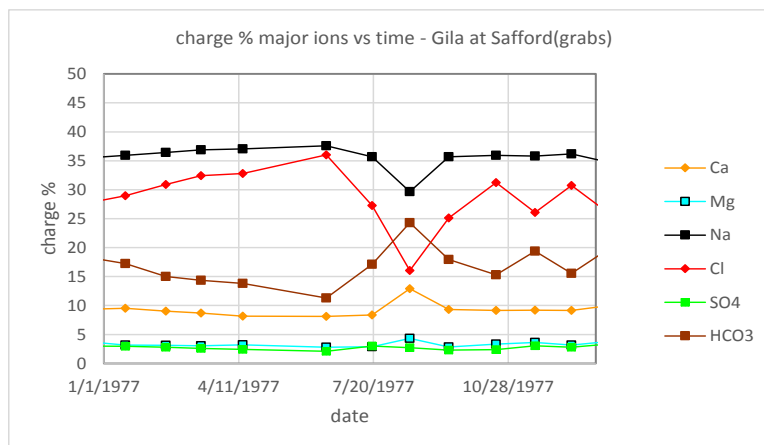


Figure 1 [\(back\)](#)

The hallmark of the inversion is that bicarbonate and chloride ion lines cross and bicarbonate becomes greater than chloride. Calcium and sodium do not usually completely ‘invert;’ they follow their preferred anion, bicarbonate and chloride respectively, but there is most often no crossing of lines – that is, calcium remains lower than sodium. Magnesium (Mg) and sulfate (SO<sub>4</sub>) remain relatively low and constant as if they wanted nothing to do with the matter.

The inversion is not always as clearly a ‘turning upside down’ as above. Witness, in the graph below, the same period in terms of the major ion concentrations themselves. It should be noted, in passing, that these are not grab sample analytical concentrations, they are specie concentrations ‘back-calculated’ from activities determined by the USGS speciation program, WATEQ4F.<sup>3</sup>

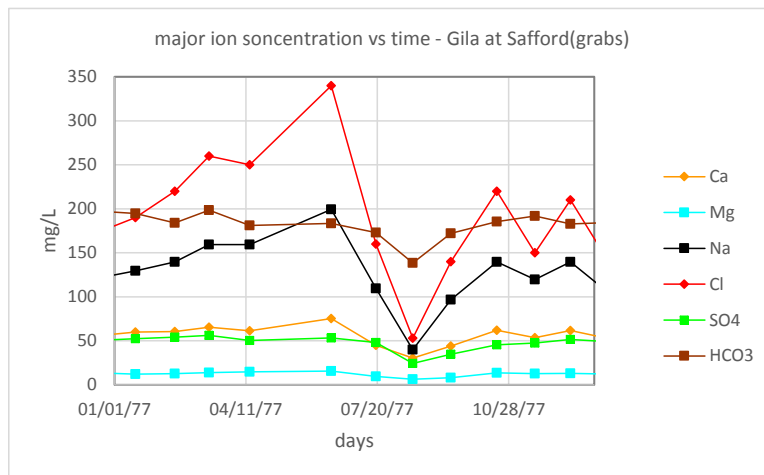


Figure 2 ([back](#))

This graph does not look like it has an ‘inversion’ at all because all concentrations are going down. But the essential requirement for inversion is that bicarbonate and chloride lines cross and that bicarbonate ends up higher than chloride and that is the case here. Bicarbonate and chloride lines going in opposite directions is the visual clue that helped reveal it initially but not a necessary part of inversion.

The graph below, which shows an inversion in early 1979, also has a different look. This extended inversion stretches out over roughly six months, with lines crossing visible only at the end (the inversion began in late 1978). Also shown in this graph is that bicarbonate and chloride can sometimes make pronounced ‘dips’ towards each other, as they do here in August. But their lines don’t cross and bicarbonate is at no time higher than chloride -- these ‘dips’ are **not** considered ‘inversions.’

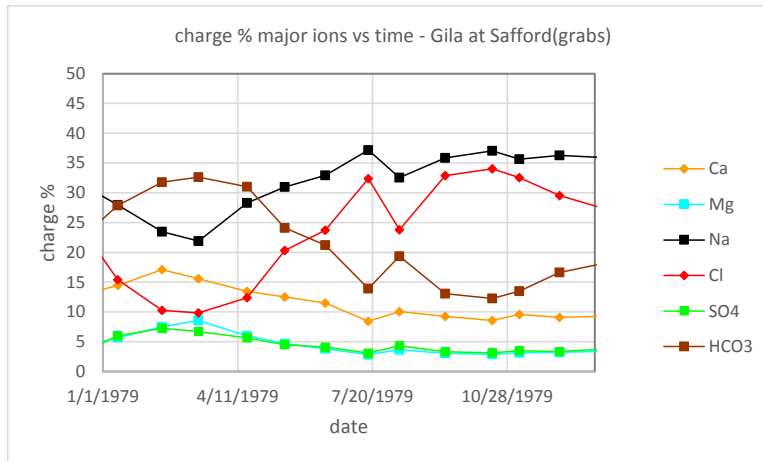


Figure 3

Analyzing inversions with graphs depends a lot on how the graphs are constructed. As an example, it is very hard to tell from the above graphs but magnesium (Mg) is following the pattern of the other ions fairly closely whereas sulfate (SO4), which is tracking so closely with Mg that they overlap, is not. Maybe a different ‘view’ of the data will help.

The table below carries the same information as Figure 1, the charge % of the major ions over the year 1977. This new view is a matrix of correlation coefficients which reflect the extent to which any two parameters are ‘moving in step.’ The closer to 1 (a direct relation) or -1 (an inverse relation) the coefficient, the more closely in step the parameters are. The patterns of the graphs are converted to numeric relations on the matrix.

intracorrelations charge % major ions 1977 - Gila at Safford(grabs)							
	Ca	Mg	Na	Cl	SO4	HCO3	
Ca	1.00	0.76	-0.97	-0.86	0.13	0.87	
Mg	0.76	1.00	-0.81	-0.66	0.20	0.72	
Na	-0.97	-0.81	1.00	0.91	-0.14	-0.89	
Cl	-0.86	-0.66	0.91	1.00	-0.25	-0.96	
SO4	0.13	0.20	-0.14	-0.25	1.00	0.42	
HCO3	0.87	0.72	-0.89	-0.96	0.42	1.00	

Sample pair count: 12 (all ions)

Table 1

For an ‘intra-correlation’ matrix such as the above, where the column and row headers are the same, the upper right corner of the matrix is a mirror of the lower left and the values of the determinant are all 1 (identities). In order that relationships of meaningful (non-determinant) values can be grasped quickly, coefficients of > 0.90 or < -0.90 are colored magenta and those between (+/-) 0.75 and 0.89 are light blue.

A correlation matrix is a less immediately graspable picture of the relations between parameters than a graph but it has several distinct advantages. The first is that it quantifies the extent of relation, replacing a ‘feeling’ that the parameters are moving together in step with a number. This number can be compared to others forming a scale with which even parameters of widely differing magnitudes can be evaluated. The second is that correlations can conveniently be used over varying time periods. This quality is particularly helpful with longer time spans whose time series graphs would appear as an unintelligible blur of points. The table below covers the major ion charge percent intra-correlations over the entire time span of the study – this will be the time frame default for correlation matrices unless otherwise specified.

intra-correlations charge % major ions -- Gila at Safford(grabs)						
	Ca	Mg	Na	Cl	HCO3	SO4
Ca	1.00	0.86	-0.77	-0.78	0.77	0.11
Mg	0.86	1.00	-0.77	-0.77	0.75	0.34
Na	-0.77	-0.77	1.00	0.92	-0.90	-0.33
Cl	-0.78	-0.77	0.92	1.00	-0.97	-0.35
HCO3	0.77	0.75	-0.90	-0.97	1.00	0.28
SO4	0.11	0.34	-0.33	-0.35	0.28	1.00

sample pair counts

charg%	Ca	Mg	Na	Cl	HCO3	SO4
Ca	161	161	161	161	161	161
Mg	161	161	161	161	161	161
Na	161	161	161	161	161	161
Cl	161	161	161	161	161	161
HCO3	161	161	161	161	161	161
SO4	161	161	161	161	161	161

Table 2

Or “sample pair count: 161 (all)”

This correlation table confirms that what is seen looking at individual annual graphs really does apply across all data. Here it can be verified that Na & Cl as well as HCO3 & Cl, the essential relations of the inversion, are highly correlated to each other, the former pair positively and the latter inversely. SO4, which does not have any high correlations, may be termed an ‘outsider’ in terms of charge% and is highlighted by a separate border.

One full set of sample pair counts for the correlation coefficients matrix above is also shown. It is entirely possible that there may be plenty of dates with data for one or the other of two parameters but few dates with data for both. Low sample pair counts can lead to high correlations by chance. With 2 sample pairs (4 values, 2 of each type) the result is always a

correlation of +/- 1, an apparent perfect correlation, which may not ‘hold up’ very long when more pairs are examined. The sample pair counts were always run as a check on correlation program results but are not usually shown here since most matrices have a full set of sample pairs (161 or 160 for sample differences).

As an example of why sample pair counts are important, note that the high inverse correlation between Na and Ca seen in 1977 does not hold up when more data is used. It is replaced by a higher correlation between Ca & Mg than seen in the 1977 matrix. The low number of samples, which would be immediately apparent on a graph, is hidden on a correlation matrix without any sample pair counts. The 1977 matrix has, as noted above, a sample pair count of only 12.

Running different analysis quantities of the major ions results in different correlation matrix patterns. The matrix below shows the intra-correlation of the major ion concentrations themselves over the entire time span of the study.

intra-correlation concentration major ions - Gila at Safford(grabs)						
	Ca	Mg	Na	Cl	SO4	HCO3
Ca	1.00	0.95	0.88	0.88	0.83	0.30
Mg	0.95	1.00	0.93	0.93	0.92	0.16
Na	0.88	0.93	1.00	1.00	0.96	0.22
Cl	0.88	0.93	1.00	1.00	0.95	0.18
SO4	0.83	0.92	0.96	0.95	1.00	0.17
HCO3	0.30	0.16	0.22	0.18	0.17	1.00

Table 3

Here all the ions are seen to be highly positively correlated to each other with the exception of HCO3 which is the outsider. This matrix provides the same information as [Figure 2](#) and leads to the same conclusion but has more weight than the graph due to the higher sample count.

Not all analyzes show high intra correlation, witness the mole fraction (% amount).

intracorrelation mole fraction major ions - Gila at Safford(grabs)						
	Ca	Mg	Na	Cl	SO4	HCO3
Ca	1.00	0.92	-0.35	-0.38	-0.02	0.36
Mg	0.92	1.00	-0.46	-0.49	0.10	0.44
Na	-0.35	-0.46	1.00	0.94	0.20	-0.66
Cl	-0.38	-0.49	0.94	1.00	0.07	-0.80
SO4	-0.02	0.10	0.20	0.07	1.00	0.10
HCO3	0.36	0.44	-0.66	-0.80	0.10	1.00

Table 4



This matrix shows little correlation among the major ions as a whole and therefore no ‘outsider’ is apparent. It does, however, include the major relations at the heart of inversion: the affinity of Na & Cl (+/-), the inverse relation between HCO<sub>3</sub> and Cl (-/-), and the affinity of Ca & Mg (+/+). These are the ‘poles’ within which the inversion oscillates.

With a large number of matrices covering different analyzers, there is a need for methods of summing the results. One technique is to calculate the percent of a perfect absolute matrix (that is, all ones). This calculation divides the sum of absolute values of the coefficients by the perfect absolute matrix sum and can be used on subsets of the matrix as well as the whole. For the above matrices, the charge % matrix is 0.65 for the whole matrix, 0.83 without the outsider SO<sub>4</sub>, the concentration matrix is 0.69, 0.92 without HCO<sub>3</sub>, and the mole fraction is 0.42 (no ‘outsider’).

With the percent of a perfect matrix calculation, the intra-correlation of the major ions can be compared across a variety of analysis quantities. In the table below the analyses are lined up from ‘simplest’ to more ‘complex’ and alternating value and corresponding percent. The results, using the same color formatting as the individual correlation matrices, are as follows

percent of perfect matrix - major ions - Gila at Safford(grabs)			
analysis	total	outsider	w/o otsdr
amount	0.83	Cl	0.90
%amount(m	0.42	none	
mass	0.83	Cl	0.90
%mass	0.68	HCO <sub>3</sub>	0.92
volume	0.82	Cl	0.90
%vol	0.67	HCO <sub>3</sub>	0.91
conc	0.69	HCO <sub>3</sub>	0.92
%conc	0.68	HCO <sub>3</sub>	0.92
activity	0.65	HCO <sub>3</sub>	0.92
%activity	0.62	HCO <sub>3</sub>	0.85
mols e	0.83	SO <sub>4</sub>	0.90
ionicity	0.83	Cl	0.90
charg%	0.65	SO <sub>4</sub>	0.83

Table 5 ([back](#))

Thus the major ions are highly intra-correlated across a wide spectrum of related but more or less distinct analyzers, not all of which are simply surrogates for concentration. The fact that this pattern persists over the entire time span of the study provides the ‘background’ pattern that makes the ‘inversion’ stand out when it occurs. The inversion appears as a break in a larger



pattern of relative positions but, as revealed by the correlational analysis, does not violate the positive and inverse relations among the individual ions to any appreciable degree. It is a change in relative position only, not a change in correlation (e.g. as from 'inverse' to 'direct').

Relations can always be improved by removing whatever doesn't agree and correlations rise when an 'outsider' is removed. The first few graphs show the central role of HCO<sub>3</sub> in the inversion so it is not surprising to see it as the most common 'outsider.' The lack of correlation of the mole fraction (% amount) makes it the 'outsider' on the level of analyzes and, being relative amount, seems particularly pertinent to inversion. The suspicion may arise that the 'outsider' may be what is causing the other parameters/analyzes to be in correlation. But a high correlation only reveals that a number of parameters are moving in step with one another. It gives no clue as to whether the cause is one of the parameters, something outside the correlation, or entirely coincidental.

The % perfect matrix approach summarizes matrices at the expense of a lot of information so it is probably worthwhile to summarize the main individual correlations potentially involved in the inversion.

intra-correlation coefficients - major ions - Gila at Safford(grabs)				
analysis	Ca&Mg	Na&Cl	Ca&HCO <sub>3</sub>	HCO <sub>3</sub> &Cl
amount	0.99	0.88	0.87	0.67
%amount(m	0.92	0.94	0.36	-0.80
mass	0.99	0.88	0.87	0.67
%mass	0.95	1.00	0.30	0.18
volume	0.99	-0.82	-0.87	0.87
%vol	0.95	-0.94	-0.87	0.14
conc	0.95	1.00	0.30	0.18
%conc	0.95	1.00	0.30	0.18
activity	0.92	1.00	0.30	0.13
%activity	0.92	1.00	0.30	0.13
mols e	0.92	-0.88	-0.87	0.67
ionicity	0.99	0.93	0.87	0.67
charg%	0.86	0.92	0.77	-0.97

Table 6

The most consistent relation is, interestingly enough, the high positive correlation between Ca & Mg. Next are the relations between cations and their preferred anions, Na&Cl and Ca&HCO<sub>3</sub>, both of which become inverse under volume, % volume, and moles e- as expected for +/- pairs. The HCO<sub>3</sub> & Cl correlation, the essence of inversion, is high and inverse for % amount (mole fraction) and charge % but high and positive for volume.

As yet another way of viewing the inversion, a different type of graph plots major ion data vs some other, single, analysis – here flow will be randomly selected. Below is a view of major ion amounts in 1977 with respect to flow. The first (left) is all the data for 1977, the second (right) is the lower quadrant, the low % charge & low flow portion, of the first.

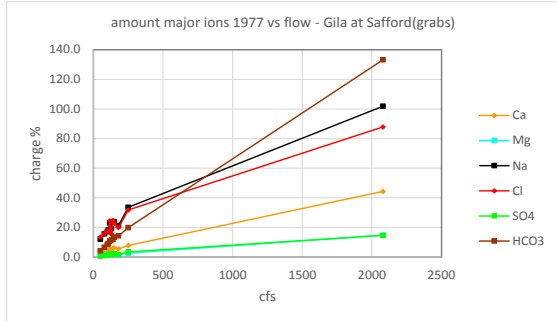


Figure 4

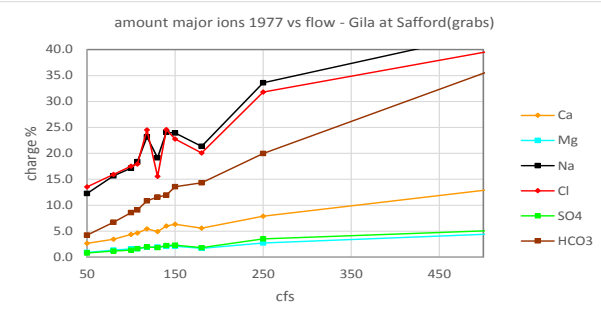
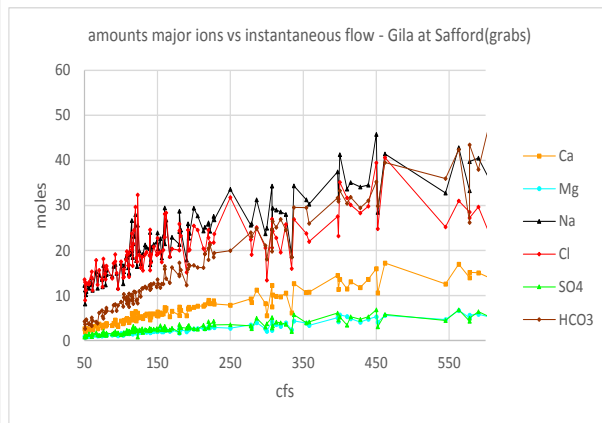
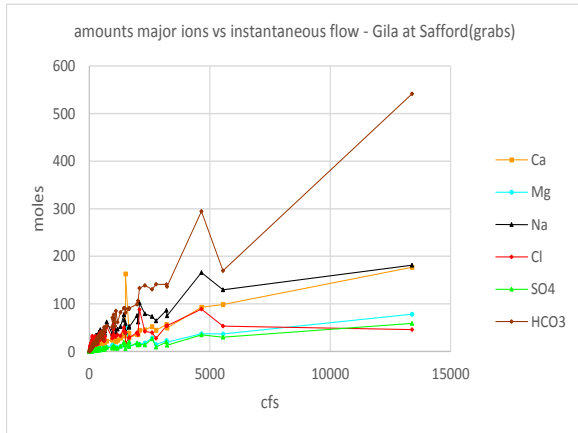
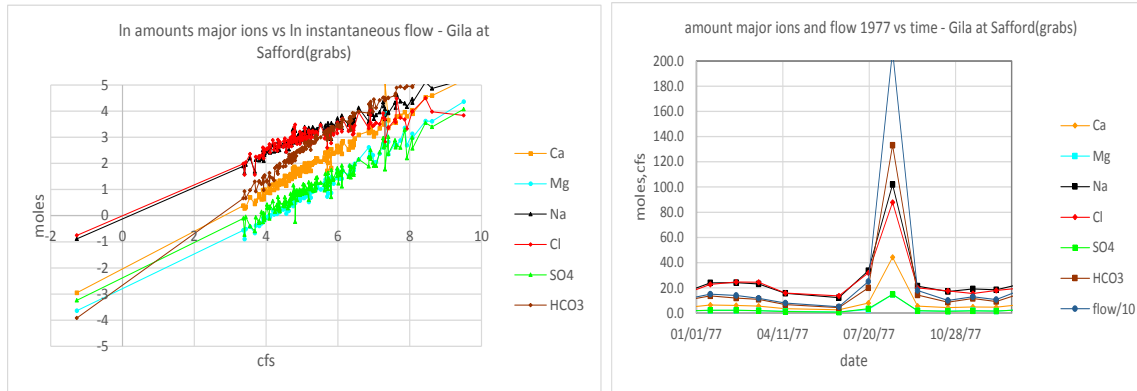


Figure 5

These graphs clearly have low sample counts (12) but do show the same patterns as seen when all available data is used (top row below). Na & Cl amounts have a logarithmic look, so the third graph (bottom row left) plots the natural log of flow vs the natural log of major ion amounts. Converting to logs makes all the relations linear but has the distressing effect of creating one set of negative flow and negative amounts which are not physically realizable quantities. Finally, going back to time-series graphing, the fourth graph (bottom row right) shows how flow and amount play out in time for the year 1977.





Figures 6-9

The time series graph shows a particular case in which amount appears to be related to flow, but tells us nothing about any other case. The single analysis graphs take the data out of its chronological time frame entirely, shows that the relationship is true across all cases, and allows focus on flow dependent relations. They present the same information as the time series graphs but with a different view at a different level of analysis.

Saying major ion inversion appears to be 'flow related' is another way of saying that the two seem to be highly correlated. The high degree of correlation can be more directly evaluated with a correlation matrix; not an 'intra-correlation' matrix of the major ions, but an 'inter-correlation' that relates them to bulk analyzes of the grab sample. The following matrix shows major ion amounts (moles) vs the bulk sample and environmental parameters of the grab samples they come from.

correlations amount major ions with bulk sample and environmental parameters							
Gila at Safford (grabs)							
values	Ca	Mg	Na	Cl	SO4	HCO3	HCO3-Cl
temp-grab/K	-0.25	-0.27	-0.38	-0.37	-0.35	-0.30	-0.25
press-grab/a	-0.18	-0.19	-0.23	-0.19	-0.21	-0.19	-0.17
flow-grab/cfs	0.86	0.91	0.87	0.57	0.94	0.97	0.98
dens(TSP)-gr	0.19	0.21	0.30	0.29	0.28	0.24	0.20
conductivity,	-0.31	-0.31	-0.41	-0.44	-0.33	-0.31	-0.25
ionicity soln/	-0.30	-0.31	-0.44	-0.45	-0.37	-0.35	-0.29
pH/SU	-0.20	-0.22	-0.19	-0.13	-0.23	-0.20	-0.20
totalk/(kg/L)	-0.59	-0.60	-0.59	-0.44	-0.60	-0.57	-0.55
D.O./(kg/L)	0.00	0.02	0.11	0.14	0.10	0.06	0.03
Eh H2O-O2/v	0.29	0.32	0.44	0.41	0.41	0.35	0.29
TDS/(kg/L)	-0.34	-0.34	-0.43	-0.44	-0.36	-0.35	-0.29
TSS/(kg/L)	0.17	0.16	0.12	0.02	0.11	0.15	0.17

(sample pair counts, TSS:117, Eh:133, all other:161)

Table 7

Unlike an intra-correlation matrix, the above matrix with different row and column headers has no determinant of identities and there is no replication of results – each coefficient is a unique major ion/analysis pair. Sample differences were evaluated but the color pattern result is the same as that of straight values. Exponentials were also run but produced no high correlations. These are therefore not shown.

The percent amounts of the major ions, however, bring out different relations when run against the sample bulk and environmental analysis parameters.

correlations % amount major ions with bulk sample and environmental parameters							
Gila at Safford (grabs)							
values	%Ca	%Lg	%Na	%Cl	%SO4	%HCO3	%HCO3-Cl
temp-grab/K	0.24	0.17	0.25	0.27	0.17	-0.06	-0.28
press-grab/a	0.11	0.07	0.07	0.06	0.09	0.17	-0.05
flow-grab/cf	-0.33	-0.24	-0.28	-0.27	-0.26	-0.55	0.22
dens(TSP)-gr	-0.07	0.01	-0.07	-0.09	0.00	0.10	0.10
conductivity,	0.68	0.70	0.76	0.76	0.73	0.25	-0.75
ionicity soln/	0.93	0.96	0.99	0.99	0.96	0.24	-0.98
pH/SU	0.05	-0.03	0.00	-0.01	-0.02	0.24	0.03
totalk/(kg/L)	0.32	0.19	0.26	0.23	0.20	0.92	-0.14
D.O./(kg/L)	-0.06	-0.03	-0.07	-0.09	0.00	0.26	0.12
Eh H2O-O2/v	-0.20	-0.10	-0.18	-0.19	-0.12	-0.05	0.19
TDS/(kg/L)	0.89	0.94	0.99	0.99	0.96	0.23	-0.98
TSS/(kg/L)	-0.23	-0.27	-0.27	-0.27	-0.28	-0.26	0.23

(Sample pair counts same as above)

Table 8

The % amounts are not highly correlated to flow, instead they are correlated to more ‘qualitative’ parameters such as conductivity, ionic strength (or ‘ionicity’), alkalinity, and TDS. While this is an ‘inter-correlation’ matrix, it is the similar physical characteristics of the ions (intra-ion) that make the correlation to the bulk quantities – i.e., they are all charged species.

Running logarithms on the values (below), yields a color pattern that pretty much combines that of the value and percent matrices above. The use of a variety of different ‘views’ of the same data is a particularly useful technique for uncovering patterns and relations and will be done repeatedly throughout the study.

correlations ln amount major ions with ln bulk sample and environmental parameters						
Gila at Safford (grabs)						
	ln Ca	ln Lg	ln Na	ln Cl	ln SO4	ln HCO3
ln-temp-grab/K	-0.44	-0.46	-0.45	-0.41	-0.48	-0.46
ln-press-grab/atm	-0.16	-0.17	-0.16	-0.13	-0.15	-0.16
ln-flow-grab/cfs	0.98	0.98	0.97	0.87	0.97	0.99
ln-dens(TSP)-grab/(kg/L)	0.32	0.33	0.31	0.27	0.35	0.33
ln-conductivity/(uS/cL)	-0.91	-0.92	-0.87	-0.76	-0.89	-0.92
ln-ionicity soln/#	-0.88	-0.88	-0.86	-0.75	-0.89	-0.92
ln-pH/SU	-0.16	-0.18	-0.11	-0.03	-0.17	-0.17
ln-totalk/(kg/L as CaCO3)	-0.55	-0.58	-0.47	-0.33	-0.56	-0.49
ln-D.O./(kg/L)	0.18	0.19	0.22	0.23	0.24	0.20
ln-Eh H2O-O2/volts	0.46	0.48	0.44	0.35	0.50	0.48
ln-TDS/(kg/L)	-0.90	-0.91	-0.85	-0.73	-0.88	-0.93
ln-TSS/(kg/L)	0.50	0.48	0.46	0.33	0.45	0.54

(Sample pair counts same as above)

Table 9

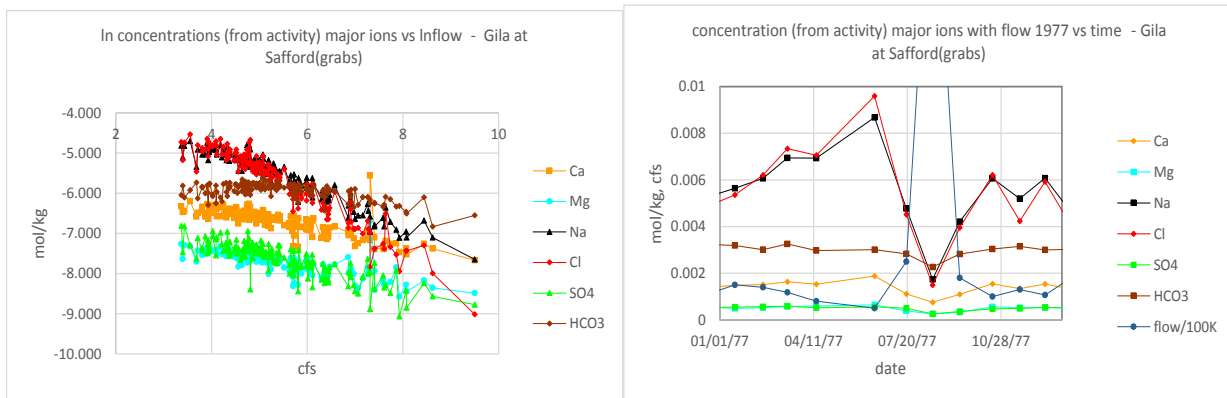
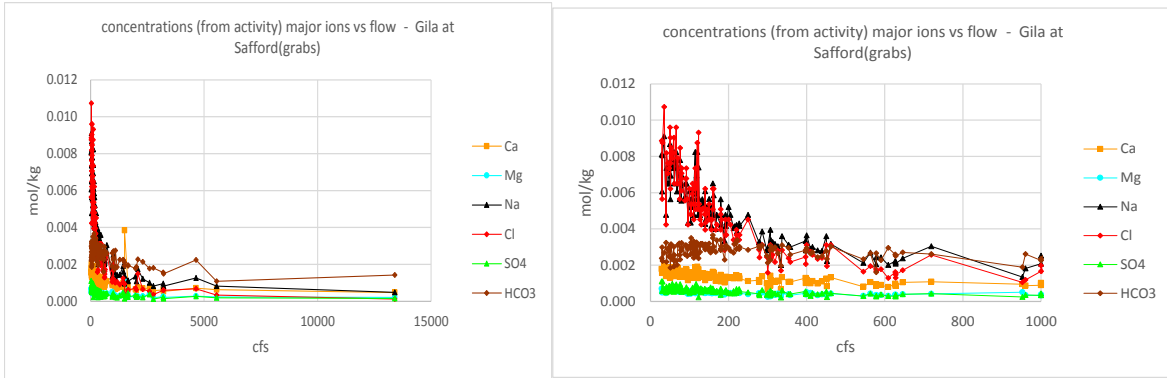
The intra-correlations of the major ions grows out of their inter-correlations to flow. This picture is particularly easy to see in the case of amounts which are usually positively correlated to flow and it follows that the ions are all positively correlated to each other as well. But how, then, can major ion inter-correlations sometimes be inverse? The answer is, of course, that different analysis quantities have different relations to flow.

Concentration, as opposed to amount, is usually inversely related to flow. The following are the correlations between major ion concentrations, calculated from activity, and the field and lab analysis parameters.

correlations concentration (mol/ kg calc from activity) major ions with bulk sample and environmental analyzes - Gila at Safford(grabs)							
	Ca	Mg	Na	Cl	SO4	HCO3	HCO3-Cl
temp-grab/K	0.24	0.17	0.25	0.27	0.17	-0.06	-0.28
press-grab/atm	0.11	0.07	0.07	0.06	0.09	0.17	-0.05
flow-grab/cfs	-0.33	-0.24	-0.28	-0.27	-0.26	-0.55	0.22
dens(TSP)-grab/(kg/L)	-0.07	0.01	-0.07	-0.09	0.01	0.10	0.10
conductivity/(uS/cL)	0.69	0.70	0.76	0.76	0.73	0.25	-0.75
ionicity soln/#	0.93	0.96	0.99	0.99	0.96	0.24	-0.98
pH/SU	0.05	-0.03	0.00	-0.01	-0.02	0.24	0.03
totalk/(kg/L as CaCO3)	0.32	0.19	0.25	0.23	0.20	0.92	-0.14
D.O./(kg/L)	-0.06	-0.03	-0.07	-0.09	0.00	0.26	0.12
Eh H2O-O2/volts	-0.20	-0.10	-0.18	-0.19	-0.12	-0.05	0.19
TDS/(kg/L)	0.89	0.94	0.99	0.99	0.96	0.23	-0.98
TSS/(kg/L)	-0.23	-0.27	-0.27	-0.27	-0.28	-0.26	0.23
	ln Ca	ln Mg	ln Na	ln Cl	ln SO4	ln HCO3	ln HCO3-Cl
ln-temp-grab/K	0.28	0.21	0.36	0.38	0.22	-0.02	0.34
ln-press-grab/atm	0.18	0.15	0.18	0.18	0.18	0.19	-0.03
ln-flow-grab/cfs	-0.84	-0.82	-0.96	-0.95	-0.86	-0.53	-0.51
ln-dens(TSP)-grab/(kg/L)	-0.16	-0.08	-0.24	-0.27	-0.10	0.07	-0.25
ln-conductivity/(uS/cL)	0.82	0.77	0.94	0.93	0.84	0.58	0.48
ln-ionicity soln/#	0.95	0.92	0.97	0.95	0.87	0.58	0.53
ln-pH/SU	0.24	0.18	0.27	0.27	0.19	0.25	0.05
ln-totalk/(kg/L as CaCO3)	0.61	0.50	0.68	0.69	0.55	0.95	0.09
ln-D.O./(kg/L)	-0.03	0.02	-0.06	-0.08	0.06	0.23	-0.17
ln-Eh H2O-O2/volts	-0.36	-0.27	-0.45	-0.47	-0.30	-0.08	-0.34
ln-TDS/(kg/L)	0.90	0.87	0.98	0.97	0.89	0.57	0.53
ln-TSS/(kg/L)	-0.53	-0.60	-0.59	-0.59	-0.61	-0.30	-0.34

Table 10

Here the percents produce the same pattern as the straight values and are not shown. Flow is not highly correlated but rather has a low negative correlation and only reappears as a high correlation when logs are taken. Put in graphical form these results plot as follows:



Figures 10-13

Notice that in the last graph, the time-series view, flow was ‘scaled’ with all values divided by 100. Without this scaling, flow would have filled up the entire graph and the major ion concentrations would have reduced to straight lines across the bottom of the graph, making it impossible to see the relation between the two.

The ‘distressing’ aspects of analysis with logarithms should not be considered overly important. While negative concentrations are not physically possible, this outcome is just a result of the fact that the relation between flow and concentration is inverse. What is important is that the underlying relationship, the shape of the data, is sometimes not linear but logarithmic, as with Cl concentration and flow.

It follows that low correlations can sometimes simply mean the correct relationship is not being used. The problem here is the use of an ‘out of the box’ function; Excel’s “correl” worksheet function is, as far as is known, exclusively linear. The true nature of the relation can often be revealed by comparing correlations and graphs. Excel graphs can produce a variety of trend lines (linear, logarithmic, exponential, polynomial (2-6 degree) and moving average) which are essentially correlations in the various views of the data. It is easy try them all out and select the one with the best fit. More sophisticated curve fitting programs are, of course, available but there

are some advantages to using simple tools -- more sophisticated programs may be making decisions the user is not aware of.

Another type of correlation used here is ‘autocorrelation’ which looks for patterns within a single parameter over time. A simple sum of the squares program was written to calculate autocorrelations. No acceptable method to reduce the results to a numerical value was found so the method remains part graphical, part numerical with neither part separately considered conclusive.

To develop and test the program a ‘seasonal test pattern’ (stp) was created. The numbers 0 through 6 were assigned to grab sample dates based on month with 0 in Jun and 6 in Dec and 5 to 1 from Jan to May to form a peak in Dec and a valley in Jun (below left). The same assignment of numbers by month can be done on all the consecutive dates (no data gaps as in the grabs) over the time span of the study to yield a stronger, more consistent signal (below right).

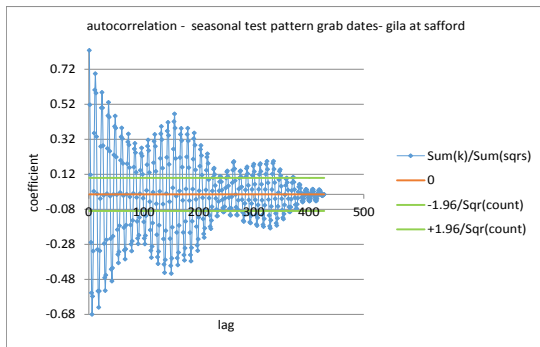


Figure 14

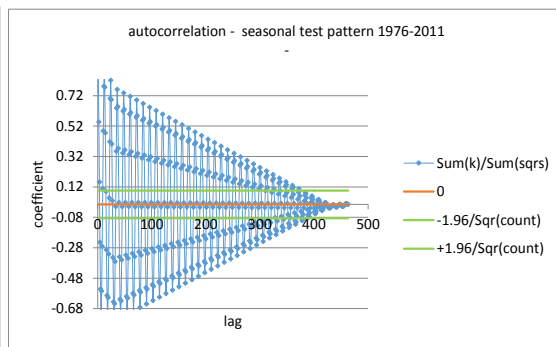


Figure 15

autocorrelation statistics - seasonal test pattern				
	% at 6&12	% at 12	$\Sigma x_1 y_2 / \Sigma sqrs$	count
grab sample dates	0.8571	0.8451	0.3041	428
all dates 1976-2011	0.8947	0.8831	0.2734	462

Table 11

The defining features of high auto correlation are the ‘damped’ oscillator pattern of the graph – decreasing amplitude with increasing lag time -- combined with maximums or minimums at regular intervals. The numbers below the graphs above are the percent of peaks for mins or maxs at months 6 and 12, ditto for 12 only, the  $\sum x_1 y_2 / \sum sqrs$ , and the process (not original) sample counts. Note that the grabs (161 original samples) have roughly the same post-processing sample count as the ‘all dates’ (13500 samples). The autocorrelation program has a built in averaging procedure to cover data gaps without which the grab samples could not be run.



The hallmark of seasonal autocorrelation is high percent mins or maxs at 6 and 12 months and that is the number most heavily relied on. Some parameters show mins or maxs in Dec. only (relative humidity being one, possibly because it is so low in the month of June in Arizona that it is difficult to accurately measure). The  $\sum x_1 y_2 / \sum s_{qrs}$  is from the program and highly regarded by statisticians but did not seem to yield consistent results. This situation is concerning because the  $\sum x_1 y_2 / \sum s_{qrs}$  is the basic output of the sum of the squares analysis while the percents by month is an added-on feature. But here, as elsewhere in this work, the usefulness and internal consistency of results outweighs the niceties of theoretical derivation (possibly at some peril).

To illustrate some of the factors involved in autocorrelation, a couple manipulations are done on the full date seasonal test pattern (Figure 15) and the results are shown on the graphs below. Removing the test pattern data in the same 6.5 year period as the data gap in the grabs (9/80-3/87) reveals the beginnings of the undulating increasing and decreasing amplitude seen in the grab dates run. Adding another factor onto the last run, dividing the test pattern numbers by 1000 from 1/1/1990 to 12/31/1999, shows the result changing magnitudes can have. Neither manipulation greatly changes the % peaks at 6 & 12.

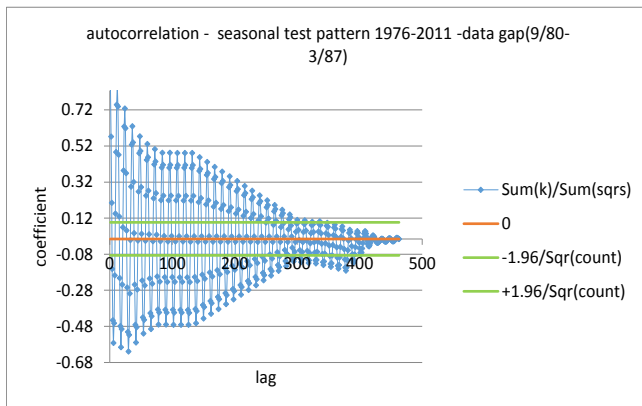


Figure 16

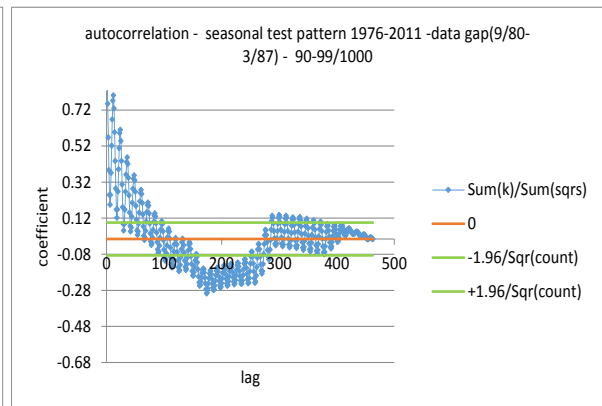


Figure 17

autocorrelation statistics - seasonal test pattern				
	% at 6&12	% at 12	$\Sigma x_1 y_2 / \Sigma s_{qrs}$	count
1976-2011-(9/80-3/87)	0.8947	0.8831	0.2647	462
ditto + (1900-99)/1000	0.8421	0.8442	0.1612	462

Table 12

All high autocorrelations look pretty much alike, including those of inversion data, so these will not be shown until some further tools have been developed. Instead, a good example of high autocorrelation using real world data is that of density. Indeed, density might well serve as test pattern itself since it is known to be highly seasonal:

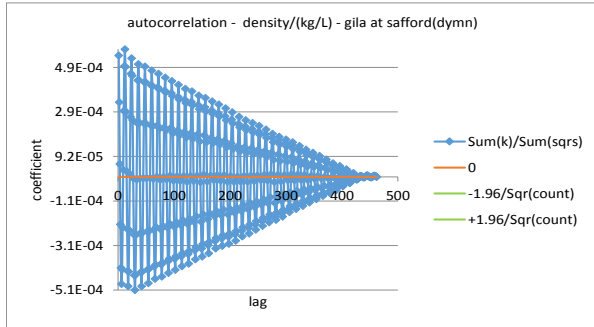


Figure 18

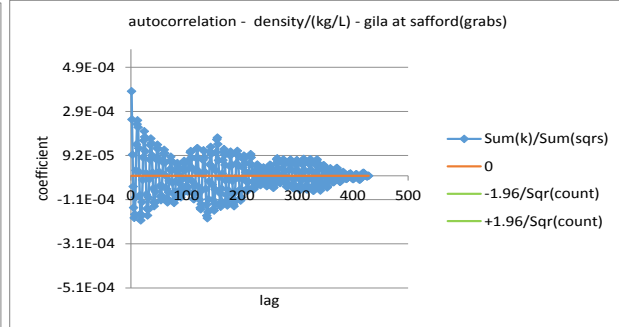


Figure 19

autocorrelation statistics - density - Safford				
	% at 6&12	% at 12	$\Sigma x1y2/\Sigma sq$	count
dymns	0.9211	0.9221	0.2825	462
grabs	0.8000	0.7465	0.3971	428

Table 13

If the density or seasonal test pattern autocorrelation is used as the standard – i.e. damped oscillator pattern of graph and roughly 0.8 % max/min at months 6 & 12 – other parameters can be run and compared to that.

These then are the basic methods used to investigate the inversion: time series (usually annual) graphs, correlation matrices (intra- or inter-), single analysis graphs, and autocorrelations. Together they provide snapshot pictures of what the inversion can ‘look like’ in terms of various analysis quantities, over various time periods, and under varying environmental conditions. The different views can be usefully contrasted and compared to each other to overcome problems or limitations in any particular single view. The hope, however, is that contrasting and comparing views with different temporal and spatial frames will also lead to some insights into how to combine the snapshots (stills) and put them into motion to create a dynamic picture of the system.

First, however, a small qualification. It might fairly be argued that major ion ‘inversion’ depends largely on which ions are considered to be ‘major.’ Indeed, the most significant criteria for inclusion of sample dates in this study is that the major ions all be analyzed and found to be present. The major ions can be determined simply by lining up the average activities of all the parameters in the database from greatest to smallest (below). H<sub>4</sub>SiO<sub>4</sub> and Fe(OH)<sub>3</sub> cannot be selected because they are not ions and are initially assumed probably not relevant to an intra-ion phenomenon such as inversion. The choice of major ions is admittedly somewhat arbitrary but

should not present any major difficulties in the analysis which will not, in any case, be limited to them.

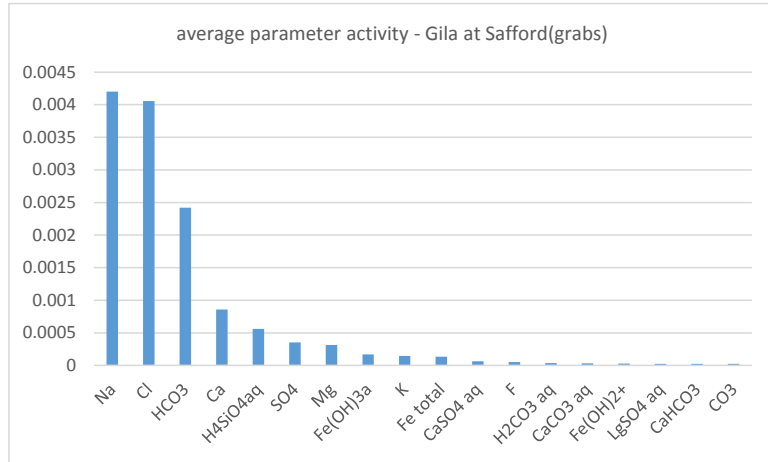


Figure 20

Inversions were initially identified with graphs but soon a need for an easier, more processing-friendly, method of spotting inversion dates was felt. The analysis of inversion can be simplified by using a 'test parameter' that highlights the most significant ions for inversion. The test parameter is simply  $HCO_3 - Cl$  for any analysis. If the quantity  $HCO_3 - Cl$  is positive the day is an inversion date, if not it isn't. (A number of other expressions were tested but none were better at differentiating inversion from non-inversion;  $HCO_3/Cl > 1$  is occasionally useful). The following table, which shows a result only when  $HCO_3 - Cl > 0$ , shows a portion of the inversion date determination worksheet covering the same analytes as used above in the same order but as column rather than row headers.

Identify inversion dates

HCO3-Cl>0

Time/date	amount	% amount mass	%mass	volume	%volume	conc	%conc	activity	%activity	mole	ionicity	charge%	
01/20/76			67	0.0023	0.0111	0.0004							
02/20/76	17	6	2229	0.0079	0.9974	0.0035	0.0006	0.0011	0.0006	0.0010	17	17	6
03/15/76			379	0.0061	0.1158	0.0019							
04/07/76			53	0.0047	0.0162	0.0014							
05/10/76			114	0.0020									
06/14/76													
08/10/76													
09/22/76													
10/12/76													
11/16/76			130	0.0041	0.0448	0.0014							
12/14/76			82	0.0028	0.0284	0.0010							
01/17/77			20	0.0005									
02/16/77													
03/14/77													
04/14/77													
06/15/77													
07/19/77			91	0.0013									
08/16/77	45	7	5011	0.0085	2.0280	0.0034	0.0008	0.0014	0.0007	0.0013	45	45	7
09/14/77			164	0.0032	0.0260	0.0005							
10/19/77													
11/17/77			154	0.0042	0.0561	0.0015							
12/14/77													
01/16/78			300	0.0055	0.1222	0.0022							
02/06/78			583	0.0063	0.2470	0.0027							
03/23/78	49	13	4079	0.0099	1.8179	0.0044	0.0012	0.0022	0.0011	0.0020	49	49	15
04/13/78	1	0	1384	0.0068	0.5444	0.0027	0.0000	0.0001	0.0000	0.0001	1	1	0

Table 14

Comparing with graphs and viewing the entire table reveals that the quantity HCO3 - Cl is positive across all analysis quantities on inversion dates (defined as (conc) HCO3-Cl>0). Mass and volume and their % counterparts show HCO3 - Cl>0 on other dates as well but, on inversion dates, HCO3 is always higher than Cl for these analyzes as well. Overall HCO3 mass is > CL about 65% of the time and volume about 59% but not always on the same days.

The test parameter as an indicator of inversion only runs into one seeming problem – on 12/3/2008, HCO3 activity is higher than Cl activity but only mass and volume follow suit. A quick check of the charge% graph indicates that HCO3 charge % is equal to Cl charge %. The test was purposefully made ‘greater than’ (>) not ‘greater than or equal to’ (>=). While the criterion for inversion is simple, HCO3>Cl, a further criterion can now be added– ‘over all selected analysis quantities’ – 12/3/08 is not an inversion date.

comparison inversion with non-inversion data - Gila at Safford(grabs)													
	amount	% amount mass	%mass	volume	%volume	conc	%conc	activity	%activity	mole	ionicity	charge%	
non-inv	-7.31007	-13.2789	30.83396	-0.00429	-0.01461	-0.00296	-0.00327	-0.00588	-0.00282	-0.00508	-7.31007	-7.31007	-12.8637
inversion	45.52975	9.455081	1966.841	0.006295	0.945848	0.002758	0.000851	0.001532	0.000793	0.001427	45.52975	45.52975	11.0776
12/03/08			490.5672	0.008057	0.210276	0.003454			1.2E-05	2.16E-05			

Table 15

In the table above, negative values mean Cl > HCO3 (non-inversion). All averages, except mass which cannot be negative, go from negative to positive between inversion and non-inversion and the differences are usually substantial. No ‘magic’ numbers or ratios, however, were found.

The inversion parameter (HCO<sub>3</sub>-Cl) correlations with flow and density for the same analysis quantities in the same order as above are shown in the table below. The partial molar volume, a representative of the ‘specific’ properties, not included in earlier correlation matrices because uniformly uninteresting (i.e. low correlations), is also shown.

correlations inversion test parameter with flow and density - Gila at Safford(grabs)				
analysis	flow		density	
	r <sup>2</sup>	type	r <sup>2</sup>	type
amount	0.95	lin	-0.04	lin
%amount	0.84	log	-0.13	lin
mass	0.96	lin	0.05	lin
%mass	0.61	log	0.20	lin
par mol vol	0.07	lin	0.97	lin
volume	0.96	lin	0.05	lin
%vol	0.82	log	0.25	lin
conc	0.71	log	-0.18	lin
%conc	0.70	log	0.18	lin
activity	0.70	log	0.18	lin
%activity	0.71	log	-0.18	lin
mols e-	0.95	lin	0.04	lin
ionicity	0.96	lin	0.04	lin
charg%	0.85	log	-0.13	lin
charg%	0.35	lin		

Table 16 [back](#) [back2](#)

These are not ‘intra-correlations’ among ions nor are they ‘inter-correlations’ with bulk sample analyzes, they are direct correlations to inversion. With the individual major ions the absolute amount/mass/volume and charge were highly correlated but their percents were not. Here, with a surrogate for the major ions specific to inversion, % amount, % volume, and % charge also show high correlations with flow when logs are used. The partial molar volume appears as the only analysis quantity low in relation to flow but high in relation with density. Its importance will be examined more closely further on.

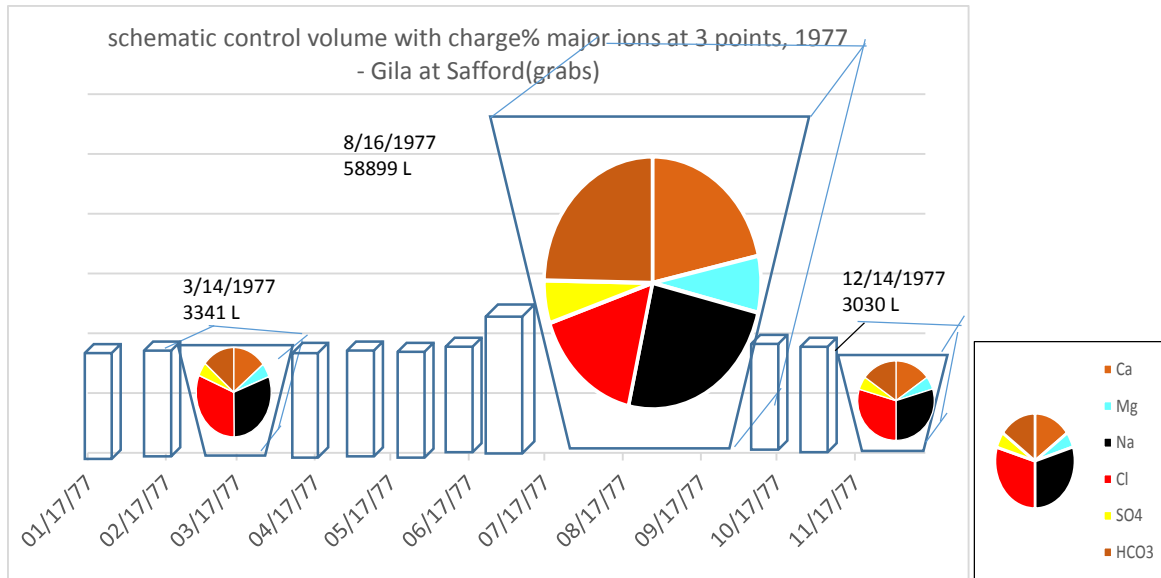
To get beyond merely identifying inversion dates, it is necessary to put the inversion into its proper context and formulate how an individual inversion can or should be analyzed. Inversion of major ions is not common in other Arizona rivers. The Colorado River at Lee’s Ferry did show inversions of SO<sub>4</sub> and Cl fairly frequently before major dam construction in the 1960s but stopped entirely afterwards. At the Colorado at Morelas there was a concentration inversion of SO<sub>4</sub> and Cl in 1993. The increased chloride in the Colorado did not, of course, spontaneously appear from nowhere. What caused the chloride concentration to go up was input to the Colorado

from one of its tributaries – the, at that point, very high chloride Gila at Dome. Inversion is, at a first approximation at least, a matter of opening and closing inputs to the system from the environment. It follows that to study inversion it is necessary to first be able to clearly differentiate the system from the environment and then be familiar with the environmental context, flow and density patterns, at any given time.

Unlike the case with the Colorado, the inversion inputs for the Gila are not known at this time. They will therefore have to be deduced from their effects on the system as represented by a ‘control volume.’ The control volume is not itself a complete system; its size and boundaries are different from those of the truly complete river system. It is a subset of the system assumed to be in 1:1 correspondence with the system as a whole. More specifically, it differs from the whole river system in absolute size and absolute size related phenomena but is 1:1 for change in size and non-size dependent phenomena. When the control volume grows the assumption is that it is because the entire system has grown. More precisely, all the control volumes (subsets) of the system grow sequentially over time from the point of input downstream until the pulse dissipates, the new material from the environment having become part of the new, larger control volumes.

The control volume is a ‘slice’ of or ‘wedge’ across the river at the sample point. All of its dimensions are more or less deformable except one which is invariant. The bottom and sides (banks) and the atmosphere are real physical boundaries which usually change relatively slowly in an established river under stable flow conditions. Work is done against and heat exchanged across these boundaries but are presumably negligible in amount at any given instant, particularly in contrast to that of the mass of water rushing downstream. The upstream and downstream sides are entirely hypothetical constructs that are rigid and impermeable and appear and disappear in time like locks, to let the next ‘wedge’ through. While they are in the line of action, they do not move but magically appear and disappear instead so no work is done. No heat is considered to pass for book-keeping reasons.

Curiously enough, the invariant dimension is not a spatial one but time – the control volume is the wedge of material that is created in one second of flow. The volume in liters is therefore equal to the flow in cfs with the appropriate conversion factor and multiplier ( $\text{cf/s} * 28.317 \text{ L/cf} * 1\text{sec}$ ). To fit the unspecified, generic volume to its shape at the site, the area of the wedge is calculated from the flow. This ‘guesstimate’ is based on 617 instantaneous area and instantaneous flow measurement pairs taken at the sample site by USGS from July of 1974 to July of 2017. An equation is created ( $r^2=0.92$ ) which is used to generate areas from flows. With the area, the length can be calculated ( $\text{velocity (or flow/area)} * 1\text{sec}$ ). The velocity is combined with the fact, derived from the literature, that the slope at the sampling point is about 9% to deduce the drop in elevation of the wedge ( $\text{vel} * 1 \text{ sec} * \tan(.002)$ ) Finally the mass is the volume (L) times the density (kg/L). The control volume represents the whole system at a specific time and place. All chemistry and thermodynamic measurements, which are ‘instantaneous’ (‘grab’) measurements as well, refer to material in the (instantaneous) control volume.



Schematic 1

The schematic above is the ‘literal’ or ‘control volume’ representation of [Figure 1](#): a series of one second snapshots of a sliver of material, average length roughly 0.03% of the Arizona portion of the river, taken at intervals of 2.5 million seconds (1 month) apart. This view should suffice to illustrate how daunting the task of using grab samples to characterize the river as a whole really is. The inversion, as seen in this view, is the difference in ion charge percent of the three pie charts shown – higher HCO<sub>3</sub> & Ca, lower Na & Cl on 8/16 compared with the opposite on 3/14 & 12/14. Unfortunately inversion analysis depends entirely on the chemical analysis done on ADEQ grab samples. Fortunately there is also another relevant dataset available for the site, the USGS daily mean flows.

There are two main, independent groups of physical measurement data in this study – the chemistry data from the Arizona Department of Environmental Quality (ADEQ) Surface Water Quality Database (SWQD) and the environmental data (flows and temperatures) mostly from USGS, University of Arizona (AZMet), Safford Regional Airport (SRA), and ADEQ-SWQD. Everything else is calculated from one or the other of these two sources. The problems encountered in correlational analysis of a large number of calculated values derived from a small number of physical measurements are probably best left to experts in statistics. Suffice it to say that, here, the distinction between a physical phenomenon and its mathematical expression is not dwelt upon unless it is apparent that some number is only the result of a mathematical manipulation with no physical significance (e.g. negative amounts or concentrations when depicted in logarithmic form).

As pointed out earlier, one of the criteria used for inclusion of data in this study is that all the major ions be present. For other parameters, each sample represents a different mix. In general, the number of parameters analyzed by ADEQ increased over the years and most of the trace metal data is from the last ten years. Arsenic, however, was always covered because it is of

concern for the water quality assessment of the Gila. For other species, like silicon and iron, coverage is sporadic because, with no applicable water quality standards, they were not always analyzed.

The ‘presence’/‘non-presence’ issue has various causes and consequences. It is very difficult, sometimes impossible, in a public records database, to know whether an analysis was run with no detectable result or simply not run at all. With limited budgets and staff, not every analysis can be run on every sample and ‘reruns’ to verify questionable results are not always feasible. A related issue is that values in a public records water quality database are not always ‘real’ numbers. Trace elements can sometimes be detected but at lower levels than can reliably be quantified. In these cases, an MDL or PQL (minimum detection or practical quantitation limit) value is assigned rather than a ‘real,’ probably unreliable, value. Zigzag patterns of trace metals can sometimes simply be artifacts as numbers switch between real and assigned values. Finally, some numbers can be derived, at least in part, from calculations done on indirect physical measurements – bicarbonate, carbonate, and hydroxide from alkalinity is one example.

The most significant cause of ‘non-presence’ is, however, not analytical but rather the data gaps resulting from sampling schedule decisions. Sampling data gaps are a more or less serious problem depending, obviously, on their length and frequency of occurrence in relation to the time length between regular sampling. A missing data point in daily sampling is less likely to be a serious issue than a missing data point in monthly sampling. The sampling intervals between the grab samples in this study are not completely random but they are not entirely consistent either and can range from 1 day to 6.5 years. Over the entire period of coverage (1976 – 2011) grab sample intervals average about 80 days with a mode of 28 days for 6.5% of the samples. Less statistical sounding but more useful: there are five years in which samples were taken monthly (1976-80), followed by a 6.5 year gap, after which samples were usually taken 3 or 4 times a year. The data in the early years, therefore, was relied upon heavily to set up the patterns for inversion while that of later years was generally used with trends from the earlier years assumed.

The intervals between grab samples on the graphs are easily bridged by straight lines but these imply a knowledge of the interval that is not available and can therefore be more or less misleading. To illustrate this point, ADEQ instantaneous flow measurements, taken at the same time as the ‘grab’ sample for chemistry, are compared to USGS daily mean flows at the sample site over the year 1977.



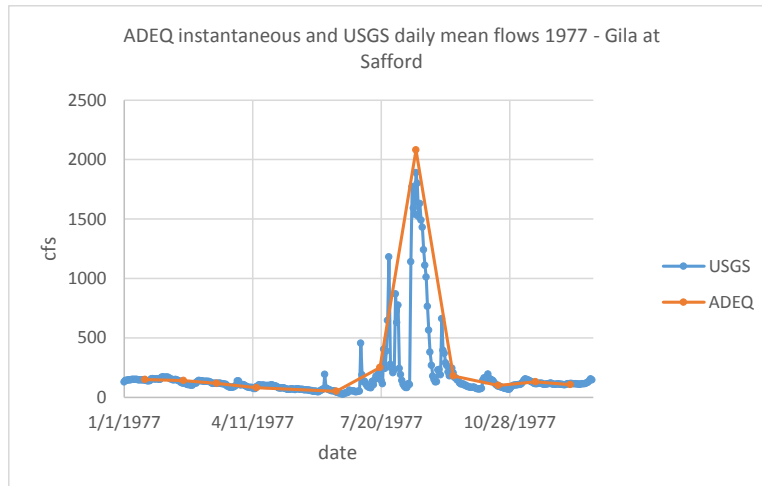


Figure 21 ([back](#))

The ADEQ instantaneous data fairly closely approximates the overall shape of the USGS daily mean data ( $r^2 = 0.76$ ) but shows a smooth ascent and descent around the large central peak that are not supported by the USGS daily means data. Strictly speaking, averaged data cannot be used to support instantaneous nor vice versa: they are two different things. But what are the implications of the difference in terms of drawing conclusions? The question is impossible to answer because it depends on what is being looked at. In some cases, such as counting the number of high flow seasons, the overall shape of the peak is usually sufficient. In others, such as wondering whether an inversion exists over an entire high flow period, it isn't.

Despite these potential difficulties, the hope here is that by comparing and contrasting instantaneous and daily mean values it will be possible to relate the behavior of the control volume to that of the river as a whole. This type of reasoning is used all the time when people speak loosely of the chemistry of a number of grab samples as that of the 'river' as a whole. The assumption is that, as the number of grab samples increases, the difference between their average and the daily mean will decrease. In practice, that is not always verified or even verifiable. One of the main approaches of this study will be to look at daily means to provide a 'context' or 'bridge' between various instantaneous chemistry and thermodynamic values of the control volume which relates them to the river as a whole.

Here are some concrete examples of why the distinction between instantaneous (grab) and daily mean values matters. Sometimes the instantaneous and daily mean data are just not 'in sync'. On 12/18/1978 the grab (instantaneous) flow was 462 cfs, the daily mean 14,800 cfs. The chemistry that day shows values of conductivity and TDS (601  $\mu\text{S}/\text{cm}$  & 426  $\text{mg}/\text{L}$  respectively) that would normally be associated, given other instantaneous data points, with a low flow not a high flow sample.

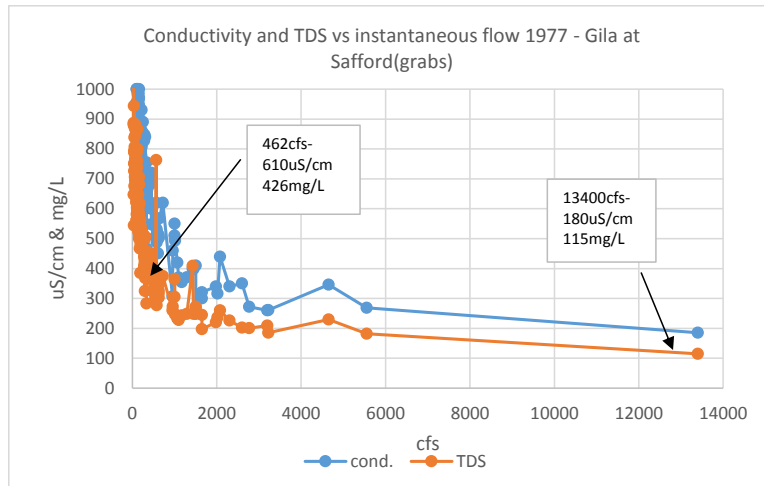


Figure 22

Looking more closely at the USGS data around 12/18/78 reveals that flows on the three previous days were 411 +/- 11 cfs while flows on the next three days were 40400 +/- 24920 cfs. Apparently the grab sample was taken early in the day; later it began to rain and rained for the rest of the day to such an extent as to send the daily average to 14800. In this case, the grab sample is not representative of average flow conditions and, more importantly, the average does not provide the correct 'context' for the grab sample chemistry. To associate the chemistry of that day with the daily mean flow would confuse the picture of the relation between flow and concentration as represented by TDS and conductivity.

Not all examples of this kind of problem are as easy to 'explain away'. On 9/20/1978, the instantaneous flow was 0.28 cfs. The daily mean flow for that day, two days before, and two days after was 77 +/- 3.4 cfs and a grab sample taken the next day was 70 cfs. For a river whose average instantaneous flow is 558 cfs and whose average USGS daily mean flow is 571, 70 is low but 0.28 cfs is really just a trickle. The conductivity and TDS (7500/4682), however, do indicate an extremely low-flow sample and the values go down the next day (1300/762) to those of a moderately low-flow sample.

The rule of thumb used here is that the instantaneous chemistry and thermodynamic data are always directly relatable to instantaneous flow. If the chemistry doesn't make sense in light of the instantaneous flow there is a problem somewhere, either in the chemistry or the flow measurement or both. But if the chemistry does not make sense when associated with the daily mean flow there is not necessarily any problem. Daily mean flow may help provide a context for instantaneous chemistry but cannot be used to test it.

Following this line of reasoning somewhat further, there is (probably) nothing wrong with either the grab sample chemistries or the daily mean flows of 9/20 or 12/18/1978. Any water quality dataset will, under close scrutiny, have its issues and these may or may not have any effect on conclusions. Grab sample chemistries here were put through a fairly rigorous set of tests that included both mass and charge balancing, the latter evaluated with seven different criteria (most from Standard Methods).<sup>4</sup> In fact, the 161 samples used here are out of 249 original samples

dating from 1965 to 2011; 88 samples did not pass tests or did not have a complete enough set of data to allow for charge balancing. The USGS speciation program used (WATEQ4F) added another layer of tests, though the few odd results that did appear were merely noted since the basic tests had been passed. The USGS daily mean flows are rigorously scrutinized and there was not felt to be any need to check their validity.

It is not necessary to ‘throw out’ data simply because grab results and daily mean flows are not in agreement. In hindsight, and in view of the constantly recurring problems it created, deleting the 9/20/78 sample might not have been a bad idea. There are, however, certain advantages to keeping outliers around and not sweeping them under the rug. On occasion a few outliers were left off graphs (and so noted) for clarity of presentation but no data that passed the initial tests was deleted.

The dichotomy between instantaneous and averaged data applies to any dataset that has a mix of the two. But it is a particularly important issue here because it is paralleled by an analogous relation between two characteristics of the physical environment of the region. The first is that erratic local precipitation patterns can lead to river flows being ‘flashy’ or changeable in both spatial and temporal scales. Meteorologists on the local network news like to point out that scattered, localized showers are the norm during the summer monsoons, particularly early on. A common phenomenon in the area during the summer is the so called ‘microburst’ -- a sudden heavy downpour over a very small area. A mainstay of neighborly conversation after a storm is how one house on the block got a ‘soaking’ while the one next to it didn’t get a drop. The term ‘intermittent flow’ had to be coined to account for the fact that some rivers flow only during periods of high precipitation. Others, perennial rivers including the Gila, will disappear into the sand only to reappear at the surface again further on downstream. In these types of situations, ‘average’ values over large periods of time or areas of space are not going to be very meaningful. The only way to deal with them is with (numerous) ‘grab’ samples taken in limited time and/or spatial frames.

The flip side of the sometimes erratic local flow patterns is the second characteristic: the larger weather patterns in the Sonoran desert of central Arizona are, overall, quite steady and predictable. This fact was noted by the earliest USGS researchers who contrasted the frontal rains of the winter, that provide a light but steady soaking for large areas over relatively long periods of time, with the sudden, localized onset and flash flooding of the convective storms of summer.<sup>5</sup> This observation immediately rings true for anyone who has lived in the area for any length of time. It immediately ‘makes sense’ of a number of seemingly unrelated phenomena associated with the differentiation of the seasons. Most of the rest of this study is, in effect, a working out of the direct and indirect implications of this sweeping, qualitative, but nonetheless brilliant, characterization. From the point of view of sampling, however, it suggests that grab samples taken in the winter are taken under conditions where most of the upstream tributaries are running, while summer grab samples have a tendency to include only a few local tributaries. Winter grab samples, instantaneous in terms of time, may thus tend to be more ‘average’ spatially and better represent the whole watershed than summer samples. Whether this supposed difference has any effect on conclusions will be explored later.

The major factors in quantifying the effects of the environment on the control volume are flow, density, and concentration. A brief overview of these will provide a very general picture of the 'stage' upon which inversion will play out and give a feel for 'average' behavior. It is here that the dichotomy between erratic local behavior and predictable seasonal behavior is first seen. The following graph shows the monthly averages for instantaneous and daily mean flows.

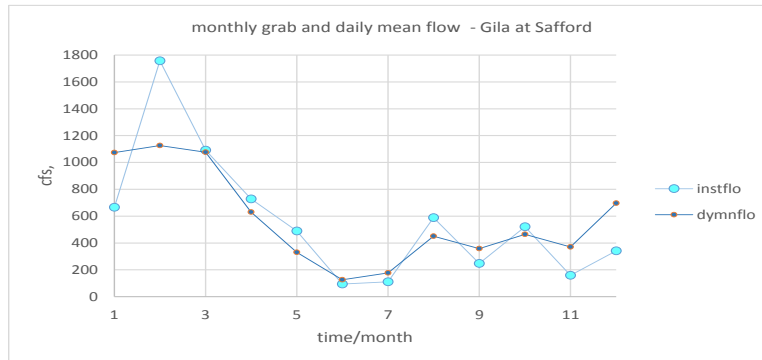


Figure 23 ([back](#))

The February instantaneous value is noticeably higher than the daily mean, possibly a result of the fact that ADEQ sampling is understandably somewhat biased toward high-flow conditions when exceedances of state water quality standards are most likely to occur. Another noticeable difference lies in the summer-fall period in which the instantaneous data indicates two high flow months (peaks) which is reflected in a less pronounced manner in the daily means. With only 161 samples divided among 12 months, the number of grab samples per month falls to 8-20. The October instantaneous peak is probably just a random effect, not indicative of a seasonal high flow period in that month.

The most predictable events of the year are the spring dry-down (May-Jun) and subsequent summer monsoons (Jul-Aug). In contrast, the fall dry-down may not even exist some years. The preceding summer high flow season may simply merge into the following year's winter high flow season. It is probably best, however, to follow the experience of locals over the last hundred years and force the data, where possible, into a two high flow season pattern. In a couple cases, 'fall' is only a nominal one-day-long to create the boundary. The decision to discount the high October flow peak, even though it is 'confirmed' by the daily means, is really a strategic one which will be put to the test by further developments. 'Forcing the data' did not, however, extend to creating high flow seasons where none exist given the criteria in that determination -- 6 of the 36 years examined were judged not to have a winter high flow season at all (1977 being one of those).

Averages of grab and daily mean density values similarly show differences. As can be seen in the graph below, grab and daily mean values differ to some extent in the value of minimums and maximums (the two types of grab samples and the labelling will be discussed later). These differences did not much affect the winter/summer season determination, which is around the yearly average, but did affect the determination of seasonal functions (also discussed later).

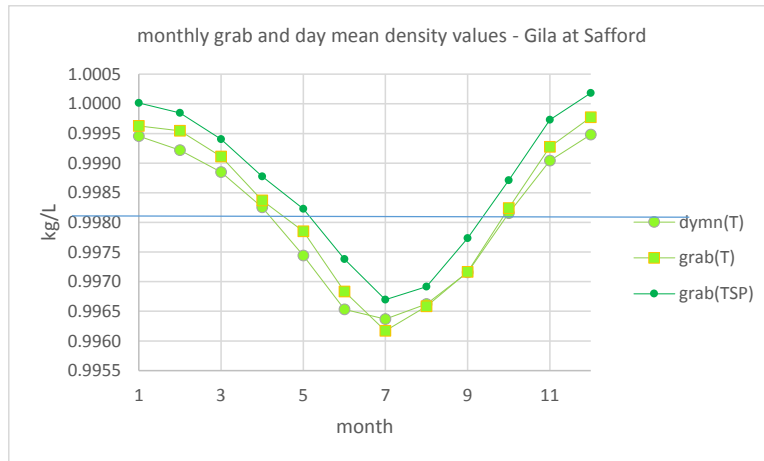


Figure 24

Both flow and density, of course, show seasonal variation but the annual curves have an important difference. The flow monthly average curve is largely defined by, or at least heavily influenced by, maximum flow values. The density curve, on the other hand, is more tightly bound around average values. It is in light of this distinction that one of the main ‘motivations’ of this study, ‘looking for a seasonal pattern in flow,’ is to be understood. Of course, everyone knows flow is ‘seasonal’ in a broad sense. The phrase merely indicates a desire to find a more extensive, explicit definition of seasonal variation (preferably an equation) to replace the loose ‘winter/summer’ or ‘high/low’ flow characterization.

There is another major environmental factor in determining the characteristics of the Gila River worth mentioning – namely concentration. The analysis of concentration relies entirely on the grabs, daily mean chemistry was not available. Below are the monthly average concentrations for solvent and solution (to left) and non-solvent as represented by the major ions (to right).

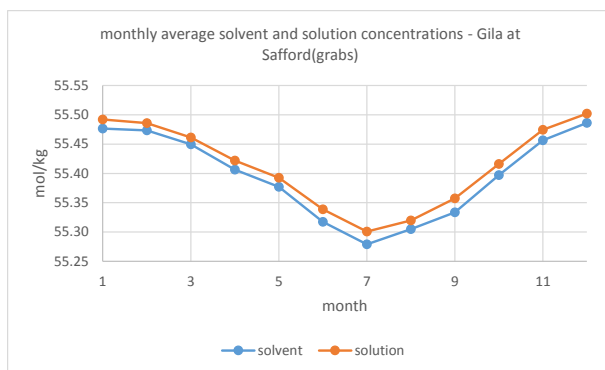


Figure 25

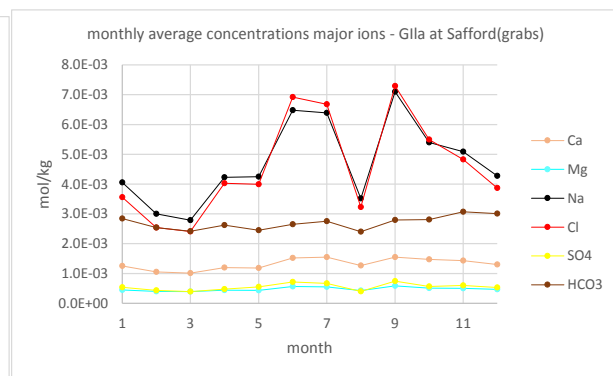


Figure 26

Solvent and solution concentration (molality) follow the pattern of density while Na & Cl concentrations are roughly the inverse of the monthly average flow pattern. Almost all the calculations in the study and the Wateq4f program results were in units of ‘molality’ (mol/kg solvent) not ‘molarity’ (mols/L solution). The word ‘molarity’ may sometimes be used loosely (and incorrectly) here as equivalent to ‘molality.’ The difference is only significant when large

temperature change is involved since solution volume is temperature dependent while solvent amount (kg) is not, i.e. with small temperature change the two are almost the same.

That the other ions follow the same pattern as Na & Cl, and to confirm the tight patterns that make inversion stand out, can be seen by scaling the other ions by constants (below left). The August dip attracts attention to itself as a discontinuity in the pattern not proportional in size with the August flow peak. But when the individual sample points are looked at, it is actually a single days very high Na & Cl values in Sept that stands out (the 0.28 cfs sample of 9/20/78). Removing that sample as well as two very low samples in August, for no good reason other than that they look suspicious, shows the dip remains but is less pronounced (below right).

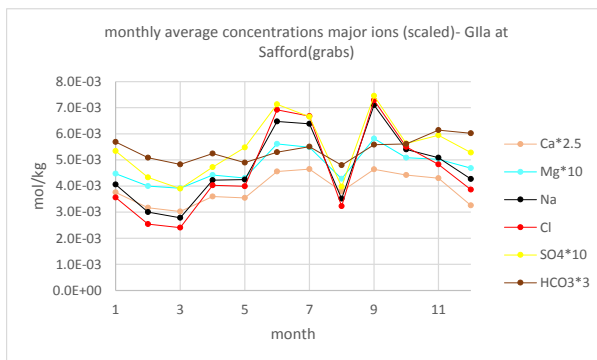


Figure 27

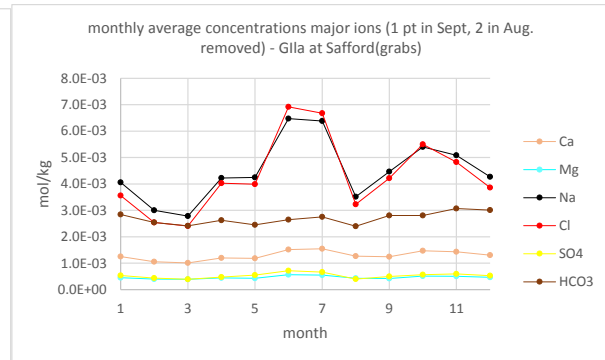


Figure 28

This brief, general look at the major environmental parameter patterns using different analyzes will suffice for now. These parameters will be used to examine inversion in its environmental context. As Lewis and Randall comment in their Thermodynamics, the fundamental quantities are usually the hardest to define.<sup>6</sup> Often used simply as in common parlance, re-definition usually only occurs if some difficulty is encountered. The terms may seem to change when viewed in different contexts. Density and concentration, for example, may sometimes seem to be the same thing – they are both after all mass/volume – and sometimes exact opposites. This dilemma will be returned to later.

No attempt at fundamental definitions will be made here, only an ‘appreciation’ of the difficulties (1) and a few operational distinctions to shape the way in which they are approached (2-4).

1. Flow is both the deformation of a body, with a certain density, and a movement or process, with a certain speed. Note, for example, the redundant-sounding phrase ‘a flowing river’ -- the ‘river’ being the body, the ‘flowing’ being the movement. Flow and density are real physical quantities but they are also abstractions of a whole that combines both in one form
2. Both flow and density are ultimately linked to temperature but the relation is much more direct and ‘tighter’ for density ( $r^2 = 0.9$  for density,  $r^2 = -0.2$  for flow).
3. Because of their different relations to temperature, flow and density reveal their effects in very different spatial and temporal domains or ‘levels’.

4. Because of their different spheres of influence, there are no high direct correlations between flow and density but there are many relations between them.

The role of the environment, largely as flow, is mirrored by its effect on the control volume. As an example, the following close up of the main peak of the summer 1977 high flow season is also a record of the volume of the control volume when converted to L. The lopsided look of flow peaks such as this one is typical and due to a relatively fast rise (flow-induced expansion) and a long tail to the right (gradually decreasing flow combined with temperature-induced contraction (via evapo-transpiration)).

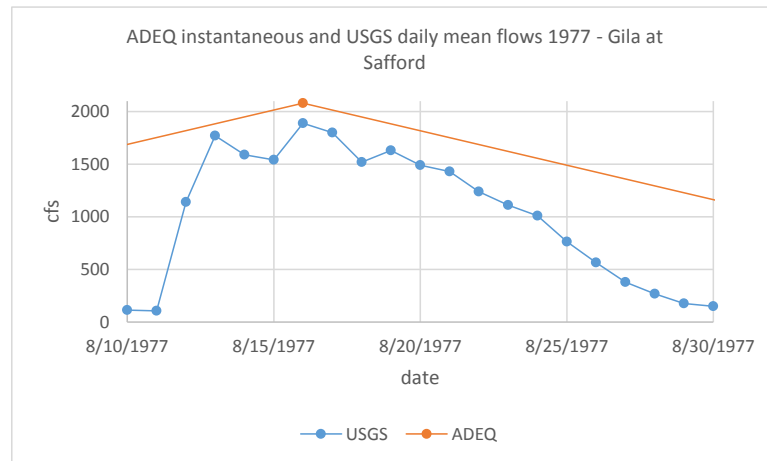


Figure 29 [\(back\)](#)

Having established in a very general way the relation of flow to inversion, it is time to take a closer look at flow patterns, how they characterize the river as a whole and what more specific information they may reveal about inversion. These are the larger context within which the inversion exists.

The location of the area has been precisely described by USGS researchers. The Safford Valley lies between the Gila Mountains on the northeast and the Pinneloa or Santa Theresa Mountains on the southwest. The valley is about 73 miles long and 12 miles wide, the width being larger than is typical for the Gila in this part of the state. The river runs from its confluence with Bonita Creek to Roosevelt Dam and meanders randomly over the relatively wide floodplain. The stream channel is a pool and riffle type with an average slope, as already noted, of about 9%. There is low annual precipitation at Safford, ranging from 3 to 17.9 inches and averaging around 8.7, with two very different precipitation regimes as already described. There is agricultural water usage in the area and extensive channel changes were made in the 1970s, examined in detail in the source from which most of the above information is paraphrased.<sup>7</sup>



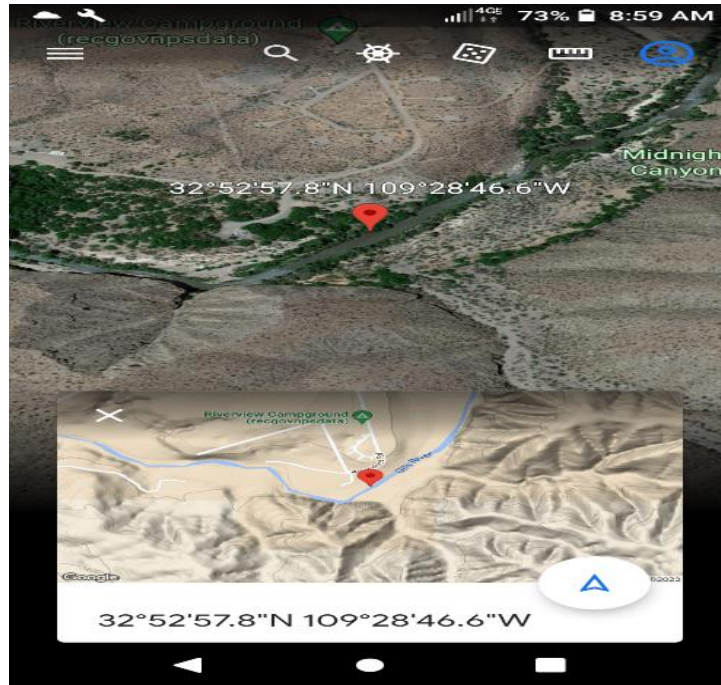


Photo1 USGS site Safford - GoogleEarth

Flow of the Gila at Safford is, therefore, that of a river in a wide floodplain at low elevation with low rolling hills and surrounding mountains not terribly high. With this kind of flow topology, the main response expected is that suspended solids are going to drop out of solution quickly and dissolved solids will concentrate to some extent. The effect of topology on flow will be elaborated on at a later points. Factoring in the effect of climate the following surmise may be made: significant dilution from local runoff sources will be a factor mostly in the summer, with local microbursts possible. In the steady, light rain winter scenario, the local runoff percentage is low and significant dilution is more likely coming down the main channel from runoff at higher elevations outside the valley. This speculation will be tested later.

The following table summarizes the statistics for instantaneous and daily mean flows over all data:



grab & daily mean flow/cfs - Gila at Safford		
	grab	day mean
average	558	571
median	170	195
mode(cnt)	80(3)	146(66)
min	0.28	26
max	13400	90000
std dev	1294	1974
rel std dev	232	346
count/#	161	13149
abs%diff		
avg&med	70	66
avg&mod	86	74
average	78	70

Table 17

Overall, the averages and standard deviations of the two groups are close which is encouraging. The big difference is in the number of samples (count/#) which is why heavy reliance will be placed on the daily means in the search for flow patterns. Note that the mode counts are quite low: 66 is only 0.05% of daily mean samples. The median, like the mode, is quite a bit lower than the average, indicating an average affected by a few high values and thus a distribution with a long tail to the right. Note also, that the percent differences between average and median as well as average and mode are of the same order for instantaneous and daily mean data, indicating that, while there are many more daily mean samples than instantaneous, both groups are equally 'normal.'

Normal data is, by definition, data whose frequency distribution plots as a bell shaped curve. Bell shaped curves divide the data up into areas of +/- multiples of the standard deviation. This property allows a probability to be assigned to any data point given the spread of values of the entire dataset. The word 'normal' is used in this study to describe data with bell-shaped frequency distributions, as in the discussions of flow and density. It was impossible, however, particularly near the end of this study, not to occasionally use the term in its looser sense as the 'usual', 'expected', 'reproducible', or at least 'predictable,' regardless of data distributions.

The frequency distributions for flow show a nearly normal (bell-shaped curve) portion and a long asymptotic tail to the right. Below are the flow distributions for daily means (left) and grabs (right) cut off to include only the first 1000 cfs (only 11% of USGS and 14% of ADEQ values are above 1000 cfs).

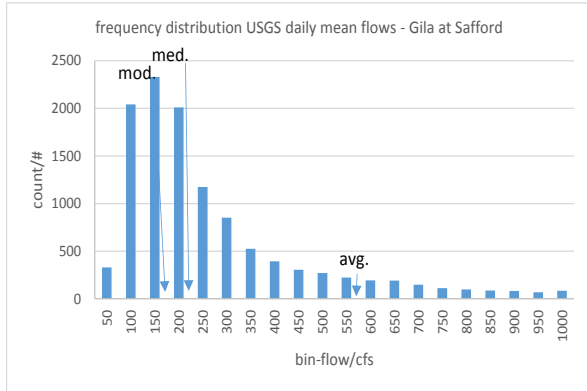


Figure 30

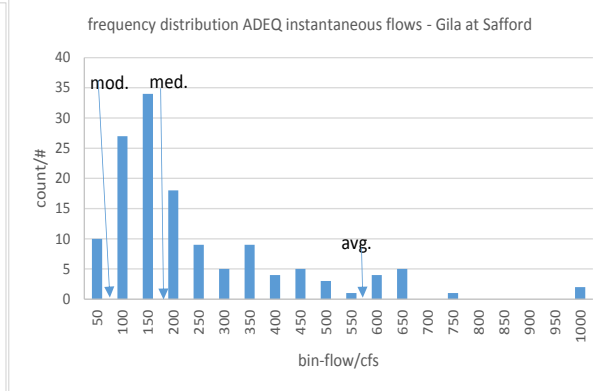


Figure 31

The overall shapes of the distributions and the positioning of average, median, and mode are the same as might be expected since the linear correlation of the two sets of data is fairly high (0.76). Note that, in both cases, the average is pretty clearly outside the bell shaped curve portion meaning that it is actually in the region of non-normal behavior. The mode and median are better indicators of the center of the distribution of values while the average is more representative of the relative weight of all values regardless of count.

Does the picture of flow patterns at this level reveal anything about inversion? To see, the instantaneous flow data can be subdivided into inversion date and non-inversion date data.

inversion and non-inversion flows/cfs - Gila at Safford(grabs)			
	all data	non-inv.	inv.
average	558	141	1408
median	170	119	719
mode(cnt)	80(3)	80(3)	1000(2)
min	0.28	0.28	278
maximum	13400	578	13400
std dev	1294	96	2009
rel std dev	232	68	143
count/#	161	108	53
abs%diff			
avg&med	70	16	49
avg&mod	86	43	29
average	78	29	39

Table 18

The division neatly separates low and high flow. While the grabs as a whole are fairly representative of the daily means, inversion and non-inversion grabs are two distinct subsets within the grabs. They are clearly but not completely distinct from each other -- there is overlap in the 278-578 cfs range. Inversion involves all flows above the average. Inversion flow shows higher standard deviation but lower relative standard deviation than all data. Also the differences between average, median, and mode decrease for both non-inversion and inversion as compared to all-data as if the division is actually making the distributions more normal.

The actual distribution of flow values for inversion and non-inversion, however, paint a somewhat different picture. The distributions are shown below are up to 1500 cfs, the larger x-scale being necessary because the inversion average value occurs at higher than 1000 cfs.

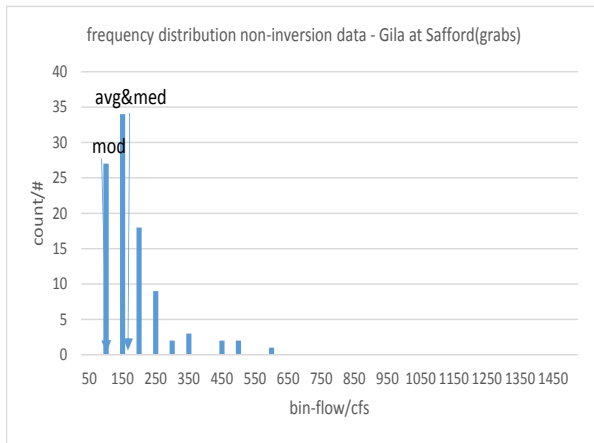


Figure 32

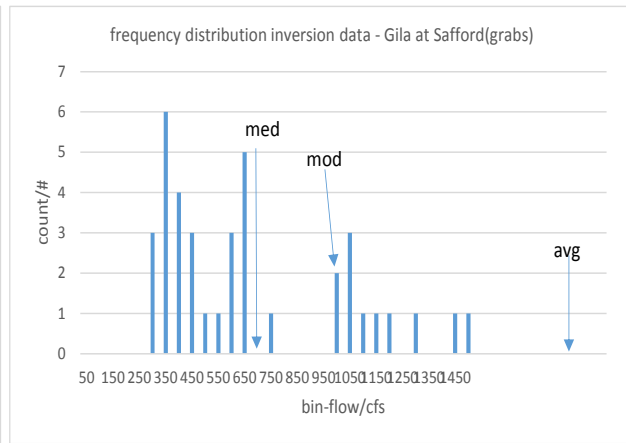


Figure 33

The inversion distribution, to the right, is clearly non-normal and looks like it might be bi- or tri-modal as well. That is probably just a random effect caused by the low number of samples (53) which leads to very low counts. The mode, for example, has a count of only 2 and the most populated bin (300-350 cfs) has only 6. (these are 'bins' of values so the values in the bin with 6 may be all different values while that of the mode with 2 must be the same value)

Non-inversion (left) is clearly more nearly normal than inversion in the position of the average, in the distances between average, median, and mode, and in overall appearance (bell-shaped curve). The effect of the inversion analysis is, at this level, one that separates normal from non-normal data.

Only a high flow/low flow distinction has been distinguished to this point. A different view may find a context into which inversion can fit. The most direct approach to finding patterns is autocorrelation which looks for patterns within a single parameter over time. The following are the results for the autocorrelation of the USGS daily mean flows (left) and flow differences (right):

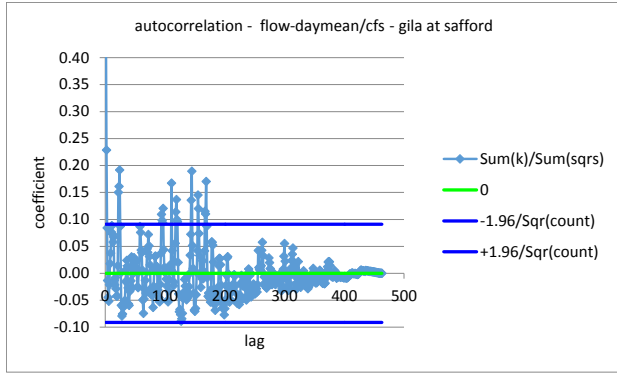


Figure 34

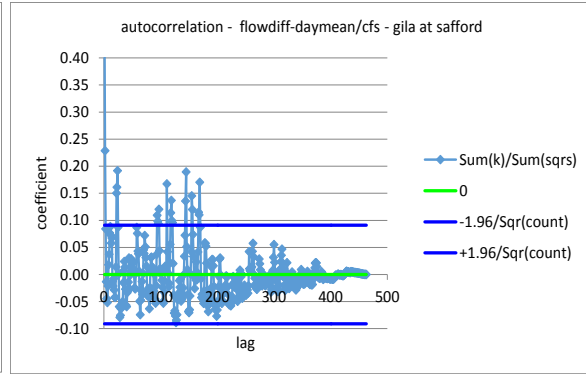


Figure 35

There is something of a damped oscillator pattern but it is not clear and the percent mins and maxs are low (table below). But if the natural logarithm of the flow and the logarithm of the absolute value of the flow differences are taken, the following results are obtained:

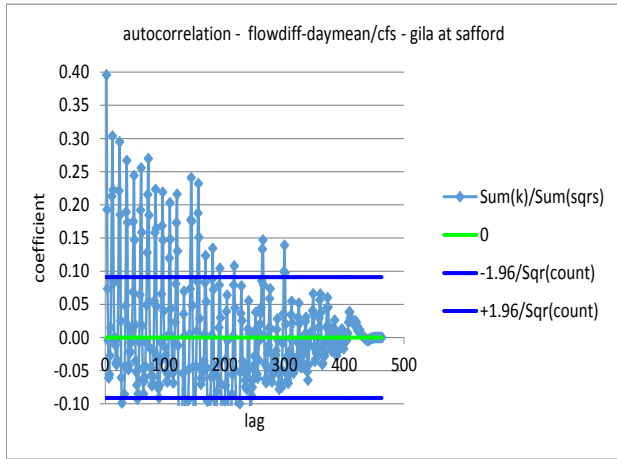


Figure 36

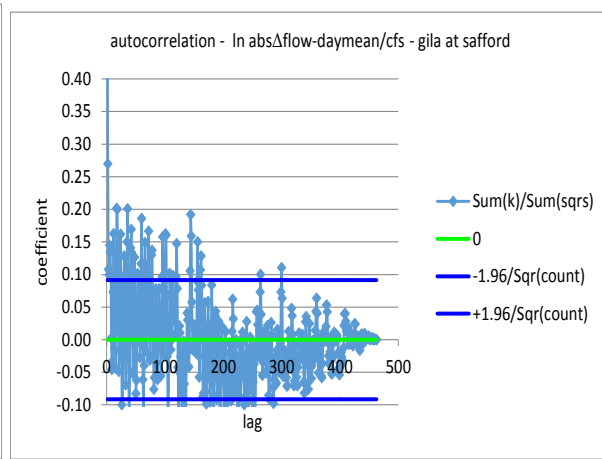


Figure 37

These graphs do not look much better than the previous but a glance at the numbers below shows the difference. Which goes to show why the form of the graph alone can't always be trusted and why there is, in practice, a heavy reliance on the %6 and 12 min/max value.

autocorrelation statistics - dymn flow/cfs - Safford				
	% @ 6	% @ 12	$\Sigma x_1 y_2 / \Sigma sqrs$	count
dymns	0.3158	0.2597	1.0668	462
dymndiff	0.4211	0.3766	2.8574	462
ln dymn	0.8947	0.5844	0.5221	462
ln abs diff	0.8421	0.4156	0.7935	460

Table 19

The autocorrelation provides some proof that there may be a more specific seasonal pattern to flow than the loose high/low designation found so far. Given the crude analytical technique used here, this discovery is open to question and begs the question: so what? At this point there is not enough related information to make it significant so the result needs to be mentally tucked away for future use.

Maybe, instead of such a broad approach as autocorrelation, a closer look at types of flow might be more helpful. To further investigate flow patterns, a simple flow function ‘labelling’ analysis is performed. Because the intervals between grab samples are inconsistent and random, the analysis is performed only on the daily means. Each daily mean flow is labelled with a two character symbol based on the direction of flow (first symbol) and the direction of flow difference (second symbol) from the previous day. Two days data are necessary for flow direction and three days data for direction of flow difference.

The resulting flow/flow difference (ffd) labels are as follows: >> (expansion), << (contraction), >< (expansion to contraction), <> (contraction to expansion), =0 (equal flow), and Δ= (equal, nonzero flow difference). If equal flow is determined first and equal flow difference determined only if not equal flow, the six labels cover all cases and are mutually exclusive. The following graph of the August 1977 flow peaks shows a few corresponding labels. The table following that gives the counts, average, and max values for the various labels for the daily means over the entire analysis period.

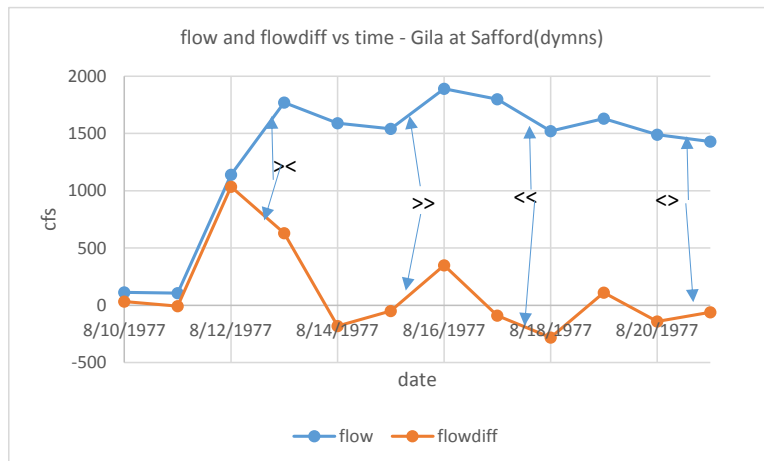


Figure 38

daily flow/flowdifference of USGS daily means - Gila at Safford					
		avg/cfs	max/cfs	count%	count/#
expansion	>>	697	62700	23	3004
	><	993	90000	6	792
contraction	<<	542	45000	30	4008
	<>	588	17000	27	3497
equal flo	=0	190	3060	8	1031
equal flodiff	Δ=	256	2640	6	816
					13148

Table 20

Expansion average values are roughly one and a half to two times that of contractions. Contractions dominate in the number of cases but expansions dominate in terms of max values. It is interesting that contraction flow averages are very close to the all-data average while equal flo or flodiff come in right around the average for low flow samples (as will be seen later on). It is also possible to take differences of labels: <<-<>, >>-><, etc., but these are difficult to deal with. It is interesting to note, however, that some of the combinations do not occur. The order of operation is significant and such combinations as >>-<> cannot occur because the logic is not correct – a ‘transition contraction to expansion’ cannot follow an expansion only a contraction.

Inversion and non-inversion dates can be looked at in terms of the daily flow/flowdiff labels. This will be a procedure followed in various places throughout the study – a labelling analysis is done on the daily means, each daily mean is given a label, the grab on that day is given the same label as the daily mean on the same date. The grab data now has a daily mean label attached to it no matter how far apart grab and daily mean flow values are. There is an inherent risk of mislabelling though hopefully such samples will be ‘averaged out.’ Here are the results showing the percentages of each function type.

count% dly flo/flodif labels applied to grab samples - Gila at Safford			
	dymn	inv.	non-inv.
>>	23	23	21
><	6	9	10
<<	30	30	35
<>	27	26	23
=0	8	8	7
Δ=	4	4	3

Table 21

The percent for each type of label on inversion and non-inversion dates of grab samples pretty well reflects the percent for all the daily means. This seems an encouraging result because it suggests that the inversion/non-inversion subsets of the grabs do have a correspondence in the daily means when they are subjected to a simple flow functional analysis.

It is somewhat disappointing, however, not to see any differentiation between inversion and non-inversion – a larger number of expansion types for inversion and contraction for non-inversion might be expected given the relation of inversion to high flow. And it is hard to get around the suspicion that the results are what they are because daily means labels have been brutally imposed onto grab sample data. A more meaningful check on the procedure may result from comparing average values rather than labels.

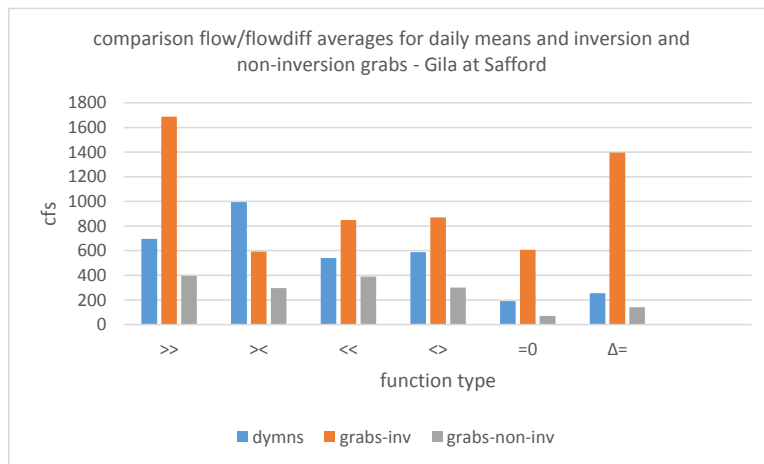


Figure 39

These results are encouraging as well but for precisely the opposite reason as the sample % count comparison. Inversion sample averages stand out as almost always higher than the daily mean while non-inversion samples are invariably lower. The only qualification required is that the grab inversion or non-inversion sample counts may be, in some cases, very low – for example, there were only 11 samples for > <, the only category in which inversion is not higher than daily mean. While being representative of the daily means in terms of proportions, grab averages reveal inversion/ non-inversion average values stand out as different from the daily means and different from each other.

There is not much more that can be done with this analysis because it looks at flow in a consistent but ambiguous context: it uses a consistent 2-3 day window but an expansion, for example, can be a 1 cfs peak during a period of low flow or a 5000 cfs peak that is a side peak to an even larger one in a wet season. What the flow/flow diff analysis does is to ratchet down the time frame to such an extent that the chance that both expansions and contractions are going on over the period is lessened. This new approach emphasizes function over chronology, allowing one to examine what all ‘expansions,’ whatever their magnitude, have in common.

At this point, however, the focus is on seasonality so the chronological approach is required. Average monthly flows have already been shown above ([Figure 23](#)) so a table of values is given here instead:

daily mean and grab flow statistics/cfs - Gila at Safford						
month	avgs		rel stdevs		counts/#	
	dymn	grab	dymn	grab	dymn	grab
Dec	697	342	421	102	1116	17
Jan	1073	667	350	155	1116	9
Feb	1125	1757	212	222	1017	11
Lar	1076	1092	137	118	1116	20
Apr	630	729	102	177	1080	13
Lay	330	489	128	104	1116	10
Jun	126	94	125	97	1080	20
Jul	177	111	133	58	1116	9
Aug	451	589	148	137	1116	16
Sep	358	248	217	107	1080	18
Oct	465	521	735	210	1116	8
Nov	370	159	311	48	1080	10

Table 22

Here the two seasons are less apparent than in the graph but the ‘wet’ months can tentatively be designated as Dec-Apr (winter), where flows and relative standard deviations are higher, and summer months (Aug-Oct) though flows there get close but do not actually exceed average flow ( $\ll 560$  cfs shown in light green). The seasons can then be calculated from the monthly averages:

seasonal from monthly flow averages/cfs - Gila at Safford		
	dymn	grab
hiflo		
winter	847	947
summer	425	453
hiflo avg	636	700
loflo	225	121



Table 23

The excellent agreement between grab and daily means for the wet seasons ('hiflo') is gratifying. But notice that the monthly averages, like the daily flow/flowdiff categories, do not change the high flow average (636,700) very much from the all-data situation (558,571). One reason for this lack of differentiation may be that the summer monsoon, which officially starts in the middle of June, may not actually start until the middle of July. The fall dry-down is also highly variable as mentioned earlier. What these factors mean is that there is still a lot of averaging over disparate values going on. The time spans for averaging, therefore, may not be optimal.

Dividing the grabs into inversion and non-inversion by month yields the following results:

inversion/non-inversion average flows/cfs by month - Gila at Safford(grabs)				
	inv	noninv	%inv	%noninv
Jan	1656	172	6	5
Feb	3009	255	11	5
Lar	1493	156	26	6
Apr	1447	113	11	7
Lay	855	123	9	5
Jun		94		19
Jul		111		8
Aug	1005	173	15	7
Sep	537	136	9	12
Oct	1809	92	4	6
Nov		159		9
Dec	855	184	8	12

Table 24

Here the division between inversion and non-inversion begins to differentiate high flow values from low flow a little more. Inversion samples do not occur in Jun, Jul, and Nov, the driest months of the year, which have only non-inversion. The high numbers in the two sets of data divide up neatly into the high-flow and low-flow months but there are low flow (non-inversion) samples even in the wettest months. There isn't much new here but it does reinforce that inversion is largely a high flow phenomenon.

But high flow seasons are, after all, seasons of extremes by definition, and it is here that the difference between daily means and grabs is most evident. The table below shows daily mean and grab minimum and maximum flows by month.

daily mean and grab min and max flow/cfs - Gila at Safford				
	mins		maxs	
	dymn	grab	dymn	grab
1	124	104	55700	3200
2	100	140	32600	13400
3	84	115	18600	5550
4	62	40	4320	4650
5	42	56	3770	1650
6	26	29	2350	450
7	27	35	2670	250
8	42	30	6710	2770
9	44	0.28	13000	1100
10	51	45	90000	3220
11	68	45	24300	307
12	104	104	62700	1170

Table 25

The grab minimums are very close to the daily mean minimums, particularly in the drier months. The maximums of the two groups, however, are often not even in the same order of magnitude, particularly in the wet months. Two separate scales, left for daily means right for grabs, need to be used to conveniently place them on the same graph.

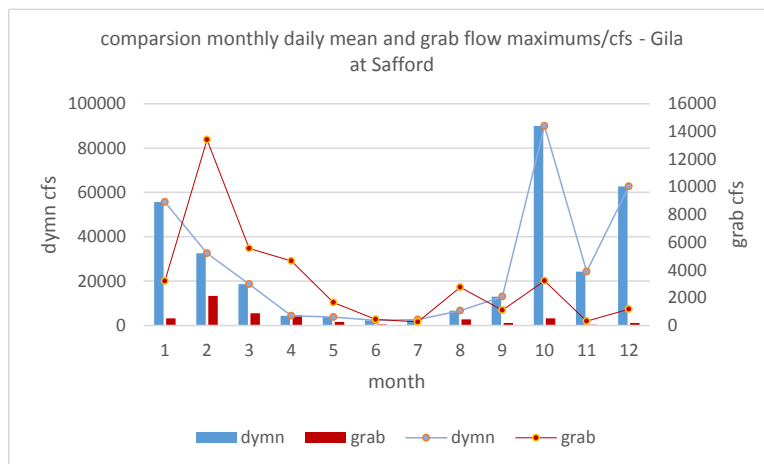


Figure 40

Not only are grab and daily mean maximum magnitudes wildly different, the relative magnitudes or patterns only have one common feature – a parabolic dip in the summer months.

If wet seasons are in some sense best defined by their extreme values, there is still have a long way to go in getting a reasonable picture of them. The maximums themselves can't be used because they are not representative of everyday behavior but the averages are just too low to provide adequate differentiation between seasons.

An approach that may provide a better picture of high flows is to determine flow-seasons. This task was accomplished using 10-day rolling averages on the USGS daily means and graphing the results onto a series of graphs with fixed x and y value scales; one year and 2000 cfs respectively. The 10-day rolling average eliminates many of the small peaks as does the 2000 cfs scale while the fixed x scale (one year) makes the graphs easy to compare with one another. The one year window was for presentational clarity only and not used in determining the seasons; 'winters' commonly start in the previous year. The resulting picture is one of grouped peaks, as seen in the 1977 graph:

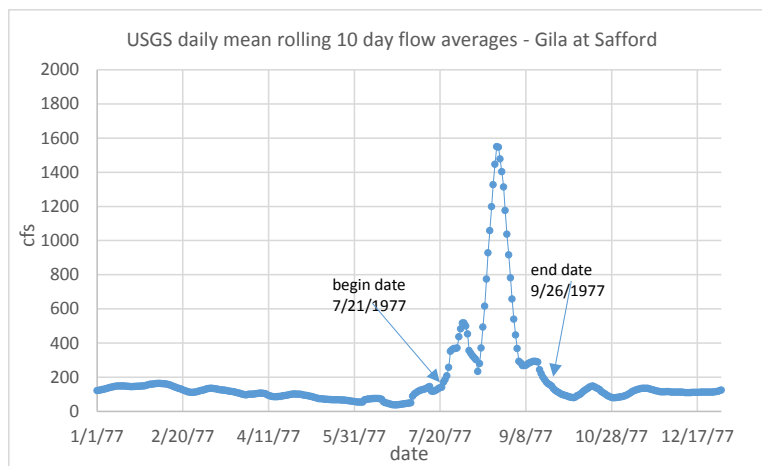


Figure 41

The begin and end dates are to some extent arbitrary, of course, but every attempt was made to make the high flow period balanced and symmetrical around the main peak(s) and ending at approximately the same flow as the begin date. It was usually much harder to fix the end than the beginning date since many seasons show tails to the right as individual peaks often do (Figure 29).

Dividing the daily mean data into seasons yields the following results.

season flow characteristics - daily means - Safford				
	avg flow/cfs	durtn/day	seas cnt/#	smp cnt/#
hiflo(w)	1345	139	30	3915
hiflo(s)	439	86	36	3129
loflo	143	93	64	6105

Table 26

The expected picture of a longer winter flow season with higher average flows and a shorter summer flow seasons with lower flows is beginning to take form. Going from monthly to seasonal analysis ‘tightens’ the context and leads to noticeably higher values for the longer season (winter), not so much for the shorter, summer season. Loflo dominates, however, in numbers of seasons and samples and more closely represents typical flow as represented by the median or the mode than the flow average of 560-570 cfs.

The seasons are, then, established using the daily means. Each days daily mean flow is given a seasonal ‘label’ and the grabs are given the same label as the daily mean for that day. The procedure is exactly the same as in flow/flowdiff but is far less brutal because it does not depend on the daily mean flow value only the date. There is no difficulty in accepting that the daily mean and grab sample taken on the same day occur in the same season. The % of inversion and non-inversion grab samples and their averages by flow season are shown in the following table.

inversion/non-inversion samples by flow season/cfs - Gila at Safford(grabs)				
	inv avg	%inver	non-inv avg	%non-inv
hiflo(w)	1664	72	241	9
hiflo(s)	796	26	152	23
loflo	278	2	#DIV/0!	#DIV/0!

Table 27

Inversion is a high-flow, non-inversion a low flow phenomenon but there are a couple of wrinkles. The first is how many non-inversion samples there are during the summer high flow season, fully 23%. This result points to the more erratic behavior of short lived summer storms underlying the flow patterns. The second is that one inversion occurred during a period designated as low flow at the minimum flow for inversion -- 278 cfs. Both are reminders that ‘high’ and ‘low’ flow are arbitrary terms and that there is a roughly 300 cfs gap between the minimum for inversion and the maximum for non-inversion. There are 20 inversion samples in this gap, one of which is designated loflo the rest ‘hiflo’, and 9 non-inversion samples all ‘loflo’. The emphasis here is on the season designation and not the individual flow values, so an inversion occurring during a low flow period is a significant problem which will be dealt with later.

The seasonal values above are averages of both increasing and a decreasing flows so it makes sense to separate the seasons into seasonal functions: expansion and contraction. Three different approaches were used in the determination of seasonal functions. The ‘instantaneous’ function is determined simply from one grab sample to the next – if the flow went up it is an expansion, otherwise it is a contraction, whether the first sample is one day or 3 months prior. (This is the only example of grab labels coming from an analysis of grab data. In all other cases, analysis is done on the daily means, daily means are given labels, and grabs are given the same label as the daily mean for that day.)

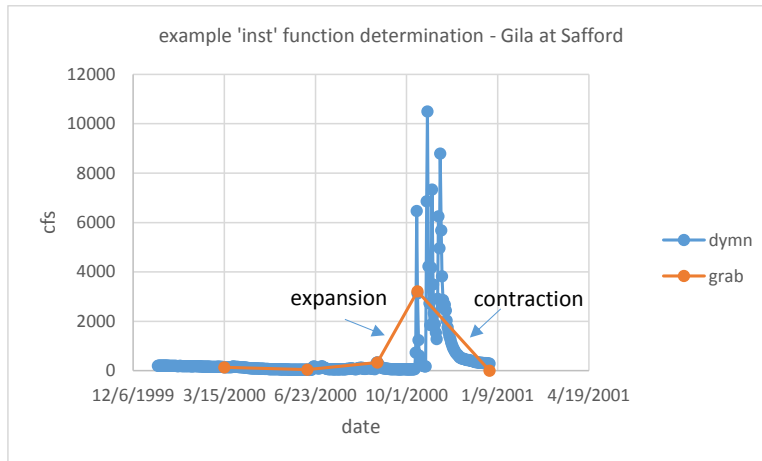


Figure 42

Because the 'inst' labels were based on a set of random intervals, the results were awful and the function was not pursued further. The following graph shows a new approach, the 'seasonal' function determination.

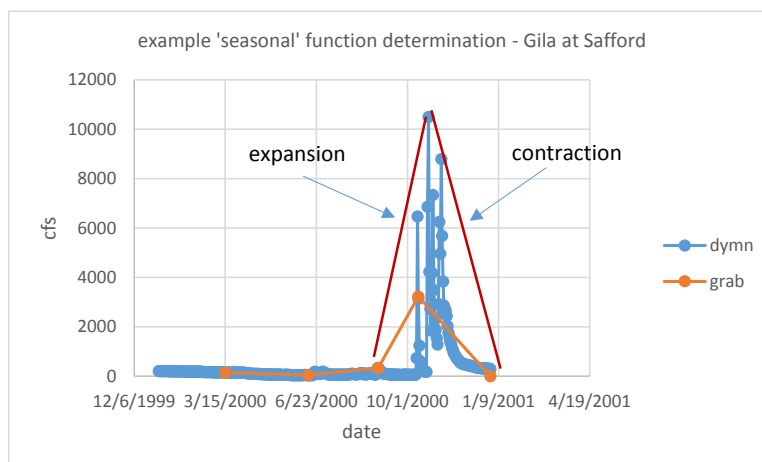


Figure 43

The function(s) approach ('s' for seasonal) treats the entire season as one expansion and one contraction around a seasonal midpoint. A couple of different methods were tried to determine the midpoint: chronological half point, point at which  $\frac{1}{2}$  seasonal cumulative volume is attained, date of max peak, and date of max pulse. In the function(s) approach the location of the midpoint is crucial and the different midpoint analyzes can yield quite different results:

summary seasonal midpoint analyzes - Gila at Safford(dymns)					
days to season midpoint					length season
	chronolog	half vol	maxpuls	maxpeak	
hiflo(w)	74	62	41	40	139
hiflo(s)	43	40	36	38	86
duration expansion & contraction/days					
exp(w)	74	62	41	40	
con(w)	-74	-74	-41	-40	
exp(s)	43	40	36	38	
con(s)	-43	-43	-36	-38	
% peaks or pulses out of sequence (increasing or decreasing)					
pulses	30	35	39	34	
peaks	33	31	35	31	

Table 28

Note that the max pulse and max peak usually occur well before the chronological midpoint, much earlier in winter (~25-30 days) less in summer (~3-5 days). The max peak and max pulse characteristics are very similar and the maxpulse was finally settled on as most likely to produce interesting results. Part of the 2001 winter hiflo season is shown as an example of midpoint symmetries.

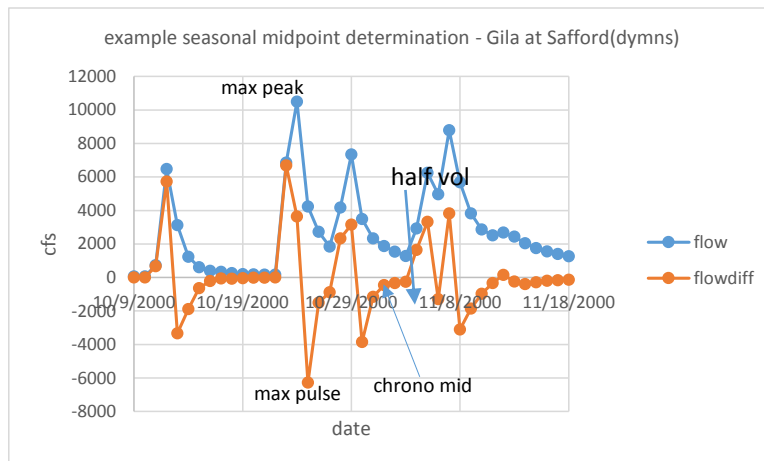


Figure 44

The logic behind the function(s) approach is the extension of the daily flo/flodiff analysis to whole seasons with one significant difference. The daily pulse in the flo/flodiff analysis is a one day event that occurs when the flow difference goes from positive to negative. There are 1488

peaks (any size) in the daily means and 1488 corresponding ‘pulses’. A seasonal pulse, by contrast, is sometimes a multiple day event and calculated by the maximum of the flow differences before minus the minimum of the flow differences after the daily pulse. Typically, particularly during low flow periods, the daily pulse and the seasonal pulse are the same. But the above definition is used to catch situations such as the following, a seasonal pulse in the summer to winter 1977 low flow season:

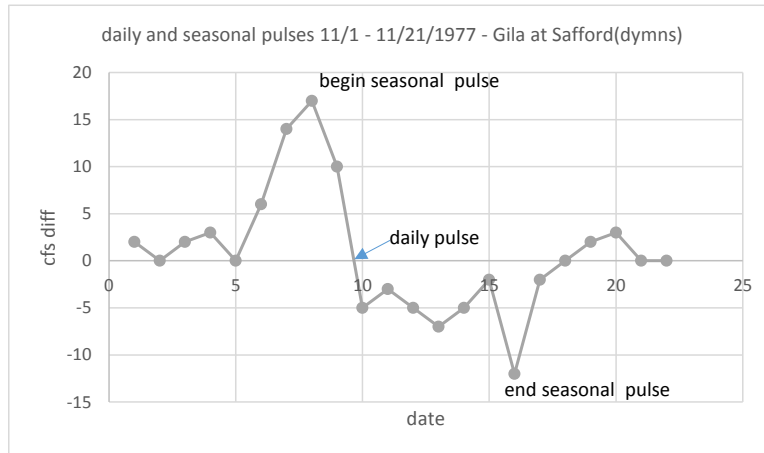


Figure 45

The seasonal pulse is therefore the full drop in cfs from peak to valley. With this definition it is possible to quantify the characteristics of the seasons further. Winter pulses are larger and longer lasting than summer and the same goes for the flow differences that they come from:

seasonal and daily flow difference characteristics in flow seasons - Gila at Safford(dymns)								
seasonal pulses	avg pls/cfs duration/days		flow differences before/after daily pulse					
	avg pls/cfs	duration/days	avg(pre)	avg(post)	cnt(pre)	cnt(post)	avgMax(pr	avgMax(post)
hiflo(w)	2502	11	905	-336	3	8	1496	-1006
hiflo(s)	652	6	189	-95	2	4	343	-309
loflo	20	5	7	-5	2	3	12	-9

Table 29

The maxpulse (mxp) is simply the maximum pulse in a given season and its statistics follow below. The seasonal pulses bear the same relation to the maxpulse as the daily flow differences do to the daily pulse. The only difference is that the count of individual pulses before/after the daily pulse)) is replaced by the count of seasonal pulses around the maxpulse and the duration of seasonal pulses around the maxpulse is the entire season (avg win-139, sum-86 days).

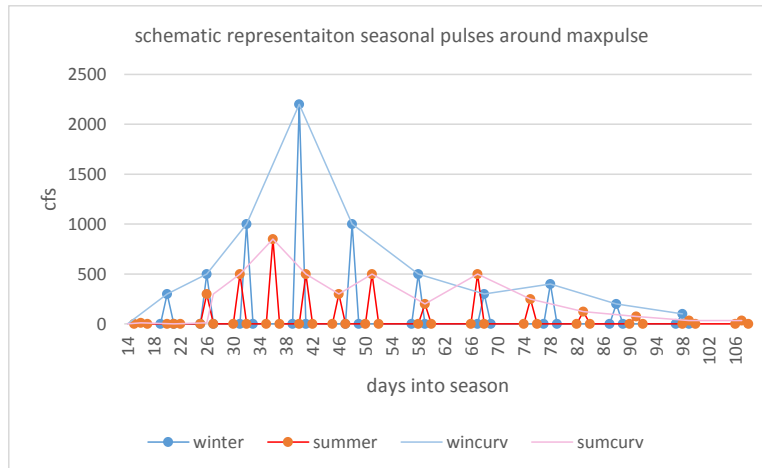
characteristics of seasonal maxpulse - Gila at Safford(dymns)											
maxpulse/cfs											
	average	median	mode	min	max	stdev	count/#				
hiflo(w)	13743	4395		33	79400	19885	30				
hiflo(s)	5222	1453		192	100000	16929	36				
avg chrono postn in seas/%			#mxp on 1st day		%	#mxp last date		%			
hiflo(w)	38		pos=0%	6	13	pos=100%	5	20			
hiflo(s)	51			2	8		4	14			
pulses before/after maxpulse											
	avg /cfs		count/#		intrvl/days		% in consec order		$\sum \text{puls}^2 \text{as} \% \text{mxp}^2$		
	pre-mxp	post-mxp	pre-mxp	post-mxp	pre-mxp	post-mxp	pre-mxp	post-mxp	pre-mxp	post-mxp	
hiflo(w)	2880	679	3	5	6	10	59	60	22	54	
hiflo(s)	224	264	7	5	5	8	58	68	34	86	

Table 30 ([back](#))

Seasonal maxpulses are larger in winter than summer though the maximum maxpulse occurs in summer. The winter maxpulse occurs earlier in the season than the summer which occurs around the chronological midpoint. In winter there are more pulses after the maxpulse but they are considerably smaller while in summer there are more pulses before the maxpulse and they are only slightly smaller than those after. The intervals between pulses are larger after the maxpulse for both winter and summer. The symmetry of pulses is the same for summer and winter – about 60% of pulses are larger (expansion) or smaller (contraction) than the previous pulse. The maxpulse stands out more from pulses before than after as can be seen by the difference in the sum of the pulses squared divided by the maxpulse squared numbers except for the post maxpulse summer season.

Putting all these pieces of information together, the following is a schematic representation of typical winter and summer high flow seasons in terms of flow pulses. The max pulse (a peak here) is the average value set on the appropriate day of the season, the number of pre- and post-season pulses, their average values, and their intervals are given above and roughly reproduced as peaks below.





Schematic 2

This schematic is the picture of a high flow season as consisting of a series of pulses starting with a group of rapid, consecutively higher frequency bursts leading up to a max pulse (max amplitude peak here) followed by longer interval, lower bursts going asymptotically to zero. The overall picture is that of an oscillator at full force to peak amplitude followed by dampening with timing and relative amplitude varying by season.

Can this picture of the flow season aid in understanding inversion? Unfortunately, no. The first and greatest difficulty is that the grab sample flows need to be converted to pulses and that means using the daily mean flow differences in one way or another. If the sample day occurred during a seasonal pulse it is assigned the seasonal pulse value, and is referred to as the 'grab pulse'. If the sample did not occur during a seasonal pulse, the daily flow difference is used. The following table shows the differences between inversion and non-inversion flows converted to pulses:

inversion/non-inversion in terms of max- and daily pulses/cfs -Gila at Safford(grabs)		
average grabpulse	avg	std
inv	1833	5070
non-inv	845	7637
grabpuls%ofmaxpulse		
inv	43	44
noninv	39	41
grabsamp-daysfromdailypulse		
inv	2	5
non-inv	1	5
grabsamp-daysfrommxp		
inv	17	37
non-inv	-5	42

Table 31 ([back](#))

The average grab pulses are a little lower for inversion and a little higher for non-inversion than the average daily seasonal pulses seen above (w/s -2502/652) and nowhere near the daily mean average maxpulses (w/s -13572/5222) but are in the right order (inv>noninv). The pulse as % of the maxpulse numbers seem a little high given the averages but offer no help in distinguishing inv and noninv.

The fact that grab sample inversion dates are on average 17 days after the maxpulse while non-inversion sampling occurred on average 5 days before seems important since in the function(s) approach the maxpulse divides seasonal expansion from contraction. 17 days after means inversion grab samples were typically taken during seasonal contraction while non-inversion grab samples, -5 days, were most commonly taken during seasonal expansion. The latter is not important because non-inversion is a low flow phenomenon and a loflo pulse is an entity of dubious significance. The former result, however, is unexpected and focuses attention on the terms 'expansion' and 'contraction' and what they mean in terms of inputs to the system. These issues will be returned to shortly.

The seasonal pulse of function(s) brings out some factors and problems of inversion/non-inversion but not a complete picture. Is the problem with the logistics of converting to pulses or the schematic picture itself? Unfortunately, as nice a picture as the schematic is, it is not borne out by the actual data; the real picture being much less symmetric and more chaotic. Plotting the

year-season pulses in terms of the number of days to/from the max pulse reveals the following composite pictures for winter (left) and summer (right) seasons:

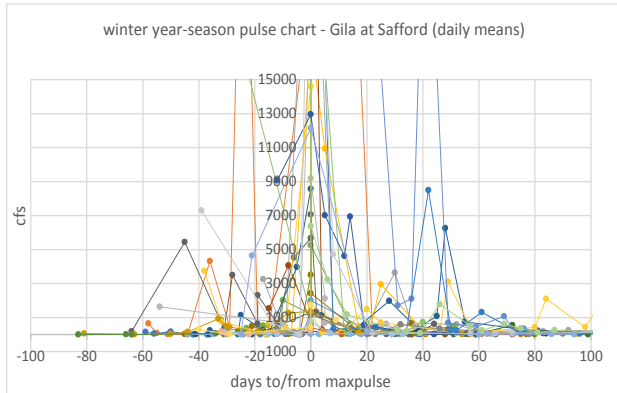


Figure 46

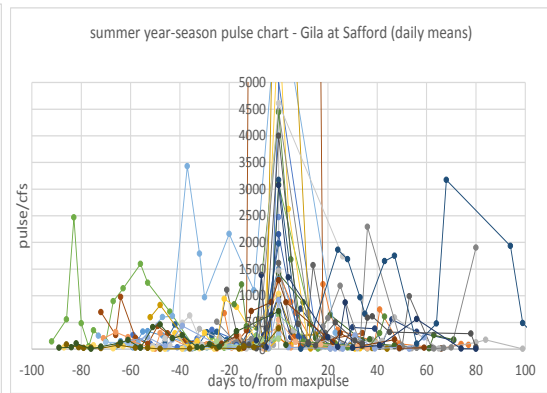


Figure 47

The dominance of the maxpulse in the graphs above is partly a visual illusion due to the fact that there is a large number of maxpulses and they are all squeezed together at the center of the graph. But the numbers (sum pre/post pulses<sup>2</sup> as % of mxp<sup>2</sup>) of [Table 30](#) above seem to bear out that the maxpulse is the dominant feature of the season – the sum of pre-maxpulses is only 20-30% of the maxpulse though post mxp can range from 50 – 80%. This dominance of the maxpulse is an affirmation that it does make sense, to a certain extent, to think of the season in terms of one expansion and one contraction.

The pattern of the above graphs, however, is not one of steadily increasing before and steadily decreasing pulses after the max at least that anyone can see (too many data points!). The final blow to symmetry comes when it is noted ([Table 30](#)) that about 11 hiflow seasons have maxpulse as the first or last pulse of the season. This is disheartening but should not be taken as an indication that flow pulses do not exist. This approach may simply not be the right way to view them.

Less cluttered graphs may help clarify things. The following graphs show the averages of the year-season pulses graphed above.

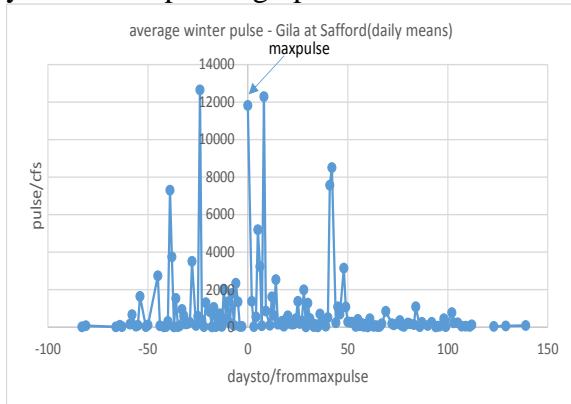


Figure 48

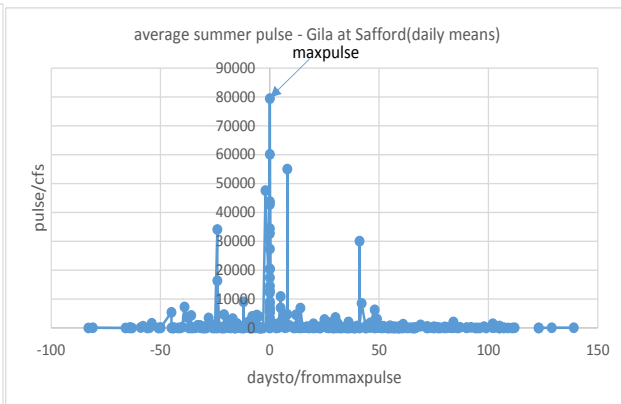


Figure 49

Actually, these graphs only show the vagaries of graphical analysis. When the winter pulse chart to the left was first created it seemed to confirm the dominance of the max pulse until it was examined more closely. The largest pulse on the original chart (47590 cfs) actually occurred two days before the max pulse for that season. That was the only value for ‘two-days-before-maxpulse’ so it became the average (it was removed from the above winter graph). The new max pulse was calculated from 30 years of pulses which ranged from 33 to 79400 cfs for an average of about 11000. The new max pulse is not even the highest on the chart. There is a bit of a symmetrical look for the winter season, but given the low counts for any particular day, that too may be just fortuitous. The summer season does seem to illustrate the dominance of the max pulse but is somewhat less symmetrical.

What is interesting here is that flow pulses do exist and can actually be seen in bunched groups of daily mean flow peaks (Figure 21). But when the focus is narrowed and the attempt made to quantify the pattern, no coherent, underlying pattern is found. It may be wondered why the pulse analysis is shown at all. The contention here is that it is always useful to look a physical data directly with simple methods first before going on to more sophisticated methods. Not finding anything does not necessarily mean there is nothing there to find. One may simply not have looked ‘hard enough.’ If another temporal, spatial, or analytical view had been tried . . . .

Despite the uncertainties encountered with the flow seasonal pulse picture, the max pulse can still be used simply as a seasonal midpoint. The table below shows average flows (not ‘pulses’ which are flow differences) around the midpoint:

seasonal function(s) averages - Gila at Safford(dymns)		
	cfs	seas avg
exp(w)	1460	1380
con(w)	1301	
exp(s)	465	443
con(s)	421	

Table 32

The seasonal daily mean averages calculated above agree well with those from (whole) season averages given above (w/s-1345/439) and the expansion/contraction difference is small but in the right order for both summer and winter.

In the table below the grab sample date flows are labelled with function(s) labels for the same date from the daily means to look for inversion/non-inversion differences in terms of the seasonal functions.

grab inversion/non-inversion samples evaluated with function(s) labels from daily means - Gila at Safford						
	dymns		grab-inv		grab-non-inv	
	avg flo/cfs	count/#	avg flo/cfs	count/#	avg flo/cfs	count/#
exp(w)	1460	1091	1338	9	275	6
con(w)	1301	2824	1765	29	190	4
exp(s)	465	1333	582	5	129	6
con(s)	421	1796	913	9	160	19
loflo	143	6103	278	1	127	73

Table 33

Inversion flows are consistently higher than non-inversion and the most common types are highlighted by blocking. But there is a distressing element. Contraction flows for inversion are higher than expansion in most seasons. This result heightens the concern raised in the full pulse analysis which showed that inversion samples were mostly taken in periods of contraction.

There are only 9 winter expansion samples showing inversion and they range from 313 to 3220 cfs. There are almost 3 times as many winter contraction samples ranging from 354 to 13400 cfs the latter of which occurred on (2/20/1993). This last high value shows the pitfalls of the function(s) approach. The daily means from three days before are 3033 +/- 283 cfs, the three following are 21000 +/- 10828 cfs. So 13400 cfs is part of an expansion at the local level. But the max pulse midpoint for the entire season (12/4/92 – 5/14/93) is 1/13/1993 so that 2/20/1993 falls in a period of contraction. While the function(s) approach leads to some interesting speculation on the nature of the seasonal pulse, it raises problems in the analysis of inversion.

Another approach is possible and it has already been used to some extent. The daily flow/ flow difference analysis lends itself easily to 'peak' analysis. A 'peak' is simply a flow value higher than that of the day before and that of the day after. A 'peak' is a one day event that can be less than 1 cfs or > 5000 cfs and occur alone or as a side-peak to a larger peak. There are a total of 1488 peaks in the daily means over the entire period and they are 69% >>, 26% ><, and 5% Δ= (a peak with a flow difference plateau). The >< or transition from expansion to contraction is theoretically always present but not always captured in the time span used – most peaks appear to go directly from expansion to contraction. The statistics for the peak analysis of the daily means are as follows:

daily flo/flodiff peak analysis/cfs			
- Gila at Safford(dymns)			
	>>	><	$\Delta=$
average	863	1622	188
Median	225	256	166
Mode	140	115	275
Min	29	48	34
Max	62700	90000	2070
count	1021	388	79
std	3681	5897	229

Table 34

Judging from the values, the  $\Delta=$  label seems to be a 'low-flow' type, while the  $><$  more likely "high-flow" but that is as far as one can go. The daily flow/flow difference is, again, a flow analysis with a very limited context.

The function(l) analysis (l for 'local') works backward and forward from each peak within a given season till the next (or previous) days flow is higher. With so many peaks in the daily means there had to be some designations to cover overlapping from one local peak to the next or intervals with no peaks and those are the 'valley' and 'steady' groups respectively. The following schematic shows how the function(l) analysis assigns expansion and contraction.

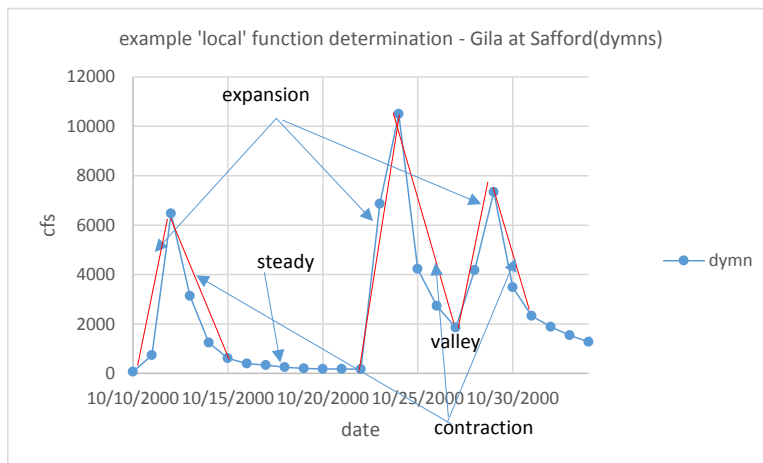


Figure 50

The context of the peaks is the previously determined chronological season in which the peaks are found (winter or summer). This analysis is therefore a seasonal-functional analysis rather than a strictly functional analysis such as the flo/flodiff analysis. The following table shows the function(l) analysis results as performed on the USGS daily means:

flow function(l) statistics		
- Gila at Safford(dymns)		
	avg/cfs	cnt/#
exp(w)	1832	1078
con(w)	1068	2721
exp(s)	627	1033
con(s)	358	1700
valley(w)	995	337
valley(s)	261	451
steady	600	203
lowflow	142	1875

Table 35

Here winter continues to be differentiated from summer and expansion continues to be differentiated from contraction. There are more winter contraction samples, almost 3 times more, than any other high flow type in the daily means which echoes what was found in the grab samples. But the function(l) approach has solved the contraction higher than expansion problem.

Can the function(l) approach tell us anything about inversion? Once again, to find out it is necessary to apply function(l) labels taken from the daily means analysis to grab samples, admittedly a somewhat questionable procedure given the possibility of disjoint between grabs and daily means.

grab sample inversion/noninversion flows with function(l) labels - Gila at Safford				
	averages		counts	
	inversion	non-inv	inversion	non-inv
exp(w)	2191	264	11	4
con(w)	1528	225	25	7
exp(s)	1040	145	6	6
con(s)	654	172	7	15
val(w)		400		1
val(s)	308	69	1	4
stdy	464	125	2	2
loflo	93	122	1	23

Table 36

These numbers are considerably higher than any seen previously. The flow analysis to this point is a 'drill down', a progressive narrowing of the time span for averaging. The vagaries produced by low sample counts in the grabs make that less clear there than with the daily means. Also significant is that expansions are now higher than contractions in all cases but one (non-inv summer).

Since there have been a lot of numbers bandied about, it may be helpful to see them all together in close proximity. A summary of the daily mean and grab sample and inversion/non-inversion average flows using the different seasonal analysis methods follows here.



flow statistics/cfs (1976-2011)		
- Gila at Safford		
	daily means	grabs
average	571	558
median	195	170
range	13400	89974
rel std dev/%	346	232
count/#	13149	161
by flo/flodiff analysis types (daily means)		
	avg	count/#
expansion >>	697	3004
><	993	792
contractio <<	542	4008
<>	588	3497
equal flow =0	190	1031
Δ=	256	816

Table 37

Over all time, daily means and grab samples have very similar averages. Dividing up the daily means with the flo/flodiff function labels shows average expansion flow to be roughly one and half to two times greater than contraction flow which comes in right around the all-data average.

flow seasonal statistics - Gila at Safford									
		monthly		seas		func(s)*		func(l)*	
		dymn	grab	dymn	grab	dymn	grab	dymn	grab
averages	hiflo(w)	822	846	1345	1368	1460/1301	913/1574	1832/1068	1667/1243
	hiflo(s)	425	453	439	383	465/421	334/402	627/358	593/326
	loflo	225	121	143	143	143	143	143	124
rel std dev	hiflo(w)	225	146	219	148	272/187	110/155	249/187	197/107
	hiflo(s)	367	151	477	154	642/244	122/155	542/278	148/111
	loflo	190	68	48	53	48	53	48	42
counts/#	hiflo(w)	1094	80	3915	481	091/2824	15/33	1078/2723	15/32
	hiflo(s)	1104	42	3129	391	333/1796	11/28	1033/1700	12/22
	loflo	1092	39	6105	74	6104	74	5627	70

\*expansion/contraction

Table 38

In seasonal analysis averages generally tend to rise as the time frame for evaluation narrows (from left to right in the analysis types (seas>funct(s)>funct(l)) and expansion is progressively more distinct from contraction. The daily means show rising relative standard deviations for expansion in the summer, something not picked up in the grabs where they are mostly the same. The only 'fly in the ointment' is the presence of higher contraction than expansion values particularly in the grab function(s) values (colored brown above).

Dividing instantaneous flows up into inversion and non-inversion processes provides another look at flow:

inversion/noninversion flows/cfs (1976-2011) - Gila at Safford(grabs)		
	inversion	non-inversion
average	1408	141
median	719	119
range	13122	577
rel std dev/%	143	68
count/#	53	108

Table 39

inversion/non-inversion process seasonal statistics - Gila at Safford(grabs)							
		season		function(s)*		function(l)*	
		inversion	non-invers	inversion	non-invers	inversion	non-inversion
averages	hiflo(w)	1664	241	338/1765	275/190	191/1528	263/225
	hiflo(s)	795	152	912/582	129/160	1040/654	145/172
	loflo	278	155	278	127	278	122
rel std dev	hiflo(w)	137	52	83/144	55/19	171/90	50/58
	hiflo(s)	99	31	89/100	51/87	105/72	42/87
	loflo	N/A	64	N/A	53	N/A	44
counts/#	hiflo(w)	38	10	9/29	6/4	11/25	4/7
	hiflo(s)	14	25	5/9	6/19	6/7	6/15
	loflo	1	73	1	73	1	69

\*expansion/contraction

Table 40

The upper table shows how inversion analysis immediately divides all the flow data into high and low. Non-inversion is, in terms of values and variability, equal to loflow with values in the 100-500 cfs range and relative standard deviations around 30-90%. The high values, ranges, and relative standard deviations of inversion over the entire time span is due to the fact that inversion occurs in both winter and summer.

The lower table (Table 40) breaks inversion numbers down into winter and summer values to show higher values in winter, lower in summer but does not show higher relative standard deviations during summer expansion as seen in the daily means. The situation for contraction values higher than expansion (highlighted with light brown) is rather worsened from the seasonal averages picture.

There are still a lot of numbers spread out over four tables so it is probably a good idea to pick out the 'best' averages in the various categories.

flow 'best' values/cfs - Gila at Safford					
over entire study time span					
		day means	%<	grabs	%<
	most representative	571	78	558	80
	most central (median	195	50	170	55
	most common (mode	146	34	80	28
averages over entire seasons					
		day means	%>	grabs	%>
winter	expansion	1832	23	1667	9
	contractio	1068	28	1243	25
summer	expansion	627	17	593	15
	contractio	358	23	326	23
low flow		143	45	124	41
inversion averages in high flow seasons					
				grabs	%>
winter	expansion			2191	9
	contraction			1528	28
summer	expansion			1040	33
	contraction			654	29

Table 41

The 'average' flow of the Gila River depends not only, of course, on the time interval used but also on where the interest lies. The flow value most commonly obtained in random visits to the site over the study time span would not be the average but the mode, which is around 146 cfs. The value most representative of both high and low flow is the average though that exact flow value is seldom actually obtained (571 cfs - 0.04% in daily means, 558 cfs - 0% in grabs). Even the range 500-600 cfs around the average represents only about 3% in both daily means and grab samples.

Inversion averages are the averages of high flows, not all flows, in a high flow season. Here, the highest numbers are the best because they are the averages that differentiate these highly variable periods the most from each other and from non-inversion flows. They are, theoretically at least, are therefore the most representative numbers available. For these reasons, function(l) values give the best results and are the ones used in the above 'best' values seasonal table.

The seasonal function(l) analysis, is actually a fairly crude analysis with no way of distinguishing side peaks from stand-alone peaks. It is not hard to imagine that the program could be elaborated by including some sort of criteria based on the height of the largest peak in the season. But what is easy to imagine is not always easy to actually do without getting very complicated and very arbitrary so the function(l) analysis was not developed further.

The dilemma related to the use of averages has already been touched on but bears 'spelling out' a bit. The more narrowly defined, the more tightly circumscribed a population is, the more likely its average will be highly representative. 2191 cfs is more representative of winter expansion flows than 570 cfs is of all flow values. But the gain in specificity is a loss in intuitive grasp. What 570 cfs means in terms of all flows is immediately known – it is the 'most' representative available number even if it is not 'highly' representative. For the 2191 cfs 'average high flow in a winter high flow season' to be meaningful, the entire process of seasonal flow determination (10 day rolling averages, 2000 cfs max, 1 year scale) has to be explained, as well as the winter/summer distinction and the expansion/contraction distinction and how they were determined.

The fact, however, that the straight seasonal function(l) analysis helps clean up the order of expansion/contraction mess of the function(s) analysis of the grabs suggests that part of the problem is the function(s) method itself. The fact that the inversion/non-inversion function(l) analysis does as poorly as function(s) shows that low total sample counts are probably also a factor. Note particularly that contractions have counts typically two or three times higher than those of expansions. With random sampling intervals, low total sample counts, more contraction than expansion samples, and more low than high expansion values, it is not surprising that the odds are skewed in favor of low expansion and high contraction averages. Analysis can divide and divide to reach more and more representative values but there is a point of diminishing returns and that is precisely at the point when sample counts get too low.

The seeming problem of contraction values higher than expansion, whatever 'explanation' is used to 'solve' it, points to a fact that may not be intuitively evident – a contraction is part of a high flow period and as such inputs are still open somewhere in the system. New, smaller inputs

may still be opening and the inputs for the main pulse, while diminishing, are not closed – that, theoretically anyway, is the situation only in low flow periods.

The big picture view of flow is a winter season with higher flows and lower variability and a summer season with lower flows but higher variability. Some numbers can now be added to the characterization of the climatology affecting the Gila made by the earliest USGS researchers.

The winter frontal pattern leads to widespread, steady precipitation activity across the state. Some areas are favored, particularly the ‘rim’ country where elevation pushes the clouds up leading to cooling, condensation, and precipitation. Others, such as the central deserts, not so much and some years it may be the only rain they will get all year. The period has variable start and end dates, as early as September and as late as March. It lasts on average about 138 days but can be as short as 16 or as long as 249. The winter high flow season reaches its zenith (maxpulse) some 40 days after the start date. Precipitation events are smaller early on, becoming progressively larger up to the zenith, then diminishing in size and occurrence until the end. Average undifferentiated winter flows are around 1350 +/- 2000 cfs (grabs). Max inversion flows, differentiated by expansion and contraction, are 2191 +/- 3912 while non-inversion min contraction flows are 225 +/- 131 cfs. Non-inversion flow is clearly less variable than inversion across the board.

The convective storms of summer follow the most predictable, least variable part of the year – the May-June, spring ‘dry down.’ They pop up suddenly, with sometimes violent outbursts of thunder and large downpour in small areas which can cause flash flooding. Typically the so-called ‘summer monsoon’ is shorter than the winter season, on average 83 days but can be as few as 8 or as long as 141 days. It can begin as early as June or as late as August. It reaches its zenith slightly earlier than the winter at around 36 days and follows the same progressively larger then smaller events going asymptotically to zero. Average summer flows are around 400 +/- 632 cfs, Inversion expansion max flows are as high as 1040 +/- 1092 and non-inversion flows as low as 145 +/- 61 cfs. The range of values is narrower in the summer than the winter but individual flows in the ‘head’ and ‘tail’ of the curve are more variable. The max max of all flows is in summer (90000 cfs) not winter.

But while the overall analysis helps quantify the seasonal picture, inversion has revealed a real problem – namely an inversion in a loflo period. The ‘solution’ to this problem is very easy and even quite reasonable. The date with the offending data, 12/8/2004, is the first day of the fall dry-down season in 2004. It is not reasonable to treat season ‘begin’ and ‘end’ dates as if they were set in stone – these are arbitrary beginning and ending points of an analysis with no particular significance beyond convenience. Make 12/8/2004 the last day of the 2004 summer hiflo season and voila – problem solved! Put it down to operator error in season determination!

The only problem with this solution is that, if there is any integrity left in this world (!), it is morally wrong. Season determinations and inversion date determinations were done separately with the intent of ‘letting the chips fall where they may.’ Altering the seasons to match inversion determination is little less than creating what you want to find. The season and inversion

determination data will be examined but not changed – there is an inversion in a loflo period and it has to be dealt with.

Looking at two views of the rolling 10 day averages of the daily means show why 12/08/2004 was determined to be in a low flow period.

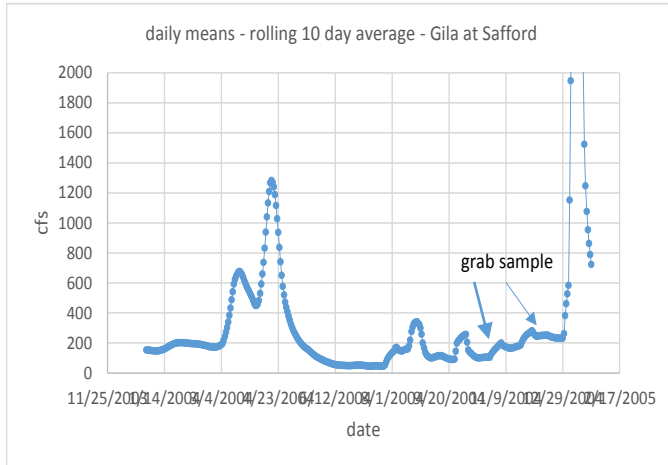


Figure 51

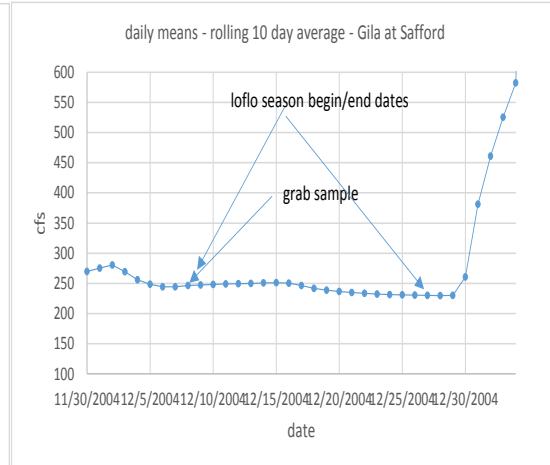


Figure 52

The grab sample follows a small flow peak which is considered the final peak of the summer 2004 hiflow season and is part of a flat section before the winter hiflow season of the next year. This interval is somewhat higher than the average loflo period (143 cfs) and it is true that the flow just previous to the summer high flow season (~200 cfs) is not reached after the season is over (~250). But the loflo designation is as much a matter of low variability as low magnitude and this is definitely low variability given the scale used. While there would be ‘no harm, no foul’ in moving the season begin date by one day, it is a very low flow for inversion and, as such, worth looking at.

Could there have been a problem in the designation of 12/8/04 as an inversion date? Comparison with the previously shown inversion/noninversion ( $\text{HCO}_3\text{-Cl} > 0$ ) data averages shows that, though the differences are low, there is no error. The charge % graph clearly shows  $\text{HCO}_3 > \text{Cl}$ .

summary of inversion/non-inversion average values over various analysis quantities with two problematic dates - Gila at Safford(grabs)													
	amount	% amount	mass	%mass	volume	%volume	conc	%conc	activity	%activity	mole	ionicity	charge%
noninvdat	-7.3	-13.3	30.8	-0.004	-0.015	-0.003	-0.003	-0.006	-0.003	-0.005	-7.3	-7.3	-12.9
inv data	45.5	9.5	1966.8	0.006	0.946	0.003	0.001	0.002	0.001	0.001	45.5	45.5	11.1
12/03/08			491	0.0081	0.2103	0.0035			1.2E-05	2.2E-05			
12/08/04	1.5	1.5	667.5	0.008	0.298	0.004	2.0E-04	3.5E-04	1.9E-04	3.4E-04	1.5	1.5	1.4

Table 42

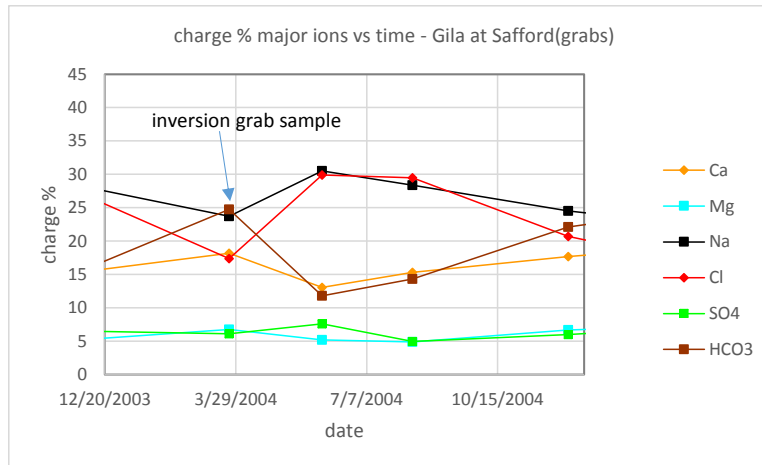


Figure 53

278 cfs is a problem because it is a “low flow” inversion sample but 279, the next higher inversion date flow value, is not because it is a “high flow” non-inversion sample. That 278 cfs shows the presence of an open input while 279 does not suggests that an increase in flow is not, by itself, enough to make the claim that a new input has opened.

The source of higher sodium and chloride on the Gila was discovered as the result of numerous investigations of various reaches of the San Francisco around the area of the Clifton Hot Springs.<sup>1</sup> For more insight into the principles and methods of ‘sourcing’ the reader is referred to textbooks in hydrology. Here only a very crude ‘sourcing’ will be done -- the speculation earlier that inversion flows are coming from outside the valley, based on a guess from the flow topology, is generally upheld by comparing the HCO<sub>3</sub>/Cl activity ratio averages by season: loflo = 0.5 - 0.7, summer hiflo = 1, winter hiflo = 2.

The distinction made by hydrologists between ‘baseflow’ and storm flow suggests a useful distinction in sources. Baseflow is the groundwater seepage that keeps some streams flowing in extended periods with no precipitation. Groundwater tends to have fairly constant composition while storm flow compositions can vary wildly because of the mingling of different tributaries. This fact means a distinction can be made between a ‘single’ source and a multi-source flow with the former being closer to a ‘closed’ system than the latter.

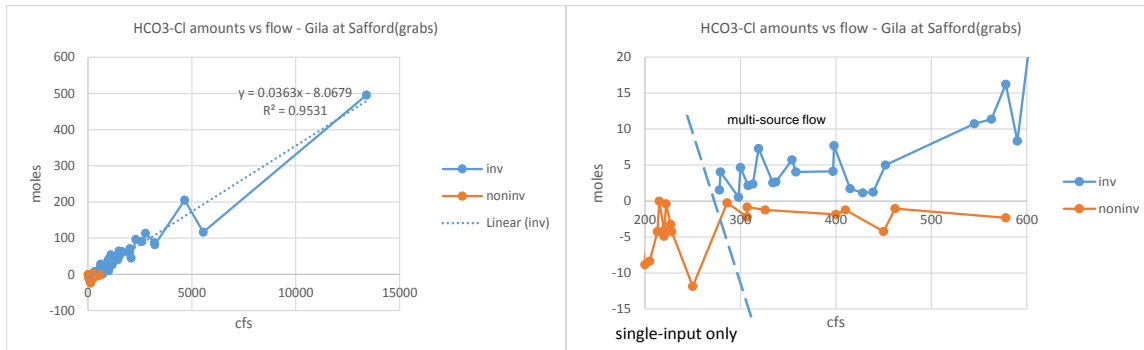


Figure 54

Figure 55

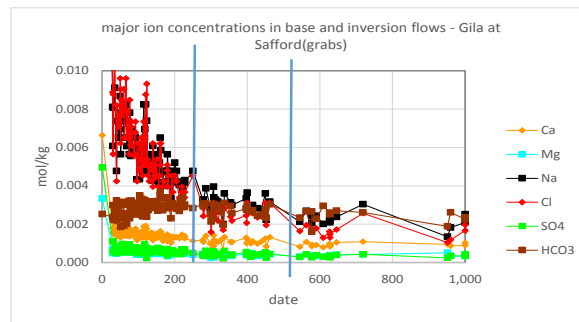


Figure 56

A problem exists because a connection has been suggested between low flow and a ‘closed’ system. What inversion shows is that that is a false identity, at least in the way low flow is currently designated. If there is any true ‘base’ flow approaching ‘closed’ system status, such as a groundwater flow (spring source), it is somewhere in the low flow region below 278 cfs or it just doesn’t exist at all (as in some Arizona rivers). Even in a closed system, a small change in volume could just be a temperature related fluctuation. A large increase in volume in a closed system, however, would probably indicate a new input and a switch to ‘open’ status.

(The reason for the somewhat obsessive insistence on finding a closed system is due to the important role of closed systems in developing the thermodynamics laws, a subject which will be discussed at a later point)

The problem of an inversion sample in a low flow regime, then, remains. It is hard to imagine new inputs at such low flow. But ‘high’ and ‘low’ flow are, after all, arbitrary designations and the relation of flow to amount is strong but not without some wrinkles. Despite this exception, inversion is still very much, at this stage, an average or above average flow phenomenon: that is, in the non-normal portion of the flow distributions.

To this point ‘inversion’ analysis has meant looking at flow on inversion and non-inversion sample dates. But flow itself has no inversions – it is the ‘things’ in the water that invert. Keeping in mind the topology of the area (p. 36) and widening the scope of analysis from major ions to TDS and TSS allows one to rationalize why the patterns of flow and dry-down are what they are. The patterns here are not of flow itself but on things affected by flow.



At Safford, relatively high TDS concentrations are a sign of what is to come for the Gila. Just as water will find the lowest spot in an area, lying there stagnant and condensing until nothing is left but a salt residue, so the rivers of Arizona head from the north, south, and east to the great central flatland bordered by Phoenix, Tucson, and Yuma. This area becomes a huge sump for water to concentrate, particularly during the hottest parts of the year.

Picking three points along the Gila in order of descending elevation, Safford – Gillespie Dam - Dome, illustrates the trends. Besides decreasing elevation (3059, 809, 10 ft above sea level respectively), there is increasing drainage area (49650, 57850, 78740 acres), increasing max temps (33, 34, 36 C) and decreasing annual rainfall (9.7, 8, 3 in (Arlington for Gillespie, Yuma for Dome)). As a result of these trends, TSS goes down (831, 179, 61 mg/L) while TDS goes up (627, 3188, 2517 mg/L) which is mirrored by average chloride numbers (163, 1078, 912 mg/L).

The major ions have different roles in these trends. Ca, Mg, HCO<sub>3</sub>, CO<sub>3</sub>, and SO<sub>4</sub> form ion pairs which can presumably join the suspended solids and, if conditions are right, precipitate out of solution (an attempt to verify these speculations will be made later). Na and Cl, however, form few ion pairs and, in accord with the so-called ‘solubility’ rules, are the last to precipitate out of solution, resisting the impulse until the water around them evaporates leaving them literally high and dry. This situation makes chloride the perfect analyte for studying water ‘cycling’ (the differential concentration and location of solids, dissolved or otherwise, in a system) – it can’t do much else than concentrate. Gila River water at Safford is almost always saturated with NaCl, the solubility index being between 5 and 8 with very little variability even in inversion periods.

The above trends can be formed into what may be called the ‘high elevation precipitation regime’. Inputs to the system coming from higher elevations are composed largely of rain water and pick up suspended solids as they flow downhill. The influx of low-TDS rain water tends to dilute receiving water bodies which are usually higher in TDS. Suspended solids are sometimes visualized as clumps or bodies afloat in the stream. These need a certain momentum of water to be kept in motion and, as drainage area increases and momentum drops, tend to fall out of the system.

The regime posited is both specific to this area and a highly generalized view with exceptions possible. The fact that average TDS is higher at Gillespie Dam than Dome may be due to the proximity of the dam to Phoenix (about 50 miles southwest and **downstream**) and possible increased domestic, industrial and agricultural water usage. Dome, about 20 miles northeast and **upstream** of Yuma, would have primarily just ag returns (Wellton-Mohawk Irrigation District).

Somewhere to the west of Gillespie Dam, the Gila sinks into the ground to reemerge at Dome, about 170 miles southwest of Phoenix. There may be underground current and/or mixing with groundwater involved. All of this is very speculative, but if general water quality can be used as a tracer, the water at Dome is the same ‘stuff’ as at Gillespie with the above trends factored in.

Every few years, the Gila floods and runs continuously from New Mexico to Yuma as it did year-round in days past. Along the way, it passes through what must be one of the loneliest, driest USGS water gages in the country at Dateland AZ. The graph below illustrates both the long dry spells and decreasing max flow over a span of more than 18 years.

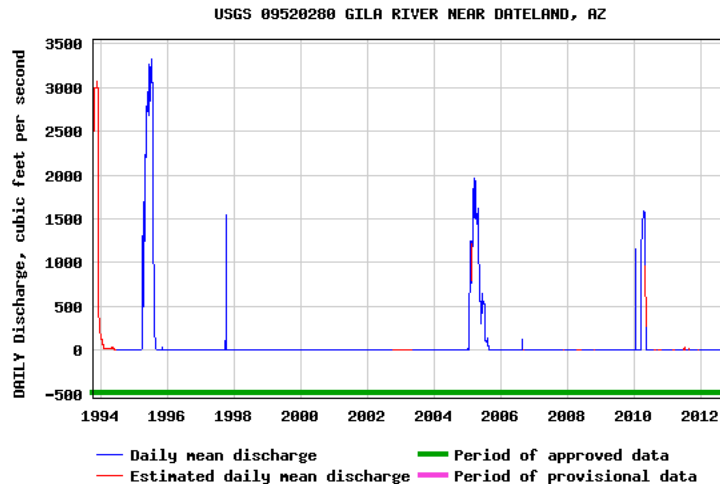


Figure 58

Looking at the high elevation precipitation regime from a low elevation point of view produces the ‘high drainage area evaporation’ regime. The two regimes are in competition with each other in terms of time and space which can be viewed along two axes. Perpendicular to the spatial (high to low elevation) axis is the time axis at any particular site. The annual wet/dry season fluctuation plays out along the temporal axis with mins and maxs set by position of the particular site along the spatial axis.

The high elevation precipitation regime would dominate the basin in the high flow years shown in the graph. That is, the high elevation regime pushes its influence into lower altitudes, maybe even across the whole river basin. Each site along the way has relatively longer wet seasons and/or higher magnitude flows than normal. In the dry periods between high flow years, the high drainage area evaporation regime dominance stretches further up into lower drainage areas (i.e. higher elevation areas) as the dry period continues. Each site along the way has a relatively longer dry-down period than normal. The alternation of wet and dry (dilution and concentration, expansion and contraction) is the same whether looked at in terms of different elevations at a particular time or in terms of a particular elevation at different times.

It may be asked what the difference is: ‘wet’ and ‘dry’ seasons vs the two regimes introduced above. The answer is that wet and dry seasons apply to the flow process as a whole with both expansions and contractions going on. The regimes, on the other hand, start to differentiate flows by function (flow change in one or the other direction only, expansion or contraction). Because flow is tightly bound to topology, high elevation flow control volumes can be characterized by slope and elevation to yield the key expansion factor: momentum. As momentum drops and water becomes relatively more stagnant, control volumes begin to take up more heat eventually evaporating. Theoretically a stream could be completely characterized at each point in time and space by an expansion potential (momentum) and a contraction potential (the change in heat content with time (temperature)). Each potential needs to be taken at each point even though the spatial extremes may not change much from year to year. The point where one regime (typically contraction) begins to predominate over the other will form a topological pattern in space over

time depending on temperatures. To reduce the jargon a bit: the line between the two regimes is where water goes from acting (diluting) to being acted upon (concentrating).

(Some proof of the above speculation may be sought for with inversion analysis. But, unfortunately, inversions are few and far between, at Gillespie (16 instances in 42 years), and rare at Dome (4 instances in 28 years). No inversions occur at Gillespie in 1987, a known high flow year, there is no 1993 data (a very high flow year) to examine, and only 1 of the 16 inversions occurs after 1994 (in 1995) with data in this dataset ending in 2001. But at Dome, 2 of the 4 inversions seen occur in 1993 and another occurs in 1987.) It is not possible to relate the flow peaks at Dateland with inversion at Gillespie Dam and Dome because the varying time frames do not allow enough data to be lined up.

To this point, flow on the Gila at Safford has been characterized in a somewhat biased manner. Interest in the inversion process has slanted the emphasis toward high flows. The low flow portion of the flow distribution frequencies graph is, it will be recalled, quite normal. Maybe using only normal flows will keep the flow/concentration response normal as well (though there is no logical reason that it should). A less important but more likely result is that the normal portion of the flow distribution will make it easier to find general flow patterns.

The results of seasonal and inversion analysis on low flow are presented below. The rationale for these analyzes have already been discussed and will not be repeated here. The low flow seasons are labelled by the high flow seasons they are bordered by: summer to winter (s-w), winter to summer (w-s), and summer to summer (s-s) if a winter high flow season was lacking. There were no (w-w).

low flow seasonal statistics - Gila at Safford					
		seas/func(s)		func(l)	
		dymn	grab	dymn	grab
averages/cfs	loflo(s-s)	130	111	130	111
	loflo(s-w)	175	169	176	169
	loflo(w-s)	123	107	119	93
rel std dev/%	loflo(s-s)	45	43	45	43
	loflo(s-w)	39	42	39	42
	loflo(w-s)	59	73	61	47
counts/#	loflo(s-s)	2167	25	2149	25
	loflo(s-w)	2002	20	1875	20
	loflo(w-s)	1936	29	1603	25

Table 43

inversion/non-inversion low flow statistics - Gila at Safford(grabs)							
	avg		rstd		cnt		#
	inv	non-inv	inv	non-inv	inv	non-inv	
loflo(s-s)		111		43			25
loflo(s-w)	278	163		41	1		19
loflo(w-s)		93		47			25

Table 44

There is little to no differentiation of the three low flow seasons. The outstanding feature of the low flow regime is that it is almost always non-inversion – that is, higher chloride than bicarbonate. The one exception has been discussed and the only thing to add is that it comes in the low flow season with the highest average flow.

Low flow periods are usually more characterized by the high drainage area model than the high elevation model. In the latter, concentrations go down as flow goes up. But there are seven examples among the grabs, most of them during low flow periods, of chloride (Cl) concentrations going up when flow goes up. This result could simply be due to higher flows from the high chloride post-Clifton Hot Springs San Francisco combined with lower flows from all other sources. A more likely example of this kind of situation are so-called ‘ag returns’ where river water is diverted to be run over crop lands. Excess water beyond the amount that is able to infiltrate the soil runs back into the river with a certain amount of new and/or condensed material in it. So there can be both loss of water from the system and addition of more concentrated materials.

It might be expected that the dates themselves would be in the hottest, driest periods of the month when the need for water would be greatest. Actually, only one date occurs in May, the others are in October(2), November(1), December(1), and January(2). Most are in low flow seasons but one October and one January are in hiflo seasons. The reason for the unexpected time of season may be that, in the hottest, driest months of the year, the water is less desirable than at other times because of higher salinity (TDS). No attempt has been made to substantiate these suggestions: people in the southwest are generally tight lipped about their water usage due to fear of regulation.

The above problems of concentrations rising when flows increase will be analyzed more fully in what follows. For now it is sufficient to note that they are small and exceptions to the rule. Below are the monthly average concentrations in mg/L for sodium and chloride. This picture shows that, in general, concentrations rise over the same months when flows are decreasing not increasing (may-jul). Thus the high drainage area evaporation regime lies at the heart of any year even in high flow years when the high elevation precipitation regime is dominant. The competition for influence between the two regimes is not only across different years but within each year. Some sort of balance between the two, in terms of area and time, is reached in any given year.

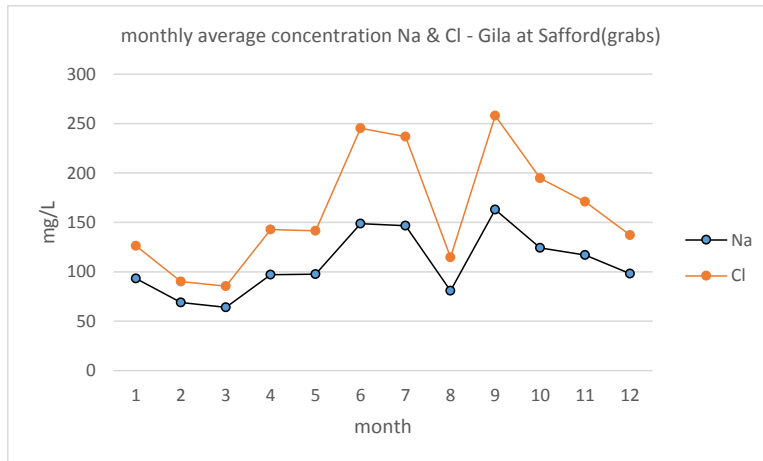


Figure 57

Reducing attention to the low flow part of the distribution helps not at all. The exceptions to the flow-concentration correlation model are usually small but they increase in number. There are new sources and inputs at work during low flow periods not apparent in high flow periods. Inputs in a low flow regime are likely to be small and uncertainty in both flow and concentration measurements increase as well. A large scale dilution is probably easier to quantify than an increase in concentration due to a small influx of highly concentrated material. But low flow periods are, in general, more representative of the every-day behavior of the Gila (median or mode vs average) and may therefore be better periods to look for larger, more general flow/amount patterns.

The graph to the left below shows the daily mean flows for each day in June, the driest month of the year, from the entire time span of the study. It might be assumed that the high values for any given day come randomly from any number of years but that is not the case. An examination of year-month values (to right) shows that the values from the three highest series come from the same years which were all 'wet' years. In other words, all the flows are coming down asymptotically but the wettest years come down more slowly and reach their lowest point later.

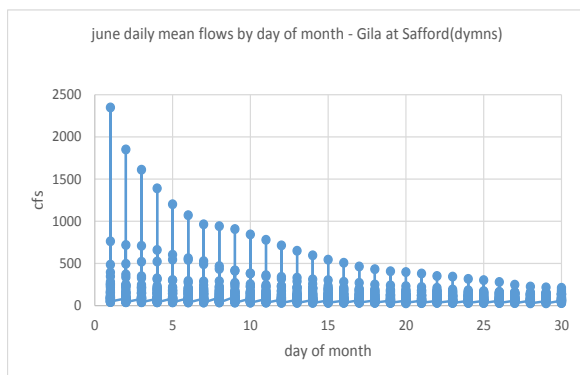


Figure 59

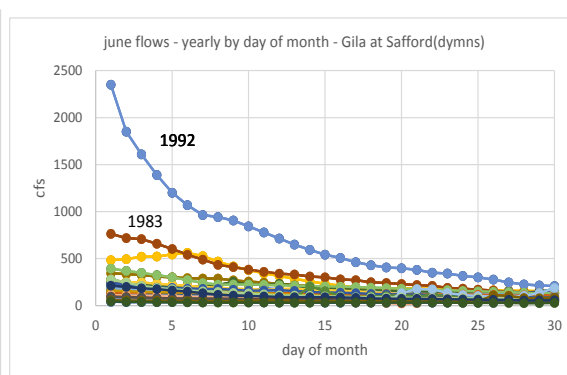


Figure 60 [\(back\)](#)

This view of June flows just begs to be extended backwards and forwards in time. Below are the daily mean flows versus the day of the year for the three years with the lowest median flows, 2002, 2009, and 2011.

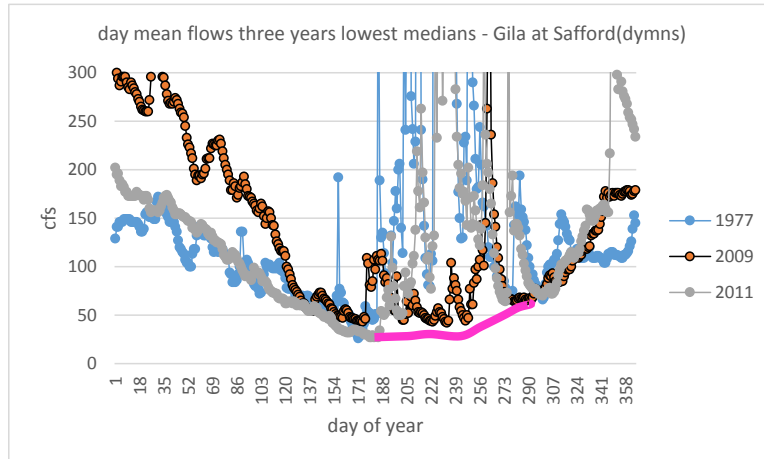


Figure 61

The picture is marred by the summer high flow season, which appears in all years, but the 'low flow' curve can be made more regular by extrapolation (magenta) to cut-out the portion affected by summer precipitation. This driest years' curve could be used as a reference to evaluate other years.

But there is easier way of finding a more generally relevant curve. It is suggested by the day of the month curve procedure used to create the June graph -- simply take the flow minimums for each day of the year over the entire time period of the study as the low flow curve. A max flow curve can be created as well for comparison but, in that case, a rolling 10 day average (r10da) is needed to reduce the noise. Below are the daily mean mins and maxs for flow values. A similar set of curves may also be generated for density.

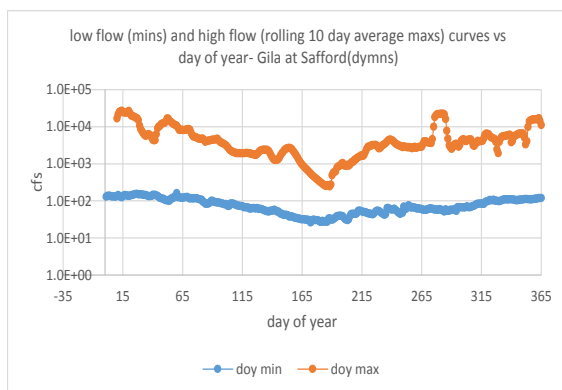


Figure 62

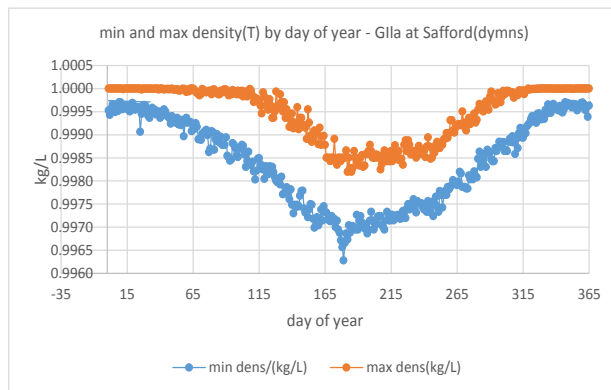


Figure 63

The low flow and low density minimums are within a week of each other – flow 6/20, density, 6/27. The max flow and max density curve minimums are both pushed to the right of their respective min curves but their minimums (min-maxs!) also fall within about a week– density 6/30, flow 7/6. The highest temperature period of the year thus coincides with both low flow and low density.

There are, however, other differences between the various flow and density curves. The max flow curve has significantly steeper slopes around its minimum (summer) than the minimum flow curve. By contrast the maximum density curve has a less steep slope in the area of the maximum(winter) than the minimum curve. The differences are enhanced in the following view of mins/ maxs and their multiples for flow (left) and density (right). Fairly realistic max density curves can theoretically be created with multiples of min density curves but realistic max flow curves cannot be created from multiples of min flow curves.

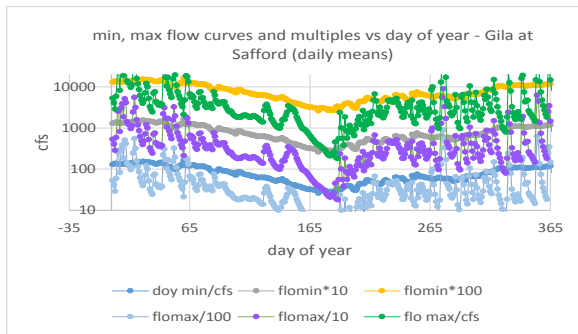


Figure 64

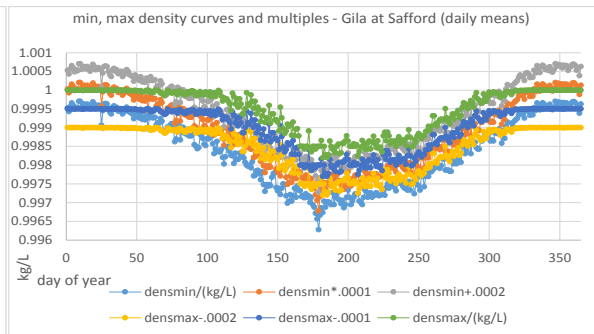


Figure 65

While the value curves have similar shapes but differ in detail, the difference of value curves show where the respective areas of high variability for flow and density lie. Below are the flow (left) and density (right) differences vs the day of year using daily mean data.

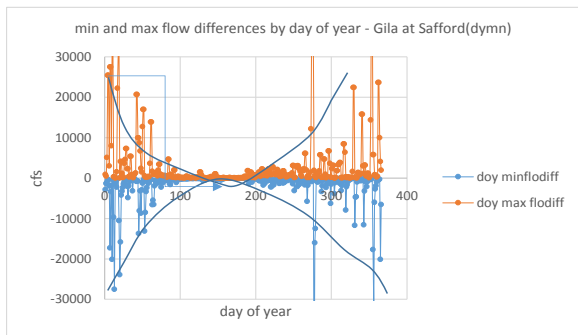


Figure 66

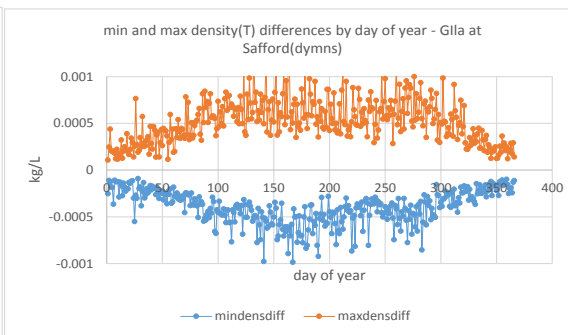


Figure 67

The differences graphs for flow and density are exact opposites, with flow difference being convex over the course of the year and density difference being concave. While flow and density have similar curve shapes, the periods of maximum range of differences (variability) are precisely the opposite with high flow variability in winter and high density variability in summer. This difference has implications in analysis – the low flow period is the best period in

which to examine a wide range of density change with less interference from flow effects or the max limit on density.

It is also possible to do a day of the year (doy) analysis on concentration but there are some difficulties. Only grab sample data is available so most doy have only one data point and 'minimums' with only one data point available are not very meaningful. Below are the solvent and sum of non-solvent concentration by day of year.

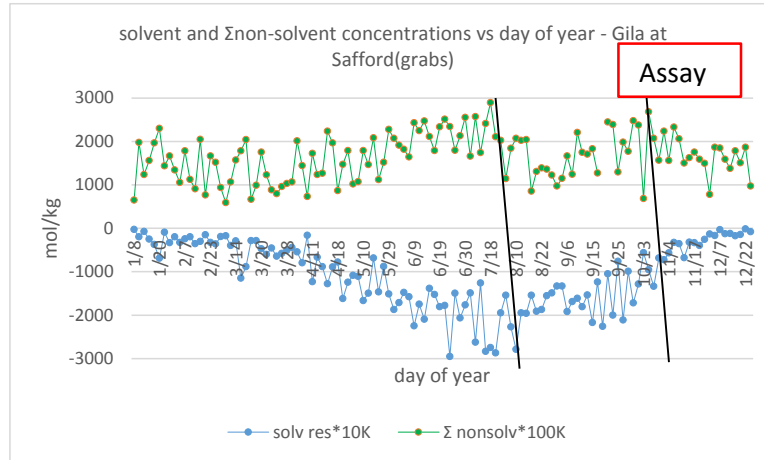


Figure 68

As has been seen before, solvent concentration closely follows the pattern of density while non-solvent concentration is pretty much a sine curve with an anomaly around Aug and Sep corresponding to the summer wet season. The August drop in non-solvent concentration is where temperature induced contraction collides with flow induced expansion and is faintly echoed in a local rise in solvent concentration.

Putting flow and density minimum curves on the same graph with non-solvent concentrations brings the three major factors, flow, density, and concentration, all together on one graph.

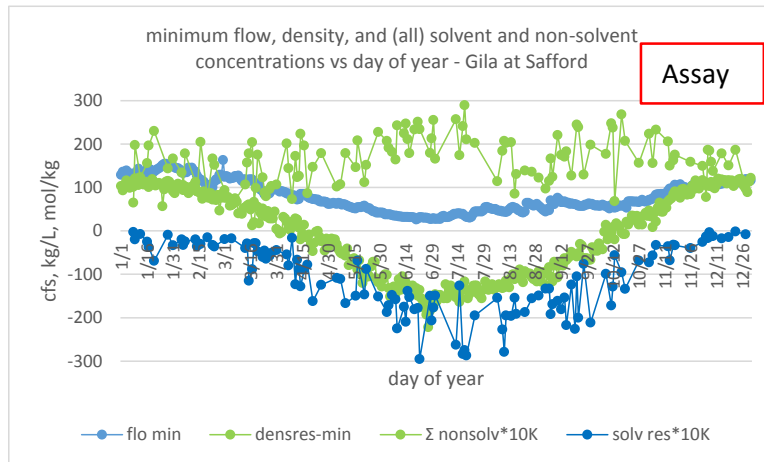


Figure 69



This is the expected picture of a dry year with minimal departure from the essential loflo season (May –July) scenario: lower solvent concentration with higher non-solvent concentration in a low density matrix. The Jul-Aug dip seems more truly anomalous here since there is no sign of higher flow on the low flow curve to explain it. The above graph covers a lot of information but is not as clear as it might be due to the use of residuals and a variety of dimensions: cfs, kg/L and mol/kg.

A better approach would be to reformulate the above in terms of the changes in volume of the control volume. Flow is highly correlated to volume ([Table 16](#)) and total relative volume can therefore be used as a surrogate for flow while the partial molar volume can be used for density, its inverse. Daily mean flow is converted from cfs to L and multiplied by one second to yield total relative volume. Daily mean density is converted to a partial molar volume with the molecular weight of water as surrogate for the solution. Both sets of numbers use the day of year minimums from the day means which are the ‘normal’ portion of the data for those distributions. It should be noted in passing that neither the grab flow nor grab partial molar volumes form the same pattern when put in day of year formatting, which result is probably just a matter of not enough days of the year represented.

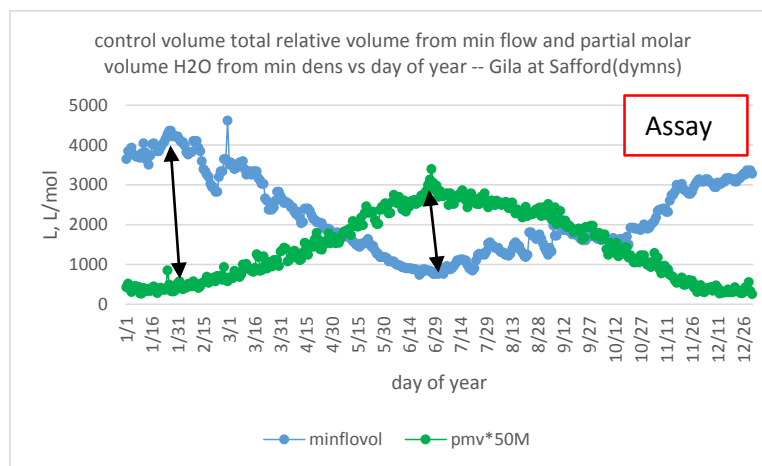


Figure 70 ([back](#)) ([back2](#))

The resulting graph suggests that a redefinition of ‘pulse’ is in order. It will still involve a change in direction but will be in terms of control volume values rather than flow differences. The new definition of pulse as the points of maximum difference of the two curves, the points of maximum amplitude, is in line with the traditional use of the term. There is one ‘pulse’ in Jul and one, much larger, pulse in Jan reinforcing the picture of a two pulse, two season year. It is with this picture in mind that the ‘discounting’ of the October high flow peak is shown to have been a good ‘strategic’ decision.

The two curves represent two aspects of volume change. The total relative volume is the volume with respect to the outside world, the ‘external’ bounds, while the partial molar volume is the internal spacing or ‘inner packing.’ The former is a matter of changing amounts of solution while the latter, the inverse of density, is a matter of temperature change. The two effects are of vastly different magnitudes with the former typically involving hundreds, even thousands, of

liters of solution while the latter are changes in the  $1 \times 10^5$  or  $^6$  L/mol range. Even when multiplied by the number of moles, the partial molar volume max change volumes are between 0.02 and 500 with an average around 40L. The winter season is characterized by total volume expansion, inner packing contraction while the summer reason is inner packing expansion and total volume contraction. The rise in flow dominates the winter season, the rise in non-solvent concentrations dominates the summer.

The above picture may be qualified by examining the variability of the parameters. The variability of the total relative volume is the same as that of flow while the variability of the partial molar volume of water does not follow that of density but looks more like that of non-solvent concentration.

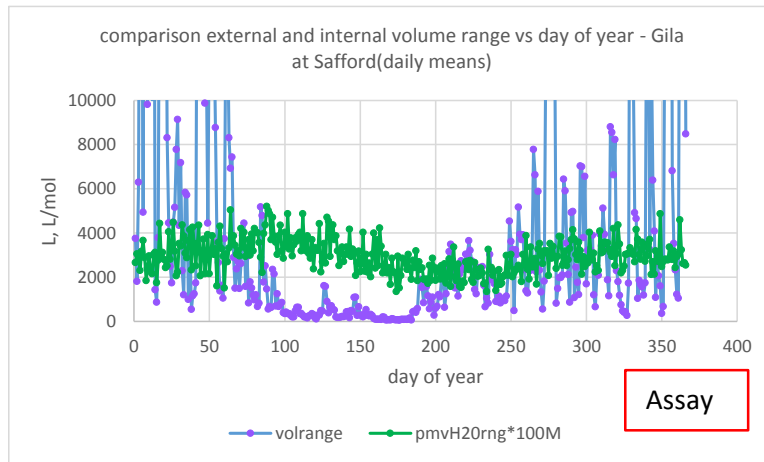


Figure 71

To elaborate further upon the relations, the points of intersection of the various curves can be examined. In the characteristic, well defined spring (May-Jun) dry down, the total relative volume of the control volume goes down in value and variability while the partial molar volume of water (the solution) goes up and variability is tending down. In the fickle fall (Oct-Nov) dry down, wide in possible span but usually narrow in practice, control volume values and variability go up while the partial molar volume values go down with variability tending up. The variability picture complements that of the values above: in spring the external volume is contracting while the internal packing is expanding and in fall vice versa. These speculations will be put to the test later.

These graphs complete the picture of the system as represented by the control volume in the hypothetical constant low flow, low density regime. They arguably give a better picture of normal flow and density patterns on the river than either 'real' flow or density graphs, just as flow mode and median are more representative of everyday values than the average. The day of the year minimums graph is a good example of a 'hypothetical' graph – the data is all 'real' (the real minimum of minimums for any given day of the year) but the context is not; stringing the values all together in one year yields a curve that has never really occurred. It is closely approximated, however, by any number of 'dry year' curves if summer precipitation is cut out.

This new view provides a clearer picture of normal behavior on the river as well as possibly providing a better scale for comparison. Rather than comparing max flows to average, as is usually done, it might actually be more meaningful to compare average flow to minimum flow. A year whose average is much higher than the minimum curve might be considered more fundamentally a 'wet' year than one in which a few maximum flows are much higher than the average. This new line of reasoning could, theoretically, lead to a complete re-definition of the 'wet' and 'dry' season dichotomy at the base of this study – a change which, at this stage in the game, is not going to happen.

While of interest in the characterization of flows and densities on the Gila, the low flow picture yields nothing about inversion. The points of minimum and maximum amplitude are too wide to make any connection with the occurrence or non-occurrence of major ion inversion. These points occur in all years, including those in which no inversion occurs, so any causal relation seems unlikely. At most these points may be part of the larger context of 'inversion,' setting the stage for it so to speak.

The low flow analysis has helped create a picture of general flow patterns but has revealed problems in the basic flow-concentration correlation model used here. New sources and outputs have to be conjured up to make sense of things. While concentrations can go either up or down with rising flow depending on relative input concentrations and volumes, amounts usually only go up with increased flow.

There are, however, 13 cases in the grabs of one or more major ion amounts going down with rising flow. In one case, 4/7 to 5/8/80, all the major ions amount differences are negative but very small in magnitude, from -0.4 to -2.3 moles. The number of moles comes from concentration differences that range from -1.6 to -5.9 mg/L for analyzed parameters and -24 for the calculated parameter (HCO<sub>3</sub>). In these cases, the differences are possibly low enough to be right around the sampling and analytical variability for the parameters. If errors in flow measurement are factored in, the whole case may just boil down to error due to analytical variability.

There are a couple other cases in the grabs, however, where the discrepancies seem too large to write off as error. For the dates 1/12 to 2/14/79, Cl goes down by about 20 moles with a flow difference of +220 cfs. A complete analysis of the change over the two dates revealed no obvious anomalies. Like the 4/7-5/8/80 case, the situation overall is a dilution, concentrations going down with increasing flow, and, probably coincidentally, pH constant. Two other cases also show large changes in amount (-6, -8 mols) with increasing flow.

Analyzing the situation with a simple mass balance approach using concentrations and volumes shows why there is a problem here. The equation for a typical fork-in-the-river scenario, using 'C' for concentration and 'V' for volume, is

$$\text{receiving} + \text{incoming} = \text{final}$$

$$C_1V_1 + C_2V_2 = C_3V_3$$

where

$$V_3 = V_1 + V_2$$

Volume is calculated from flow multiplied by time (cf or L/sec times secs) so that time 'falls out' of the equation. Amount is found by multiplying C (mg/L or mol/L) by V(L) in the first equation, liters cancel above and below the line, leaving

$$M_1 + M_2 = M_3$$

where M is mass in mg or amount in mols. If amounts are going down with increasing flow then M3 is less than M1 which means M2 has to be negative, which is not possible. Both concentration and volume can only be positive values (or zero), so no amount of fiddling with either is going to alter the situation.

The above equation is, of course, an expression of the first law. The first law applies to the entire universe, not necessarily to any particular portion of the universe. It has no time factor - the 'seconds' in flow can be removed with the distributive law and cancelled on either side of the equation. There is, however, a spatial distinction necessarily involved - M1 occurs before the fork and M3 occurs after. This distinction raises a sampling decision that has to be made - how close to the fork are the before and after samples to be? Time creeps back into the practical evaluation of the equation because, in a flowing river, how close to the fork is a question of time to and from the fork. In fact, for the grab sample analysis here, the initial (M1) and final (M3) sample points are spatially the same point and what separates them is time, incoming (M2) being the sum of all inputs in the interim. The further apart two sample points are in space and/or time, the harder it is to show the first law at work because - well, things change.

The mass balance is often used in water treatment systems. For example, it was used to calculate concentrations in a reservoir holding treated wastewater effluent used for cooling tower water at a major nuclear facility. The equation is modified slightly to  $C_1V_1(\text{inputs}) - C_2V_2(\text{outputs}) = C_3V_3(\text{final})$  to suit the new situation. Knowing plant effluent (inputs) and reservoir (final) concentrations and flows, it was possible to compare calculated to analytical concentrations. In general, percent differences were around 0.7 to 2 (+/- 5 to 8) % for Ca, Mg, SiO<sub>2</sub> and 2.5 +/- 12% for PO<sub>4</sub>. PO<sub>4</sub> results were particularly bad at two times of the year - spring (Jun) and fall (Nov) - where differences between calculated and analytical concentrations rose to 30% or above. It was theorized that, PO<sub>4</sub> being a nutrient, the rise in variability might be due to "bugs" absorbing it in spring and releasing it as they died off in winter. The theory was, however, never tested and the results became merely an interesting footnote in a larger problem of phosphate removal which will be referred to again later.

Another apparent violation of the first law occurs when materials precipitate out of solution. Here the necessary change is to expand the 'system' to include not just the solution but also the solution boundary where the precipitates have gathered. In all cases, widening the system spatially, temporally, or analytically brings back the 'completeness' envisioned by the first law.

It should come as no surprise, therefore, that when the final sample is taken at least a month and sometimes three or four months after the initial, it may not be easy to demonstrate the first law. But while the first law may not always be easily demonstrated, the verbal expression is easily

stated and intuitively obvious – matter at a macroscopic level has never been known to spontaneously appear or disappear, it always comes from ‘somewhere else’. It follows that negative amounts are not possible, so if flow is going up, amounts must also be rising or at least remain constant. ‘Else there has to be a mighty good explanation.

While the M2 (change to the initial system) in the equation above cannot be negative, there is no law that says it can’t be a sum of two terms, M2.1 and M2.2. These two terms could be inputs (2.1) and outputs (2.2) and bingo! – systems analysis would make outputs (M2.2) a negative number. The new equation, with altered numbering for ease of viewing, is:

$$\text{Initial} + (\text{inputs} - \text{outputs}) = \text{final}$$

$$M1 + (M2-M3) = M4$$

$$C1V1 + (C2V2-C3V3) = C4V4$$

Where

$$V4 = V1 + (V2-V3)$$

The trick here is to make the output amount (C3V3) greater than the input (C2V2) with V4 exceeding V1 so that the overall situation is a dilution. The initial and final data, concentrations and volumes (from flow) are taken from the grab sample flows and chloride data for 1/12/79 and 2/14/79.





the trick				
	initial	(data from 1/12 and 2/14/79)	final	
cfs	1650	flow goes up	2600	
L in 1 sec	46723		73624	
mg/L	44		22	
1)	V1	$(V4-V1)=(V2-V3)$	V4	
	46723	26901	73624	
L in 1 sec	46723		73624	
mg/L	44		22	
mg	2055814	amount goes down	1619732	 
2)		$(M4-M1) = (M2-M3)$		
		-436082		
calculator		inputs	outputs	
	cfs	1683	cfs	732.5 
	c2	10	c3	44
	v2	47643	v3	20742
checks		v2-v3	26901	compare to 1) above
		c2v2-c3v3	-436223	compare to 2) above
	$c1v1 + (c2v2-c3v3) = c4v4$		1619591	compare to equal sign above

Table 45

First, expressions for the requisite volume increase and amount decrease are worked out (1 & 2). The input concentration (c2) is arbitrarily set to a low value, here 10 mg/L Cl. The output concentration (c3) can be set to any convenient number but a number larger than the input and lower than or equal to the initial keeps the results reasonable. An output flow (cfs) (marked by big arrow) is plugged in, converted to output liters, input liters (via 26901+output L), and input cfs (input L / 28.317/1sec). Using the calculator, output flow is manipulated until c2v2-c3v3 (in box) is close to M4-M1 (the #2 requirement) to any desired level of agreement. When the requirement has been met, c1v2 + (c2v2-c3v3) in the bottom line will be close to c4v4, the final amount of material (marked by big equal sign).

Without any experience in water usage quantities in the area, it is hard to know if 1683 cfs input and 732.5 cfs output are very realistic. These would have to be actual water withdrawals such as irrigation where water infiltrates the soil and goes down to groundwater (that is, is removed from the river system entirely) – all of this is purely speculative. And even if the situation is realistic, this calculation is hardly proof that such withdrawals actually occurred. The model shows only that amounts can decrease with increasing flow under certain circumstances without violation of the first law.

The low flow analysis has found some interesting general flow patterns (as volume) but has also raised a host of questions. The questions first appeared in the ‘exceptions’ to the flow trends derived from topology (pp.69-70). They suggest that the simple flow-concentration correlation used here has problems and these have been dealt with individually one by one.

Another approach, one that deals summarily with the above problem, is to normalize concentrations with respect to flow. With this approach, results do not depend on the normality of the underlying data (i.e. it is a ‘non-parametric’ approach). An example of such an approach is the Kendall seasonal tau test used by USGS researchers<sup>8</sup>. If concentration is normalized to flow, then flow effectively drops out of the picture as a cause. If a trend is observed it is not the result of a change in flow and requires some other explanation.

This approach allows trends to be picked up that might be otherwise have been missed with the flow-concentration correlation model. Examples are above and below reservoirs (where the local flow regime is changing rapidly) and near mine slag piles (small flows of highly concentrated material.) This method makes possible the accurate and precise determination of trends at specific sites. Increased precision, however, comes with a loss in scope. There are no trends for the river as a whole such as those visualized by the regimes introduced above. The method is actually too ‘sensitive’ for viewing the general patterns and relations that are of interest here.

It must be admitted that the hope was that a flow pattern would be found out of which inversion would be seen to ‘grow’ and that has not happened. Hope springs eternal, however, and another attempt will be made to find such a flow pattern. This one will start with the most fundamental relations of amount/activity. Rather than looking directly at flow, the approach, inspired by the topological trend analysis, will examine amounts and activities in order to look at flow indirectly. The results of the attempt will be used to set up some new ‘rules’ to approach the problem which will enable a more direct search for a more extensive, explicit ‘seasonality’ in flow.

The definitions of inversion that have been developed all still apply here but the formulations will be somewhat different. Beginning again with the major ions, the focus will shift to groups of parameters. There will also be some changes in presentation such as, for example, shifting from strictly annual time-series graphs to graphs bounded by inversion status. A new method combining correlation and autocorrelation analysis will also be presented.

The correlations of the major ions with flow for a number of analyzes have already been shown. Here the analysis is repeated for amounts and activities of four of the major ions and extended to cover five ‘views’ of the ions and of flow: straight values, differences of values, the natural log of values, the difference of the natural log of values, and the natural log of the difference of

values. At this point, the different ‘views’ will simply be used; the way in which they operate will be considered at a later time. The analysis uses all available grab data over the whole time frame of the study.

When it is said that flow and amount are highly correlated to one another it is generally understood that the relation is between the ‘straight values’ of the two. It is easy to accept, further, that ‘corresponding views’ (i.e. the same ‘view’ of both analyzes e.g. ln (flow) and ln (amt)) should also correlate. The correlations that form a diagonal pattern between flow and Na amount (Table 46 below) are such ‘corresponding’ views. But Cl has high correlation for only a couple of the pairs, the others do not correlate in spite of being ‘corresponding views’. A correlation is attempting an intersection between two sets of chronological data and it is not always known how that connection is being made. About all that can be said is that flow at any given point is a product of multiple inputs each of which varies in time. Here the multiples of Cl amount appear to be less consistent, i.e. more variable, than, for example, those of Na.

relation flow and amount major ions - Gila at Safford(grabs)						
	flow	Δflow	ln(flow)	Δln(flow)	lnΔflow	
flow	1.00	0.58	0.65	0.33	0.33	
Δflow	0.58	1.00	0.27	0.54	0.55	
ln(flow)	0.65	0.27	1.00	0.53	0.47	
Δln(flow)	0.33	0.54	0.53	1.00	0.83	
lnΔflow	0.33	0.55	0.47	0.83	1.00	
Clmol	0.57	0.08	0.79	0.35	0.31	
ΔClmol	0.31	0.34	0.41	0.70	0.59	
lnClmol	0.44	0.10	0.87	0.44	0.32	
ΔlnClmol	0.22	0.28	0.48	0.85	0.60	
lnΔClmol	0.31	0.34	0.47	0.75	0.71	
Namol	0.87	0.31	0.83	0.37	0.35	
ΔNamol	0.55	0.78	0.44	0.78	0.72	
lnNamol	0.59	0.21	0.97	0.49	0.40	
ΔlnNamol	0.31	0.46	0.53	0.96	0.76	
lnΔNamol	0.37	0.56	0.50	0.86	0.90	
HCO3mol	0.97	0.47	0.73	0.36	0.35	
ΔHCO3mo	0.59	0.95	0.34	0.66	0.64	
lnHCO3mc	0.60	0.23	0.99	0.52	0.45	
ΔlnHCO3rr	0.29	0.46	0.53	0.99	0.80	
lnΔHCO3rr	0.34	0.62	0.41	0.85	0.96	
Camol	0.86	0.46	0.69	0.40	0.36	
ΔCamol	0.48	0.79	0.30	0.61	0.58	
lnCamol	0.64	0.26	0.98	0.53	0.45	
ΔlnCamol	0.33	0.52	0.52	0.97	0.80	
lnΔCamol	0.36	0.67	0.39	0.83	0.86	

Table 46 [\(back\)](#)

While there is no doubt ‘flow’ and ‘amount’ are strongly directly related, this closer look reveals that the different parameters vary in the closeness of the relation. All the ions show a diagonal pattern of ion analysis view with the ‘corresponding’ view of flow except Cl which is blocked to highlight the difference from the other ions. This disparity does not seem to be due to the overall variability of ion amounts (as opposed to the variability of individual inputs which may be off-setting or self-cancelling). As can be seen in the standard deviations and relative standard deviations over all dates below, Cl moles actually has by far the lowest relative standard deviation with an unexceptional standard deviation. Na, on the other hand, has by far the lowest standard deviation and a typical relative standard deviation.



variability MI amounts - Gila at Safford(grabs)			
	std	relstd	
Ca	2.3	1.7	
Mg	9	1.7	
Na	0.002	1.5	
Cl	13	0.5	
SO4	7	1.4	
HCO3	56	1.7	

Table 47

The diagonal patterns of Table 46 above are, of course, artifacts caused by the selection of row and column headers: any desired pattern could be achieved by rearranging columns and rows. But the corresponding views relation, which will not go away with different arrangements, is probably an indication of a strong relationship. This is particularly true if the corresponding views include high correlation between the straight values and/or differences and flow, the most basic signs of a strong relation.

relation flow and %amount major ions - Gila at Safford(grabs)							
	flow	$\Delta$ flow	ln(flow)	$\Delta$ ln(flow)	ln $\Delta$ flow		
flow	1.00	0.58	0.65	0.33	0.33		
$\Delta$ flow	0.58	1.00	0.27	0.54	0.55		
ln(flow)	0.65	0.27	1.00	0.53	0.47		
$\Delta$ ln(flow)	0.33	0.54	0.53	1.00	0.83		
ln $\Delta$ flow	0.33	0.55	0.47	0.83	1.00		
%Clmol	-0.61	-0.28	-0.91	-0.50	-0.51		
$\Delta$ %Clmol	-0.27	-0.49	-0.44	-0.88	-0.83		
ln%Clmol	-0.76	-0.41	-0.87	-0.49	-0.51		
$\Delta$ ln%Clmol	-0.38	-0.70	-0.38	-0.81	-0.79		
ln $\Delta$ %Clmol	-0.25	-0.45	-0.38	-0.80	-0.82		
%Namol	-0.66	-0.36	-0.87	-0.52	-0.53		
$\Delta$ %Namol	-0.30	-0.59	-0.37	-0.83	-0.79		
ln%Namol	-0.69	-0.41	-0.82	-0.51	-0.52		
$\Delta$ ln%Namol	-0.32	-0.64	-0.33	-0.76	-0.74		
ln $\Delta$ %Namol	-0.24	-0.53	-0.33	-0.80	-0.78		
%HCO3mc	0.50	0.15	0.87	0.44	0.43		
$\Delta$ %HCO3m	0.19	0.31	0.46	0.84	0.74		
ln%HCO3n	0.41	0.12	0.88	0.46	0.40		
$\Delta$ ln%HCO3	0.15	0.23	0.48	0.86	0.66		
ln $\Delta$ %HCO3	0.14	0.21	0.42	0.73	0.70		
%Camol	0.32	0.16	0.53	0.37	0.29		
$\Delta$ %Camol	0.15	0.25	0.25	0.51	0.42		
ln%Camol	0.42	0.16	0.73	0.41	0.34		
$\Delta$ ln%Camol	0.21	0.32	0.38	0.71	0.58		
ln $\Delta$ %Camol	0.01	0.19	0.08	0.37	0.20		

Table 48

In terms of % amount (the mole fraction, above), the major ions form a different pattern with respect to flow. Here all the views of all the ions, except Ca, are highly correlated only to those views of flow that use the natural log. There is also a sub-pattern with the straight value % and

natural log of % of the ions correlating with the natural log of flow while differences correlate with differences. This alternating line pattern is a different, looser ‘corresponding views’ pattern within the natural log area.

The difference of the logarithm and the logarithm of the difference are not the same thing, yielding different numeric results, but often have similar correlations. The situation of % amount correlating to the natural log of flow is judged to be a less direct correlation because it is assumed to be a correlation to a part of, not the whole flow. Only ln%mol of chloride correlates with flow as a whole. (The subject of the natural logarithm and underlying patterns will be worked out more explicitly in what follows)

The activities of Na & Cl (below left), but not Ca & HCO<sub>3</sub>, show the same high correlations with the natural log of flow as the % amounts. Taking the percent of the activities (below right), however, shows that Ca & HCO<sub>3</sub> also take part in the correlation to a pattern in the flow though to a lesser extent. Both activity, a relative amount, and % activity, a relative relative factor, correlate more like % amount than amount.

relation flow and activity major ions - Gila at Safford(grabs)						relation flow and %activity major ions - Gila at Safford(grabs)					
	flow	Δflow	ln(flow)	Δln(flow)	lnΔflow		flow	Δflow	ln(flow)	Δln(flow)	lnΔflow
Clact	-0.29	-0.09	-0.79	-0.44	-0.29	%Clact	-0.61	-0.28	-0.91	-0.50	-0.52
ΔClact	-0.09	-0.16	-0.40	-0.73	-0.43	Δ%Clact	-0.27	-0.50	-0.44	-0.88	-0.83
lnClact	-0.70	-0.34	-0.95	-0.52	-0.50	ln%Clact	-0.42	-0.76	-0.87	-0.50	-0.51
ΔlnClact	-0.35	-0.62	-0.47	-0.93	-0.84	Δln%Clact	-0.38	-0.71	-0.38	-0.81	-0.79
lnΔClact	-0.11	0.01	-0.21	0.06	0.05	lnΔ%Clact	-0.26	-0.46	-0.39	-0.81	-0.85
Naact	-0.31	-0.11	-0.79	-0.45	-0.29	%Naact	-0.66	-0.37	-0.86	-0.54	-0.54
ΔNaact	-0.10	-0.17	-0.40	-0.73	-0.43	Δ%Naact	-0.30	-0.59	-0.37	-0.84	-0.79
lnNaact	-0.66	-0.32	-0.96	-0.53	-0.50	ln%Naact	-0.70	-0.43	-0.81	-0.52	-0.52
ΔlnNaact	-0.31	-0.57	-0.47	-0.95	-0.84	Δln%Naact	-0.33	-0.66	-0.33	-0.77	-0.75
lnΔNaact	0.02	-0.01	0.00	0.06	0.02	lnΔ%Naact	-0.24	-0.53	-0.33	-0.80	-0.78
HCO <sub>3</sub> act	-0.53	-0.31	-0.43	-0.23	-0.24	%HCO <sub>3</sub> act	0.50	0.15	0.87	0.43	0.43
ΔHCO <sub>3</sub> act	-0.26	-0.49	-0.09	-0.29	-0.37	Δ%HCO <sub>3</sub> act	0.19	0.30	0.46	0.84	0.74
lnHCO <sub>3</sub> act	-0.58	-0.35	-0.45	-0.24	-0.26	ln%HCO <sub>3</sub> act	0.42	0.11	0.88	0.45	0.40
ΔlnHCO <sub>3</sub> act	-0.30	-0.56	-0.11	-0.31	-0.40	Δln%HCO <sub>3</sub> act	0.15	0.23	0.49	0.86	0.66
lnΔHCO <sub>3</sub> act	0.18	0.00	0.17	0.01	0.05	lnΔ%HCO <sub>3</sub> act	0.08	0.15	0.42	0.74	0.71
Caact	-0.38	-0.14	-0.70	-0.33	-0.29	%Caact	0.37	0.16	0.61	0.38	0.32
ΔCaact	-0.11	-0.21	-0.30	-0.55	-0.40	Δ%Caact	0.17	0.27	0.28	0.55	0.47
lnCaact	-0.55	-0.25	-0.80	-0.41	-0.40	ln%Caact	0.45	0.16	0.80	0.41	0.35
ΔlnCaact	-0.21	-0.40	-0.34	-0.68	-0.60	Δln%Caact	0.21	0.33	0.43	0.77	0.63
lnΔCaact	0.03	-0.03	0.01	0.04	0.02	lnΔ%Caact	0.00	0.14	0.06	0.28	0.10

Table 49

Table 50

Cl shows one high correlation to flow as a whole, ln%act Cl, analogous to ln%molCl for amount. So do the natural logs of the % amount and the % activity of Cl correlate with each other?

correlation Cl amt/act -Gila at Safford(grabs)		
	ln%Clamt	ln%Clact
ln%Clamt	1.00	1.00
ln%Clact	1.00	1.00

## Table 51

This example seems to show that two functions that correlate to another (flow), correlate to each other. But the correlation is a little too good: a correlation of 1.00 is always a little suspicious (except among the molar functions). Here particularly so since the original correlations of the two with flow are not perfect and are actually on the low side for ‘high’ correlations (-0.76). This result may just be an artifact of the analysis but it is one that has been seen before.

Early on, a large matrix of the fundamental quantities was created to show the expected high correlations between such related quantities as mass and amount. Such high correlations can be pointed to as trivial, or ‘merely’ mathematical. The same inter-correlation matrix of fundamental quantities can be produced using 1) inversion dates and 2) non-inversion dates only. Under inversion, not only are concentration and activity highly correlated to each other, as expected, but they are also highly correlated with the mole fraction whereas that is not the case with non-inversion. That means that, under inversion, the activities (i.e. concentrations) have among themselves the same interrelations as the individual ions. What that in turn means for system function is not clear and is left to stronger heads to determine. The opposite result, having the high correlation in non-inversion samples where Na+Cl is seemingly ‘dominating’ and the ‘norm’, would have fit preconceived notions of the situation better. Inversion is, after all, not the norm . . . is it?

Two factors in evaluating correlations are at play here. First, some correlations are more interesting than others because of the analyzes involved – finding a good correlation between mole fraction and activity seems important. Second, some correlations are more significant than others because of the nature of the relation. As a simple example, percentages are always highly correlated to each other – they have to be because raising the percentage of one item necessarily lowers the percentage of another or multiple others. The correlation is therefore considered trivial. But when values correlate with their percentages, it seems to be saying something about both the values and the percents – namely, that changes in the two are proportional which means that they relate as one ‘complete’ set to another.

It does not appear, no matter how meaningful the correlation may be, that if A correlates with B and B correlates with C, A will always necessarily correlate with C. The amount of sodium is highly correlated to flow (0.87) and to the amount of chloride (0.88) but the amount of chloride is not highly correlated to flow (0.57) except in the form  $\ln\%Cl$  amount. Whether chloride amount is highly correlated with flow, and whether the ABC relation holds, depends, it appears, on how strictly the corresponding views are stuck to.

Shifting attention to the group Na+Cl (below) reveals some new relations. (In the remainder of the study, Na and Cl are sometimes labeled as ‘NaCl’ or ‘Na&Cl’ but are operationally ‘Na+Cl’ or the sum of the two for whatever analysis quantity is being looked at) Most of the high correlations involve logarithms, differences of logarithm, and logarithms of differences as with Na & Cl ions. Below are the correlation coefficients for flow vs amount (top) and activity (bottom) of Na+Cl in the same five different views.

relation flow and amount/activity Na+Cl - Gila at Safford(grabs)						
	flow	Δflow	ln(flow)	Δln(flow)	lnΔflow	
amt Na+Cl	0.79	0.24	0.84	0.37	0.35	
Δ(amt Na+Cl)	0.49	0.65	0.45	0.78	0.71	
ln(amt Na+Cl)	0.55	0.18	0.94	0.48	0.38	
Δ(lnamt(Na+Cl))	0.29	0.42	0.52	0.93	0.71	
ln(Δ amt Na+Cl)	0.37	0.42	0.52	0.81	0.83	
actNa+Cl	-0.30	-0.10	-0.79	-0.45	-0.29	
Δ(actNa+Cl)	-0.10	-0.16	-0.40	-0.73	-0.43	
ln(actNa+Cl)	-0.68	-0.32	-0.96	-0.52	-0.50	
Δ(lnactNa+Cl)	-0.32	-0.58	-0.47	-0.94	-0.84	
ln(ΔactNa+Cl)	-0.25	-0.35	-0.48	-0.71	-0.76	

Table 52 ([back](#))

The high correlation of amount to flow of the group Na+Cl presumably comes from the same relation with amount Na not found with amount Cl. The relations between ln %amt and ln % act of Cl ion with flow are, if not lost, at least diminished (blocked below). It seems that if one parameter is correlated to flow and one isn't, the one that is brings some correlation to the group that contains both but it may be diminished in value. Blocked areas are where it might be expected, based on the ions, to find high correlations but where they are less than might be expected.

relation flow & %amount/activity Na+Cl - Gila at Safford(grabs)						
	flow	Δflow	ln(flow)	Δln(flow)	lnΔflow	
flow-grab/	1.00	0.58	0.65	0.33	0.33	
Δflo	0.58	1.00	0.27	0.54	0.55	
lnflo	0.65	0.27	1.00	0.53	0.47	
Δ(ln(flo))	0.33	0.54	0.53	1.00	0.83	
ln(Δ(flo))	0.33	0.55	0.47	0.83	1.00	
amt %Na+	-0.64	-0.31	-0.91	-0.52	-0.53	
Δ(amt %N)	-0.29	-0.54	-0.43	-0.88	-0.83	
ln(amt %N)	-0.72	-0.40	-0.86	-0.51	-0.52	
Δ(lnamt(%	-0.35	-0.66	-0.38	-0.82	-0.80	
ln(Δ amt %	-0.29	-0.50	-0.45	-0.85	-0.91	
act %Na+C	-0.64	-0.32	-0.91	-0.53	-0.53	
Δ(act %Na	-0.29	-0.55	-0.43	-0.89	-0.83	
ln(act %Na	-0.73	-0.41	-0.86	-0.52	-0.53	
Δ(lnact(%N	-0.35	-0.67	-0.38	-0.83	-0.80	
ln(Δ act %I	-0.26	-0.41	-0.43	-0.73	-0.86	

Table 53

Two sets of patterns for correlations with flow have thus far been found– the diagonal, corresponding views of amount which is considered a strong correlation and the natural log correlations of %amount and (%)activity with their own looser, corresponding views of ln and differences, which are considered more indirect and therefore possibly weaker correlations. The correlations with flow of the group Na+Cl seem to grow out of similar correlations of the individual ions, with some differences. There is both correlation to flow as a whole (Na & Na+Cl mols) but more correlations to underlying patterns in flow (ln).

Do the high correlations between flow and major ion amount/activity have anything to do with whether there is any relation to high autocorrelation? Autocorrelations of major ion amounts and activities will be run and then compared to high correlations to flow for the respective views. Below is the autocorrelation graph for the activity difference of Na+Cl and a table of %max/min at 6&12 mos. results for it and other views showing fairly high autocorrelation. (> 0.70).

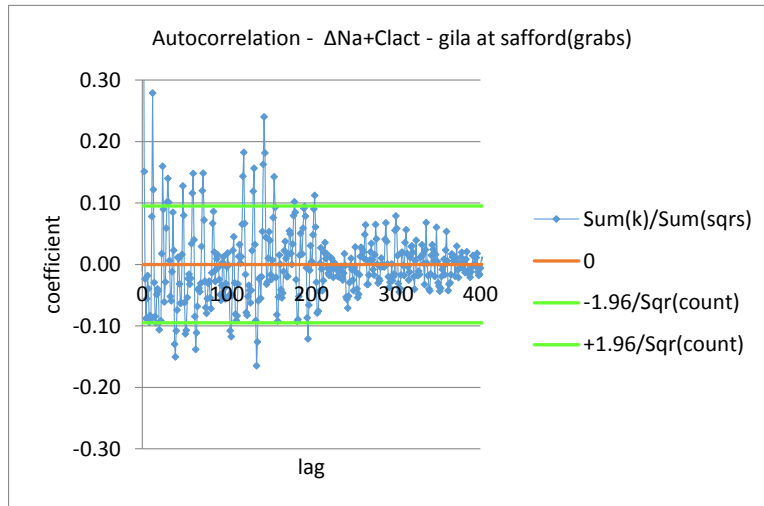


Figure 72

autocorrelations Na+Cl %6&12 mos peaks				
- Gila at Safford(grabs)				
		amount	activity	
values		$\Delta(\text{actNa+Cl})$		0.9143
		$\Delta(\text{lnactNa+Cl})$		0.8857
percents	$\Delta(\text{amt \%Na+Cl})$	0.8571	$\Delta(\text{act \%Na+Cl})$	0.8571
	$\ln(\Delta \text{ amt \%Na+C})$	0.8571	$\ln(\Delta \text{ act \%Na+Cl})$	0.7143
	$\Delta(\text{lnamt}(\%Na+Cl))$	0.7429	$\Delta(\text{lnact}(\%Na+Cl))$	0.7714

Table 54

The only high autocorrelations among the straight values are for activity and involve differences.  $\Delta(\text{act}(\text{Na+Cl}))$ , however, shows no high correlations with any view of flow, let alone with the corresponding view,  $\Delta(\text{flow})$  (Table 52 above). On the other hand,  $\Delta(\text{lnact}(\text{Na+Cl}))$  is highly correlated to both  $\Delta(\text{lnflow})$  and  $\ln(\Delta(\text{flow}))$ . The highest autocorrelation therefore shows no corresponding high correlation to flow while the next highest shows high correlations not only with the corresponding view but also with another, seemingly unrelated, view. If high activity autocorrelation does not come from high correlation with flow, where does it come from?

The %Na+Cl amount and activity autocorrelations are a notch lower than straight value autocorrelations but there seems to be the same 'related view' relationship to flow as seen with  $\Delta(\text{lnact}(\text{Na+Cl}))$ . The amounts correlations (Table 46) clearly show the 'block' of high inter-correlation between  $\Delta(\text{ln})$  and  $\ln(\Delta)$  for all the ions but Cl. The block is diminished in the percent

amounts for all but Cl, lost in the activities, but reappears for Na and Cl and Na + Cl in both % amount and % activity. The highest autocorrelation for ion activity has no corresponding view high correlation with flow, but lower autocorrelations have high correlations to two views of flow that are highly correlated to each other (0.83). The  $\Delta \ln$  and  $\ln \Delta$  block is, it seems, a nexus of high autocorrelation and high correlation to flow and it is significant that the two are the only views of flow that correlate with each other.

To avoid confusion between ‘high correlation’ (to flow for example) and ‘high autocorrelation’ (of amount or activity) one small change in terminology will be made. Rather than speaking of ‘high autocorrelation’, the terms ‘highly seasonal’ or ‘high seasonality’ will be used except where the autocorrelation calculation itself is being referred to. Confusion is less likely with ‘high correlation’ and ‘high seasonality’ since it is obvious that all parameters that are highly correlated to each other are not necessarily seasonal as well.

Using a group like Na+Cl may obscure things, so here is the seasonality of the different views of the major ions sorted from largest to smallest. Lines are used to (arbitrarily) divide high from low with ‘interesting’ seasonalities that are slightly lower blocked to complete the Na+Cl picture. Na & Cl, as expected, dominate all but amount. Note also that activity is unique in having the highest two seasonalities being simple differences while the highest % amt and %act are diff%Cl for both. Activity also has a large drop from high to low seasonality not seen in mols, %mols, or %activity which show very gradual decline.

autocorrelations major ions - Gila at Safford(grabs)							
mols	%mols	act	%act				
$\ln \Delta \text{Namol}$	0.89	$\Delta \% \text{Clmol}$	0.86	$\Delta \text{Naact}$	0.91	$\Delta \% \text{Clact}$	0.86
$\ln \Delta \text{HCO}_3\text{r}$	0.83	$\Delta \ln \% \text{Clmol}$	0.83	$\Delta \text{Clact}$	0.89	$\ln \Delta \% \text{Clact}$	0.86
$\ln \Delta \text{Camol}$	0.80	$\ln \Delta \% \text{Clmol}$	0.83	$\Delta \ln \text{Clact}$	0.89	$\Delta \ln \% \text{Clact}$	0.80
$\Delta \ln \text{HCO}_3\text{r}$	0.74	$\Delta \% \text{Namol}$	0.77	$\Delta \ln \text{Naact}$	0.86	$\Delta \% \text{Naact}$	0.77
$\Delta \ln \text{Namol}$	0.71	$\Delta \ln \% \text{HCO}_3$	0.77	$\Delta \ln \text{Caact}$	0.54	$\Delta \ln \% \text{Naact}$	0.74
$\Delta \ln \text{Camol}$	0.69	$\ln \Delta \% \text{HCO}_3$	0.77	$\text{Clact}$	0.49	$\Delta \% \text{HCO}_3\text{a}$	0.74
$\ln \Delta \text{Clmol}$	0.60	$\Delta \ln \% \text{Namc}$	0.69	$\Delta \text{Caact}$	0.49	$\Delta \ln \% \text{HCO}_3$	0.74
$\Delta \text{Namol}$	0.60	$\Delta \% \text{HCO}_3\text{r}$	0.69	$\text{Naact}$	0.46	$\ln \Delta \% \text{HCO}_3$	0.71
$\Delta \ln \text{Clmol}$	0.57	$\ln \Delta \% \text{Namc}$	0.66	$\Delta \ln \text{HCO}_3\text{a}$	0.46	$\ln \Delta \% \text{Naact}$	0.66
$\Delta \text{HCO}_3\text{mo}$	0.51	$\% \text{Clmol}$	0.46	$\ln \text{Naact}$	0.43	$\Delta \% \text{Caact}$	0.51
$\Delta \text{Camol}$	0.51	$\ln \% \text{Clmol}$	0.46	$\ln \text{Caact}$	0.43	$\% \text{Clact}$	0.49
$\Delta \text{Clmol}$	0.40	$\% \text{Namol}$	0.43	$\Delta \text{HCO}_3\text{act}$	0.40	$\ln \% \text{Clact}$	0.49
$\ln \text{Namol}$	0.37	$\Delta \% \text{Camol}$	0.43	$\text{Caact}$	0.40	$\Delta \ln \% \text{Caact}$	0.49
$\text{Namol}$	0.34	$\ln \% \text{Namol}$	0.40	$\ln \text{Clact}$	0.37	$\% \text{Naact}$	0.43
$\ln \text{HCO}_3\text{mc}$	0.34	$\Delta \ln \% \text{Camc}$	0.40	$\ln \text{HCO}_3\text{act}$	0.31	$\ln \% \text{Naact}$	0.43

Table 55

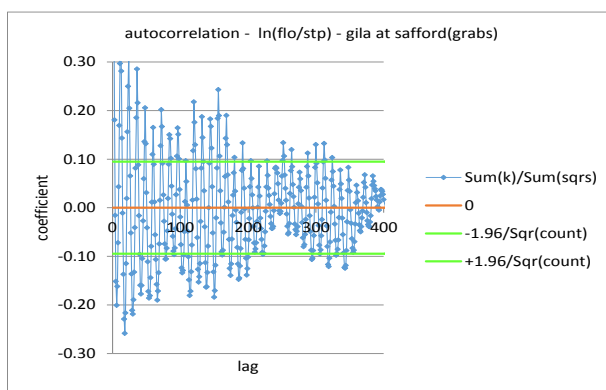
The seasonality of the Na+Cl group seems to grow out of similar seasonality of the ions but viewing those does not clear up any of the questions on the relation between correlation to flow and seasonality. There is, however, one ‘view,’ the natural log, which has a meaning that it may be possible to exploit to get more information.

Finding high correlations with logarithms has been said to be finding an ‘underlying’ pattern. In other words, the mole fraction is not directly related to flow or change in flow but rather to a distinct subordinate pattern within the flow (a flow within a flow). The idea of functions within

functions is due to Fourier who found that a sine wave is made up of a combination of ‘inner’ sine waves. A logarithm, by analogy, is a simple de-convolution of patterns of multiples.

Since the natural log of day mean flows is highly seasonal (0.89) but the natural log of grab flows is not (0.37), there must be an underlying pattern in the day means not present in the grabs. It is natural to wonder if data could not be added to create such a pattern in the grabs. Assume constant flow, say 1000 cfs (autocorrelation = 0), on the grab sample dates, add the seasonal test pattern (stp) values, and take the log (ln(1000+stp)): the result is a high autocorrelation, 0.86, with a damped oscillator pattern as expected. But a similar procedure, adding stp directly to the grab sample flows (grbflo+stp), yields only low autocorrelation, the weak signal of the added flow (stp=0 to 6) is lost due to the higher magnitude and variability of the grab flow.

If the seasonal test pattern is modified slightly by changing 0 to 0.01 (which does not change the autocorrelation result but does avoid problems with the log), then the log taken and divided by the grab flow, the resulting function also shows high seasonality (%6&12peaks = 0.94) (below left). Shown to the left below are the stp pattern and, to the right below, the ‘underlying’ pattern flows for 1977, which brings out an interesting aspect of the natural log.



ln(flo/stp) 0.9429 0.7746 0.5961 428

Figure 73

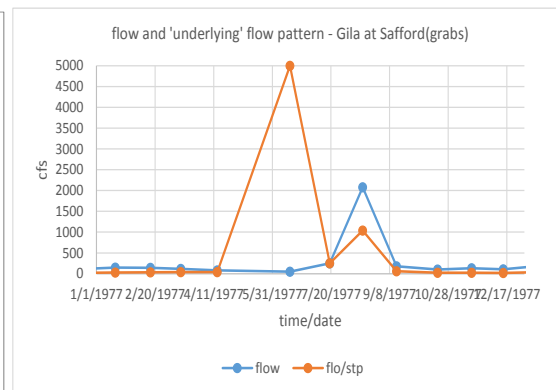


Figure 74

The fact that the ‘underlying’ flow can be greater than the receiving flow is one of those distressing aspects of the use of logs. Mathematically it is just the result of dividing the flow by a number smaller than one. But it suggests that high autocorrelation using logs may mean two different things. While ln(grbflo+stp) does not yield high autocorrelation, multiplying the seasonal test pattern by 1000 does (ln(grbflo+stp)\*1000). But comparing the original receiving flow with the new shows that the latter is not revealing an ‘underlying’ pattern at all but rather imposing a new pattern by a huge influx of new flow. It is still necessary to look at the magnitude of receiving and incoming flows to know whether the high autocorrelation of a log function is picking up an underlying or an imposed pattern.

A more direct approach with a better chance of finding ‘underlying patterns’ would be to examine the natural log of the daily mean flows of a tributary of the Gila. The USGS daily mean flows from the San Francisco at Clifton were downloaded from the internet, some 36000 values

from 1911 to the present with gaps. Average flow on the San Francisco is, over the period of record, about 209 cfs or less than half that of the Gila. Daily mean flows on the San Francisco, with a min of 1 and a max of 4680, are at times greater than those of the Gila but only about 0.65% of the time. It was hoped that the straight flow values would show high seasonality but they do not. The natural log of the flow, however, does show high seasonality (0.97) suggesting that the underlying pattern in the Gila may be coming from an underlying pattern in the San Francisco.

Is the pattern found in the San Francisco the same as that found in the Gila? The answer brings out some of the factors involved in autocorrelation analysis and a finding of ‘highly seasonal’. A first run of Inflow of the Gila day means (seasonality 0.89) with Inflow of the San Francisco day means (0.97) using all available data for both has a correlation of only 0.62. What is being done here is the autocorrelation output of coefficient vs lag time of the two runs are being correlated to each other.

Sometimes removing long data gaps from data to be autocorrelated improves the results so this was done for the San Francisco data. It did not change the San Francisco autocorrelation much (0.96) and only improved the correlation with the Gila values (no data gaps) slightly (0.66). The graph below shows the results of the first run attempt to correlate autocorrelations with different time frames (0.66).

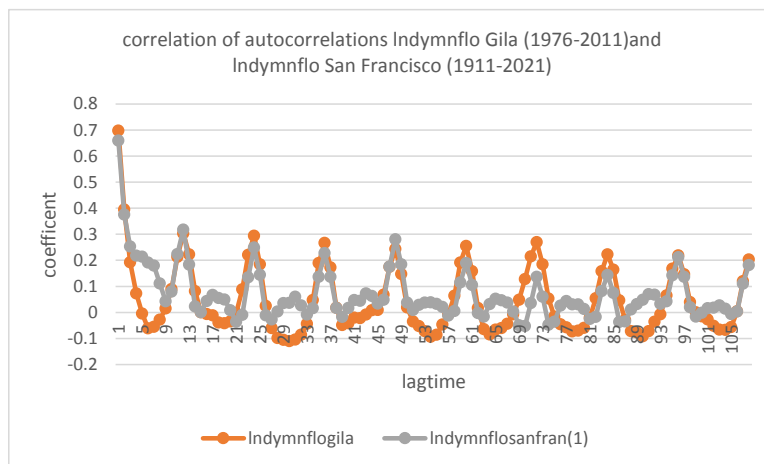


Figure 75

What did greatly improve the correlation was to make the time frames involved the same for both – 1/1/1976 to 12/31/2011. Now the correlation between the two is 0.93 but the seasonality of the San Francisco data drops to 0.84, presumably due to lower number of input data points compared to the full time frame. When the time frames are the same, the two sets of data plot on top of one another (below). Comparing the above graph with that below brings out the fact that, if the time frames are the same, high correlation results are a matter of lining up two consistent patterns with each other and all high autocorrelations are the same pattern.



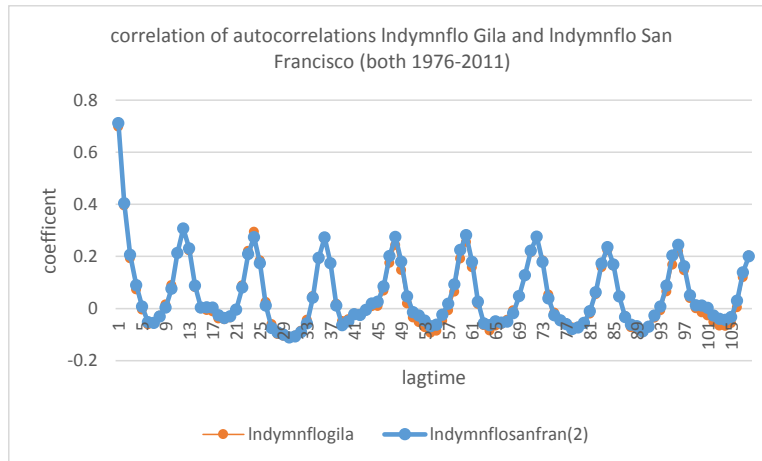


Figure 76

Theoretically, it should be possible to track down an underlying pattern to a seasonal source – i.e. one in which flow itself, rather than the log of flow, would be highly seasonal. Discharge values for Clifton Hot Springs, however, were not found. Hem calculates an average flow of 2.5 second-feet with supposedly ‘little variation’ but no daily statistics are available<sup>1</sup>. The magnitude of incoming flow compared to the receiving (San Francisco then Gila) is small but the concentrations are undoubtedly high which may explain why seasonality may be easier to pick up with activity than flow. It may be a result of differing sensitivity of two analyzes, chemistry results and flow measurements.

As mentioned earlier,  $\ln(\text{flow})$  of the Gila grabs has a seasonality of 0.4 while  $\ln(\text{flow})$  of the Gila daily means has a seasonality of 0.9. There are no time frame issues here since the time frames of the two are the same, 1976-2011. If the two sets of autocorrelations run ‘as is’ are correlated the result is a correlation of only 0.65. If the day means are run with day mean values on grab sample dates only, the correlation with the grab samples is 0.98 – but the seasonality of the day means drops to 0.34, about the same as the grabs. The daily mean values on grab sample dates only do not have any higher seasonality than the grab values. The two low seasonality results are, however, highly correlated to each other and the pattern is the same. The graphs below show the low correlation of a high and a low autocorrelation (left) and the high correlation of two low autocorrelations (right). Note that the low autocorrelation,  $\ln(\text{grbflo})$ , actually follows the pattern as the high,  $\ln(\text{dymnflo})$ , but the signal is not as strong, there is less amplitude.

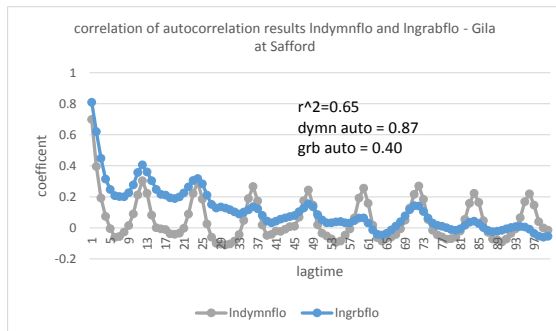


Figure 77

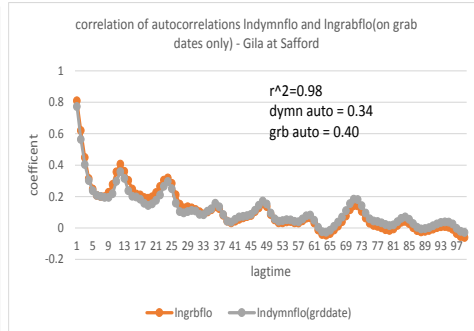


Figure 78

This example is important because it shows that the grab and day mean flows, relatively highly correlated to each other (~0.73) and with the same time frame, can still have quite different seasonality. The two sets of data above have about the same number of counts after processing (427 & 462) so it must be the total number of data points before processing that makes the difference (dymns 13149, grabs 161). Only full sets of data like the USGS daily means, covering at least about ten years, should be used for autocorrelations. Smaller sets like ADEQ grabs, even if highly correlated to the larger set, are likely to miss the pattern altogether or have it turn up in another view (grab Indiff = .80, grab diffln = .83).

Another way of looking for ‘underlying patterns’ would be to break down the daily means into components and see if any patterns can be picked up among them. Day of year curves for minimums, averages, and maximums of the daily mean flows were constructed and autocorrelations were run with the five views used above. The day of year curves adamantly refused to produce any high autocorrelations – most produced %min/max at 6-12 values of 0, occasionally a 0.33 or a 0.66. This result is particularly disheartening since the minimums curve was used in the low flow analysis. These results suggest it is a very artificial construct with little connection to real world flow. It is depressing to find no seasonality in a curve that was supposedly a general pattern in flow!

Now it is quite possible that these autocorrelation numbers are being looked at a little too closely, Two factors, data gaps and changes in value, were originally shown to be involved and now two others, time frame issues and original sample counts, also seem involved. Autocorrelations, as done here, are only good for distinguishing ‘high’ from ‘low’ seasonality not for quantification. The fact that the highest autocorrelation of ion activities (0.91) is considerably higher than the highest flow autocorrelation (lnΔabsflow-0.83 for grabs) is not, therefore, really an issue – they’re both just ‘high.’

About all that can be said at this point is that flow and ion amount/activity show some high correlations and ion amounts/activities show high seasonality in certain views but usually not those which are highly correlated to flow. There seems to be no rhyme or reason as to which views correlate with flow and/or which are highly seasonal.

Two ‘rules’ will be used in an attempt to salvage the situation. 1) All high autocorrelations are the same – there is only one seasonal pattern and the only difference is how completely it is

expressed which is a matter of amplitude not pattern. Flow and ion amount/activities both show high seasonality in some views and not others and correlations of corresponding view autocorrelations are usually low except within the related view 'block' ( $\Delta \ln$  and  $\ln \Delta$ ). 2) All views are therefore considered the same – if any view has high autocorrelation then the parameter as a whole has a seasonal pattern. These 'rules' open up the possibility of (arbitrary) mixing and matching rather than being limited to 'corresponding' views.

Since all autocorrelations are the same pattern, any parameters that show high seasonality must, in some sense, be correlated to each other. This argument is simply an 'end-run' around the problem. It is loosely based on the success in forcing different views of flow or different flows to correlate with each other - maybe the same thing would be possible for ion activities and flows. Below are four graphs that relate grab flow to grab Na autocorrelations showing the first 100 lag times. The first two insist on 'corresponding' views using the highest autocorrelation for Na activity (left) and flow (right) with the corresponding view for the other. The results are, as expected, visibly low correlation between the two autocorrelation runs.

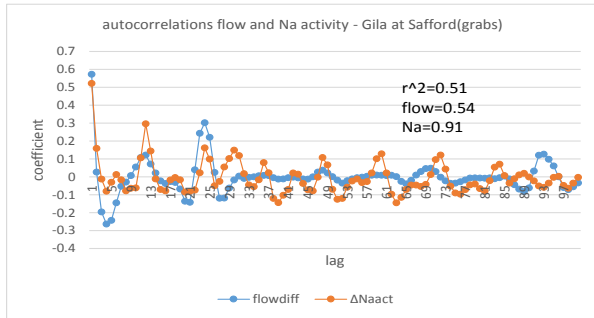


Figure 79

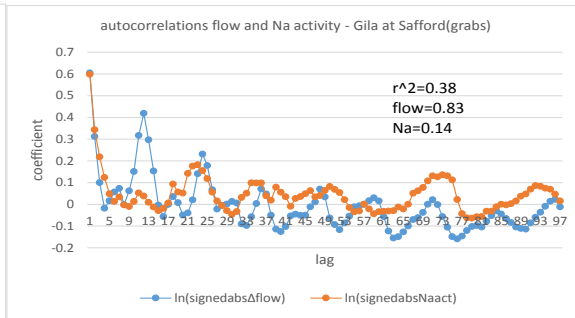


Figure 80

The next graphs use 1) the highest autocorrelations of both regardless of view and 2) the highest view autocorrelations that use diffln or Indiff. Picking a lower autocorrelation view for Na, one that is somewhat more related to the view of flow in that both use differences and the natural log, at last leads to the desired result – both ion activity and flow are, in these views, highly seasonal and highly correlated to one another. While the preferred 'corresponding' views' analysis does not work with just any autocorrelations, there is an indication that correspondence of some sort is still a factor of importance in making the connection between high correlation to flow and high seasonality.

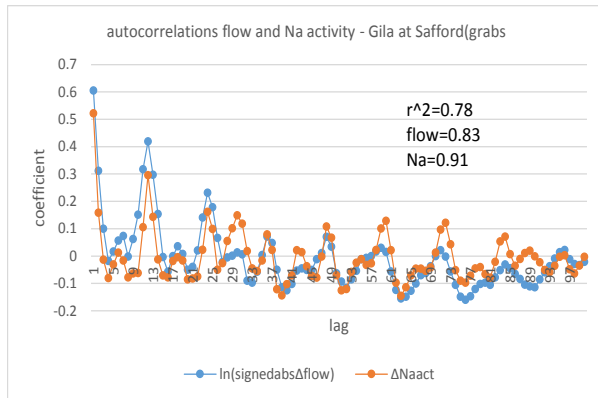


Figure 81

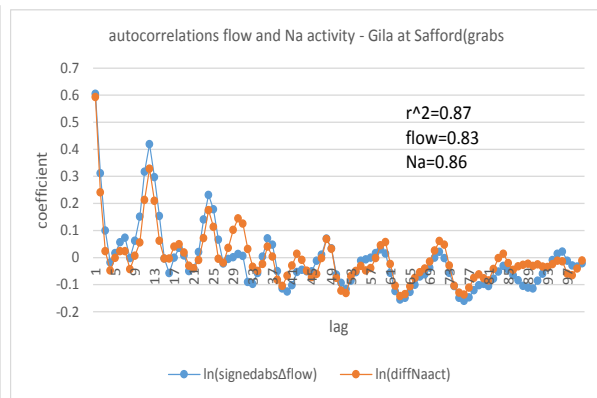


Figure 82

Note that these comparisons were done with Na, the ion that most closely follows flow: similar results would not be expected with Cl given previous results. It is, however, always a good idea to run things even if the outcome is ‘known.’ Running the analysis of the graph to the left above for Cl yields an  $r^2$  of 0.71, slightly lower than with Na at .78, while with the analysis of the graph on the right the result for Cl is 0.77, considerable lower than Na at 0.87 but still in the ‘middling high’ range. None of these values, however, come close to the correlation of the Na with the Cl autocorrelation data which is 0.97.

But the burning question is, will inversion present with a seasonal pattern as well? The correlations of the inversion test parameters with flow do not look very promising – there is only one high correlation with activity and five with amount forming a diagonal with the ‘corresponding’ view of flow (see below). If high seasonality is a result of high correlation with flow, the inversion parameter should not show high seasonality. The percents, however, do show the same relation of log to log as seen above.

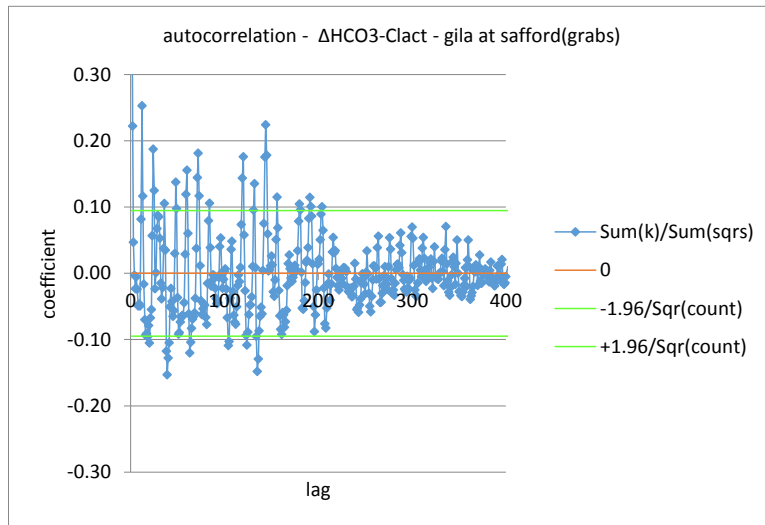
relation flow & inversion test parameter - Gila at Safford(grabs)						
	flow	Δflow	ln(flow)	Δln(flow)	lnΔflow	
amt HCO <sub>3</sub> -Cl	0.98	0.53	0.64	0.32	0.32	
Δ(amt HCO <sub>3</sub> -Cl)	0.57	0.97	0.27	0.55	0.56	
ln(amt HCO <sub>3</sub> -Cl)	0.62	0.27	0.79	0.41	0.45	
Δ(lnamt(HCO <sub>3</sub> -Cl))	0.27	0.48	0.35	0.71	0.73	
ln(Δ amt HCO <sub>3</sub> -Cl)	0.34	0.63	0.28	0.65	0.78	
HCO <sub>3</sub> -Clact	0.24	0.06	0.75	0.42	0.27	
ΔHCO <sub>3</sub> -Clact	0.07	0.11	0.39	0.70	0.39	
lnHCO <sub>3</sub> -Clact	-0.42	-0.15	-0.66	-0.35	-0.38	
ΔlnHCO <sub>3</sub> -Clact	-0.16	-0.26	-0.30	-0.56	-0.59	
lnΔHCO <sub>3</sub> -Clact	-0.05	-0.07	-0.28	-0.51	-0.57	

Table 56

relation flow & %inversion test parameter - Gila at Safford(grabs)						
	flow	Δflow	ln(flow)	Δln(flow)	lnΔflow	
amt %(HCO3-Cl)	0.58	0.23	0.92	0.48	0.49	
Δ(amt %(HCO3-Cl))	0.25	0.42	0.47	0.89	0.82	
ln(amt %(HCO3-Cl))	0.53	0.21	0.86	0.46	0.48	
Δ(lnamt %(HCO3-Cl))	0.21	0.38	0.40	0.80	0.77	
ln(Δ amt %(HCO3-Cl))	0.25	0.42	0.45	0.84	0.89	
%HCO3-Clact	0.58	0.22	0.92	0.48	0.49	
Δ%HCO3-Clact	0.24	0.42	0.47	0.89	0.82	
ln%HCO3-Clact	0.54	0.21	0.87	0.46	0.49	
Δln%HCO3-Clact	0.21	0.37	0.40	0.81	0.77	
lnΔ%HCO3-Clact	0.25	0.42	0.45	0.84	0.89	

Table 57

Given the discussion to this point, however, it should not come as a surprise to see that high seasonality results for the inversion parameter, HCO3-Cl, over different analyzes can be achieved (with some finagling). The high correlation with flow for amounts do not turn into high seasonality of amount – just the opposite. But various views of activity do show high seasonality. The autocorrelation graph for difference in activity (HCO3-Cl) and the %6&12mos peak results are shown below.



parameter %max/min %max/min sumxmy2/ count(pts  
diff(act HC 0.8857 0.4930 0.8372 427

Figure 83

autocorrelations HCO <sub>3</sub> -Cl %6&12 mos peaks - Gila at Safford(grabs)			
	amount		activity
values		$\Delta(\text{actHCO}_3\text{-Cl})$	0.8857
percents		$\Delta(\text{act \%HCO}_3\text{-Cl})$	0.8571
		$\ln(\Delta \text{ act \%HCO}_3\text{-Cl})$	0.8857
		$\Delta(\ln\text{act}(\%\text{HCO}_3\text{-Cl}))$	0.8857

Table 58

Note that simple differences of values, not high in the original Na + Cl correlations with flow, have come back as very high seasonality, in fact higher than the highest grab flow autocorrelation ( $\ln(\text{absdiff flow}, 0.83)$ ).

Can the inversion activity high seasonality be forced into high correlation with flow as was done with sodium activity? Skipping the testing and using the lessons learned above, shows that the percent inversion test parameter is highly correlated to the corresponding view of grab flow. (These use the signed natural logs of abs differences (i.e. if the difference is negative, use  $-\ln(\text{abs}(\text{diff}))$  otherwise  $\ln(\text{diff})$ ).

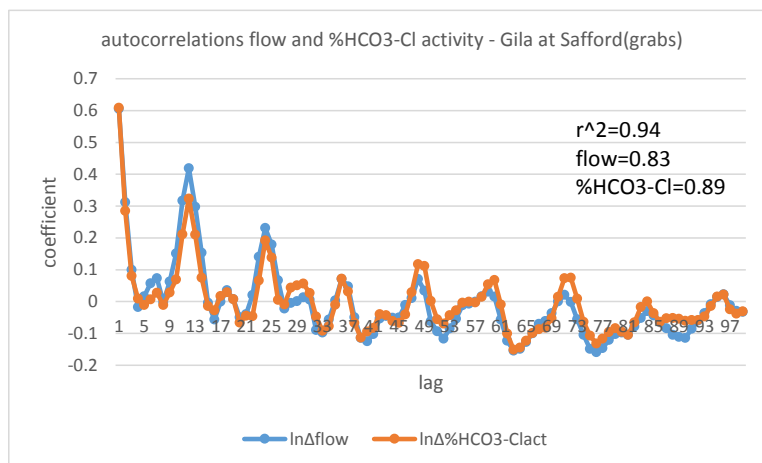


Figure 84

If two parameters, one of which is flow, are highly seasonal in any view, then two views can be found that are highly correlated to each other and these may or may not be a ‘corresponding’ views. The initial argument that was attempted is rather turned on its head. Run backwards, the argument is: if a view of Na+Cl correlates with flow and a view of HCO<sub>3</sub>-Cl correlates with flow, the two should correlate with each other since both are highly seasonal. The result should

not come as a surprise since the inversion has been presented from the beginning as the response to the drop in Na+Cl activity.

relation flow & %inversion - Gila at Safford(grabs)					
	flow	Δflow	ln(flow)	Δln(flow)	lnΔflow
flow	1.00	0.58	0.65	0.33	0.33
Δflow	0.58	1.00	0.27	0.54	0.55
ln(flow)	0.65	0.27	1.00	0.53	0.47
Δln(flow)	0.33	0.54	0.53	1.00	0.83
lnΔflow	0.33	0.55	0.47	0.83	1.00
ΔlnNa+Clact	-0.32	-0.58	-0.47	-0.94	-0.84
Δln%HCO3-Clact	0.21	0.37	0.40	0.81	0.77

Table 59

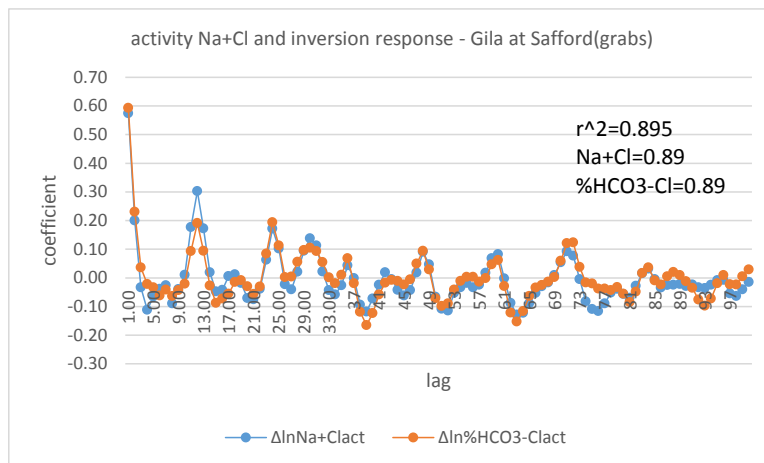


Figure 85

This picture of two surrogates for flow reveals the ‘underlying pattern’ first seen in the autocorrelation of the logarithm of the daily mean flows. Relatively high flows occur every year though they are not visible in the analysis before this point due to the low sensitivity of the flow analysis used (one year x-scale, 0 to 2000 cfs y-scale). The high elevation precipitation regime has some possibility of occurring in any year and competes with the high drainage area evaporation regime in every year as well as across different years.

There are a couple factors of interest to be noted here. The first is that, while amount may be useful in unraveling problems in the flow-concentration correlation analysis, it is activity (a kind of ‘corrected’ concentration) that is come back to in the final picture. The second is that, while

the discovery of a more explicit flow pattern was what was being sought for, flow effectively drops out of the picture in the correlation of autocorrelations method.

Inversion itself seems, therefore, to be a seasonal phenomenon. That is to say that autocorrelations and views have been mixed and matched, in an appropriate time frame, to yield (fairly) high autocorrelations that correlate with a view of flow and with each other. It is now possible to say: ‘inversion is a seasonal phenomenon more or less related to seasonal flow patterns’ and leave it at that. This statement could, of course, have been made on a hunch at the onset of this study. But at least some ‘steps’ and ‘guidelines’ for coming to that conclusion that can be tested and evaluated for soundness have been presented.

Finding the patterns of activity change for the inversion means that a shift from looking for context for inversion to looking for patterns within the inversion response itself is now possible. Having found what was being looked for, it is tempting to just ‘go on’ to other topics. But the difficulties and finagling required show that autocorrelation analysis, at least as done here, has some issues and it is best to lay them out fully. While the exercise will, in general, only throw more doubt on the previous analysis, there is some very interesting information found along the way.

Autocorrelations were done on three sites on the Colorado River using USGS daily mean stream flows. The sites are, from north to south, Lee’s Ferry, Parker Dam, and Morelas Dam. The %min/max 6&12 values are first given for these sites in the all available data time frame, which is a different time span for each site.

autocorrelations - colorado river sites		
		alldata %6&12
N	leesferrydymn	0.80
↓	leesferryIndymn	0.78
	parkerdymn	0.39
	parkerIndymn	0.67
↓	morelasdymn	0.37
S	morelasIndymn	0.72

Table 60

Lee’s Ferry is clearly much more seasonal than either Parker or Morelas with the latter two becoming considerably more but not highly seasonal when the natural log is taken. Note also that the Lee’s Ferry straight value stream flows are actually a little more seasonal than the log flows making this apparently something of a ‘seasonal source’ flow (though that may be reading these numbers too closely). These findings make sense because not only is Lee’s Ferry much further north, where seasonal effects are more pronounced, than the other two, it is also closer to the source and further from the closest upstream dam (Glen Canyon, start date 1965) than they are.

The three sets of autocorrelations cannot be compared to each other, however, because they have different time frames. The same three sites were therefore autocorrelated in a common time frame, the study time-frame 1/1/1976 – 12/31/2011.



autocorrelations - colorado river sites		
1976-2011		
N	leesferryd	0.50
↓	leesferryln	0.68
	parkerdym	0.87
	parkerlndy	0.89
	morelasdy	0.17
S	morelasln	0.50

Table 61

Seasonality in this time frame goes down from the all-data situation for Lees Ferry and Morelas but up for Parker. If these numbers are to be believed, there are seasonal flows at Parker which seems highly unlikely. The USGS site at Parker is directly below the dam and stream flow can be assumed to be regulated following a water demand/usage schedule not a seasonal pattern.

To investigate further, a second autocorrelation program was written, called autocorrelation(2). Unlike the first program, this one has no coding to first resolve all data into monthly averages and/or cover data gaps. Instead the program does the sum of the squares analysis on daily data first and then locates peaks wherever they may be, calculating days between. It was tested with numeric test patterns for weekly, biweekly, and monthly daily data and passed all tests and was able to find the correct days between peaks for each.

Using the old and new autocorrelation programs to examine various time frames within the 1976-2011 span used above, however, only adds to the headaches involved with autocorrelation. The apparent high autocorrelation at Parker over the period 1976-2011 does not 'grow out' of any periods of high autocorrelation.

results auto(1) & (2) runs colorado at parker dymn flows 1976-2011		
	auto(1)	auto(2)
1976	0.000	13.1
1977	0.000	8.6
1978	0.000	12.5
1979	0.000	16.8
1980	0.000	32.1
1981-85	0.000	27.8
1986-90	0.143	6.9
1991-95	0.571	7.9
1996-2000	0.000	20.8
2001-05	0.429	14.6
2001	0.000	10.0
2002	0.000	11.6
2003	0.000	12.4
2004	0.000	9.0
2005	0.667	10.2
2006-10	0.429	16.6
average		14.4

Table 62

How then, can a high seasonality result for a certain time span develop? Shown below is a different type of autocorrelation(2) result for daily mean flows at Parker from 1976-2011.

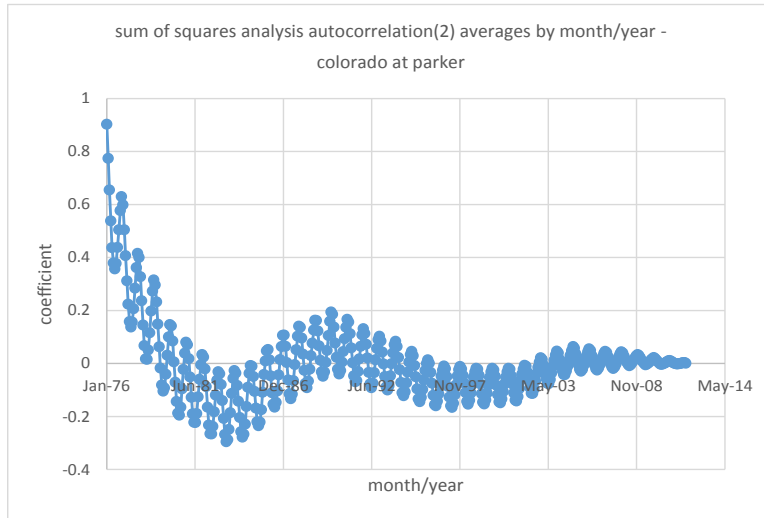


Figure 86

What has been done in the above graph is that the original run (daily) sum of the squares result from the autocorrelation(2) run has been averaged by month and displayed by month/year (rather than lag time). The peaks on the graph are one year apart but there is another curve as well. This inner curve can be seen in the original (not averaged by month) autocorrelation2 run of the same data showing, to the right, only the first 100 lag times.

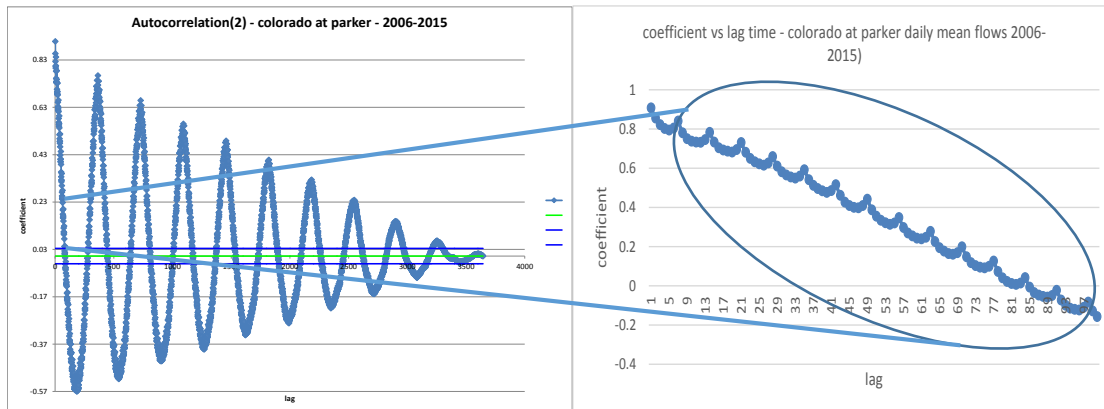


Figure 87

Figure 88

A manual evaluation of the peaks in the month averaged autocorrelation(2) run shows that there were 36 valleys and 36 peaks but not all valleys were Jun or peaks in Dec. The actual percent peaks at 6 & 12 was 0.85 or a fairly high autocorrelation1 result. What this finding seems to be saying is the autocorrelation(1) program may mistake a weekly for a monthly pattern and that may be the case for biweekly or other patterns. In certain time frames, it may be that peaks from one pattern line up perfectly with monthly peaks to give a false positive for seasonality.

Repeating autocorrelation 1 & 2 runs for all dates reveals a very reproducible average days apart for flow peaks of seven (below) which is half of the far more variable 1976-2011 yearly averages of about 14 (above). The time frame therefore has a major effect on auto(2) results as well as auto(1). Water usage changes with some variability from year to year but may average out to a quite different number over longer time spans.

autocorrelation(1&2) results - %6/12 - colorado at parker			
auto(1)		auto(1)	
same start date 1/1/1935		same end date 12/31/15	
(35-45)	0.08	(36-15)	0.43
(35-55)	0.09	(46-15)	0.69
(35-65)	0.21	(56-15)	0.98
(35-75)	0.37	(66-15)	0.96
(35-85)	0.42	(76-15)	0.81
(35-95)	0.39	(86-15)	0.88
(35-05)	0.39	(96-15)	0.86
(35-15)	0.39	(06-15)	0.58
auto(1) reruns		auto(2)	days apart
(36-15)		(36-15)	6.5
(46-15)		(46-15)	7.0
(56-15)	0.91	(56-15)	7.3
(66-15)	0.88	(66-15)	7.0
(76-15)	0.81	(76-15)	7.1
(86-15)	0.88	(86-15)	6.8
(96-15)	0.86	(96-15)	6.5
(06-15)		(06-15)	6.9

Table 63

It might be expected that the above mentioned lining up of patterns would be more prevalent for shorter time spans but this supposition does not hold up. In fact, shorter time frames of known high autocorrelation patterns in a longer time frame do not autocorrelate highly. A year run of daily mean density on the Gila at Safford shows, of course, no autocorrelation because the comparison is over a number of years, the more the better. A five year run of the same data shows a perfect damped oscillator pattern but a %6-12 value of only 0.62. Subsets of high seasonality do not necessarily have high seasonality themselves. It seems likely that the overall time frame, particularly the end date, and its relation to the peak to peak time spans (7 & 30) is probably what is responsible for the false positive problem (blocked above). But attempts to 'fool' the autocorrelation(1) program with all possible permutations of numeric 7 or 14 day test patterns failed.

The seasonal autocorrelation(1) program passed a seasonal test pattern test and correctly identified a highly seasonal parameter, density. It is, however, subject to both false negative and false positive results. The false negative is less of a concern and easier to explain – it's probably just due to lack of data. False positives are less easy to explain and much more troublesome to deal with. About all that can be done, as with any analysis or instrument that sometimes produces erratic results, is to rerun 'suspicious' looking runs until results begin to find some average value. False positives are just a random event in the analysis and will either go away with repetition, if a procedural error, or need to be tested by similar time frame runs or outside information.

After all these 'discouraging' words, it may seem presumptuous and/or foolhardy to proceed further with the results of autocorrelation analysis. The following case, however, is different because there is supporting evidence which is, in itself, very interesting. If the Lee's Ferry data is divided into two (large) parts and each autocorrelated separately the results are startling.

autocorrelation1 - lee's ferry		
	1926-60	1960-2011
leesferrydymn	0.93	0.16
leesferryIndymn	0.93	0.18

Table 64

The fact that Lee's Ferry showed highly seasonality before extensive dam construction in the 1960s (Glenn Canyon 1965) and less afterwards is mirrored in water quality Piper Plots. <sup>9</sup> In the diagram to left below, 1926-1965, the change in seasons can be seen, appropriately enough, in the changing colors (spring-green, summer-yellow, fall-red, winter-blue) spread across the diagram while in the diagram to the right, 1966-2008, all the seasons plot on top of one another in tightly clustered groups.

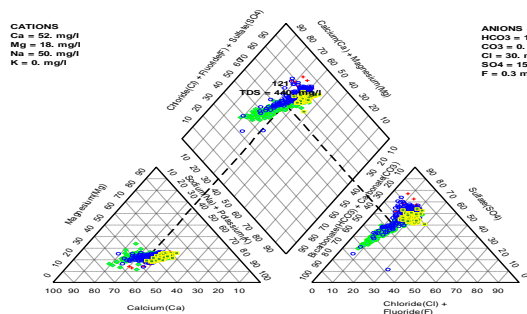


Figure 89

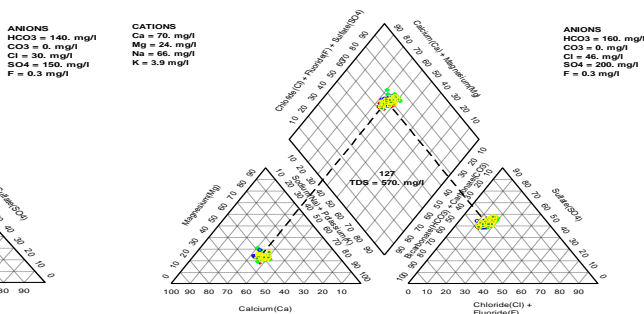


Figure 90

This view of a site along the Colorado just begs for a comparison with the Gila whose Piper Plot, seen below, can be evaluated for signs of seasonality.

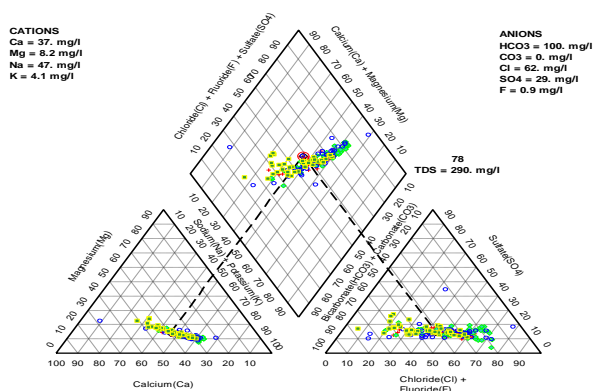


Figure 91 (back)

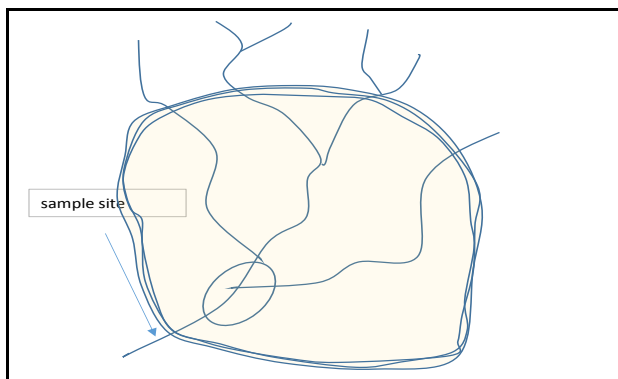
At first glance the plot shows summer plotting on top of the other seasons as in the low seasonality Lee's Ferry plot. But note that the spread is wider for the groups on each plot, an indication of changing water quality not seen in the Lee's Ferry 1960-2008 plot. The various seasons are visible as patches of different color but the patches are not as

distinct from each other as those at Lee's Ferry 1926 to 1965. Water quality is variable in each season but the overall spread of values is not as great. The Gila is quite a bit further south than Lee's Ferry so signs of the season are not as pronounced.

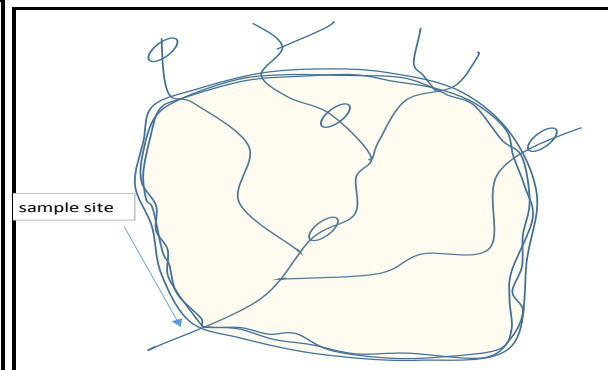
While the foundation, the relation of seasonality and high correlation to flow, is not as strong as might be wished, it is always possible, if dangerous, to run with what has been found. After indulging in some speculation on the wider implications of finding seasonality in major ion activities, the inversion process itself will finally be investigated.

To this point, 'presence' has been primarily understood as an analytical problem largely when it presents (sic) in the form of 'non-presence'. The wider implication of the results above, however, is that 'presence' has a pattern, at least in the case of the major ions. The wet seasons vary from year to year in start and end dates, intensity of precipitation, and areas affected. But over the course of many years, certain days of the year, intensities, and areas affected will begin to form an average. The sources of new material will also change from year to year. But over the course of many years, ephemeral sources (e.g. small slag piles) will disappear while the large area, higher concentration sources (i.e. vast salt beds) will begin to predominate.

Some of the major factors involved in the pattern of 'presence' are illustrated in the schematics below. The two charts show two extreme situations with location of sampling site and point sources (ovals) as well as 3 years 'wet' rings for the hypothetical watershed, i.e. the area affected by precipitation. One, to the left, is presumably what the Na & Cl case looks like – a large area, high concentration source close to the sampling site. The other, to the right, might be more representative of a parameter such as a trace metal – smaller sources scattered over a large area, some further from the sampling site than others, some within the wet ring only in extremely high precipitation years.



Schematic 3



Schematic 4

While there may be an underlying pattern to flow over long periods of time, it is not to be found by looking directly at flow itself. It is found, instead, by looking at amounts, concentrations, or activities. Secondly, if there is a pattern to Na or Cl presence there is, in theory at least, a pattern for the presence of every other parameter whether or not it can actually be seen. With a robust enough algorithm relating flow to source concentrations, it should be possible to determine

sample concentrations from flow values alone. But the algorithm involved would be very complex and require an almost infinite amount of information. The more information an algorithm requires, the less advantage it has over simple manual tabulation. In the real world, ‘presence’ for most parameters remains a problem.

Just as on a typical July day in Arizona the whole landscape seems to lie shimmering and simmering in the summer sun, so the entire earth can be envisioned as a conglomerate of pulsating objects in constant motion. From the light, flighty patterns of breezes to the ponderous, millennium-long movement of continents, amounts of material are constantly being transported from place to place. The process is ultimately fueled by heat input from the sun which engenders responses in and on the earth. Heat input and pressure have no direct effect on amount though they may change form (e.g. moles C(graphite) = moles C(diamond) at certain pressures and/or temperatures). Changes of form can be accompanied by large changes in volume which are often involved, either directly or indirectly, in change in amount, i.e. material transport.

Changes in volume have an effect on almost all other properties and are at the heart of what is going on in the river’s response to the environment. The following graph shows the total volumes of the major ions in 1977 which has a volume inversion of HCO<sub>3</sub> & Cl on the same day as major ion concentration inversion.

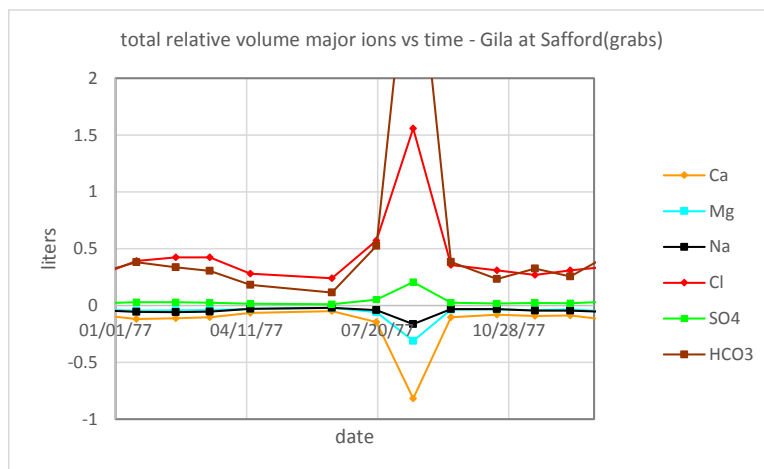


Figure 92

Note that the ‘volumes’ of the cations are negative. The presence of these parameters causes contraction of the solution as a whole. ‘Volume’ here is therefore really a ‘relative volume’. The volumes of the various constituents of the solution are not ‘real’ physical volumes until they are all added up. Then they become the total (relative) volume and are equal to the actual physical volume of the solution in the control volume.

The intra-correlations of the total relative volumes of the major ions has already been shown (.82 % of perfect matrix, .90 without outsider (Cl) [Table 5](#)). The inter-correlation coefficients with flow and density for the inversion test parameter volume, which acts just like one of the major ions, has also already been given (flow-0.96 lin, dens-0.05 lin, [Table 16](#)). Everything that

has been said about flow, from the possible patterns to the drilled down averages, applies to relative volume.

Total relative volume is calculated with moles times the partial molar volume and so follows 'moles' (amount) and is an extensive property. The partial molar volume, on the other hand, is 'per mole' rather than 'times moles' and a 'specific' or intensive property. It is dependent on both concentration and temperature. The partial molar volumes used here, however, are 'at infinite dilution' as is commonly done. Even though the partial molar volume is both concentration and temperature dependent, only the temperature dependence is being looked at here.

Partial molar volumes were largely taken from the compilations of Frank J. Millero.<sup>10</sup> Some values were not available and had to be worked out from temperature and density measurements (HCO<sub>3</sub> being one). Here are the partial molar volumes of the major ions and correlations over all data:

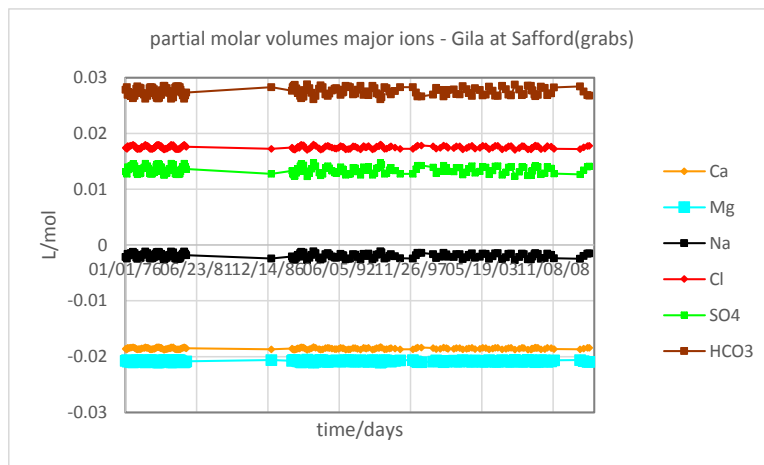


Figure 93 [\(back\)](#)

The graph above is one of very few in which the whole time span of the study can be shown on one graph with no apparent loss of information. There simply are no inversions of any sort – a realm of uniformity. HCO<sub>3</sub> is clearly the dominant factor with the highest values all the time. There are relations between HCO<sub>3</sub> and Cl and HCO<sub>3</sub> and Mg but that is not apparent from the graph.

Seemingly invariant parameters are sometimes seen to actually be changing if examined more closely. One way to do this is to change the graph x and/or y scale. The following graphs zero in on the years 1976-1980 and the y-scale values enclosing the HCO<sub>3</sub> (left) and Cl (right) curves.

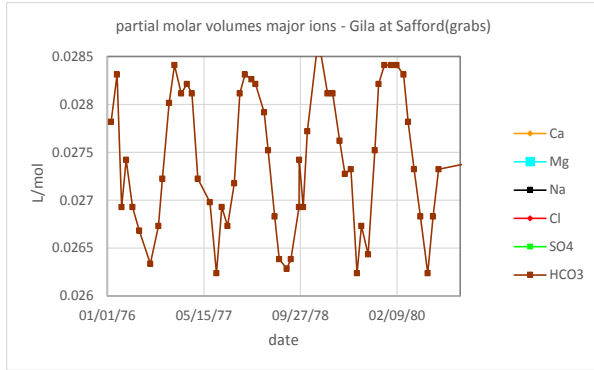


Figure 94

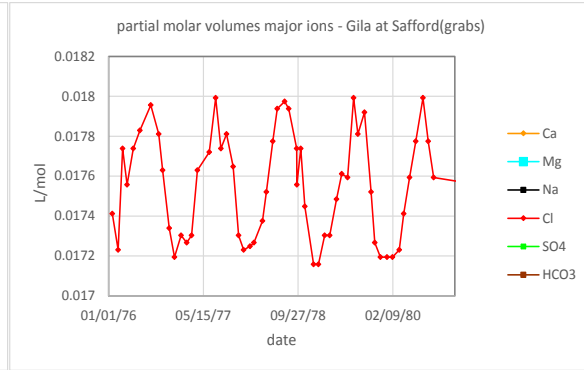


Figure 95

The above graphs bring out the slight undulations in the curves of Figure 92 and reveal that HCO<sub>3</sub> and Cl both do change over time in a regular pattern. Note that the variation around the average is very small, 0.0003 and 0.0007 L/mol for Cl and HCO<sub>3</sub> respectively which explains why the change is barely visible at the scale of Figure 92. But it is difficult to see what the relation is between change in HCO<sub>3</sub> and change in Cl. Do peaks in HCO<sub>3</sub> occur when there are peaks in Cl or is the relation inverse, peaks of one with valleys in the other?

To compare the patterns with each other can be accomplished by ‘scaling’ the various curves so that they all appear in the same y-scale frame. Using this method, the various curves are juxtaposed against one another so that common patterns can line up with each other and points of intersection examined. These are the so-called ‘residuals’ of the major ion partial molar volumes for the year 1977.

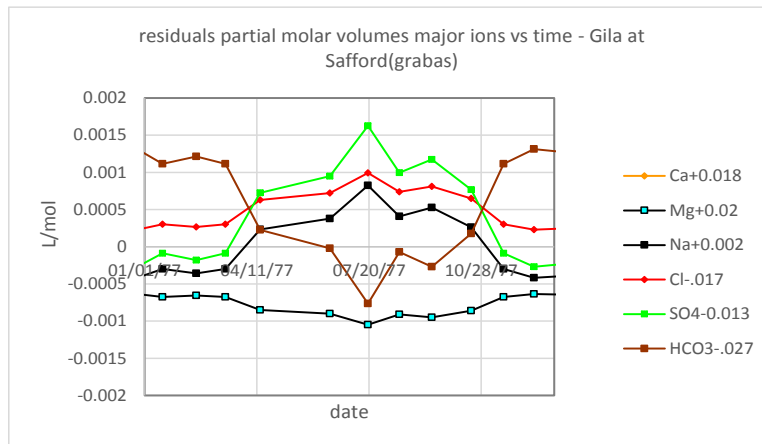


Figure 96

The most common ‘scaling’ method uses linear transformation,  $mx + b$ , where  $x$  is a value on the curve,  $m$  is the slope, and  $b$  is the intercept.  $m$  and  $b$  can be used separately ( $mx+0$ ,  $0x+b$ ) or together as needed. Each and every value on the curve is multiplied or divided by the same slope number and/or has the same intercept added or subtracted.

Multiplying by a large number expands the curve out across the y axis while dividing by a large number flattens it down to, ultimately, a straight line. Multiplication does not affect the



correlation, the relation of the points with each other, but does change the slope. So multiplication is only acceptable when the overall shape or direction, not the rate of change, needs to be ascertained. Adding a constant only moves the entire curve up or down the y-axis without, again, altering the relations of the points with each other.

There are various ways to find the numbers used to scale curves. All the calcium partial molar volumes in liters start with -0.018. If +0.018 is added to each value what is left is the portion that is changing from point to point. This procedure was used to produce the residuals of the figure above and the scaling factors are noted in the legend. In other cases, where there is more variability in the numbers, the point of reference can be the first or last, minimum, or average values, the result being differences around the point of reference, These are the residuals of HCO<sub>3</sub> and Cl partial molar volume for the period 1976-80.

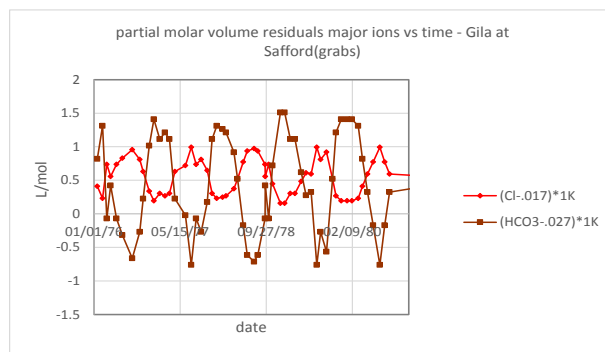


Figure 97

According to this graph, there appears to be four inversions of HCO<sub>3</sub> > Cl over the period. The points of intersection of the curves are, however, entirely determined by the ‘scaling’ factors chosen and are therefore just ‘artifacts’ of the analysis. The residuals merely confirm the inverse correlation coefficient for HCO<sub>3</sub> and Cl partial molar volume but with a lot more effort.

intra-correlations partial molar volumes major ions - Gila at Safford(grabs)							
	Ca	Mg	Na	Cl	SO4	HCO3	
Ca	1.00	-1.00	1.00	1.00	1.00	1.00	-1.00
Mg	-1.00	1.00	-1.00	-1.00	-1.00	-1.00	1.00
Na	1.00	-1.00	1.00	1.00	1.00	1.00	-1.00
Cl	1.00	-1.00	1.00	1.00	1.00	1.00	-1.00
SO4	1.00	-1.00	1.00	1.00	1.00	1.00	-1.00
HCO3	-1.00	1.00	-1.00	-1.00	-1.00	-1.00	1.00

Table 65 [\(back\)](#)

Scaling is useful, and sometimes absolutely necessary, for example in visualizing curves of widely differing magnitudes. Its primary use here, however, will be in looking for portions of

curves that correspond with portions of other curves – something correlation matrices cannot easily do. But scaling can also cause problems as seen above. The manipulation of x and y axis values is a safer method of investigating lower magnitude change but may require multiple graphs, making comparisons more difficult. A change of ‘view,’ a mathematical manipulation of the graph data, is often a better way to handle the problem.

To find real physical inversions, a residual-like quantity will instead be used – the point to point differences of the partial molar volumes. Anyone who has done even a little reading in thermodynamics may be tempted at this point to ask ‘difference?! What difference?!’ There are various ‘differences’ in thermodynamics with the major ones being ‘changes in energy because absolute values are not known’ ( $dE = dq - dw$ ) and ‘adjusted values from a standard reference point’ ( $dH - Cp(T-T_0) = dH_0$ ). The partial molar volumes are already ‘differences’ in the latter sense. They are also calculated by the additivity principle (i.e. difference from a salt compound) and are, by convention, +/- the absolute partial molar volume of the proton to make them comparable to one another.

But the difference to be used here is a point to point difference of partial molar volume values on consecutive grab sample dates. This new factor will be called  $\Delta dX_m$  or delta-‘d’=‘X’-‘m’ or ‘delta-d-molar-‘X’ where ‘Xm’ is a molar function. The use of  $\Delta dX_m$  is justified by the fact that  $dX_m$  is a state function: i.e. change in  $dX_m$  can be evaluated with two points, a beginning and an end value, ( $\Delta dX_m$ ), which adequately represents the change in state because it is independent of path. The inconsistent, largely random, intervals between grab samples, so often railed against above, are not a problem at all here.

Here are the differences in major ion partial molar volumes for the same year as the residuals, 1977.

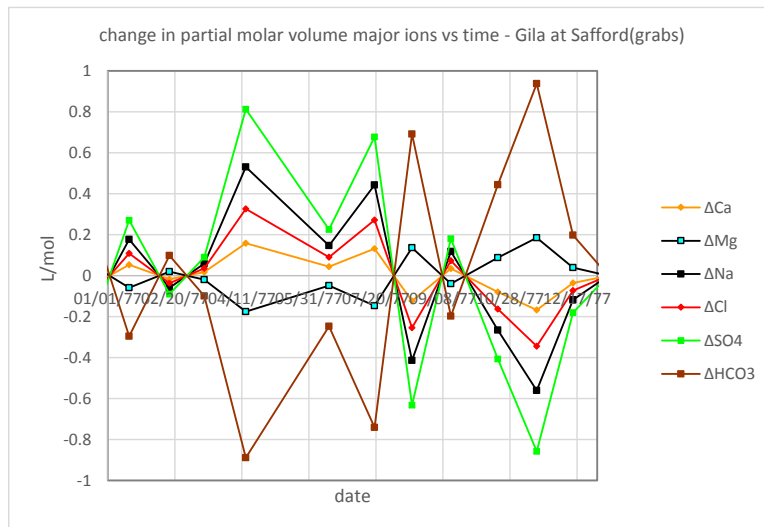


Figure 98 ([back](#))

While this graph does not look at all like the residuals of the graph above, the differences are largely a visual illusion and the relations between the ions are the same. This sameness can be

demonstrated by taking the difference of the residuals, rather than of the partial molar values themselves, which yields a graph (not shown) that is the exact copy of Figure 98 above. When differences are taken, the scaling constants drop out. That the relations between the points remain the same is also attested by the fact that the intra correlations for differences and residuals (not shown) are identical to those above for the original partial molar values (Table 65). Note that, as with the straight partial molar values,  $\Delta\text{HCO}_3$  is positively correlated to only  $\Delta\text{Mg}$  and negatively correlated to all the other ions and that this relationship is evident on the graph.

The new view with differences reveals the possibility of ‘inversions’ in the partial molar volume. In fact, there is indeed an inversion with  $\text{HCO}_3 > \text{Cl}$  on the same day as major ion concentration inversion, 8/16/77. Never mind that there appear to be other similar inversions on other dates that have no major ion concentration inversion. While inversions in the sense of ‘crossing lines’ are present, the pattern does not seem at this point to match that of major ion concentration inversion.

Since correlations in this realm tend to be identities or at least all very high, some format changes seem to be in order. First of all, a new definition of the correlation ‘outsider’: rather than the parameter with low correlation values, the ‘outsiders’ are from the lowest number of parameters in a given direction – usually the inverse relation but can be a solitary positive or two as well. For partial molar volume the outsiders are both  $\text{HCO}_3$  &  $\text{Mg}$ . Second, a new color formatting will be used: values  $> 0.85$  are light blue and values  $< -0.85$  are light green. Determinant values, which are non-meaningful (tautologies), are colored so as not to break up the pattern. The above partial molar volume matrix, but in terms of differences, does duty again in its new colors:

intercorrelations difference in partial molal volumes major ions - Gila at Safford(grabs)							
	$\Delta\text{Ca}$	$\Delta\text{Mg}$	$\Delta\text{Na}$	$\Delta\text{Cl}$	$\Delta\text{SO}_4$	$\Delta\text{HCO}_3$	
$\Delta\text{Ca}$	1.00	-1.00	1.00	1.00	1.00	1.00	-1.00
$\Delta\text{Mg}$	-1.00	1.00	-1.00	-1.00	-1.00	-1.00	1.00
$\Delta\text{Na}$	1.00	-1.00	1.00	1.00	1.00	1.00	-1.00
$\Delta\text{Cl}$	1.00	-1.00	1.00	1.00	1.00	1.00	-1.00
$\Delta\text{SO}_4$	1.00	-1.00	1.00	1.00	1.00	1.00	-1.00
$\Delta\text{HCO}_3$	-1.00	1.00	-1.00	-1.00	-1.00	-1.00	1.00

Table 66

For completeness, % partial molar differences are also shown:

intracorrelations % partial molar volume differences major ions - Gila at Safi						
	$\Delta\%Ca$	$\Delta\%Mg$	$\Delta\%Na$	$\Delta\%Cl$	$\Delta\%SO_4$	$\Delta\%HCO_3$
$\Delta\%Ca$	1.00	1.00	1.00	-1.00	-1.00	-1.00
$\Delta\%Mg$	1.00	1.00	1.00	-1.00	-1.00	-1.00
$\Delta\%Na$	1.00	1.00	1.00	-1.00	-1.00	-1.00
$\Delta\%Cl$	-1.00	-1.00	-1.00	1.00	1.00	1.00
$\Delta\%SO_4$	-1.00	-1.00	-1.00	1.00	1.00	1.00
$\Delta\%HCO_3$	-1.00	-1.00	-1.00	1.00	1.00	1.00

Table 67

The differences of percent partial molar volume divides up not by individual ions, as the values, but by groups with anions inversely related to cations. Percents were calculated over the sum of the major ions (sumMI) with mixed positive and negative numbers and can therefore be higher than 100. The relationships between the numbers remain the same as if absolute values were used and the sum is still 100%. Calculating percent with absolute values changes the correlations so was not an option here. There is a potential problem if the numbers in the average calculation sum to 0 but that did not occur. (More on the topic of percent calculations to follow)

To discover what might be causing the pattern of intra-correlations among the major ions, an 'outside' view (inter-correlational) is always useful.

correlations partial molar volume difference major ions and basic bulk and environmental analyzes differences - Gila at Safford(grabs)						
	$\Delta Ca$	$\Delta Mg$	$\Delta Na$	$\Delta Cl$	$\Delta SO_4$	$\Delta HCO_3$
$\Delta temp-grab/K$	1.00	-1.00	1.00	1.00	1.00	-1.00
$\Delta press-grab/atm$	0.00	0.00	0.00	0.00	0.00	0.00
$\Delta flow-grab$	-0.16	0.16	-0.16	-0.16	-0.16	0.16
$\Delta dens(TSP)-grab/(kg/L)$	-0.94	0.94	-0.94	-0.94	-0.94	0.94
$\Delta conductivity/(uS/crr$	0.05	-0.05	0.05	0.05	0.05	-0.05
$\Delta ionicity soln/\#$	0.11	-0.11	0.11	0.11	0.11	-0.11
$\Delta pH/SU$	-0.08	0.08	-0.08	-0.08	-0.08	0.08
$\Delta totalk/(mg/L as CaC$	0.02	-0.02	0.02	0.02	0.02	-0.02
$\Delta D.O./(mg/L)$	-0.65	0.65	-0.65	-0.65	-0.65	0.65
$\Delta Eh H_2O-O_2/volts$	-0.05	0.05	-0.05	-0.05	-0.05	0.05
$\Delta TDS/(mg/L)$	0.12	-0.12	0.12	0.12	0.12	-0.12
$\Delta TSS/(mg/L)$	0.09	-0.09	0.09	0.09	0.09	-0.09
$\Delta cvlen-grab/ft$	-0.31	0.31	-0.31	-0.31	-0.31	0.31
$\Delta cvarea-grab/ft^2$	-0.16	0.16	-0.16	-0.16	-0.16	0.16
$\Delta cvvol-grab/L$	-0.16	0.16	-0.16	-0.16	-0.16	0.16
$\Delta cvmass-grab/kg$	-0.16	0.16	-0.16	-0.16	-0.16	0.16
$\Delta cv\Delta h-grab/ft$	0.31	-0.31	0.31	0.31	0.31	-0.31

Table 68

Note that the dimensions of the control volume are in no way related to the partial molar volume of the major ions. The external dimension of the control is related to the total relative volume (an extensive property) while the internal packing of the control volume is related to density. The

‘control volume’ external volume, the real physical volume of a partly hypothetical entity, falls into the extensive side of the relation and is a function of flow/amount as seen below.

relations control volume and bulk and environmental parameter: - Gila at Safford(grabs)					
	$\Delta cvlen-grab$	$\Delta cvarea-gr$	$\Delta cvvol-grab$	$\Delta cvmass-gi$	$\Delta cv\Delta h-grab$
$\Delta temp-grab$	-0.31	-0.16	-0.16	-0.16	0.31
$\Delta press-gra$	-0.11	-0.06	-0.06	-0.06	0.11
$\Delta flow-grab$	0.68	1.00	1.00	1.00	-0.68
$\Delta dens(TSP)$	0.25	0.12	0.12	0.12	-0.25
$\Delta conductivity$	-0.32	-0.14	-0.14	-0.14	0.32
$\Delta ionicity s$	-0.33	-0.17	-0.17	-0.17	0.33
$\Delta pH/SU$	-0.16	-0.10	-0.10	-0.10	0.16
$\Delta totalk/(r$	-0.63	-0.50	-0.50	-0.50	0.63
$\Delta D.O./(mg$	0.06	0.05	0.05	0.05	-0.06
$\Delta Eh H2O-C$	-0.01	0.17	0.17	0.17	0.01
$\Delta TDS/(mg,$	-0.35	-0.17	-0.17	-0.17	0.35
$\Delta TSS/(mg/$	0.15	0.17	0.17	0.17	-0.15

Table 69

The direction of correlation of the partial molar volumes of the major ions, however, is a reflection of their differing direction of correlation with temperature via density. Mg and HCO<sub>3</sub> are inversely related to the other ions because they are positively related to density while the others are inversely related to density. The percent partial molar volumes of the major ions, if calculated with the sum solution (SS) or sum dissolved solids do not correlate with density. If calculated with the sum of the major ions (MI), however, they do have a high correlation to density. Summarizing the important relationship of the partial molar volume with density in the new formatting:

correlation partial molal volume major ions with density - Gila at Safford(grabs)							
	$\Delta Ca$	$\Delta Mg$	$\Delta Na$	$\Delta Cl$	$\Delta SO4$	$\Delta HCO3$	
$\Delta dens(TSP)-grab/(kg/L$	-0.94	0.94	-0.94	-0.94	-0.94	0.94	
	$\Delta \%Ca(SS)$	$\Delta \%Mg(SS)$	$\Delta \%Na(SS)$	$\Delta \%Cl(SS)$	$\Delta \%SO4(SS)$	$\Delta \%HCO3(SS)$	
$\Delta dens(TSP)-grab/(kg/$	-0.10	-0.10	-0.07	0.10	0.10	0.10	
	$\Delta \%Ca(MI)$	$\Delta \%Mg(MI)$	$\Delta \%Na(MI)$	$\Delta \%Cl(MI)$	$\Delta \%SO4(MI)$	$\Delta \%HCO3(MI)$	
$dens(TSP)-grab/(kg/L$	-0.93	-0.93	-0.93	0.93	-0.93	0.93	

Table 70

Summing up ‘everything’ in a solution to calculate percentages is easily done and presents no problems. The mole fraction, for example, is the moles of a particular parameter divided by the moles of ‘everything,’ including the parameter of interest, in the solution. ‘Moles’ above and below the line cancel leaving a unit-less number to express the percentage. But summing partial molar quantities of different parameters is not as simple and straightforward for several reasons. First, these are ratios whose dimensions do not cancel and to add ratios a common denominator is required. There seems to be one here, ‘mol,’ but the denominator is really mol X or mol Y not just mols of anything or everything. What is the change in solution volume when 1 mol of X is added?

Second, and as if to underline the mathematical problem, partial molar values are differences for a parameter taken when all the other parameter amounts in the solution as well as solution

temperature and pressure are held constant. To sum them all up, willy-nilly, means creating a mish-mosh of self-contradictory conditions. One value is the change in liters caused by X when Y is constant, another is change in liters caused by Y when X is constant; both these conditions cannot hold at the same time.

But the constraints involved in the experimental determination of partial molar values may not have any bearing on how the values are related to one another in solution. Indeed, the assumption made here is that partial molar values are simply additive with no interferences or multiplier effects involved. If a solution (water) contains 1 mol X and 1 mol Y, and 1 mol X reduces solution volume by (-)5 liters while 1 mol Y increases solution volume by 2, the result will be found by simply adding the two --  $-5+2 = -3$ . If they all act the same way, it is not important to know exactly which one is causing the change. An end-run around the problem, additivity effectively converts all denominators to 'mols something.' The sum of all the 'somethings' in a solution will be simply the sum of the signed values of all the constituents.

If the assumption held completely the sum solution of the partial molar volumes should be zero since the constant amount, temperature, pressure solution at any particular moment is neither contracting nor expanding. Most of the sum solution partial molar volumes on grab sample dates are negative and the average is around -0.27 L/mol. This result probably points to limitations in the analysis; there are one or more incorrect values or some parameter has been left out.

Actually, there is a parameter missing here – H<sub>4</sub>SiO<sub>4</sub> partial molar volume could not be found anywhere in the literature (nor could H<sub>2</sub>CO<sub>3</sub> for which CO<sub>3</sub> is sometimes substituted with unknown effect). The total relative volume of H<sub>4</sub>SiO<sub>4</sub>, by difference with the sum solution total relative volume, appears to be about 3-5% of total differences in volume depending on conditions. Here, a 'reason' for the sum of the partial molar volumes not summing to zero has been found and the assumption of additivity seems safe. In other cases, more elaborate 'reasons,' ones that cast a suspicion on how the system 'slice' is made, will be necessary to save the assumption.

The link between the partial molar volumes of the various parameters and density is important for several reasons. The first is that it links the partial molar volume, a calculated value, to a physical factor that can theoretically be measured experimentally, density. Second, it opens up the possibility of studying partial molar volume difference inversion with density data. Since all that is required for a calculated density is a temperature, this step is significant because it means that, at some point, daily mean temperatures can be used rather than being limited to grab samples.

The relation between partial molar volume and density can be found with inversion analysis. First it is necessary to determine which dates represent partial molar volume difference inversion and which do not. From the graph above ([Figure 98](#))  $\Delta\text{HCO}_3 > \Delta\text{Cl}$  seems an appropriate test parameter to use. Shown below are a portion of the inversion date determination worksheet showing the test parameter and the corresponding change in density on the same date and a graph of the density differences over the same time period.

partial molar volume inversion/ non-inversion date determination - Gila at Safford(grabs)			
	$\Delta\text{HCO}_3\text{-}\Delta\text{Cl}$	inv $\Delta\text{dens(T)}$	non-inv $\Delta\text{dens(TSP)}$
1/17/1977	-0.0004		-0.0003
2/16/1977	0.0001	0.0002	
3/14/1977	-0.0001		-0.0001
4/14/1977	-0.0012		-0.0016
6/15/1977	-0.0003		-0.0005
7/19/1977	-0.0010		-0.0023
8/16/1977	0.0009	0.0018	
9/14/1977	-0.0003		-0.0004
10/19/1977	0.0006	0.0012	
11/17/1977	0.0013	0.0017	
12/14/1977	0.0003	0.0003	

Table 71 [\(back\)](#)

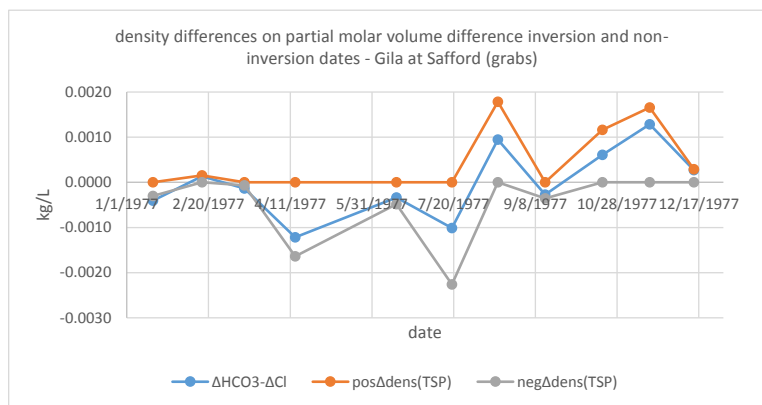


Figure 99

In accord with the correlations, inversion dates are positive change in density while non-inversion are negative. This crucial finding opens up a whole new range of analytical possibilities. But if density is going to be used as a surrogate for the partial molar volume, it is important to have the best average values available and to be aware of any patterns and/or anomalies that may influence the picture of molar function difference inversion that emerges.

‘Density’ can be either a physical measurement (with a hydrometer for example) or a calculated value. Calculated densities from temperature are used here because direct physical measurements of density were not available. As mentioned previously, temperature data was gathered from different sources. The online AZMet dataset (University of Arizona) covered average daily air temperatures at Safford for the period 1989 – 2011. Average daily air temperatures from 1976 to 1988 are from the Safford Regional Airport dataset which is online at WeatherUnderground.com.

For the calculation of daily mean density, air temperatures need to be converted to water temperatures. Two datasets of instantaneous water and instantaneous air temperature pairs at the Safford site were available from ADEQ. One set, possibly a special study, contained 101 pairs from 1965 to 2011. Another set, from the surface water quality database, contained 102 pairs from 1988 to 2012. These datasets were used to create equations relating air to water

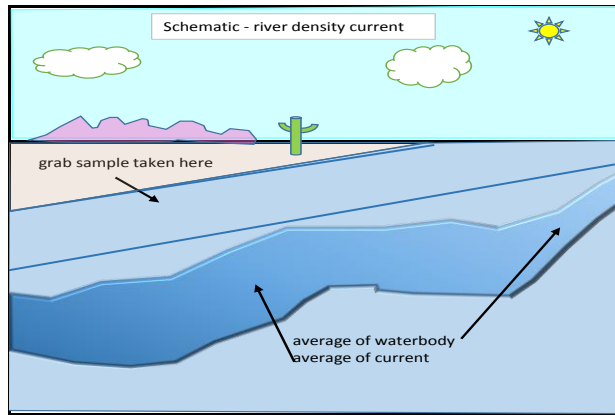
temperature. Unfortunately, when compared to actual water temperatures at the site, one equation gave consistently higher while the other gave consistently lower predicted water temperatures. A compromise equation using the average slope and average intercept of the two equations was therefore used. The correlation coefficient associated with the original air/water data for this equation was 0.78. The correlation coefficient for calculated and actual water temperatures, however, was 0.92.

Grab sample densities were calculated with ADEQ instantaneous water temperature(T), salinity(S), and barometric pressure(P) measurements where available. There are actually two sets of grab sample densities: both use ADEQ instantaneous water temperatures (not guesstimates from air temperature) but one set is calculated with temperature, salinity, and pressure dependence '(TSP)' while the other set is calculated with temperature dependence only '(T)' for comparison with the daily means which are all temperature dependent only. (A few 'TSP' may be just 'TS' or 'TP' but are not designated separately).

On the plus side, a density calculation, though it does not have the weight of a physical measurement, is about as good as it gets for a calculation. The density calculation used here is the Thermodynamic Equation of Seawater (TEOS-10).<sup>11</sup> This equation has been evaluated as producing values within +/- 0.004 kg/m<sup>3</sup> at atmospheric pressure for salinities up to 42 g/kg at temperatures up to 45C.<sup>12</sup> A 0.004 kg/m<sup>3</sup> difference at a density of 999 kg/m<sup>3</sup> produces a very low percent relative standard deviation ( $4 \times 10^{-4}$ ). For this reason, an assumption will be made here that a density measurement is 'as good as' a physical measurement for comparison with other calculated values.

On the negative side, using a single daily density for a moving body of water, whether average (over time) or instantaneous, is a great simplification. Examples of daily density fluctuations in rivers are very hard to come by and what information there is refers to formation of river 'density currents'. The situation seems analogous to that of temperature/density stratification in a lake with the important difference that a river is a moving body which implies mixing, the inverse of stratification. Single day density values apply only to a spatial average density of unknown extent and variability. A bottle of river water can be shaken in the lab, a river cannot. The best that can be done with the original water sample is through the use of a composite sampler of some sort. A grab sample has one density, a river is inherently more or less heterogeneous for density. A schematic 'appreciation' of the situation is presented below:





Schematic 5

An average can always be taken, the question is: how representative of the system as a whole is that average? A good example is the river flow average of about 558 cfs - pages have been spent trying to place that number in the context of the whole river over time with the result that the mode or median were found to be more representative than the average. The average continued to be used though because its 'weighted' characteristic give it meaning even if it is not highly representative.

How representative a single instantaneous or daily mean density is of the entire water body or even the entire control volume, the dataset provides no clues. There is one density per day, no indication of whether it was taken in the morning or the evening, or exactly at what point in the flow it was taken. Even if this information were available with the grabs, it would not be sufficient. It would take numerous density and location measurements at numerous times on numerous days over the entire year to develop the type of 3d picture of density in the river so cavalierly depicted above. The analysis would have to be done at each point, an overwhelming task whose result would probably be so complex as to be virtually impossible to visualize. So, for lack of a better alternative, the investigation will continue using a single daily value for density.

The distributions of density values for the three analysis types are as follows:

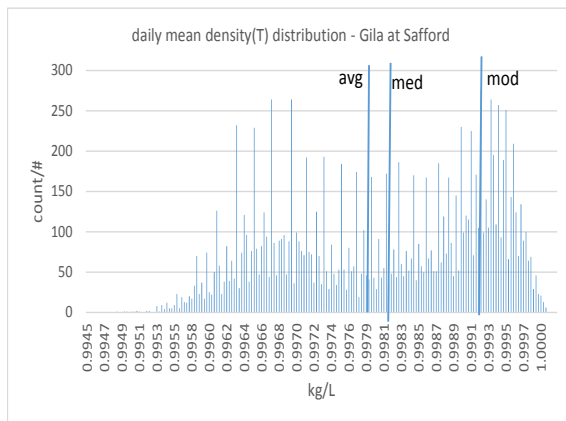


Figure 100

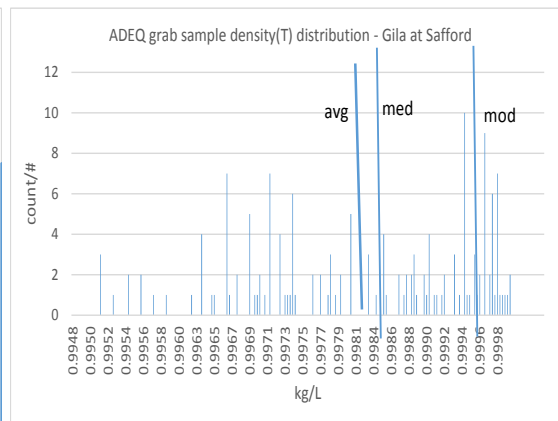


Figure 101

The above graphs compare the daily mean densities with the ADEQ grab sample densities using temperature only (dens(T)). Both show what appears to be a roughly bi-modal pattern with a bell curve in the center and a bunching of values at the high end. The average and median are found between the two ‘modes’ and the numeric mode is in the bunched section at the right. This is where the first wrinkle comes in – grab sample T (above) and TSP (below) densities have somewhat different distributions.

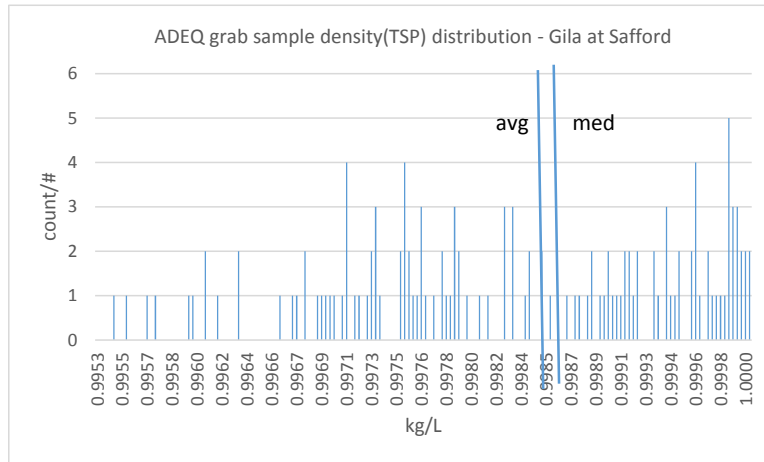
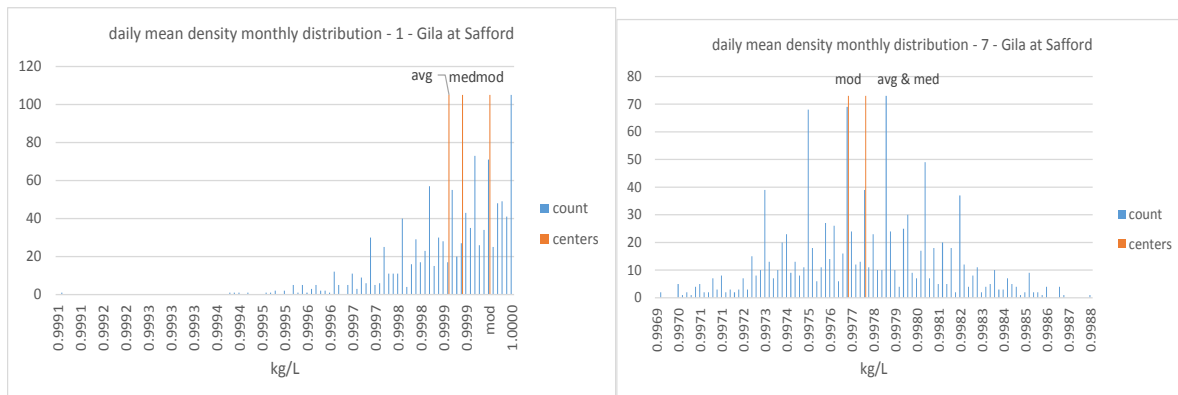
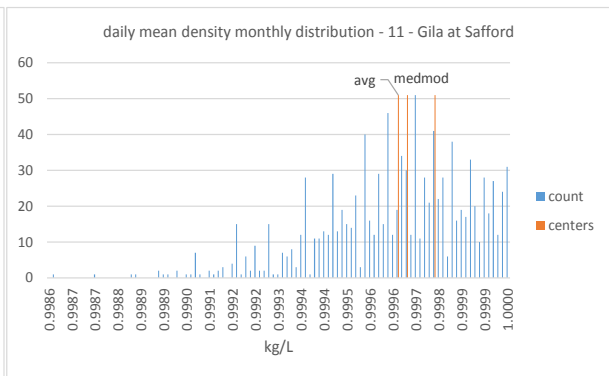
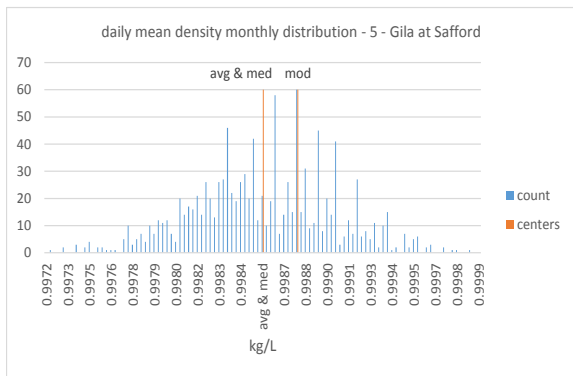
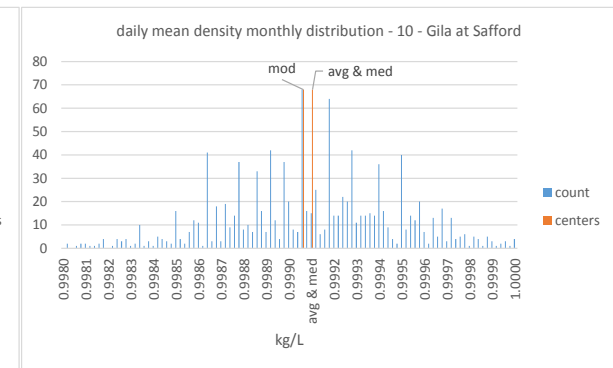
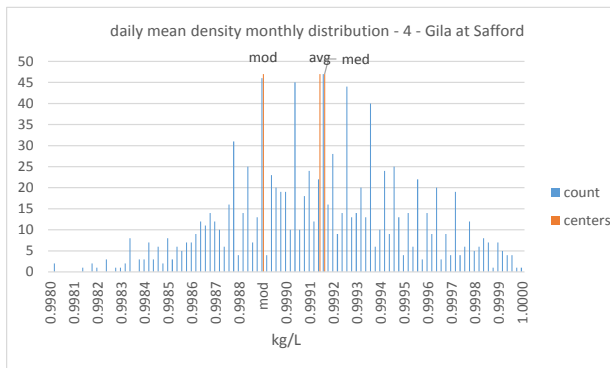
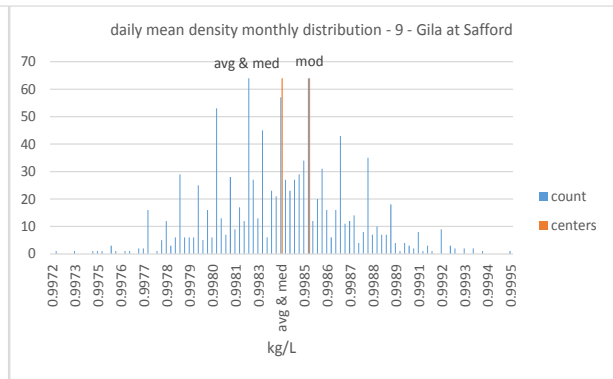
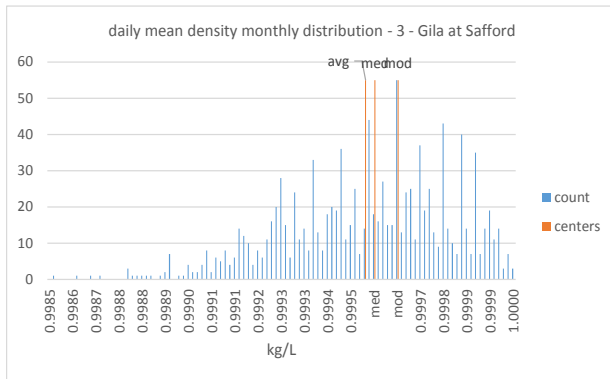
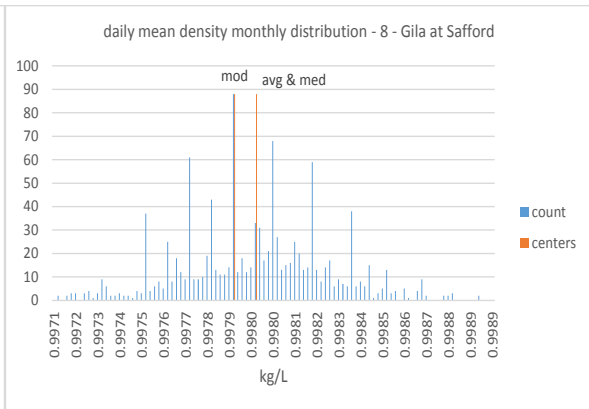
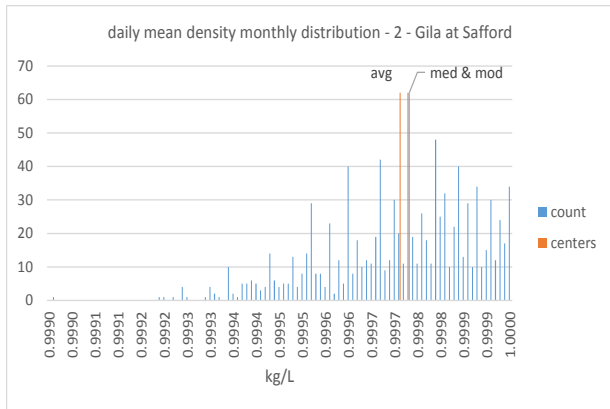


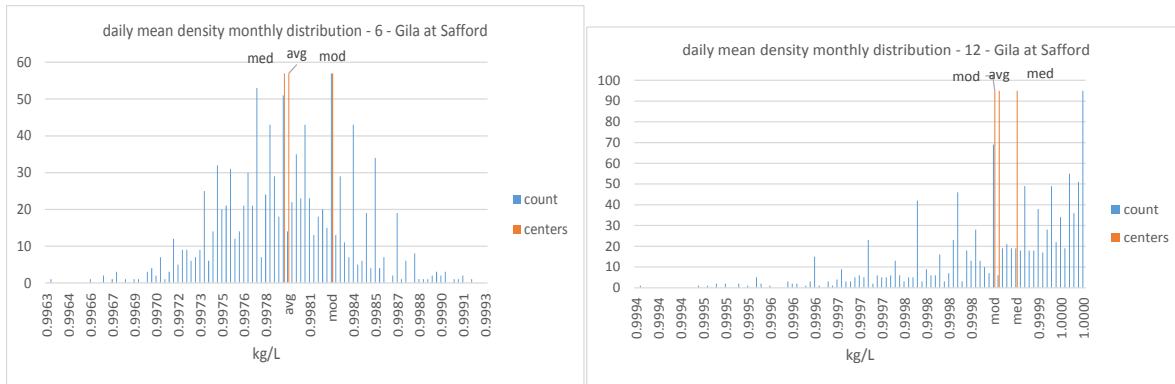
Figure 102

TSP densities are distributed more evenly over the entire scale with less apparent central bell shape or bunching to the right. The mode, furthermore, is non-existent. This disjoint between the daily mean or ADEQ densities (T) and ADEQ densities (TSP) needs to be kept in mind whenever the two are being compared.

Does the bunching to the right of density values indicate a non-normal distribution? No, it is sort of an optical illusion brought on by superimposing data from different times all together. Here are the monthly distributions for daily mean densities (T), with Jan-Jun from top to bottom in the left column and Jul-Dec in the right column.







Figures 103 to 114

Scanning the first column from top to bottom, then the second, it becomes apparent that it is the shifting of the distribution over the year that gives the all-data distribution its bi-modal appearance. The bell shaped curve appears early in the year (Mar) and marches steadily towards lower values until mid-summer (Jul). Then it shifts in the other direction and finally bunches up at the right end. This ‘bunching’ is not so much a non-normal distribution as one half of a normal distribution up against a physical limit, i.e. the max density of water.

What are the distributions for density differences? The following graphs are intended to show just that.

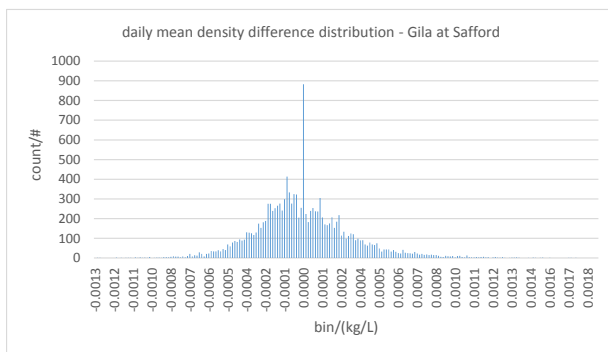


Figure 115

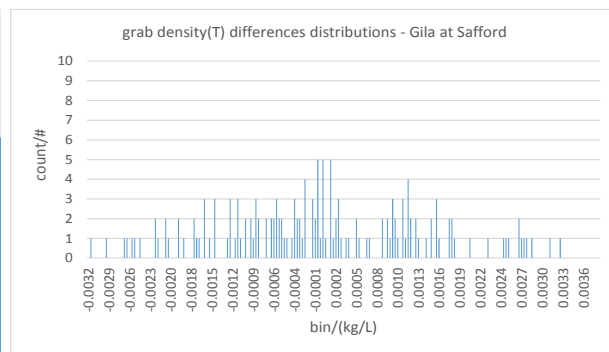


Figure 116

These look like perfectly normal distributions and the slight variation between daily mean and grab is probably due to the low sample count of the grabs. Once again, however, TSP densities (below) have a slightly different look with a wider x-scale and a less distinct center value. These differences correspond to the same distinctions seen in the values. But the TSP distribution of the differences is a little more normal looking, more of a bell shaped curve, than it was for the values.

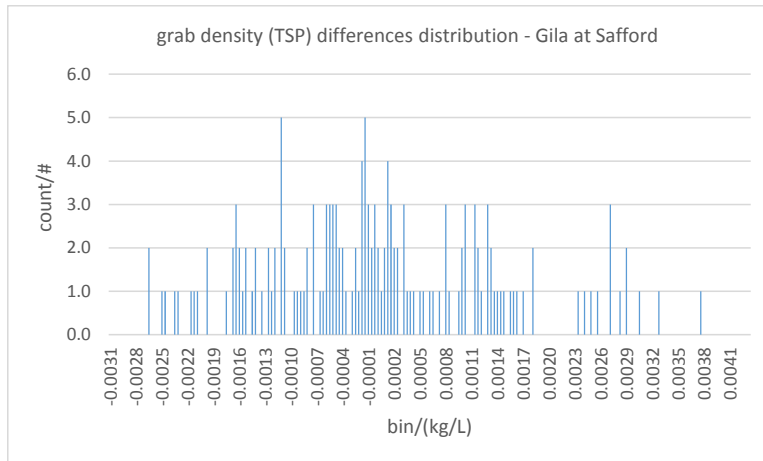


Figure 117

There is really no need to look at monthly density difference distributions – they are all very normal and very much alike. But the center of distribution of the differences do change over the course of the year as the values do.

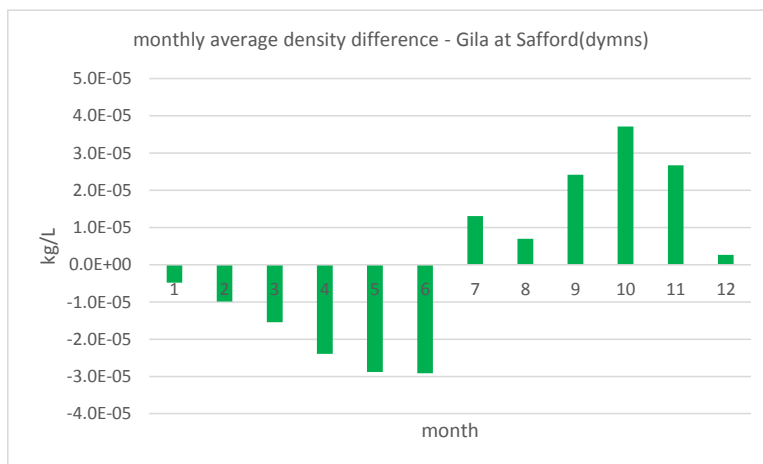


Figure 118

What the averages show is that the center of density difference distributions too will shift over the course of the year. Also the look of the above graph suggests that it may be useful to plot average monthly daily mean density differences with monthly grab density differences.

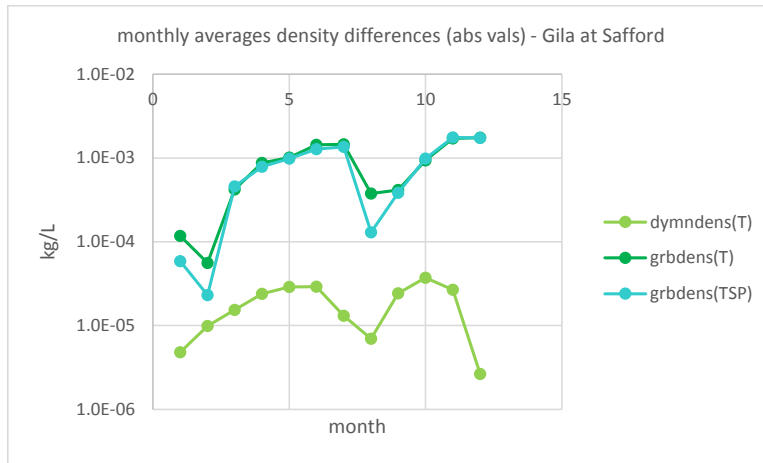


Figure 119 (back)

Amazingly enough, grab sample differences seem to capture the form of the daily mean difference curve even though they are orders of magnitude apart in values and counts and do not represent the same time intervals. The curious thing here is that grab(TSP) densities, while values are higher, sometimes show smaller monthly average differences as in Feb and Aug above. Overall, the agreement of grabs and daily means is a good sign even though it took absolute values and a logarithmic scale to show it.

The following table summarizes the statistics for density values and density differences over all data. The following graphs show the values (left) and differences (right) in density for the various sample and analysis types over the year 1977 (all in gr/ml or kg/L).

density statistics over all data/ kg/L - Gila at Safford						
	values			differences		
	dymn(T)	grab(T)	grab(TSP)	dymn(T)	grab(T)	grab(TSP)
average	0.9980	0.9982	0.9986	-3.0E-08	-1.4E+05	-1.6E-05
median	0.9982	0.9985	0.9989	-1.8E-05	-6.7E-05	-1.4E-04
mode	0.9992	0.9996	N/A	0.0E+00	0.0E+00	N/A
min	0.9945	0.9948	0.9953	-1.3E-03	-3.2E-03	-3.1E-03
max	1.0000	1.0000	1.0006	1.7E-03	3.8E-03	4.5E-03
stdev	0.0012	0.0014	0.0014	3.1E-04	1.4E-04	1.4E-03
count	13149	161	161	13148	160	160

Table 72

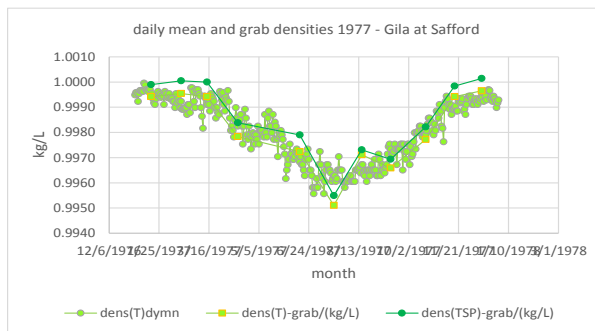


Figure 120

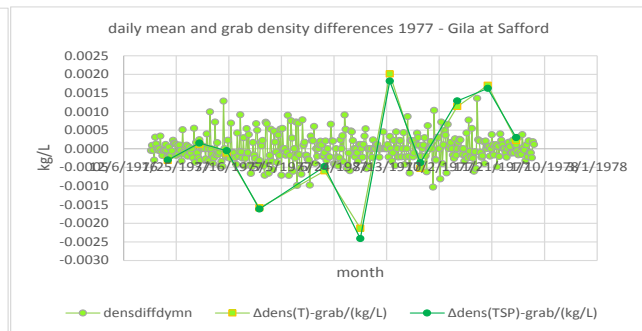


Figure 121

The three sets of data have average values and their standard deviations fairly close to one another even though the sample counts differ by several orders of magnitude. The relative percent standard deviation between grab dens(T) and dens(TSP) ranges from 0.016 to 0.36 bit averages about 0.05 indicating that there are a few high values. The difference, it will be seem, is variable at different times of the year.

But density differences (graph to right) reveal what may very well prove to be a problem – the differences of the grabs (from one grab sample to the next) are in some cases four orders of magnitude larger than the daily mean differences. Densities, like flow, are not state functions as the thermodynamic functions are, so there will have to be a heavy reliance on averages to bridge data gaps if processes are to be investigated. Differences are less familiar, may even look a little strange, so it is probably a good idea to compare side by side both values and differences to help maintain bearings.

Can molar function difference inversion yield any insights at this high level picture of density? The following tables show the results of sorting the density parameters over all data by inversion/non-inversion before taking averages. This table uses a new, morphed sort of formatting with magenta – high values (>0.9990), plum – low values, light blue – positive difference, light green – negative difference.

daily mean and grab densities under molar volume inversion over all data - kg/L - Gila at Safford						
values	dymn(T)	dymn(T)	grab(T)	grab(T)	grab(TSP)	grab(TSP)
	inv	non-inv	inv	non-inv	inv	non-inv
average	0.9981	0.9980	0.9987	0.9977	0.9991	0.9982
median	0.9983	0.9981	0.9990	0.9974	0.9994	0.9980
mode	0.9992	0.9992	0.9996	0.9994	N/A	N/A
min	0.9950	0.9945	0.9956	0.9948	0.9961	0.9953
max	1.0000	1.0000	1.0000	0.9998	1.0060	1.0002
std	0.0012	0.0012	0.0012	0.0014	0.0012	0.0013
count	5536	7613	69	91	69	91
differences	dymn(T)	dymn(T)	grab(T)	grab(T)	grab(TSP)	grab(TSP)
	inv	non-inv	inv	non-inv	inv	non-inv
average	2.7E-04	-2.0E-04	1.3E-03	-1.0E-03	1.2E-03	-9.7E-04
median	2.0E-04	-1.6E-04	1.1E-03	-8.7E-04	1.1E-03	-7.7E-04
mode	2.2E-04	0.0E+00	1.2E-03	0.0E+00	N/A	N/A
min	-1.7E-05	-1.3E-03	4.1E-05	-3.2E-03	-1.7E-03	-3.1E-03
max	1.7E-03	2.3E-05	3.8E-03	0.0E+00	4.5E-03	9.2E-05
std	2.4E-04	1.8E-04	9.0E-04	8.2E-04	1.1E-03	7.8E-04
count	5535	7613	70	90	70	90

Table 73 [\(back\)](#)

Inversion/non-inversion for the grabs roughly divides high from low density average values though this result is not seen in the daily means and modes, minimums, and maximums reveal that there is overlap. The expected division into positive and negative density differences for inversion and non-inversion is also evident. There is a rise in daily mean difference values from the all data average (-3E-8) to close to the level of the grab differences (E-4). But the division between positive and negative differences is not as perfect as one might expect from the above snippet of the partial molar volume inversion date determination table. Why not?

Partial molar volume and density have different relations to temperature. The partial molar volume vs temperature relation as used here is a linear equation that is either always directly or always inversely related to temperature depending on what parameter is being examined and what temperature range is being considered. In the range of common interest (276-306 K) for water the two are inversely related. The partial molar volume of water vs temperature is shown below right. The density of water on the other hand, has a more complicated relation to temperature: positive at temperatures below 277.15 K (4C) and inverse above (left graph below)

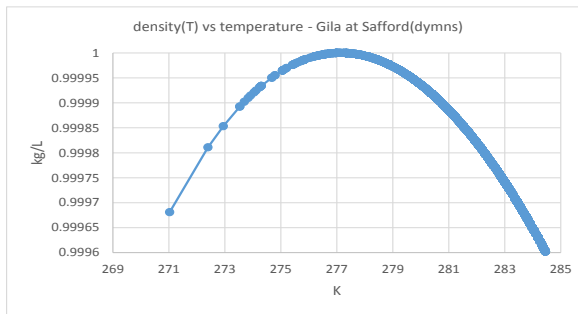


Figure 122

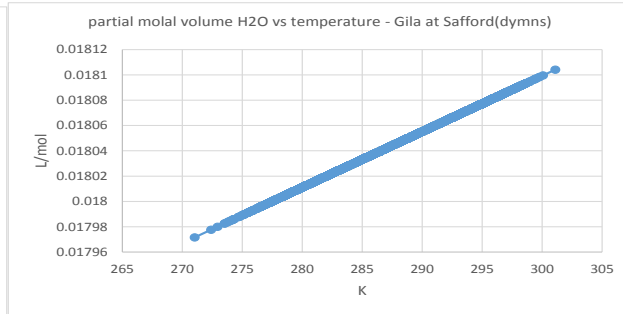


Figure 123

Density differences in the area around 277.15 may straddle the line and therefore split into two groups– if the temperature ‘ $\Delta$ from277.15’ is negative, the relation is positive, if the difference is positive the relation is inverse. (‘ $\Delta$ temp’ and ‘ $\Delta$ dens’ in the graph below are the point to point sample differences). Of the daily mean density differences under inversion (positive HCO3-Cl) there are 43 negative values (0.33%). These all correspond to negative temperature differences between 271.02 and 276.98K.

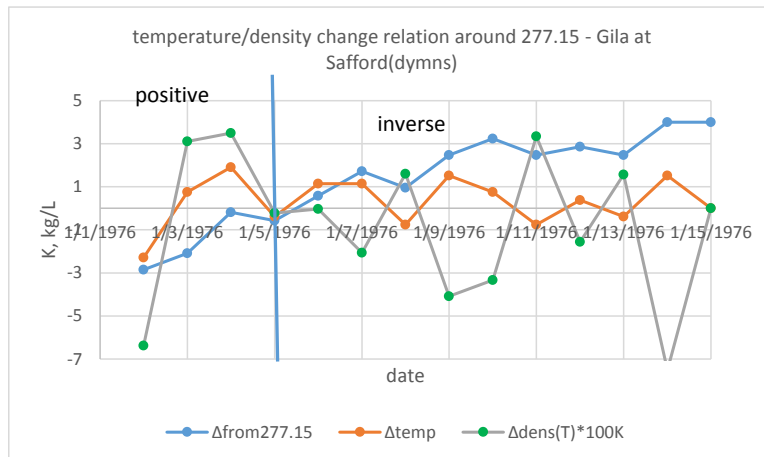


Figure 124

The errant negative grab(TSP) difference minimum under inversion in [Table 73](#) is caused by something else. All grab densities are at or above 279 K so the arguments made for the daily mean discrepancies do not apply. The minimum TSP difference in question is from 9/20-21/1978 – the same dates looked at before because the flow went from 0.28 to 70 cfs in a single



day and, more significantly, TDS went from 4620 to 767 mg/L. Higher salinity raises density values but does not change the relation to temperature. When differences are taken, however, the difference between a very high density (caused by high salinity) and a very low (temperature related) can cause an apparent anomaly in the temperature/density difference relationship.

high to low TDS reverses normal inverse temperature/density relation 9/21/78 - Gila at Safford(grabs)							
date	temp-grab/t	dens(TSP)-	dens(T)-gra	TDS/(mg/L	Δtemp	Δdens(TSP	Δdens(T)
05/16/78	299	0.9973	0.9969	554	+	-0.0015	-0.0016
06/09/78	304	0.9962	0.9956	794	+	-0.0011	-0.0013
07/18/78	305	0.9960	0.9953	944	+	-0.0002	-0.0003
08/09/78	304	0.9961	0.9956	647	-	0.0001	0.0003
09/20/78	298	1.0006	0.9971	4620	-	0.0045	0.0015
09/21/78	293	0.9989	0.9983	767	-	-0.0017	0.0012
10/11/78	298	0.9977	0.9971	787	+	-0.0011	-0.0012
11/02/78	290	0.9994	0.9988	726	-	0.0017	0.0017

Table 74

Here the difference between TSP and T densities are apparent – the dens(TSP) for 9/21 is the only one where a negative temperature difference is accompanied by a negative density difference (a positive rather than the normally inverse relation between temp and density). This anomaly would not have been picked up if the sample had been deleted as an ‘outlier’ and /or only dens(T) values had been used. It is, in general, a good idea to keep as wide a scope as possible in what is being looked at and this is particularly true if finding exceptions that test the ‘rule’ are of particular interest.

The monthly averages are shown below with borders to distinguish high from low values and positive from negative differences.

monthly average density/ (kg/L) - Gila at Safford					
	values			counts	
	dymn(T)	grab(T)	grab(TSP)	dymn	grab
Jan	0.999456	0.999627	1.000016	1116	9
Feb	0.999218	0.999543	0.999847	1017	11
Mar	0.998849	0.999112	0.999404	1116	20
Apr	0.998252	0.99837	0.998775	1080	13
May	0.997442	0.997848	0.998228	1116	10
Jun	0.996532	0.996833	0.997381	1080	20
Jul	0.996368	0.996169	0.996696	1116	9
Aug	0.996624	0.996586	0.996916	1116	16
Sep	0.997158	0.997164	0.997733	1080	18
Oct	0.998154	0.998242	0.998712	1116	8
Nov	0.999041	0.999272	0.999732	1080	10
Dec	0.999482	0.999775	1.00018	1116	17

Table 75

monthly average density differences/ (kg/L) - Gila at Safford					
	values			counts	
	dymn(T)	grab(T)	grab(TSP)	dymn	grab
Jan	-4.8E-06	1.2E-04	5.9E-05	1115	8
Feb	-9.9E-06	5.6E-05	-2.3E-05	1017	11
Mar	-1.5E-05	-4.2E-04	-4.6E-04	1116	20
Apr	-2.4E-05	-8.7E-04	-7.9E-04	1080	13
May	-2.9E-05	-1.0E-03	-9.8E-04	1116	10
Jun	-2.9E-05	-1.4E-03	-1.3E-03	1080	20
Jul	1.3E-05	-1.5E-03	-1.4E-03	1116	9
Aug	6.9E-06	3.8E-04	1.3E-04	1116	16
Sep	2.4E-05	4.2E-04	3.9E-04	1080	18
Oct	3.7E-05	9.4E-04	9.9E-04	1116	8
Nov	2.7E-05	1.7E-03	1.8E-03	1080	10
Dec	2.6E-06	1.7E-03	1.7E-03	1116	17

Table 76

The months divide up roughly into hidens (>0.9990, nov-mar) and lodens (apr-oct) while the differences divide up roughly into negative density change (feb-jun) and positive density change

(aug to jan). The monthly timespan raises the daily mean difference but not to the level of the grabs. Both monthly values and differences are in accord with the average yearly value and difference curves seen above.

Below are tables showing the average monthly values and differences of the various forms of daily mean and grab densities (T&TSP) under molar volume inversion/non-inversion.

monthly densities under inversion/non-inversion partial molar volume - Gila at Safford						
values	dymn(T)	dymn(T)	grab(T)	grab(T)	grab(TSP)	grab(TSP)
	inv	non-inv	inv	non-inv	inv	non-inv
Jan	0.9999	0.9998	1.0000	0.9999	1.0003	1.0001
Feb	0.9998	0.9997	0.9999	0.9999	0.9999	0.9999
Mar	0.9996	0.9995	0.9998	0.9996	0.9996	0.9994
Apr	0.9993	0.9991	0.9992	0.9992	0.9987	0.9988
May	0.9987	0.9985	0.9995	0.9987	0.9994	0.9981
Jun	0.9980	0.9978	0.9991	0.9979	0.9987	0.9973
Jul	0.9979	0.9977	0.9993	0.9972	0.9990	0.9965
Aug	0.9981	0.9979	0.9980	0.9975	0.9972	0.9966
Sep	0.9985	0.9983	0.9986	0.9978	0.9983	0.9971
Oct	0.9992	0.9990	0.9992	0.9989	0.9989	0.9984
Nov	0.9997	0.9996	0.9998		0.9998	
Dec	0.9999	0.9999	1.0000		1.0003	

Table 77

monthly densities under inversion/non-inversion partial molar volume - Gila at Safford						
differences	dymn(T)	dymn(T)	grab(T)	grab(T)	grab(TSP)	grab(TSP)
	inv	non-inv	inv	non-inv	inv	non-inv
Jan	6.9E-05	-5.1E-05	1.6E-04	-4.2E-05	4.2E-04	-1.8E-04
Feb	1.1E-04	-8.0E-05	2.4E-04	-4.7E-05	3.8E-04	-3.5E-04
Mar	1.8E-04	-1.3E-04	3.7E-04	-3.1E-04	5.3E-04	-6.7E-04
Apr	2.5E-04	-1.7E-04	8.9E-04	-6.4E-04	1.2E-03	-1.0E-03
May	2.4E-04	-1.9E-04	7.1E-04	-8.6E-04	1.1E-03	-1.2E-03
Jun	2.3E-04	-2.0E-04	5.2E-04	-1.3E-03	7.8E-04	-1.5E-03
Jul	2.3E-04	-1.7E-04	7.0E-05	-1.3E-03	1.2E-04	-1.5E-03
Aug	2.1E-04	-1.5E-04	9.7E-04	-7.7E-04	9.7E-04	-1.1E-03
Sep	2.2E-04	-1.5E-04	7.9E-04	-3.8E-04	9.0E-04	-4.5E-04
Oct	2.1E-04	-1.3E-04	1.2E-03	-6.9E-04	1.6E-03	-9.6E-04
Nov	1.3E-04	-8.4E-05	1.2E-03		1.8E-03	
Dec	7.0E-05	-5.0E-05	1.1E-03		1.8E-03	

Table 78

The monthly average values divide up roughly into high (winter) and low (summer) density regimes in accord with the yearly average picture. Inversion/non-inversion has no effect other than not having any non-inversion grab samples in Nov & Dec. But inversion/non-inversion divides up the differences neatly into positive (inversion) and negative (non-inversion) in contrast to the picture seen in the average density curve. So, at this stage, it is possible to

generate some general ‘rules’: among the values, season predominates over inversion/non-inversion, while among the differences, inversion/non-inversion predominates over season.

The seemingly innocuous monthly difference averages, however, show some interesting relations among themselves when graphed together as seen below.

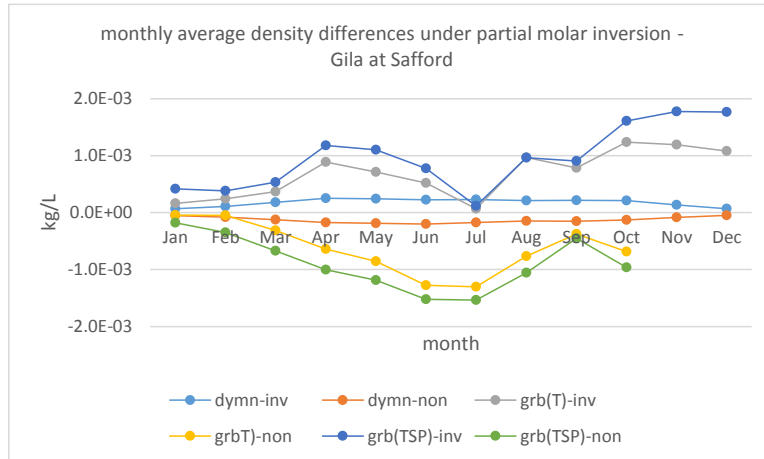


Figure 126

Inversion densities are positive, non-inversion negative, but the grab curves look quite different from the daily means. With the daily means, inversion and non-inversion are, as expected, the inverse of one another. This is not the case with the grabs where dens(T) and dens(TSP) inversion are highly correlated to each other but not at all correlated to their corresponding non-inversion partners. The grab inversion curves are reminiscent of the monthly average density differences curves (Figure 125) but the characteristic dip there was in Aug. here it is in July.

correlations monthly average density differences under pmv inversion - Gila at Safford

	dymn-inv	dymn-non	grab(T)-inv	grab(T)-non	grab(TSP)-inv	grab(TSP)-non
dymn-inv	1.00	-0.96	0.10	-0.75	-0.08	-0.78
dymn-non	-0.96	1.00	0.05	0.86	0.20	0.87
grab(T)-inv	0.10	0.05	1.00	-0.13	0.95	-0.16
grab(T)-non	-0.75	0.86	-0.13	1.00	-0.11	0.98
grab(TSP)-inv	-0.08	0.20	0.95	-0.11	1.00	-0.15
grab(TSP)-non	-0.78	0.87	-0.16	0.98	-0.15	1.00

Table 79

The grab non-inversion curves, indeed, look like a totally new beast and bear no relation to their corresponding inversion curves as the correlations bear out. In fact, they are more closely related to both the daily mean curves, which they little resemble, than their own corresponding inversion

curves. The red bordered boxes above show where high correlations would be expected to be if the grabs inversion/non-inversion pairs were correlated to each other as the daily means are.

To visualize the above results a bit further, in the graphs below the grab non-inversion (left) and inversion (right) differences are plotted along with the daily mean differences as residuals around their average. Grab non-inversion curves resemble both daily mean inversion and non-inversion curves while grab inversion curves resemble neither of the daily mean curves.

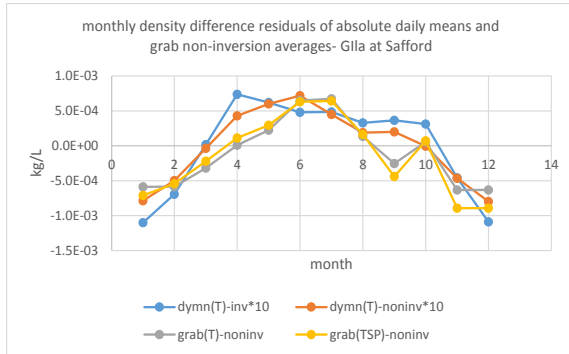


Figure 127

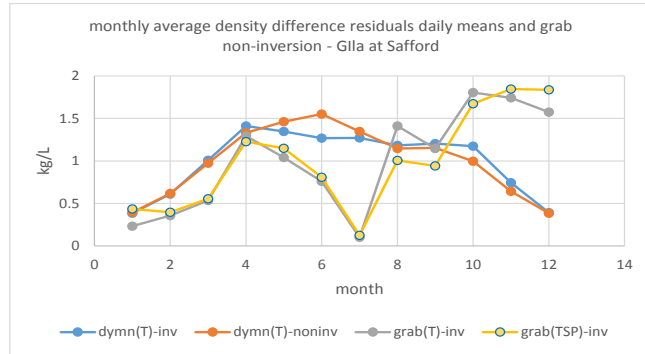


Figure 128

These graphs accentuate the similarity of grab non-inversion density differences (left) and the lack of similarity of inversion density difference curves with either daily mean inversion density difference curve. There is a definite lack of symmetry here that is, as always, a little disturbing. It suggests that something is missing in the analysis or that the ‘view’ is not correct.

In the functional analysis of density which follows, what has been termed ‘negative density change’ will be referred to as ‘dilution,’ positive as ‘concentration.’ It might have been wiser to choose terms less closely associated with flow to avoid the inevitable confusion between two very different things: flow-induced and temperature-induced expansion or contraction. It is just too late at this point, however, to go back and change all the labels and references to ‘dilution’ and ‘concentration’ with respect to density so a caveat will have to suffice.

The terms ‘densification’ and ‘un-’ or ‘de-densification,’ as clumsy as they may sound, do help explain how distilled water can have various states of density. The CRC has a table with different densities of distilled water at different temperatures. How is it possible for distilled water, virtually ‘pure’ water with nothing else in it, to have different densities? The answer is that these multiple densities are not the result of any additions or subtractions of dissolved constituents but rather due to volume change of the water caused by temperature difference -- the same mass in a larger or smaller volume. ‘Densification’ is therefore a change in density due solely to change in volume caused by temperature change, amount remaining constant, while the process of ‘concentration’, as commonly used, is due to a change in amount with the change in volume proportional to the increase or decrease of amount. Here, however, ‘concentration’ as used in reference to density change is understood as ‘densification,’ ‘dilution’ as ‘de-densification.’

The flow/flow difference analysis lends itself easily to the study of density but here it is called, of course, ‘daily dens/densdiff.’ (dddd) The flo/flodiff difference labels follow the direction of flow (increase in flow - >, decrease - <) not concentration, which is the opposite. The dens/densdiff labels follow the direction of density (increase in density - >, decrease in density - <) not temperature, which is the opposite. Because the one follows a ‘cause’ while the other follows a ‘result’, the labels ‘flip’ -- >> is a flow induced expansion (dilution) while >> for density is a temperature induced contraction (concentration or densification) as seen in the Sep-Dec slope of the average density graph.

A dens/densdiff analysis of the daily mean densities yields the following results.

density averages values - dens/densdiff analysis - kg/L - Gila at Safford							
values		dymn(T)	grab(T)	grab(TSP)	dymn-cnt	grab(T)-cnt	b(TSP)-cnt
concentration	>>	0.9981	0.9982	0.9986	4181	50	49
	><	0.9983	0.9984	0.9988	1375	20	20
dilution	<<	0.9980	0.9980	0.9984	5226	66	66
	<>	0.9978	0.9984	0.9988	1500	18	18
equal	=0	0.9979	0.9981	0.9986	866	7	7
<b>differences</b>							
concentration	>>	3.1E-04	3.9E-04	4.2E-04	4181	50	49
	><	1.5E-04	-3.7E-05	3.9E-05	1375	20	20
dilution	<<	-2.4E-04	-2.4E-04	-2.3E-04	5226	66	66
	<>	-1.4E-04	-2.6E-04	-2.9E-04	1500	18	18
equal	=0	-2.1E-07	-1.0E-04	-4.7E-04	866	7	7

Table 80

The dens/densdiff analysis is so ‘close’ to the data that it reduces almost everything to the average value of all-data (0.99804-dymns). This outcome is good in the sense that it confirms that the three sets of data, despite great differences in sample counts, are populations with similar values under a simple functional analysis.

The analysis also raises the magnitude of the daily mean differences to that of the average grab differences over all data (from dymns: -7.5E-9, grab(TSP): -1.6E-5). The preference for straight dilution (<<) or concentration (>>) seen in the values holds for the differences as seen in the sample counts. Note also that the direction of change are largely correct here: concentration types are usually positive, dilution types negative, though that may be entirely by chance (see below).

The dens/densdiff analysis runs into problems when trying to deal with density differences. A difference label really should have all the information for the two dates involved so a proper label would be something like <<-< or >>->. This type of labelling, however, leads to a proliferation of labels, 36 to be exact, and they are hard to analyze and/or manage. Sorting by label doesn’t help because there are too many, sorting by average values doesn’t help because they are all too small and close together. And the only result of using full labels is confirmation of the preference for straight concentration or dilution types as was the case with the values. For the analysis here, the daily label of the ‘to’ date is given rather than a full ‘from-to’ label.

The grab difference is a difference of two consecutive grab samples whereas the daily mean difference is the difference of the daily means on the same day as the grab and the day before. Applying a label that was created by the difference of the daily means to the grab led to a situation in which 36% of the grab differences were going in the ‘wrong’ direction from that indicated by the label (the daily mean difference). That is, for example, the difference of two consecutive grabs might be a dilution but the difference of the daily means, and therefore the grab sample label, would indicate that it was a concentration.

Because of the above considerations, only the daily means will be used in density difference seasonal and functional analysis. Since inversion/non-inversion is, to this point, known only for the grab samples it will also not be possible to pursue that analysis further. Or is it? In fact, since a partial molar volume only requires a standard state reference value and a temperature, it should be possible to determine inversion/non-inversion dates for the daily means using the partial molar function test parameter,  $\Delta HCO_3 - \Delta Cl$ , as described above. The following tables show a dens/densdiff analysis done after daily mean samples were divided up by partial molar volume inversion/non-inversion.

density/dens diff analysis under partial molar volume inversion/non-inversion - Gila at Safford(dymns)					
		inv		non-inv	
		kg/L	count%	kg/L	count%
values	concentrat >>	0.9990	75	1.0000	1
	><	0.9991	24	1.0000	0.3
	dilution <<	1.0000	1	0.9989	68
	<>	0.9999	0.1	0.9988	20
equal	=0			0.9989	11
differences	concentrat >>	2.1E-04	75	1.4E-05	0.3
	><	9.7E-05	24	3.1E-05	1
	dilution <<	-2.5E-05	1	-1.6E-04	68
	<>	-4.7E-05	0.1	-9.5E-05	20
	equal	=0		0.0E+00	11

Table 81

Once again, all the values come in close to each other though at a higher magnitude than the all-data situation. What is different here, in contrast to the even spread of types in all data, is the preference for certain types as seen in the counts. Inversion prefers relatively lower magnitude concentration types while non-inversion prefers lower magnitude dilution.

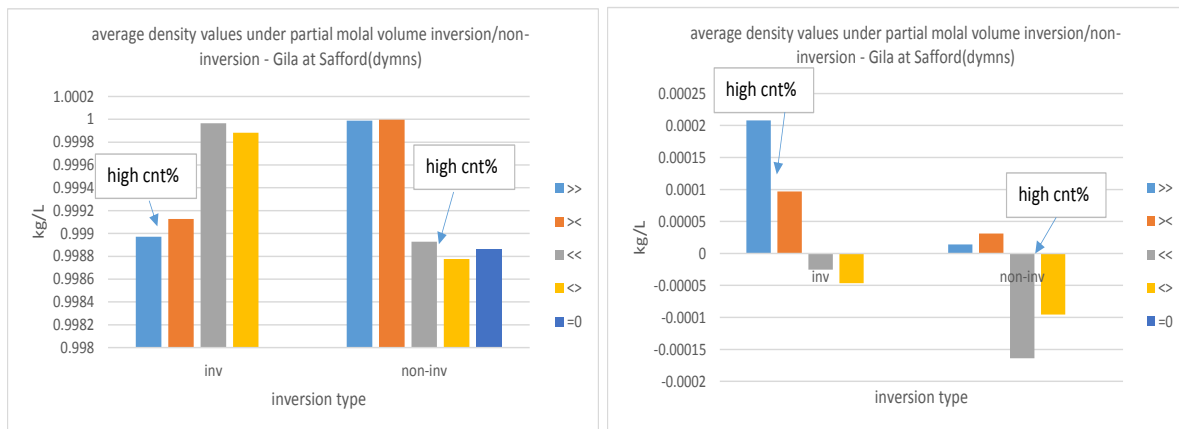


Figure 129

Figure 130

The differences, slightly lower in general than the all data, are also all close to each other. Preferred types line up with higher values so that inversion is a matter of high concentration differences (positive density change) while non-inversion is a matter of high magnitude dilution differences (negative density change). These are the same distinctions as seen in the monthly values under inversion/non-inversion.

Unlike flow, it is not very hard to find pattern for density. Density is closely correlated to temperature and the auto correlation is, like temperature, quite high. The graphs for daily means and grabs were shown previously as an introduction to autocorrelation. They are repeated here as a starting reference point.

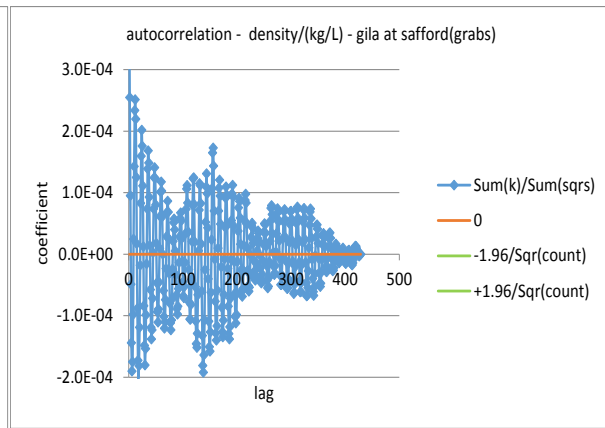
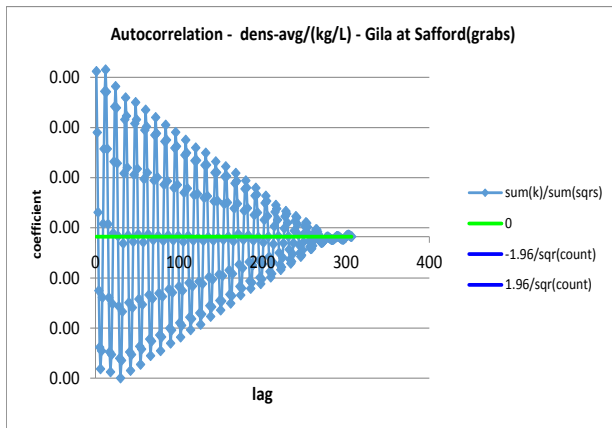


Figure 131

Figure 132

autocorrelation statistics - density - Safford				
	% at 6	% at 12	$\Sigma x_1 y_2 / \Sigma sq$	count
dymns	0.9211	0.9221	0.2825	462
grabs	0.8000	0.7465	0.3971	428

Table 82

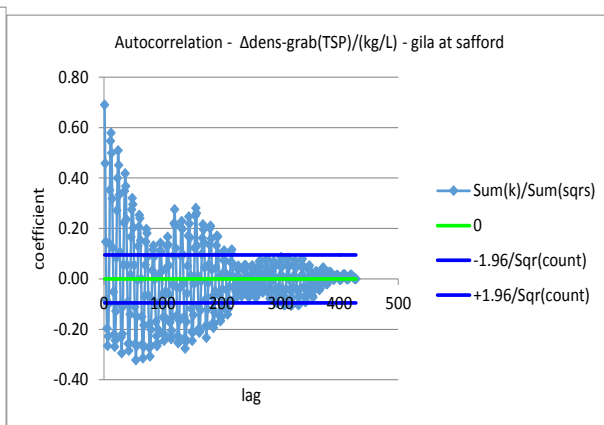
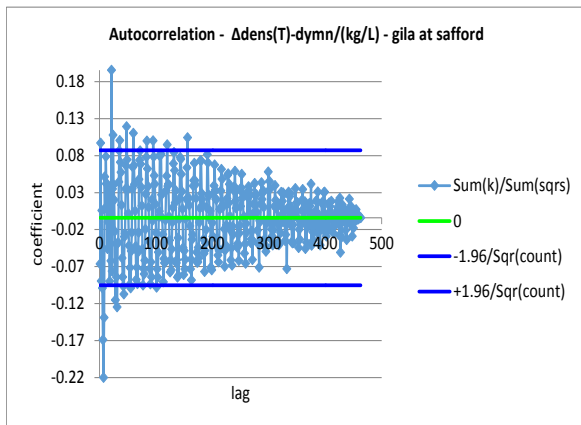




Figure 133

Figure 134

autocorrelation statistics - density - Safford				
	% at 6	% at 12	$\Sigma x_1 y_2 / \Sigma sq$	count
$\Delta dymns$	0.5526	0.4026	2.1249	462
$\Delta grab(TSP)$	0.6857	0.7465	0.6287	427

Table 83

There is quite a drop in autocorrelation with differences from values, and running the natural logarithm of the absolute value of the density difference doesn't help (# peaks at 6 & 12 - 0.6579 daily means, 0.4000 grab(TSP)). (The same things are true for temperature difference, 0.4700, grabs, 0.3684 daily means) Just because one view of the data is highly auto-correlated does not mean any mathematical manipulation of those same numbers will also be.

Fortunately the way density values work out over time is a clear enough pattern: a sine wave over the entire year with max in Dec-Jan and min in Jun-Jul. The close relation of grab(T) to daily mean densities(T) suggests that the use of a guesstimated water temperature from air temperature for the daily means is a bit more of an issue in the first half of the year than the second but not a large factor in either case. Since both grab(T) & (TSP) calculations use actual water temperatures, the fact that grab(TSP) are consistently higher than grab(T) densities is a result of the fuller calculation using salinity and pressure.

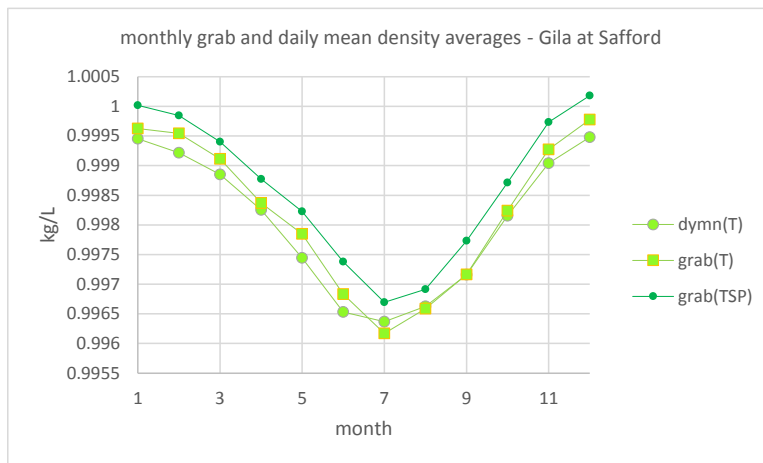


Figure 135

A closer look at the daily mean density curve in any given year (below), shows that there is a structure within the curve – it is like a twisted cord of smaller curves within a larger one. What the inner curve reveals is that there are plenty of concentrations, for example, in what is, according to the average view, a period of dilution (jan to jul ). The partial molar volume difference inversion/non-inversion analysis is, it appears, simply more in tune to the inner than the average density curve.

The inner curve has a fairly consistent peak to valley duration. A simple peak analysis reveals that peaks are about 4.7 +/- 2.5 days apart. Here is the daily mean density curve for 1977 (left) and the monthly peak to valley durations for all the daily means (right).

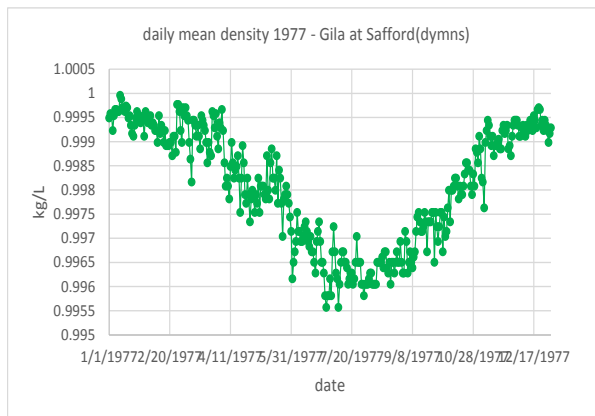


Figure 136

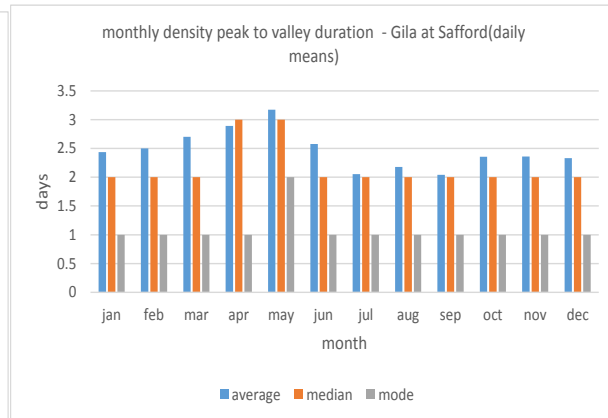


Figure 137

The graph on the right shows that the inner curve has a fairly consistent mode for peak to valley duration of one day (gray) except in May when it jumps to 2. The median (red) is very consistent at 2 days except in Apr and May when it jumps to 3. The average (blue) hovers between 2 and 3.5 following the pattern of the maximums which range from 8 to 14 days.

The inner density curve is not perfectly symmetrical with respect to the year average curve and peak to valley dips are longer in spring than any other time. The grab samples cannot, of course, pick up this deeper structure but do capture the overall shape of the average curve ( $r^2 = 0.92$ ) which varies little in overall shape from year to year.

Could there be an 'inner' inner curve? That is, could there be an even tighter pattern within the inner curve? That would be, presumably, the daily density curve that was sought for earlier. If density is temperature dependent and there is a daily temperature pattern then there must be a daily density pattern as well. But, for reasons mentioned above, we have no physical evidence for that curve and will have to rely on a hypothetical curve based on temperature change.

The season/function modes of analysis have already been developed under the discussion of flow and only differences specific to the density analysis will be commented on here. Graphs and tables are presented with comments limited to highlights. The yearly average is used to divide low and high density seasons. The graph below shows the year average (green) and seasonal averages (hi-blue, lo-red) for daily mean density in 1977.

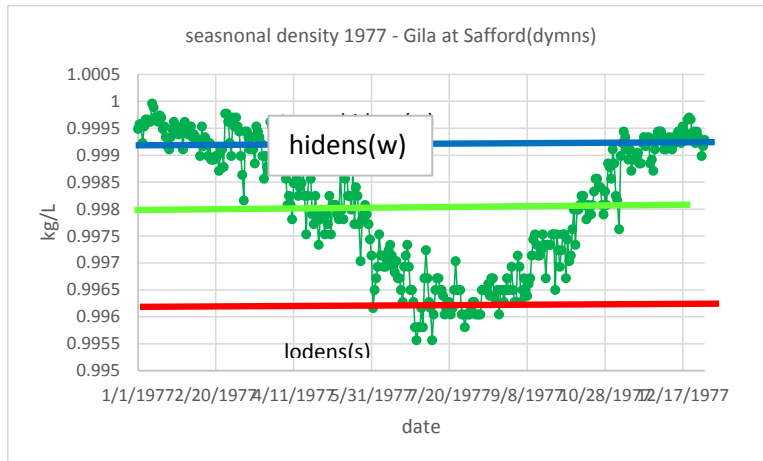


Figure 138

seasonal density average values/ (kg/L) - Gila at Safford					
	averages		counts		
	dymns(T)	grab(T)	grab(TSP)	dymns	grabs
hidens(w)	0.9990	0.9992	0.9996	7068	84
lodens(s)	0.9969	0.9970	0.9975	6081	77

Table 84

With seasonal density, the division between high and low density is small but clear and extends across the board (median, mode, min, max (not shown) except that TSP has no mode). The labelling is a bit redundant, there being no need to add a (w) or an (s) to hidens and lodens for winter and summer except as a flourish and a nod to the flow analysis.

seasonal daily mean density average differences (kg/L) - Gila at Safford			
	averages	relstdev	counts
hidens(w)	1.94E-07	144331	7067
lodens(s)	-2.9E-07	-116584	6081

Table 85

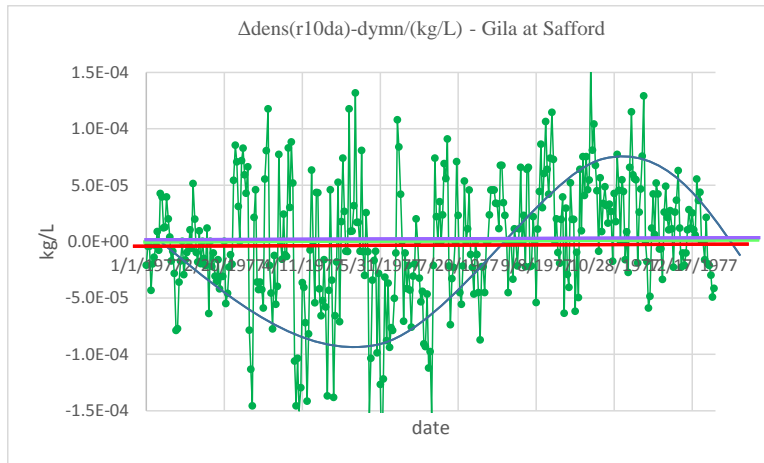


Figure 139

Seasonal average differences are of the same magnitude as the day mean all-data level in contrast to the larger magnitudes of the daily dens/densdiff analysis. The yearly average for all daily mean differences is  $3.4E-7$  with hidens being slightly above 0 and lodens slightly below but essentially the averages just plot one on top of the other. Ten day rolling averages help a little in visualizing that there is a slight difference between high and low density seasons represented by the blue and red arrows respectively. The sine curve is an artistic aid to distinguish a possible but barely visible greater number of points below zero (left) and above (right).

Applying density seasonal labels to densities on molar volume difference inversion and non-inversion dates yields the following tabulation.

daily mean density values and differences under partial molal volume inversion/non-inverison/(kg/L) - Gila at Safford				
<b>values</b>				
inv			non-inv	
	avg	cnt	avg	cnt
hidens(w)	0.9991	2906	0.9989	4162
lodens(s)	0.9970	2629	0.9968	3452
<b>differences</b>				
inv			non-inv	
	avg	cnt	avg	cnt
hidens(w)	$2.5E-04$	2906	$-1.7E-04$	4161
lodens(s)	$3.0E-04$	2629	$-2.3E-04$	3452

Table 86

With the seasonal approach, the distinction between high values in the winter and low values in the summer remains clear under inversion analysis. With the differences, inversion is picking out concentrations across seasons in which both concentrations and dilutions are present (the inner curve).

The division into periods of concentration and dilution forms the basis of the function(s) approach for density which is shown schematically below.

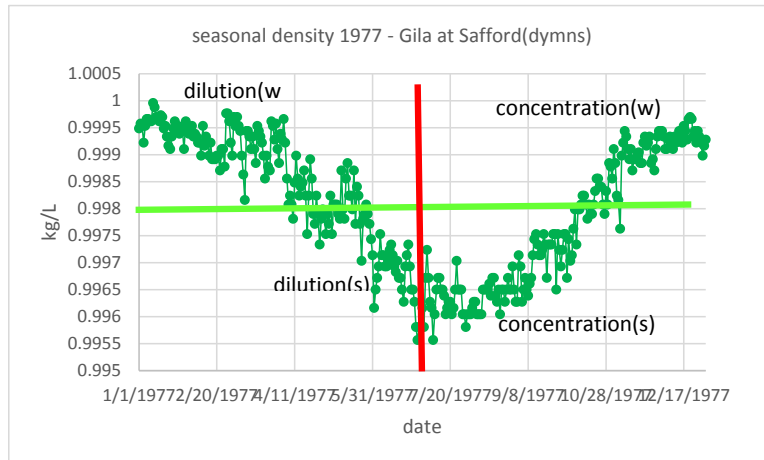


Figure 140

In the function(s) definitions, concentration and dilution are defined by the direction of change of average density around a seasonal midpoint. The (w) and (s) labels now become necessary to differentiate the functions in different seasons. The midpoint used here is the chronological midpoint (red line) of the year not the minimum value to avoid situations such as that illustrated below. This graph shows how a potential problem in the function(s) approach can easily be avoided with a good choice in methodology.

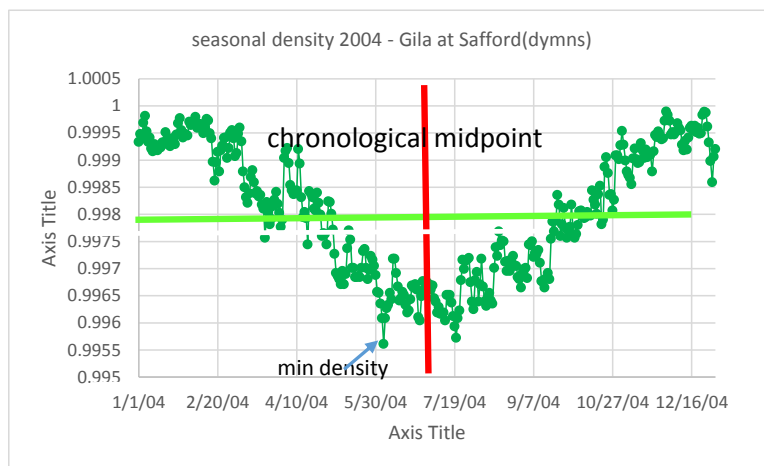


Figure 141

With the function(s) approach, it becomes necessary to make a distinction between a sample that is 'dilute' and a group of samples that are undergoing 'dilution' or becoming progressively more dilute – i.e. 'dilution' is both a noun and a verb, a relative state and a process. The confusion can

be dispelled somewhat by realizing that the functions here are relative to the season – a concentration(s) sample, for example, is a dilute (summer) sample among other dilute samples that are in the process of becoming more concentrated. The process is emphasized here over the state.

Only the dens/densdiff analysis is fully functional, the others are really ‘seasonal-functional’ with the seasonal label attached prior to the functional analysis. The confusion might have been alleviated with different labelling – winter(dil), summer(conc) – but the flow labels (exp(w), etc.) provided the template and it is too late to go back and re-label everything which would not, moreover, change any of the results.

Using the function(s) labels, the daily mean and grab sample densities can be evaluated.

function(s) values - density - Gila at Safford					
	averages/(kg/L)			counts	
	dymn(T)	grab(T)	grab(TSP)	dymn	grab
dilution(w)	0.9989	0.9990	0.9994	3534	48
dilution(s)	0.9968	0.9971	0.9976	3084	30
concentration(s)	0.9970	0.9969	0.9974	2997	47
concentration(w)	0.9991	0.9995	0.9999	3534	36

Table 87

The functions are listed in chronological order from top to bottom and summer (s) values are clearly lower than winter. The various functions seem to have fairly similar sample counts with a somewhat larger number of winter than summer samples.

It is at this point that the difference between the inner and outer sine curves really comes into play. A label like dilution(w) (or winter(dil), describing the time period and functional direction of the outer sine curve, actually covers both increasing and decreasing densities (of the inner curve). The averages have to deal not only with the numbers of differences going in a certain direction but also their magnitudes. A dilution(w) may include many low negative values and a few large positive values and the average may end up positive.

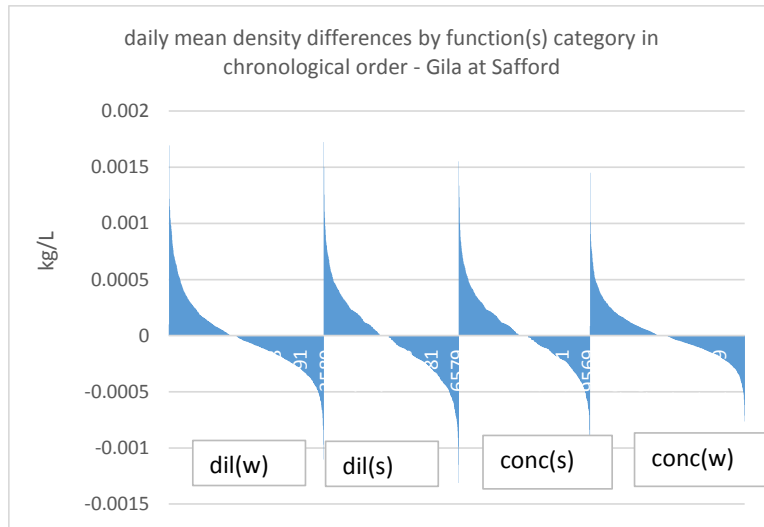


Figure 142

In the above graph, daily mean density differences are grouped by function(s) category and, within categories, are sorted from largest to smallest to separate positive from negative density change. The areas, which give the percent positive or negative, appear quite similar with only concentration(w) standing out as being a bit smaller and having a larger gap between negative and positive (zero density difference). Here are the numbers:

areas positive/negative density differences daily means (inner sine curve) - Gila at Safford				
	type	$\Sigma$ absdiffs	count	equal
dilution(w)	conc	0.24		
	dil	0.26	171	
dilution(s)	conc	0.29		
	dil	0.34	213	
concentration(s)	conc	0.29		
	dil	0.25	234	
concentration(w)	conc	0.17		
	dil	0.15	247	

Table 88

The averages for density difference come out, as might be expected from the even mix of types, in accord with the all data averages. Note that dilution is negative differences, concentration is positive differences. So the function(s) 'slice' of the system is one that aligns correctly with the regime designations which follow the annual curve.

function(s) values and differences of daily means/(kg/L) - Gila at Safford				
	values	cnt	differences	cnt
dilution(w)	0.9989	3534	-1.2E-05	3533
dilution(s)	0.9968	3084	-2.1E-05	3084
concentration(s)	0.9970	2997	2.1E-05	2997
concentration(w)	0.9991	3534	1.2E-05	3534

Table 89

Dividing up function(s) densities into molar volume difference inversion and non-inversion categories first, yields the following average values and differences. The function(s) approach yields both positive (inv) and negative (non-inv) differences in both dilution and concentration periods. The inversion analysis is picking up the ‘inner curve’ values within the annual curve.

function(s) daily mean density values and differences under partial molal volume inversion/non-inversion (kg/L) - Gila at Safford						
values			differences		counts	
	inv	noninv	inv	noninv	inv	non-inv
dilution(w)	0.9990	0.9988	2.9E-04	-2.0E-04	1376	2158
dilution(s)	0.9969	0.9968	3.0E-04	-2.5E-04	1272	1812
concentration(s)	0.9971	0.9969	2.9E-04	-2.0E-04	1357	1640
concentration(w)	0.9992	0.9991	2.1E-04	-1.4E-04	1531	2003

Table 90

Season still takes precedence over inversion/non-inversion for the values. The function(s) average differences are divided into dilution and concentration across all seasons by inversion analysis. As a result there are periods of dilutions with positive values and concentrations with negative values, the opposite of the functional direction for the season. Inversion at the function(s) level, produces an un-symmetric ‘cut’ that creates positive differences in dilution and negative differences in concentration regimes.

The function(l) (l for local) approach is exactly the same as in flow: “The function(l) analysis works backward and forward from each peak till the next (or previous) days” density “is higher. With so many peaks in the daily means there had to be some designations to cover overlapping from one local peak to the next or intervals with no peaks and those are the ‘valley’ and ‘steady’ groups below”. The following figure shows how the function(l) analysis assigns dilution and concentration.

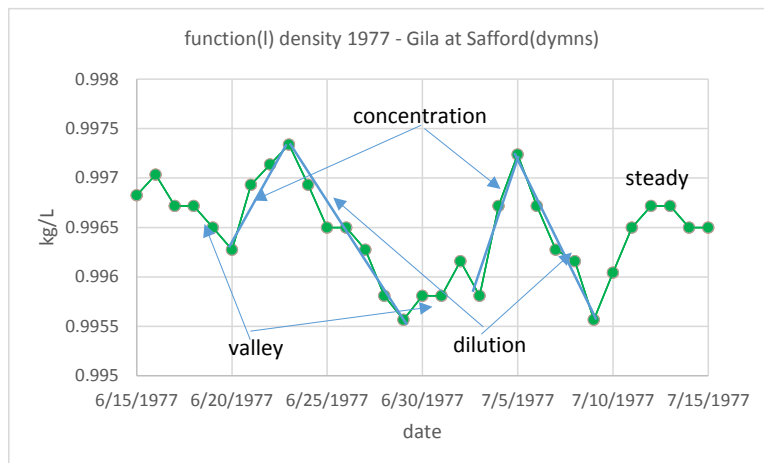


Figure 143

The function(l) approach is somewhat different in density than in flow because the context is different. Unlike flow, density does not present with long intervals of steady values interspersed with short bursts of pulses. Density is more of a constant pulsing and though there are higher



peak to valley drops in the spring than in the winter there are few 'steady' states and those there are of short duration.

The daily mean average values and differences under the function(l) approach have, like the function(s) approach, differences in line with the regimes of the annual curve.

function(l) density average values and differences/(kg/L) - Gila at Safford(dymns)				
	value	cnt	difference	cnt
dilution(w)	0.9990	2254	-1.7E-04	2254
dilution(s)	0.9969	1646	-2.4E-04	1646
concentration(s)	0.9970	2616	2.6E-04	2616
concentration(w)	0.9991	2940	2.2E-04	2940
steady	0.9981	874	6.3E-05	874
valley(s)	0.9967	1346	-2.4E-04	1346
valley(w)	0.9988	1472	-1.9E-04	1472

Table 91

Under inversion/non-inversion the daily mean function(l) density values are largely what would be expected. As with function(s), function(l) picks up both the positive and negative differences of the inner curve as opposed to the averages picture (to right below) of the annual curve.

function(l) density average values and differences under inversion /non-inversion (kg/L) - Gila at Safford(dymns)					func(l) avgs values
values	inv	cnt	non-inv	cnt	
dilution(w)	0.9999	13	0.9989	2241	0.9990
dilution(s)			0.9969	1646	0.9969
concentration(s)	0.9970	2435	0.9966	181	0.9970
concentration(w)	0.9991	2699	0.9991	241	0.9991
steady	0.9981	361	0.998038	513	
valley(s)			0.996653	1346	
valley(w)	0.9999	27	0.998806	1445	
differences	inv	cnt	non-inv	cnt	
dilution(w)	9.4E-05	13	-1.7E-04	2241	-1.7E-04
dilution(s)			-2.4E-04	1646	-2.4E-04
concentration(s)	2.9E-04	2435	-1.4E-04	181	2.6E-04
concentration(w)	2.5E-04	2699	-1.0E-04	241	2.2E-04
steady	3.0E-04	361	-1.1E-04	513	
valley(s)			-2.4E-04	1346	
valley(w)	6.6E-05	27	-2.0E-04	1445	

Table 92

What is new in the function(l) inversion process picture is that the seasonal distinction in values is beginning to blur a little and the preference for certain types is pronounced. Rather than simply an average value, the function(l) inversion analysis distinguishes preferred type by sample type count. In values, under inversion, concentration is the preferred type in both winter and summer, non-inversion prefers dilution. The differences split into positive and negative across all seasonal-functional groups and the inversion preference for concentration types, non-

inversion for dilution, is expressed in the counts. Inversion now represents concentration regardless of season while non-inversion represents dilution. The only apparent problem is the disappearance of dilution(s) samples under inversion for reasons not immediately apparent.

What follows is a summary of density values and differences from the all-data situation through seasonal/functional analysis to inversion/non-inversion process analysis. Grab(T) densities have been eliminated from all except the 'all-data' portion to keep the tables smaller and easier to read.

density statistics over all data/ (kg/L) - Gila at Safford						
	values		differences			
	dymn(T)	grab(T)	grab(TSP)	$\Delta$ dymn(T)	$\Delta$ grab(T)	$\Delta$ grab(TSP)
average	0.9980	0.9982	0.9986	-3.0E-08	-1.4E-05	-1.6E-05
median	0.9982	0.9985	0.9989	-1.8E-05	-6.7E-05	-1.4E-04
mode	0.9992	0.9996	N/A	0.0E+00	0.0E+00	N/A
min	0.9945	0.9948	0.9953	-1.3E-03	-3.2E-03	-3.1E-03
max	1.0000	1.0000	1.0006	1.7E-03	3.8E-03	4.5E-03
stdev	0.0012	0.0014	0.0014	3.1E-04	1.4E-03	1.4E-03
count	13149	161	161	13148	160	160

Table 93

average density values/ (kg/L) using different analysis methods - Gila at Safford								
values	dymn(T)				grab(TSP)			
	month	season	funct(s)*	funct(l)*	month	season	funct(s)*	funct(l)*
hidens(w)	0.9992	0.9990	0.9991	0.9991	0.9998	0.9996	0.9989	0.9997
			0.9989	0.9990			0.9994	0.9995
lodens(s)	0.9972	0.9969	0.9970	0.9970	0.9978	0.9975	0.9974	0.9978
			0.9968	0.9969			0.9976	0.9974
rel std. dev								
hidens(w)	0.0003	0.056	0.053	0.053	0.0003	0.065	0.052	0.065
			0.057	0.057			0.066	0.063
lodens(s)	0.051	0.068	0.062	0.067	0.001	0.101	0.105	0.076
			0.073	0.067			0.096	0.094

\* = concentration/dilution

Table 94

The distinction between high and low density is apparent at the seasonal level and does not change significantly with functional analysis. Grab(TSP) values are higher than daily means across the board, as expected. The relative standard deviations for density values remain fairly constant, a little higher for grabs than daily means but mostly all in the same ballpark and very low.

It is with the differences (below) that the advantages of narrowing the field for averaging become apparent. A tighter context produces larger differences. This outcome can be seen in the table by scanning the daily mean differences in the order suggested by the blue arrows, with the tip of the arrow towards higher values. There is a difference of three orders of magnitude in the daily mean differences from  $E^{-7}$  to  $E^{-4}$ .

daily mean density differences under different analysis methods - kg/L - Gila at Safford

difference	monthly	seasonal	func(s)*	func(l)*
hidens(w)	5.40E-07	1.90E-07	1.20E-05 -1.20E-05	2.20E-04 -1.70E-04
lodens(s)	1.60E-07	-2.90E-07	2.10E-05 -2.10E-05	2.60E-04 -2.40E-04
relstddev				
hidens(w)	1150	144331	1878 -2633	112 83
lodens(s)	4952	116584	1521 -1692	101 75

\* = concentration/dilution

Table 95

Even more dramatic and possibly more significant is the lowering of relative standard deviations. The astronomical values for daily mean seasonal relative standard deviations are a result of dividing a very small number (the standard deviation) by another very small number (the average difference). Narrowing the field for averaging both decreases the standard deviations (the numerator in the relative standard deviation equation) and increases the average difference (the denominator) both of which contribute to making the relative standard deviation a smaller number. To explicitly grind out the numbers, here are the numerical inputs for seasonal and function(l) relative standard deviations.

grinding out the numbers (rel std dev calc)

	seas-hidens(w)	func(l)-hidenavg
stdev(numerator)	2.74E-04	2.80E-05
avg(denomintor)	1.90E-07	2.50E-05
rel std dev	144331	112

Table 96

Inversion analysis yields consistent, higher difference averages and consistent, lower relative standard deviations all in one step. It thus sidesteps the question, first posed by the instantaneous/average value dichotomy: what is the most meaningful time span for averaging? It assumes that the time interval used in inversion analysis is meaningful and there are no inconsistencies or anomalies to suggest otherwise. Only viewing the process in a different time-frame will raise that question. More to follow.

daily mean average density differences using different analysis methods and inversion									
non-inversion - kg/L - Gila at Safford									
differences	inversion				non-inversion				
	monthly	season	function(s)	function(l)	monthly	season	function(s)	function(l)	
hidens(w)	2.1E-04	2.5E-04	2.1E-04	2.5E-04	-1.5E-04	-1.7E-04	-1.4E-04	-1.0E-04	
			2.9E-04	9.4E-05			-2.0E-04	-1.7E-04	
lodens(s)	3.1E-04	3.0E-04	2.9E-04	2.9E-04	-2.3E-04	-2.3E-04	-2.0E-04	-1.4E-04	
			3.0E-04				-2.5E-04	-2.4E-04	
abs rel std									
hidens(w)	88	95	91	94	83	88	90	126	
			93	100			82	82	
lodens(s)	82	82	82	83	85	87	90	149	
			83				84	78	
*concentration/dilution									

Table 97

The average daily mean density values and differences for the various seasons on the Gila River at Safford can now be identified with very 'tight' (precise) numbers. These are the function(l) values and the inversion/non-inversion differences both of which have relatively low relative standard deviations. The only fly in the ointment is that explaining how these numbers were arrived at, given the numerous assumptions and 'guesstimates' made along the way, may take a while.

The winter hi-density season on the Gila usually begins in October, only once in September and once in November in the analysis here. It typically lasts 190 days but can be as few as 85 or as many as 227. The average winter density is 0.9990 +/- 0.00056 kg/L (kg/L=gr/ml). The average day to day difference in winter density is 1.9E-7 +/- 2.7E-4. Inversion/non-inversion differentiation yields a day to day inversion difference of 2.5E-4 for concentration, 9.7E-5 for dilution while non-inversion concentration and dilution are both around -1.0E-4.

The summer lo-density season is shorter with a shorter range as well, average 165 days, min 129 max 189. It begins either in April or May with about as many starts in one month as the other. The average seasonal summer density is 0.9969 +/- 0.00068 kg/L. The average day to day difference in summer density is -2.9E-7 +/- 3.4E-4. Inversion/non-inversion differentiation yields a day to day inversion difference of -2.9E-4 for concentration periods, while non-inversion varies from -1.4E-4 to -2.4E-4 kg/L. In both seasons, inversion/non-inversion analysis not only separates positive from negative density change but lowers the relative standard deviations from astronomical numbers to around the same value as the difference itself (100%).

The appearance of April and October as pivotal dates is probably a function of the annual change in density just as January and July are the months of max winter high and min summer low flow periods respectively. Flow amplitudes are at their max in Jan and min in Jul but the total relative and partial molar volume lines of the low flow analysis cross in April and October. So there are general points of correspondence between flow and density patterns but they depend largely on the data used and scaling of the graph. These are, at best, circumstantial but continued scrutinizing of these points of contact may lead to new, more fundamentally meaningful ties.

The 'inversions' found to this point, whatever view is used to find or evaluate them, fall into two groups that seem quite distinct the one from the other. Major ion concentration inversion is a flow related process that involves a difference in groups of inputs during certain flow periods.

Molar volume inversion is a density related process that involves changes in a system in more or less constant flux. Eventually the question of whether these two types of inversion have any connection will have to be answered. That will be done after the energy patterns of the system have been examined.

Before continuing the analysis with the thermodynamic functions, there is type of energy relation that needs to be considered first for completeness – namely the overall mechanical energy of the control volume in time and space. The following graph shows the kinetic ( $1/2mv^2$ ) and the potential (mGdh) energy of the control volume in 1977.

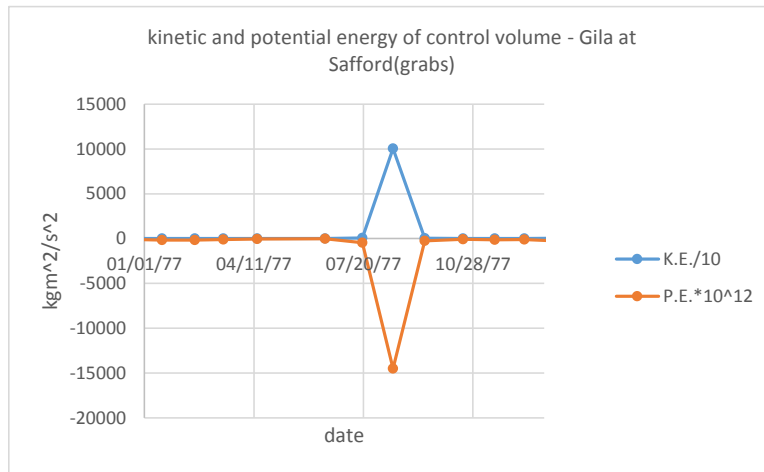


Figure 144

The correlation between kinetic and potential energy are quite high and, significantly, so are those with flow but not with density. What the peaks of K.E. and valleys of P.E. correspond to are periods of maximum conversion of potential to kinetic energy (that is, high flow).

correlations mechanical energy control volume with flow and density - Gila at Safford (grabs)				
	K.E.	P.E.	flow-grab	dens(TSP)-grab
K.E.	1.00	-0.99	0.97	0.14
P.E.	-0.99	1.00	-0.99	-0.17
flow-grab	0.97	-0.99	1.00	0.20
dens(TSP)-	0.14	-0.17	0.20	1.00
pair counts (all)		161		

Table 98

Since the external energy is related to flow, it seems it might also be related to major ion concentration inversion. That, however, does not appear to be the case. There are 42 KEpeak/PEvalleys pairs and 53 major ion concentration inversions but only 28 examples occurring on the same date. Since the connection here would presumably be causal, anything less than 100% disproves the idea entirely.

It may be wondered why density is even being evaluated here. The reason is that this study is an ‘exploration’ of a dataset rather than a summary of established fact. Things were still being discovered and ‘worked out’ (or not) as it was being written. And it is always a good idea to check relations even when it is fairly certain there is none: it is always possible to be surprised.

The internal energies too are highly intra-correlated and highly correlated to flow. Here the total thermodynamic functions are used, H or enthalpy, S or entropy, and G or free energy to represent the internal energy. These are calculated by the amount (number of moles) times the molar functions (dHm, dSm, dGm). The amount of water is so overwhelmingly large in comparison with that of any or even all of the lesser constituents that it totally dominates the solution. What follows are the total thermodynamic functions for water, as a surrogate for the solution, using the standard functions of formation for water from the CRC.

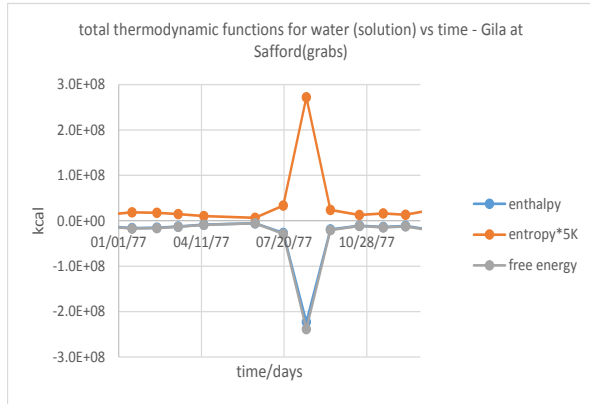


Figure 145

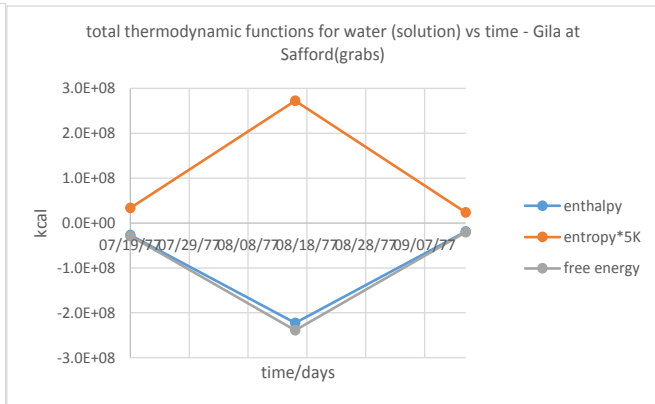


Figure 146

The correlations are high and bring out the circular nature of the calculations but the connection to flow (via amounts) is 'real.'

correlations thermodynamics functions of water (solution) with flow and density - Gila at Safford(grabs)					
	enthalpy	entropy*5K	free energy	flow-grab/cf	dens(TSP)-grab/(kg/L)
enthalpy	1.00	-1.00	1.00	-1.00	-0.20
entropy*5K	-1.00	1.00	-1.00	1.00	0.20
free energy	1.00	-1.00	1.00	-1.00	-0.20
flow-grab/cfs	-1.00	1.00	-1.00	1.00	0.20
dens(TSP)-grab/(kg/L)	-0.20	0.20	-0.20	0.20	1.00
pair counts (all)	161				

Table 99

The correlations between external and internal energy are quite high (below). There are 42 enthalpy/free energy valleys and 43 entropy peaks. There is already a 'problem' with a lone entropy peak with no corresponding enthalpy/free energy valley. Closer inspection of the offending date, 8/22/02, shows no obvious problems, just that the values differ only slightly than those of the following date, 11/3/02 – these are very small peaks and valleys. Other than that, KE/PE peaks and valleys line up perfectly with internal energy peaks and valleys.

correlations external and internal energy - Gila at Safford(grabs)					
	K.E.	P.E.	H	S	G
K.E.	1.00	-0.99	-0.97	0.96	-0.97
P.E.	-0.99	1.00	0.99	-0.99	0.99
H	-0.97	0.99	1.00	-1.00	1.00
S	0.96	-0.99	-1.00	1.00	-1.00
G	-0.97	0.99	1.00	-1.00	1.00
pair count:	161				

Table 100

The high correlations above would seem to suggest that the internal energies of the control volume have some relation to the external. But the accepted wisdom is that the external energy of the system as a whole has no influence on the internal energy. The reason is that the internal energy of the system is related to the internal degrees of freedom (rotational, vibrational, and electronic).<sup>13</sup> These are intrinsic aspects of the system not changed by changes in kinetic energy or gravitational potential of the system as a whole. For this reason, the accepted wisdom will be followed and the relations between external and internal will not be further considered. Only the internal energy changes are relevant to what is being looked at here – i.e. the internal changes in a system caused by the environment.

There is a serious consequence to these considerations. Nearly perfect correlations are being dismissed as irrelevant and, worse, are seen to be potentially misleading. This conclusion does not bode well for a study based largely on correlations. Which are meaningful and which are not? Does the answer lie in preconceived notions that lie outside the system description? Or is it possible to build up a structure of relations that support one another to such an extent as to be able to stand up on its own? That, of course, remains to be seen.

To further investigate internal energy patterns, the thermodynamic molar functions of formation for the aqueous ions were taken from the CRC (63<sup>th</sup> ed.) and other accepted sources (Lange's, Stumm, Hepler and Hovey, Wateq4f and Phreeqc datasets, Vemulapali, Atkins). Values for compounds of these ions were deduced with Hess' Law. Values from these accepted sources are the best numbers available, developed by authorities and rigorously checked and rechecked. Numbers taken from different sources, however, will have been developed with different experimental set-ups and calculated in different ways. Across parameters in the dataset used here there are undoubtedly mis-matches, one source may have a different number than another for the same factor. The thermodynamic values used here are a hodge-podge and may lack internal consistency at any number of levels.

To adjust for temperature, the equations  $dH_m = dH_m^o + C_p(T-T_o)$  and  $dS_m = dS_m^o + C_p \ln(T/T_o)$  were used where the small m denotes a molar function (for H, kcal/mol, for S, kcal/mol\*K) and the small o denotes the standard state temperature and pressure (STP). The heat capacities are considered constant, a reasonable assumption with the limited temperature range involved at Safford (grabs, 279-306 K). Free energy was calculated with  $dG_m = dH_m - TdS_m$  which is from the definition.

What follows is a review of basic thermodynamic theory. It is neither complete nor definitive. Instead it is an adaptation of some of the principles of thermodynamics to suit the needs of the analysis. Function meanings are kept as 'conservative', as close to text-book definitions, as possible. There is, moreover, an attempt to 'build up' the principles from the 'ground' to provide adequate 'motivation' for analysis procedures. But sometimes interpretation is needed if the analysis is to proceed at all and there is always a danger that the range of applicability of the laws will be exceeded. If the review seems a bit 'spelt-out' and repetitious at times, that's because the laws need to be tested in their new context to make sure they still 'sound right.'

The thermodynamic functions are all expressions of two things, heat and work, related by a common expression:

$$\Delta E(\text{energy}) = \Delta q(\text{heat}) + \Delta w(\text{work})$$

The first law thus stated sets up a proportional relation between a certain amount of work and a certain amount of heat, the so-called 'mechanical equivalent.' Work can be of many different forms, all of which can be represented generically as the lifting of a weight somewhere in the environment by a work-performing system. Work takes effort and ends when effort ends. But heat gain or loss does not necessarily end with work-related effort. Any work performing system needs to maintain a certain ratio of heat gain/loss to survive.

Entropy looks at changes in the system in order to ensure that work-related can be distinguished from system-maintenance heat loss/gain. The magic formula is  $dq(\text{rev}) = TdS$ . The way to ensure the boundary between the two types of heat loss/gain has not been passed to any great extent is to approach it gradually or 'reversibly.' The presence of the border is continually verified by passing back and forth across it. It turns out that the reversible process that guarantees that only work-related heat loss/gain is being considered also yields the max work that can be done by the system.

Adding the idea of reversibility and a generic definition of work with a sign convention to go with it results in

$$dE = TdS - pdV$$

Working in the definition of enthalpy  $dH = dE + d(PV)$  yields

$$= dE + d(PV) = TdS - pdV + pdV + Vdp$$

$$dH = TdS + Vdp$$

etc.

All the thermodynamic function differential equations can be derived from the first two equations which embody the first and second laws. The main problem in practice is either finding the equation that best fits the circumstances and available data (the 'student' approach) or manipulating the situation and/or the data and checking the fit with a particular equation (an 'experiment.').

Each of the partial molar thermodynamic functions has a specific meaning at the reaction level. The molar free energy, for example, shows whether a reaction, as written from left to right (i.e. reagents to products), can move spontaneously, at an indeterminate rate, towards equilibrium conditions ( $G_m = -RT \ln K$  where  $K$  is the equilibrium constant for the reaction). Equilibrium is the state of no (apparent) change, in which the rate of reaction in one direction (say product formation or to the right) is equal to the rate in the other direction (product dissociation or to the left).

The full differential equation for reversible change in free energy is the Gibbs equation:  $dG_m = -S_m dT + V_m dP$ . The last term is easily calculated being the volume times the difference in pressure (day2-day1) with L-atm of the parameters in this dataset converted to kcal to match the dimensions of the other term. It is the first term,  $S_m dT$ , wherein lie all the problems. The following is a discussion of the relations of entropy in different contexts and with different factors which can be used to handle the term operationally.



The universal imperative, first enunciated by Clausius, states that the 'energy of the universe is a constant but entropy tends towards a maximum'. The upshot is that spontaneous processes in closed systems can only raise entropy ( $dS \geq 0$ , the equality is for equilibrium conditions). The 'closed' system envisioned here is the (thermodynamic) universe. As 'everything,' it is so complete that nothing can be added to it (i.e. no inputs are possible). A number of alternate terms can be used to describe the 'universe': closed, complete, isolated, having non-permeable boundaries, functionally complete. Though 'complete completeness' was necessary as the starting point to develop them theoretically, the thermodynamic laws are really about functional completeness under a given set of circumstances.

There can only be one thermodynamic universe or the imperative falls apart. How would anyone ever know that a process in one universe didn't actually lower the entropy in another? Since the full extent of the universe is not known, how can it be used in analysis? To deal with this 'universe' and its relation to the real world, it is divided into two parts: a 'system' of interest and the 'environment' which is everywhere else in the universe other than the system. The 'environment' is just as nebulous as the 'universe' but that's not a problem because the interest is in its inter-action with the system (the difference it makes) not the extent of either. The 'environment' is, as far as anyone knows, an inexhaustible source of 'anything' and 'everything' that could possibly be needed by the system of interest.

The main thrust of the universal imperative is the maximization of positive entropy. Since  $\Delta S$  is always pushing toward a maximum, it is necessary to make sure that the heat loss or gain of the system corresponds to only the amount of work being considered and that is what  $q(\text{rev}) = TdS$  does. No matter how the entropy of a work performing system changes, the overall change in entropy of the universe must be positive or zero. Negative entropy change in a system is possible but it must be 'local' in time and/or space (i.e. the system must be smaller than the universe). It must be 'made up for' or 'resolved' by an input of positive entropy from some other part of the system or from somewhere in the environment outside the system.

The input must be 'large enough' to offset the negative and then a 'little more' to make sure the change in the universe stays positive. The argument here is beset by fuzziness – how much larger? what is 'a little' more? 'Infinitesimal' is usually highly recommended, particularly when it leads to a 'reversible' situation (i.e. a small change that results in a measurable change of direction). In a reversible situation, the answer to the question of 'how much' is in the context of back and forth change around an equilibrium position. In the real world, the question is open and it is much more difficult to determine where work-related heat loss ends and system maintenance heat loss begins.

A quick glance at the of grab sum solution molar entropies ( $dSm$ ) shows an average value of -0.45 kcal/K and a sum of -71.66 with 160 negative values and 1 positive. If the grab sample sum solutions are the 'system,' entropy is not 'resolved' at the grab sample level. But there is a problem here because it is not clear what the energy 'difference' is. For a function to be recognized as such it must produce some measurable change in the system. It must have a starting state, a change to another state, and an end point. For the cycle to be complete, the end

point must be a return to the original state to make sure the system has not flown off into another, a third state. The sign of completeness of the energy 'cycle' is the return to the original state.

The universal imperative applies at all levels of time and space but it may or may not apply at any particular time and place. Besides the consideration of whether the system under consideration is complete, the energy differences must make up a complete cycle. The completeness of the system is an intrinsic property of the system while the completeness of the cycle is a transitory property of the process which the analysis must capture. It is not known if a system and a cycle are complete until a complete analysis reveals that negative entropy has been resolved in a complete cycle.

Change in entropy is intimately related to volume change. The basic equation for the entropy of a perfect gas in free expansion under isothermal conditions is  $\Delta S = nR \ln(V_f/V_i)$ . If  $V_f > V_i$  the expression is positive, if  $V_f < V_i$ , the natural log of a ratio less than one makes the expression negative. Even with the multitude of conditions possible in the grab samples, total entropy most often follows the pattern of total relative volume with expansion equaling positive entropy. Since most substances expand when heated, the relation expansion = positive entropy, while not the only one possible, is most common. (Why this is so and a notable exception will be examined later when what entropy really 'is' is discussed – at this point we are dealing only with the relations of entropy with other factors and how it is dealt with operationally).

Things get more complicated with real gases. The quintessential free expansion gas experiment is that used to determine the Joule-Thomson coefficient. This experiment is the isothermal, isobaric, isenthalpic expansion of a gas into a vacuum –  $dH_m/dT = uC_p$ . (The traditional use of the word 'inversion' is the temperature at which a gas under these conditions goes from releasing to absorbing heat or vice versa).  $C_p$ , the constant pressure heat capacity, is related to entropy so that, at moderate temperature ranges,  $dS_m(T_2) = S^0_m + C_p \ln(T_2/T_1)$ . Here the sign of the temperature compensation portion is a combination of the log portion with the sign of the heat capacity. For parameters with positive heat capacity, entropy goes down when  $T_1 > T_2$  up when  $T_2 > T_1$ , for negative heat capacity parameters, entropy goes down when  $T_2 > T_1$  up for  $T_2 < T_1$ .

This equation brings heat into the picture which, in some ways, implies another, more 'virtual' type of volume change. In the quantum mechanical picture, the application of heat moves molecules (i.e. they expand into) higher energy levels. This interpretation leads directly into the view of entropy as a maximization of probabilities: ( $S = k \ln W$ , where  $W$  is the number of microstates and  $W$  maximum is the condition of equilibrium). Beyond this, and how it applies to non-equilibrium states, the reader is referred to textbooks on statistical thermodynamics, a subject that goes beyond the scope of this study.

The phrase 'the resolution of negative entropy' can have two meanings. The first is that a period of negative entropy can be 'resolved' over time when followed by an equivalent or slightly larger or longer period of positive entropy. The connection between the heat capacity and entropy opens up the possibility of a second meaning: negative entropy can be resolved by an input of heat to the system. The idea is that negative can be changed to positive entropy with positive enthalpy (heat gain by the system). Negative entropy is permitted to exist indefinitely if

simultaneously combined with positive enthalpy. Note that process direction is entirely temperature dependent, with no dependence on amount.

In the case of a solution, however, it is necessary to expand the scope of ‘the resolution of negative entropy’. It is important to remember that most of the time in this study we are not looking at entropy per se but ‘change in entropy’ – that is not ‘negative entropy’ itself but ‘a change in direction towards negative entropy’. The ‘entropy’ of the solution as a whole, which is not known, may be positive while the change in entropy from one point to another may be negative. Some species, when added to the solution, favor the positive while others favor the negative direction. If the change from one point to the next in sodium entropy increases solution entropy and the change in chloride decreases it then the two are inversely related and, if proportional in magnitude, cancel each other out. The end result is that solution entropy does not change. Note that here process direction depends on relative amounts at a single temperature and that the time can be assumed to be instantaneous. This interpretation does make an assumption of simple ‘additivity’ but it does make sense in the ‘ion affinities’ perspective.

Much of the rest of the analysis will be devoted to looking at different ‘views’ of the data to show the different ways in which negative entropy may be resolved. These ‘views’ will, with a couple notable exceptions, usually be of parts of a solution. But the resolution of negative entropy is only assured in the context of a complete energy cycle in a complete system. So the challenge is to fit the parts together in such a way that the response of the whole system can be deduced. To aid in putting the pieces together into a whole, a view of the system can be posited as complete and the various patterns of parts compared to it. Here there are two posited ‘complete systems’ – the sum solutions of constituents and water – neither is truly ‘complete’ but they provide a reference for comparison.

The ‘completeness’ of the system is important in how negative entropy is resolved. An input of heat causes in most materials a volume expansion. When the heat input ends and/or as a ‘recoil’ there is a contraction of volume. Since all emanations eventually dampen and die, each succeeding ‘pulse’ is smaller than the previous meaning that, over time, there is a slight residual of positive entropy. A ‘universe’ moves heat or material around within itself, resolving its own negative entropy over time. Most earthly systems require an input of heat (enthalpy) or amount of material with sum positive entropy to contribute from the environment, i.e. from outside the system.

Another thing touching entropy can be said, though it is often over looked in standard textbooks probably because it is considered too obvious. It is that the ‘somewhere else’ in the environment (outside the system) that provides the offsetting entropy must be contiguous and in physical contact. It is not expected that a drop in entropy on the Gila be ‘made up for’ by a rise in entropy on a river somewhere in China. This assumption comes from analogy with what is seen in mass-heat transfer. A cup of coffee on a hot plate will only be warmed if it is actually in close physical proximity i.e. on top of it. Furthermore, the rate of heat transferred is proportional, not only to the temperature difference, but also to the area of physical contact between the two.

The assumption of physical contact suggests another, related assumption that local negative entropy change is taken care of as quickly and as much at the same 'level' as possible. It is not expected that a negative entropy change involving a compound of arsenic be resolved by raising entropy of one of the major ions. There has to be a sameness of magnitudes, something sometimes referred to as the 'economy' of nature.

The resolution of S can be examined in its relation to free energy (G) via the relation  $\Delta G = \Delta H - T\Delta S$ . Mathematically, the equation works around the sign of entropy – if entropy is negative  $T\Delta S$  adds to enthalpy and free energy is positive, if entropy is positive and  $T\Delta S$  larger than H, free energy is negative. We therefore expect free energy to be usually negative at higher temperatures. Free energy is both a number indicating spontaneity and a (particular type of) heat content in kcals. The above equation is at the heart of the thermodynamic argument because it sets up a relation between an experimental result (H from a calorimetric analysis for example), the entropy state of the system (S), and a number that reconciles the two in kcals, (G). The relation is, again, based on the change in reversible heat content being equal to  $T\Delta S$  for a given amount of work.

The above equation is just one among several possible for free energy. It can also be calculated with  $dG^0_m = RT\ln(K)$  or  $dG_m = dG^0_m + RT\ln(a)$ , or  $dG_m = nFE$ . These calculations yield different numerical values and do not correlate with one another. They 'start' from different places and look at different dependencies. The calculation with activity ( $\ln(a)$ ) starts at the level at which the parameter is when the activity is taken and changes with change in activity. It yields values quite different from other equations some of which concentrate on temperature dependence only. All of the calculations are, however, ultimately reconcilable with each other should one wish to take the time and effort. In expanding on  $dG = nFE$ , Atkins<sup>11</sup> shows it to be equal to  $\Delta G_m = \Delta H_m - T\Delta S_m$  which is the form most used here.

There are rather too many options when all that is wanted is a quick and easy way to calculate free energy. Using the definition,  $G = H - TS$ , seems like a safe bet and plugging in the tabulated standard values seems like the right thing to do but  $dG^0_m = dH^0_m - TdS^0_m$  does not yield the accepted value for free energy at STP (standard temperature and pressure). While the  $X^0_m$  are the sums of the products minus the sums of the reagents for the reaction ( $\Delta X$ ),  $G = H - TS$  is interpreted as  $\Delta G = \Delta H - T\Delta S$  and  $\Delta S$  is not the tabulated value for molar entropy,  $dS^0_m$ .

A spreadsheet calculation showing how the equation is worked out for water, illustrates how  $\Delta S$  fits the standard values together.<sup>14</sup> Inputs, in blue, are the stoichiometric coefficients, the standard values of molar enthalpy and entropy, the latter bordering in red, and third law entropies of reagents. The inputs in blue are the data in the available dimensions and formulas do the calculations to keep all dimensions the same.

		H2 + 1/2 O2 = H2O							
		products	reagents					diff sums	
ΔH	stoich	1	0	1	0.5	0	0		
	kJ	-285.5	0	0	0	0	0	-285.5	
	kcal	-68.2726	0	0	0	0	0	-68.2726	
ΔS	stoich	1	0	1	0.5	0	0		
	J	70	0	130.6	205	0	0	-163.1	-0.1631 kJ
	cal	16.73935	0	31.23084	49.02238	0	0	-39.0027	-0.039 kcal
	kcal	0.016739	70.03223						
ΔG	kcal	0.0167							
									-236.872
								-56.644 -73.2635 (incorrect)	
T=								298.15	

Table 101

The values in the next to last column to the right are the sum of the products minus the sum of the reagents. The values for enthalpy and free energy are the tabulated standard values for enthalpy and free energy but the entropy number (-163 J) is not the tabulated molar entropy for water (70 J/mol\*K).

‘ΔG’ in this section, and others like it, will refer to free energy calculated with ΔS while ‘dGm’ refers to free energy calculated from dSm. Either free energy equation sets up a complete analysis – any one of the functions can be calculated from the other two with nothing left over or left out. But only the calculation with ΔS reconciles the three functions at STP (298 K, 1 atm) with one another. So the tabulated values, dG°m, are equal to ΔG not dGm. That is why the ΔG calculation is a ‘touchstone’ analysis and the value of dGm is labelled as ‘incorrect.’

Is the ΔS calculation a ‘zeroing out’ of the system maintenance entropies so that all parameter’s free energy calculations start out from the same place? It seems likely but the claim has not been examined for support in the literature. The ΔS as calculated above does, however, reconcile the standard values at STP. This statement was only actually verified for water. In most cases, Third Law entropies could not be found. In one case where all the numbers were available (AgCl3), the calculated ΔG did not agree with the tabulated value. This case is probably just due to inconsistency in the dataset and the assumption here is that the tabulated values (ΔG) come from a calculation with ΔS not dSm.

From the calculation above, it is seems obvious that ΔS will always be larger than dSm, with the difference being the Third Law entropies. A quick glance at the thermodynamic data dataset, however, reveals that there are 16 examples of absolute dSm larger than absolute ΔS. Since S or dSm subtract from G or dGm, one would expect dGm > ΔG but there are 17 examples of where that is not the case and they are not all the same parameters that have dSm > ΔS, Finally there are 15 examples of ΔG > ΔH which raises the question ‘how can the free energy, the max work available from reversible work, ever be greater than the total energy that can be converted to work?’

It is to be noted, in passing, that one of the first pieces of advice given to students using the thermodynamic values is that they verify the consistency of the dataset they are using. In this case, consideration of dataset consistency was about the last thing to be done. The initial response to that excellent advice was effectively ‘why?’ and ‘how?’ But when the dGm

calculation ran into the  $\Delta G$  calculation, the dataset was examined because of the implications for entropy change.

The Third Law entropies are, according to Atkins<sup>11</sup>, not exact due to the existence in samples at 0 K of random distributions of isotopes and should be considered ‘conventions’. The extent of variability is not known and is assumed not ‘large’ but it is transferred to  $\Delta S$  and from there to  $\Delta G$ . The probably slight variability in each of the two free energy calculations is, however, less important than the existence of a variable amount of entropy in one of them.

Free energy values reconciles enthalpy and entropy but different values of free energy may divide the influence of the two differently. There is, it seems, an uncertain proportion of entropy to enthalpy depending on the circumstances. The line between a certain amount of work and work-related heat gain/loss moves about in different cases. And the proportion, uncertain but constant for a given parameter, is variable between different parameters.

The above calculator can be used to determine  $\Delta S$  but, for a solution with many parameters, each with different reagents, involves quite a lot of work. If the values of enthalpy and free energy are known at any given temperature, however, entropy can be calculated as  $\Delta S = -(\Delta G - \Delta H)/T$ , en masse, without having to know the specific third law entropies involved. To examine its behavior over a wide temperature range,  $\Delta S$  was calculated at 298.15 with the standard values of enthalpy and free energy. Another point was needed and 0 K served the purpose. At 0K,  $\Delta S$  goes to zero in accord with the ‘Third Law,’ and  $\Delta G = \Delta H$ . A calculator was created with the standard values at 298 and making the free energy at 0K equal to the enthalpy. With these two points, the rest of the  $\Delta G$  values were determined with the slope between 298 and 0 and an intercept =  $\Delta H(0)$ . This procedure meets all the requirements but did not and could not produce the correct relation. With it,  $\Delta S$  is a constant so entropy, in effect, does not change. Just distributing enthalpy and free energy values equally between two points does not work. Even though the relation between the three functions is linear, the underlying relationship between enthalpy and free energy is not.

A better solution is to use the Gibbs-Helmsholtz equation,  $\Delta G/T = G^{(0)}/T - ((H/T^2 - G^{(0)}/298^2)*(T-298.15))$ . Times 1K is added to resolve the dimensional difference. This equation meets the requirements at 298 and 0K and gives a non constant  $\Delta S$  at each temperature. There is some strange behavior at the lower end of the relation with temperature for both  $\Delta S$  and  $dSm$  (left below). But the important thing is that, in the 279-306 K range encountered here, the two slopes are very small in magnitude and quite linear. The percent  $dSm$  of  $\Delta S$  (right below) is also a curious curve with  $dSm$  becoming an increasingly large proportion of  $\Delta S$  as temperatures rise.

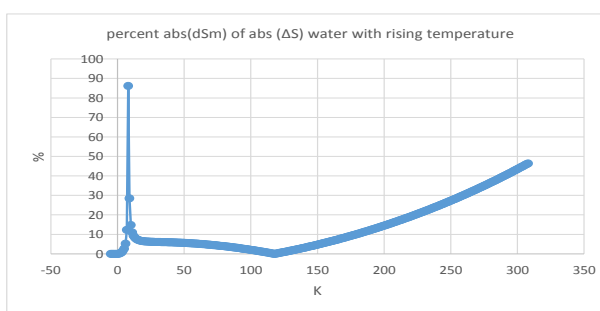
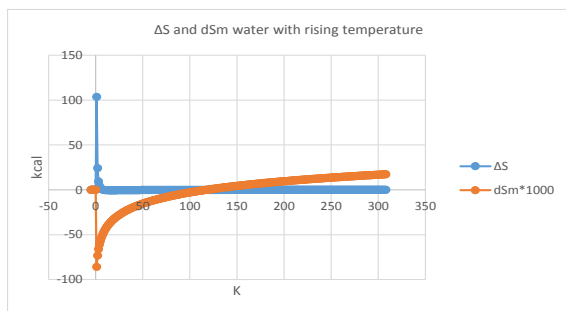


Figure 147

figure 148

The en masse calculation of  $\Delta S$  allows the free energy equation to be easily used on different parameters. How  $\Delta G$  changes depends on the relative magnitudes of H and  $T\Delta S$  and their signs.  $dH^{\circ}_m (= \Delta H)$  is usually negative (144 out of 157 parameters here) and larger than  $dS_m$  which is probably always smaller than  $\Delta S$ . There are different combinations but it all comes down to one thing – either entropy or enthalpy is driving the reaction. The table below works out the various combinations with a simple numeric example to verify conclusions.

relationship $\Delta G = \Delta H - T\Delta S$			
$\Delta H$ & $\Delta T\Delta S$			
	$\Delta H^-$	$\Delta H^+$	
$T\Delta S^-$	$\Delta G$	$\Delta G$	decr
$T\Delta S^+$	$\Delta G$	$\Delta G$	incr
			decr    incr
			$\Delta$ $\Sigma$
			$\Sigma$ $\Delta$
$absT\Delta S > abs\Delta H$		$abs\Delta H > absT\Delta S$	
	-1    1		-3    3
-3	2    4	-1	-2    4
3	-4    -2	1	-4    2
if $absT\Delta S > abs\Delta H$ then positive $T\Delta S =$ negative free energy entropy driven		if $abs\Delta H > absT\Delta S$ then negative $\Delta H =$ negative free energy enthalpy driven	
if $absT\Delta S > abs\Delta H$ if $T\Delta S > 0 =$ entropy driven else NS1            (not spontaneous) end if else ( $abs\Delta H > absT\Delta S$ ) if $\Delta H < 0 =$ enthalpy driven else NS2 end if end if			

Table 102

The labels  $absT\Delta S > abs\Delta H$  and  $abs\Delta H > absT\Delta S$  refer to the table structure, the  $dG$  results within the table are the result of placing the signed values of  $T\Delta S$  and  $dH$  into the equation. Because of the minus sign in the equation the H and  $T\Delta S$  expressions work inversely to one another. When both are increasing or both are decreasing the result is the difference, when they are going in opposite directions the result is the sum of their values. With these relations a test can be derived to identify entropy and enthalpy driven reactions and that is given at the bottom of the table.

The above test seems a bit more straightforward than that proposed by Atkins on p. 269 of his Physical Chemistry. There he uses the fundamental equation in the form  $-G/T = -H/T + dS$  and one has to struggle with whether the minus signs are from the function or the equation. If H is negative (exothermic reaction) then  $-H/T$  is  $H/T$  so, if  $dS$  is negative and larger than  $H/T$ , then the result is negative and equal to  $-G/T$  making  $G/T$  positive (non-spontaneous). If  $dS$  is positive,  $-H/T$  adds to it and  $-G/T$  is positive so  $G/T$  is negative (spontaneous-enthalpy driven). Similarly if H is positive (endothermic reaction) then  $-H/T$  subtracts from  $dS$ . If  $dS$  is positive and larger than  $-H/T$  then  $-G/T$  is positive so  $G/T$  is negative (spontaneous-entropy driven). If  $dS$  is negative, then the two add and  $-G/T$  is negative so  $G/T$  must be positive (non-spontaneous). But the two tests come to the same thing: note that  $-dG$  (magenta in the boxes) is a result of either positive  $T\Delta S$  or negative  $dH$ .

Recourse is had here to the reaction level meaning of negative free energy being the sign of a spontaneous reaction. This relation is explained with the equation  $dG = RT\ln(Q)$  where  $Q$  is the so-called 'reaction quotient.'  $Q$  is basically a ratio of the concentrations of products and reagents. More exactly, it is the product of the concentrations of the reaction products to their stoichiometric coefficients divided by the product of the concentrations of the reagents to their coefficients in any given circumstance.  $K$  is the reaction quotient at the point at which equilibrium has been reached. If the denominator of  $Q$  (reagents) is greater than the numerator (products), the natural log makes the whole expression negative and the reaction proceeds spontaneously toward the formation of products until  $Q = K$ . If the numerator is larger than the denominator, free energy is positive and the reaction is not spontaneous in the left to right direction as written.

The magnitude of free energy indicates only the ability to change spontaneously and says nothing about the speed of change. Rising temperature always speeds up reactions (roughly 10x for every degree C according to the Arrhenius principle) but effects spontaneity variously through the changing inter-relations among the thermodynamic functions.

$dH$  and  $T\Delta S$  were calculated for each major ion and  $H_2O$  using the standard values of formation from 0 to 308K. How the function relations play out with rising temperature depends in part on the sign of the heat capacity. The following graph shows the temperature compensation portion of the enthalpy ( $C_p*(T_2-T_1)$ ) and entropy ( $C_p*\ln(T_2/T_1)$ ) calculations for  $H_2O$  (positive  $C_p$ ) and  $HCO_3$  (negative  $C_p$ ). As expected, heat content (enthalpy) and entropy of water have a positive slope with rising temperature while with  $HCO_3$  they have a negative slope. They all meet at 298.15, the temperature difference reference point ( $T_1$  above).

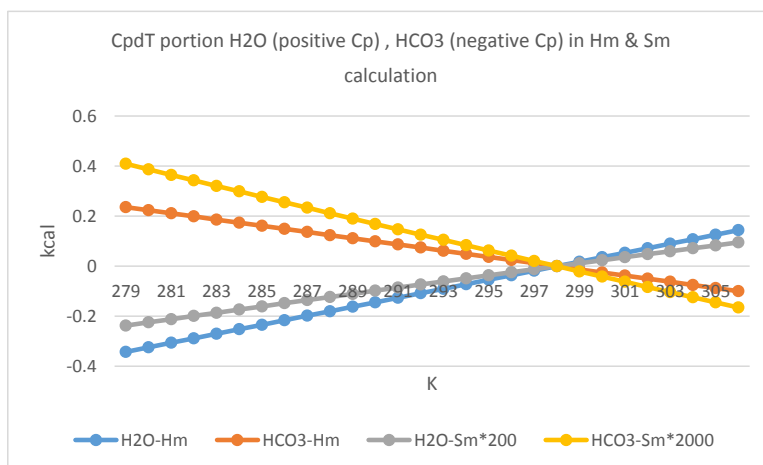


Figure 149 [\(back\)](#)

While the slope of the heat content function is determined by the sign of the heat capacity, whether the values are negative or positive is determined by the sign of the standard value. The temperature compensation portion of the equation is usually a small factor added or subtracted to the standard value. In the views below the parameters go to their standard values, rather than zero, at 298. Through the interplay of entropy and enthalpy, two parameters, one with negative



heat capacity the other positive and therefore heat loss and heat gain with rising temperature respectively, can both have (numerically) decreasing free energy.

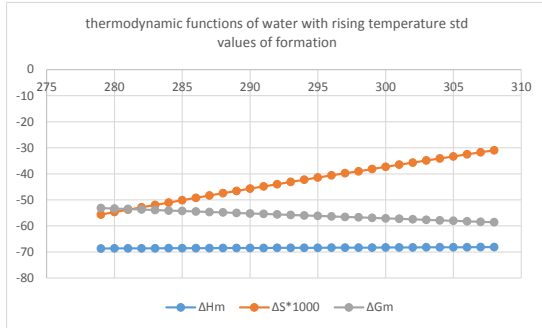


Figure 150

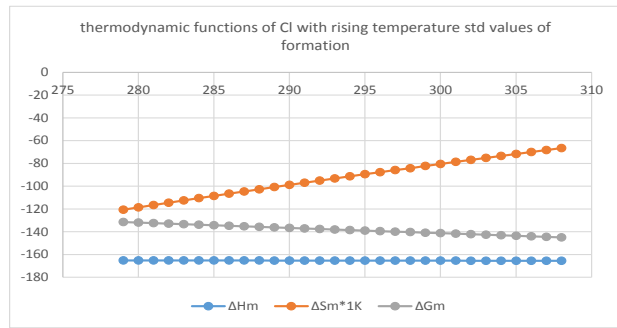


Figure 151

	change in thermodynamic functions with rising tempe std vals		
	$dHm = \Delta H_r$	$T\Delta S$	$\Delta Gm = dGm$
H2O	incr	incr	decr
HCO3	decr	incr	decr

Table 103

In some cases the values and the overall change is very small so residuals are used to make them visible and the table makes the direction explicit. The X(m)/T results of the G-H equation have been multiplied by the temperature because X(m)/T can have a different slope than X(m). The original free energy and enthalpy data for the graph are negative numbers. Free energy, however, increases in a negative direction (i.e. a larger negative number) which is termed a ‘functional’ increase.

The following reasoning applies when the standard values of enthalpy and free energy are negative numbers. Negative enthalpy, or rather ‘heat content,’ increases when its absolute value becomes smaller – i.e. when it becomes a smaller negative number which is to say it increases in a positive direction. This interpretation is in line with the convention that heat gain from the environment is positive. Less heat-loss is heat-gain.

Free energy, on the other hand, increases when its absolute value becomes larger – i.e. a larger negative number which is to say it ‘increases’ in a negative direction. So the negative slope of the dGm curve on the graphs above, which means a larger negative number, really represents a increase in free energy. Numeric increase/decrease was determined by a simple slope calculation but while a negative slope means decreasing enthalpy/entropy, it means increasing free energy. No slopes, correlations, or relations were reversed: the ‘functional’ direction correction will always be explicitly identified.

One may wonder how all the functions can be increasing when the fundamental relation between them is inverse:  $dG - dH = -T dS$ . Part of the reason is that slopes change magnitude and direction depending on the temperature range chosen. Below shows the thermodynamic functions of water over the extended temperature range 0 – 500 K.  $dH$  is a slightly increasing but consistently linear function,  $TdS$  and  $dG$ , however, are nonlinear and change slope around 50K. Slope directions and function correlations are shown in a table below the figure. Note that overall the inverse relation among the functions is maintained but in different ways depending on the slopes. The inverse relation disappears only when free energy is ‘flipped’ to make all the functions increase in the same direction. The rest of the discussion in this section and other similar sections deals exclusively with slope directions (numeric or functional) not correlations.

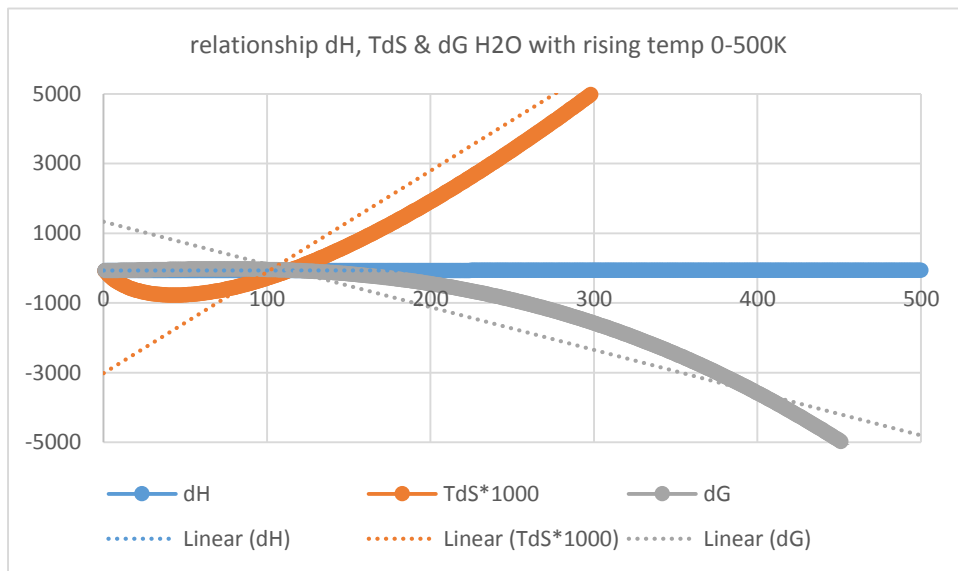


Figure 151.5

slopes and correlations H2O at two temp ranges				
slopes	$\Delta H_m$	$TdS*1000$	$\Delta G_m$	
0-50K	0.018	-11.9	0.867375	(H,G/S)
279-306K	0.018	0.848647	-0.18799	(H,S/G)
correls	H&TdS	H&G	G&TdS	
0-50K	-0.9005	0.998185	-0.88068	invTDS
279-306K	0.999683	-0.99997	-0.99967	invG

Table 103.5

The Wateq4f program uses thermodynamic values of reaction in the aqueous phase. This set was also used at times in this study, except for the case of water which is not defined in the reaction

in the aqueous phase. Using reaction in the aqueous phase dataset gives a quite different picture of the relations between  $\Delta H$  and  $T\Delta S$ .

The reaction in the aqueous phase reference values of  $H^{\circ m}$  and  $S^{\circ m}$  of the major ions, except  $HCO_3$ , are zero so using them is like using only the temperature compensation portion. If the non-zero reference value parameters are analyzed with their corresponding values of reaction in the aqueous phase, the result is that 58 out of 100 of them have  $298 \cdot dS_m$  greater than  $dH_m$ . But when dealing with  $\Delta S$  things become more complicated.

The following graphs show the relations of the thermodynamic functions for Na and Cl when reaction in the aqueous phase values are used. Na has a positive heat capacity while Cl a negative. The increasing slope of Na free energy indicates a decrease in free energy, just the opposite for Cl in line with the reasoning above. When the free energy value is greater than zero, the reaction is not spontaneous no matter what the magnitude or direction of the slope. This picture clearly shows how ‘complementary’ Na and Cl are, something that is presumably more important when they are ‘dominant’ in the solution.

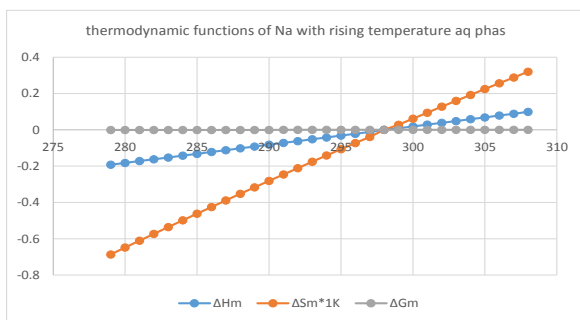


Figure 152

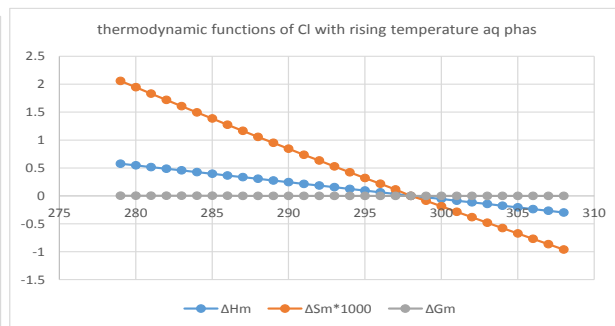


Figure 153

change in thermodynamic functions with rising tempe			
aq phas			
	$dH_m = \Delta H_r$	$T\Delta S$	$\Delta G_m = dG_m$
Na	incr	incr	incr
Cl	decr	decr	decr

Table 104

The following table summarizes the relations among the thermodynamic functions using both standard values of formation and reaction in the aqueous phase and adds some defining tests. The reactions being considered are, in the standard values view, the formation of water or the ions, in the reaction phase view, the formation of the aqueous forms of the ions. Slope directions are now indicated with +/-1 rather than ‘incr’ or ‘decr’ except for functional G for emphasis. The standard values of formation picture (top) is divided from the reaction in the aqueous phase picture (bottom) with parameters other than  $H_2O$  in corresponding order.

major ion and water thermodynamic functions with rising temperature									
std vals	H2O Na Cl Ca Mg HCO3 SO4	sign slope**, correl with T			functional relations	$\Delta H > T\Delta S^{**}$	$dG > dH^*$	$T\Delta S > S\Delta T^*$	
		$\Delta H$	$T\Delta S$	$\Delta G$ funct $\Delta G$					
	H2O	1	1	-1 incr	H,S,G	$\Delta H$	-S(h)	$T\Delta S$	
	Na	1	1	-1 incr	H,S,G	$\Delta H$	-S(h)/+S(g)	$T\Delta S$	
	Cl	-1	1	-1 incr	G,S/H	$\Delta H$	-S(h)	$T\Delta S$	
	Ca	-1	1	-1 incr	G,S/H	$\Delta H$	-S(h)/+S(g)	$T\Delta S$	
	Mg	-1	1	-1 incr	G,S/H	$\Delta H$	-S(h)/+S(g)	$T\Delta S$	
	HCO3	-1	1	-1 incr	G,S/H	$\Delta H$	-S(h)	$T\Delta S$	
	SO4	-1	1	-1 incr	G,S/H	$\Delta H$	-S(h)	$T\Delta S$	
aq phas	Na	1	1	-1 incr	H,S,G	$\Delta H/NS2$	-S(h)/+S(h)	$T\Delta S$	
	Cl	-1	-1	-1 incr	H,S/G	$NS2/\Delta H$	+S(h)/-S(h)	$T\Delta S$	
	Ca	-1	-1	1 decr	H,S,G	$NS2/\Delta H$	+S(h)/-S(h)	$T\Delta S$	
	Mg	-1	-1	1 decr	H,S,G	$NS2/\Delta H$	+S(h)/-S(h)	$T\Delta S$	
	HCO3	-1	1	-1 incr	G,S/H	$T\Delta S$	+S(g)	$T\Delta S$	
	SO4	-1	-1	1 decr	H,S,G	$NS2/\Delta H$	+S(h)/-S(h)	$T\Delta S$	

\*\*slopes 279-308K

\*\*tests 5-308K

\* abs vals

Table 105 [\(back\)](#)

The way the thermodynamic functions are related to each other (column 7) follows from their correlation to temperature. The functional relations are derived from the slope directions (279-308K) of enthalpy, entropy and functional free energy to the left. There are two combinations in the standard values view, either H,S,G or G,S/H. H,S,G is predominant in the aqueous phase view, only bicarbonate and Cl are different (G,S/H) and (H,S/G) respectively. When all three are not directly related, entropy is directly related to free energy and inversely related to enthalpy or directly to enthalpy, inversely to free energy. These combinations will appear again under different circumstances and at different levels of the analysis.

The tests in the last three columns, as do the slopes, ignore results around 0 K. In the standard values of formation view, all the parameter reactions are enthalpy driven and show increasing (functional) free energy with rising temperature. In the reaction in the aqueous phase picture, most of the major ions are non-spontaneous at lower temperatures, enthalpy driven at higher. The non-spontaneous/enthalpy switch temperature is the same as the negative to positive entropy switch temperature – 298.15. The exception are Na, which is enthalpy driven at lower temps, non-spontaneous at higher, and HCO3 which is entropy driven at all temps considered here.

The last column shows the results of a test that turned out to be largely uninteresting:  $T\Delta S > S\Delta T$  predominates above 5 K,  $S\Delta T > T\Delta S$  only appears sporadically around 0K. The next to last column relates the sign of entropy to whether abs G or abs H is higher. The ions in standard values view all show enthalpy representing negative entropy at lower temps to which the cations add on a stretch of positive entropy from higher free energy at higher temps. HCO3 is unique in having positive entropy coming from free energy at all temps. Do these relations set up a link between HCO3 and Na, across the poles of the inversion, as well as with Ca & Mg, within the inversion?

The fact enthalpy and free energy ‘increase’ in different directions, the one positively as heat gain the other negatively as a larger negative number, makes for another test for monitoring change in entropy. The various possible combinations are worked out below with a simple numeric example for verification.

relationship (H-G)/T			
$\Delta H$ & $\Delta G$			
	$\Delta H-$	$\Delta H+$	
$\Delta G-$	$\Delta S$	$\Delta S$	
$\Delta G+$	$\Delta S$	$\Delta S$	
			decr      incr
			$\Delta$ $\Sigma$
			$\Sigma$ $\Delta$
$abs\Delta G > abs\Delta H$			$abs\Delta H > abs\Delta G$
	-1	1	
-3	2	4	
3	-4	-2	
			-3      3
			-1      -2      4
			1      -4      2
if $absG > absH$ then negative free energy = positive entropy		if $absH > absG$ then positive enthalpy positive entropy	
<pre> if <math>absG &gt; absH</math>   if <math>G &lt; 0</math> = positive entropy   else, negative entropy1   end if else (<math>absH &gt; absG</math>)   if <math>H &gt; 0</math> = positive entropy   else, negative entropy2   end if end if </pre>			

Table 106

When enthalpy and free energy are increasing or decreasing both together, the result is a summation of their absolute values. When one is increasing and the other decreasing, the result is a difference. The differences flip sign when  $dG > dH$  or  $dH > dG$ . This difference of differences makes for an easy test to determine if entropy is positive or negative. If  $absG > absH$  then negative free energy means positive entropy, else if ( $absH > absG$ ) positive enthalpy means positive entropy. In the table above, the notation under the  $dG > dH$  column header denotes only the sign of  $T\Delta S$  and the source, not whether it is increasing or decreasing with temperature.

The relations above are for individual formation reactions seen at two different perspectives. The relations of interest here are those of a solution in which they are all going on at the same time. Most, but not all, of the major players are here. The cumulative result predicted for the solution, given the weights seen in the table above, will be that, in the standard values view, free energy largely increases with rising temperature but mostly splits in the reaction in the aqueous phase view: three increasing (Na, Cl,  $HCO_3$ ) and three decreasing (Ca, Mg,  $SO_4$ ),

But why calculate these functions at all if what they 'mean' at the solution level is not known? Solution total free energy is probably **not** anything quite as simple as 'something the solution seeks the lowest possible value for in order to come as close to equilibrium as possible'. The analogy between the reaction and solution level is quite possibly a faulty one. On the other hand, it is not unreasonable to assume at least a general sameness of function between reaction and solution levels and that is what will be done here. We form our notions, rightly or wrongly, of what to expect at the solution level by what we see at the reaction level.

Using the thermodynamic functions to analyze a solution, where many reactions and physical inter-relations are going on simultaneously, is, it seems, fraught with danger. The

thermodynamic functions of the solution are, undoubtedly, not anything quite as simple as the solution sum of the thermodynamic functions of all its constituents. There are apparently problems, possibly similar in nature to those involving ideal and real gases, in going from reaction to solution level. Authorities on the subject make use of 'mixing rules' and a variety of 'excess' functions to cover 'non-ideal' behavior, both of which are much too involved for the present discussion. Vemulapalli presents a fairly simple equation that can be used for complex, open systems but is careful to note that it applies only to reversible processes. <sup>15</sup>

Nonetheless simple sum solutions of constituents will be used here. The emphasis will therefore have to be on parts or aspects of the solution, their relative importance and interrelations, to set up a web of patterns rather than to attempt to calculate a single number for the whole solution. The scope of analysis will be further limited by using averages and differences of percents or percents of total differences. This is all well and fine, but dealing with parts of a system is not the same as dealing with a complete system and it may take different 'views' to find the balance being sought for.

Two major assumptions have been made and need to be underlined due to their importance in the rest of the analysis: the thermodynamic functions have the same general function in solution that they have at the reaction level and the simple sum solution of constituents is an adequate representation of the solution as a whole. Both these assumptions are necessary to allow the analysis to continue but neither should be accepted wholesale and they will be tested as the analysis proceeds.

The identification of enthalpy and entropy driven reactions will not be a major part of the ensuing analysis. That is, in part, because inversion is not a chemical reaction it is a relation. The thermodynamic laws apply to relations, phase change is often used as an example, but they are not usually characterized as enthalpy or entropy driven. Instead they are investigated in terms of change in free energy with the resolution of negative entropy understood.

The inversion relations involve changes in activity and therefore free energy which balances enthalpy and entropy. But the resolution of negative entropy will be examined not through calculations but primarily visually. The inversion relations will be put into the context of a complete energy cycle and presented as patterns on a graph. The interest here is in the parameters existing in solution (the products) at the time of inversion and the energy they bring to or take out of the solution, not in their formation from the elements.

For most of the rest of the analysis  $dS_m$  or  $\Delta dS_m$  will be largely used rather than  $\Delta S$ . The main reason is that  $\Delta(\Delta S)$  cannot be resolved from the free energy equation. That is to say,  $G_2 - G_1 = (H_2 - T_2 S_2) - (H_1 - T_1 S_1)$  cannot be expressed in terms of differences because  $T$  &  $S$  cannot be separated ( $T$  would but  $T_2$  and  $T_1$  do not factor out leaving  $(S_2 - S_1)$ ).  $\Delta dS_m$ , however, is an indicator of the molar function response to temperature that has a consistent relation to enthalpy and free energy. So the values for entropy will be different and, while the three functions can be calculated the one from the others, they do not give the correct standard values at 298. The loss in completeness of analysis is made up for the increased clarity of focus on the temperature dependence of the function of interest.

The discussion of the energy of the system has, to this point, been in terms of the relations of the thermodynamic functions with each other. These relations could apply anywhere at any time if the complete system and complete cycle requirements are met. The only temperature dependence seen to this point is the effect of rising temperature not the actual patterns of temperature change at Safford.

The two major patterns of temperature change are the daily and the seasonal. Hourly temperatures were not found and so a hypothetical daily temperature curve is developed and the 8/16/77 result is shown below left. The annual or seasonal pattern, shown for 1977 to the right, is the inverse of the annual density curve already seen. There is an ‘inner’ curve within the annual, similar to and the cause of the inner density curve, and the daily curve is an ‘inner-inner’ curve within that.

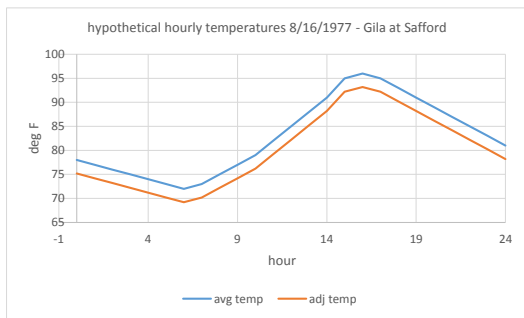


Figure 154

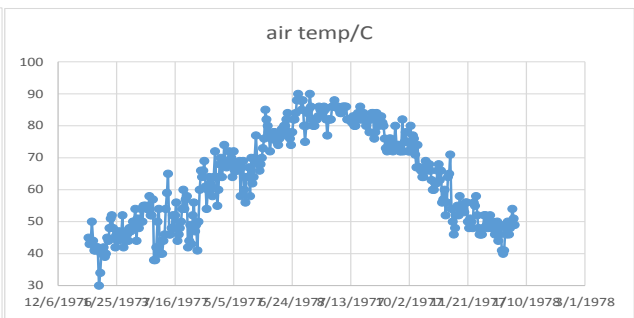


figure 155

There are several water temperature ranges and differences that come up repeatedly. The average absolute difference between two grab samples is about 5.8K while the absolute difference between two daily means is about 1.2K. The latter is a solid physical number denoting the day to day water temperature difference of the average. The former is the difference of instantaneous water temperatures taken at largely random times of the day and sampling intervals. The difference of absolute monthly average temperatures of the grabs is about 3.1K, a little less for the daily means at about 2.5 K. With averaging, the grab differences ‘settle down’ to close to the daily mean difference but the variability of the former remains much higher than that of the latter.

The overall average daily temperature range is around 13 +/- 3 C. This value can be compared to the 12.9K difference of daily mins and maxs derived from the SRA temperature dataset (all dates, 1976-89). The average difference between a single day minimum and maximum derived from the hypothetical hourly temperature analysis (to be developed later) is a little higher at 13.8K. The monthly average daily temperature range is also 13 but with +/- 0.91 standard deviation. So the daily temperature range is quite stable over the course of the year.

The difference in radiant energy input with a 13 degree change in temperature is, however, not the same in June as it is in December because the absolute temperature scale has moved up. The energy difference of the December minimum air temperature and that value plus 13 K is 45.4 J. The energy difference of the June maximum temperature and that value minus 13 K is 69.9 J. These values are obtained with the emissivity of the atmosphere equal to 0.80 and are for an area

of  $1 \text{ m}^2$ . A temperature difference of 13 degrees, therefore, can mean a radiant energy input 24.5 J or .0058 kcal higher in June than in December.

The daily ranges and monthly differences look slightly different depending upon how they were formulated – grabs and hypotheticals use grab sample dates only, daily means use all dates 1976-2011 or, in the case of the SRA temperature dataset, all dates 1976-89. Notice in particular that the large drop in daily temperature range in August for the hypotheticals is not seen in the SRA dataset view (left below). In the monthly differences to the right below, the slight dip in May for the grabs is not seen in the full day mean temperature picture. Both of these differences may be just coincidental in the grabs and hypotheticals, the result of the lower number of samples. The larger dataset provides a check that keeps the analysis from making too much of slight (or even rather large) changes that may not be significant.

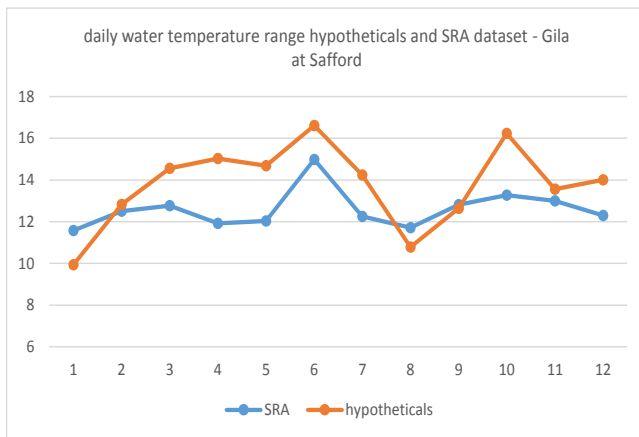


Figure 156 [\(back\)](#)

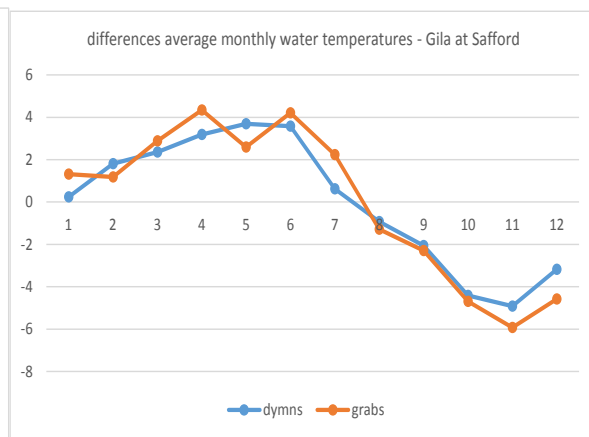


Figure 157 [\(back\)](#)

The daily temperature range is relatively large and stable over the year while the monthly average temperature difference is small but changes quite a bit, including a change in sign. The monthly difference is affected by the difference in radiant input reflected in the absolute temperature while the daily is not. A daily temperature range, whether real or hypothetical, is always positive. The seasonal temperature curve is of temperature differences and so can be either negative or positive. The seasonal curve is a complete cycle as is the daily temperature curve but the daily temperature range is not a cycle.

There are therefore two distinct ways in which temperature can influence the thermodynamic functions – either as a difference (the daily temperature range) or by absolute value (radiant energy input). These two cases can be investigated further but the way in which they are formulated affects the analysis.

The average grab sample temperature difference corresponds roughly to the average grab sample chronological difference calculated earlier. This number can be deduced from temperature differences by creating hypothetical ‘grab’ temperature differences over various time intervals with daily mean temperatures. Below are the temperature differences from 7 to 30 days apart (left) and 60 to 360 days apart (right).



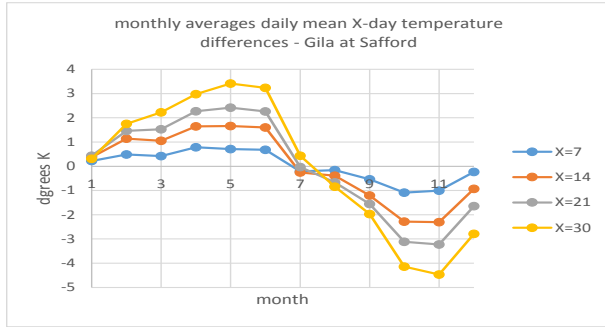


Figure 158

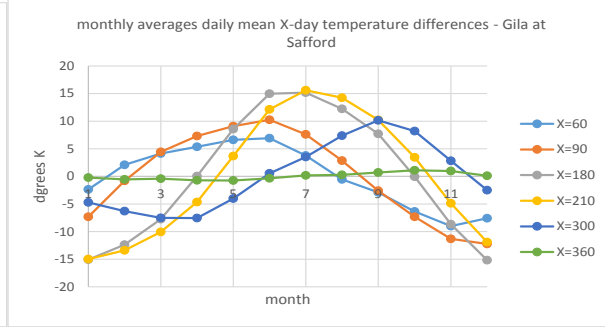


Figure 159

As would be expected, the largest temperature differences are for samples 180 to 210 days apart. After that the differences become smaller until 360 which is almost a straight line. With an absolute temperature difference of 6 K, the ‘real’ grab sample time interval is between 60 and 90 days apart (80 days was calculated earlier).

Note that an ‘inversion’ of sorts seems to occur in July with sample time intervals between 7 and 30. It shifts to August with sample differences between 60-90 days before splitting in two for 180-210 (April and Nov). Then it shifts to Jun for 300 days and, just barely visible, back to Jul for 360. The ‘inversion’ here is an artifact, simply the combination of a sampling decision (how many days apart samples are taken) acting on an annual temperature curve that changes in direction. The ‘artifact’ is the change in sign of temperature change itself, an ‘inversion’ involves two different responses to that change in sign.

Temperature creates the patterns of thermodynamic function response but the final inversion picture also depends on which parameters are dominant. This study began with an intuitive feel that Na & Cl were ‘controlling’ things and rising HCO<sub>3</sub>, the major ion concentration inversion, was disrupting that dominance. Here are the ‘straight’ molar function average values, dXm (not ΔdXm), sorted in order from largest value to least using absolute values where all are negative, with the major ion graph color formatting to make changes in position easier to see:

hierarchy of molar function average values; - Gila at Safford(grabs)				
dVm	dSm	abs(dHm)	abs(dGm)	legend
0.028	0.022	217	219	Ca
0.018	0.014	165	172	Mg
0.013	0.014	130	126	Na
-0.002	0.006	112	102	Cl
-0.019	-0.013	57	61	SO <sub>4</sub>
-0.021	-0.033	40	44	HCO <sub>3</sub>

Table 107

The partial molar volume is included with the thermodynamic functions as a check and reference and because it has a pivotal role with the others. All of the findings concerning the partial molar volume apply to the other thermodynamic functions as will be seen. But there is now the possibility of correlations with and among the other thermodynamic functions.

The four molar functions seem to divide naturally into two groups as emphasized by the bordering. The visual clue is the similar positions of Ca, Mg, HCO<sub>3</sub> and Cl across two functions in each group: only Na & SO<sub>4</sub> differ in the first group (to left). Note that HCO<sub>3</sub> is high in both groups, while Na & Cl fall in position when going from one group to the other and Ca & Mg rise. These are precisely the main parameter relations in major ion concentration inversion (although with only 6 major ions this may just be what ‘shakes out’).

The differences, however, suggest a new division, one that places Sm and Hm in one group and Vm and Gm, curiously intra-related, in the other.

hierarchy of molar function average differences - Gila at Safford(grabs)				legend
$\Delta dSm$	$\Delta dHm$	$\Delta dVm$	$\Delta dGm$	
1.082	317	0.474	106	Ca
0.494	145	0.094	67	Mg
0.204	60	-0.085	67	Na
0.106	31	-0.174	29	Cl
0.063	18	-0.284	-60	SO <sub>4</sub>
-0.165	-48	-0.434	-158	HCO <sub>3</sub>

Table 108

Note that, in the new Sm/Hm group, cations (bottom) are separated from anions (top) with a large separation between Na & Cl. This hierarchical grouping is one that is based on a functional difference. Going from Vm to Gm, HCO<sub>3</sub> goes from top to bottom while Ca & Mg flip and rise and Na & Cl, now close together, flip but stay in the same low position. There may be some functional meaning to the groupings here too but it is harder to interpret.

The percents and differences of percents (not shown) divide up as nicely as the straight values into the two groups with, however, different players in different positions. What is not seen is high HCO<sub>3</sub> in both groups, dropping Na & Cl, and rising Ca & Mg. In a word, the intra-relations of the ions are quite different for the percent molar functions and do not seem as pertinent to inversion.

To see how the dominant roles play out with temperature differences gives a better feel for the roles of the thermodynamic functions. Below are graphs for molar entropy difference values (top) and percents (bottom) as they occur over the year 1977 (left) and vs change in density (right).

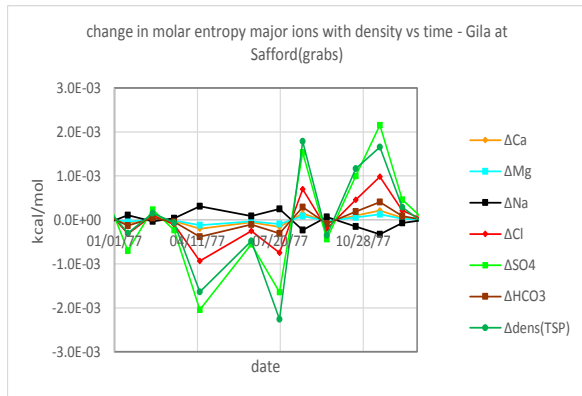


Figure 160 [\(back\)](#)

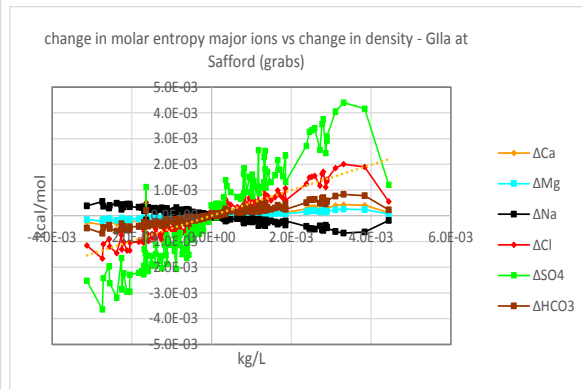


Figure 161

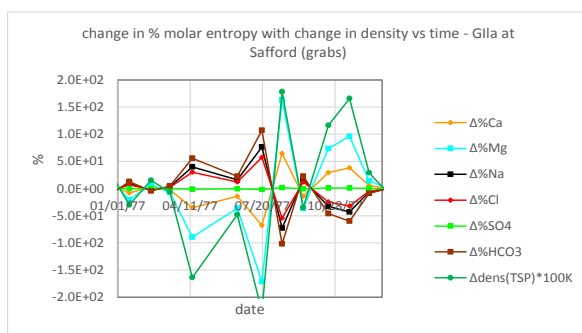


Figure 162

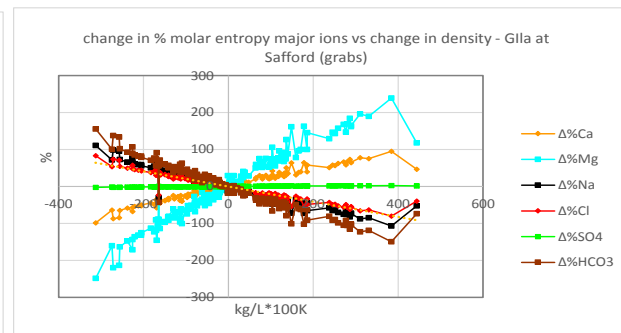


Figure 163

In the straight values, Na is balancing the other ions, in the percents, Ca and Mg play that role. The consequence is that Na is balancing Cl in the straight values while it is moving in direct relation with Cl in the percents. These relationships will be seen again in the total thermodynamic functions but in different form and in a different context.

A full set of all the molar function differences as time series graphs was created but are not shown here. The graphs all look pretty much alike – the pattern is set by density and the ions merely change roles. The graphs were not ‘scaled’ in the sense of different data series being multiplied by a constant to make changes in their values stand out. But when different graphs have different y-scales then some are effectively ‘scaled’ relative to others. The straight value graphs are scaled + to – 3E-3 kcal and the percents -300 to 300, so these can be tiny changes in value and huge changes in (signed not absolute) percent.

It may be, in fact, that it is the magnitude not just the direction of change that matters. The data for the above graphs is regrouped to produce new graphs, each of which shows the varying influence of change in density on the magnitudes of molar function differences of a single ion. Since there is no ‘scaling’ of individual data series, some functions plot on top of one another – the emphasis here is on both the direction and the magnitude of change not just the direction. The molar function difference graph below has a y-scale of -1 to +1 (L/mol or kcal/mol), the % molar function difference graph has a scale of -200 to 200 (%).

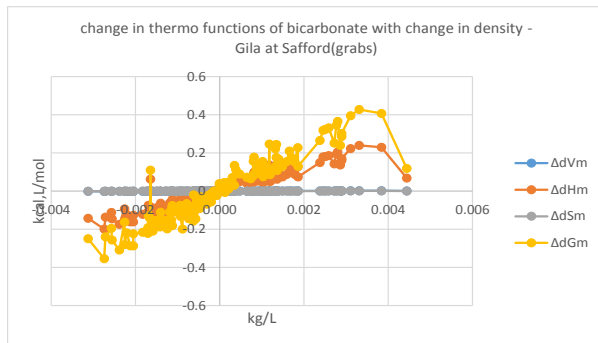


Figure 164

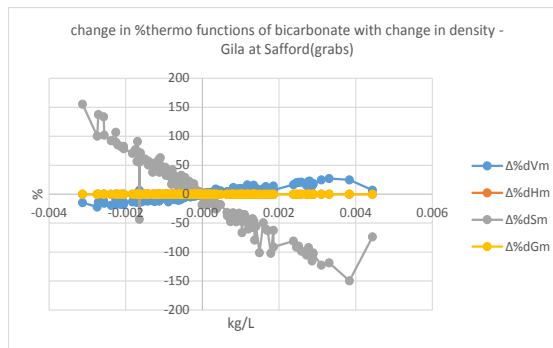


Figure 165

The above graphs show the straight molar function differences (left) and percent molar function differences (right) with respect to density for bicarbonate. Both dGm and dHm values rise with increasing density (left) while on the right only d%Sm drops and d%Vm rises slightly. The full series of major ion magnitude of molar function difference with change in density (not shown) show the same patterns seen above but with different functions in different roles. One intra-function relation that holds in most cases is the inverse relation of dGm and d%Sm. Only in the case of SO4 are the two functions directly related.

The graphs above (Figure 160-163 and others like them) can be conveniently summarized by correlation matrices. Here are the intra-relations for major ion molar entropy (left) and free energy differences (right). The pattern for enthalpy is exactly that of entropy. Again, the contrasting roles of Na and Ca&Mg is seen here but the relations are different between values and percents.

intra-correlations change in molar entropy/enthalpy major ions - Gila at Safford(grabs)							intracorrelations change in molar free energy major ions - Gila at Safford(grabs)						
	ΔCa	ΔMg	ΔNa	ΔCl	ΔSO4	ΔHCO3		ΔCa	ΔMg	ΔNa	ΔCl	ΔSO4	ΔHCO3
ΔCa	1.00	1.00	-1.00	1.00	1.00	1.00	ΔCa	1.00	1.00	-1.00	-1.00	-0.99	-1.00
ΔMg	1.00	1.00	-1.00	1.00	1.00	1.00	ΔMg	1.00	1.00	-1.00	-1.00	-0.99	-1.00
ΔNa	-1.00	-1.00	1.00	-1.00	-1.00	-1.00	ΔNa	-1.00	-1.00	1.00	1.00	0.99	1.00
ΔCl	1.00	1.00	-1.00	1.00	1.00	1.00	ΔCl	-1.00	-1.00	1.00	1.00	0.99	1.00
ΔSO4	1.00	1.00	-1.00	1.00	1.00	1.00	ΔSO4	-0.99	-0.99	0.99	0.99	1.00	0.99
ΔHCO3	1.00	1.00	-1.00	1.00	1.00	1.00	ΔHCO3	-1.00	-1.00	1.00	1.00	0.99	1.00

Table 109 [\(back\)](#)

Table 110 [\(back\)](#) [\(back2\)](#)

The fact that the entropy and enthalpy tables are the same is significant. That means, obviously, that Na is balancing all the other ions for both entropy and enthalpy. But it also means that Na enthalpy is inversely related to the entropy of all the other ions. Free energy, which represents the balancing of entropy and enthalpy, shows Ca and Mg inverting with the rest of the major ions, not Na. This little dilemma will be expanded upon further.

The connection with density is also seen with the molar functions of the major ions (see below) as it was with the partial molar volume. The cations, negatively correlated with the anions above, have dGm and dSm differently correlated to density and to each other while the anions, positively correlated with each other above, have dGm and dSm positively correlated with each other and with density.

correlations difference in molar free energy and entropy major ions with density - Gila at Safford(grabs)							
correl with $\Delta$ dens(TSP)	$\Delta$ Ca	$\Delta$ Mg	$\Delta$ Na	$\Delta$ Cl	$\Delta$ SO4	$\Delta$ HCO3	
$\Delta$ dGm	-0.95	-0.95	0.95	0.94	0.90	0.94	
$\Delta$ dSm	0.94	0.94	-0.94	0.94	0.94	0.94	

Table 111

The percents should also be looked at but a couple of important notes on how they are calculated are required here. These are almost always differences of percents not percent differences:  $\Delta\%dXm$  not  $\% \Delta dXm$  unless stated specifically. The percents are signed not absolute, the implications of which has already been addressed above. Most of the percents in this study are over the sum of all solution constituents (dissolved solids, gases, solvent but not suspended solids or organics). In the case of the molar functions, however, percents are also done over the (signed, not absolute) sum of the major ions (sumMI) for the particular function.

The reason percents over the sum of the major ions are used is because there is a relation to density not seen when sum solutions are used. Replacing dSm with  $\% dSm$ , the above table is expanded to show the difference of the two methods of calculation.

correlations molar free energy and percent entropy major ions with density - Gila at Safford(grabs)							
	$\Delta$ Ca	$\Delta$ Mg	$\Delta$ Na	$\Delta$ Cl	$\Delta$ SO4	$\Delta$ HCO3	
$\Delta$ dGm	-0.95	-0.95	0.95	0.94	0.90	0.94	
	$\Delta\%$ Ca	$\Delta\%$ Mg	$\Delta\%$ Na	$\Delta\%$ Cl	$\Delta\%$ SO4	$\Delta\%$ HCO3	
d%Sm(SS)	0.13	0.13	-0.13	-0.16	-0.22	-0.14	
d%Sm(MI)	0.96	0.96	-0.96	-0.96	0.96	-0.96	

Table 112

The four matrix tables that follow further illustrate how different the relations between the % partial molar thermodynamic functions of the major ions can be when sumMI (left) or sum solution (right) is used. The top row shows entropy, the bottom row shows enthalpy relations.

correlations % change in molar entropy and density - Gila at Safford(grabs) (over sum major ions)								correlations % change in molar entropy and density - Gila at Safford(grabs) (over sum solution)							
	$\Delta\%$ Ca	$\Delta\%$ Mg	$\Delta\%$ Na	$\Delta\%$ Cl	$\Delta\%$ SO4	$\Delta\%$ HCO3	$\Delta$ dens(TSP)		$\Delta\%$ Ca	$\Delta\%$ Mg	$\Delta\%$ Na	$\Delta\%$ Cl	$\Delta\%$ SO4	$\Delta\%$ HCO3	$\Delta$ dens(TSP)
$\Delta\%$ Ca	1.00	1.00	-1.00	-1.00	1.00	-1.00	0.96	$\Delta\%$ Ca	1.00	1.00	-1.00	-1.00	-0.99	-1.00	0.13
$\Delta\%$ Mg	1.00	1.00	-1.00	-1.00	1.00	-1.00	0.96	$\Delta\%$ Mg	1.00	1.00	-1.00	-1.00	-0.99	-1.00	0.13
$\Delta\%$ Na	-1.00	-1.00	1.00	1.00	-1.00	1.00	-0.96	$\Delta\%$ Na	-1.00	-1.00	1.00	1.00	0.98	1.00	-0.13
$\Delta\%$ Cl	-1.00	-1.00	1.00	1.00	-1.00	1.00	-0.96	$\Delta\%$ Cl	-1.00	-1.00	1.00	1.00	0.99	1.00	-0.16
$\Delta\%$ SO4	1.00	1.00	-1.00	-1.00	1.00	-1.00	0.96	$\Delta\%$ SO4	-0.99	-0.99	0.98	0.99	1.00	0.99	-0.22
$\Delta\%$ HCO3	-1.00	-1.00	1.00	1.00	-1.00	1.00	-0.96	$\Delta\%$ HCO3	-1.00	-1.00	1.00	1.00	0.99	1.00	-0.14
$\Delta$ dens(TSP)	0.96	0.96	-0.96	-0.96	0.96	-0.96	1.00	$\Delta$ dens(TSP)	0.13	0.13	-0.13	-0.16	-0.22	-0.14	1.00

Table 113

Table 114

correlations % change in molar enthalpy and density - Gila at Safford(grabs) (over sum major ions)							
	Δ%Ca	Δ%Mg	Δ%Na	Δ%Cl	Δ%SO4	Δ%HCO3	Δdens(TSP)
Δ%Ca	1.00	1.00	1.00	-1.00	-1.00	1.00	0.94
Δ%Mg	1.00	1.00	1.00	-1.00	-1.00	1.00	0.94
Δ%Na	1.00	1.00	1.00	-1.00	-1.00	1.00	0.94
Δ%Cl	-1.00	-1.00	-1.00	1.00	1.00	-1.00	-0.94
Δ%SO4	-1.00	-1.00	-1.00	1.00	1.00	-1.00	-0.94
Δ%HCO3	1.00	1.00	1.00	-1.00	-1.00	1.00	0.94
Δdens(TSP)	0.94	0.94	0.94	-0.94	-0.94	0.94	1.00

Table 115

correlations % change in molar enthalpy and density - Gila at Safford(grabs) (over sum solution)							
	Δ%Ca	Δ%Mg	Δ%Na	Δ%Cl	Δ%SO4	Δ%HCO3	Δdens(TSP)
Δ%Ca	1.00	1.00	1.00	1.00	1.00	1.00	0.09
Δ%Mg	1.00	1.00	1.00	1.00	1.00	1.00	0.09
Δ%Na	1.00	1.00	1.00	1.00	1.00	1.00	0.10
Δ%Cl	1.00	1.00	1.00	1.00	1.00	1.00	0.06
Δ%SO4	1.00	1.00	1.00	1.00	1.00	1.00	0.08
Δ%HCO3	1.00	1.00	1.00	1.00	1.00	1.00	0.09
Δdens(TSP)	0.09	0.09	0.10	0.06	0.08	0.09	1.00

Table 116

Note that the intra ion pattern for % molar entropy using sum solutions (Table 114 above) is the same as that of the straight value free energy (Table 110) highlighting the important relation between %Sm and Gm and Ca & Mg. These are the same two functions seen above to have common patterns across all major ions. It seems reasonable to surmise that the sum solution relations are ‘deeper,’ more fundamental to the system, while the sumMI are focused on individual ion ‘affinities’. But the correlation %dSm with density is only in the sum MI table, not in the sum solution table.

The basic equation relating entropy and the heat capacity is  $dSm = dSm^{\circ} + Cp \cdot \ln(Tf/Ti)$ . Of the 130 parameters with entropy data, the heat capacities for 8 could not be found meaning these parameters are constant at the standard state entropy value. Removing these 8 parameters did not, however, did not much improve the correlation of the (new) sum solution entropy with density.

The answer to this dilemma seems to be in a combination of two things. First, the temperature compensation portion of the molar entropy ( $\ln(Tf/298.15)$ ), that is to say the portion of the entropy function that is changing, is positively related to temperature, therefore inversely related to density (left graph below). Second, most of the parameters (122) have negative heat capacity which turns the sign of entropy with respect to density around (right graph below). The result is that most major ion molar entropies, Na being the only exception, are positively correlated to density (Figure 167 below shows Ca)

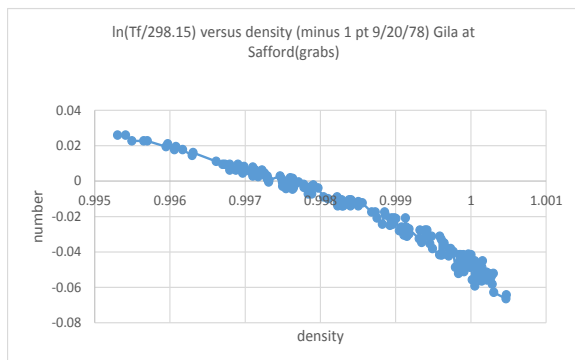


Figure 166 (back)

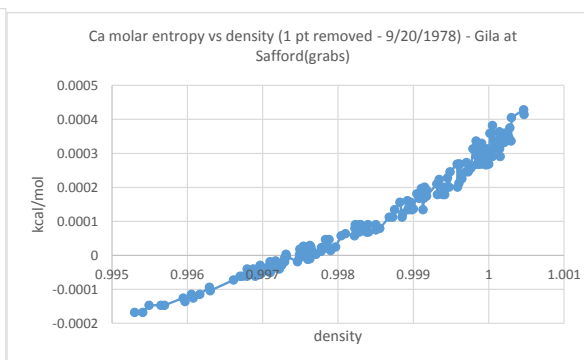


Figure 167

What appears to be happening is that, as long as negative heat capacity parameters are in the majority (as in sumMI), the sign of the heat capacity flips the normally inverse  $\ln(T_f/298.15)$  relation with density and the correlations are high and positive. In the sum solution with all parameters, a few positive heat capacities (15) are enough to change the relation with density. There are no noticeably higher positive heat capacity values and the count favors the negatives, but the weights of the two trends must be very evenly matched. With half the weight indicating 'inverse' and half indicating 'direct', the result is little or no correlation.

The lack of correlation between entropies and density when percents are of sum solution suggests that the 'complete' systems used here are probably not really complete. No different 'view' of the sum solution %molar entropies could be found that correlated with any view of density. All the relations deduced for the sumMI percents fit well together and agree with basic thermodynamic principles but that does not guarantee that they are correct. In fact, all the conclusions that were reached using the sumMI rather than the sum solution percents are doubly suspect because the sumMI are even less likely to represent the whole solution than the sum solution.

To concentrate on the molar functions themselves, the intra-correlations of the molar functions of just one parameter,  $\text{HCO}_3$ , are shown below in both old and new formats. These matrices use a new column/row grouping in which differences of percents (calculated with sum MI) are added in a seemingly random manner. The new groups may be called the 'molar volume difference' and the 'molar heat content difference' groups after the functions that have both straight values and percents in the same group. This new grouping will be further explained in what follows.

Intra-correlation molar functions bicarbonate - Gila at Safford(grams) (percents over sum major ions)									Intra-correlation molar functions bicarbonate - Gila at Safford(grams) (percents over sum major ions)								
	dVm	d%Vm	%dSm	%dGm	dHm	%dHm	dSm	dGm		$\Delta$ dVm	$\Delta$ %dVm	$\Delta$ %dSm	$\Delta$ %dGm	$\Delta$ dHm	$\Delta$ %dHm	$\Delta$ dSm	$\Delta$ dGm
dVm	1.00	0.99	-0.95	-1.00	1.00	1.00	1.00	1.00	$\Delta$ dVm	1.00	0.99	-0.95	-1.00	1.00	1.00	1.00	1.00
d%Vm	0.99	1.00	-0.93	-0.99	0.99	0.99	0.99	0.99	$\Delta$ %dVm	0.99	1.00	-0.93	-0.99	0.99	0.99	0.99	0.99
%dSm	-0.95	-0.93	1.00	0.95	-0.95	-0.95	-0.94	-0.94	$\Delta$ %dSm	-0.95	-0.93	1.00	0.95	-0.95	-0.95	-0.94	-0.94
%dGm	-1.00	-0.99	0.95	1.00	-1.00	-1.00	-1.00	-1.00	$\Delta$ %dGm	-1.00	-0.99	0.95	1.00	-1.00	-1.00	-1.00	-1.00
dHm	1.00	0.99	-0.95	-1.00	1.00	1.00	1.00	1.00	$\Delta$ dHm	1.00	0.99	-0.95	-1.00	1.00	1.00	1.00	1.00
%dHm	1.00	0.99	-0.95	-1.00	1.00	1.00	1.00	1.00	$\Delta$ %dHm	1.00	0.99	-0.95	-1.00	1.00	1.00	1.00	1.00
dSm	1.00	0.99	-0.94	-1.00	1.00	1.00	1.00	1.00	$\Delta$ dSm	1.00	0.99	-0.94	-1.00	1.00	1.00	1.00	1.00
dGm	1.00	0.99	-0.94	-1.00	1.00	1.00	1.00	1.00	$\Delta$ dGm	1.00	0.99	-0.94	-1.00	1.00	1.00	1.00	1.00

Table 117

Table 118

All the major ion thermodynamic functions show the same everything- highly-correlated-to-everything-else situation as  $\text{HCO}_3$ . The newer formatting, however, shows a certain color pattern for bicarbonate molar functions which is not reproduced by the other major ions. There is no rhyme or reason apparent for why the patterns are what they are. The 'gain' in being able to link the percents to density enabled by using the sum major ions in the percent calculation leads to a loss in generality.

Going back to the sum solution method (table below), most of the correlations of the percents are lost, only the relations of the straight differences remain and the pattern is the same (+/-1) for all



the major ions. Shown below are the intra-correlations of the thermodynamic functions of HCO<sub>3</sub> using sum solutions for percents.

intra-correlations molar functions HCO <sub>3</sub> - Gila at Safford(grabs)									
( % as sum solution)									
	$\Delta dV_m$	$\Delta \%dV_m$	$\Delta \%dS_m$	$\Delta \%dG_m$	$\Delta dH_m$	$\Delta \%dH_m$	$\Delta dS_m$	$\Delta dG_m$	
$\Delta dV_m$	1.00	0.03	-0.15	0.06	1.00	0.06	1.00	1.00	
$\Delta \%dV_m$	0.03	1.00	-0.15	0.16	0.03	0.16	0.03	0.03	
$\Delta \%dS_m$	-0.15	-0.15	1.00	0.07	-0.15	0.07	-0.16	-0.16	
$\Delta \%dG_m$	0.06	0.16	0.07	1.00	0.06	1.00	0.05	0.05	
$\Delta dH_m$	1.00	0.03	-0.15	0.06	1.00	0.06	1.00	1.00	
$\Delta \%dH_m$	0.06	0.16	0.07	1.00	0.06	1.00	0.06	0.06	
$\Delta dS_m$	1.00	0.03	-0.16	0.05	1.00	0.06	1.00	1.00	
$\Delta dG_m$	1.00	0.03	-0.16	0.05	1.00	0.06	1.00	1.00	

Table 119

The members of the heat content group (lower right block), with the exception of %dH<sub>m</sub>, the only percent in the group, are highly correlated to each other. The molar volume group (upper left block), containing mostly differences of (sum soln) percents, show no high intra-group correlations. But dV<sub>m</sub> is also highly correlated to the straight functions in the heat content group (upper right and lower left blocks).

The above matrix pattern for HCO<sub>3</sub> is reproduced exactly for all the other major ions rather than there being a different pattern for each ion. It is the relations between the thermodynamic groups that is being shown rather than the relation between the individual functions. This finding somewhat strengthens the speculation on sum solution percents being more ‘fundamental.’

But note that almost all the correlations are positive. The only exceptions are  $\Delta \%dS_m$  and one  $\Delta \%dV_m$  both of which are always low in value. This is a very strange view of the thermodynamic functions, one with which inverse relations only appear sporadically in low (or no) correlation situations.

correlations molar functions HCO <sub>3</sub> with bulk sample and environmental parameters									
- Gila at Safford(grabs)									
	$\Delta dV_m$	$\Delta \%dV_m$	$\Delta \%dS_m$	$\Delta \%dG_m$	$\Delta dH_m$	$\Delta \%dH_m$	$\Delta dS_m$	$\Delta dG_m$	
$\Delta temp\text{-grab/K}$	-1.00	-0.03	0.15	-0.06	-1.00	-0.06	-1.00	-1.00	
$\Delta press\text{-grab/atm}$	0.00	0.41	-0.05	-0.07	0.00	-0.07	0.00	0.00	
$\Delta flow\text{-grab}$	0.16	-0.05	0.08	-0.12	0.16	-0.12	0.16	0.16	
$\Delta dens(TSP)\text{-grab/(kg/L)}$	0.94	0.09	-0.11	0.07	0.94	0.08	0.94	0.94	
$\Delta conductivity\text{/(uS/cm)}$	-0.05	0.07	0.03	0.04	-0.05	0.04	-0.05	-0.05	
$\Delta ionicity\ soln/\#$	-0.11	0.05	0.00	0.02	-0.11	0.02	-0.11	-0.11	
$\Delta pH/SU$	0.08	0.11	-0.14	0.18	0.08	0.18	0.08	0.08	
$\Delta totalk\text{/(mg/L as CaCO}_3\text{)}$	-0.02	0.18	0.03	0.02	-0.02	0.02	-0.02	-0.02	
$\Delta D.O.\text{/(mg/L)}$	0.65	0.07	-0.16	0.13	0.65	0.13	0.65	0.65	
$\Delta Eh\ H_2O-O_2\text{/volts}$	0.05	-0.03	-0.08	-0.37	0.05	-0.37	0.05	0.05	
$\Delta TDS\text{/(mg/L)}$	-0.12	0.05	0.00	0.04	-0.12	0.04	-0.12	-0.12	
$\Delta TSS\text{/(mg/L)}$	-0.09	-0.05	0.22	-0.22	-0.09	-0.22	-0.09	-0.09	

Table 120

The above table shows the correlations of the inversion group parameters with the bulk sample analyzes. Note that the groups that are highly correlated to each other above (heat content group non-percents and the partial molar volume difference) are highly correlated to density while the



percents are, for the most part, not. The same relation to density exists between the molar functions groups as between the individual ions.

Can a more comprehensive and balanced-looking matrix of molar function differences be created by pursuing the new relations between them seen above? In order to find out, it is necessary to do the inversion analysis on the molar function differences. This process is essentially just an extension of the procedure followed for partial molar volume inversion determination ([Table 71](#))

The first task in the inversion analysis is the selection of suitable test parameters. What follows is a summing of groups of inversely related major ions which is then ‘winnowed’ down to a few representative species.

development molar function inversion test(s) - Gila at Safford(grabs)						
opposing forces						
	Δ			Δ%		
Δ(%)dVm	HCO3&Mg	rest including Cl		HCO3&Cl	rest including Na	
Δ(%)dSm	Na	rest including Cl		Mg&Ca	rest including Cl	
Δ(%)dHm	Na	rest including Cl		Cl&SO4	rest including Na	
Δ(%)dGm	Ca&Mg	rest including Cl		Ca&Mg	rest including Cl	
inversions						
	Δ		'rest'	Δ%		'rest'
invV	HCO3	Cl		inv%V	HCO3	Na
invS	Na	Cl		inv%S	Mg	Cl
invH	Na	Cl		inv%H	Na	SO4
invG	Ca	Cl		inv%G	Ca	Cl

Table 121

The ‘rest’ of the ions can usually be represented by Na or Cl, the ‘outsider’ is determined from the inversely related ions and narrowed down by selecting the one with the greatest difference from the ‘rest.’ Here, underneath the calm surface of uniformity implied by the straight-line partial molar volume values graph ([Figure 93](#)), is the inversion embarrassment of riches evident in the time series graphs. There are no less than eight different types of inversions corresponding to each of the straight and percent molar function differences. Furthermore, there no way of knowing which, if any, are ‘best’ for the purposes of this study.

Maybe seeing how they play out in time will provide some answers. Below is a portion of the inversion(s) dates determination spreadsheet which shows the results of running the inversion/non-inversion test with the appropriate test parameter for each molar function difference. A result is shown only if the test parameter is positive.

inversion(s) dates determination -Gila at Safford(grams) - L/mol, kcal/mol, %								
	$\Delta dV_m$	$\Delta \%dV_m$	$\Delta \%dS_m$	$\Delta \%dG_m$	$\Delta dH_m$	$\Delta \%dH_m$	$\Delta dS_m$	$\Delta dG_m$
01/20/76								
02/20/76	0.000675	9.299533	51.4567	0.025873				
03/15/76					0.562141	0.100931	0.001932	0.331262
04/07/76	0.000675	8.505716	91.96924	0.025803				
05/10/76					0.200765	0.035998	0.000679	0.118308
06/14/76					0.100382	0.017979	0.000335	0.059154
08/10/76					0.140535	0.025147	0.000465	0.082815
09/22/76	0.00054	6.394854	128.0554	0.020602				
10/12/76	0.000675	8.343141	107.4903	0.025788				
11/16/76	0.00108	14.22636	108.8426	0.041341				
12/14/76	0.00054	7.553626	37.85696	0.020708				
01/17/77					0.120459	0.021671	0.000423	0.070985
02/16/77	0.000135	1.878615	9.696186	0.005176				
o o o o								
full table								
count	70	70	70	70	85	85	85	85

Table 122

The reason for the ‘new’ grouping of the functions mentioned above is now apparent. This new grouping with %Sm and %Gm in the same group as Vm and %Vm and Sm and Gm in the same group as Hm and %Hm might be called the ‘inversion’ as opposed to the ‘hierarchical’ groupings of Tables 83-4. The differences are all relatively small and the percent differences high only for %entropy.

From the sample counts it is clear that each of these types of inversion occurs in roughly half the 160 difference samples. In fact, on only five dates were there no molar function differences at all. What is immediately apparent upon viewing the entire table is that, even though each type of inversion is defined differently (above), there are two sets of inversion dates and they are mutually exclusive with a randomly alternating pattern.

correlations molar function difference test parameters - Gila at Safford(grams)								
	$\Delta dV_m$	$\Delta \%dV_m$	$\Delta \%dS_m$	$\Delta \%dG_m$	$\Delta dH_m$	$\Delta \%dH_m$	$\Delta dS_m$	$\Delta dG_m$
$\Delta dV_m$	1.00	1.00	0.86	1.00				
$\Delta \%dV_m$	1.00	1.00	0.83	1.00				
$\Delta \%dS_m$	0.86	0.83	1.00	0.86				
$\Delta \%dG_m$	1.00	1.00	0.86	1.00				
$\Delta dH_m$					1.00	1.00	1.00	1.00
$\Delta \%dH_m$					1.00	1.00	1.00	1.00
$\Delta dS_m$					1.00	1.00	1.00	1.00
$\Delta dG_m$					1.00	1.00	1.00	1.00
sample	70	70	70	70	0	0	0	0
counts	70	70	70	70	0	0	0	0
	70	70	70	70	0	0	0	0
	70	70	70	70	0	0	0	0
	0	0	0	0	85	85	85	85
	0	0	0	0	85	85	85	85
	0	0	0	0	85	85	85	85
	0	0	0	0	85	85	85	85

Table 123

The high correlations for the percent functions reveals that sum MI percent calculations have been slipped back into. This strange looking matrix table makes it possible to see that, using all the data as the correlation matrices do by default, the two types of inversion really are mutually exclusive as suggested by the small portion of the inversion date determination sheet shown. The

intra-group correlations (lower right & upper left quadrants) are more balanced at the expense of any correlations at all between the two groups (upper right, lower left). And the strange situation of having no inverse relations remains. Overall, this matrix looks both too balanced in parts and too unbalanced overall, leaving one with the feeling that things cannot be left in this state.

Turning now to inter-correlations with bulk and environmental samples, it is possible to run the same analyzes as above with the various test parameters appropriate to each molar function difference.

correlations molar function difference test parameters and basic sample bulk and environmental parameters - Gila at Safford(grabs)									
	ΔdVm	Δ%dVm	Δ%dSm	Δ%dGm	ΔdHm	Δ%dHm	ΔdSm	ΔdGm	
Δtemp-grab/K	-1.00	-1.00	-0.86	-1.00	1.00	1.00	1.00	1.00	1.00
Δpress-grab/atm	0.07	0.07	0.10	0.07	0.06	0.06	0.06	0.06	0.06
Δflow-grab/cfs	-0.07	-0.07	-0.02	-0.07	-0.20	-0.20	-0.20	-0.20	-0.20
Δdens(TSP)-grab	0.82	0.80	0.87	0.82	-0.91	-0.91	-0.90	-0.91	-0.91
Δconductivity/(t	0.03	0.02	0.05	0.03	0.15	0.15	0.15	0.15	0.15
Δionicity soln/#	0.07	0.06	0.09	0.07	0.37	0.37	0.36	0.37	0.37
ΔpH/SU	0.13	0.13	0.02	0.13	-0.06	-0.06	-0.06	-0.06	-0.06
Δtotalk/(mg/L a	0.13	0.13	0.07	0.13	0.12	0.12	0.12	0.12	0.12
ΔD.O./(mg/L)	0.63	0.63	0.46	0.63	-0.32	-0.32	-0.32	-0.32	-0.32
ΔEh H2O-O2/vo	0.16	0.15	0.19	0.16	0.13	0.13	0.12	0.13	0.13
ΔTDS/(mg/L)	0.07	0.06	0.08	0.07	0.32	0.32	0.31	0.32	0.32
ΔTSS/(mg/L)	-0.19	-0.21	-0.01	-0.19	-0.25	-0.25	-0.25	-0.25	-0.25

Table 124

The relations between the molar function differences and density is, with the use of inversion test parameters, again seen to be at the core of the inter-relations between the two groups as it was for the separate ions. The molar volume group is directly correlated with density, inversely related to temperature, while the molar heat content group is inversely related to density, directly to temperature. Here, each molar function is representative of the difference of two ions.

The following table, created using a new analysis method to be discussed later, shows the test parameter inversion relations on a single day (8/16/1977). The results were checked by running a number of other days and were always the same as, indeed, they had to be. (This somewhat cryptic statement will be clearer when the full results worksheet of the new analysis is shown).

intra-correlations molar function difference test parameters (8/16/77 results*) - Gila at Safford(hypo)								
	invVm	inv%Vm	inv%Sm	inv%Gm	invHm	inv%Hm	invSm	invGm
invVm	1.00	1.00	1.00	1.00	-1.00	-1.00	-1.00	-1.00
inv%Vm	1.00	1.00	1.00	1.00	-1.00	-1.00	-1.00	-1.00
inv%Sm	1.00	1.00	1.00	1.00	-1.00	-1.00	-1.00	-1.00
inv%Gm	1.00	1.00	1.00	1.00	-1.00	-1.00	-1.00	-1.00
invHm	-1.00	-1.00	-1.00	-1.00	1.00	1.00	1.00	1.00
inv%Hm	-1.00	-1.00	-1.00	-1.00	1.00	1.00	1.00	1.00
invSm	-1.00	-1.00	-1.00	-1.00	1.00	1.00	1.00	1.00
invGm	-1.00	-1.00	-1.00	-1.00	1.00	1.00	1.00	1.00

\* percents over sumMI

Table 125 [\(back\)](#) [\(back2\)](#)

Creating the above table was not as easy as might have been expected. These are, after all, state functions so it should be possible to take the multiple differences involved over any time span with any parameter. In fact, the above table depends on the use of the inversion test parameter, individual ions did not work, and on the percents being over the sum of the major ions, sum

solution did not work. What the above table shows is that inversion can exist at different levels. The individual test parameters ‘encloses’ the inversion difference. The connection with density (i.e. temperature) brings back the inversion relations at the molar function level.

The table to the left below shows the daily means using the new analysis method, the table to the right uses the grab samples. The un-highlighted, ‘low’ correlation parameters, %dSm on the right %dVm on the left, are not a great problem: the signs are correct in both cases. The cutoffs for highlighting high correlation are entirely arbitrary and the values here are only marginally lower. But these slight imperfections do suggest that the ‘perfect’ matrix of table 125 above is something of an ideal, limiting value picture.

intra-correlations molar function difference test parameters (daily averages of hour by hour*) - hypotheticals								
	invVm	inv%Vm	inv%Sm	inv%Gm	invHm	inv%Hm	invSm	invGm
invVm	1.00	0.95	0.71	1.00	-1.00	-1.00	-1.00	-1.00
inv%Vm	0.95	1.00	0.56	0.96	-0.95	-0.95	-0.96	-0.96
inv%Sm	0.71	0.56	1.00	0.67	-0.71	-0.71	-0.66	-0.67
inv%Gm	1.00	0.96	0.67	1.00	-1.00	-1.00	-1.00	-1.00
invHm	-1.00	-0.95	-0.71	-1.00	1.00	1.00	1.00	1.00
inv%Hm	-1.00	-0.95	-0.71	-1.00	1.00	1.00	1.00	1.00
invSm	-1.00	-0.96	-0.66	-1.00	1.00	1.00	1.00	1.00
invGm	-1.00	-0.96	-0.67	-1.00	1.00	1.00	1.00	1.00

\* percents over sumMI  
signs reversed for %Sm & %Hm

Table 126

intra-correlations molar function difference test parameters (grab samples*) - Gila at Safford(grabs)								
	invdVm	inv%dVm	inv%Sm	inv%dGm	invdHm	inv%Hm	invSm	invdGm
invdVm	1.00	0.75	0.95	1.00	-1.00	-1.00	-1.00	-1.00
inv%dVm	0.75	1.00	0.70	0.75	-0.75	-0.75	-0.75	-0.75
inv%Sm	0.95	0.70	1.00	0.94	-0.95	-0.95	-0.94	-0.94
inv%dGm	1.00	0.75	0.94	1.00	-1.00	-1.00	-1.00	-1.00
invdHm	-1.00	-0.75	-0.95	-1.00	1.00	1.00	1.00	1.00
inv%Hm	-1.00	-0.75	-0.95	-1.00	1.00	1.00	1.00	1.00
invSm	-1.00	-0.75	-0.94	-1.00	1.00	1.00	1.00	1.00
invdGm	-1.00	-0.75	-0.94	-1.00	1.00	1.00	1.00	1.00

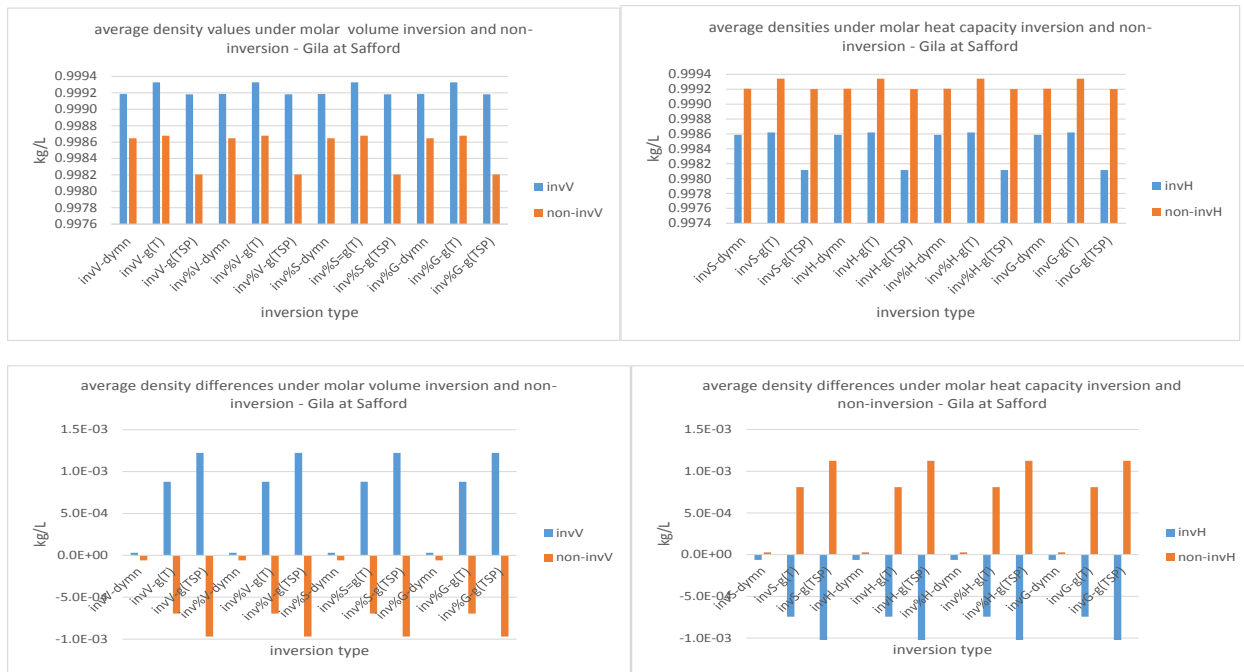
\* percents over sumMI  
signs reversed for %Hm

Table 127

The prevalence of balance is high everywhere in the molar function arena but here perfect balance seems the only ‘logical’ outcome. The pattern goes from being an experimental output to becoming a check on the correctness of the analysis. Parameters that don’t fit are not called ‘outsiders’ -- they are either errors or a sign that not all scenarios work even for state functions.

The intra-correlation of the molar function differences depends on the relations of the individual functions with density when the test parameter is used. This is strictly analogous and depends on the fact that the major ion molar function difference is dependent on the individual ion relation to density.

Given the fundamental linkage between density and molar function difference relations it is clear that molar function inversion/non-inversion can also be framed in terms of density. Density values on inversion and non-inversion dates for the various molar functions are shown below. These are the average density values (top) and differences (bottom) for molar volume (left) and molar heat content inversions (right). Each function is represented along the x axis by 3 values, daily mean(T), grab(T) and grab(TSP) densities as determined by the appropriate molar function difference test parameter.



Figures 168-171

The alternating pattern of inversion/non-inversion (blue/red) make the relations easy to grasp. In the graphs above note that the molar volume pattern of inversion (blue) is repeated in red in the heat content group. The daily mean average differences are tiny but all in the right direction.

What the repeating of patterns means, with respect to density on inversion and non-inversion dates, is that the two types of inversion are the inverse of one another. This pattern grows out of the positive and inverse relation to density of the two groups which also causes the occurrence on alternate days or mutual exclusivity of inversion in the two groups. The same date that is a molar volume inversion date is a molar heat content non-inversion date so the two groups very neatly divide up positive and negative density values in two ways. In examining density on inversion and non-inversion dates, it is only necessary to look at one set of inversion/non-inversion knowing that the other type is in the opposite state.

inversion/non-inversion grab density values			
- Gila at Safford(grabs)			
inversion date = 1		non-inversion = 0	
Vm grp	Hm grp	$\Delta$ dens(TSP	$\Delta$ dens(TSP
#####			
#####	1	0	0.000383
#####	0	1	-0.00238
4/7/1976	1	0	0.00118
#####	0	1	-0.00116
#####	0	1	-0.00045
#####	0	1	-0.00113
#####	1	0	0.001198
#####	1	0	0.001268
#####	1	0	0.001341
#####	1	0	0.000475
#####	0	1	-0.0003
#####	1	0	0.000153
oooo			

Table 128

Now the above developments, while encouraging, have some consequences. In fact, molar function difference inversion reveals some new aspects of density change, but it not only side-steps seasonal/functional analysis but, ultimately, blows up the whole concept of inversion analysis as developed to this point. To substantiate this claim, it is necessary to look again at how molar function difference inversions play out in time. Below is the time series graphs of the partial molar volumes inversion parameter ( $\text{HCO}_3^- - \text{Cl}$ ) and density difference over the month in 1977 in which the summer major ion concentration inversion took place, August.

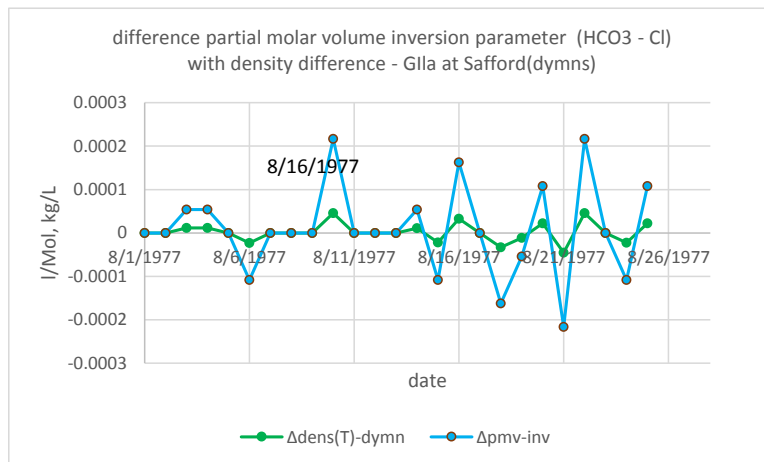


Figure 172 [\(back\)](#)

The choice of a month long time span, rather than the full year span usually used elsewhere, is absolutely necessary because the full year span using the daily means is too closely packed with data points to be intelligible. The graph brings out some important relations: while the partial molar volume value is usually inversely related to density (i.e.  $\text{H}_2\text{O}$ ), the partial molar volume

inversion parameter (a difference) is directly related to density difference. This fact will rear its ugly head later in the analysis.

The temperature dependence of density has its anomalies but is, in general, very straightforward. With the molar function inversions, however, it becomes clear that a new approach is needed. It is possible to expand the analysis using the new analysis technique, referred to earlier, which was used to produce the ‘perfectly balanced’ correlation matrix for the thermodynamic functions ([Table 125](#)). The mechanics for a new, partly ‘hypothetical’, approach, will be built up from the ground. The reason for this new approach is to replace ‘patterns’ of largely unknown significance with numbers that quantify the effects of ‘inversion’ at different levels.

The following graph is from the internet<sup>16</sup> and shows the average low and high temperatures across the year at Safford.

### Average Weather for Safford, Arizona, USA

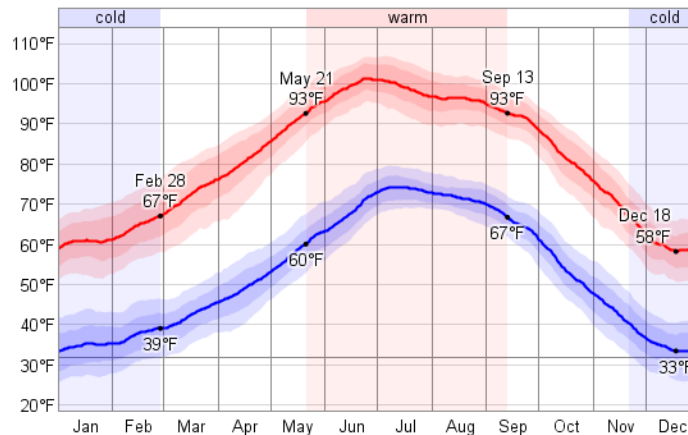


Figure 173 ([back](#)) ([back2](#))

August 16, 1977 had an average daily air temp of 80 F (from AZmet dataset) and the graph shows the average low to be about 72 and the high about 96 which means that the average average calculates out to be 82.8. With this information it is possible to create a hypothetical reconstruction of temperature rise and fall over the course of the day that is probably not too far off the actual. The low average temperature is placed at 6:00 am and the high average at 4:00 pm with the other temperatures filled in in such a way as to mimic day time heat acceleration. Then the whole curve is lowered to make the average around 80.

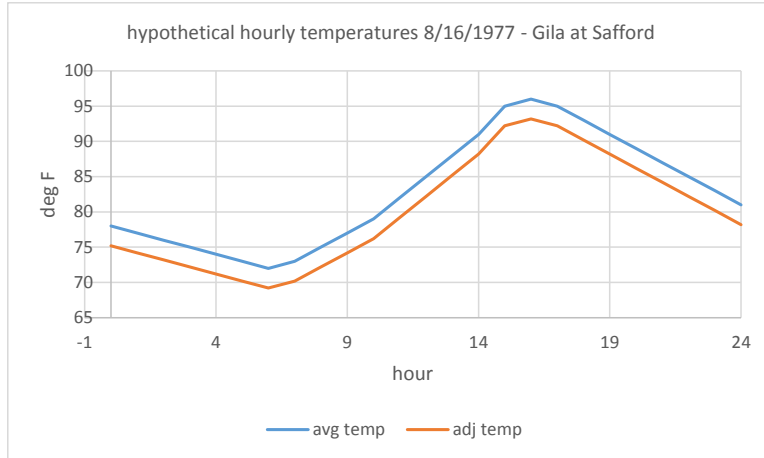


Figure 174

With these air temperatures converted to water temperatures in Celsius using the ‘guesstimate’ equation referred to above, the partial molar volumes of HCO<sub>3</sub> and Cl can be calculated on an hourly basis. Below are the partial molar volumes (dVm) by temperature in chronological order (left) and the molar volume differences (ΔdVm) vs temperature in chronological order (right) for 8/16/1977.

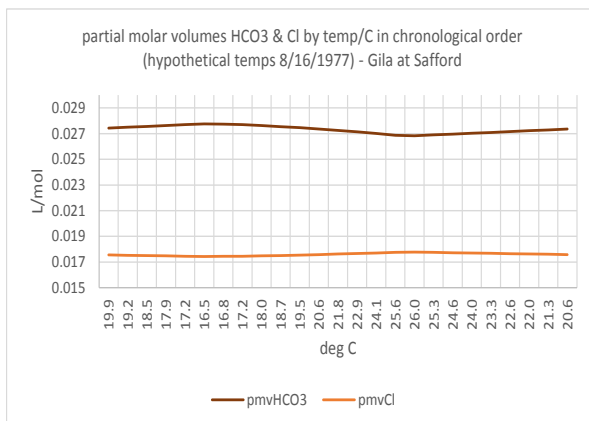


Figure 175

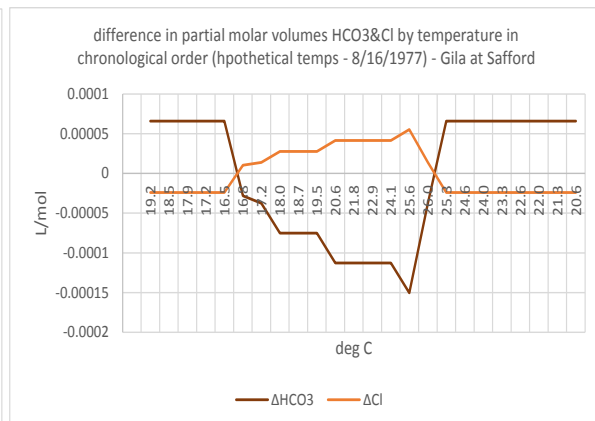


Figure 176

The partial molar volume of HCO<sub>3</sub> is inversely related to temperature difference while Cl is positively related as evidenced by the slight bends in the graph to the left. (Here the switch is made from density to temperature dependence to avoid the hobgoblins around 4C that might occur on other sample dates) These small changes in slope, at 6:00 am and 4:00 pm, are enough to produce inversions of ΔHCO<sub>3</sub> and ΔCl as seen in the differences graph to the right above.

To simplify the picture a bit, the above right graph is converted to the partial molar volume test parameter, ΔdVm(HCO<sub>3</sub>) - ΔdVm(Cl). By the look of the data with just a visual estimate, 8/16/1977 appears to be a ‘non-inversion’ date (test parameter predominately < 0) but it’s really hard to tell.



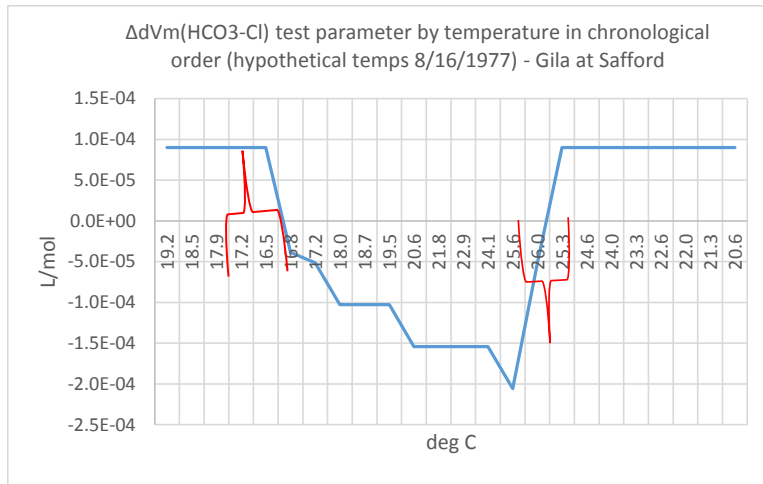


Figure 177 (back)

The red brackets are used to highlight an assumption that creates an area of uncertainty. The analysis sets the minimum temperature at 6:00 am and the maximum at 4:00 pm, typical min and max temperature hours respectively. But the lines will cross zero at the actual time of min and max temp in which there will be some variability over the course of the year.

It is not too hard to imagine continuing the analysis down to the minute by minute and second by second level. True it would become increasingly arbitrary and require more and more information that is not readily available. Water temperatures are less likely to move inexorably in one direction than air temperatures because there are many more factors at different levels involved. There can be inflows of waters at different temperatures, canopy cover or the lack thereof, possible heating or, more likely, cooling caused by air contact in riffles, areas of channel deepening leading to slowing down and onset of temperature stratification, etc. All of these factors make it reasonable to believe that the single lines in the hourly graph above may be analogous to the yearly average density. There may be an inner set of curves within analogous to the 'inner' curve of the yearly average density graph.

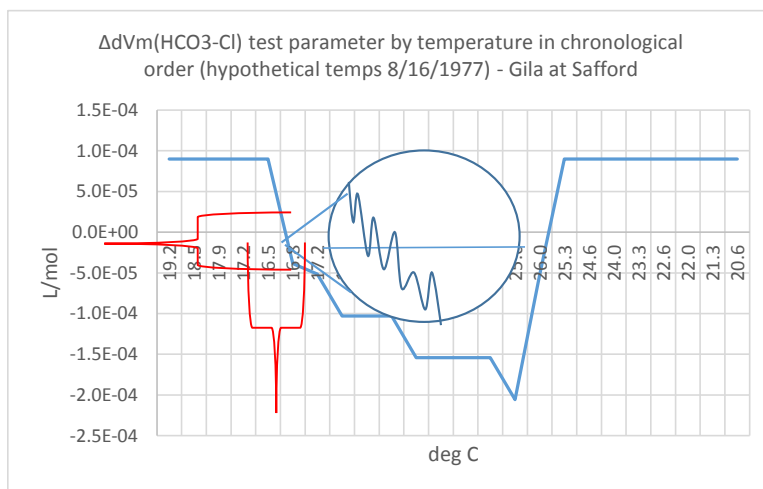


Figure 178

The straight line downward and upward slopes at 6 & 4 may really contain areas of twisting back and forth across the inversion boundary and only take a particular direction in a cumulative sense. The zig-zag line in the insert view above is not only a problem in itself but may be actually occurring somewhere to the left or the right. Bottom line,

there is uncertainty in both the x- and the y-scale. The same arguments would apply for other molar function differences such as dHm (not shown), the positions of inversion and non-inversion are merely flipped.

But how far can these arguments be pushed? Every time there is a difference in temperature is there is a difference in density and the molar functions? There is, of course, a limit to the sensitivity of the instrumentation used and there must be a minimum temperature difference at which no change in density is observed.

Despite these considerations, the most appropriate time span over which to average molar functions has at last been found. The minute by minute or second by second analysis might pinpoint the exact time of lines (first) crossing zero but would not change the bigger picture of inversion. And the daily hour by hour temperature curve is not likely to change overall shape in any drastic manner over the course of the year or in different seasons.

There is a dilemma, however, in that the month of August graph (Figure 172) clearly indicates 8/16/1977 to be an inversion date whereas the test parameter graph (Figure 177) seems to suggest a 'non-inversion' date. Running through the partial molar volume difference test parameter calculation shows how 8/16/77 on the month of August 1977 graph ends up an 'inversion' date.

calculation inversion/non-inversion partial molar volumes using daily mean temps							
- Gila at Safford(dymns)							
	temp/C	pmvHCO3	pmvCl	$\Delta$ pmvHCO	$\Delta$ pmvCl	$\Delta$ temp	test parameter value
8/14/1977	26.8	0.0268	0.0178				
8/15/1977	27.6	0.0267	0.0178	-0.00008	0.00003	0.80	-0.00011 (non-inversion)
8/16/1977	26.4	0.0268	0.0178	0.00012	-0.00004	-1.20	0.00016 (inversion)
8/17/1977	26.4	0.0268	0.0178	0.00000	0.00000		
8/18/1977	27.6	0.0267	0.0178	-0.00012	0.00004	1.20	-0.00016 (non-inversion)

Table 129

The key is the change in direction of temperature change. Although the numeric temperature difference is not used in the calculation or the graph, it is captured in the volume difference. The partial molar volume comes from an empirically derived equation that relates dVm and temperature. Columns three and four are the resulting pmv for HCO3 and Cl at the temps in column two. Then the differences of consecutive dates are taken for HCO3 and Cl ( $\Delta$ pmv) and finally the difference of HCO3 minus Cl, the test parameter, for each date is in the last column ( $\Delta$ pmvHCO3- $\Delta$ pmvCl). The temperature difference is almost simply an aside or a label which just happens to coincide with the fact that the pmv test parameter is inversely related to temperature change. In fact, the test parameter graphs above are all 'line' graphs not x-y scatterplots and anything could have been placed along the x-axis.

Using hypothetical temperatures (below) with the same calculations may make things a little clearer. The test parameter stays negative or positive until the temperature difference changes sign at which time the test parameter also changes sign.

calculation inversion/non-inversion partial molal volume using hypothetical temperatures							
	temp/C	pmvHCO3	pmvCl	$\Delta$ pmvHCO	$\Delta$ pmvCl	tempdiff	pmvtestparameter
day1	21.0	0.0273	0.0176				
day2	20.0	0.0274	0.0176	9.9E-05	-3.6E-05	-1.0	1.4E-04 inversion
day3	19.0	0.0275	0.0175	9.9E-05	-3.6E-05	-1.0	1.4E-04 inversion
day4	18.0	0.0276	0.0175	9.9E-05	-3.6E-05	-1.0	1.4E-04 inversion
day5	20.0	0.0274	0.0176	-2.0E-04	7.3E-05	2.0	-2.7E-04 non-inversion
day6	21.0	0.0273	0.0176	-9.9E-05	3.6E-05	1.0	-1.4E-04 non-inversion
day7	22.0	0.0272	0.0176	-9.9E-05	3.6E-05	1.0	-1.4E-04 non-inversion

Table 130

Now this is all well and fine but if 'grab' differences were being taken over this period, problems would develop.

hypothetical 'grab' samples using hypothetical temperatures							
	temp/C	pmvHCO3	pmvCl	$\Delta$ pmvHCO	$\Delta$ pmvCl	tempdiff	pmvtestparameter
day4	18.0	0.0276	0.0175	9.9E-05	-3.6E-05		
day5	20.0	0.0274	0.0176	-2.0E-04	7.3E-05	2	-2.7E-04 non-inversion
day1	21.0	0.0273	0.0176	2.7E-02	1.8E-02		
day5	20.0	0.0274	0.0176	9.9E-05	-3.6E-05	-1	1.4E-04 inversion

Table 131

Is day 5 an inversion or a non-inversion date? It depends entirely on the grab sample interval chosen and the temperatures on those dates. As long as the sampling interval is consistent, be it hourly, daily, or monthly, the results will be consistent but the moment it becomes random, inversion/non-inversion dates also become random. The patterns seen on the inversion date determination worksheet, alternating dVm and dHm on different days, would remain the same but there would be different days marked as 'inversion' or 'non-inversion'. In a word, these developments reinforce the general concept of an inversion/non-inversion pattern but blow up the whole idea of an 'inversion date' as such.

Note that the same reasoning would apply if the first column in the table above read min4, min1, min5 but in that case the reference would be to inversion hours rather than dates. Below is the complete 8/16/1977 hypothetical hourly data set using the molar function difference test parameter method.

hourly partial molar volume difference test parameter inversion/non-inversion analysis using hypothetical temperatures - Gila at Safford

	temp/C	pmvHCO3	pmvCl	ΔpmvHCO	ΔpmvCl	tempdiff	test parameter
hour 1	19.7	27.45572	17.54456				
hour 2	18.9	27.52823	17.51791	7.3E-02	-2.7E-02	-0.7	9.9E-02 inversion
hour 3	18.2	27.60074	17.49127	7.3E-05	-2.7E-05	-0.7	9.9E-05 inversion
hour 4	17.5	27.67325	17.46463	7.3E-05	-2.7E-05	-0.7	9.9E-05 inversion
hour 5	16.7	27.74576	17.43799	7.3E-05	-2.7E-05	-0.7	9.9E-05 inversion
hour 6	16.0	27.81827	17.41134	7.3E-05	-2.7E-05	-0.7	9.9E-05 inversion
hour 7	16.0	27.81827	17.41134	0.0E+00	0.0E+00	0.0	0.0E+00
hour 8	17.0	27.71676	17.44864	-1.0E-04	3.7E-05	1.0	-1.4E-04 non-inversion
hour 9	18.0	27.61524	17.48594	-1.0E-04	3.7E-05	1.0	-1.4E-04 non-inversion
hour 10	19.1	27.51373	17.52324	-1.0E-04	3.7E-05	1.0	-1.4E-04 non-inversion
hour 11	20.1	27.41222	17.56054	-1.0E-04	3.7E-05	1.0	-1.4E-04 non-inversion
hour 12	21.1	27.3107	17.59784	-1.0E-04	3.7E-05	1.0	-1.4E-04 non-inversion
hour 13	22.2	27.20919	17.63514	-1.0E-04	3.7E-05	1.0	-1.4E-04 non-inversion
hour 14	23.2	27.10768	17.67244	-1.0E-04	3.7E-05	1.0	-1.4E-04 non-inversion
hour 15	24.2	27.00616	17.70974	-1.0E-04	3.7E-05	1.0	-1.4E-04 non-inversion
hour 16	25.2	26.90465	17.74704	-1.0E-04	3.7E-05	1.0	-1.4E-04 non-inversion
hour 17	26.3	26.80314	17.78434	-1.0E-04	3.7E-05	1.0	-1.4E-04 non-inversion
hour 18	25.5	26.87565	17.7577	7.3E-05	-2.7E-05	-0.7	9.9E-05 inversion
hour 19	24.8	26.94816	17.73106	7.3E-05	-2.7E-05	-0.7	9.9E-05 inversion
hour 20	24.1	27.02067	17.70441	7.3E-05	-2.7E-05	-0.7	9.9E-05 inversion
hour 21	23.3	27.09318	17.67777	7.3E-05	-2.7E-05	-0.7	9.9E-05 inversion
hour 22	22.6	27.16568	17.65113	7.3E-05	-2.7E-05	-0.7	9.9E-05 inversion
hour 23	21.9	27.23819	17.62449	7.3E-05	-2.7E-05	-0.7	9.9E-05 inversion
hour 24	21.1	27.3107	17.59784	7.3E-05	-2.7E-05	-0.7	9.9E-05 inversion

Table 132 (back)

It is now easy to see why the hourly results are perfectly correlated as seen in [Table 125](#). With the model used, the change of direction in temperature difference occurs in exactly two places, 6:00 am and 4:00 pm, and the inversion test parameters follow suit. The ‘mystery’ of no molar function difference values on five grab dates is now also easily dispelled – there was no difference in temperature from the previous (grab) sample date as is the case in hours 6-7 above. Two instantaneous temperatures being the same on two different days is just a random event in the analysis. Molar function differences are always going on at or above some minimum time interval even if they can’t always be calculated with the crude +/- 1C temperatures used here.

Using the hypothetical hour by hour analysis shows that 8/16/77 is neither an inversion nor a non-inversion day, it is actually both over the course of the day. If both molar heat content and molar volume groups are considered, it is also both at any particular time of the day as well. During the daylight hours, there is heat content inversion going on at the same time as molar volume non-inversion and the nighttime is just the reverse, molar volume inversion and heat content non-inversion. (Note that ‘inversion dates,’ like averages that have been shown to be unrepresentative, will continue to be used later in the analysis since they are the ‘real’ quantities here.)

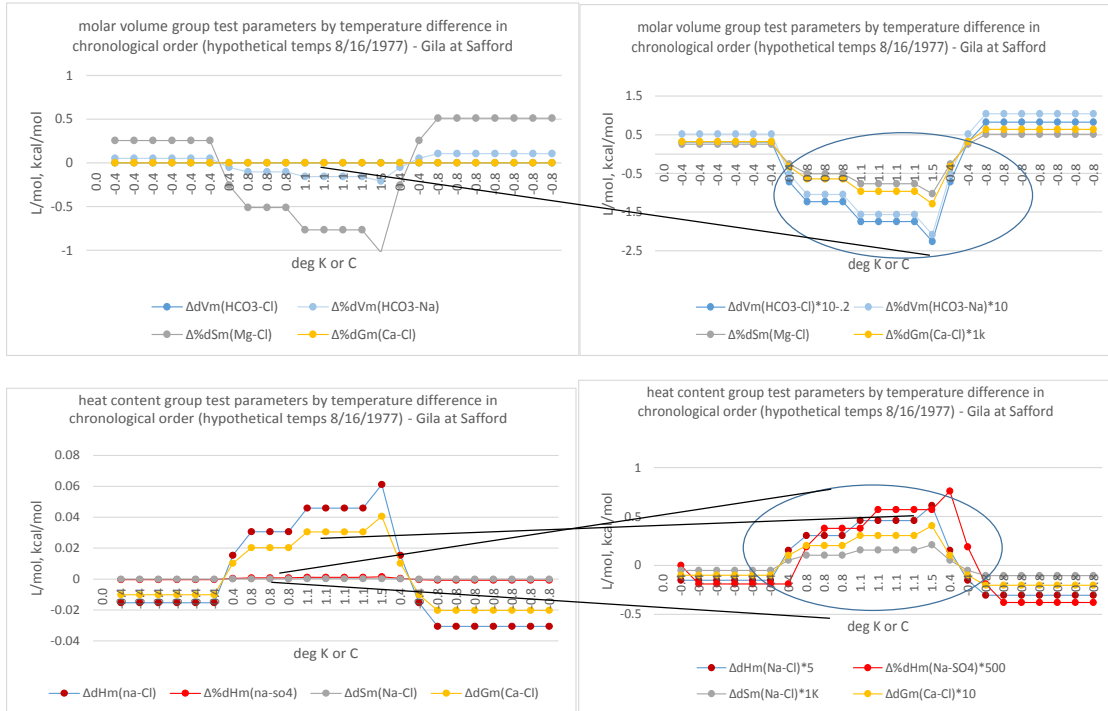
‘Non-inversion’ does not, of course, mean that nothing is going on, it only means that what is ‘going on’ has a different sign or is going in a different ‘direction’ than what has been defined as ‘inversion’. And what ‘going on’ means in terms of molar volume is a constant expansion and contraction with implications in entropy and a concomitant adjustment in the energy of the system.

It is important to emphasize that the functions within each group are moving directly with one another as seen in the correlations. There are no inversions of individual test parameters within the two larger molar function group inversions. This finding is significant because it means that molar entropy and molar enthalpy, both in the heat content group, are moving in direct relation to one another not inverting the one with the other. In the molar function test parameter inversion group picture, entropy is inverting with volume not enthalpy or free energy. This strange relation will be examined at a later point.

A process can be defined as any change in the analytical parameters of a system. In a practical sense, a process has to have an ‘up’ and a ‘down’ signal to read with an analytical instrument and a beginning and an end in a time frame that is easily apprehended. The major ion concentration inversion is a process in this sense. Some processes are more difficult to apprehend than others but can at least be comprehended intellectually if not intuitively (e.g.,

geological processes). Any process, however, that has both up and down signals at the same time and is going on all the time without any particular beginning or end is probably best considered not as a process but as a state in constant flux.

A 'constant flux' needs to be treated somewhat differently than a process particularly when it is going on in so many analysis quantities at the same time. For major ion concentration inversion, one test parameter covered about a dozen analysis quantities. With molar function difference inversion there are eight pairs of ions making up the test parameters, no one of which is necessarily representative of the solution as a whole. The various molar function difference test parameters can be cast into the hour-by-hour mold. Here are the molar volume (top) and heat content (bottom) groups on 8/16/1977 in both a full scale view for relative magnitudes (left) and a zoomed-in, scaled view for direction of change (right).



Figures 179-182

The correlated movement of all the parameters can be seen to the right, which is what the test parameter is designed to bring out, and relative magnitudes are evident to the left. But it is not clear what to do with the multiple parameters going in the same direction. Are they to be summed or averaged? No, this is not a quantitative but a qualitative analysis. Running the creation process step by step from the full major ion picture to the test parameter graph for the heat content group illustrates how the test parameter concept reduces the problem to a simple change of sign.

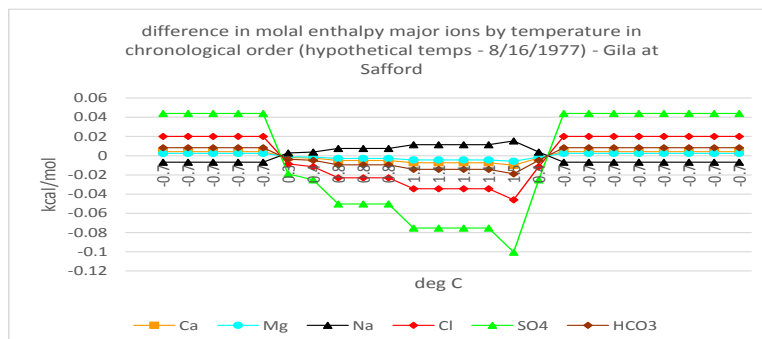


Figure 183 ([back](#))

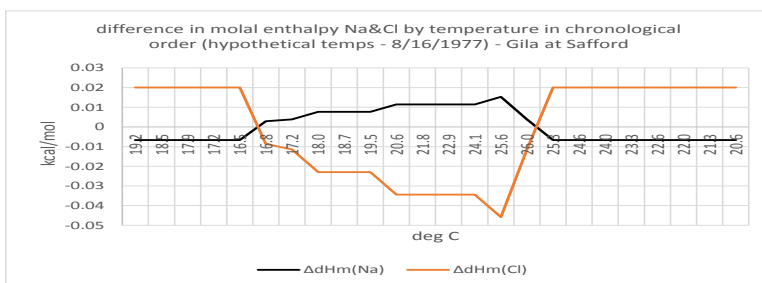


Figure 184

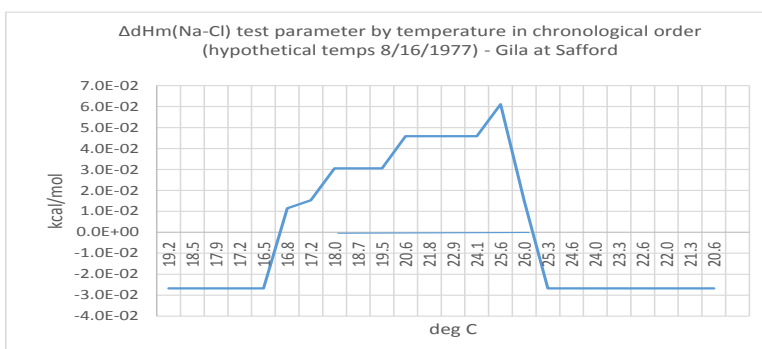


Figure 185

The test parameter, which excludes four of the six ions, creates an area which clearly brings out changes in direction with respect to temperature change. For enthalpy the majority of the major ions are actually becoming increasingly negative during the day-time. The exception is Na which, significantly, is like H<sub>2</sub>O in having rising heat content with rising temperature (i.e. positive heat capacity).

The inversion analysis needs to change. Simple crossing lines and ‘up’ and ‘down’ will no longer do. One way that suggests itself from the above graphs is to take areas above or below the curve.  $\Delta dX_m(T)$  (e.g.  $dH_m(T_2) - dH_m(T_1)$ ) will be used as a simplified version of  $\int dX_m(T)dT$ . This can be calculated as  $C_p \cdot (T_2 - T_1)$  either with  $T_1$  &  $T_2$  as begin and end temperatures of the inversion period or by using the hour by hour differences and summing over the inversion period. These different methods of calculation all yield the same answer (see below). But the important thing here is that they can be thought of as areas rather than point to point differences.

sign enthalpy and direction of temperature difference - Gila at Safford(grabs)						
H2O						
temp-grab/	dT	dHm= dHo+CpdT	$\Delta dHm(T2-T1)$	$\Delta dHm(\text{day})$	$\Sigma \Delta dHm$	$Cp(T2-T1)$
293			-68.408			
298	5		-68.318	0.090		
301	3		-68.273	0.045		
304	4		-68.210	0.1979	0.063	0.1979
301	-4		-68.273	-0.063		
298	-3		-68.318	-0.045		
293	-5		-68.408	-0.1979	-0.090	-0.1979

Table 133

Thinking in terms of areas changes things entirely. Worrying about exactly when and where lines cross is a thing of the past. The focus here is on area above and below zero. Whether the incoming radiant energy is added from 6:00 am to 4:00 pm or some other min-max pair makes no difference, at least to the analysis as currently conceived. The concern here is the total quantity of heat absorbed not the rate of application. As a result, it makes no difference if the polygons generated are 'realistic' and complex (as left below) or if the heat is applied all at once in a simple rectangular form (to right). The simple rectangular form is, however, easier to calculate the approximate area of than that of the more 'realistic' form.  $\int dXm(T)dT$  for the latter needs a function to adequately quantify the area, the addition of 'inner' polygons being not only clumsy and difficult but also yielding only an approximate result.

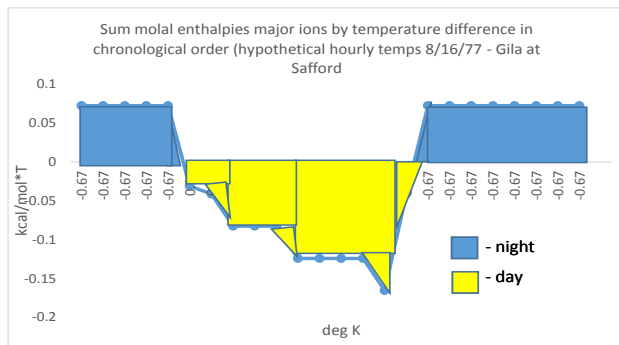


Figure 186

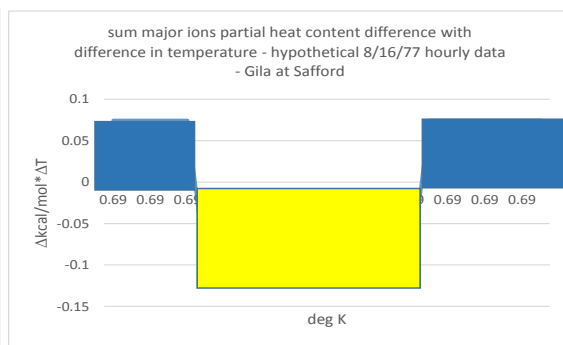


Figure 187

Any given day will have a total area, defined by the max – min temperature range, and two places in which the direction of temperature change changes: either from minus to plus or plus to minus. The different min/max hours are a seasonal effect and, for any given total, simply change the height and width of the rectangles, the areas above and below remain the same. This can be shown schematically as below but is also directly verified by calculating the areas using not only the 6-4 but also the 7-3 and 5 to 5 scenarios.

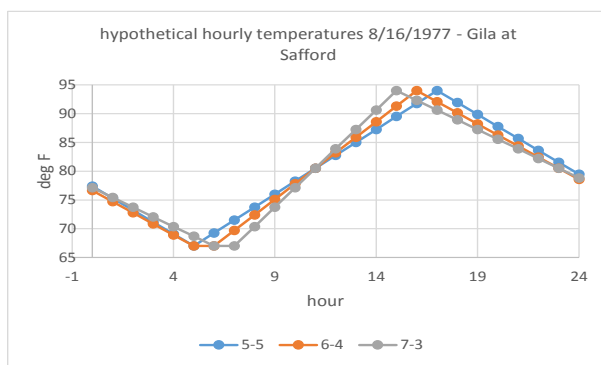


Figure 188

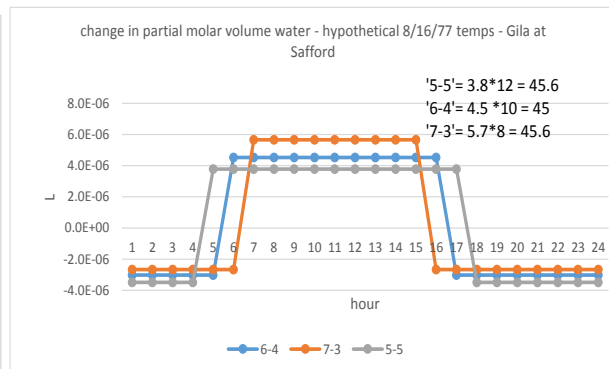


Figure 189

$\Delta dV_m - H_2O$		hypothetical 8/16/77 hourly data		
		sum differences		
		5-5	6-4	7-3
day		4.9E-05	5.0E-05	5.1E-05
night		-3.8E-05	3.9E-05	4.0E-05

Table 134

The sum values do change slightly with scenario but the differences are probably small enough to be ignored and analysis will proceed with the 6-4 scenario only. Notice that day and night values do not balance as exactly as they should: this is just a result of the crudeness of the analysis which was intended only to show the sameness of area of the central polygon. Whatever the specific configuration of the polygons, what uniquely determines the areas is not the daily absolute temperature but the daily temperature range, in this example about 27 degree F.

The molar functions themselves can be evaluated either with the sum solution of parameters or the inversion test parameters (listed on Table 132) to reveal their daily inversions. The functions are calculated on an hourly basis, hourly differences taken, and finally the sum or the difference of the differences. The graphs below use the hypothetical daily temperatures and real grab parameter amounts for 8/16/77 to calculate the change in density and partial molar volume (left) and molar entropy, enthalpy, and free energy (right) for that day. (The moles of each parameter are not used in any calculation, they are used only to determine whether or not to calculate the molar function for a given parameter (mols > 0 = 'presence')). The thermodynamic results use the Gibbs-Helmholtz equation and  $\Delta S = \Delta H / T - \Delta G / T$ . The daytime values are those of the central area while the nighttime are the sum of the two outer areas.

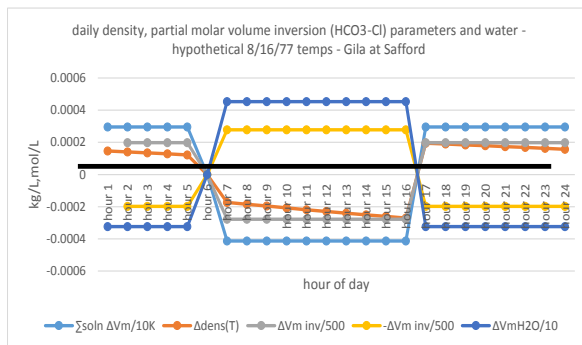


Figure 190

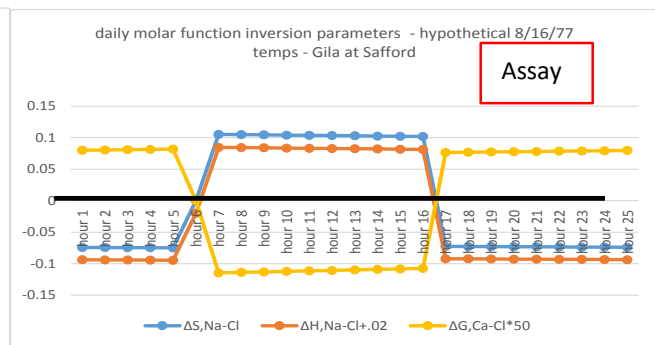


Figure 191

Figure 191, the thermodynamic functions picture, is a distinct improvement over Figures 186-187 above. There the major ion molar enthalpy differences sum to a negative number during the



day. If the major ions represent the solution, then there is heat loss during the day, heat gain at night (coming from some unknown source). This result seems odd but makes sense with the characteristics of major ion enthalpy – all their standard enthalpy values are negative and five of the six have negative heat capacities.

But water temperatures do rise during the day so the heat content of the solution must also rise, no matter how many individual parameters have negative enthalpies. Fortunately, the Gibbs-Helmholtz equation picture of the sum of solution constituents' enthalpy is the same as the above inversion test parameter view, increasing during the day decreasing at night. Since free energy increases in a negative direction, all three functions increase during the day and are directly related to one another. In summary, heat input from the environment causes the system to expand and work is done on the environment to an equivalent extent. At night, the environment works on the system with an equivalent amount of heat loss from the system. Solution enthalpy rising with daytime heat increase, decreasing at night is seen here as a 'touchstone' analysis result.

It may be that our understanding of the intensive behavior of the solution is being influenced by our knowledge of its extensive properties. Our expectations of solution behavior are usually based on the way the total functions of water behave. Water is so overwhelmingly greater in amount than any other parameter that its behavior can reasonably be used as a surrogate for the total functions of the solution in many cases. In the molar function view, water may be just one among many others with no special significance or weight. On the other hand, the molar values of water are 'different' because water is the 'medium' in which all the other parameters exist. Density is not calculated with any other parameter. The molar volume of water is also a reasonable surrogate for the solution and is inversely related to its density (another touchstone relation).

Given these relations, Figure 190 raises some questions. The sum solution molar volume and that of water as well as density are given as references. But there are also two versions of the molar volume inversion test parameter, one the negative of the other, and only one can be correct. The only real, functional view of the solution as a whole that can be used to decide which is correct is density.

If density is calculated for each hour using the same 8/16/77 hypothetical temps the resulting values are the inverse of the daily temperature curve. The density differences have a negative slope with increasing temperature as expected from the basic relation of the density of water with temperature above 4 C. The daily density curve, even though a hypothetical construct, is another 'touchstone' analysis. Recall that while the partial molar volume is, in general, inversely related to the density, the partial molar volume inversion parameter is directly related to the difference in density.

Is there any way to connect the daily density fluctuation to the molar volume function inversions? The same basic procedure that produces the inversion test parameters can be followed for grab densities. Each date is labeled as a 'concentration' or a 'dilution' with respect to the previous date, then the differences taken: 1) a conc to a dil, 2) dil to conc, 3) dil to dil, 4) conc to conc. The groups for the partial molar volume inversion test parameter are the same as

density with ‘inversion’ substituted for ‘dilution’ and ‘non-inversion’ substituted for ‘concentration.’ Density on average goes down during the day with increasing temperature so grab sample status 3 & 1 (below) represent the daytime situation, 4 & 2 the night. The graph below shows the relation between density change, the partial molar volume inversion test parameter, and the other molar function inversion test parameters.

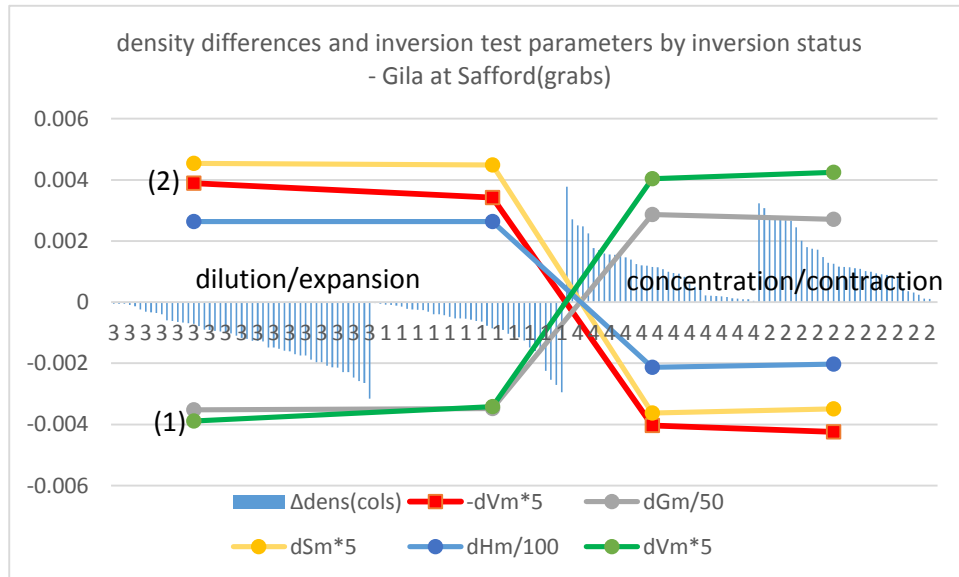


Figure 192

There are really two sets of inversions going on at the same time on any given day. The three thermodynamic functions are differently related to density change than the partial molar volume: ‘inversion’ substitutes for ‘concentration’ and ‘non-inversion’ substitutes for ‘dilution’, the opposite of the partial molar volume inversion test parameter relations. The result is that if the inversion parameter for partial molar volume is run as is, ( $HCO_3-Cl > 0$ ), there is one set of inversion statuses per sample date and it is the opposite of those for the other thermodynamic functions on that date. For example, a date with an inversion status of 1 (conc to dil) for the partial molar volume is a “2” (dil to conc) for the other functions. The upshot is that the two sets of relations cannot be sorted together so the date as a whole cannot be evaluated.

The partial molar volume inversion test parameter functionalizes the data through its relation to density change but it has no basic, fundamental meaning – it is not set in stone and parameters and directions can be changed at will. Converting the partial molar volume to a negative without changing the definition - ( $HCO_3-Cl > 0$ ) flips the partial molar ‘inversion’ to ‘concentration’ and makes the inversion status to density change the same across all functions. The negative partial molar volume inversion test parameter is, coincidentally, of the same form as the partial molar volume of water.

The final result, Figure 192, presents two options for the partial molar volume. With (1), the partial molar volume is directly related to the change in density as in the sum solution or uncorrected inversion test pattern view. The result is that the solution is contracting at the same time as the density indicates an expansion (dilution). In view (2), the solution partial molar

volume rises inversely to density change so that the dilution is now understandable as an expansion of volume.

But there is more. In (1) positive entropy occurs with a contracting partial molar volume. While not impossible, this result cannot be explained with a simple volume/entropy picture and requires information from outside (or deeper within) the system. With (2), positive entropy is simply the result of volume expansion.

One more view will be shown although it uses a procedure and a format to be developed later. The above graphs were created with hourly sample differences. The new view takes grab sample ‘inversion differences:’ inversion status 1s – inversion status 4s, inversion status 2s – inversion status 1s, inversion status 3 and 4 differences within themselves (an inv3-another inv3, an inv4-another inv4). The density differences are swept up in the procedure merely being the density on any given inversion status day. If the inversion statuses are lined up in a ‘beginning to end’ of an inversion (4,1,3,2,4) the results are the two graphs below. These improve the view of Figure 192, showing expansion and contraction more clearly and revealing the proportionality of peaks and valleys.

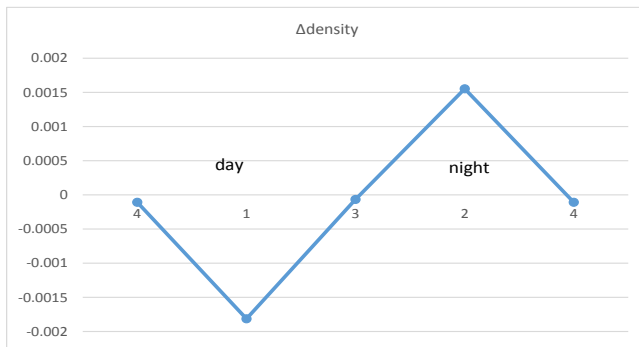


Figure 193

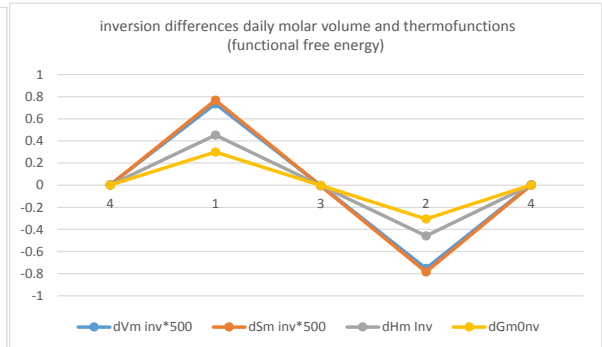


Figure 194

The above ‘corrected’ pictures of the thermodynamic function daily inversions meet all expectations. The negative entropy of nighttime is resolved over time by the positive entropy of the following day. There is one constant heat input signal: it is the alternating on/off switching of day/night that creates the alternating expansion/contraction, positive/negative entropy. What makes the molar view ‘molar’, the normalization by amount, is the same thing that makes the thermodynamic universe ‘complete’ – constant amount/energy. When amount is taken out of the picture and only temperature considered (and normalized - ‘H/T, G/T’), negative entropy is resolved over time.

The above picture is, of course, highly generalized. It depends entirely on the hypothetical daily temperature curve which changes monotonically like an ambient temperature curve. The real temperature of interest, the water temperature curve on any given day, is too complex with deviations occurring randomly over time and space. There is no ‘rule’ like the relation between flow and elevation to define spatial change. We are left with a picture that ‘must be right’

because it agrees with certain preconceived notions and does not disagree with the other pictures that evolve when averaging has smoothed things out.

The various molar function inversion groupings and patterns found to this point should be mutually reconcilable though actually doing so may not be easy. Where the molar function groups, molar volume and molar heat content, are in relation to the daily inversion parameter curves and how they intersect is not completely clear. It may be significant, however, that the group picture and the daily inversion picture has all three thermodynamic functions directly related to one another and to volume, though the sign of volume is flipped in the daily inversion picture (Tables 119 and 125).

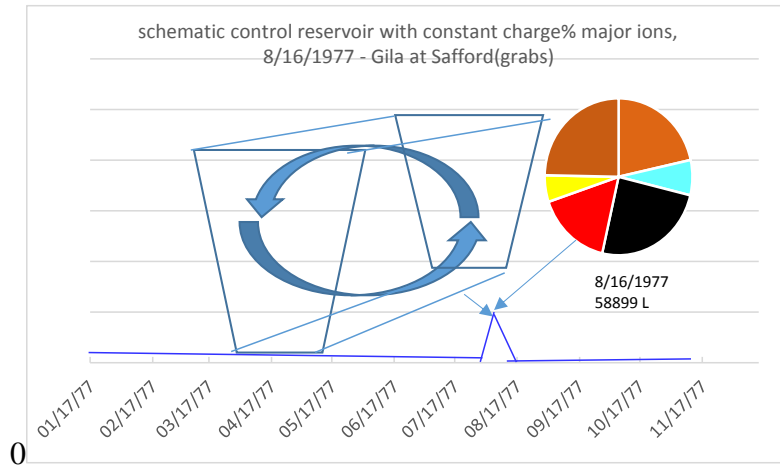
The fact that the daily inversion test parameter entropy and enthalpy patterns are the same is reminiscent of the fact that Na balances the other major ions for both molar functions (, [Figure 185](#)) in the grab sample correlations. There is no surprise here since one of the test parameter parameters in each of the two tests is Na (with entropy or enthalpy data as needed). But the free energy ion correlations ([Table 110](#)) show Ca and Mg related inversely to the rest of the ions including Na. So it appears that the balance of free energy, and hence the resolution of negative entropy, may require a shift from Na to Ca-Mg as the primary balancer. This speculation will be tested later when the proper context has been developed.

The effect of changes in the molar functions are to be seen in the total functions so the former will be examined to quantify the latter. But to do so with a control volume that only exists for one second is not possible. Instead, a 'control reservoir' is needed. The control reservoir is created when the rigid and impervious downstream (cross-stream) boundary, rather than appearing and disappearing every second, remains open for exactly one full day. When the volume of one full days flow has been reached, flow is directed backwards for exactly one half day (43200 seconds). When the backward flowing river just hits the upstream boundary, the backward directed flow is joined to the last of the incoming flow. The upstream boundary becomes impervious and stationary, cutting off all further flow into the system. At this point the 'lights are flipped on', the experiment begins, and the control reservoir contains an endless loop of flowing water with a period of one day.

The result is a conveyor belt arrangement of 86400 identical control volumes, moving but not changing in amount. All control volumes in the reservoir are subject to the same environmental factors whatever their position in the loop. Incipient precipitation and dissolution are noted but not allowed to proceed. The physical boundaries are rigid and impervious, with the result that stream deepening and widening is not possible.

The goal of this 'thought experiment,' however misguided it may be, is to create a closed system. In order to achieve this goal it is necessary to stipulate not constant flow, which would imply constant volume, but constant amount. The big picture here is a system with no open inputs, this in turn means that all control volumes, or subsets of the system, must remain identical in amount. They are allowed to change in volume which, since the effects of physical factors have been expressly forbidden, can only be a function of temperature change. It is easy to enumerate the

logical requirements for this experiment which would, however, be nearly impossible to actually construct in the real world.



Schematic 6

Maximum changes in value that can be expected due to temperature change alone can't be compared to average values that change due to a lot of different factors. To make matters worse there is no comparable dataset available, as far as is known, to compare results against. It is also clear that the molar functions may lack the 'completeness' necessary to do the analysis so seeing the effect on the total functions is not just nice it is necessary.

In addition, heavy reliance will be placed on volume and density relations of H<sub>2</sub>O. It is easier, with H<sub>2</sub>O, to get a 'feel for' which results may be correct and which are 'out of whack'. The partial molar volume of water may be just one of many partial molar volumes with no particular special significance. It is, however, easier to use than the sum of solution constituents' partial molar volumes which should theoretically add up to zero (though it doesn't in practice) and could cause numerical annihilation and explosions (DIV/0!) wherever it goes.

To generate 'experimental' results, the hypothetical hourly analysis is done on each grab sample day and averaged over all grab sample days. For example, the density of water on each grab sample date can be put through the hypothetical hourly analysis procedure described above and the result averaged with similar results for the other grab sample dates. The difference in density numbers, given below, are the difference of the density at 4:00 pm minus the density at 6:00 am and are per degree Celsius. The total function results are given since it is the effect on them that makes changes in the molar functions significant. The change in total kilograms, the change in density per C times the temperature range and the sample volume, is per day or, more specifically, the cumulative total over the twelve hours of increasing daytime heating.

hourly H2O density change analysis using hypothetical temperatures - Gila at Safford			
$\Delta(\text{kg/L})/\text{C}$	$\Delta\% \text{dens}$	$\Delta\text{kg/day}$	$\Delta\% \text{kg}$
-0.0002	-0.02	-23	-0.19

Table 135

The signs are correct for water, decreasing density with increasing temperature, but some explanation of what they mean may be in order. The negative  $\Delta\text{kg}$ , for example, does not mean that twenty three kilograms were 'lost.' It means that the volume change causes a change in density equivalent to an apparent loss of twenty three kilograms compared to the mass if the volume had not changed. This interpretation will be verified by calculation below.

Turning to the partial molar volume of H2O, the same analysis as for density can be run yielding the following results. The result in (L/mol)/degC to the left below agrees roughly with that found previously (Table 134) though the latter was a much cruder analysis and derived from data on a single date (8/16/77) ( $5.0 \text{ E-}5 / 27 = 1.8 \text{ E-}6$ )

hourly H2O volume analysis using hypothetical temperatures - Gila at Safford			
$\Delta(\text{L/mol})/\text{C}$	$\Delta\%(\text{L/mol})$	$\Delta\text{L/day}$	$\Delta\% \text{L}$
4.4E-06	0.024	40.8	0.298

Table 136

The change in the partial molar volume per degree C is very small amounting to only a 0.024% change at 4:00 pm from the partial molar volume value at 06:00 am (function max/min). The volume in liters, the same as above but with negative sign, is really 'lost' at night though it is immediately regained the next day.

The analysis at this point is not just hypothetical, it is actually a mish-mosh of hypothetical and real data. The temperatures are established as described above and the thermodynamic molar function differences are calculated with the temperatures generated. To calculate total function areas, however, the number of moles of each constituent is necessary. To calculate percents it is necessary to have the solution sums of the various molar and total functions. This data is taken from the grab sample data. The analysis is therefore limited to grab sample dates even though hour by hour straight function calculations could be done with the daily means. Only instantaneous data is used therefore and, further, is assumed to be, not average, but constant.

The effect of daily heating is very small on a percentage basis for both density and partial molar volume change as would be expected. But how variable are the results? For the difference in total relative volume, each days' analysis uses a constant value for moles of water. But over

different sample dates the amount of water will vary. So the difference in liters (dV) has to be understood as that of the hourly analysis run on the average of grab sample moles of water. Over all 161 samples with widely differing amounts of water, there is an expansion of about 41 liters. The averages over different grab sample used above for the sake of clarity, are replaced with ranges to give a better idea of the variability involved.

hourly H2O density change analysis using hypothetical daily temperatures - Gila at Safford				
	$\Delta(\text{kg/L})/\text{C}$	$\Delta\%\text{dens}$	$\Delta\text{kg/day}$	$\Delta\%\text{kg/day}$
min	-0.0003	-0.03	-298	-0.41
max	-0.00001	-0.001	-0.02	-0.01

Table 137

hourly H2O volume analysis using hypothetical daily temperatures - Gila at Safford				
	$\Delta(\text{L/mol})/\text{C}$	$\Delta\%(\text{L/mol})$	$\Delta\text{L/day}$	$\Delta\%\text{L}$
min	4.41E-06	0.0244	0.025	0.11
max	4.408E-06	0.0245	551	0.43

Table 138

The average cumulative change in mass corresponds to an apparent loss of 23 kg but can range from 0.02 to 298 kg, a maximum five orders of magnitude range. The change in cumulative increase in volume is similarly about five orders of magnitude. What makes water overwhelmingly representative of the solution are the amounts involved, the moles that cause all the problems in variability here.

It is clear that averaging over grab sample amounts undermines the hypothetical analysis. The varying number of moles on different grab sample dates undercuts the purpose of a constant amount analysis. The percent total difference min/max, however, are of the same order of magnitude as opposed to the total function differences which differ by orders of magnitude. The former are the numbers to focus on, however small they may be.

The effect of different daily temperature ranges on the molar functions is not a problem when results are reported by degree C. Over all grab samples the temperature at 04:00 pm ranges from 8 to 32 C while the minimum at 06:00 am ranges from -2.5 to 18. The difference between the two, the daily temperature range, however, is very constant as already noted. For the grabs, in one calculation, it averages 12.2 +/- 3 C though the range of ranges is from 4 to 17. For the daily means converted to water temperatures, the range is 13.4 +/- 3.4C.

If the average hypothetical temperature range of 13 C is used, the average cumulative change in density for one day is -0.00201 kg/L. If the sample starts on in the morning with the average winter dens(T) value of 0.9992, then by the end of the day the density will have changed to 0.99769 which is only slightly higher than the average summer dens(T) value of 0.9970. (Dens(T) values are used here because they are the density of pure water rather than density of solution (TSP)). Since the difference in density per C and the temperature range are averages, there will probably be large areas of overlap between daily density difference and seasonal density difference meaning the two cannot be told apart by magnitude alone.

With the change in density and the change in volume available, it is possible to examine the two to see if the results corroborate one another. First, the partial molar volume method: on 8/22/11 the original control volume dens(T) was 0.99672. The control reservoir expanded by 34.03 L

and dividing the original number of kg (12760) by the original number of liters (12799) plus the expansion liters yields a new density of 0.99431 (not a realistic grab density - this will be addressed later). Multiplying the new density by the original volume (as if there had been no expansion) yields a value of 12726 kg which is 33.83 kg lower than the original control volume mass. Second, using the density analysis, multiplying the change in density by the sample volume, the control reservoir change in mass is -34.02 kg. The results are an apparent 0.265% (pmv method) or 0.27% (dens) change in mass with a 0.56% difference between the two answers.

The excellent agreement of the two methods is a little suspicious, as if the argument were circular. It isn't, but it seems so because, if the density is exactly 1.0000, the change in kg will always be equal to the change in liters. Example  $(100\text{kg}/(100+2)\text{L} = 0.98\text{kg/L}, 0.98\text{kg/L} * 100\text{L} = 98\text{kg}, 100\text{kg}-98\text{kg} = \underline{2\text{kg}})$

To address the question raised above of 'unrealistic' densities being generated by the analysis, the above procedure will be repeated on an 'extreme' day. The maximum daily minimum grab water temperature (18.8 C on 8/9/79) sets the lowest possible morning daily density(T) value (0.99658). The control reservoir expanded by 8.77 L and dividing the original number of kg (5365) by the original number of liters (5380) plus the expansion liters yields a new density of 0.99522. Multiplying the new density by the original volume (as if there had been no expansion) yields a value of 5354 kg which is 9 kg lower than the original control volume mass. Using the density analysis, the control reservoir change in mass is -8.2 kg. The results are a 0.16% (pmv method) and 0.15% (dens) change of the original masses.

More straightforward analyzes comparing densities are also possible. The cumulative change in pmv H<sub>2</sub>O for 8/9/79 is  $4.4\text{E}-6 * 6.71$  or  $3.0\text{E}-5$  L/mol. The number of moles of water on that day was calculated to be 296421 which means that the control volume expanded by 8.8 liters. Dividing the original mass by the original volume plus the expansion liters yields a new density of 0.9952. Subtracting average density change (-.0002 kg/C) times the 8/9/79 day temperature difference (6.71) from the original dens(T) value of 0.99658 yields a density of 0.99524. All the densities calculated on 8/9/79 are higher than the lowest grab sample density(T) of 0.99478 kg/L. This means that the 'unrealistic' density of 8/22/11 is probably the result of a wider than normal temperature range (10.9 as opposed to 6.7 for 8/9/79)

The highest daily temperature range, 17.62 occurs on 3/20/02. On that date the control volume dens(T) was 0.99917 and the change in volume 14.74. Going through the calculations yields a new density of 0.995425 and an apparent loss of 14.24 kg. The change in density method would have predicted only -6.52 kg. Here, the agreement between methods is not good (0.19% & 0.42% or a 77% difference between the two) but the low density is within grab sample limits.

It is hard to decide how much to weigh 'unrealistic' density values in evaluating the analysis. Densities lower than the lowest grab density(T), 0.99478, do occur as seen on 8/20/11, so the analysis is generating density values not seen in the 'real world'. But the grabs are not daily minimums, they are instantaneous values whose difference from the daily minimum is entirely unknown. It is like randomly picking a density during the day and saying 'the daily minimum



cannot be lower than this or it is unrealistic,' which is absurd. If the daily mean day of year (doy) minimum minimum density(T) is used, the bar would be even higher (0.996495). The graphs below, which essentially remake the initial temperature range at Safford graph (Figure 173) but in water temperatures/C, shows the more variable grab min/maxs ( $r^2 = 0.859$ ) versus the daily mean day of year average daily densities ( $r^2 = 0.975$ ).

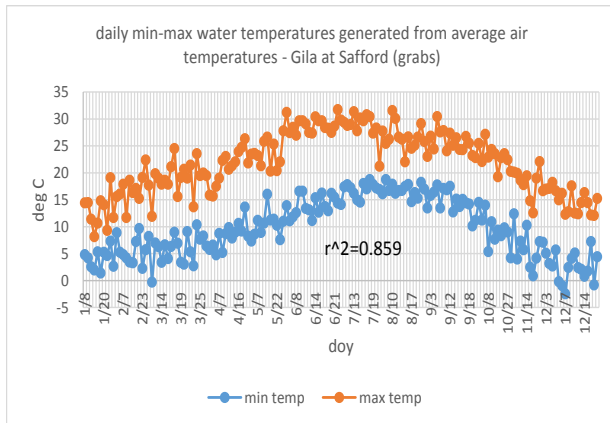


Figure 196

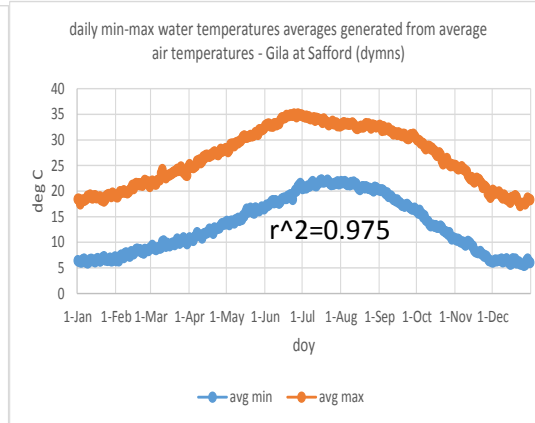


Figure 197

The analysis of extreme values to judge how realistic hypothetical results are is a logically sound method but it has to be done correctly. Here grab sample values were used as a matter of convenience rather than the more correct, daily minimum density values. Given the fact, however, that the daily minimum densities need to be calculated from air temperatures converted to water temperatures with a 'guesstimate' equation, they are not 'real' values either. For what it's worth and with only 1976-1989 daily air temperature maximums and minimums available (the SRA temps dataset), the minimum daily minimum density of grab sample dates comes out to be 0.9934 and the whole 'problem' just goes away.

The other molar and total thermodynamic functions can be processed to yield the following results using the new format, ranges rather than averages. Notice how a difference that is so small as not to be apparent at either the straight molar level (column 1) or percent molar level (column 2) can translate into a huge difference at the total level (column 3).

hourly H2O thermodynamic functions/kcal- using hypothetical daily temperatures - Gila at Safford				
	$\Delta(dX_m)/C$	$\Delta\%(dX_m)$	$\Delta X/day$	$\Delta\%X$
dH-min	1.7994741873804E-02	-0.0264	103	-0.46
-max	1.7994741873807E-02	-0.0262	2248734	-0.11
dS-min	6.04E-05	0.35	0.4	1.62
-max	6.47E-05	0.41	7840	6.80
dG-min	-1.67E-02	0.0212	-2	0.10
-max	-1.55E-02	0.0228	-0.4	0.39

Table 139

The change in molar functions for water is extremely small when reported by degree C. The direction of change agrees with those found in table 105 with enthalpy and entropy increasing and free energy decreasing with rising temperature. The change in the total enthalpy is huge, thanks to the overwhelmingly large amount of water.

To see how these numbers are generated by the analysis, four graphs are shown. Below are the graphs of grab (blue) and hypothetical (red) analysis results for change in molar enthalpy and percent molar enthalpy (top) and total and % total enthalpy (bottom) with change in temperature for water.

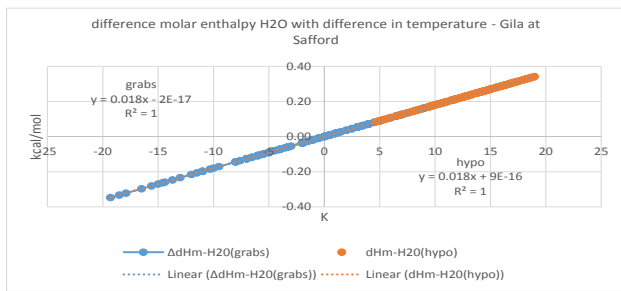


Figure 198

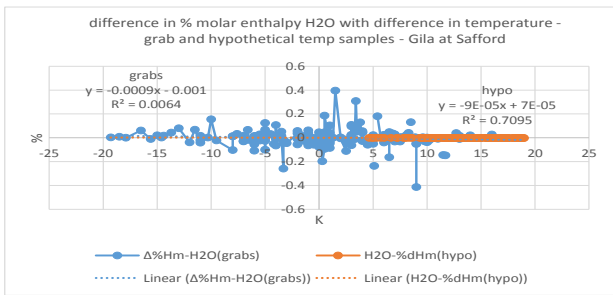


Figure 199

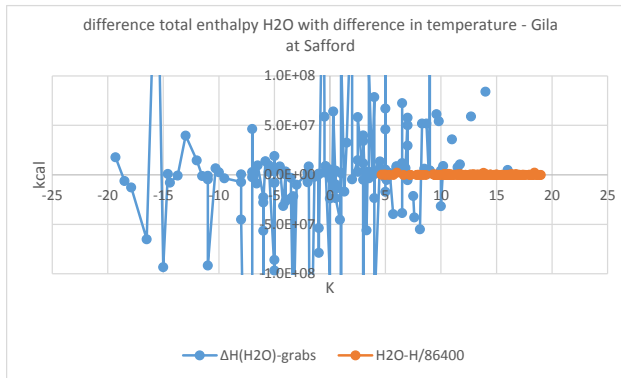


Figure 200

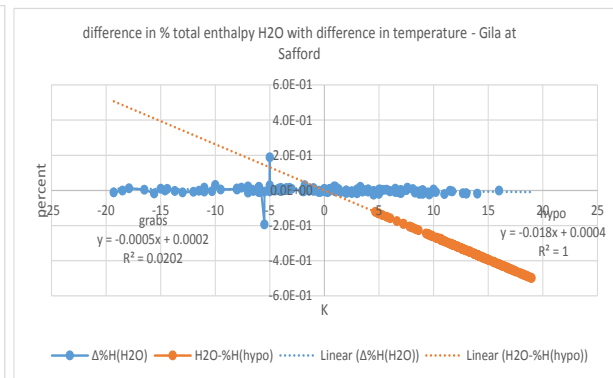


Figure 201

Molar enthalpy (top left) is highly correlated to temperature and the grab and hypothetical results agree with a common slope equal to the heat capacity of water. The hypothetical analysis appears as simply an extension of the enthalpy calculation into a higher temperature range. For the percent molar enthalpies (top right), hypothetical results are more linear ( $r^2=0.70$ ) than grab but have no relation with temperature (zero slope). The same applies to total enthalpy (bottom left): having the total number of moles of the grab samples in the calculation obscures any dependence on temperature there might be in the grabs.

But with the % total enthalpy (bottom right) a new relationship is set up with the hypotheticals, a relationship entirely lacking in the grabs. This new relationship with temperature is inverse and

quite linear. It is, of course, a direct result of holding amounts constant and is visible only in the percent total view.

Entropy gives basically the same picture as enthalpy with only the relation to temperature change in the percent total view being positive. The difference in % molar entropy and total entropy vs difference in temperature graphs (not shown) are carbon copies of the enthalpy graphs. In neither of those cases do the hypothetical results show any more relation to temperature than the grabs.

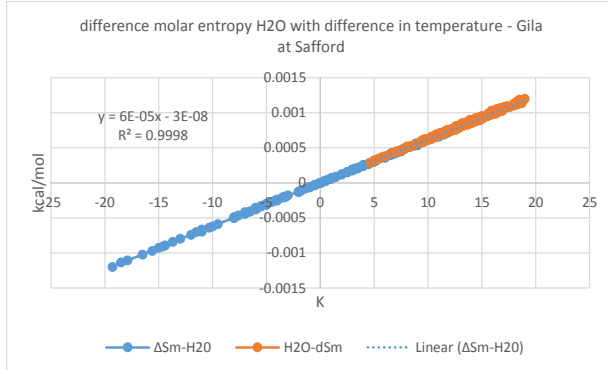


Figure 202

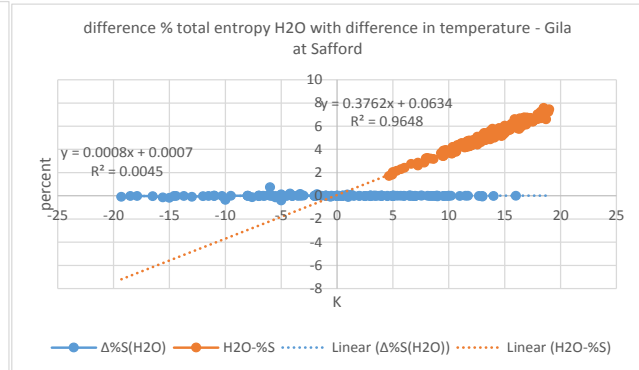


Figure 203

The molar entropy graph (above left) shows, once again, the hypothetical analysis to be just an extension of the basic entropy calculation carried out to a higher temperature range. The difference in percent total entropy vs difference in temperature graph to the right above again shows a new relationship for the hypothetical results that is entirely lacking for the grab samples, positive with temperature change as expected.

Free energy follows enthalpy but flips the direction of increase.

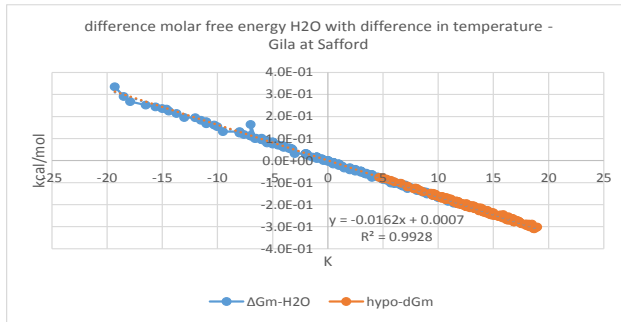


Figure 204

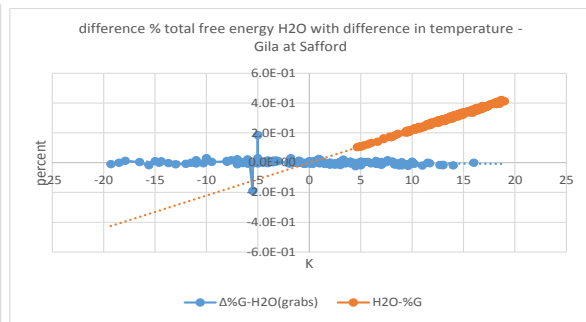


Figure 205

The new relationship is the direct outcome of the decision to hold the number of moles constant. The question whether this new relationship will yield any verifiable and useful information is still very much open. What has been shown to this point is that the various calculations are in accord with each other not that they are in accord with patterns that real samples would assume under the same conditions. The new relationship does, however, set bounds for the evaluation of the analysis. If the patterns of the grabs agree with the hypotheticals in partial molar, % partial molar, and total function, the spatial average assumption will be to some extent vindicated. It is not expected that

the grab percent total results will resemble the hypotheticals, indeed it is the difference that is the goal of the analysis.

The results of Tables 137-9 above look unobjectionable enough but there is no way to establish whether they are correct or not beyond the crude methods of checking self-consistency and looking for 'unrealistic' results. More information is required to provide a larger context by which to judge them. One way of establishing such a context is to compare them to the grab samples monthly averages. The monthly average partial molar and total relative volume of water for the grabs are shown below.

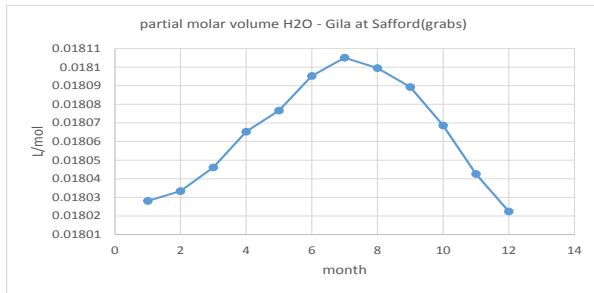


Figure 206

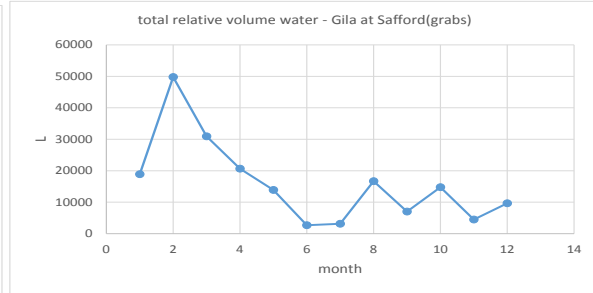


Figure 207 (back)

As noted before, the monthly partial molar volume pattern is the inverse of monthly density and identical to the temperature curve, while the total relative volume follows the flow pattern. The output of the hypothetical analysis is all differences, but it is possible to go back and pull out the hour by hour partial molar volume values that went in to calculating the differences. Below are the partial molar volume of water monthly averages by hour (top, left) and the averages of the hour by hour results by month (top, right) and ditto for total volume (bottom).

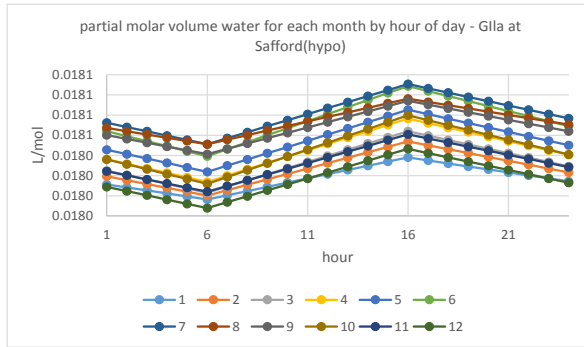


Figure 208

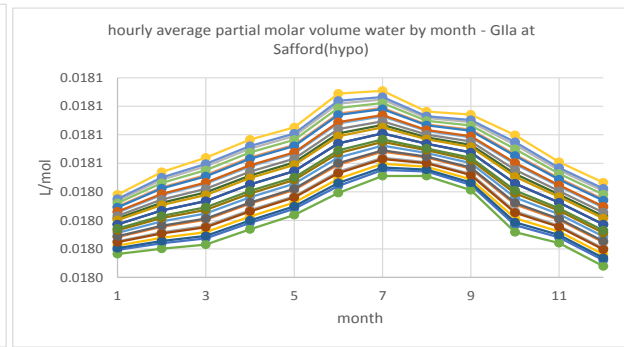


Figure 209

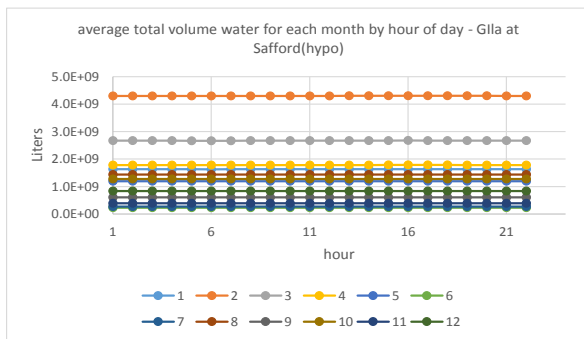


Figure 210

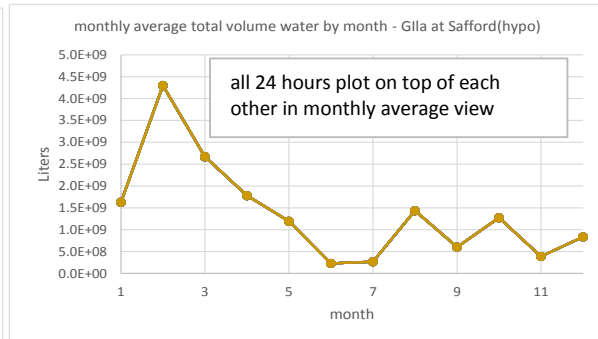


Figure 211

In the hour by hour daily results by month, top left, the (hypothetical) daily temperature curve is apparent. Reversing rows and columns, the monthly averages (top right), reveal that the hypothetical samples follow the same inverse density pattern as the grabs. Multiplying by a constant (as in 'moles') (bottom left) gives the total volumes which, when flipped rows to columns, reveals the flow annual pattern (bottom right) with the hour by hour results plotting on top of each other as monthly averages.

Here it is possible to see how simple the analysis is: an hour by hour calculation of the partial molar volume which varies slightly by month and the multiplication by a constant for any given day to calculate the total volume. Reversing rows and columns reveals that the basic underlying inverse density and direct flow patterns seen above still hold, it just takes a different 'view' to bring them out.

The analysis, however, produces as its output differences of molar functions and so it with differences, not values, that the grab and hypothetical results need to be compared. It is important to keep in mind in what follows that the 'differences' of grabs and hypothetical samples are two different things: differences in instantaneous temperatures from one grab sample date to the next vs differences in minimum and maximum hypothetical temperatures in a single day. The only reason these two sets of differences can be compared is that these are state functions and the result depends only on the difference of the two temperatures not on when, how, or why the differences are taken. If the temperature difference is the same between two grab sample dates as it is between the minimum and the maximum of a single day, the molar function result will be the same regardless of the different situations. The total function will also be the same but only if amounts are the same and constant. Differences in volume in this analysis are a function of temperature change only as explained above.

The monthly average differences of partial molar volume (left) and total volume of water (right) for the grabs (blue) and hypothetical (red) samples are seen below.

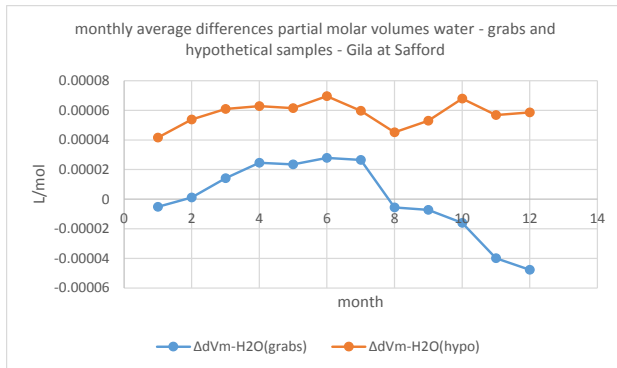


Figure 212

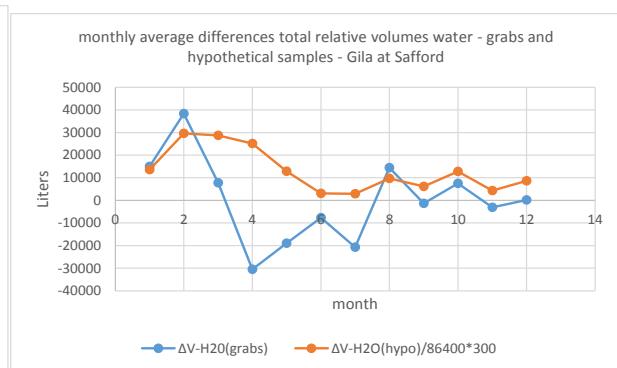


Figure 213 (back)

Grab and hypothetical total volume results (right) agree in following the flow pattern, the grabs in a rather exaggerated form, hypothetical samples in a rather muted form reminiscent of the daily mean flow curve. Note that the hypothetical samples had to be multiplied by 300 (after division by 86400) to be comparable to the grabs.

The partial molar volume grab and hypothetical differences (above left) follow the monthly temperature difference pattern but present several small but important differences. The hypothetical results are larger than the grab because the temperature differences are larger. A graph with exactly the same appearance can be generated by plotting partial molar volume differences vs **temperature** differences, rather than by month (not shown). The pattern is exactly the same as that above because the partial molar volume equation is just a linear transformation of the temperature curve. The fact that the grabs partial molar volume from Aug to Dec is basically going down while the hypotheticals are steady or going up is unexpected and may point to some 'other' factor in the grabs not accounted for in the hypothetical analysis.

The percent change in partial molar volume for water for grabs and hypothetical results are shown in monthly average form below left. Grab and hypothetical results are in good agreement for the difference in percent molar volume with peaks in April and November, but there is little else of interest.

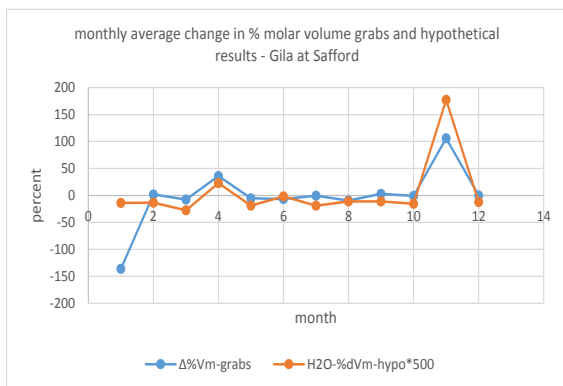


Figure 214

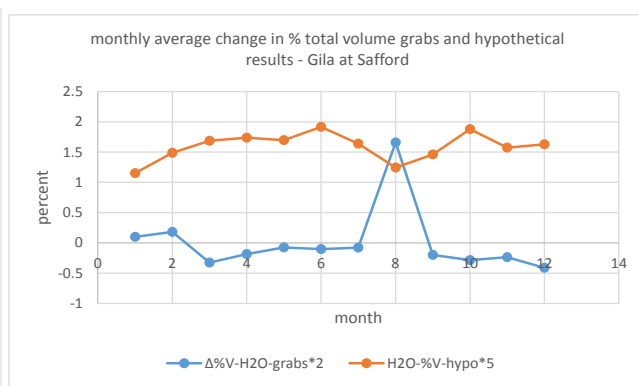


Figure 215

The difference in percent total volume (above right) for the hypothetical results (red) are quite distinct from the grab results (blue) as they should be. There is a small but gradual increase in the first six months in the hypotheticals, expansion corresponding to increasing temperature, with a dip in July-Aug as summer monsoons increase the total amount of water, decreasing the percent expansion number. Note that the grab curve, despite the excessively large August peak, starts out as a very weak, watered down form of the flow curve while the hypothetical curve, with the exception of the August dip, seems to be a very flattened out temperature curve. A total function seems to be showing temperature dependence, as opposed to being entirely a function of amount/flow, even if it is only a percent and is a rather 'flattened out' curve.

The analysis continues with the other thermodynamic functions. The monthly average thermodynamic functions proper are shown (below): first a view of the grab molar values (in residuals) and differences and then total values and differences.

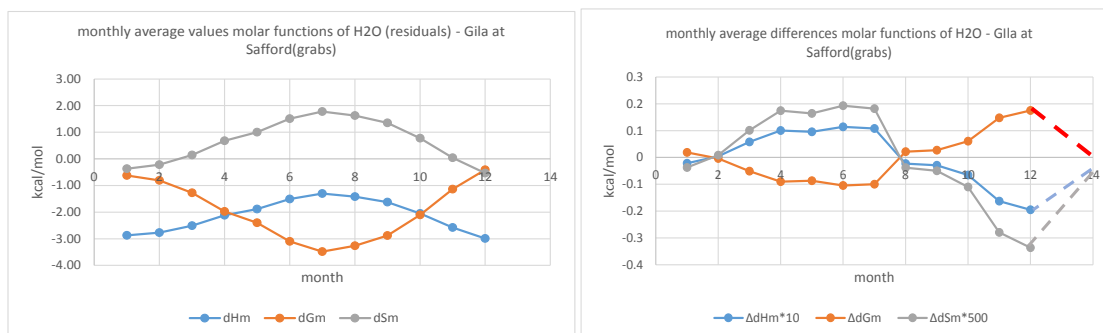


Figure 216

Figure 217

The molar functions of water quite clearly follow the temperature pattern either positively, enthalpy and entropy, or inversely, free energy. The differences of the molar functions clearly follow the monthly temperature difference curve (Figure 156) but is not an artifact but rather an 'inversion' because there are two different responses to the change in sign of temperature difference.

Any temperature dependent function is going to follow the daily or the annual temperature curve and will therefore show change in direction when the sign of temperature difference changes. The min and max temperature curves (Figure 172), when cast in monthly form, each show the artifact 'inversion' of monthly differences but at no time during the year do (or rather can) the functions cross one another. For the thermodynamic functions, only in the 'differences' view where the standard values drop out leaving just the temperature compensation portion, is there the possibility of true inversion. It is the difference in response to temperature change of the various parameters that causes the inversion not the temperature change itself, i.e. positive and negative heat capacity (or, for the partial molar volume, direct and inverse relation to density). Inversion is view dependent but not necessarily an 'artifact' for that reason – the view must simply incorporate the inversion relation and be worked out in the relations of the functions to one another.

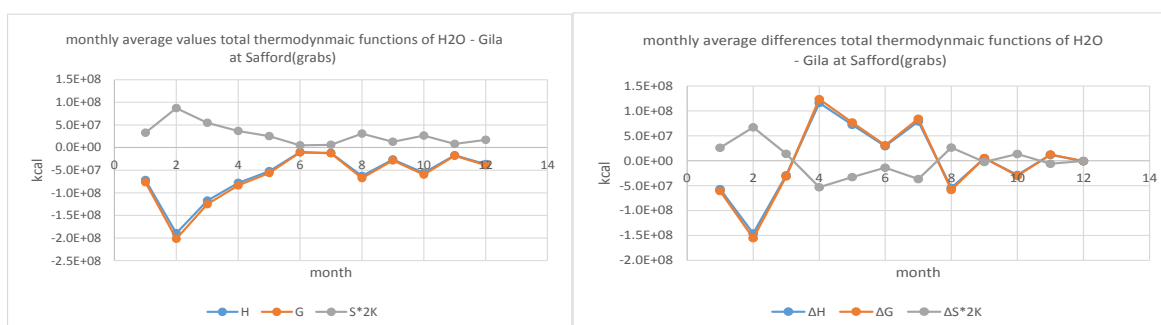


Figure 218

Figure 219

The grab sample total function values (above left) and differences (above right) above follow the flow pattern with entropy inversely related to enthalpy and free energy, the latter two largely plotting on top of one another.

The total enthalpy hypothetical sample differences (below) are calculated from the positive molar differences and show the total change brought about by the daytime positive temperature change, positive as well. So, when grabs (blue) are compared to hypotheticals (red), the analysis flips the sign while the effect of the numbers of moles part of the calculation remains apparent in the largely flow-like appearance of the curve.

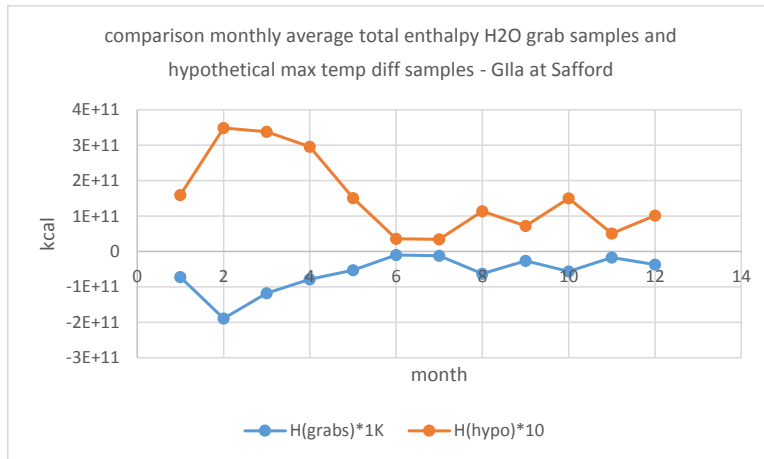


Figure 220

The differences of molar and total thermodynamic functions of water for the grabs and hypothetical samples are not shown since they are carbon copies of the flow graphs (Figure 206).

The percent molar thermodynamic functions are less well known and therefore bear showing in their 'untouched' form ('values') with the grab sample monthly averages. The percent molar functions (left below) are rather nondescript copies of the water partial molar volume graph. They show only slight responses in March and November with the November dip in entropy and enthalpy accompanied by an inverse movement of volume not seen in the smaller March response.

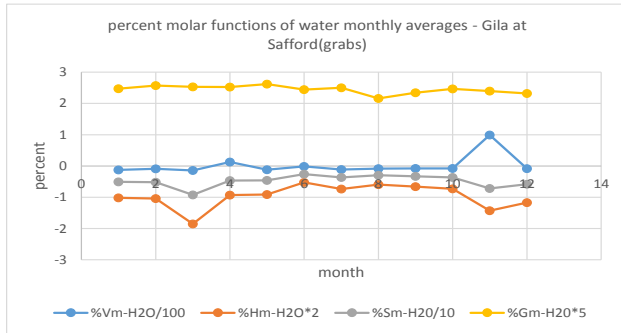


Figure 221

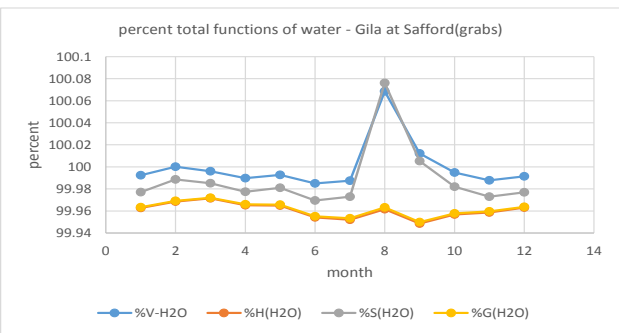


Figure 222

The percent total functions (right above) show a single large peak in August which is a volume/entropy peak, enthalpy and free energy plotting on top of one another in a much subdued peak below. But there is a bit of a problem here— thermodynamic functions, unlike football players, cannot give '110%': being limited by reality they can only be 100% or less. There is no doubt that there is something going on in August, and the volume-entropy combination is perfect to describe the expected meaning of the summer flow expansion, but values greater than 100% do suggest error.

It is again in the percent differences of the total thermodynamics functions that consistent temperature patterns begin to creep into the picture. The total volume percent differences have already been shown (Figure 212); below are similar graphs for free energy and enthalpy (top), and entropy (bottom), with grabs (blue) compared to hypotheticals (red).

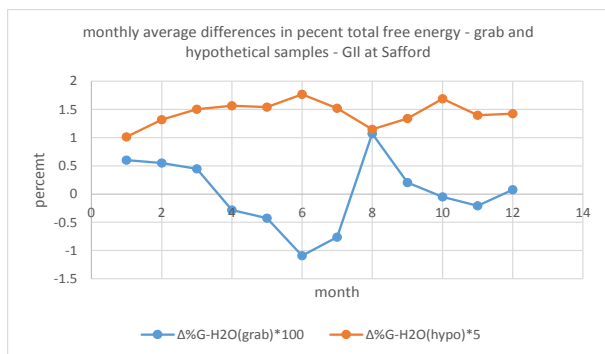


Figure 223

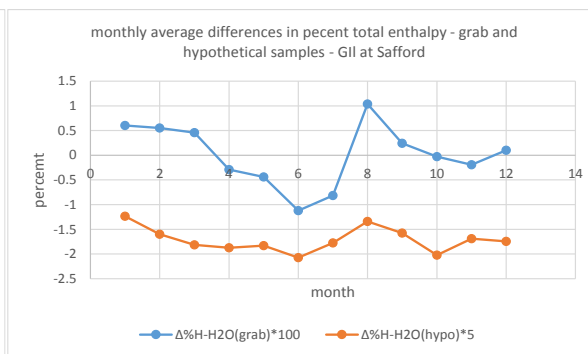


Figure 224

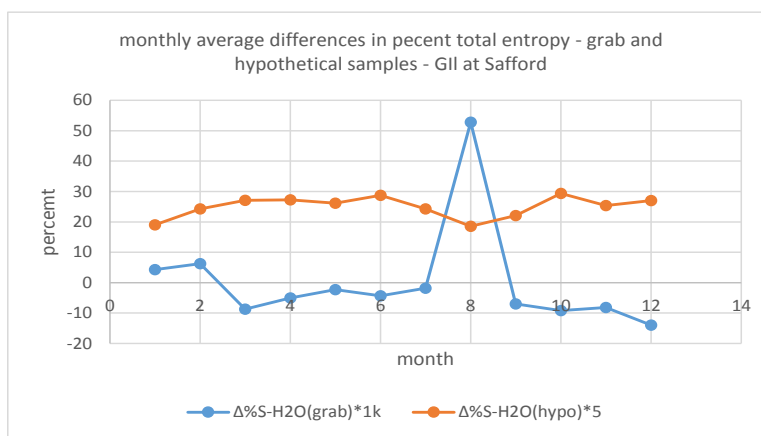


Figure 225

The grab samples (blue) all show the expected flow peaks (August) and valleys (June) though the entropy curve is pretty flat around June. The hypothetical curves (red) are quite distinct from the grabs, with free energy and entropy replacing the August peak with a valley and the June valley with a peak while enthalpy (top left) follows the direction of the grabs in June and August. In general, the hypothetical enthalpy curve is roughly the inverse of the entropy and free energy curves. Once again, total functions seem to be showing temperature dependence thanks to the stipulation of constant amount and are replicates of the hypotheticals daily temperature range (Figure 156).

Can any more refined seasonal analysis of the grabs show the same 'seasonal' temperature pattern seen in the monthly hypothetical samples? The short answer is 'no' and the testing will be summarized briefly here.

The grab percent thermodynamic functions were subjected to seasonal analysis to see if any influence of temperature can be found. The same seasonal analysis was done on the corresponding hypotheticals. Finding signs of seasonality in either would be good in itself but also help verify the original (rather flat) seasonal pattern supposedly found in the hypothetical monthly averages. Since the analytical methods and rationales for them have already been described the analysis will be done in summary fashion.

The first step is to do frequency distributions: the results are significant but not very interesting to look at, and so are not shown. The grab difference in percent total thermodynamic functions are all quite normal with perfect bell shaped curves. The hypotheticals are not normal distributions and are instead flat curves with low numbers in each bin. But hypothetical analysis is by definition an artificial construct and there is no reason why the results should be normal. It is, after all, very much the extrication of a 'part' of a larger whole: parts do not have the same expectation of normality that 'wholes' often do.

Another analysis of interest is autocorrelation to look for patterns. To summarize the results: grab difference values in %total volume and entropy show no autocorrelation (peaks at 6 and/or 12 mos = 0.40) which number rises a little for the hypothetical samples (0.65 to 0.71). The grab difference in % total enthalpy and free energy are, surprisingly enough, fairly highly auto-correlated (0.80) which number declines a little for the hypothetical samples (0.65-0.78). The hypothetical samples are, therefore, all in the same fairly narrow but low range 0.65-0.78 for autocorrelation whereas the grab samples are either highly auto-correlated (%enthalpy and %free energy) or not at all (%volume and %entropy).

Another view is provided by a simple density functional analysis (dddd). There are differentiations by magnitude and by sign among the % total thermodynamic functions for both the grabs and the hypotheticals but it is not clear what they mean. And more refined seasonal analyzes (season, function(s), function(l), also provide no clear clues. Both magnitude and sign have been pre-determined by the temperature range and the analysis procedure so there is really nothing to compare.



How has the transformation of an extensive function to show temperature dependence been brought about? Aren't these apples and oranges? To some extent, yes. Conceptually, the big difference between grab and hypothetical results is that the main factor in the grab total function differences is the difference in number of moles of the two samples. The number of moles, constant for each days' analysis but different for different days, appear in the hypothetical result total averages. Taking the percent total change eliminates the effect of different amounts on different days. With the hypothetical results, the difference in the molar function (usually small) is used with the moles for that day to show that portion of the total function that can be attributed to positive temperature change and this is relatively constant on a percent basis.

daytime molar function max differences			
H2O (soln) - Gila at Safford			
$\Delta dV_m$	$\Delta dH_m$	$\Delta dS_m$	$\Delta dG_m$
4.8E-05	0.20	6.6E-04	-0.18

Table 140

The relationship between the two types of inversion can now be dealt with at least qualitatively. The molar function inversion is seen to be a very small effect, as expected. Some 'views' may be better in finding such an 'underlying' pattern than others. But the main factor in amplifying or diminishing the intersection between the two is the timing of events.

These considerations lead to the big picture view, then, of the relation between major ion concentration inversion and the various molar function inversions. The two groups are related as a well-defined and consistent pattern with a tiny effect (the molar function inversions) with a largely random pattern occurring at a much higher magnitudes (hi-flow and input requirements of major ion concentration inversion). The intersection of the two is also largely random.

Things can either go in the same or in opposite directions or switch from one to the other depending on the point of intersection. The huge expansion in volume implicit in major ion concentration inversion can be heightened slightly if it occurs in the day-time and is accompanied by a slight rise in molar volume or lessened if it occurs in the night time and is accompanied by a slight decrease in molar volume. An extended period of major ion concentration inversion will show a slight expansion during the day, a slight contraction at night. This slight daily 'pulse' within the flow pattern changes over the year and so becomes a 'seasonal' effect though a very 'weak' one.

Less intuitive than volume change but potentially more interesting from the viewpoint of energy are the same scenarios in terms of entropy. Here differences in direction of the two types of inversion leading to either gradual or sweeping changes in entropy has implications in terms of 'reversibility'/'irreversibility' which in turn implies an approach or retreat from some sort of equilibrium. The difference in magnitudes of the two types of inversion, however, mean that any potential equilibrium at their intersection is going to be a very small effect, very deep in the system.

The control reservoir approach, with constant amounts subjected to a hypothetical daily temperature change, has provided some useful information on a possible underlying more extensive seasonal pattern for flow and the inter-relation of the two types of inversions (flow and density related). But attempts to find more specific, unambiguous temperature patterns in the grab total functions largely fail. The ‘flattened out’ temperature curve formed by the percent total function differences of the hypotheticals may just be an illusion and it may be the ‘scaling’ that leads to mistaking what is just a straight line for a curve.

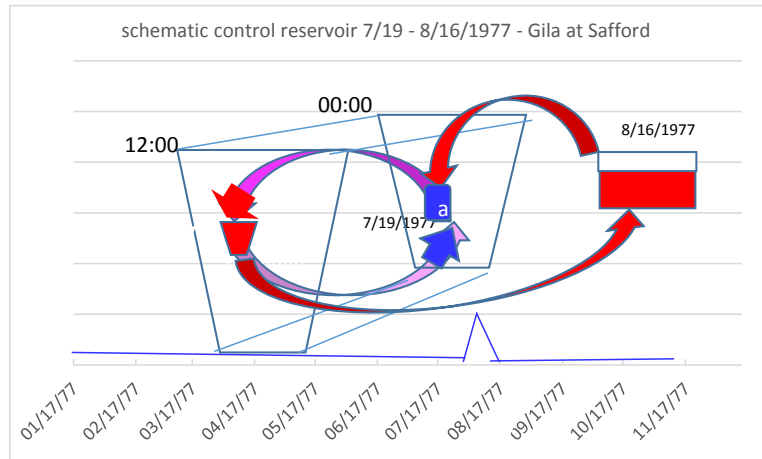
While the molar function inversions have been shown to have a small effect on the total functions, one that may change slightly by season, what major ion concentration inversion means for the system as a whole at any given incidence has not been dealt with. The question is, how does the system response called inversion play out on an individual event basis and what patterns unique to inversion evolve?

It is natural to wonder if major ion inversion has any effects ‘lower’ in the hierarchy of concentrations. A massive intra correlation matrix was constructed of all parameter concentrations with sample counts > 20. The major ions were in the upper left hand corner and the ‘other’ species, including major ion compounds, made up the rest of the matrix. The ‘other’ portion of the matrix was first examined by creating ‘identity’ blocks around the various species with a common cation. High correlations within these blocks were ignored as trivial – the concentrations of compounds are all calculated from single values of the cation and anion so if one goes up, another must go down. The result is that some groups are highly intra correlated (Cu, Mn, Zn) and others are only weakly intra correlated (Na, K).

Going up and down the matrix to examine non-identity block correlations shows a random mix of high and low correlations and no particular patterns. Cu and Zn tend to correlate with many other species while others correlate with few species, Pb compounds for example only with Cd compounds. No noticeable high areas of intra correlation among the other compounds that could create a nexus for another type of inversion was found but it is possible that the gaps between data points was just too wide and/or values just too low to count on (questions of ‘presence’). Higher correlations between trace metal compounds apparently only indicate that ‘where A is found, there B is also found.’

Having quickly reached a dead-end with this somewhat ‘shotgun’ approach, it is time to consider whether the use being made of the ‘control reservoir’ is not too limited. It is not a great step logically, even if it is a potentially problematic one, to imagine the introduction in a controlled manner of a set amount of new material from the environment. The new material is added as analytical input concentrations in a step-wise fashion as the difference of each parameter on the two days divided by the number of hours into which it is being applied. The result is a linear stepwise addition and subtraction going from first day values at 00:00 hours to second day values at 12:00 hours and back to the first. (The analysis was initially run with data from pairs of grab sample dates while later averages over groups of inversion or non-inversion dates were used. Also the hypothetical inversion or non-inversion peak was initially set at noon while later the peak is at 5 am or 5 pm. Examples are drawn randomly from earlier and later runs.)

The schematic below is an artistic rendition of what is going on. In between the ‘real’ values at 00:00 and 12:00, the hypothetical incremental values go from one date to the other. Day 2 values are gradually blended into the system up to noon, then gradually removed in the time back to 0 hours. The analysis therefore speeds up the chronological process from several days to over one day but allows the analysis over that period to be spread out in a series of steps.



Schematic 7

The USGS wateq4f program was used originally to generate activities, speciation, and solubility data for each of the 161 individual grab sample dates. Now pairs of dates provide the first and second day data input values for another run of the program whose output creates a dynamic picture of sample differences between the two dates. Varying wateq4f parameters in different runs, a variety of possible pathways between non-inversion and inversion can be examined.

In the initial runs, any parameter missing data on either day 1 or day 2 was zeroed out entirely. In later runs, averages of parameters are used. The wateq4f program runs into problems using parameter maximums, predictably yielding warning flags that input concentrations and conductivity are ‘out of sync.’ But it has no problems running minimums or averages of all parameters. To deal with the problem of ‘non-presence’, only averages of the major ion (MIavgs) were used initially. The idea for subsequent runs was to add averages of one new parameter at a time (“MIavgs+K”). Averaging ensures that there will almost always be a value for both day 1 and for day 2.

The averaging referred to here is over groups of paired dates. The dates are chosen by inversion status and include four possible ‘scenarios’: 1) non-inversion to inversion, 2) inversion to non-inversion, 3) inversion to inversion and 4) non-inversion to non-inversion. The choice of sample dates within each group was made to be mutually exclusive; each sample date could only be a day1 or a day2 not both. For example, scenario 3 are inversion dates followed by another inversion date. Of an inversion lasting over three dates, only date1 and date2 could be used because date2, once used, could not be a day1 for a date 3’s day2. (Sorry!) Date1 could be preceded by a non-inversion date because what is of interest here is the interval between date1 and date2. There are some dates that belong to more than one group, noticeably in scenarios 1 &

2, but as a whole the dates are not the same in both scenarios. Each category contains about 25-7 date pairs except 3 which contains only 16.

The most important parameter for inversion is, of course, flow. Scenario 1 are all flow up, scenario 2 are all flow down but scenarios 3 & 4 can be either. To cut down on the number of runs, scenarios 3 & 4 were run only with flow in an 'interesting' direction – flow down for scenario 3 and flow up for scenario 4. The flow directions are 'interesting' in that they 'test' flow going in the opposite direction indicated by inversion analysis. In scenario 4 (non-inversion to non-inversion) flow going up tests if any inversion-type responses are elicited. With scenario 3 (inversion to inversion) flow going down tests whether, on average, there is any indication that inversion may not last over the extended period.

The wateq4f program requires additional information beyond input concentrations such as TDS, conductivity, and salinity. These were initially derived from stepwise addition between the TDS, conductivity, and salinity of the two dates but later changed to calculations done on the stepwise added input concentrations. This change was theoretically necessary because not all parameters from the two dates were being used -- TDS of the two dates were of all parameters not just major ions (there were, however, no warnings from wateq4f when the two date TDS was used, so close enough). TDS is a straight addition of input concentrations (mg/L), salinity is estimated as TDS/1000, and conductivity is calculated from an equation derived from grab sample TDS and conductivity ( $r^2=0.97$ ) run on the newly calculated (input) TDS.

The wateq4f program also requires inputs for temperature, density, pH, and dissolved oxygen and these are far more difficult to model than the amount related bulk analyzes referred to above. To cope with these difficulties, some changes were made to the original setup. The time frame for hypothetical daily temperature increase was changed from 6:00 am to 4:00 pm to 5:00 am to 5:00 pm min/max. This change in time frame puts the daily temperature curve, a stepwise addition itself, in line with the (hypothetical) amount addition curve. It then becomes necessary to change the name of the analysis from a "hypothetical inversion in one day" to a "hypothetical inversion in 24 hours." The graphs generated are now from 5 am or 5 pm of one day to 5 am or 5 pm of the next – that is, two half-days with full inversion or non-inversion occurring at the center of the graph at either 5 am or 5 pm. There is no way of telling, other than by looking at temperature, whether the '5' at the center of the graph is 5 am or 5 pm so this information is sometimes included in the chart title (inv5am(Tdn)). The x-axis also changes from "hour" (of the day): to "time of day" (over two days). (Again, the analysis was performed many times over an extended period of time so these changes are not seen in all runs from which examples here are randomly chosen.)

The program was run with redox values all set to 'full' oxidation using the 'classical' H<sub>2</sub>O/O<sub>2</sub> couple which was deemed most appropriate for surface water. (The wateq4f program was originally designed for groundwater studies but test examples show it can be used with surface water as well.)<sup>17</sup> There is also another assumption here, probably a particularly good one for surface water, that one redox couple is 'dominant'<sup>18</sup> so that others can be ignored. Because 'full' oxidation is used, and there seemed little need for a 'deprived oxygen' scenario, dissolved oxygen was generated by a calculation using temperature, pressure, saturation vapor pressure,

and relative humidity rather than using field values. The result is dissolved oxygen values that follow temperature inversely and, remaining between about 7-8 mg/L, look more like Henry's Law values than field values which can range erratically from 6-12. There is at least one distinct disadvantage to using a calculation for D.O. which will be dealt with later.

For pressure the average of day 1 and day 2 was used with +/- 0.003 bar minimums and maximums at 4 and 10 am/pm in accord with daily fluctuations seen in the tropics (even though Arizona is not, of course, in the tropics!). This tiny pattern is really just a flourish and a nod to the 'daily' in 'daily context' having little effect on either density or dissolved oxygen values. The saturation vapor pressure was calculated from its relation to temperature and pressure. Relative humidity doesn't even qualify as a wild guess, being more a 'placeholder' than anything else, and is merely thrown in as the minimum of one day to the maximum of the other day. In scenarios 1 & 2, relative humidity goes from high for the inversion date to low for the non-inversion date but is in the 'interesting' ('test') direction for scenarios 3 & 4 or set to a low constant (25%) if not available. Dissolved oxygen was thus effectively eliminated as a factor in spite of its important role in the determination of Eh, the feeling being that 'full' oxidation covers the situation sufficiently. Using the same 'guesstimate' as for DO to calculate pressure, it is an easy matter to calculate the TSP density at each hour. A few runs were made with field D.O. values to see if any major changes could be provoked but there were no interesting results.

Temperature and pH are not so easily disposed of and here strategic decisions had to be made. The 'daily' context used here, it was decided, is not designed to produce the picture of a 'typical' day. It is designed to achieve two interrelated goals: 1) letting the amounts interact with the widest range of temperature and pH possible and (in part therefore) 2) heighten or diminish the possible effects of or on inversion.

The question becomes, however, whether any use can be made of grab sample temperature differences themselves in the model. The actual temperature difference values are of little use, being entirely a function of sample date difference as has already been seen. The very consistent daily temperature range of about 12-13C apparent in the min/max temperature graphs for Safford was also not used since that would lead to 'typical' results and not heighten the possible effect of temperature on inversion. The example of relative humidity was therefore used and temperatures range from the minimum of day 1 to the maximum of day2. This method results, in all cases but scenario 3, in an average hourly increase of a roughly 1C per hour. Only a careful examination of temperature y-scale values shows that these are occasionally 'impossible' days ranging, in one case, from 7 to 32C in a single day.

The final additional parameter is pH which has too profound an effect on speciation, in particular, to be relegated either to a set daily pattern (if one could be found) or the difference of averages on different days. Instead it is handled like temperature and relative humidity, going from the minimum of one day to the maximum of the other, to provide the largest possible 'daily' context for inversion. Because pH is so important, increasing and decreasing pH from day1 to day2 were done as separate runs of each scenario (pHup, pHdn). The modelling of pH is probably the most problematic step in the hypothetical scenarios. pH is, after all, a concentration and as such depends on all the other concentrations so changing it independently in willy-nilly

manner seems inviting trouble. The wateq4f program is relied on to pick up any major errors, but in itself, uses pH to make up differences, so . . . .

It is important to emphasize, before marching on, that a hypothetical scenario cannot ‘prove’ anything. The most telling example is scenario 3, from an inversion date to another inversion date. The pattern produced does not ‘prove’ that the inversion really lasted from date 1 to date 2. In fact, it **assumes** that it did in order to generate patterns around the inversion. Some of these patterns may be used to test the assumption. The real question is whether the newly generated patterns tell us anything about the real physical patterns of inversion. In this kind of game, about the only thing that can really be ‘proven’ occurs when a pattern is evolved that could not possibly exist in the real world, such as a violation of the first law.

Finally, it is necessary to make mention of some of the nitty-gritty detail of how the analysis was processed. While the endless qualifications and caveats may be annoying to read, an awareness of the logistical difficulties involved in the analysis should help the reader evaluate the results more critically. This study is ‘raw’ work as it developed not a polished product. The reader will not be spoon fed well-established pabulum but must make the best of it on his own.

An Excel workbook was used to put together the input for the wateq4f program and then create graphs from wateq4f output. A ‘wateq4ftemplate’ sheet was created and the rows of data from day one and day two input averages placed on two rows while the stepwise incrementations in between were performed by formulas copied from left to right over the entire data area between the day1 and day2 rows. The additional bulk parameter calculations referred to above were then ‘overwritten’ (over the stepwise incrementation formulas) as formulas on a column by column basis as needed. Both input and output values are graphed, the input mostly as a check to make sure no input errors were made. In addition a number of parameters that test the inputs and their relations are also graphed. Whenever possible, spreadsheet calculations were performed to see if wateq4f results could be reproduced. For example, ionic strength calculations are done by the wateq4f program and formulas in the Excel spreadsheet are used to try to reproduce the wateq4f results.

The workbook structure beyond the wateq4ftemplate is as follows: the wateq4f output file is opened on an ‘input’ sheet (i.e. input for the rest of the Excel workbook) and converted from fixed width text into Excel columns. The desired data is then extracted by string formulas, a process that depends highly both on the regularity of output formatting and correct selection of column widths. Errors at this level are easy to spot, usually producing unintelligible ‘garbage.’ The data is placed into columns first on one sheet, then converted into rows on another. The prepped data in columns A to Y of the second sheet (in rows) is then copied en masse onto A-Y of another sheet. This final sheet has sorting instructions and prepared graphs to the right of column Y so that the newly entered data merely has to be resorted with the sorting instructions provided to produce the majority of the graphs.

The basic data generated by the wateq4f program are concentrations (from activities), speciation, and solubility indices. Amounts are generated by concentration (mols/kg) times kg solvent and mols e- (moles of electrons) are generated from the amounts and charge. Percent “mols e-/2” are 50% cations, 50% anions. Later ionic strength, calculated from concentrations and charge, was substituted for mols e-. The data is replicated in different areas of the final worksheet in order to produce graphs of 1) the major ions 2) ion pairs by anion, 3) ion pairs by cation, and 4) high to low values (all parameters).

Additional ‘cleaning up’ and checking has to be done manually. At this stage checking is largely done by looking at the graphs. This is virtually the only way to easily check a workbook that is full of ‘linked’ cells many of which contain formulas and are therefore quite susceptible to corruption. Errors in not properly selecting the correct cells when using the ‘replace’ function, for example, can wreak havoc on such a workbook and lead to some outstandingly absurd looking garbage: The only remedy, if the error is spotted in time, is to exit without saving or face the possibility of endless manual corrections.

The analysis is done by a number of macros run in a specific sequence and requires a large number of manual checks and adjustments to be made along the way. The process is, however, streamlined to the point that an entire scenario, from data input to production of about 100-150 graphs, can be done in about 5-10 minutes if the checks are done in a cursory manner. Running three or four scenarios in a single day, however, is likely to leave the analyst in a mental state that makes checking results difficult. One of the most common errors is in chart titles when the analyst may lose track of whether, for example, the temperature of the current run is going up or down (or was that the run before?!) While most problems are easily spotted by looking at the graphs, deciding whether those ‘problems’ are just design or input errors or actually reflective of what is going on physically is often not. (One needs to be aware, in looking at some of the supporting data files, that many runs were done to look at specific things and were not completely checked in all areas for correctness – there may be ‘garbage.’ The danger is considerably heightened by that fact that outdated runs and sometimes even runs with errors were kept for future reference rather than deleted – although some attempt was made to clearly label failed attempts. (Caveat investigator!))

In spreadsheet chemistry calculation such as that done here, location is everything. The main program tasks of sorting and running calculations were done on data at a set location and arranged in a set order. The idea is to cut the coding down by eliminating the searching required when data is in random locations. The final arrangement of data for graphing or tabulation, other than the standard processed graphs, is usually done by manual cutting and pasting and errors can occur here although this type of error is usually spotted pretty quickly with graphs.

There are a couple of useful principles of coding used here. One is a modular approach – a series of macros run in a set order each of which does a limited amount of work on the data. Each macro in the module works only on a certain, named sheet and a new analysis requires a new sheet. Intermediate results are kept on separate sheets which can be returned to if further analysis runs into problems.

The coding within each macro is also modular and sequential. The use of overarching structure is minimized, instead the data is put through a sequence of analyzes which may build on previous analysis or be on the original data. One way of minimizing error within the individual macros is making analysis loops do nothing if conditions are not correct (If A=B (do something), Else (do nothing), End if). Error messages, either in the Else clause (msg: A<>B) or, better, independent (If A<>B (msg), Else (nothing), End if), are also useful in stopping analysis so that errors are not propagated.

No matter the precautions taken, the more processing of data the greater the chance of error. Work can be done pretty quickly with a spreadsheet and it is difficult to always keep up with annotation and tempting to just press on to see what ‘develops’. The situation is made worse by the habit of keeping for reference rather than immediately deleting erroneous analyzes as mentioned above. The result is that past work can be highly enigmatic, even for the author.

With this rather discouraging assessment of the difficulties involved, it is probably a good idea to jump ahead a bit and see what advantages, if any, the hypothetical scenario method may have – otherwise, why bother? With this new, looser, form of analysis a radically new definition of ‘inversion’ becomes possible. Inversion will include any trend or pattern that occurs on or around a major ion concentration inversion. This definition seems hopelessly wide but actually brings a more realistic approach to the analysis. With it, it is not necessary to see a parameter peak on the same day as inversion or have a curve that correlates with another curve before the two are considered potentially related. A parameter that peaks before the inversion may actually be a cause that has a certain ‘time lag’ before its effect is apparent.

Below is a graph from the study of a wastewater treatment phosphate removal problem. Volatiles in the reaction zone, the apparent cause of the problem, peak well before (1/16) and are on the way down when phosphate values (red) begin to rise above the control line (dashed red) to a peak on 2/12.

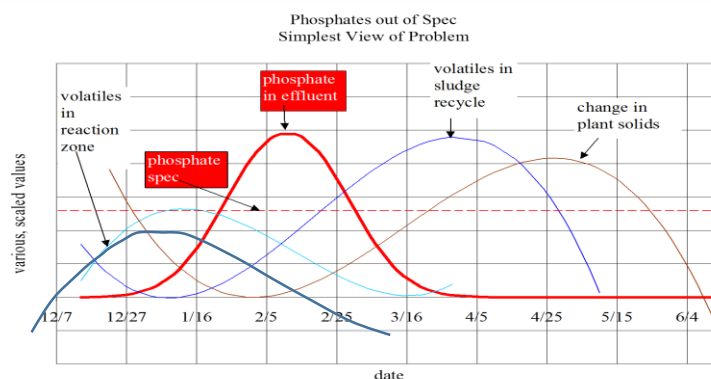


Figure 226

Peaks do not coincide and there is almost zero correlation between the curves. But peaks that occur near or around an event can be combined to form a logically complete picture. This

example shows a ‘slug’ passing through the plant – as the volatiles that were trapped in the reaction zone were gradually passed to the sludge recycle and removed from the plant, phosphate gradually returned to normal levels. This slow change is typical for solids-related change which is not nearly instantaneous as are pH or density change. It is the rise in sludge recycle volatiles combined with the drop in phosphate that points to the reaction zone volatiles as the cause. The analysis was not considered complete, however, until the dip in plant % solids that underlies the other curves was seen to correspond to a ten degree change in water temperature. The temperature-induced change in density forms a logical bedrock ‘linking’ the other curves to a well-known, confirmed physical phenomenon.

The success achieved in the wastewater study, which provided all the information needed to effectively end the phosphate removal problem at a major nuclear facility, was on a practical level only. The volatiles had already been fingered as possible suspects so the study only confirmed that. Two key factors, however, pointing towards a practical solution were discovered: the viscosity of plant solids and their location (# of cycles) in the system were shown to be involved. The discovery was made when a clarifier, running on (recycled) lime re-calcined at the plant, was seen to recover normal PO<sub>4</sub> values more quickly than other clarifiers on purchased lime brought in by railcar. Plant operators were then able to create techniques to put an end to the problem. No actual mechanism linking volatile concentrations with disruption of phosphate precipitation was ever found. One can only broadly speculate that differences in the matrix caused by the two types of lime being used was responsible.

But, to return to the proposed new line of inquiry, it is best to first see what is entailed in the mechanics. Below are the input concentrations of the major ions, using the stepwise addition method from day one to day two and back (left), and the output concentrations derived from them occurring during a hypothetical single day (right). These graphs show, in the simplest possible manner, the transformation of input to output concentrations from 7/19 to 8/16/77 placed in a single day (an example of non-inversion to inversion (scenario 1)). Note that there would be no inversion, i.e. in the sense of crossing of lines, if the input analytical concentrations had been used – inversion is a matter of activities.

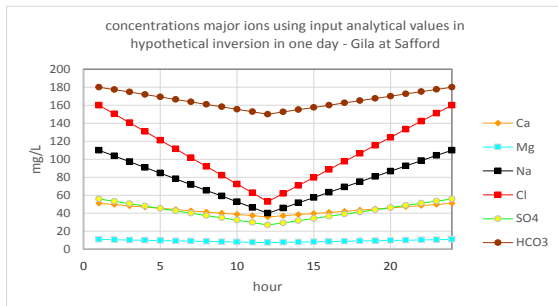


Figure 227

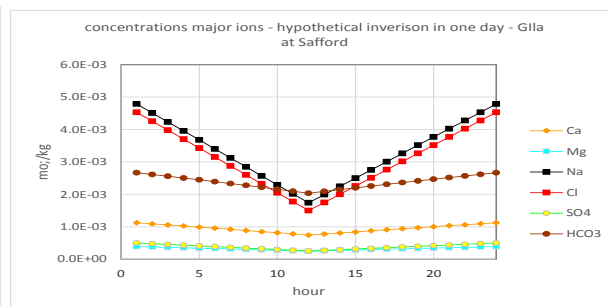


Figure 228

While concentrations can go either up or down with rising flow depending on relative input concentrations and volumes, amounts cannot, as has already been seen in the examination of low



flow regimes. Examining amounts helps highlight an important factor in the hypothetical scenarios. If grab amounts from the original analysis of the two dates are used and incremented in a stepwise manner from day one to day two, the graph to the left below is the result. But if amounts are calculated using the output concentrations (mol/kg) above right with stepwise added kg solvent over the two dates, the graph to the right below is the result.

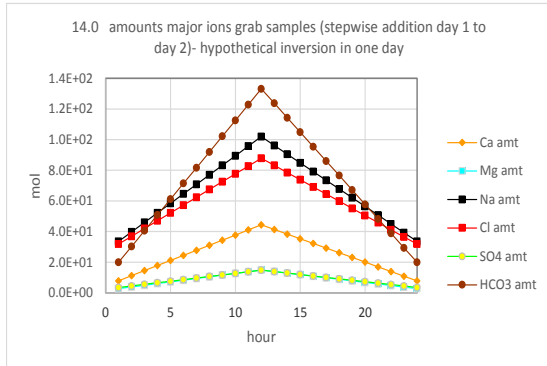


Figure 229

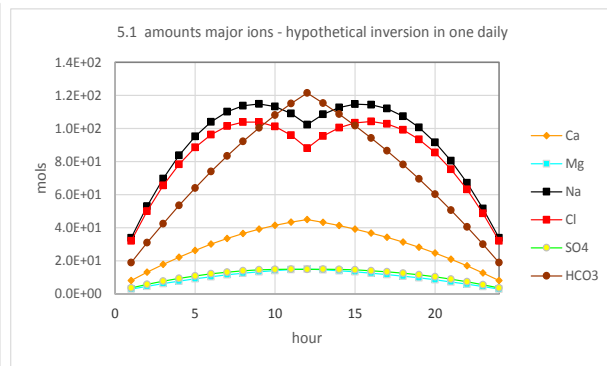


Figure 230

At first it might be assumed that the curious bending pattern of Na & Cl to the right might be an ‘activity’ effect. But if the **input analytical amounts** are converted to concentrations in mg/L with the stepwise added grab data for liters between the two days, the same pattern is obtained showing that it cannot possibly be an activity effect. Just for good measure, though hardly necessary, a run with constant temperature was made to make sure that it is not a temperature effect either and the result was a graph (not shown) exactly like that below.

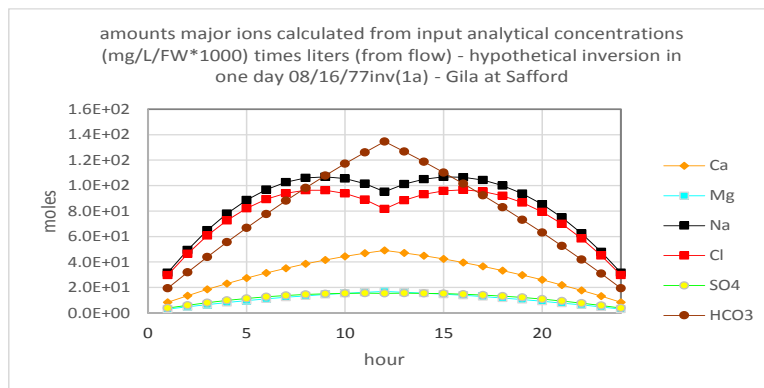


Figure 231

The above graphs are all ‘pictures’ of inversion but need some explanation. Flow, in the hypothetical one day scenario1 picture (date 1 non-inversion, date 2 inversion), is always going up from 0 hours to 12:00. The following graph shows the relationship between moles Cl and flow in chronological order over that time span. The curious thing here is that increasing flow is apparently accompanied by decreasing amount in the last three or four points on the graph.

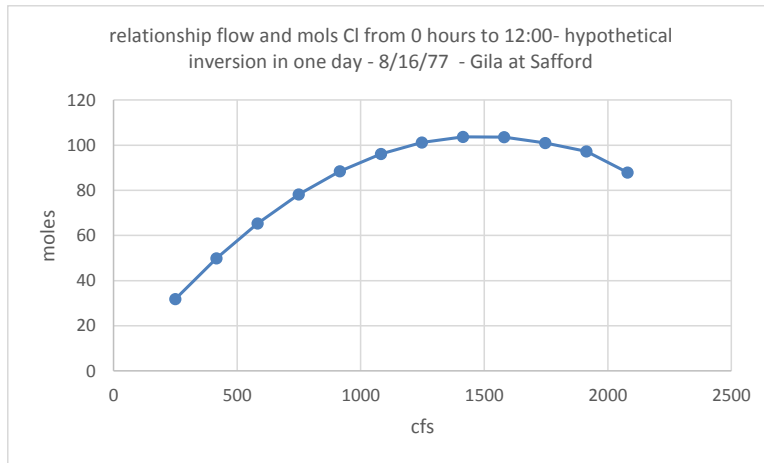


Figure 232

The bending pattern of sodium and chloride is easily explained in purely mathematical terms. The graph to the left below shows the volume vs time function while the graph to the right shows the output concentrations of the major anions vs time function. If time is plugged into the two sets of linear functions between 00:00 and 12:00 and the two multiplied together, the third graph below is obtained.  $(\text{flowslope} \cdot \text{time} + \text{flowint}) \cdot (\text{concslope} \cdot \text{time} + \text{concint})$

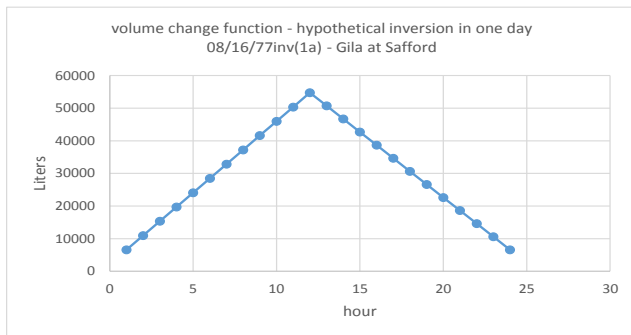


Figure 233

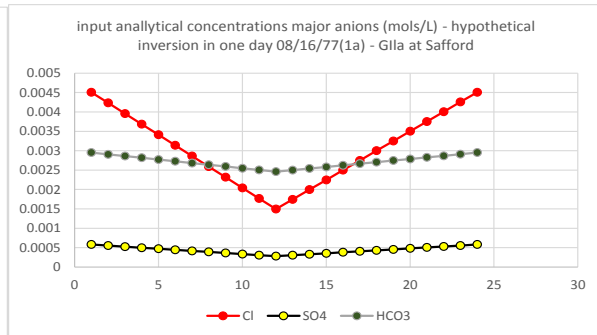


Figure 234

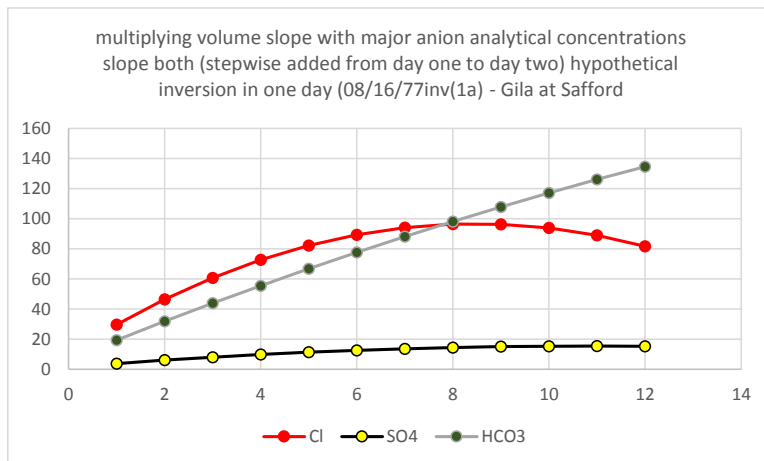


Figure 235

The multiplication of two linear equations yields a parabolic equation -- whether a parabola is actually seen or not depends on the 'scaling' of the graph. The bending effect is due simply to the interaction of two widely different slopes going in opposite directions. HCO<sub>3</sub> and SO<sub>4</sub> form much wider parabolas and the parts that are visible appear linear. Increasing the rate of volume change makes the parabolic shape apparent for these parameters as well.

But knowing the mathematical reasons in no way solves the physical problem of having rising flow associated with decreasing amount which is, as seen earlier in the analysis of low flow periods, an apparent violation of the first law. The 'fork in the river' version of the mass balance equation discussed above, is, once again:

$$M1 + M2 = M3$$

$$C1V1 + C2V2 = C3V3$$

$$V3 = V1 + V2$$

$$C3 = (V1/(V1+V2))*C1 + (V2/(V1+V2))*C2$$

As the last formulation shows, the equation is essentially a volume weighted addition of concentrations. C<sub>3</sub> can never equal either C<sub>1</sub> or C<sub>2</sub>, unless C<sub>1</sub> = C<sub>2</sub>, in which case C<sub>3</sub>=C<sub>1</sub>=C<sub>2</sub> or no change in concentration, which is not useful in studying inversion. Other than that case, C<sub>3</sub> has to be some value between C<sub>1</sub> and C<sub>2</sub> and no amount of manipulating the volumes can change that. If C<sub>3</sub> is to go from a non-inversion concentration of C<sub>1</sub> to a different concentration of C<sub>2</sub> for inversion, the **amount** has to be decreased while simultaneously increasing the final volume. There is only one way in which C<sub>3</sub> can equal either C<sub>1</sub> or C<sub>2</sub> and that is when one concentration is volume weighted at 100% while the other is 0%. This process is accomplished by decreasing and increasing flow.

two mass balance scenarios -- constant and changing flow							
	receiving 100 ppm	incoming 10 ppm			resulting		
L from flow	C1V1	C2V2			C3		
7079.25	707925	70792.5			55		
11790.169	1179016.9	117901.69			55		
16501.088	1650108.8	165010.88			55		
21212.007	2121200.7	212120.07			55		
25922.926	2592292.6	259229.26			55		
						flow1	flow2
7079.25	707925	0			100	100%	0%
11790.169	884263	29475.423			38.75	75%	25%
16501.088	825054	82505.441			27.5	50%	50%
21212.007	530300	159090.05			16.25	25%	75%
25922.926	0	259229.26			10	0%	100%

Table 141

What leads to confusion in the graphs above is that it is total flow that is being looked at and there is no indication of how receiving and incoming flows have been manipulated. Rather than a typical dilution or concentration with relatively constant, non-equal, flows, the hypothetical

scenario is actually a replacement of one flow with a certain amount of material for another with another amount. The same result might have been effected with water withdrawals, as in the low-flow period analysis, but that seemed a bit of a stretch even for an artificial construct such as this. While not impossible, the hypothetical scenario is not very commonly seen, with one stream going down in concentration to zero at the same rate that the other is going up. Whether such a change can actually occur, however, is less of an issue than that the analysis itself is creating a change from one system to another rather than showing a continuum change in one system.

Looking at what actually is going on under inversion conditions, it is immediately apparent that there are a variety of different responses. About the only things common to all inversions are the rise in flow, the decreasing activity of Na & Cl, and a drop in ionic strength. Everything else changes from one case to the next. The drop in ionic strength, however, provides a nexus around which a number of different strands of the story can be brought together.

The following discussion is a summary of findings in scenarios run with the major ion averages. Focusing on the major ions lowers the overall number of ion pairs and limits them to those mostly likely to have an important role. Later the major ions were expanded to include potassium (K), carbonate and hydroxide (calculated by wateq4f) to use as a reference baseline (“nuMI”) from which to evaluate changes caused by ion pairs. Finally the ions were lumped into groups to provide the most generalized picture possible.

It is necessary, when viewing the graphs, to keep in mind that changes in inversion status can occur twice on each graph, between 00:00 and 12:00 and 12:00 and 00:00. It will often be necessary to focus on just one half or the other of the full scenario graphs. Scenario 1 is the ‘non-inversion to inversion’ scenario but the actual non-inversion to inversion transition occurs on the left hand side, the right hand side is inversion to non-inversion or, more correctly, non-inversion to inversion run backwards. ‘Under inversion’ is often used loosely to mean the 00:00 to 12:00 transition whether there is an actual change in inversion status (scens1&2) or, less correctly, not (scens3&4).

Unlike moles e-, which follows amount, ionic strength is a function of the concentration of certain species – namely charged species. The major ions are, of course, all charged species. Examining the change in ionic strength of the major ions in scenario 1 values and percentages (left and right graphs below respectively) reveals that the percent of ionic strength of most of the major ions follows their values with decreasing ionic strength yielding decreasing % ionic strength. Calcium and sometimes bicarbonate, however, can have decreasing ionic strength but increasing % ionic strength. Bicarbonate is not as clear as calcium because it tends to form flat curves – little or no change in ionic strength or % ionic strength, particularly in scenario 3 and 4. The drop in ionic strength of Na & Cl (scen1 below) is so much larger and faster that Ca and/or HCO<sub>3</sub> can drop in value (left) while rising in percentage (right). This relation between values and percents is termed a ‘disproportionate’ relation.

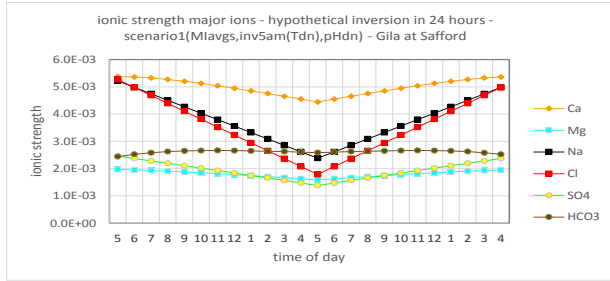


Figure 236 ([back](#))

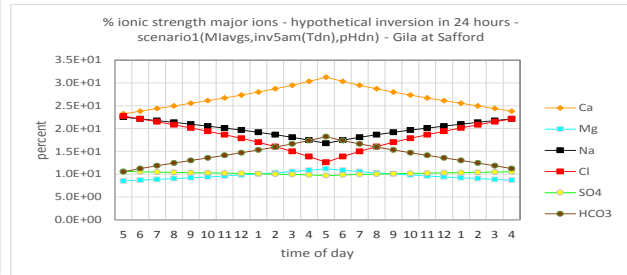


Figure 237

All the so called ‘free’ ions, which includes the “major” ions, are charged whereas ion pairs, which can also be referred to as ‘bound’ forms, can be either charged or uncharged (neutral). So that the bound forms can be added up as a group, they are converted to moles of free ion using formula weights. For example ‘CaSO<sub>4</sub> (reported) as Ca’ is the amount of CaSO<sub>4</sub> multiplied by the formula weight of Ca over the formula weight of CaSO<sub>4</sub>. CaSO<sub>4</sub> can also be converted to ‘CaSO<sub>4</sub> as SO<sub>4</sub>’ using the weight of SO<sub>4</sub> over CaSO<sub>4</sub>. The new formulations give the amount of free ion represented by the ion pair and can be summed up with the corresponding free ion to give ‘total’ ion. Finally, another group can be distinguished – ‘excess’ free ion is free minus bound – to quantify how much greater than bound forms the amount of free ion is.

In the following discussion the ‘bound’ forms being discussed are invariably the ion pairs of Ca, Mg, HCO<sub>3</sub>, and SO<sub>4</sub>. Na, K, and Cl form very few ion pairs (Cl <<<< Na,K) and those they do are in very low amounts. Below are graphs of amounts (moles) of total, free, bound and excess SO<sub>4</sub> in scenarios 1 and 2.

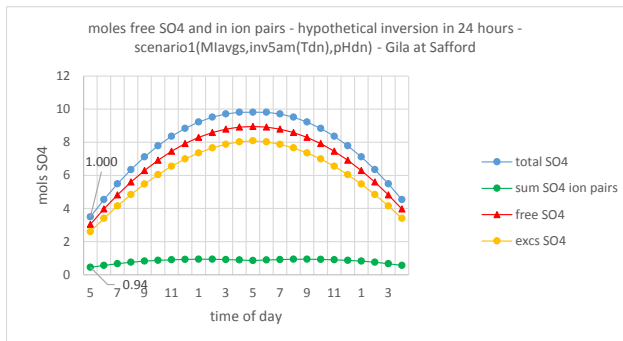


Figure 238

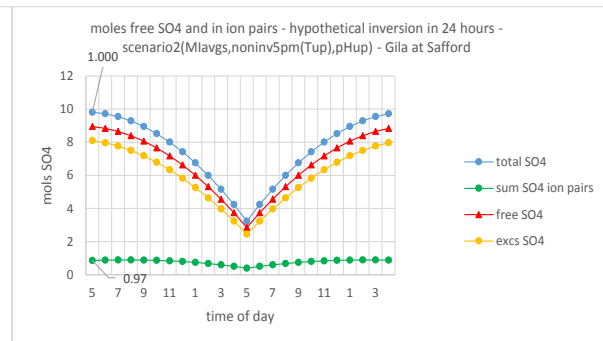


Figure 239

The relative amounts are typical of all the major anions with bound forms a very small percentage of the total. The bound forms do, however, change in the same direction with total and other forms - the data labels are correlation coefficients with the ‘free’ form. The direction of change is entirely dependent on flow and not affected by either pH or temperature. Scenarios 1 & 2 appear as the time shifted images of one another; the peak to valley of the right side of scenario 1 being the left side peak to valley of scenario 2 -- but only because the temperature and amount patterns are the same. Either scenario can peak or valley at 5 am or 5 pm, but the temperature change will be in sync with the amount change at only one time: 5 am for non-inversion to inversion and 5 pm for inversion to non-inversion.

Scenarios 3 & 4 show the same flow dependence but the y-scales are very different, scenario 3 being much higher and 4 much lower than either scenarios 1 or 2. Scenario 3 is the maintenance of the conditions at the center peak of scenario 1 (12:00) while scenario 4 is the maintenance of conditions at the center valley of scenario 2. Neither are straight lines because still affected by the direction of flow change within the scenario (flow down for 3, flow up for 4) whatever the magnitude of flow may be.

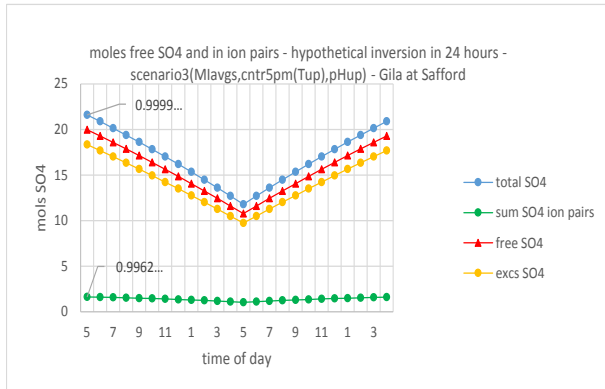


Figure 240

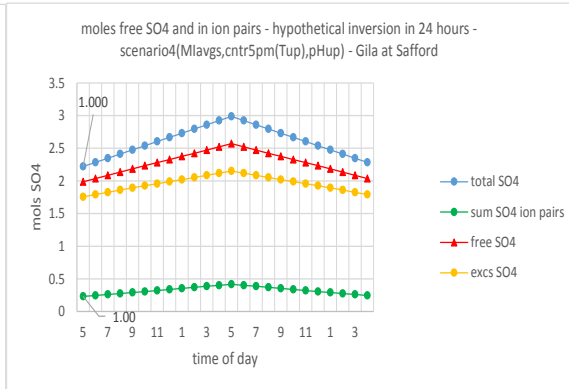


Figure 241

The overall patterns of free and bound ions of the cations (not shown) are very similar to those of the anions. Here also the direction of change is determined by flow. Total, free, and excess ions are generally so close that they plot on top of one another. The bound forms, which are positively correlated to the others, are very low percentage-wise as with the anions. Once again the y-scale is much higher for scenario 3 (max 60), much lower for scenario 4 (max 6) than either scenario 1 or 2 (max 30-35)

The same approach can be taken with oxygen but the results are very different. Here bound forms predominate over free (D.O.) though again the different forms are all highly correlated to one another. The direction of change follows flow as expected and scenario 3 y-scale is high, scenario 4 low as one would expect with the highflow/lowflow distinction implied in inversion status.

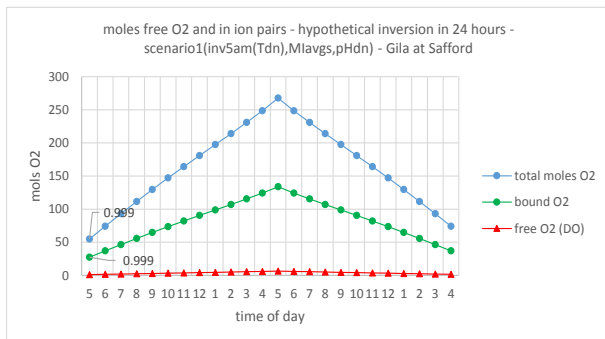


Figure 242

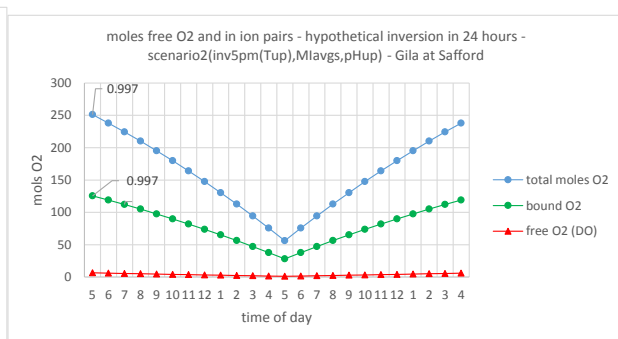


Figure 243

It is worth expanding a little on the distribution of oxygen in terms of combinations with the major ions. In the graphs below it is clear that HCO<sub>3</sub> is the predominant bound form and that it

follows total O2 closely. The correlations with free O2 are less evident in the other forms and become increasingly lower in scenarios 3 & 4.

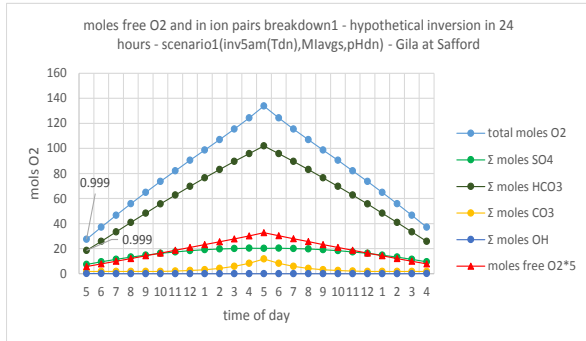


Figure 244

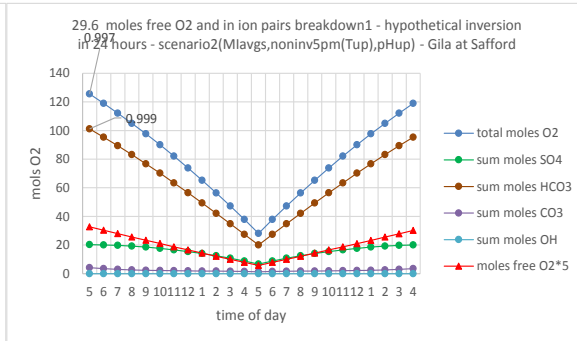


Figure 245

Dipping down further in the hierarchy of amounts, the effect of varying pH becomes apparent, particularly in the case of CO3. Hydroxide (OH) is affected along with CO3 though that is not visible on the graphs below due to scaling issues. Below are two views of scenario 3 O2 bound and free with pH going down (left) and up (right). Note in particular that CO3 amounts go up at the center of the left hand graph even though flow is going down and the opposite for the right hand graph.

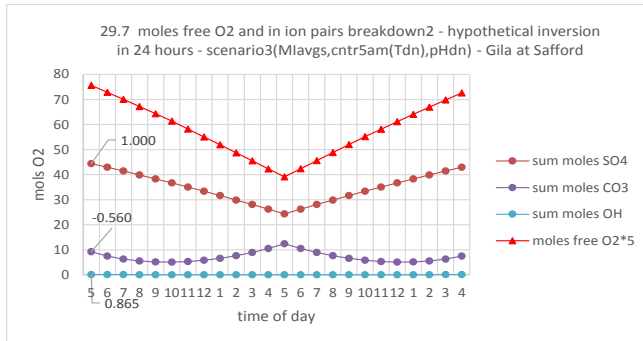


Figure 246

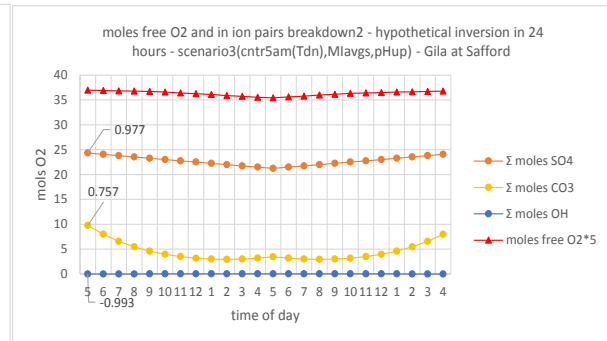


Figure 247

The above graphs show how different relations can be when viewed at different levels. The free cations and anions are a very low proportion of the total ion but, when viewed as compounds of oxygen, some are much higher than free oxygen.

To get at the relations between the forms, the major ion bound forms can also be viewed in terms of percentages, the sum of the ion pairs (as free ion) divided by total ion. The high dependence of %CO3 on pH and the relative inertness to pH of all the other anions is evident here. O2 bound forms are very steady at 50% while the others are also steady but lower at 0-12%. % bound forms of HCO3 is noticeably a very low portion of total HCO3 though, as already seen, it is a high proportion of total O2. Below are the percentages for two views of scenarios 1(pHdn) & 2(pHup)

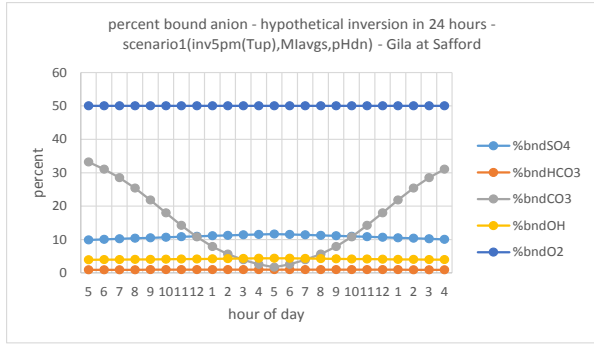


Figure 248

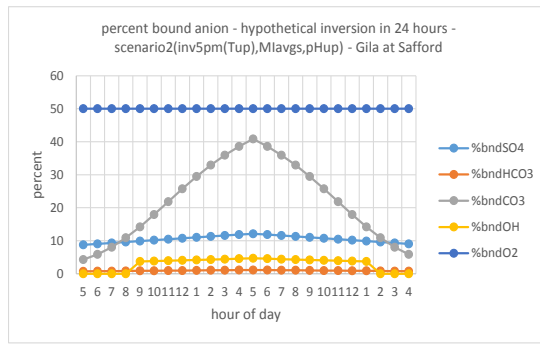


Figure 249

On the other hand, inversion/non-inversion (from 0:00 to 12:00) changes the gap between free and bound form amounts dependent upon flow quite a bit for HCO<sub>3</sub> and O<sub>2</sub> which are inversely related to one another, while SO<sub>4</sub>, CO<sub>3</sub> and OH are not noticeably affected. Scenario 3 has the widest gaps while scenario 4 has the lowest and is also not highly effected by flow (low flow regime). Below are the gaps for two views of scenarios 1(pHdn) & 2(pHup).

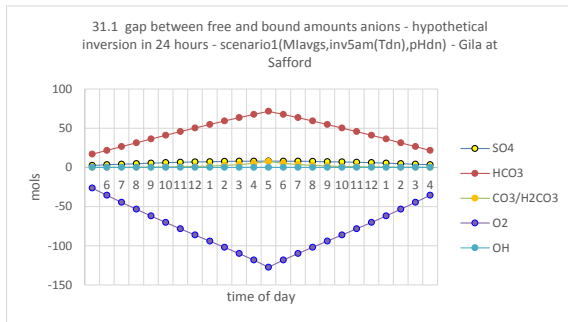


Figure 250

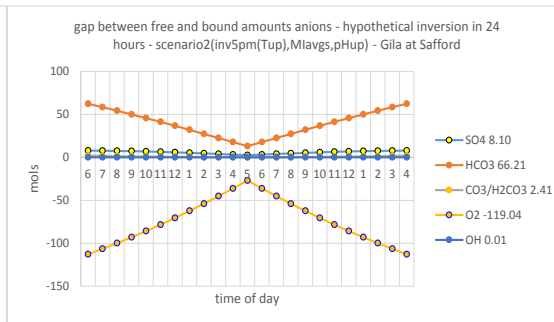


Figure 251

While the percentages of most of the bound species remain fairly steady for the major ions, changing significantly only for CO<sub>3</sub> and OH, the gap between free and bound for some increases with inversion. The reason for this result is that the ion pairs are returning free ions to solution as they are, themselves, dissolving.

The cations show slight differences from the anions in terms of the percentage bound and gap between free and bound views. There is variability caused by what percent of bound cation is associated with CO<sub>3</sub>. The y-scale for percentages is invariably around 3 to 6 across all scenarios. The gaps between free and bound are highest for Ca, next Mg, finally Na and are dictated by flow with the typical high y-scale for scenario 3, low for 4 and intermediate for 1 & 2.

In order to put the various strands developed together into some sort of coherent picture, two new 'views' are developed for the major-ion ion-pairs (the 'results' of the process). First, constituent ions (reagent) concentrations and percent speciation are on one graph. Then, on a second graph, ion pairs (products) of those ions and others competing with them. As an example here are the scenario 1 & 2 pictures for CaSO<sub>4</sub>, with the base ion view on top and the competing ion pairs below.



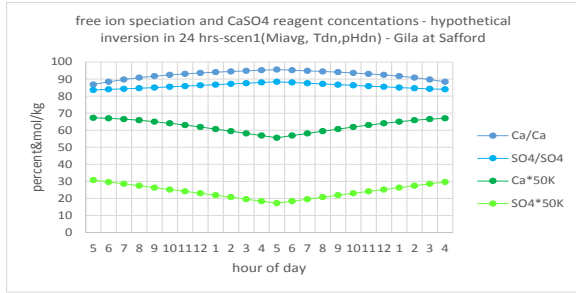


Figure 252

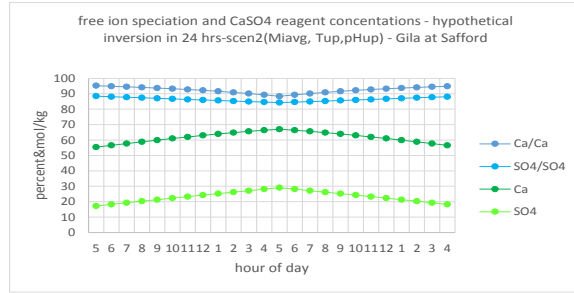


Figure 253

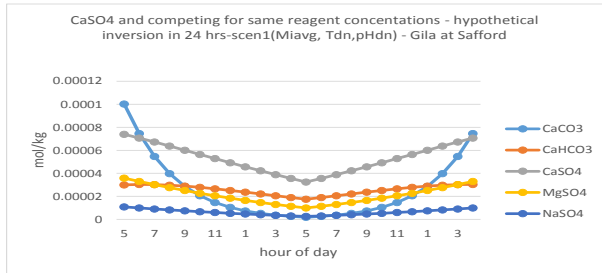


Figure 254

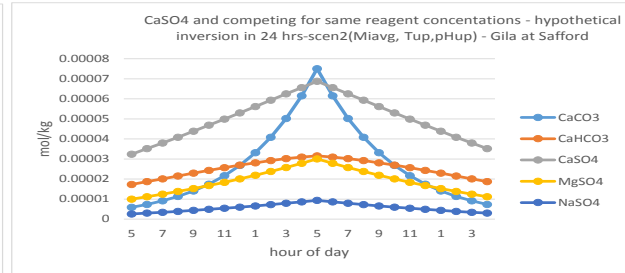


Figure 255

Scenarios 3 and 4 speciation and concentration of Ca and SO4 have much the same look but form flatter curves with SO4 concentrations, low in scenario 3 and high in scenario 4.

The shift in view here has turned everything ‘upside down’ from the earlier graphs using amounts. With increasing flow, amounts almost invariably go up. An incoming water can raise amounts or not change them but cannot lower amounts in a receiving water (unless water is being withdrawn). But increasing flow usually causes **concentrations** to go down by dilution effect (unless incoming concentrations are so high as to overcome the added volume). When free ion concentrations go down, so do bound form concentrations in accord with mass action.

Scenario 1 is flow up from 00:00 to 12:00, flow down from 12:00 to 00:00, and the regime is dilution, so concentrations go down with rising flow and up with decreasing flow. On the left half of scenario 1 above free ion concentrations (green lines) are seen to be falling with increasing flow. A fall in concentration of the constituent ions pushes the formation equation for CaSO4 in the direction of the reagents (constituent ions) to relieve ‘stress’ on the system in accord with LeChatelier’s principle.



Dissolution of CaSO4 is favored as long as Ca and SO4 concentrations keep dropping. This fact is mirrored in the rise in % speciation of Ca/Ca and SO4/SO4 (blue lines) since these must rise as % CaSO4/Ca and % CaSO4/SO4 fall.

When Ca and SO4 concentrations plateau and begin to rise once again, as seen on the left side of scenario 2 above, the mass action equation is pushed in the opposite direction – formation of CaSO4.



Concomitantly, % speciation of Ca/Ca and SO<sub>4</sub>/SO<sub>4</sub> drop because %CaSO<sub>4</sub>/Ca and % CaSO<sub>4</sub>/SO<sub>4</sub> are rising. The percent speciation of the reagent ions is inversely related to the concentration and % speciation of their ion pair products. As reagent ion concentrations go up and the CaSO<sub>4</sub> equation is pushed in favor of product, the concentration and speciation % of CaSO<sub>4</sub> goes up while the speciation % of Ca and SO<sub>4</sub> go down – they are being ‘used up’ in the formation of product.

The falling major ion concentrations caused by increase in flow during inversion lead to the favoring of the dissolution of ion pairs and subsequent increase in free ions. The newly freed ions, Ca & Mg and SO<sub>4</sub> & HCO<sub>3</sub>, are +/-2 (except HCO<sub>3</sub> which is -1) so ionic strength might be expected to go up. Why then does ionic strength invariably drop as inversion proceeds? The answer is that Na & Cl concentrations are so much greater and fall so much quicker than that of any of the other ions that that is the dominant factor in change in solution ionic strength.

The nice elementary-chemistry picture of free ion speciation/ concentration and ion pair concentrations may strike some as too neat and something that would probably not be apparent in real world situations. But the above mechanisms can clearly be seen in the following graphs for Boulder Creek. The SO<sub>4</sub>/SO<sub>4</sub>, Ca/Ca and Mg /Mg percents go down (graph to left below) and CaSO<sub>4</sub>, MgSO<sub>4</sub> and NaSO<sub>4</sub> concentrations over the same period go up (graph to right). Formation apparently went on more or less steadily for about 8 months.

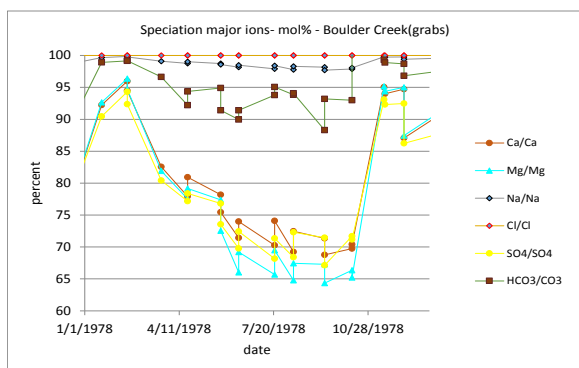


Figure 256

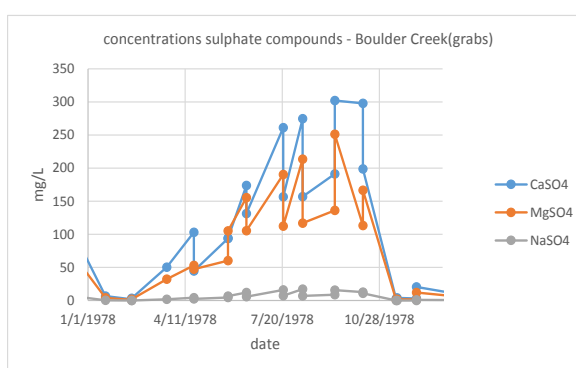


Figure 257

Note that %HCO<sub>3</sub>/HCO<sub>3</sub>, in the left hand graph, does not correlate as tightly with that of the other ions as they do with each other. Growth of ion pairs, in the right hand graph, is generally exponential, though appearing linear or logarithmic at times, and the order of magnitudes is usually CaSO<sub>4</sub> > MgSO<sub>4</sub> > NaSO<sub>4</sub>.

Though the percentage of sulfate as sulfate is decreasing, sulfate concentrations actually have to be rising because that's what is pushing formation of the ion pairs. Ion pair formation is self-regulating in accord with the law of mass action (sulfate input in an open system in a steady state).

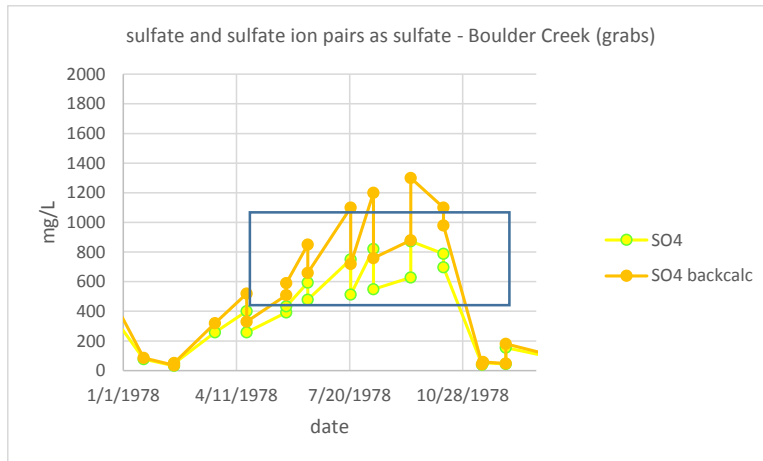
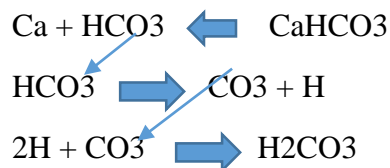


Figure 258 [\(back\)](#)

The above graph shows free sulfate concentration in yellow with ‘sulfate backcalc’ (sulfate plus sulfate ion pairs as sulfate or ‘total’ sulfate) in orange. The divergence of yellow and orange lines shows the accelerating growth of ion pair concentrations. Ion pair formation continues as long as sulfate ion concentration is rising and, in itself, serves to lower sulfate concentration. This may be termed a ‘deceleration’, the ion pair formation conceived as acting as a brake on the rise of sulfate. Similar decelerations occur for Ca and Mg but very little if at all for Na. The rectangle shows approximately where CaSO<sub>4</sub> precipitation is expected if conditions are right. Precipitation of CaSO<sub>4</sub> out of solution can potentially speed up the deceleration process by providing an additional stress pushing the equation further in the direction of product. Boulder Creek was used because the role of sulfate, the major anion, is so clear.

The situation with bicarbonate is more complex than that of sulfate. The reason is that the formation of carbonate from bicarbonate provides additional ‘stresses’ to the system that must be accounted for.



This state of affairs makes it less likely that both free calcium and free bicarbonate concentrations will be rising or falling simultaneously. In fact, the speciation of HCO<sub>3</sub> follows D.O. (free O<sub>2</sub>) ( $r^2 = 0.92$ ) more closely than it follows the concentration of HCO<sub>3</sub> ( $r^2 = 0.73$ ).

Given the more complicated situation for bicarbonate speciation, it seems even less likely that the above mechanisms can be seen at work in nature. But that is not the case. The percent speciation of free HCO<sub>3</sub> follows the same general pattern as SO<sub>4</sub> with some minor but important wrinkles. The same drop in free major ion percent speciation with subsequent rise in ion pair formation can be seen in the grab data for the Verde at Perkinsville.

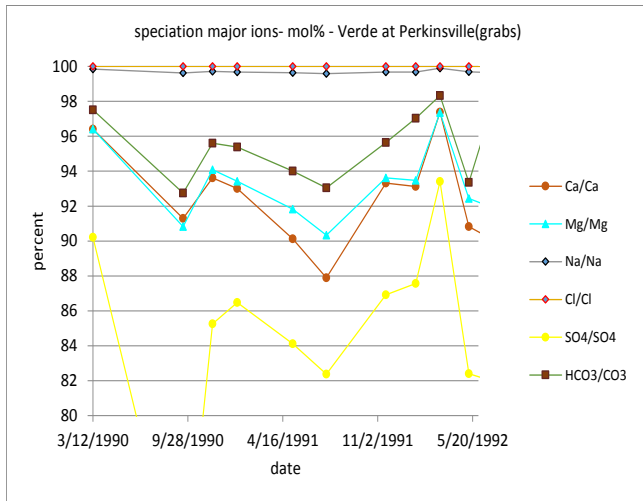


Figure 259

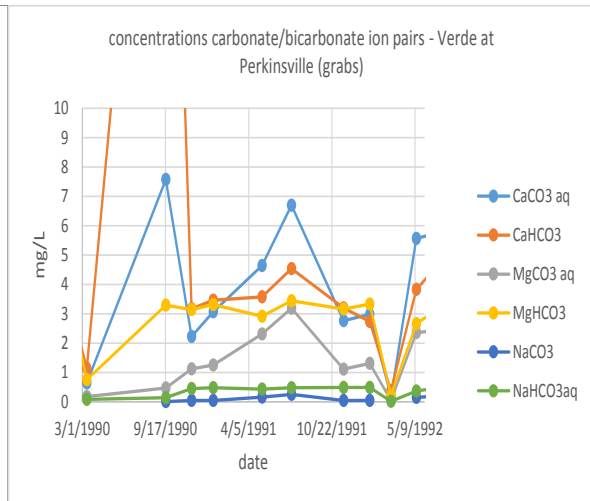


Figure 260

CO<sub>3</sub> actually provides a better picture of what inversion can potentially lead to. With CO<sub>3</sub> the effects of flow direction increasing or decreasing amounts is seen but pH can change things dramatically. In scenario 3 (flow down) pH apparently trumps the change in flow (~ 1000 cfs), causing CO<sub>3</sub> amounts to increase with decreasing flow in another apparent violation of the first law. The upshot is that bound amounts go up while free go down and vice versa (i.e. bound CO<sub>3</sub> is inversely related to free) the opposite of the mass balance argument being developed. Here are two views of bound/free CO<sub>3</sub> in scenario 3 (both flow down) with pH up (left) and down (right).

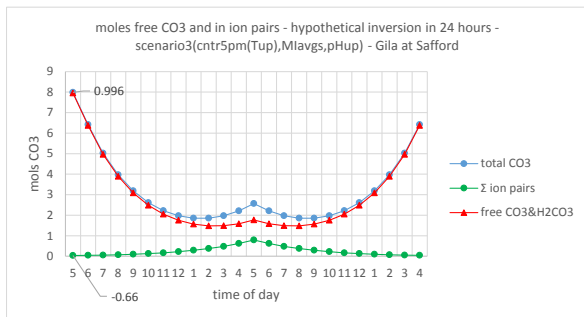


Figure 261

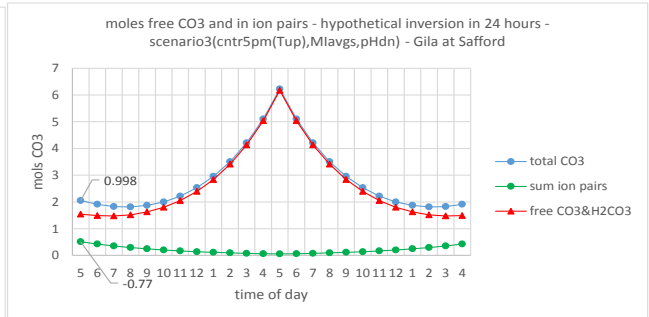


Figure 262

The above issues may be due to the fact that 'free CO<sub>3</sub>' here is the sum of H<sub>2</sub>CO<sub>3</sub> and free CO<sub>3</sub>. It was decided not to place the ephemeral H<sub>2</sub>CO<sub>3</sub> into the bound forms but this decision was probably not a good one. CO<sub>3</sub> and H<sub>2</sub>CO<sub>3</sub> are exact opposites in terms of pH so that the 'free' form is actually composed of two groups with opposing tendencies. Placing H<sub>2</sub>CO<sub>3</sub> into the bound forms, however, does not straighten out the relationship between free and bound forms.

One reason why % speciation is positively related to concentration for CO<sub>3</sub> might be that wateq4f provides speciation in the form of CO<sub>3</sub>/HCO<sub>3</sub>. But converting all CO<sub>3</sub> compounds to %CO<sub>3</sub> does not help the situation. What does resolve the issue is removing H<sub>2</sub>CO<sub>3</sub> from the ion

pairs of CO<sub>3</sub>. Then the relationship between % speciation and ion pair concentrations for CO<sub>3</sub> becomes inverse as mass balance arguments suggest it should be.

These developments leave H<sub>2</sub>CO<sub>3</sub> in a no-man's land. H<sub>2</sub>CO<sub>3</sub> is generally inversely related to CO<sub>3</sub> and CO<sub>3</sub> ion pair concentrations and positively to HCO<sub>3</sub> but the correlations are not strong in either case. The strong correlation for H<sub>2</sub>CO<sub>3</sub> is with pH.

correlations HCO<sub>3</sub> and CO<sub>3</sub> ion pair concentrations - Verde at Perkinsville(grabs)

	HCO <sub>3</sub>	CO <sub>3</sub>	H <sub>2</sub> CO <sub>3</sub> aq	CaCO <sub>3</sub> aq	CaHCO <sub>3</sub>	MgCO <sub>3</sub> ac	MgHCO <sub>3</sub>	NaCO <sub>3</sub>	NaHCO <sub>3</sub> aq
HCO <sub>3</sub>	1.00	0.67	0.07	0.73	0.94	0.71	0.97	0.59	0.94
CO <sub>3</sub>	0.67	1.00	-0.63	0.99	0.52	0.98	0.70	0.90	0.73
H <sub>2</sub> CO <sub>3</sub> aq	0.07	-0.63	1.00	-0.56	0.21	-0.54	0.02	-0.45	-0.04
CaCO <sub>3</sub> aq	0.73	0.99	-0.56	1.00	0.63	0.97	0.75	0.87	0.76
CaHCO <sub>3</sub>	0.94	0.52	0.21	0.63	1.00	0.59	0.90	0.47	0.84
MgCO <sub>3</sub> ac	0.71	0.98	-0.54	0.97	0.59	1.00	0.77	0.95	0.80
MgHCO <sub>3</sub>	0.97	0.70	0.02	0.75	0.90	0.77	1.00	0.67	0.98
NaCO <sub>3</sub>	0.59	0.90	-0.45	0.87	0.47	0.95	0.67	1.00	0.74
NaHCO <sub>3</sub> a	0.94	0.73	-0.04	0.76	0.84	0.80	0.98	0.74	1.00

Table 142

The same relations seen between ion pair and free ion concentrations for SO<sub>4</sub> apply equally well to HCO<sub>3</sub> though the separation is not as great, does not grow as fast, and there would be little or no precipitation predicted for HCO<sub>3</sub> ion pairs.

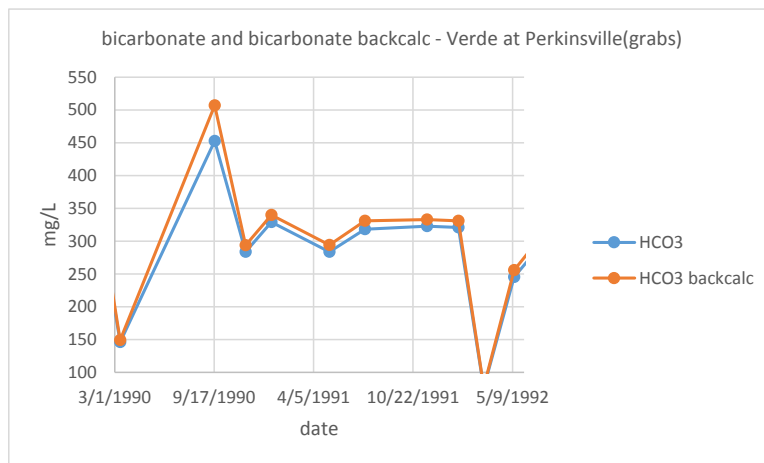


Figure 263

It is important to point out that neither Boulder Creek nor the Verde at Perkinsville exhibit major ion concentration inversions of any sort. The result of mass action on ion pair concentrations serves generally as a moderating effect on flow related free ion concentration increase and hence has an influence on ionic strength.

Is there any evidence of sulfate or bicarbonate ion pair formation on the Gila at Safford and can it be linked to inversion? The evidence for it is there but not overwhelmingly strong. %SO<sub>4</sub>/SO<sub>4</sub>

correlates with Cl concentration with an  $r^2$  of -0.73 and with  $\text{HCO}_3^-$  concentration at +0.73. % $\text{HCO}_3^-/\text{HCO}_3^-$  correlations are considerably lower (-0.38 Cl, 0.40  $\text{HCO}_3^-$ ). The graphs below show grab sample anion concentrations (as represented by charge %) and percent speciation  $\text{SO}_4^{2-}/\text{SO}_4^{2-}$  (yellow) and  $\text{HCO}_3^-/\text{HCO}_3^-$  (brown).

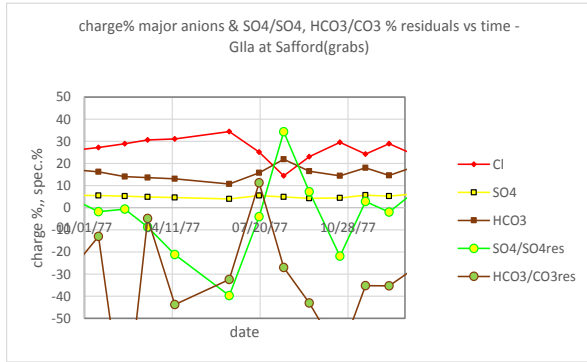


Figure 264

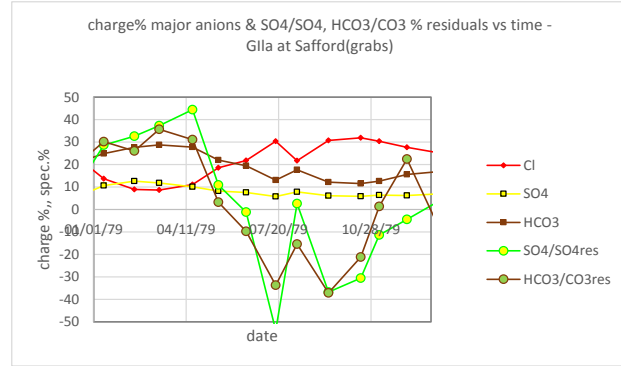


Figure 265

As can be seen in the 1977 graph (to left),  $\text{HCO}_3^-/\text{HCO}_3^-$  begins declining before the inversion date (8/16). The 1979 graph (to right) shows a more extended inversion period where rising percent speciation during inversion and declining after are more clearly seen. But both  $\text{SO}_4^{2-}/\text{SO}_4^{2-}$  and  $\text{HCO}_3^-/\text{HCO}_3^-$  dip before the end of inversion in early 1979 and rise well before the next inversion, off graph to the right in 1980. While the pattern is there in a general sense, the ‘fit’ with inversion is not ‘tight’.

Another view uses the activities of  $\text{CaCO}_3$  and  $\text{CaSO}_4$  in place of the % speciation. The fit is a little better and the more straightforward presentation makes it easier to remember and work with. But without the % speciation there is no ‘motivation’ for why this occurs – i.e. mass action.

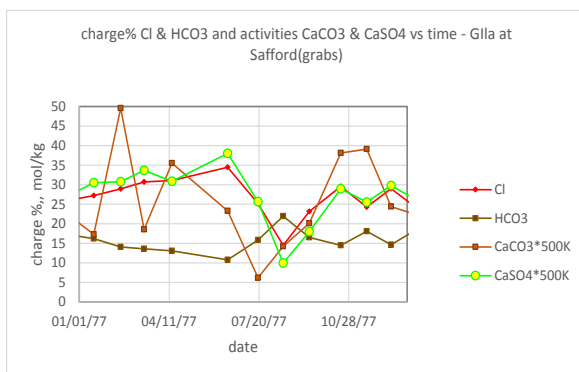


Figure 266 [\(back\)](#)

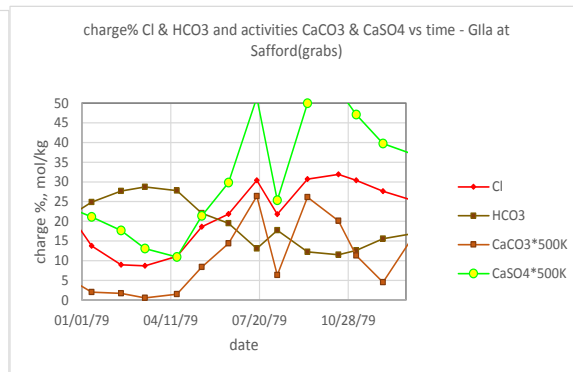


Figure 267

To judge the relation, it is unfortunately necessary, because of the time shifts referred to above, to go through the graphs a year at a time. It is best to focus on  $\text{SO}_4^{2-}$  because of the vagaries in  $\text{HCO}_3^-$  already noted. Most cases are like the above two: rises and dips may not occur at precisely the right moment but the overall shape is falling  $\text{CaSO}_4$  or  $\text{CaCO}_3$  activity for inversion and rising for non-inversion.

The rising concentration of ion pairs in the transition from inversion to non-inversion brings some other matters to the fore. Ion pairs may remain dissolved (NaSO<sub>4</sub> especially) but they may also reasonably be expected to enter the suspended solids portion, or precipitate out of solution depending on conditions. Another aspect of what the major ion inversion may ‘mean’ is a shift from a highly dissolved, ionic matrix of one sort to one of another sort, accompanied by a growing share of at least potential solids in the second.

Unfortunately these highly reasonable suggestions are not borne out by the evidence, at least in the quick checks on the grabs that were run. The tables below are an attempt to relate the speciation percents and ion pair concentrations seen above to TSS and, as is seen, they fail miserably to produce any high correlations with TSS.

correlations TSS with selected concentrations and solubility indices - Gila at Safford(grabs)

	TSS/(mg/L	SO <sub>4</sub> /SO <sub>4</sub>	CaSO <sub>4</sub>	MgSO <sub>4</sub>	NaSO <sub>4</sub>	CaSO <sub>4</sub>	CaSO <sub>4</sub> ú2(H <sub>2</sub> O)	MgSO <sub>4</sub> ú7(H <sub>2</sub> O)
TSS/(mg/L)	1.00	0.20	-0.30	-0.25	-0.24	0.35	0.36	0.40
SO <sub>4</sub> /SO <sub>4</sub>	0.20	1.00	-0.72	-0.72	-0.65	0.74	0.72	0.61
CaSO <sub>4</sub>	-0.30	-0.72	1.00	0.96	0.97	-0.94	-0.93	-0.88
MgSO <sub>4</sub>	-0.25	-0.72	0.96	1.00	0.97	-0.85	-0.83	-0.77
NaSO <sub>4</sub>	-0.24	-0.65	0.97	0.97	1.00	-0.86	-0.84	-0.80
CaSO <sub>4</sub>	0.35	0.74	-0.94	-0.85	-0.86	1.00	1.00	0.96
CaSO <sub>4</sub> ú2(H <sub>2</sub> O)	0.36	0.72	-0.93	-0.83	-0.84	1.00	1.00	0.97
MgSO <sub>4</sub> ú7(H <sub>2</sub> O)	0.40	0.61	-0.88	-0.77	-0.80	0.96	0.97	1.00

Table 143

correlations TSS with selected concentrations and solubility indices - Gila at Safford(grabs)

	TSS/(mg/L	HCO <sub>3</sub> /CO <sub>3</sub>	CaCO <sub>3</sub>	MgCO <sub>3</sub>	NaCO <sub>3</sub>	Ca(CO <sub>3</sub> )	MgCO <sub>3</sub>
TSS/(mg/L)	1.00	-0.04	-0.02	0.01	-0.08	-0.03	0.48
HCO <sub>3</sub> /CO <sub>3</sub>	-0.04	1.00	-0.64	-0.64	-0.60	0.56	0.05
CaCO <sub>3</sub>	-0.02	-0.64	1.00	0.99	0.83	-0.89	-0.11
MgCO <sub>3</sub>	0.01	-0.64	0.99	1.00	0.81	-0.88	-0.10
NaCO <sub>3</sub>	-0.08	-0.60	0.83	0.81	1.00	-0.72	-0.02
Ca(CO <sub>3</sub> )	-0.03	0.56	-0.89	-0.88	-0.72	1.00	0.08
MgCO <sub>3</sub>	0.48	0.05	-0.11	-0.10	-0.02	0.08	1.00

Table 144

The grabs do not support any conclusions on the relation of ion pair formation with suspended solids or potential precipitates. These are located in other ‘domains’ so to speak and arguments generated here will have to be limited to the dissolved portion of the solution.

Can what has been seen as a possible role for CaSO<sub>4</sub> and CaCO<sub>3</sub> in inversion be generalized and analyzed with the hypothetical inversion analysis to yield further insights? Both CaSO<sub>4</sub> and CaCO<sub>3</sub> are neutral ion pairs that are directly related to major ion concentration and speciation.

Major ion concentration is a large factor in ionic strength therefore neutral ion pairs have a relation, if only an indirect one, to ionic strength as well.

There are three different ways in which ionic strength can change. The first is the change in (free) major ion concentrations themselves: Na & Cl concentrations are higher and drop faster than Ca & HCO<sub>3</sub> concentrations during the inversion and ionic strength (or 'ionicity' (in slang)) follows. The second is the replacement of charge by certain ion pairs. For example, a NaSO<sub>4</sub> molecule has a -1 charge and can replace a chloride while a CaHCO<sub>3</sub> molecule has a +1 charge and can replace a sodium. Finally, neutral ion pairs, such as CaSO<sub>4</sub> and CaCO<sub>3</sub>, contribute to ionic strength.

The neutral ion pairs themselves have an ionic strength of zero so they do not, as ion pairs, contribute at all to ionic strength. But the dissolution or formation of ion pairs does have an effect on ionic strength; adding free ion charge with dissolution, removing free ion charge with formation. The ionic strength of the constituent ions of a neutral ion pair can be added up to give the **potential** change in ionic strength with the change in concentration of the ion pair. Since ionic strength is always positive due to the definitional squaring of charge, a negative change means a reduction of ionic strength. Note that here, and in the following discussion, ionic strength is sometimes loosely referred to as 'charge' but plus or minus is strictly addition or removal of ionic strength not the sign of charge.

The addition or removal of charge of the neutral ion pairs is calculated as follows. The change in concentration of an ion pair from 00:00 to 12:00 is calculated first. If the concentration has gone down, the absolute concentrations of the two ions are multiplied by their charge squared, following the definition of ionic strength, and added together. A drop in the concentration of CaSO<sub>4</sub>, for example, results in an increase in charge; the dissolution of 1 mol CaSO<sub>4</sub> producing 1 mol free Ca and 1 mol free SO<sub>4</sub>. If the change in concentration is positive, the calculation is the same but the whole expression is made negative to show removal. The formation of 1 mole of CaSO<sub>4</sub> removes 1 mol free Ca and 1 mol free SO<sub>4</sub>.

The potential difference in ionic strength of neutral ions is shown below along-side the other groups even though its effect is already reflected in the major ion concentrations. If CaSO<sub>4</sub> concentration is higher on day 2 than day 1, there had to be a reduction in free Ca and free SO<sub>4</sub> and that is why Ca and SO<sub>4</sub> are lower on day 2. The three groups mentioned above, therefore, do not add up to 100% of all cases, they are more like, say, 110%, because the neutral ion pairs have in effect been 'double-counted.' The groups on the graphs below (scenario 1 left, 2 right) are those mentioned above plus the 'net' change or the sum of the other three groups.



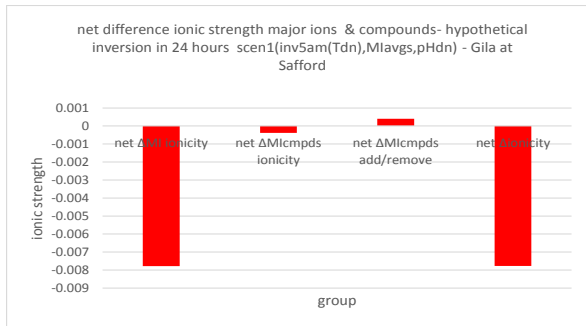


Figure 268

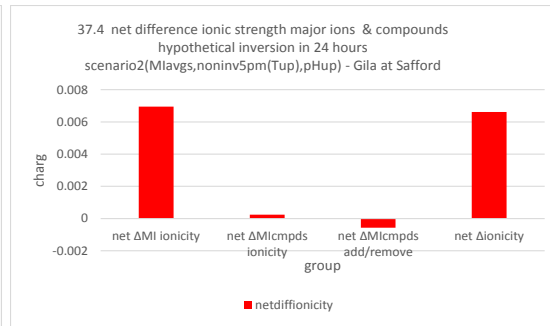
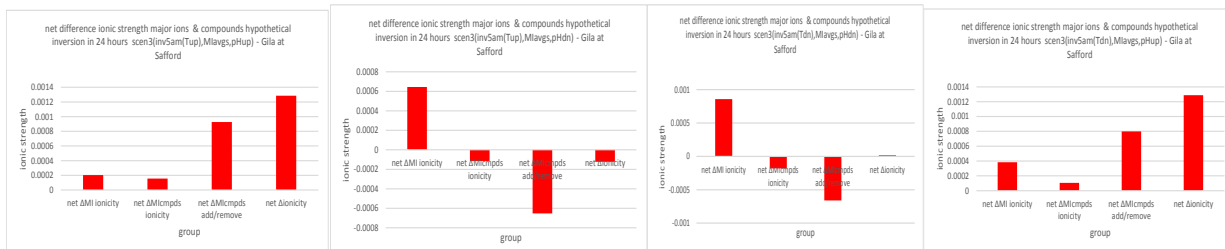


Figure 269

All the ‘views’ of scenario 1, 2, and 4 are similar to the two shown above and reveal major ion concentration difference (first group to left) to be the overwhelmingly major factor, virtually equal to net change. Ion pair replacement and neutral ion pair addition/removal (groups 2 & 3) are, by contrast, negligible factors. The changes in ionic strength **from 00:00 to 12:00**, that is the change to inversion or non-inversion conditions, are what would be expected: scenario 1 shows a decrease in ionic strength, scenario 2, an increase. The total change in ionic strength for scenarios 1 & 2 is about +/- 0.008 while scenario 4 drops a bit to +/- 0.005-6.

Scenario 3, the maintenance of the inversion condition, looks quite different from 1 & 2. The total change in ionic strength is much lower at around +/- 0.002. More significantly, the relative heights of the three groups are also quite different with neutral ion pair addition/removal (group3) becoming a major factor even at times exceeding that of the major ions themselves (group1).



Figures 270-273

With pH going down (the center two graphs above), the neutral ion pairs are removing charge to such an extent as to offset the major ion contribution and the result is low net charge. In the lab, adding a little acid is a common method of breaking down compounds such as  $\text{CaPO}_4$  or  $\text{CaSO}_4$  to their constituent ions to get ‘total’ (dissolved) ion amounts. The ‘dissolved’/‘solid’ distinction is arbitrary: ‘dissolved’ is often understood in the lab to be ‘what passes through a 0.45 micron filter.’ A sample that has been passed through a 0.45 micron filter, however, can be acidified and will often yield higher results than the initial sample that was only passed through the filter. In general, though, low pH, acidic conditions, dissolves ‘solids’ to their free ion form. It would seem, therefore, that, when pH goes down, there should be addition to, not removal of, charge.

Notice, however, that there is both addition and removal of charge in the center two graphs above. The problem is that the neutral ion contribution is a sum of differences, not all of which are necessarily going in the same direction. pH is inversely related to hydrogen ion concentration. As the pH goes down the H ion concentration goes up, pushing the equation in the direction of product – here H<sub>2</sub>CO<sub>3</sub> – in accord with mass action. That accounts for the removal of charge. Na & Cl are very low so largely out of the picture as far as major ion contribution which means the first column must be made up mostly of Ca, Mg, HCO<sub>3</sub>, CO<sub>3</sub>, or SO<sub>4</sub>. The other neutral ion pairs in the MIavg system, are actually dissolving, at a lower percentage, under the influence of low pH. This addition of charge results in the higher major ion contribution of the center two views (pHdn).

With pH going up (outside two graphs above) the hydrogen ion concentration is going down pushing the formation reaction for H<sub>2</sub>CO<sub>3</sub> in the direction of reagents (dissolution to ions, adding ionic strength +0.00122). Most of the other neutral ions are actually removing charge because, with flow going down and free ion concentrations going up, the formation equation is pushed toward formation of product. But they do so at levels much lower than H<sub>2</sub>CO<sub>3</sub> (sum all but H<sub>2</sub>CO<sub>3</sub>, -0.00029) so H<sub>2</sub>CO<sub>3</sub> is the predominate factor for the column as a whole. The major ion contribution is low because they are being ‘used up’ to form neutral ion pairs.

To get a better view of what is going on, the neutral ion pair constituent ion changes in ionic strength are added (as plus or minus) to the appropriate free ion. The change in ionic strength of Ca, for example, is that at 12:00 minus that at 00:00 (that is with the ion pair change included) plus the negative or positive contribution caused by dissolution or formation of CaCO<sub>3</sub> and CaSO<sub>4</sub>. Now the original free ion concentration can be calculated separately with and without the contribution to ionic strength of neutral ion pair’s dissolution or formation.

To gain this new information, additions and removals of ionic strength are tallied for each constituent ion separately. These changes make the total of all groups now equal to 100%. The highlighted boxes below show what is being summed. The blue boxes are the 100 % calculation for ionic strength addition (+) or removal (-) and the light blue background is the sum of the neutral ion pair potentials. (Note that here, potassium (K) was added to Na & Cl to create ‘nuMI’, a variation on MI that is used occasionally). FI = free ions, NIP = neutral ion pairs, CIP = charged ion pairs

reconciliation Δ % ionic strength - hypothetical inversion in 24 hrsscen4(nuMI,Tdn,pHdn)-Gila at Safford					
		free(+)	ion pair(+)	free(-)	ion pair(-)
FI	NaKCl	53.4			-0.2
	other MI	34.6	11.8	-27.5	-70.3
NIP	H <sub>2</sub> CO <sub>3</sub>		10.9		
	ΣotherMIneut		0.9		-70.3
CIP	Σreplace		0.11		-2.23
ΣFI + ΣNIP + ΣCIP			100.0		-100.0
ΣNIP			11.8		-70.3

Table 145

The worksheet section above constitutes a ‘reconciliation’ center for the analysis. Since the actual change in free ion should equal the ion pair potential, the bottom number ( $\Sigma$ NIP), should equal that in the second row (ion pair (+ or -)) which is the ion pair contribution to free ion change in ionic strength. In this particular example a  $1.25E-4$  mol/kg drop in  $H_2CO_3$  concentration corresponds to a  $+7.5E-4$  addition (+) to ionic strength due to the release of  $H^+$  and  $CO_3^{=}$  ions. The  $H^+$  (actually  $2H$ ) contribution and  $CO_3^{=}$  contribution are calculated separately and yield  $+2.5E-4$  for  $H$  and  $+5.0E-4$  for  $CO_3^{=}$  which turn out to be 3.6 and 7.3% of the total charge addition respectively or 10.9% together (the ‘potential’). The other positive change in ionic strength comes from a +0.89% potential due to  $MgSO_4$ , 0.448% due to  $Mg$  and 0.448% due to  $SO_4$  additions. The 11.8 % charge addition to the free ions is the result of the dissolution of 2 ion pairs whose total potential to change ionic strength is 11.8.

So, for the table as a whole, the neutral ion pairs are once again being shown twice, but this time one tabulation, as ion pair potentials, is a different calculation and serves as a check on the other, the percent of free ion ionic strength change due to ion pair formation and dissolution. The initial ‘lumped-together’ tabulation of the graphs above was still run and provided a check for the total amount of signed neutral ion pair potential difference in ionic strength.

First, to provide some orientation, the results for the NaKCl system is shown on the graphs below. The stacked groups are free ion (dark blue) and free ion from neutral ion pair dissolution (light blue) A new format will be used here to provide more of a narrative approach – the order of scenarios is no longer numeric but ‘chronological’, 1,3,2 and 4 from left to right. (back) Scenario 3 values are flipped (plus for minus) because scenario 3 was run from day 2 to day 1 to make flow go down. Note that the ion pair contributions (only  $NaHCO_3$  here) are very small and have to be multiplied by 100 to be visible but are invariably working in the opposite direction from the free ions (a ‘moderating’ effect).

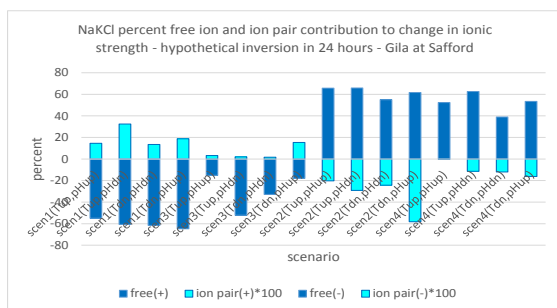


Figure 274

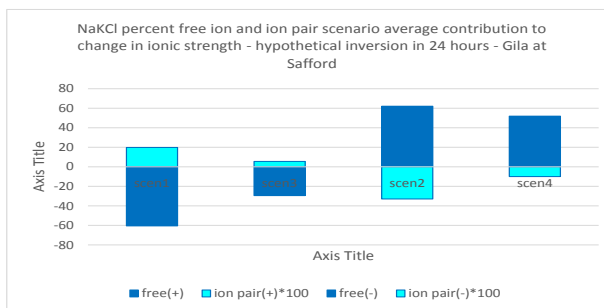


Figure 275

The full view (left) shows little or no consistent temperature dependence (left 2 vs right 2 in each group of 4) or pH dependence (inner 2 vs outer 2 in each group of 4). There is, therefore, no loss in information with the average scenario view (right). Na, K, & Cl concentrations themselves are seen to account for about 60% contribution to change in ionic strength, removing charge in scenario 1, adding in scenario 2 (Na & Cl always have the same sign depending on concentration change). These are apparently the ‘motivating’ changes that start the inversion process and this is the baseline view for further development.

To see the ramifications of changes in the NaKCl system, all the other ions, at this point the other ‘major ions,’ can be examined in the same manner and compared and contrasted to the NaKCl system.

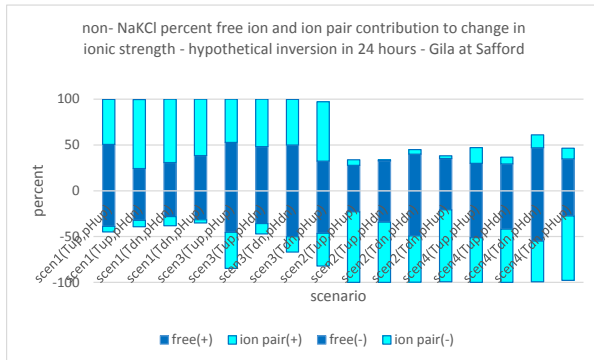


Figure 276

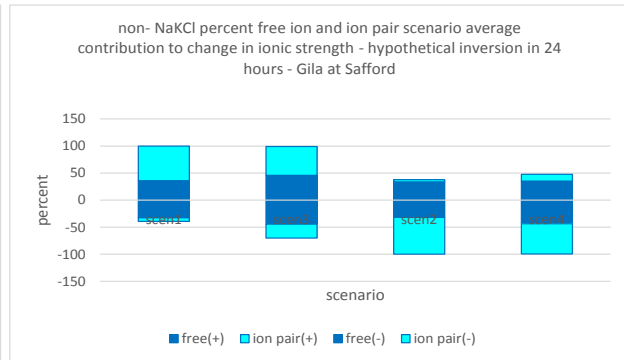


Figure 277 [\(back\)](#)

The ‘big picture’ here is that the neutral ion pair contribution (light blue) adds in opposition to the direction set by NaKCl free ions, adding charge in scenario 1 & 3 and removing charge in scenario 2 & 4. The free ion percent contribution is slightly larger in scenarios 3 & 4 but fairly even across all scenarios. The ion pair contribution in scenarios 1 and 3, however, is mostly on the positive side, addition of charge, while in scenarios 2 and 4 it is mostly negative, removing charge and favoring the return to higher %Na & Cl ionic strength. Scenario 3 & 4 are slightly more evenly balanced, bidirectional situation – i.e. both addition and removal of charge, as might be expected for these ‘maintenance’ scenarios.

Two groups of ions can be distinguished: the sulphates which are neither pH nor temperature dependent (below left), and the carbonates (right) which are pH dependent (center 2 different from outer 2 in each group of 4). The picture of average sulfate role in charge addition/removal, differing only in magnitudes not in direction, is therefore much more certain than that of the carbonates whose average is one of two opposing tendencies. Fortunately, the magnitudes are larger in one direction than the other so the result is not an average of zero.

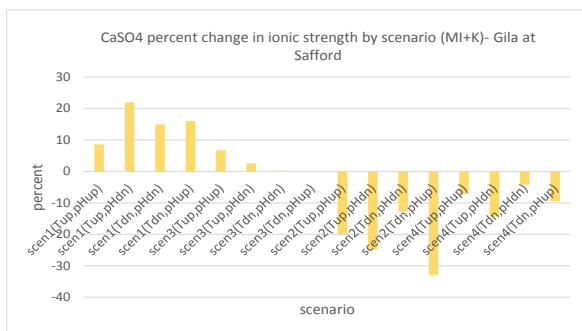


Figure 278

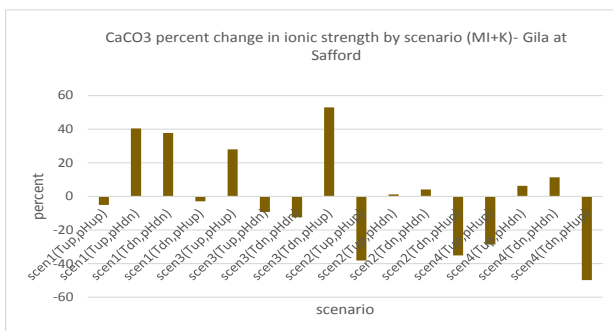


Figure 279

Finally, the various individual neutral ion pairs can be looked at to see the contribution that each makes to change in ionic strength. At this stage, only major-ion ion pairs are presented. Note

that one ( $\text{NaHCO}_3$ ) is actually a link between the two systems that have been opposed to one another but is a very low magnitude one so that the two systems are almost entirely independent.

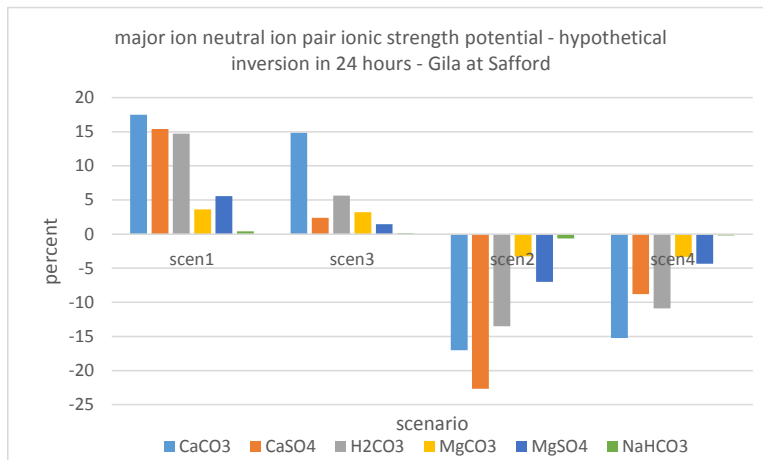


Figure 280 ([back](#)) ([back](#))

The direction of change agrees with the direction of charge addition/removal seen above and the only new information is the relative contributions of the various pairs. Scenarios 1, 2 & 4 seem to have fuller representation of all the ion pairs whereas scenario 3 seems depleted, as if there was something missing in the response. Other than  $\text{CaCO}_3$ , which seems to be doing all the work in 3, the other ion pairs contribute little.

At this point, the plan was to proceed adding one new species at a time. This method is the only way to provide ‘control.’ It is like adding just one reagent at a time to a flask in the laboratory and observing any changes at each new addition. But in this situation, dealing with a whole system, one change is liable to have more responses than can be easily tabulated. And one does get a little worried as graphs and charts proliferate madly and one does lose patience after a while. The species added to the  $\text{Na(K)Cl}$  baseline were iron (Fe), silicon (Si), NBP (nitrogen, boron, phosphate) and ‘all parameter averages’ in that order. Each addition is understood to be on a system with all previous additions. ‘+NBP’, for example, is ‘add NBP in the presence of the major ions and Fe and Si’.

The addition of iron (Fe) immediately changes things. The effect on the  $\text{NaKCl}$  system is minor – scenario 2 goes from 60% to 55% free ion. The effect on the ‘other’ ion neutral ion pair contribution in scenario 2 also changes but very little. It is in the relative roles of the neutral ion pairs, however, that iron really stands out.

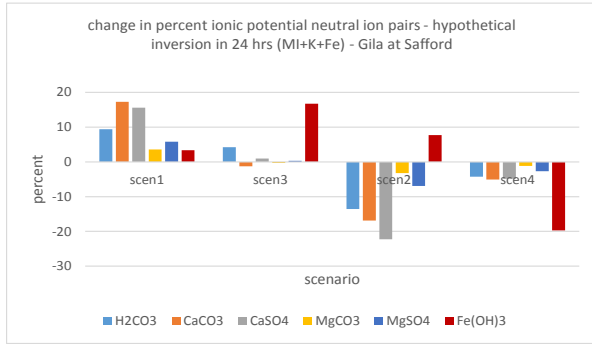


Figure 281

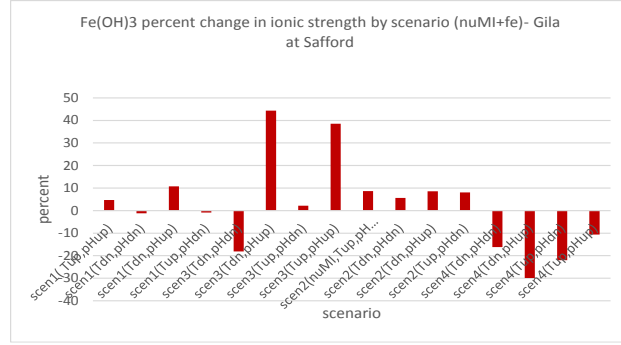


Figure 282

Fe(OH<sub>3</sub>) immediately appears as the major factor in scenarios 3 & 4, working in the same direction but dwarfing the percents of the major ion ion pairs. It only has a small, supporting role in the shift to inversion (scenario 1). In scenario 2 (the return to non-inversion) it works opposite in direction to the major ion ion pairs. Fe(OH<sub>3</sub>) becomes a major factor in the maintenance scenarios and plays a balancing role compared to the major ion ion pairs in the return to non-inversion.

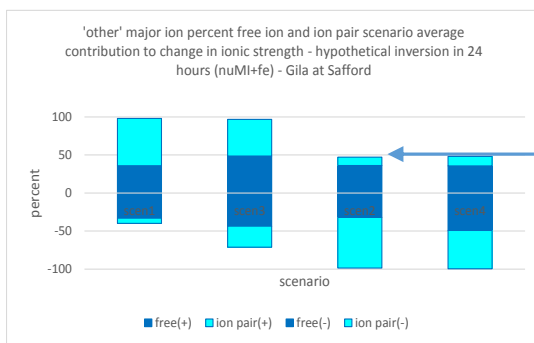


Figure 283

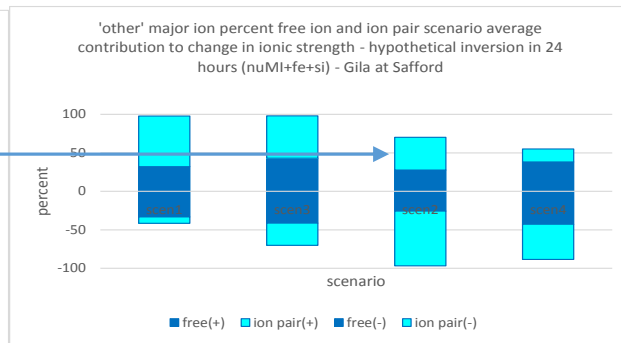


Figure 284

Adding a little silicon (H<sub>4</sub>SiO<sub>4</sub>, above right) also changes the simple up-in-scen1&3, down-in-scen2&4 picture given by the major ion neutral ion pairs. Unlike Fe (left above), Si makes major changes in the % contribution to the 'other' free ions from their neutral ion pairs in scenario 2. The change is from about 10% to 30% (blue arrow above). With this change, scenario 2, the return to 'normal' scenario, has a much more balanced, maintenance-like look.

H<sub>4</sub>SiO<sub>4</sub> usually adds charge, working in the same direction and overshadowing Fe in all but scenario 4 (below left) where it works against and is not as important as Fe. Note that in scenario 3, the direction of change of the other major-ion ion pairs changes from addition (Fe only) to removal (Fe+Si). Low to begin with, the ion pairs of the major ions are largely replaced by Fe & Si in scenario 3.

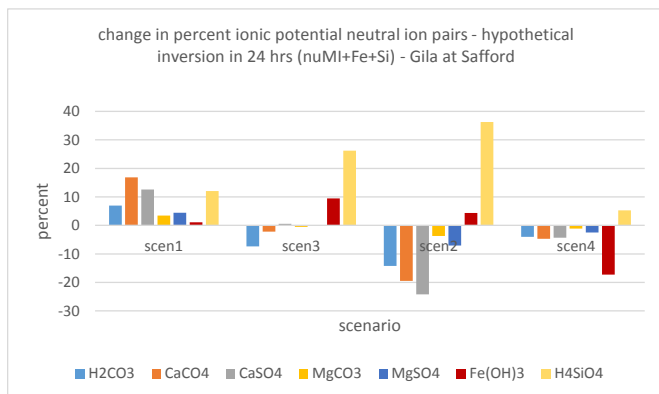


Figure 285

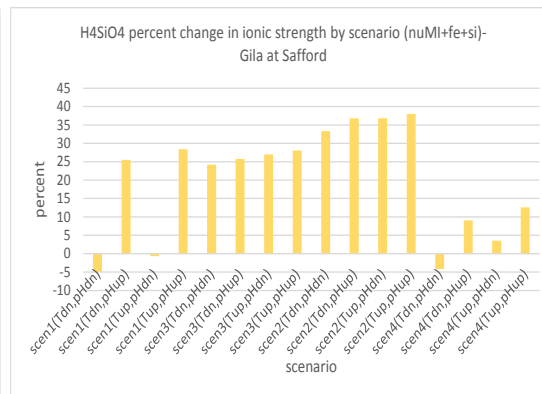


Figure 286

The full view of Fe(OH)<sub>3</sub> in the presence of Si (not shown) remains the same as above (Figure 282 above) suggesting that their roles are not interdependent. Just to make sure, however, Si was added to the nuMI system without Fe being present. The results are as expected: The graph generated (not shown) has the same relative heights for H<sub>4</sub>SiO<sub>4</sub> as that on the graph to the left above while the graph to the right is identical. Si, then, seems to play its role largely independently of Fe, in all cases but one and it is a curious one. The ion pair of the NaKCl system, i.e. NaHCO<sub>3</sub>, which is always a very small factor, with Si addition (alone) is diminished even more, needing multiplication by 1 million instead of 100 (when Fe is present) to be visible. Only in this apparently minor effect does the presence of Fe seem to have any effect on the function of Si.

The addition of NBP (nitrogen, boron, phosphorus) was to make sure an important ion (nitrate) and the other components of non-carbonate alkalinity (H<sub>3</sub>BO<sub>3</sub>, H<sub>3</sub>PO<sub>4</sub> (in addition to H<sub>4</sub>SiO<sub>4</sub>)) were represented. These components made no change in the proportions of free ion and ion pairs in either system but did lead to an explosion of minor species containing phosphate (PO<sub>4</sub> or HPO<sub>4</sub>).

Finally, the scenarios were run with the averages of all possible species. There was, again, little change in the free ion/ion pair contributions in either system and the ion pair potentials show exactly the same patterns as above. The only effect is, again rather curiously, a drop in NaHCO<sub>3</sub> contribution as seen with the addition of Si without Fe but not noticeable in either nuMI+Fe+Si or +NBP.

In the 'all averages' scenarios there are about 108 to 120 species represented. The number of species per grab sample, however, ranges from 33 to 104 but averages only about 66. Now, of course, the scenarios are sample date pairs but it might be expected that both dates would have mostly the same species. The day to day species count absolute difference across all grab sample dates ranges from 0 to 47 and averages 10. While the all average species count is almost reached in the grabs and the day to day difference average is only about 10, the average grab sample species count is only 66, or roughly half the all-parameter situation, and the day to day absolute difference can range from 0 to 47.

These results suggest that the all-average scenarios are really no more realistic than those that use only the major ions. It is, once again, a question of 'presence' which is random for most parameters and there is no way around it. About all that can be done is to group and tabulate the species which can 'take each others places' and see how they may influence each other, always with the caveat 'if present'.

To briefly summarize the process: it begins with a drop in solution ionic strength caused by a large influx of water dilute in Na & Cl. The ion pairs of most of the other ions respond by favoring dissolution. The response is not an attempt to maintain any particular ionic strength; there is no 'law' requiring it and solutions can exist indefinitely at a number of different ionic strengths. Ionic strength is simply the result of the coming together of charged species at different concentrations. The 'other' ion ion pairs are acting in accord with mass action. In the change from non-inversion to inversion, the neutral ion pairs are for the most part adding charge to the system through dissolution. Mass action returns some free ions to solution, moderating the drop in Na and Cl concentrations caused by increasing flow.

The return to non-inversion is not just a function of rising Na & Cl concentrations but is also accompanied by removal of charge (formation of ion pairs) by most of the 'other' ions. This response also is consistent with mass action since flow is going down, free ion concentrations go up, favoring ion pair formation. It reduces non-NaCl free ions and returns control of the system to the free ion concentration change of Na & Cl. Iron flips its role vis a vis Na & Cl, adding charge in scenario 2, removing charge in scenario 4. Silica almost invariably adds charge, usually working in the same direction and dwarfing the effect of iron in all but scenario 4 where it works opposite and is less of a factor.

But it is in scenario 3 that the effects on the system wrought by inversion can most clearly be seen. The maintenance of inversion at lower % Na & Cl and higher % 'other' free ion ionic strength is a sea-change for the system. Average flow differences between day 1 and day 2 are an average of 742 cfs for scenario 1 and 1155 cfs for scenario 3. But the change in ionic strength for scenario 1 is on the order of 0.008 that of scenario 3 is on the order of 0.002. A larger change in flow, which translates into a larger change in concentrations, is responded to with a smaller change in ionic strength.

In fact, small changes in concentration of the ion pairs, as opposed to large swings in free ion concentrations, become the norm in scenario 3. The maximums of the 'other' free ions with respect to the new, lower ionic strength of Na & Cl are probably developed pretty quickly and the ion pair response becomes the 'fine tuning' necessary for small fluctuations. (There is some fuzziness here but note that time (timing) is part of the equation). Fe from  $\text{Fe}(\text{OH})_3$  and  $\text{SiO}_4$  from  $\text{H}_4\text{SiO}_4$ , with concentrations multiplied by 9 and 16 (their charges squared) respectively, have important roles because they can add or remove a lot of charge with relatively small changes in concentration.

To verify the preceding picture of average behaviour in a hypothetical construct will require returning to the grabs. The term 'scenarios' of the hypothetical analysis will be replaced by the term 'inversion status' with the same numbers meaning the same situation. The term 'scenario'



may hang around (inadvertently) but does not imply a hypothetical analysis – these are calculations done on grab samples, all parameters present, averaged by inversion status.

The focus will be on inversion status 3 and the role of the neutral ion pairs. There are 13 inversion status 3 situations in the grabs and they range from 2 to 5 grab samples over from 21 to 587 days apart with the average around 144 (one inversion status 3 straddles the 6.5 year data gap (2996 days), is not considered in the average). Much of the analysis will be done with graphs and these will no longer be annual, instead they will stretch across the inversion status 3 event only.

Examining the neutral ion pairs themselves over extended time periods does not reveal any general trends or relations. They do not intra-correlate in any grouping or any view and their autocorrelations are uniformly low. They also adamantly refuse to inter-correlate with anything else – their ionic strength potentials, amounts, and activities show no high correlations with flow or with any group or individual parameter ionic strength, amount, or activity investigated. They do, however, correlate to their corresponding free ions so the basic mass action arguments do seem to be confirmed.

correlations free ions and neutral ion pair concentrations (mol/kg solv) - Gila at Safford(grabs)										
	Na	Cl	Ca	SO4	CO3	OH	OH calc	Fe calc	BO3 calc	SiO4 calc
Na	1.00	1.00	0.87	0.96	0.15	0.08	0.14	0.14	-0.21	-0.17
Cl	1.00	1.00	0.87	0.95	0.14	0.10	0.14	0.14	-0.21	-0.17
Ca	0.87	0.87	1.00	0.82	0.18	0.03	0.23	0.23	-0.21	-0.17
SO4	0.96	0.95	0.82	1.00	0.10	0.05	0.13	0.13	-0.16	-0.06
CO3	0.15	0.14	0.18	0.10	1.00	0.68	0.29	0.29	-0.30	0.02
OH	0.08	0.10	0.03	0.05	0.68	1.00	0.26	0.24	-0.26	0.25
OH calc	0.14	0.14	0.23	0.13	0.29	0.26	1.00	1.00	-0.05	0.11
Fe calc	0.14	0.14	0.23	0.13	0.29	0.24	1.00	1.00	-0.05	0.11
BO3 calc	-0.21	-0.21	-0.21	-0.16	-0.30	-0.26	-0.05	-0.05	1.00	0.25
SiO4 calc	-0.17	-0.17	-0.17	-0.06	0.02	0.25	0.11	0.11	0.25	1.00
CaCO3 aq	0.27	0.27	0.34	0.20	0.95	0.80	0.28	0.27	-0.40	-0.07
CaSO4 aq	0.97	0.96	0.85	0.98	0.05	0.02	0.11	0.11	-0.06	-0.09
Fe(OH)3a	-0.15	-0.16	-0.25	-0.15	-0.33	-0.27	-1.00	-1.00	0.07	-0.09
H2CO3 aq	-0.01	-0.01	-0.02	0.00	-0.57	-0.49	-0.46	-0.46	0.01	-0.30
H3BO3 aq	0.83	0.81	0.80	0.76	0.26	0.22	0.08	0.08	-1.00	-0.24
H4SiO4aq	0.11	0.12	0.19	0.01	0.24	0.31	0.27	0.26	-0.44	-1.00

Table 146

Overall, the correlations for most of neutral ion pairs with their corresponding free ions are positive which is what mass action says. The exceptions, labelled as ‘calc’ values, can easily be explained. These concentrations are deduced from the free ion concentration differences used to calculate ionic strength addition or removal. They are the values needed to balance the total amount of free ion when neutral ion pairs dissolve or form. The wateq4f predicts no free iron, in all instances, on either day 1 or day 2 so presumably whatever amount of free iron there was between the two days is totally used up in the iron ion pairs of day 2. Note that these correlations are also ‘too perfect’ (-1) -- usually an indicator of a mathematical construct not experimental data. While the result can be explained, these ‘calc’d’ neutral ion pairs cannot really be used to either confirm or deny mass action.

Wateq4F also predicts about 14 species, most of them iron species, for which all sample dates are blank. Apparently these are ‘possible’ but not ‘probable’ species. Early runs contained these 14 blank rows which were later eliminated. As the analysis proceeded, their elimination was forgotten leading to some very strange results. The entire calculation process is highly dependent on things being where they are supposed to be so additions or deletions of rows of data have to be adjusted for or it’s ‘garbage in, garbage out.’

There are also some small details that there may be more than just mass action involved. Note that CaCO3 correlates less with Ca than it does with CO3 and OH, the latter two of which are weakly correlated to each other (0.68). H2CO3 does not correlate with anything even with CO3, a

situation that has already been addressed if not very satisfactorily explained.  $\text{Fe}(\text{OH})_3$  correlates with calculated OH but not experimental OH, usually a bad sign. Finally  $\text{H}_3\text{BO}_3$  correlates with all the major ions for no apparent reason. None of these comments are to suggest that mass action does not apply but simply that it cannot always be demonstrated to the nth degree and other factors appear to be involved when a simple correlational analysis is used.

The proposed mechanism related to inversion seems to be intact in terms of its underlying structure but is not supported in toto by experimental evidence. And there is no insight forthcoming with respect to whether the switch from ion pair dissolution to formation occurs during or after inversion status 3. Since correlations with flow and autocorrelations have failed to find any general patterns or relations, graphing of grab samples will be used to examine the response on an individual event basis.

The graph below shows flow, for orientation with respect to inversion, and the neutral ion pair ionic strength potentials over the extended inversion period of 2/79 to 5/79. The x-axis is the chronological grab sample number and extends from 12/78 to 7/79. The first and last dates are inversion status 4. The second date (36) is inversion status 1 and the second to last (41) is inversion status 2. The extended inversion status 3 is therefore only the four central samples 37-40, marked with arrows on the graph. The example is then a complete inversion cycle from a non-inversion through inversion back to non-inversion.

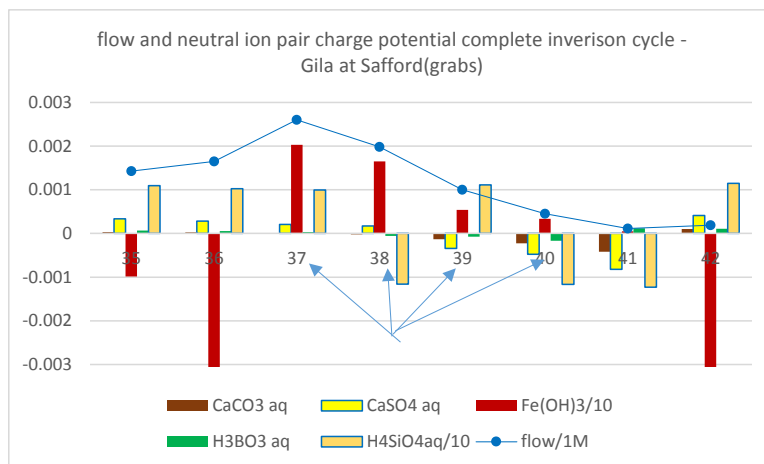


Figure 287

Breaking the chart down into individual ion pairs or groups, below, makes it easier to see relations. In the inversion status 4 samples (35&42), iron is removing charge in accord with the average picture. And in inversion status 3, iron is seen to be adding charge throughout in accord with the average view. But the switch to adding charge should have taken place in inversion status 1 (#36) which, not in line with the averages picture, is here seen to be removing rather than adding charge.

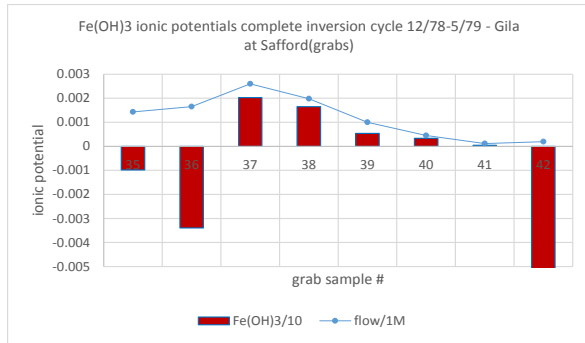


Figure 288

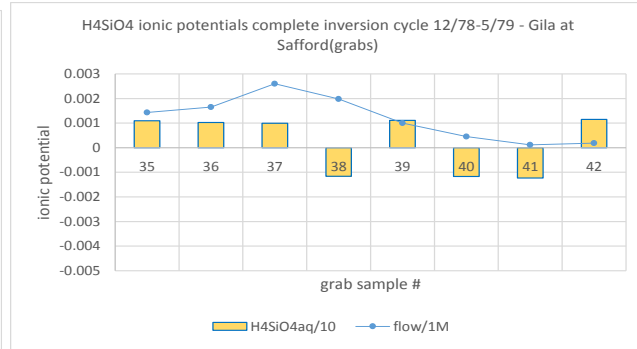


Figure 289

Silica in the averages picture primarily adds charge at a relatively constant level across all scenarios. In the current example, however, H4SiO4 uncharacteristically flips back and forth over the scenario3 period and is removing charge in scenario2.

H3BO3 (below, left) also primarily adds charge but flips direction after the first inversion status 3 sample. CaSO4 and CaCO3 move as expected starting by adding charge in a gradually diminishing manner before switching to removing (formation of CaSO4 etc.) in the last and afterwards but the switch from dissolution to formation occurs half way through inversion status 3.

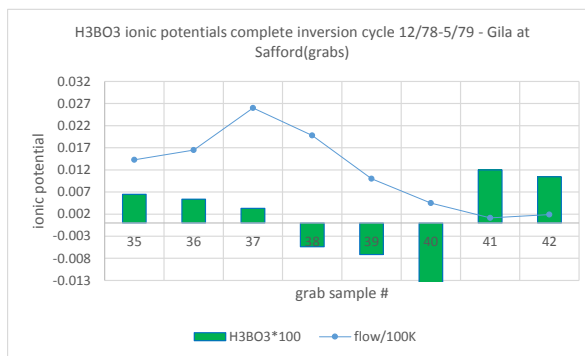


Figure 290

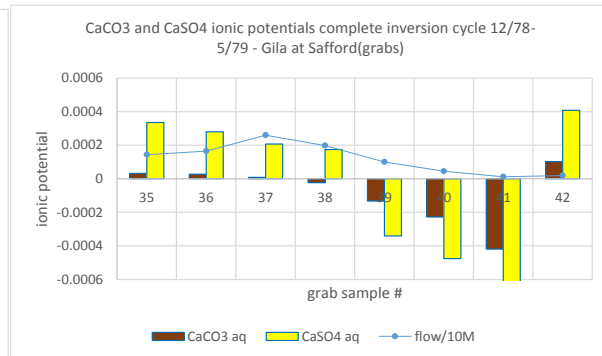


Figure 291

This example of an extended inversion status 3 is, unfortunately, the only good, if not satisfactorily explainable, one available. All the difficulties associated with this type of analysis come together here in a perfect storm. There needs to be a certain number of data points to establish trends and most of the inversion status 3 have only 2 or 3 dates. Only three inversion status 3 examples stretch across 4 or more grab sample dates. Two of these extend over such long periods of time that it seems highly unlikely that the inversion actually lasted from the first to the last date (587 and 2996 days apart). In addition, these examples also have issues of ‘non-presence’ for iron and silica.

With so little information available, none should be thrown out. Further useful information may be gleaned by examining the two and three date inversion status 3 examples. Here ionic potential differences are taken between dates 1 and 2 and 2 and 3, if available, unlike the hypothetical

averages where only the 1-2 date interval was used. The graphs below show the 1-2 (left) and 2-3 (right) intervals sorted by days apart to give some idea of where in the (assumed) extended inversion status 3 interval the difference date is. The results for iron pretty much reflect what was found in the 2-5/79 example above: there is some charge removal on later dates in the 1-2 set but in the 2-3 set things have settled down to mainly charge addition. Over both sets of data charge addition clearly outweighs charge removal which is in accord with the averages picture for scenario 3.

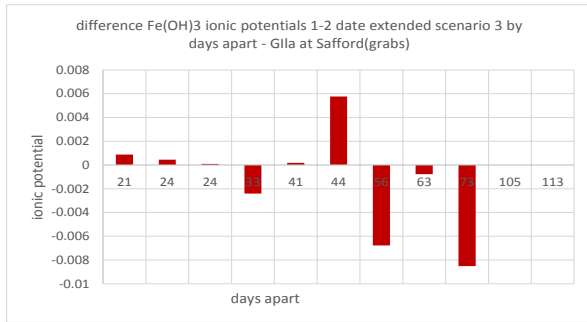


Figure 292

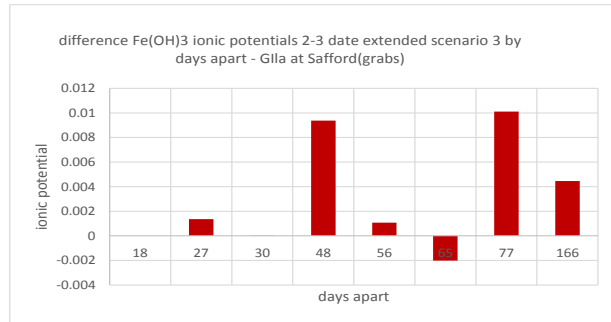


Figure 293

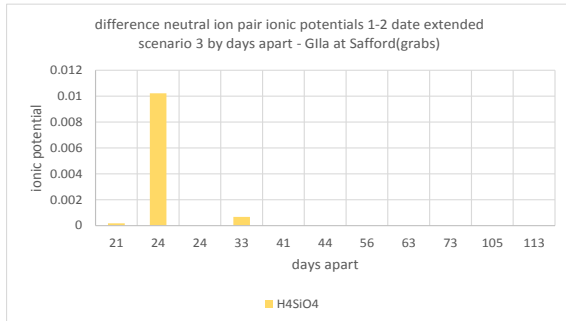


Figure 294

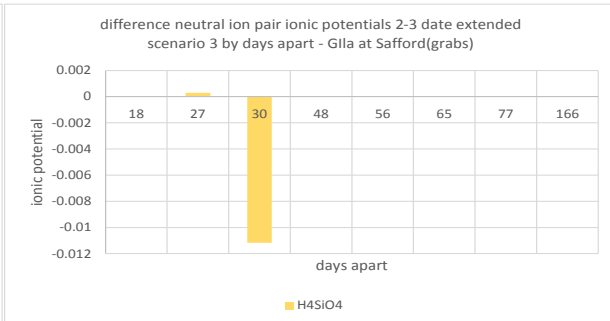


Figure 295

The results for silica only indicate that there are deficiencies in the analysis here. There are problems of ‘non-presence’ as well as an indication that the averages picture may be skewed by a few high values.

The result for the other major ion neutral ion pairs (below) also shows a variable result but it can be put down to the fact, mentioned earlier, that the ‘fit’ with inversion is not ‘tight,’ so that there may be an overlap and a blurring of function in the earlier and later stages of the inversion. The middle section of the 1-2 set is pretty uniformly addition of charge while the later section of the 2-3 set is largely removal.

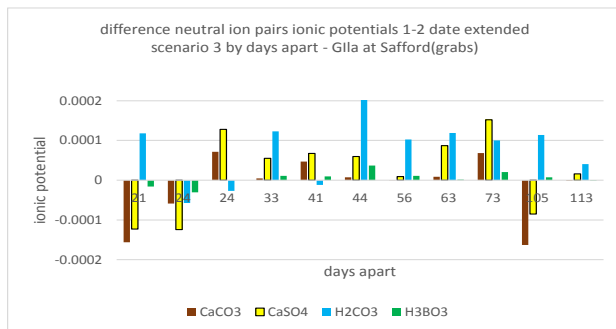


Figure 296

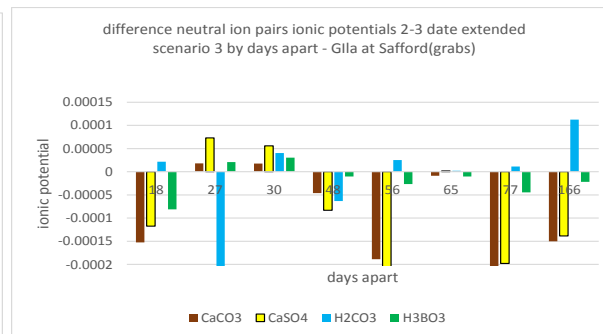


Figure 297

One reason the averages picture is not highly corroborated by the grab sample analysis may be that an important factor has been left out. Increased flow leads to the dilution of the free ions, but it also usually results in an increase in one parameter (besides H<sub>2</sub>O): dissolved oxygen.

Dissolved oxygen is a reagent in the formation of the anions so an increase in oxygen leads to an increase in anions which promotes the formation of metal ion pairs. Note that the scenario 3 ion pair ionic strength contribution ([Figure 277](#)) is not entirely addition of charge (dilution effect) and includes a roughly 25% contribution to reduction of charge as well, indicating ion pair formation.

How equally balanced the two effects, increasing dilution and increasing D.O., are is not known. The dissolved oxygen average values by inversion status do not differ from one another by much: inversion status 1 comes in at 8.85 mg/L, a little higher than 4 at 8.6. (One suspicious value of 15.4 mg/L in the low flow status 4 was removed before calculating that average). Scenario 3, where the highest values might be expected, is actually slightly lower than 1 at 8.79 while scenario 2, not unexpectedly, sees the largest drop to 8.51.

Unfortunately this is about as far as the analysis can go. The D.O. values in the final dataset were picked from 1) field values, 2) wateq4f values and 3) monthly averages in that order of preference. The latter are sometimes calculated from dry air composition, or climate factors (temp, press, dens, RH, SVP) or Henry's Law depending on what information was available. With such a mish-mosh of sources, the values of D.O. are not a coherent set of numbers that can be used to evaluate other trends with any degree of confidence.

As often happens, seeking more information to 'verify' previous averaged results only brings out the weakness of the averages picture. About all that can be added to the previous statement of common themes in inversion, is that the drop in ionic strength of inversion status 1 can be further characterized as accompanied by a general shift towards dissociation of the ion pairs, most noticeably the neutral ion pairs of Ca and Fe(OH)<sub>3</sub>. The roles of the other ion pairs are just too changeable to yield meaningful trends, though H<sub>4</sub>SiO<sub>4</sub> probably has an important role, if a largely unspecifiable one at this point.

Maybe looking at the neutral ion pairs from a thermodynamic rather than an ionic strength viewpoint will provide some insights into their roles. The dissociation of ion pairs that starts in scenario 1 is a very small effect. The following table was constructed by calculating the average

moles of each of the neutral ion pairs by inversion status, then subtracting the inversion status 4 average from the inversion status 1 average to give the max inversion status difference in amount. The average amount differences were then multiplied by the negative of the standard molar value of formation to give the amount of energy involved in the dissociation of the ion pair. There is no meaningful 'average' temperature for inversion states so the entropy values are in kcal/K.

average total thermodynamic function max difference at dissociation			
	entr/(kcal/	enth/kcal	free/kcal
Fe(OH) <sub>3</sub>	0.750	1592	1027
CaCO <sub>3</sub>	0.007	81	72
CaSO <sub>4</sub>	0.003	150	134
H <sub>3</sub> BO <sub>3</sub>	-0.003	21	19
H <sub>2</sub> CO <sub>3</sub>	-0.039	145	129
H <sub>4</sub> SiO <sub>4</sub>	-0.691	5640	5030

Table 147

Here one sees immediately the relative importance of Fe(OH)<sub>3</sub> and H<sub>4</sub>SiO<sub>4</sub> but it is hard to tell from just the numbers themselves whether ion pair dissociation is a significant quantity in the inversion process or not. One way of evaluating the effect is to compare it with the max difference under inversion of HCO<sub>3</sub>. These are calculated as above with the standard values of formation for HCO<sub>3</sub> which serves as the denominator for the percent ratio.

average total thermodynamic function % max diff at dissociation (%HCO <sub>3</sub> diff)			
	entr/(kcal/	enth/kcal	free/kcal
Fe(OH) <sub>3</sub>	70	-20	-12
CaCO <sub>3</sub>	1	-1	-1
CaSO <sub>4</sub>	0	-2	-2
H <sub>3</sub> BO <sub>3</sub>	0	0	0
H <sub>2</sub> CO <sub>3</sub>	-4	-2	-2
H <sub>4</sub> SiO <sub>4</sub>	-65	-71	-61

Table 148

The max dissociation difference of Fe(OH)<sub>3</sub> ion pairs, for example, is about 70% of the total entropy inversion difference of HCO<sub>3</sub> under the same conditions, i.e. going from inversion status 4 to inversion status 1. Looked at the other way, only Fe(OH)<sub>3</sub> and H<sub>4</sub>SiO<sub>4</sub> would markedly change scenario 1 entropy difference if they did not dissociate. That is to say, they have a high

potential to change entropy depending on the extent to which they dissociate in addition to the entropy they add or subtract as intact ion pairs.

Another way of gauging the importance of ion pair dissociation is to compare the above dissociation numbers to the values obtained with the ion pairs intact. Put another way, how does the dissociation amount compare to the amount they add by their presence as intact ion pairs?

average total thermodynamic function max diff at dissociation (/diff intact)			
	entr/(kcal/	enth/kcal	free/kcal
Fe(OH) <sub>3</sub>	-1.42	-1.41	-1.05
CaCO <sub>3</sub>	-1.05	-0.97	-0.89
CaSO <sub>4</sub>	-1.34	-0.88	-0.79
H <sub>3</sub> BO <sub>3</sub>	-0.95	-0.95	-0.82
H <sub>2</sub> CO <sub>3</sub>	0.00	-0.96	-0.79
H <sub>4</sub> SiO <sub>4</sub>	-0.98	-0.98	-0.85

Table 149

Most values come in right around 1, indicating that the dissociation effect is roughly equal to the intact ion pair effect. A ratio greater than 1 means the parameter is removing more energy by dissociating than it is contributing as an intact ion pair. This is the case for iron across all functions and CaCO<sub>3</sub> and CaSO<sub>4</sub> entropy. Of course, the comparison is not really 'fair' – with the grabs the amount added by the intact pair is that added by however much of the ion pair remains as ion pair – it is 'post' ion pair dissociation.

This last qualification suggests that maybe a summation of the two contributions is a more meaningful number. The relative importance of the different ion pairs remain largely the same but Fe(OH)<sub>3</sub> emerges as by far the leader in entropy and enthalpy contribution while H<sub>4</sub>SiO<sub>4</sub> is by far the highest in free energy contribution, things not apparent in the straight number tabulations of Table 147 above.

summation total thermodynamic function dissociation + intact pair contributions			
	entr/(kcal/	enth/kcal	free/kcal
Fe(OH) <sub>3</sub>	0.223	460	49
CaCO <sub>3</sub>	0.000	-2	-9
CaSO <sub>4</sub>	0.001	-20	-36
H <sub>3</sub> BO <sub>3</sub>	0.000	-1	-4
H <sub>2</sub> CO <sub>3</sub>	0.002	-6	-33
H <sub>4</sub> SiO <sub>4</sub>	0.013	-103	-915

Table 150

But all these relative estimates do not alter the fact that, in comparison with the entropy change due to the amount difference of water, the effect is, of course, very small. In terms of the solution as a whole, the effect on total entropy of ion pair dissociation is minuscule.

average total thermodynamic function % max diff at dissociation (%H2O diff)			
	entr/(kcal/	enth/kcal	free/kcal
Fe(OH)3	4.E-03	-2.E-03	-1.E-03
CaCO3	4.E-05	-9.E-05	-8.E-05
CaSO4	2.E-05	-2.E-04	-1.E-04
H3BO3	-2.E-05	-2.E-05	-2.E-05
H2CO3	-2.E-04	-2.E-04	-1.E-04
H4SiO4	-3.E-03	-6.E-03	-5.E-03

Table 151

But if the magnitude of dissociation is not large on a solution scale, its effect in terms of changing relations between parameters is large. The main cause of neutral ion pair dissolution during inversion is mass action as described above. But the equations of dissolution and formation must also follow the thermodynamic laws and can be categorized in terms of being enthalpy or entropy driven.

The table below summarizes the molar functions for formation of the neutral ion pairs for which information was available. The analysis uses the same rising temperature (279-306) scenario as Figures 149 thru 153 and [table 105](#). The reference values are signed as their tabulated values for formation.

formation neutral ion pairs with rising temperature (279-306K)										
		slope sign, correl T			functional functional					
		$\Delta H_m$	$T\Delta S$	$\Delta G$	$\Delta G_m$	relations	$\Delta H > T\Delta S$	$dG > dH$	$T\Delta S > S\Delta T$	
std vals	CaSO4	1	1	-1	incr	H,S,G	dH	-S(h)	$T\Delta S$	
	CaCO3	1	1	-1	incr	H,S,G	dH	-S(h)	$T\Delta S$	
	MgSO4	1	1	-1	incr	H,S,G	dH	-S(h)	$T\Delta S$	
	MgCO3	1	1	-1	incr	H,S,G	dH	-S(h)	$T\Delta S$	
	Fe(OH)3	1	1	-1	incr	H,S,G	dH	-S(h)	$T\Delta S$	
aq phas	CaSO4	-1	-1	-1	incr	H,S/G	$T\Delta S$	+S(g)	$T\Delta S$	
	CaCO3	-1	-1	-1	incr	H,S/G	$T\Delta S$	+S(h)/+S(g)	$T\Delta S$	
	MgSO4	-1	-1	-1	incr	H,S/G	$T\Delta S$	+S(h)	$T\Delta S$	
	MgCO3	-1	-1	-1	incr	H,S/G	$T\Delta S$	+S(h)/+S(g)	$T\Delta S$	
	Fe(OH)3	-1	-1	-1	incr(pos)	H,S/G	NS2	+S(h)	$T\Delta S$	

Table 152



Formation of the neutral ion pairs is enthalpy driven in the standard values view, entropy driven in the reaction in the aqueous phase view. For the enthalpy driven reactions, entropy is a negative number but moves in the direction of positive entropy (becomes a smaller negative) as temperatures rise and functional free energy increases. For the entropy driven reactions, entropy is positive but moves in the negative direction as do enthalpy and functional free energy increases. Relations change from H,S,G in the standard view to H,S/G in the aqueous phase. The exception is Fe(OH)<sub>3</sub> whose formation is not spontaneous in this temperature range and has increasing functional free energy nullified by being a positive value.

Fe(OH)<sub>3</sub> is, like the oxygen compounds examined earlier, a parameter for which the reagents, the free ions, are a smaller percentage of the total than the bound forms. In fact, Wateq4f predicts no free Fe<sup>3+</sup> in solution on all grab sample dates. While the thermodynamic functions apply to all levels of time and space, they do make an assumption that there is a sufficient amount of reagent to complete the reaction. That is, they cannot deal with relative scarcity.

Mass action grows directly out of LeChatelier's principle. While of less general scope and applicability, it provides in its relation to the thermodynamic laws a larger context. In cases where reagents are in abundance, mass action follows the thermodynamic laws and the result is, depending on the view and circumstances, the enthalpy or entropy driven formation of product. But the reverse direction of mass action, that is products to reagents which implies reagent scarcity, is outside the sphere of the thermodynamic laws and labelled simply as 'no change.' In fact, there is change and that is dissociation of the products but it is not fueled by temperature change and only occurs with change in relative amount.

The above conclusions help explain why, from the thermodynamic point of view, most neutral ion pair dissociations are labelled 'not spontaneous.' The following table is created from the same calculations as the above but the signs of the reference values are the opposite of their values of formation. Here all entropy is decreasing, positive with decreasing enthalpy and functional free energy in the standard values view, negative with decreasing enthalpy and functional free energy in the aqueous phase view. Apparently nature can be lavish with negative entropy when "it's not going to happen." Fe(OH)<sub>3</sub> is unique being enthalpy driven with increasing functional free energy and entropy moving in a positive direction.

dissociation neutral ion pairs with rising temperature (279-306K)									
		correl T			functional functional				
		$\Delta H_m$	T $\Delta S$	$\Delta G$	$\Delta G_m$	relations	$\Delta H > T\Delta S$	dG > dH	T $\Delta S > \Delta T$
std vals	CaSO <sub>4</sub>	-1	-1	-1	1 decr	H,S,G	NS2	+S(h)	T $\Delta S$
	CaCO <sub>3</sub>	-1	-1	-1	1 decr	H,S,G	NS2	+S(h)	T $\Delta S$
	MgSO <sub>4</sub>	-1	-1	-1	1 decr	H,S,G	NS2	+S(h)	T $\Delta S$
	MgCO <sub>3</sub>	-1	-1	-1	1 decr	H,S,G	NS2	+S(h)	T $\Delta S$
	Fe(OH) <sub>3</sub>	-1	-1	-1	1 decr	H,S,G	NS2	+S(h)	T $\Delta S$
aq phas	CaSO <sub>4</sub>	-1	-1	-1	1 decr	H,S,G	NS1	-S(g)	T $\Delta S$
	CaCO <sub>3</sub>	-1	-1	-1	1 decr	H,S,G	NS1	-S(g)	T $\Delta S$
	MgSO <sub>4</sub>	-1	-1	-1	1 decr	H,S,G	NS1	-S(h)	T $\Delta S/\Delta T$
	MgCO <sub>3</sub>	-1	-1	-1	1 decr	H,S,G	NS1	-S(g)	T $\Delta S$
	Fe(OH) <sub>3</sub>	1	1	1	-1 incr	H,S,G	dH	-S(h)	T $\Delta S$

Table 153

Note that almost all neutral ion pair dissociation reactions are associated with decreasing functional free energy. The fact that it is decreasing is not significant. The positive values indicates the reactions are not spontaneous. The opposite of spontaneity is ‘stability’ and the neutral ion pairs do not have any tendency to dissociate with rising temperature. Fe(OH)<sub>3</sub> is different with its functional free energy increasing with rising temperature. This combination of factors brings out the unique role of Fe(OH)<sub>3</sub>, stable in the standard values and unstable in the aqueous phase picture, opposite the other neutral ion pairs. Note also that all the thermodynamic function are directly related to one another in both views though things are obviously going nowhere (“NS”),

The daily fluctuations of ion pair dissociation are very easy to handle – they don’t exist. Ion pair dissociation is not primarily temperature dependent. Ion pair formation, on the other hand, will wax and wane on a daily basis in accord with the daily temperature fluctuation when conditions are right (namely, no scarcity of reagents). The motivations are in accord with the above Table 152, enthalpy driven in the standard values of formation view, entropy driven in the reaction in the aqueous phase view with the exception of Fe(OH)<sub>3</sub>. Below are the standard values view (top) and reaction in the aqueous phase view (bottom) of entropy (left) and (numeric) free energy differences (right).

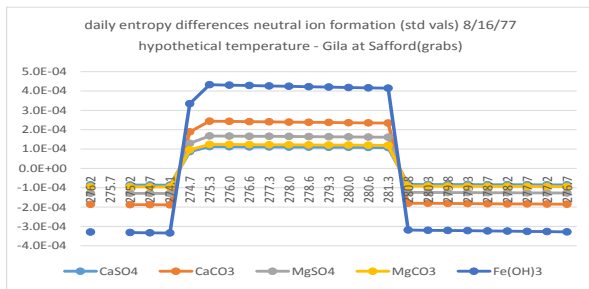


Figure 298

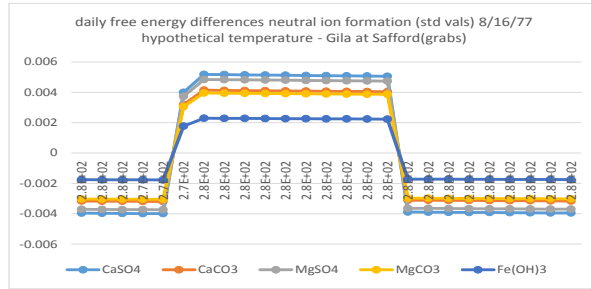


Figure 299

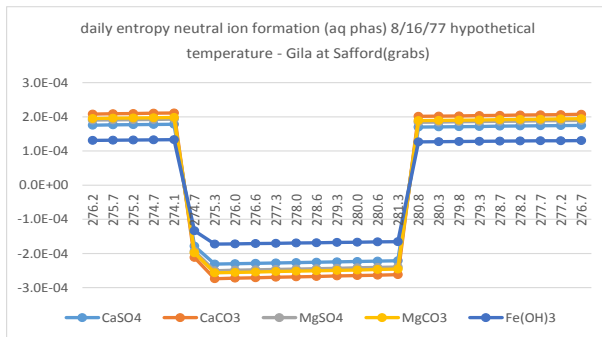


Figure 300

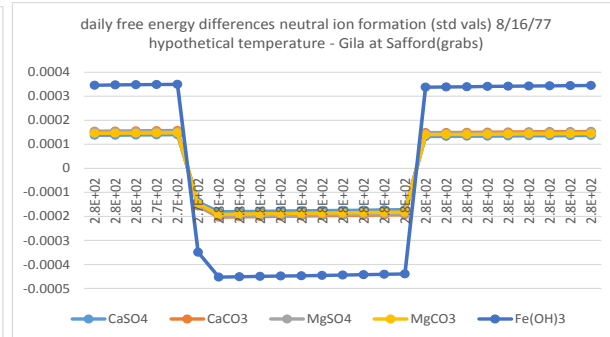


Figure 301

Despite the set-backs, a fuller picture of major ion concentration inversion has emerged thanks to the patterns of formation/dissolution of the ion pairs. It remains only to see how this new picture fits into the larger context of system energetics. Specifically, do the patterns in the

thermodynamic functions yield any insights into the timing and /or significance of ion pair dissolution and formation in the system during inversion? To answer this question it is necessary to once again 'start all over' and examine the relationships between system energetics and fundamental quantities. Unlike ionic strength which changes with concentration, the total thermodynamic functions change with change in amount. Both concentrations and amounts here are 'back-calculated' from activity so carry the changing inter-relations between constituents with them.

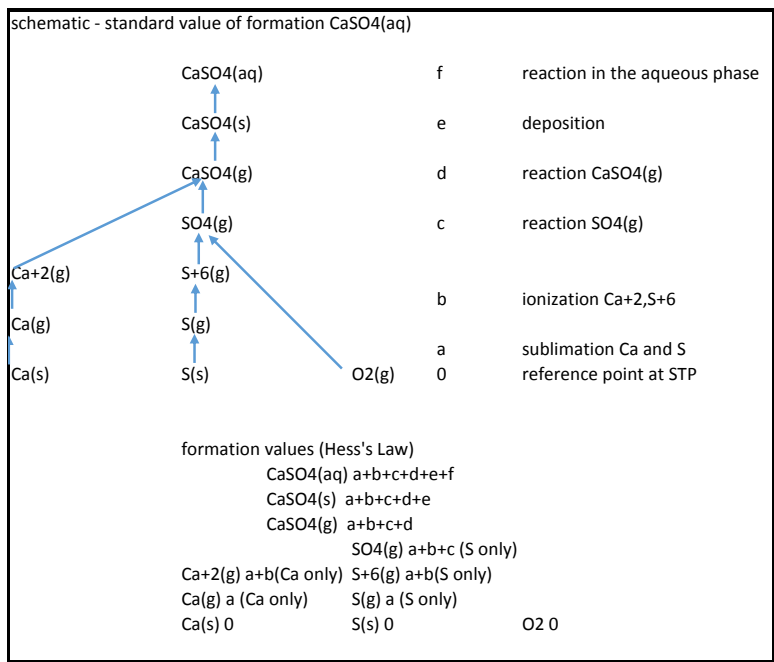
The molar thermodynamic functions are intensive properties, i.e. uniform across the system (like temperature), and say nothing about amounts. The partial molar functions of water are no more significant in describing the system in this sense than those of any other parameter. Only when multiplied by the number of moles of water do they become very significant indeed. In fact, the total thermodynamic functions of water are as close as it is possible to get, here, to a picture of the solution as a whole.

It seems obvious that to understand the changes in energy of a system in the real, material world, it is necessary to use the total not the molar thermodynamic functions. The total thermodynamic functions are very easy to calculate being simply the molar function times the number of moles of the parameter of interest. Such a simple, fundamental value must have some meaning. But, as has already been seen, the introduction of the number of moles creates difficulties in obtaining results that can be compared to one another. Another set of assumptions will have to be made that the total thermodynamic functions have the same general function as the molar and that they are adequately represented by the sum solution of constituents.

The two sets of thermodynamic standard values will be used as focal points from which to evaluate inversion. The thermodynamic values are 'instantaneous', not averages over time, and represent the system for one moment only. But they are also 'state' functions – the result does not depend on the path taken but is a difference of the value at the moment from that at a previous moment. Because they are state functions, they are 'instantaneous' values with 'history.' A grab flow says absolutely nothing about the flow that went before. But a free energy gives the value at a particular instant relative to a previous value. (Free energy 'values' here are therefore really differences and differences of 'values' are really differences of differences or 'accelerations' -- the rate of change of a changing process. The original terminology using 'values' ( $dH$ ) and 'differences' ( $\Delta dH = dH_2 - dH_1$ ) will, however, continue to be used for ease of understanding.)

The basis for evaluating the 'history' in a thermodynamic value is Hess's Law of Heat Summation which breaks a reaction down into sub-reactions and then tallies their molar values all up for the molar value of the overall reaction. The diagram below is a schematic for hypothetical energy steps in the formation of  $\text{CaSO}_4(\text{aq})$  from the most stable forms of the reagents,  $\text{Ca}(\text{s})$ ,  $\text{S}(\text{s})$  and  $\text{O}_2(\text{g})$  at the conventional reference point, the so-called 'standard temperature and pressure' (STP). Letters are used to represent the kcal of energy involved in each step because numeric values could not be found for all steps. These are sometimes summations but only in the sense of being across all parameters involved i.e. 'b' is the sum of all

ionizations (Ca & S) at that step, but is completely separate and independent of 'a,' the sum of all sublimations.



Schematic 8

There are two types of values here. Each 'reaction' or phase change has its own energy requirement; a thru f are the energy required for each step individually. A 'formation' value, on the other hand, is the sum of all the pertinent previous steps. The reaction in the aqueous phase value is the energy difference of CaSO<sub>4</sub>(aq) from CaSO<sub>4</sub>(s), i.e. step f only, while the standard value of formation of CaSO<sub>4</sub>(aq) is the sum of a through f, that is the sum of the individual steps from the reagents at STP to CaSO<sub>4</sub>(aq).

That the reaction in the aqueous phase values used by Wateq4f are the energy requirement to go from CaSO<sub>4</sub>(s) to CaSO<sub>4</sub>(aq) only is immediately apparent since they are much smaller than the standard energy of formation for CaSO<sub>4</sub>(aq). The reference starting point is not the reagents at STP but the aqueous ions which are set to zero.

The standard values of formation are 'padded' with a lot of information that may not be of interest. The amount of energy needed to sublime Ca(s) to Ca(g) is not of much concern in studying inversion. When differences are taken, such values become constants and fall out of the calculation. For this reason, any step may be picked as a reference starting point for a value of formation. Many of the thermodynamic values of the ion pairs here, for example, are calculated with the aqueous phase of the ions as the starting reference point of zero. This procedure, which involves creating an extra step 'aquating' the reagent ions not seem in schematic 8, essentially makes a single step reaction into a value of formation.

schematic - standard and reaction in aqueous phase values of formation CaSO4(aq)

reaction aqueous

```

      Ca2+(aq)      SO4(2-)(aq)
       /      \
        CaSO4(aq)
  
```

Ca2+(aq)	-129.74	-132.3	-0.0127
SO4(2-)(aq)	-217.32	-177.97	0.0048
CaSO4(aq)	-347.06	-310.27	-0.0079

standard formation

formation from reagents at STP, m = 1 CRC 63rd ec.

CaSO4(aq)	-347.06	-310.27	-0.0079
-----------	---------	---------	---------

Schematic 9

Because the aqueous ion formation values contain all the energy information up to their creation from the most stable forms at STP, the result is the same as the full calculation. In any case, it gives immediately the dissociation energy from ion pairs to aqueous ions.

The usual textbook presentation of Hess' Law shows how it can be used to find unknown values. For example, if the value for the deposition of CaSO4(s), step (e), was not known but the standard value of **formation** of CaSO4(aq) and all the values up to the formation of CaSO4(g) plus the reaction in the aqueous phase (a thru d and f) were available, 'e' could be calculated as  $= (a+b+c+d+e+f) - (a+b+c+d+f)$  thanks to Hess's Law. The input requirement is steep – every value but one must be known or at least estimated. Here Hess's Law will be used in a somewhat different way, in conjunction with the two sets of thermodynamic standard values, as a way of analyzing inversion.

The total thermodynamic picture of inversion can be seen in the percent total thermodynamic functions using the standard values of formation. The graphs below show the percent total free energy for the major ions for inversion status 1 (left) and inversion status 2 (right).

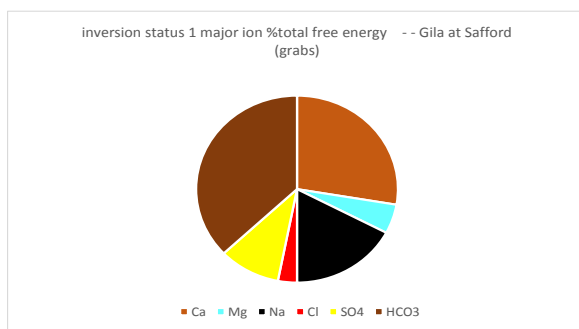


Figure 302

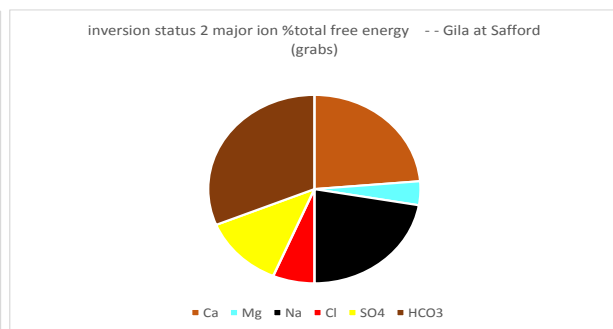


Figure 303

The interesting thing from the point of view of analysis is not the (straight) percent values but the differences of percent between inversion statuses. The inversion status differences procedure, first used in the ionic potential analysis, restores the familiar picture of inversion (below, with scenarios in chronological order). Scenario 3 & 4 values are so low they had to be scaled up to be

visible (right graph). The inversion relations clearly seen in the graphs below would be fairly hard to make out comparing slices of pie on the two graphs above.

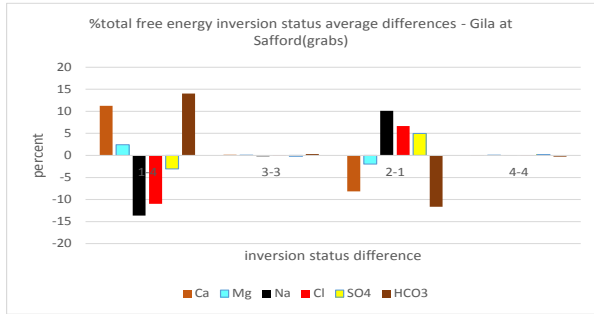


Figure 304

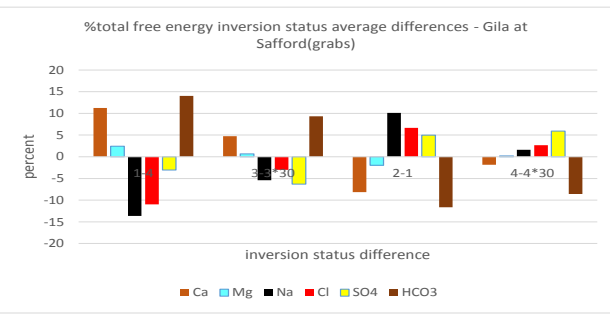


Figure 305

The % thermodynamic functions show the roles of the various ions but provide no indication of how the straight values (kcal) play out in time. The dominance of bicarbonate in amount is clearly seen in the straight value thermodynamic functions time series graphs. Shown below are the total entropies (left) and enthalpies (right) of the major ions for 1977 using the standard values of formation.

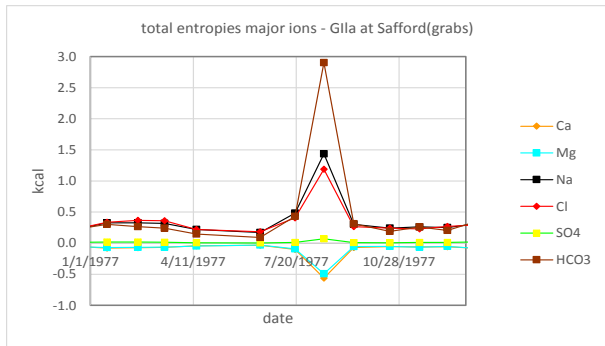


Figure 306

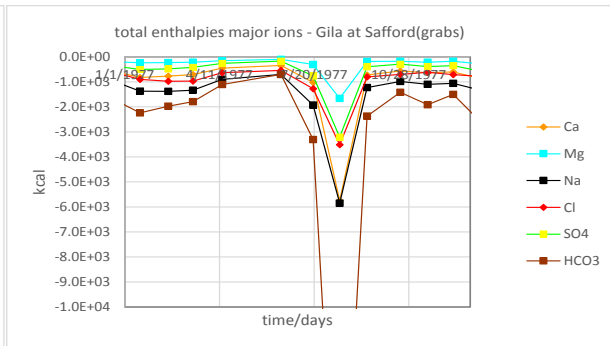


Figure 307

Free energy (not shown) has the same pattern as enthalpy. Note that the absolute values for enthalpies are magnitudes higher than those for entropy. Bicarbonate is the dominant player here in both entropy and enthalpy and  $HCO_3 > Cl$  (in absolute values) is the norm not the exception. Notice that enthalpies are negative while entropies are positive values with the exception of Ca and Mg. These two are unique in the major ions in having negative molar entropy standard values of formation.

The picture of inversion is quite different if the thermodynamic values of reaction in the aqueous phase are used. Below are the inversion status 1 (left) and inversion status 2 (right) views of major ion % total free energy.

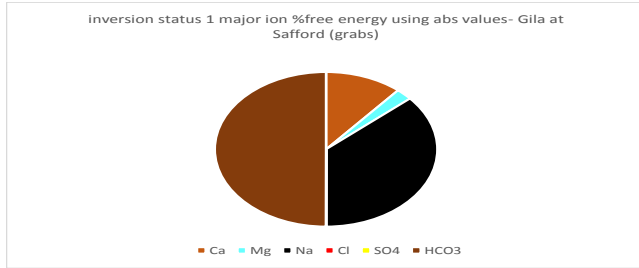


Figure 308

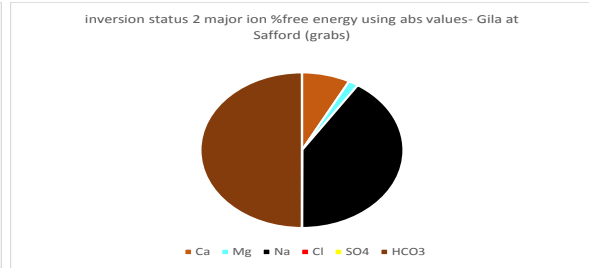


Figure 309

HCO<sub>3</sub> completely takes over the picture for the anions thanks to TS being a huge factor. On 2/20/76,  $H - TS = -36 - 105 = -141$  kcal: this result is the tip-off that these graphs were made using reaction in the aqueous phase values. The patterns seen above are quite similar to those for inversion status 3 & 4 and for all inversion status entropies and enthalpies. The inversion difference picture shows the dominant players in the reaction in the aqueous phase picture to be calcium and sodium. So while the dominant player overall is bicarbonate, the changes in status are more a function of calcium-magnesium and sodium.

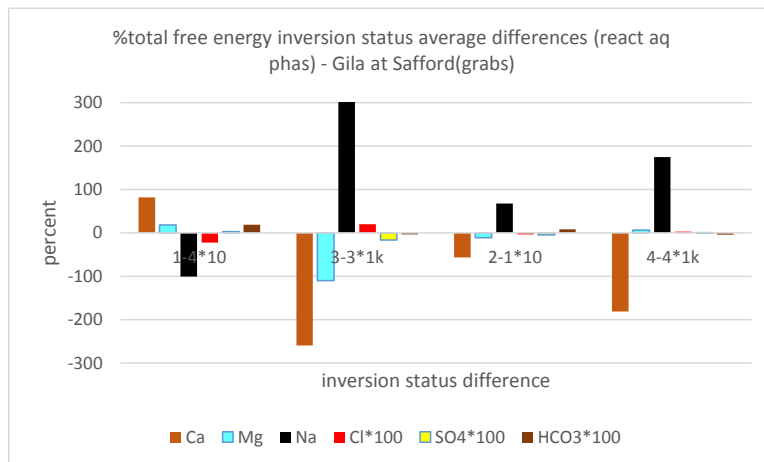


Figure 310

If the reaction in the aqueous phase values are used to create the same major ion total entropy over 1977 graph as above, the patterns formed are completely different from those generated with the standard values of formation. HCO<sub>3</sub> still peaks on 8/16/77 but there is no crossing of lines with Cl so there is no inversion. In fact, Na and Cl, as shown in the 'blown-up' scale (without HCO<sub>3</sub>) to right, seem to have no role at all to play during the inversion (8/16) while they have balanced, contrary roles during non-inversion.

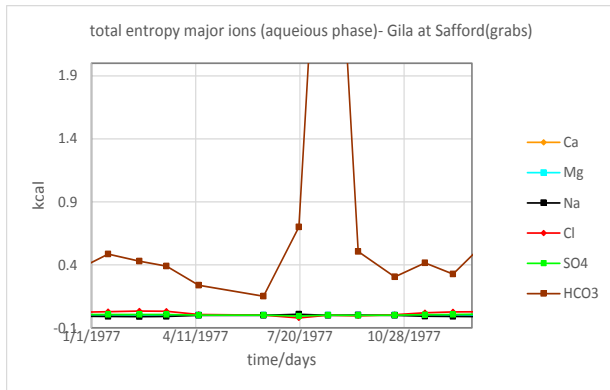


Figure 311

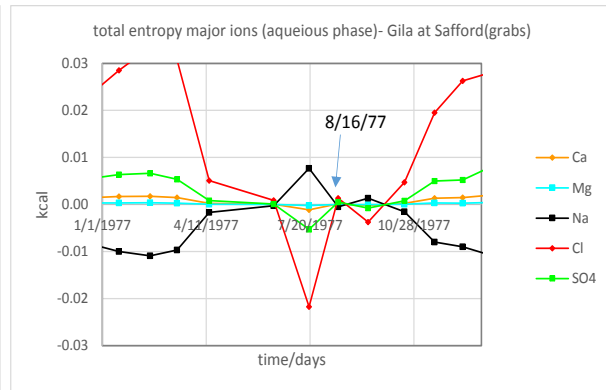


Figure 312

To quantify the intra-relations among the major ions over the entire expanse of data and see if the (implied) correlation with flow apparent in 1977 extends beyond, two matrices are given. The first shows major ion total entropies using standard values of formation, the second shows the same with the reaction in the aqueous phase values.

total entropy major ions - std vals of form - Gila at Safford(grabs)										
	Ca	Mg	Na	Cl	SO4	HCO3	flow/cfs	dens(TSP)/(kg/L)		
Ca	1.00	0.99	-0.82	-0.59	-0.82	-0.87	-0.86	-0.18		
Mg	0.99	1.00	-0.85	-0.60	-0.89	-0.92	-0.91	-0.20		
Na	-0.82	-0.85	1.00	0.89	0.92	0.93	0.87	0.28		
Cl	-0.59	-0.60	0.89	1.00	0.70	0.69	0.59	0.36		
SO4	-0.82	-0.89	0.92	0.70	1.00	0.95	0.93	0.34		
HCO3	-0.87	-0.92	0.93	0.69	0.95	1.00	0.97	0.23		
flow-grab/	-0.86	-0.91	0.87	0.59	0.93	0.97	1.00	0.19		
dens(TSP)-	-0.18	-0.20	0.28	0.36	0.34	0.23	0.19	1.00		

Table 154

total entropy major ions - react aq phas - Gila at Safford(grabs)										
	Ca	Mg	Na	Cl	SO4	HCO3	flow/cfs	dens(TSP)/(kg/L)		
Ca	1.00	1.00	-0.94	0.72	0.99	0.92	0.94	0.38		
Mg	1.00	1.00	-0.92	0.69	0.99	0.93	0.95	0.35		
Na	-0.94	-0.92	1.00	-0.91	-0.95	-0.83	-0.80	-0.60		
Cl	0.72	0.69	-0.91	1.00	0.76	0.59	0.52	0.78		
SO4	0.99	0.99	-0.95	0.76	1.00	0.91	0.90	0.41		
HCO3	0.92	0.93	-0.83	0.59	0.91	1.00	0.97	0.23		
flow-grab/	0.94	0.95	-0.80	0.52	0.90	0.97	1.00	0.19		
dens(TSP)-	0.38	0.35	-0.60	0.78	0.41	0.23	0.19	1.00		

Table 155

The total entropies of the major ions are highly intra-correlated and highly correlated to flow in either view with aqueous phase correlation coefficients slightly higher. Cl is the outsider here with high correlations only to Na though it picks up a slightly higher correlations with SO4 and, interestingly enough, a much higher correlation with density in the aqueous phase view. Total enthalpy and total free energy correlation matrices are almost identical to those of entropy, with just changes of sign. But total enthalpy has the same high relations of Cl with SO4 and density while total free energy keeps the SO4 relation but loses the density relation. The relation with density, if not just coincidental, may be related to the low correlation of Cl to flow.



The total thermodynamic functions themselves are intra-related via the molar function relations. The correlations matrix below relates solution sums for each of the total thermodynamic functions to each other and to flow and density. The intra correlations show the same relations between V&S and H&G that prompted the definition of the two molar function inversion groups – volume and heat content. But the correlation here is with flow not with density (temperature).

sum solution total thermodynamic functions (std vals form) - Gila at Safford(grabs)						
	$\Sigma$ soln V	$\Sigma$ soln S	$\Sigma$ soln H	$\Sigma$ soln G	flow/cfs	dens(TSP)/(kg/L)
$\Sigma$ soln V	1.00	1.00	-1.00	-1.00	1.00	0.19
$\Sigma$ soln S	1.00	1.00	-1.00	-1.00	1.00	0.19
$\Sigma$ soln H	-1.00	-1.00	1.00	1.00	-1.00	-0.19
$\Sigma$ soln G	-1.00	-1.00	1.00	1.00	-1.00	-0.19
flow-grab/	1.00	1.00	-1.00	-1.00	1.00	0.19
dens(TSP)-	0.19	0.19	-0.19	-0.19	0.19	1.00

Table 156

Though they do not validate the use of sum solutions, the nice, neat relations with each other and with flow, are encouraging. It seems that these entities are in some sense ‘complete’ if not necessarily accurately representing the solution as a whole. But the above picture is highly dependent on how the system is ‘sliced,’ using reaction in the aqueous phase values gives a very different picture as seen in the table below.

sum solution total thermodynamic functions (react aq phas) - Gila at Safford(grabs)						
	$\Sigma$ soln V	$\Sigma$ soln S	$\Sigma$ soln H	$\Sigma$ soln G	flow/cfs	dens(TSP)/(kg/L)
$\Sigma$ soln V	1.00	-0.08	-0.66	-0.68	0.00	0.25
$\Sigma$ soln S	-0.08	1.00	0.77	-0.62	0.98	0.18
$\Sigma$ soln H	-0.66	0.77	1.00	0.03	0.69	0.00
$\Sigma$ soln G	-0.68	-0.62	0.03	1.00	-0.67	-0.28
flow-grab/	0.00	0.98	0.69	-0.67	1.00	0.19
dens(TSP)-	0.25	0.18	0.00	-0.28	0.19	1.00

Table 157

Using reaction in the aqueous phase values, all the intra correlations between the functions vanish and only the positive correlation of entropy and flow remains. Water is not defined for the reaction in the aqueous phase. The decision not to use water in the sum solution for **volume**, however, is not necessitated by any ‘law.’ The decision is more a reflection of the desire that all the calculations should be done the same way, which is usually a good idea. But the result is a disjoint between amount and volume. The average sum solution volume with water is 15812 L while the average without water is 0.73

If water is added to the sum solution for volume while still not included in the other functions because they use aqueous phase standards, the relation between entropy and volume is restored but there is no effect on H or G.

sum solution total thermodynamic functions - react aq phas - using full vol w/H2O - Gila at Safford							
	$\Sigma\text{soln V(+H2O)}$	$\Sigma\text{soln S}$	$\Sigma\text{soln H}$	$\Sigma\text{soln G}$	flow/cfs	dens(TSP)/(kg/L)	
$\Sigma\text{soln V(+H2O)}$	1.00	0.98	0.69	-0.67	1.00	0.19	
$\Sigma\text{soln S}$	0.98	1.00	0.77	-0.62	0.98	0.18	
$\Sigma\text{soln H}$	0.69	0.77	1.00	0.03	0.69	0.00	
$\Sigma\text{soln G}$	-0.67	-0.62	0.03	1.00	-0.67	-0.28	
flow-grab/cfs	1.00	0.98	0.69	-0.67	1.00	0.19	
dens(TSP)-grab/	0.19	0.18	0.00	-0.28	0.19	1.00	

Table 158

If water is **not** used for the sum solution volume but still used in the other functions with standard values of formation, H & G become highly correlated to each other and to flow and V & S remain highly correlated but their correlation to flow is lost and the correlations of the two groups with each other are noticeably lowered.

sum solution total thermodynamic functions - std vals form - volume w/o H2O - Gila at Safford(grabs)							
	$\Sigma\text{soln V-H2O}$	$\Sigma\text{soln S}$	$\Sigma\text{soln H}$	$\Sigma\text{soln G}$	flow/cfs	dens(TSP)/(kg/L)	
$\Sigma\text{soln V-H2O}$	1.00	0.90	0.01	-0.01	0.00	0.25	
$\Sigma\text{soln S}$	0.90	1.00	0.38	0.36	-0.39	0.15	
$\Sigma\text{soln H}$	0.01	0.38	1.00	1.00	-0.97	-0.19	
$\Sigma\text{soln G}$	-0.01	0.36	1.00	1.00	-0.97	-0.20	
flow/cfs	0.00	-0.39	-0.97	-0.97	1.00	0.19	
dens(TSP)/(kg/l)	0.25	0.15	-0.19	-0.20	0.19	1.00	

Table 159

These various, somewhat strange looking, views of the system make clear that it is both the amount and the volume of water that tie the sum solution total thermodynamic functions to each other and to flow. The relations depend on the ‘history’ included in each function and on the amount-volume relation between the functions. These two factors are pertinent in the question of whether a system and/or a cycle are ‘complete’. The reaction in the aqueous phase view is a ‘stripped to the bone’ picture that brings out the importance of entropy relations.

Which set of thermodynamic standard values is most appropriate depends on where the interest lies. If the interest is in the energy change over the entire inversion process, the standard values of formation need to be used. If the interest is in the formation or dissociation energy of ion pairs like  $\text{CaSO}_4$ , that value also is included in the standard value of formation of  $\text{CaSO}_4$ .

The reaction in the aqueous phase standard values start with the creation of the aqueous ion and do not have any specific information about anything that occurred before that, just a summation. But if the interest is in the ‘end states’ of the inversion process, then these are the values to use. The reaction in the aqueous phase picture, being the last energy step that occurred just before the inversion, is the one most pertinent to the state of the system at that moment.

The order of events to this point has been hypothetical analysis followed by analysis of the grabs to verify hypothetical results. Here the process will be reversed – grab sample analysis will be done first to set the stage for the hypothetical analysis that follows. This particular hypothetical analysis is so ‘outside the bounds’ of normal modelling that it is best to first have some idea of the actual state of affairs to set limits on what is acceptable in the model and what is not.

For reasons stated above, most of the analysis from this point on will be of differences. Unlike ionic potential which is always positive, the thermodynamic partial molar functions have a sign which can be either negative or positive depending on the sign of the standard reference value and on the temperature adjustment of that value. The sign of the partial molar function value is carried over to the total function value. The difference between total function values on two days are calculated with the signs allowed to work themselves out following the rules of algebra. But the final sign is ultimately set by the context. All HCO<sub>3</sub> total entropy straight values are positive because the partial molar value is positive and amount for a straight value is always positive. But the differences change sign by inversion status because HCO<sub>3</sub> total entropies are higher in inversion status 1 than in inversion status 4, lower in 2 than in 1, etc. An average then gives the overall tendency for gain or loss of energy by inversion status.

Rather than continuing with time-series graphs, the survey switches back to the inversion status difference diagram format. Inversion status 4 is at the beginning and the end, and 1, 3, and 2 in left to right order in the middle. The analysis is now, at least in format, like a thermodynamic experiment: allowing input from the environment to a system seemingly at rest, noting the reaction, and allowing the system to return to rest. The patterns created map the different end states of the inversion process not, as the time series graphs, the process itself.

The inversion status difference procedure expands on the 'chronological' order format of the ionic potential analysis ([see earlier discussion](#)). First the samples are sorted by inversion status then the inversion status 1s are subtracted from inversion status 4s, inversion status 2s from inversion status 1s, and inversion status 3s & 4s within themselves. The first of one group is subtracted from the first of the other with the samples within each group in no particular order (unless Excel chooses one 'on its own'). The result is a random set of differences with some samples left out since the scenarios have different numbers of samples. The averages here are averages of differences as opposed to the ionic potential analysis which used differences of averages. The output presents the inversion statuses in the 'chronological' order of a complete cycle, 4-1-3-2-4. The 'zero' being created here is scenario 4

It is important to point out that, in this section, the 'scenarios' occasionally referred to are only used in the selection of grab sample dates. While the terms will be used synonymously, 'scenario' is a term more appropriate to the 'hypotheticals' with 'inversion status' being the preferred term for the grabs. There is nothing at all hypothetical about the analysis here: these are actual grab total thermodynamic function values or differences over the selected dates averaged by inversion status. Any relative values or solution sums are over all parameters present in the grab samples, not just, for example, the major ions.

As an example of the sorting by inversion status technique, the graph below left shows the grab flow differences sorted as described above. The averages picture to the left is neat and clear and agrees with what is known about flow change in the different scenarios. The full picture to the right, with individual flow differences sorted from highest to lowest, as well as their averages as points, reveals that inversion status 1 & 2 are unidirectional while 3 & 4 are bidirectional. Inversion status 3 is a time of high, variable change in flow. It is averaging over an evenly

distributed set of bidirectional values that makes inversion status 3 look like a system at rest when it is, in fact, quite the opposite.

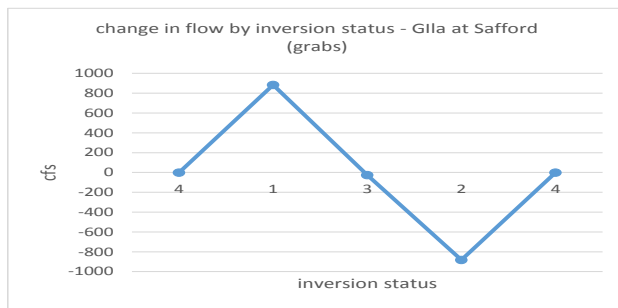


Figure 313 [\(back\)](#)

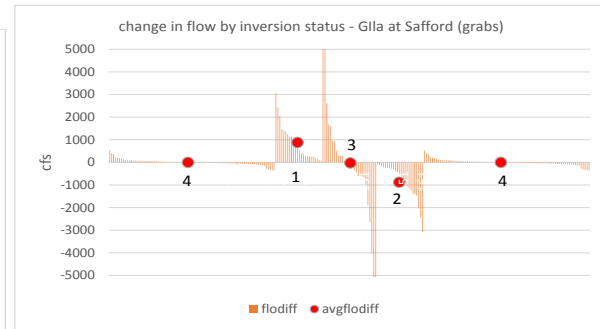


Figure 314

It has been stated that the inversion starts with the drop in activity of sodium and chloride. This statement is true enough but is rather ‘out of the blue’ and arbitrary. There is not the ‘linkage’ to something else that would be expected at this level. It might as well be said that the inversion starts with the formation of clouds somewhere over the Pacific or the Gulf of Mexico.

Nature is all of one piece. Analysis, the description of sequences of events in time, however, demands a starting and an ending point. The end point is simply the first appearance of the phenomenon of interest. The starting point, since it is necessarily arbitrary, might as well be convenient as long as it is pertinent. The main factors in pertinence are encompassing as many potential causes as possible and uniqueness to the phenomenon being analyzed. The clouds over the oceans are the first cause of many phenomena, most of which have nothing to do with inversion on the Gila.

For these reasons, increased flow along the Gila is designated the ‘primary action’ of inversion. Flow is not linked to any particular change in water quality and some cases of rising flow do not show inversion. But all inversions occur during rising flow so factors associated with flow are the likeliest causes of inversion.

The pattern seen in Figure 313 above, a peak at inversion status 1 and a valley at inversion status 2, is designated the pattern of ‘primary action and reaction’ or just ‘primary action’ for short. Action and reaction at a particular level, here ‘primary’, happen over extended periods of time (multiple grab samples) and there is no information on what may have gone on before or after (the clouds over the ocean are out!).

The terminology here is obviously borrowed from Newton’s Third Law, which relates bodies in motion (i.e. with a certain momentum or force) to other bodies as action and reaction pairs. The usage here is somewhat different; the ‘forces’ are no longer only bodies in motion and can be something like a ‘flow’ or a ‘concentration’ and they are no longer necessarily balanced. In fact, it may very well be the lack of balance that provides ‘motivation’.

Action is more like ‘causal motion’ or, in less loaded terms, ‘a change in the system that motivates another change’, the ‘other’ change here called the reaction at that level. The reaction

may really be just the cessation of action, i.e. diminished flow over time. Each action (i.e. single peak or valley) is both a cause of a reaction on its own level and, after the arbitrary primary level, an effect of action at another level. The whole scheme is merely a way of keeping track (tabulating, categorizing, prioritizing, and linking) of a series of events in which the system changes.

Using the same inversion status difference procedure as for flow, the total thermodynamic functions of the solution (water) are calculated and the results are shown below with volume/entropy to the left and enthalpy/numeric free energy to the right. The percents (not shown) follow the straight values with the only difference that percent relative volume and percent entropy flip direction and follow the enthalpy/numeric free energy pattern instead. These are considered to be the directions of energy change of the solution as a whole and are the patterns that all others will be compared to.

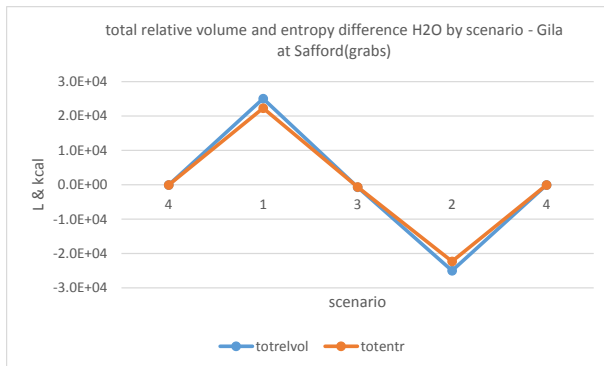


Figure 315 [\(back\)](#) [\(back2\)](#)

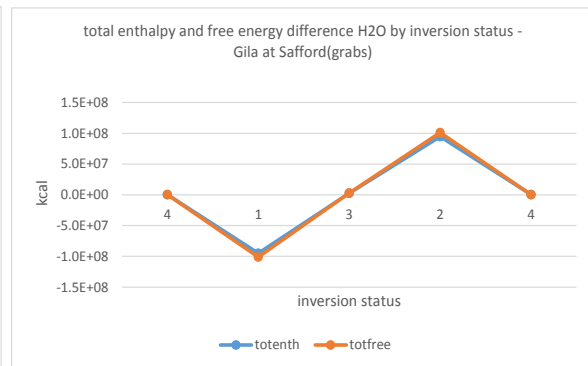


Figure 316 [\(back\)](#)

Average flow ([Figure 313](#)) and the volume of water ([Figure 315](#)) obviously have the same pattern which suggests that patterns, in general, can be related to each other. An individual pattern is, by itself, entirely unique and coincidental with itself only. It is in the relation of patterns to each other that they are not only verified but also made significant. It is not always clear, however, whether similar patterns are linked by cause and effect or are rather identical, two aspects of the same thing, or just coincidental. Often some arbitrary decision has to be made.

The volume of water is clearly related to primary action (flow) since the amount and volume of water as they change in time **are** flow. But what about the enthalpy and free energy of water? Should their pattern be considered to be in 'reaction' to primary action? The answer is 'no' because the change in pattern is not based on a change in the (physical) system but is due rather to the inverse relation of entropy and enthalpy-free energy,  $(G-H)/T = -S$ . The 'flipped' direction of enthalpy, free energy, %entropy, and %volume are, therefore, all simply ignored. The total thermodynamic functions of the solution (water) follow primary action (flow) with, let us say, non-significant 'variations'.

But why do the patterns look the way they do? A negative sign for enthalpy is considered by convention to mean heat loss to the environment by a reaction as written from reagents to products, positive to mean heat gain from the environment. If the relation can be applied to our solution, it makes 'sense' because the scenario 2 picture is one of negative entropy which, to be maintained for any length of time, needs an input of heat from the environment. And voila' – the enthalpy change for water is positive in scenario 2. Unlike the individual major ions, water is in a position to change things on a big scale due to its overwhelmingly larger amount. At the solution level, negative entropy at scenario 2 is resolved by the positive enthalpy of water.

If the sign of free energy has anything to do with spontaneity of change in a solution, then that too makes sense in the picture that has been built up to this point. Inversion status 1, its high positive entropy generated by the rapid, large increase in volume, is energetically favored as evidenced by its negative free energy. Inversion status 2 is not favored energetically, i.e. has a high positive free energy, because of negative entropy apparently due to a large volume contraction.

The 'thermodynamic experiment' look of the above graphs is encouraging. The symmetry and/or 'balance' are expected – the free energy peak at inversion status 2 is roughly proportional to the valley at inversion status 1 – which is what the conservation laws say. Or rather, the process has been dissected in time and space to show the complete analysis cycle of a complete system and the conservation laws can be seen to hold. It is the symmetric, balanced look of the graph that confirms the completeness of the cycle which in turn confirms that it is a complete system that is being looked at.

Proportionality is seen on the graphs but can be evaluated numerically as well. The proportional relationship between scenario 1 and scenario 2 for any given analysis can be checked simply by calculating  $\text{abs}(\text{scen1}) - \text{abs}(\text{scen2})$  or as a percent difference  $((\text{abs}(\text{scen1}) - \text{abs}(\text{scen2})) / \text{abs}(\text{scen2}))$ . The two views are helpful because a high difference, that might suggest a major role for a particular parameter, may have the same percent difference as others. The closer to zero either of these numbers is, the closer the two scenario areas are to being equal. Especially close attention was paid to the scen1-scen2 proportionality of entropy and the scenario 1 percent relations between volume/entropy and enthalpy ( $H/T$ )/entropy. The differences and percent differences scen1-scen2 for water are zero across all functions. Scen 1 entropy is 0.89 percent of total scen1 volume and  $H/T$ ,  $G/T$  are roughly 15 times scen1 entropy.

Using the inversion status procedure and taking differences with entropy as  $dS_m$ , the first completely 'functional' view of the system during inversion has been created. This new formulation maps out the various inversion states not in terms of the magnitudes and directions of parameters during the process itself but as the energy end-states of the process. As such, each diagram in the survey that follows is the 'energy footprint' of the parameter being examined at any particular level.

The above graphs could be created in several ways. The original straight values can be sorted by inversion status and the inversion differences (random differences as described above) taken and averaged. Or the grab sample date chronological differences can be sorted by inversion status

and averaged. These two methods produce different ‘differences,’ but they lead to the same result.

What is more significant is that the relations between the total functions of water seen above (H,G/S or, functionally, S,G/H) do not agree with those seen in the daily sum solution molar function inversions (H,S/G or, functionally, H,S,G). The former have come about through relations of amount while the latter are the result of temperature dependence only (Table 105). Both amount and temperature change are incorporated in change of volume though in different time and spatial contexts. It is the amount-volume of water that changes the relations of the thermodynamic functions with one another. Note that the numeric H,G/S relation seen here is not seen anywhere else and may be presumed to be a signature relation for amount.

The other big difference with table 105 is the use of  $\Delta S$  in the table,  $dSm$  for the above graph. Recreating the above graphs with the  $\Delta S$  of water rather than  $dSm$  would produce two graphs (not shown) that differ from the above in two ways – free energy has the same pattern but different values and, more importantly,  $\Delta S$  is now a large **valley** at scenario 1 with a corresponding peak at scenario 2. Why should, or rather how can, a period of expansion show negative entropy? Setting that question aside for the moment and assuming that only water, with its overwhelmingly large amount, can resolve its own negative total entropy – how is that done? Enthalpy in the new  $\Delta S$  picture is directly not inversely related to entropy, only free energy is (functionally) inversely related to entropy. So how would negative entropy be resolved?

There are many ways in which the system can be ‘sliced’ but it is probably a good idea to use only one and be consistent about it. The  $\Delta S$  calculation, while necessary to distinguish enthalpy from entropy driven reactions, doesn’t suit the analysis here as well as the  $dSm$  calculation. The picture of the solution  $\Delta S$  creates seems to lead into another realm where all the basic patterns have changed.

While all questions have not been answered and many dilemmas remain, a simple picture of river function emerges that makes ‘sense’ in terms of the basic meaning of the thermodynamic functions. But changes in water cannot explain everything, the changing functions and patterns of the constituents are too regular to be dismissed as coincidental as will be seen shortly.

The patterns evolved all fall into two groups: an expansion at inversion status 1 (a peak) and a contraction at 2 (a valley) as in volume/entropy above or a contraction at 1 (valley) and an expansion at 2 (a peak) as in solution enthalpy/free energy above. The differences lie in four areas. First is the proportionality of peaks and valleys. Second the ‘level’ at which the parameter exists (magnitudes). Generally speaking, the lower (deeper) the level the less proportionality. The third are the interrelations with other parameter patterns and, most importantly, whether the pattern is working in the same direction or against that of the solution as a whole (water). The fourth is whether there are any anomalies, instances where the diagram is not a simple as advertised. With the different standard value datasets, the time-span frame of reference of each status can be altered to reveal the here-and-now, instantaneous as well as the full historical, energy summation end state.

The question – can inversion status 3 & 4, with their apparent look of ‘no change’, be characterized as ‘equilibrium’ situations? – can now be answered, at least for the thermodynamic functions. The answer is ‘no’ for several reasons. The system is hardly ‘at rest’ during these periods, the magnitude of change is not infinitesimal though it can be very low in inversion status 4. And the direction of change, while bidirectional and roughly equal in both directions (which is one definition of equilibrium) in 3, is definitely not subject to change in direction by a small change in the environment (i.e, is not ‘reversible’).

Wiser heads than the authors' have surmised that equilibrium is not possible in natural systems and deduced that all natural phenomena are 'irreversible'. That is to say, all reactions go in one direction only rather than balancing around an equilibrium position. Inversion status 3 & 4 are more properly described as periods of 'maintenance of (different) non-equilibrium states'. Having no equilibrium position to relate them to, they can only be related to each other and to the 'motivational' scenarios (1, 2). At best they constitute a quasi-equilibrium situation, a period of relative balance, which can be exploited by analysis. Between the four states, they provide a 'complete' picture of the system, every possible energy change is covered.

Delving further down into the system with the solution sum of the dissolved solids (graphs below), things change immediately. Here the entropy and free energy changes are relatively high and in the same direction as those of the solution (water). But the volume and enthalpy changes are relatively low and enthalpy no longer follows the same direction as (numeric) free energy. Each of the four functions have scen1-scen2 differences and percent differences of zero but the percent relations with volume and H/T of entropy (2.9 and 0.116 respectively) are different from those of water (the solution).

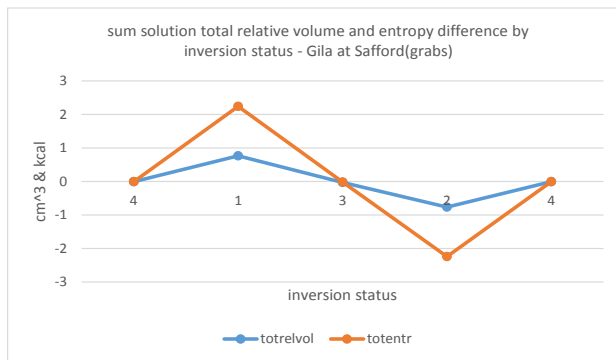


Figure 317 ([back](#)) ([back2](#))

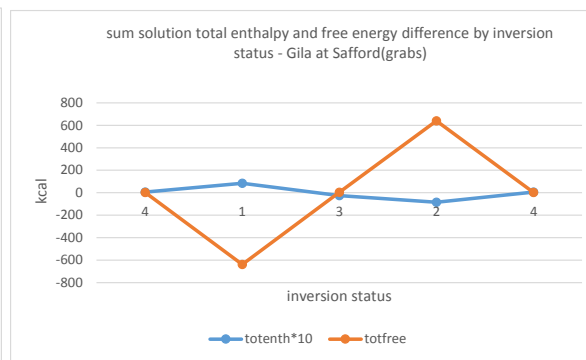


Figure 318

There is a slight amount of heat gain in inversion status 1 (8.5 kcal - multiplied by 10 to be visible on the graph to the right), heat loss in inversion status 2. Most of the dissolved solids cause contraction of the solution, hence the lower total relative volume. Heat is apparently needed to maintain the high positive entropy of inversion status 1 at the dissolved solids level given the small change in volume. This situation is 'local,' applying only to the dissolved solids, and is opposite that of the solution as a whole as represented by water where entropy is proportional to volume. The assumption here is that an entropy imbalance is made up as quickly as possible and from the closest source or level. While the dissolved solids are a 'complete' subsystem in terms of charge balancing and the resolution of negative entropy (over time), the results above shows that they don't have the correct amount-volume ratios to be complete at the level of energy balance.

Using reaction in the aqueous phase values for the dissolved solids thermodynamic functions shows a different situation from the standard formation values in terms of relative (unscaled) magnitudes (left) but the same patterns as the solution (right) when scaled appropriately. Because many parameters are more affected by TS than H, G is much lower, a product of two factors



going in opposite directions. But the fact that the patterns, when appropriately scaled, are the same for aqueous phase as standard values of formation points to the general relevance of the inversion status difference diagram whatever time factor is included in the end state picture.

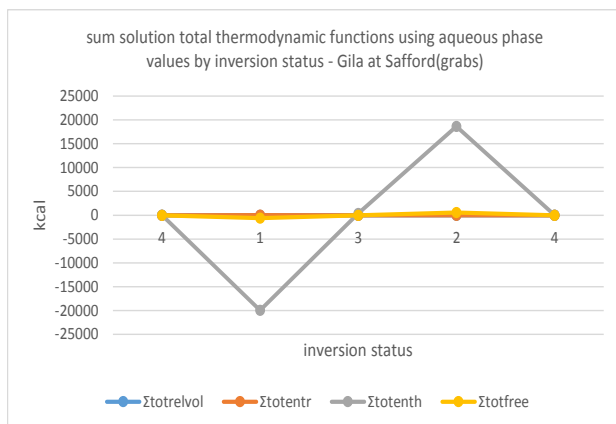


Figure 319

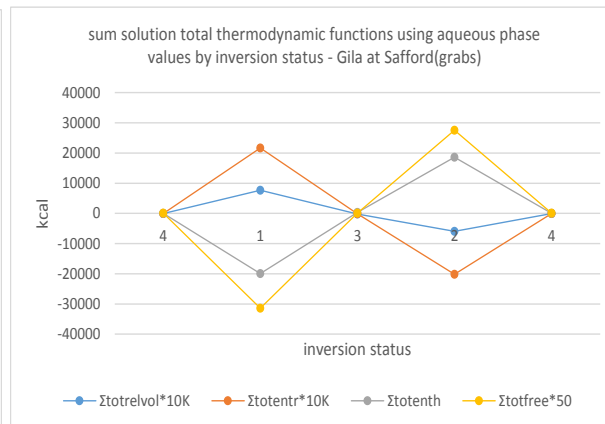


Figure 320

The scen1-scen2 differences and percent differences are not zero for reaction in the aqueous phase so the various functions do not resolve themselves over time. But the percent relations between volume, H/T and entropy are similar to those seen in the standard values view.

Relating the major ion activities to the primary action reveals a significant new pattern. The transformation of action at one level to action at another can often reasonably be linked together. The new pattern is designated the 'secondary action and reaction' or 'secondary action' for short. This secondary 'action,' a valley at inversion status 1, is itself a reaction to the primary action of increased flow. Levels of action, as conceived here, are analysis, the dissection of levels of matter, of instantaneous phenomena and are in the opposite direction from the level above, i.e. an action on the secondary level is a reaction to an action at the primary level.

The picture of falling Na & Cl activity in inversion status 1 and rising in inversion status 2, opposite the change in flow, is clearly seen in the change in major ion activities (left) and percent activities (right) by inversion status. But while the patterns follow, the proportionality of scen1 and scen2 is largely lost here and in all the following views of the major ions. The differences and percent differences scen1-scen2 are not zero meaning the peak/valleys are not proportional. The sum of the ions at scen 1 and scen 2 differences and percent differences can also be calculated and these are not at all what one would expect from the individual ions results but never equal zero. So the sum the ions as a group is functionally different but does not achieve complete system status.

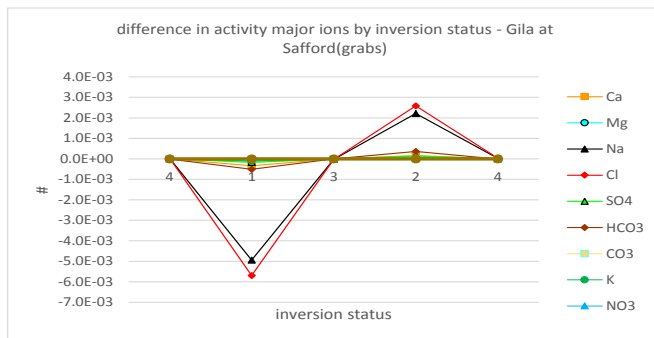


Figure 321

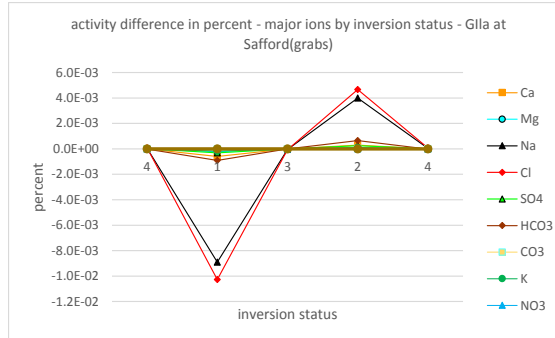


Figure 322

The activities were calculated with the WATQ4F program which is used here, admittedly, as a ‘black box.’ The activity is understood to incorporate inter-ion attractions and repulsions in a unit-less number that stands in place of a concentration. (Part of the equation has units of  $(I/\text{mols kg}^{-1})^{0.5}$  where  $I$  is the ionic strength, and  $\text{mols/kg}$  is a concentration). It says nothing about amounts or volumes though the result of the interplay between these two factors is incorporated into the number via the concentration.

The interesting thing here is that the pattern of the straight values of activities and the percent activities are exactly the same. A rise in value accompanied by a rise in percent means the two are proportionate while a fall in value with a rise in percent, as seen in ionic strength of  $\text{HCO}_3$  and  $\text{Ca}$  (Figures 236-7), means a disproportionate change is occurring in the system. The picture above, however, is not perfectly balanced, with the valley of inversion status 1 being considerably larger than the peak of inversion status 2. Summing the major ions at inversion status 1 and 2 does not change the situation – the values above and below the line are not balanced. Like the total dissolved solids, the major ions do not represent a complete system for energy balancing.

When percents follow straight values directly there is a sense that the analysis quantity is in some sense ‘complete’ and it is even better when there is balance as well. For this reason, situations in which values and percents show the same pattern are often used as ‘starting’ points for analysis and/or considered adequate ‘end’ points. In any case, both views need to be examined for completeness of analysis.

Amount values and percents of the major ions are, on the other hand, quite different. The major ion amount values picture (left) shows  $\text{HCO}_3$  change as the dominant factor in inversion while percent amounts (right) show change in  $\text{Na}$  &  $\text{Cl}$  to be the dominant factor. Put into the new parlance, amounts can be said to follow primary action. Percent amount (the mole fraction) at first glance seems to follow secondary action but is only a change of ‘view’ for amount and does not represent a change in the physical system. The mole fraction is, itself, a kind of concentration so having a pattern similar with that of activity, another ‘concentration’-like number, makes sense.

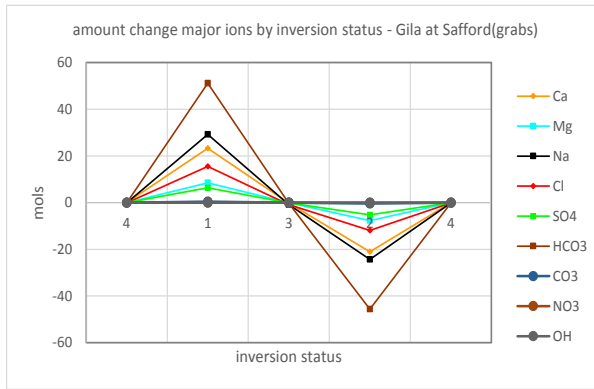


Figure 323

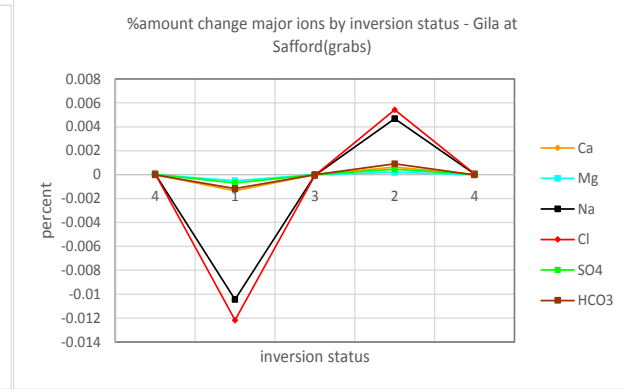


Figure 324

The amount of the major ions picture is not perfectly balanced but better than the percent amount view. Amount percent differences ((scen 1 – scen 2)/scen2) are very consistent at around 0.17 +/- 0.08 while the percent percent differences are 0.1 +/- 0.55. In neither case does summing the ions at 1 and 2 achieve perfect proportion, in fact the averages of the individual ions come closer to zero.

The total relative volume of the major ions looks a lot like amount but with a twist – the largest change in volume is HCO3 (below left) but the largest percent change is for Cl (below right). The sign of the partial molar volume keeps the cations and anions on opposite sides of the zero line so there is something like a ‘built-in reaction’ here. Total relative volume change, like amount change, is considered part of primary action.

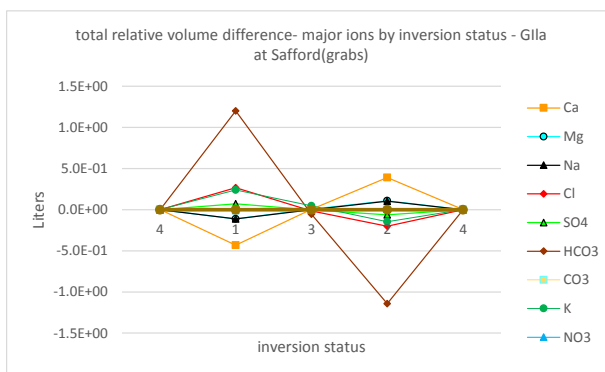


Figure 325

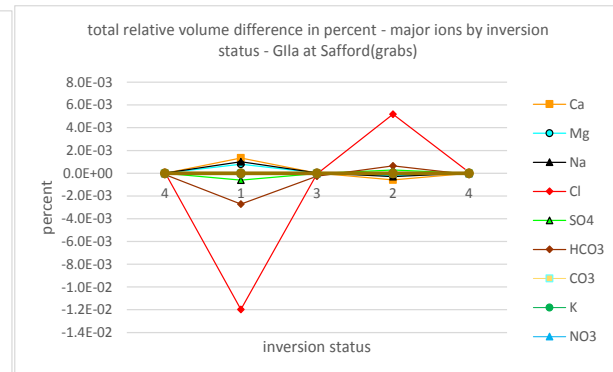


Figure 326

The total relative volume picture is, like the amount, not perfectly balanced. Individual ion scen1/scen2 percent differences are 0.17 while the sum of the ions at scen1 and scen 2 is 0.6, The percent differences for the percent relative volume are around 1.3 almost the same as the sum of the ions (1.4).

Volume is calculated from a linear equation relating partial molar volumes to temperature. The different thermodynamic values calculated by two sets of standards have to apply to one set of volumes, the only difference are those of magnitude. A 1.2 L contraction in volume of HCO3 in inversion status 2 will correspond to a numerically different drop in entropy with the standard

values of formation (-1 kcal/K) than it will with the reaction in the aqueous phase values (-2 kcal/K). This difference is caused by water dropping out of the (**analytical**) picture and becoming the medium of reaction and is not a change in the system itself. But the important thing here is that not just any old volume will do, there is a ‘thermodynamic volume’ that is appropriate to any given set of thermodynamic function values.

The amount and volume of water tie the total thermodynamic functions to flow. There is no problem believing they are part of the primary level since the amount and volume of water as they play out in time **are** flow while amount and volume of major ions are not. Amount and volume of the major ions are, instead, solution patterns that have been translated down in level as a ‘complete’ system to an incomplete system.

To jump ahead a bit, it is necessary to motivate the following discussion a bit. Since the activity, amount, and volume of the major ions were shown not to represent complete systems, it does not seem possible, certainly, that their entropy, enthalpy, or free energy will all of a sudden appear to be complete systems. But it is possible to see patterns of relative balancing – i.e. balancing at a certain level of analysis. The inversion is worked out differently at different levels. An imbalance at one level is presumably made up for by a corresponding imbalance at another level and the two presumably balance each other.

Entropy of the major ions using the standard values of formation largely follows primary action but there are a few wrinkles. HCO<sub>3</sub> is dominant, Na & Cl are moving in the same direction, and all are balanced by Ca and Mg. This picture is close to the original flow/amount relationships above except that Ca and Mg have flipped direction thanks to their negative molar entropies – the tip-off that standard values of formation have been used here. This picture of the complete inversion process is made possible by the fuller energy ‘history’ contained in the standard values of formation.

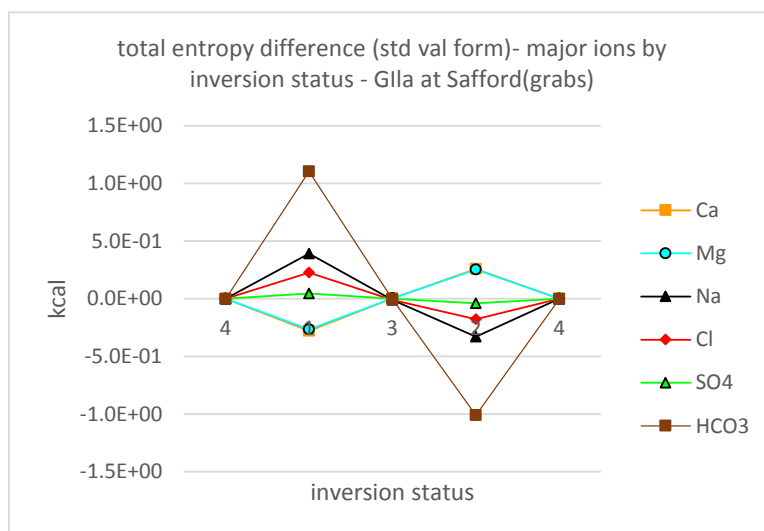


Figure 327

The percent thermodynamic functions can be handled the same way. The resulting patterns for the percent entropy are the exact opposite of those of the straight values. Percent Na & Cl roles change the most while percent HCO<sub>3</sub> changes less, recalling the inter-relations of major ion percent activity. The flipping of patterns between straight values and percents do not correspond to any change in the physical system, they are the result of a change in ‘view’ only.

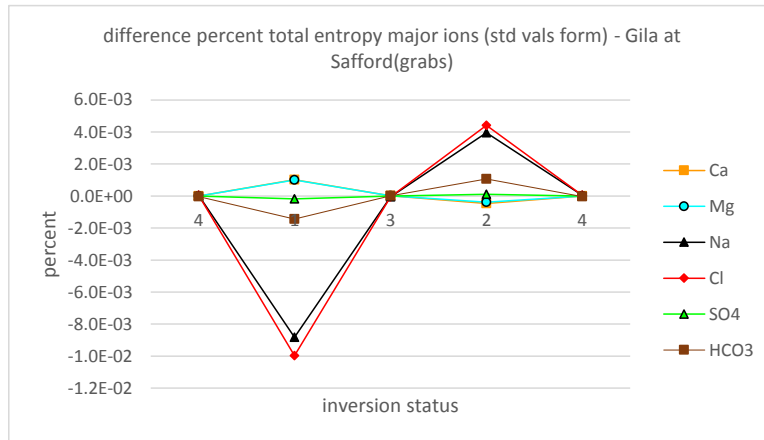


Figure 328

The above entropy graph can be recreated (below) using reaction in the aqueous phase standard values. Because of differences of scale, two graphs become necessary. The pattern for HCO<sub>3</sub> is the same as with the standard values of formation. The blown-up view of the other major ions, however, shows that their relations to each other have changed. When standard values of formation are used, Na and Cl go in the same direction at each inversion state and balance is across inversion state 1 & 2 with the flip in direction. With reaction in the aqueous phase values, the two balance each other at each inversion 1 or 2 peak or valley. At the lower level, Na is the primary balancer for the other ions while Ca and Mg take lesser roles following the direction of chloride.

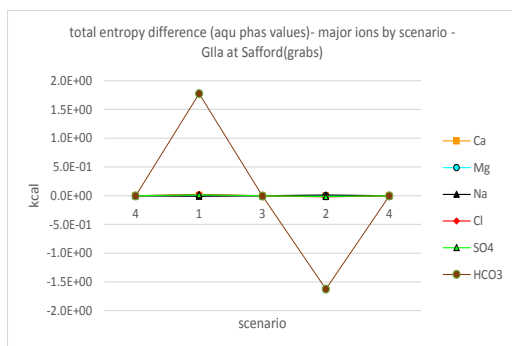


Figure 329

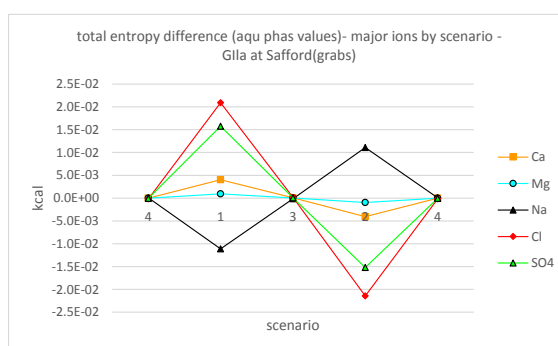


Figure 330 [\(back\)](#)

Percents using reaction in the aqueous phase values present yet another view. The fairly symmetrical look of inversion 1 & 2 peaks and valleys seen in the graphs above dissipate in the lower level, blown up view to right. Na stays on the positive side, quite flat in inversion status 1, and Cl stays on the negative side of zero so there is no characteristic flipping of direction between inversion status 1 & 2 for them although the other ions continue to flip. Notice also that the ions do not all pass directly through zero at inversion status 3, there is a slight stacking up of values there, indicating that the distribution of values is not symmetrical as it is in flow. Sulfate emerges as a major player, attempting but not succeeding in balancing HCO<sub>3</sub>.

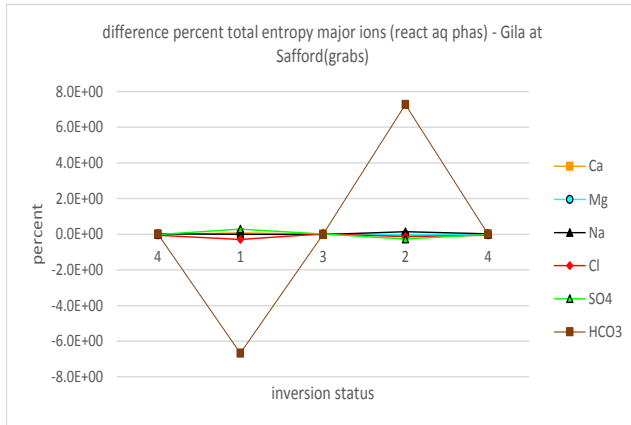


Figure 331

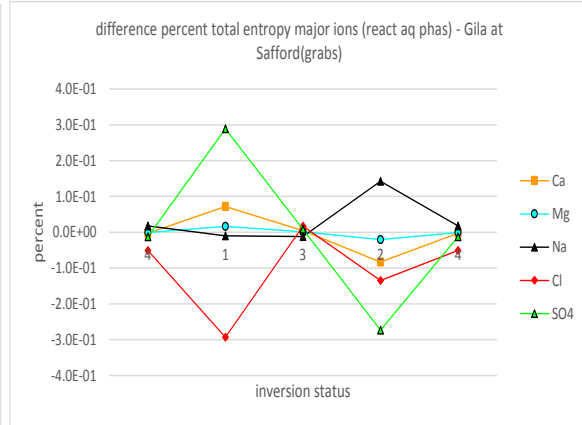


Figure 332 (back)

The picture for major ion enthalpy with the standard values of formation has the expected look with HCO<sub>3</sub> dominant in secondary action pattern, Na & Cl having minor roles following the same pattern.

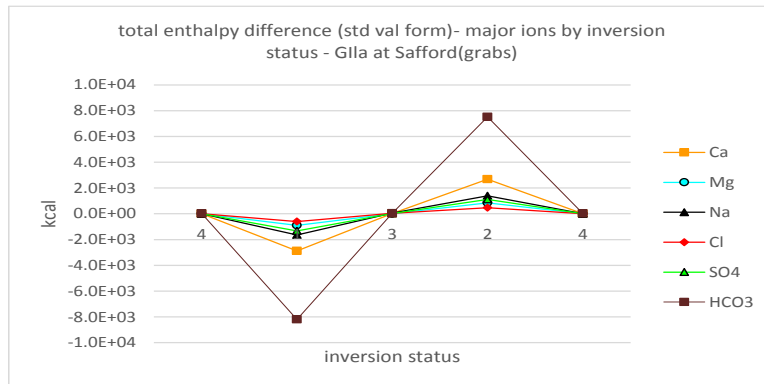


Figure 333

As with solution enthalpy, major ion percent enthalpies do not change pattern from that of the straight values. Once again, in the percent picture, Na & Cl make the greatest change.

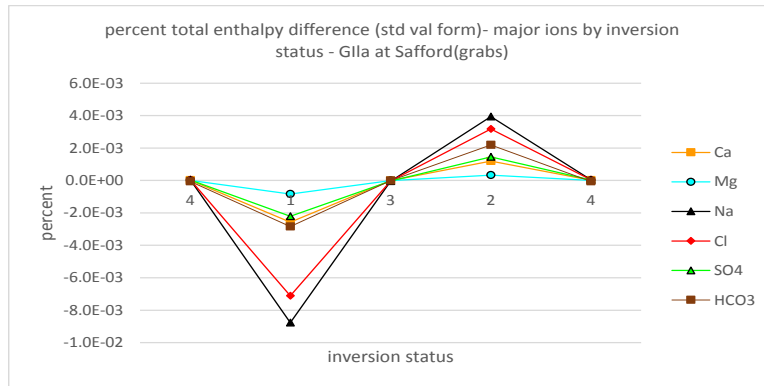


Figure 334

Using aqueous phase values (below left) shows the dominance of HCO<sub>3</sub> for total enthalpy. A closer view (right) shows the opposite direction of Na and Cl, with SO<sub>4</sub> and Ca following Cl as in the entropy picture, Cl is high in inversion status 1, low in 2, while Na is the opposite. In terms of enthalpy, the dominant balancing position is again that of sodium. Sodium, like water and the dissolved gases, has a positive heat capacity which makes it different from most of the other parameters. Note that here, unlike entropy, all major ion enthalpies pass through 0 at inversion status 3.

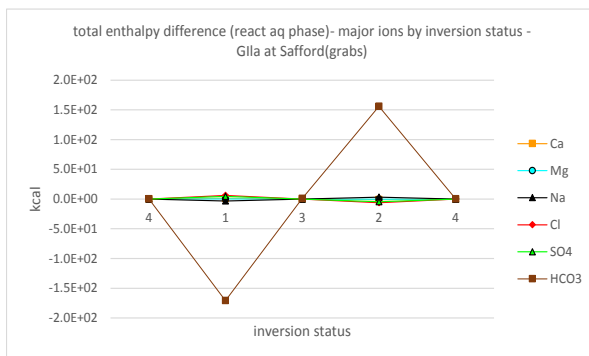


Figure 335

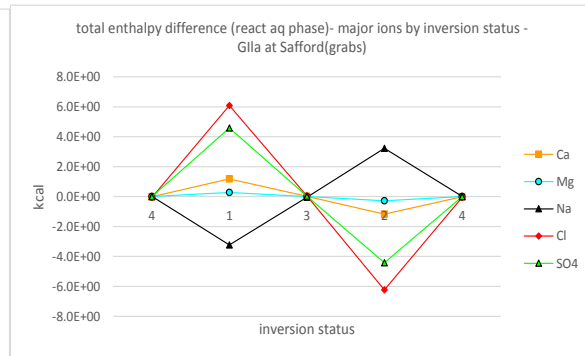


Figure 336

As was the case with entropy, the percent total enthalpies using reaction in the aqueous phase values are very unsymmetrical looking. Inversion status 2 has a very deflated look possibly because that end state is the closest to the inversion status 4 end state that all are being compared to. The balance of Na & Cl across each inversion state peak or valley remains but which side each is on has flipped compared with entropy (compare below to [Figure 332](#)). This flipping of sides indicates a change in function between entropy and enthalpy for Na & Cl, Note also that HCO<sub>3</sub> % total enthalpy has flipped to primary action; there is usually no flipping of pattern for enthalpy. The relative scale is different here as well with one graph largely sufficient to show all patterns.

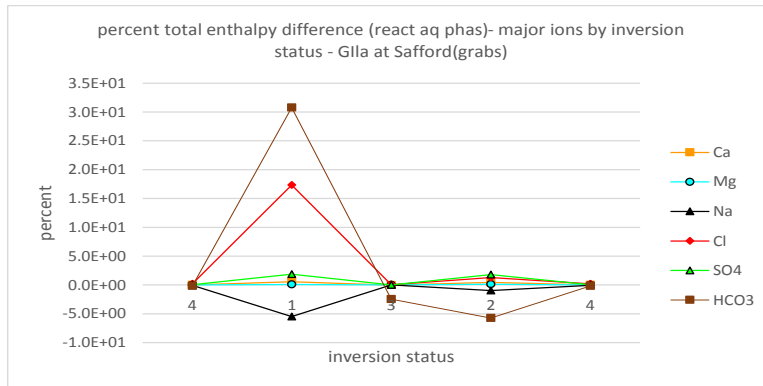


Figure 337

Finally major ion total free energy graphs when standard values of formation are used (not shown) have similar patterns to the enthalpy graphs above. Major ion total free energy graphs using reaction in the aqueous phase standard values (not shown) are also similar to enthalpies with that view.

But the percent total free energies using reaction in the aqueous phase standards are a new sort of beast. HCO3 % total free energy (below left) does not flip to primary action but does lose its peak at inversion status 2. The lower level relations of Na and Cl (below right) are the same as in enthalpy with only differences of scale. Sulfate emerges as a major player, particularly in inversion status 2, as it was in % entropy but not % enthalpy.

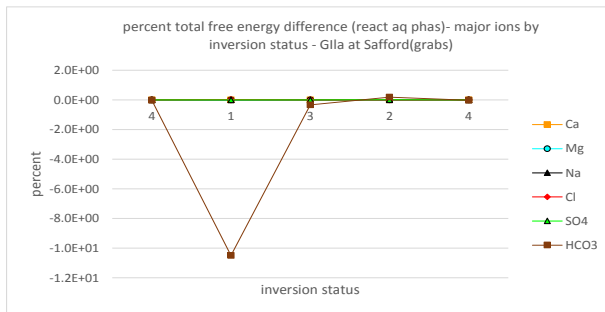


Figure 338 [\(back\)](#) [\(back2\)](#)

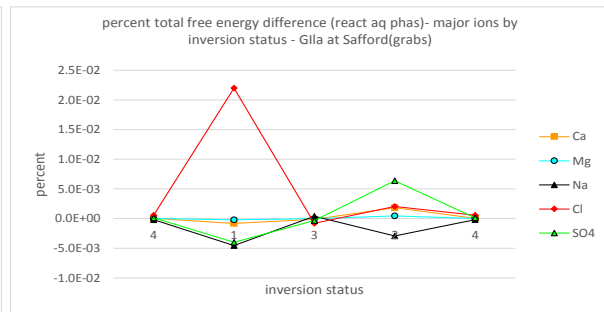


Figure 339

Note that there is about a 3 degree of magnitude drop in range from the full scale graphs to the 'blown up' scales -- HCO3 is by far the dominant player. In earlier graphs, the enthalpy y-scale decreased from  $10^4$  for H2O to  $10^0$  for the dissolved solids and HCO3 and goes down even more for the ion pair thermodynamic functions. The magnitude of change is undoubtedly the most important factor in determining causation but one should not be too cavalier in discounting small magnitude changes at certain critical levels and times.

The differences of scale for the two sets of standard values are summarized in the table below.



HOC3 max scale/ kcal - Gila at Safford		
	std val form	aqu phas
entr	1	2
enth	7000	150
free	8000	600

Table 160

The big picture view of total thermodynamic functions shows that HCO<sub>3</sub> is the dominant factor in amount, relative volume, and entropy. The amount and volume difference of HCO<sub>3</sub> follow the pattern of primary action (flow) while percent amount (mole fraction) and percent total relative volume follow the pattern of secondary action (MI activities). All of these views are equivalent in importance as expressions of inversion. Inversion is intimately related to changes in amount and volume of HCO<sub>3</sub> & Cl and the changes in system enthalpy and entropy these bring about which are all 'worked out' as it were in free energy via 'activity.'

If the dominant parameter, HCO<sub>3</sub>, is the most important then the major ion total thermodynamic functions follow the same pattern as those of the solution (water) - entropy in primary and enthalpy/free energy in secondary with percent entropy flipping direction but not percent enthalpy/free energy. The direction of change of HCO<sub>3</sub>, following primary action in amount, volume, and entropy, is considered tertiary action and reaction. There is a bit of the old 'chicken and the egg' dilemma with Na & Cl, but HCO<sub>3</sub> is commonly viewed as the 'interloper' here because it only enters with new flow. The pattern of alternating action and reaction is, however, clear and simple with tertiary following primary action (flow) and in reaction to secondary action (Na&Cl activity). The dissolution and formation of ion pairs is considered quaternary action and reaction which follows secondary action (Na&Cl) and is in reaction to tertiary action.

While four levels have been distinguished, there are only two patterns and so references will usually be to 'primary' and 'secondary' action patterns even at tertiary or quaternary levels. There is some ambiguity in whether the 'primary action' is being used as short for 'primary action and reaction' or means only the 'action' in 'primary action and reaction' - the peak at inversion status 1. This ambiguity is just the translation of the 00:00 to 12:00 vs 00:00 to 00:00 dilemma of the hypothetical analysis mentioned previously. Context will hopefully make the appropriate choice clear. The main problem, however, is to make sure that whatever label is applied, it corresponds to a change in the physical system not to a change in 'view' or other similar distraction. Assuming the correctness of the analysis, all level patterns reduce to 1) a peak at scenario 1 and a valley at scenario 2 or 2) a valley at scenario 1 and a peak at scenario 2.

Going further down in level, the more there appears to be reaction within action meaning that, operationally, action is more subject to change. Flow direction and change in amount are not easily altered but ion pair formation as a whole is because there is more than one ion pair and they don't all change in the same direction. The 'balanced' look of the patterns in the 'blown up' (lower level) pictures can be interpreted as being 'built in' reaction at the same level. It would be

nice to consider the relations of Na & Cl at lower levels as a 'bedrock' or possibly even 'remnants' of another time beneath the surface of change.

There may, however, be problems with the idea of 'built-in reaction' at a single level. The 'actions' and 'reactions' are depicted horizontally across the graph. The 'built in reaction' being posited here is in a different line of motion, the vertical. 'Built-in reaction,' action within an action peak or reaction valley, may represent 'no-change' which can exist within change just as friction exists within motion. Friction works in direction opposite to that of motion (is in 'reaction' to it), but it ends with motion and does not send the body into motion in another direction (it is 'built-in').

While the attempt to fit them in logically may be weak, there are definite differences in pattern in the underlying web of relations visible when HCO<sub>3</sub> is deleted and the y-axis blown up which have logical ties to other views. When the standard formation values are used most ions flip in direction between peak and valley following the direction set by HCO<sub>3</sub>. When reaction in the aqueous phase values are used HCO<sub>3</sub> has its peaks and valleys at one level and, at a lower level, the other ions have a very balanced look to them. With the straight entropy change values using aqueous phase values ([Figure 330](#)), for example, Na & Cl have balanced, contrary roles, flipping sides between inversion status 1 and 2 positions and clearly going through zero at inversion status 3 even with a highly blown up scale.

Part of the inversion process, it appears, is an exploration of new roles for sodium, chloride, and bicarbonate with respect to the direction of solution thermodynamic functions. More precisely, the changing context makes the result of their roles, their functions, different. The return to dominance of Na & Cl in the percents using the reaction in the aqueous phase values (i.e. at the here-and-now end state) of inversion status 2 may not be a function of changes in their % free energy but rather that of 'other' parameters, which is interesting to say the least.

The sample count situation is good here being over all possible samples and, while they differ by several orders of magnitude, none stand out as particularly high or low. But the percent values here are truly minuscule. That is because the total free energy of the ion is being divided by the sum solution of total free energies including that of water when standard values of formation are used.

There are reasons to find the change in direction of Na & Cl % total free energy at inversion status 2 significant but the safe interpretation is that the influence of Na & Cl is simply zero. A difference of percent gives no clue as to the original magnitudes – a drop of 10% can mean a change from 90 to 80 or 10 to 0. Here, it is assumed that Na & Cl dominate in inversion status 2 because they are assumed to dominate in inversion status 4 whatever their percent contribution to change.

With some idea of the changing roles of the major ions, it remains to be seen what the roles of the ion pairs are. Fe(OH)<sub>3</sub> dominates the picture for the total relative volume of the neutral ion pairs (left below). At the lower level, CaCO<sub>3</sub> and CaSO<sub>4</sub> also follow secondary action, the other ion pairs going in the opposite direction (right). Values for H<sub>4</sub>SiO<sub>4</sub> were not available so the picture is far from complete.

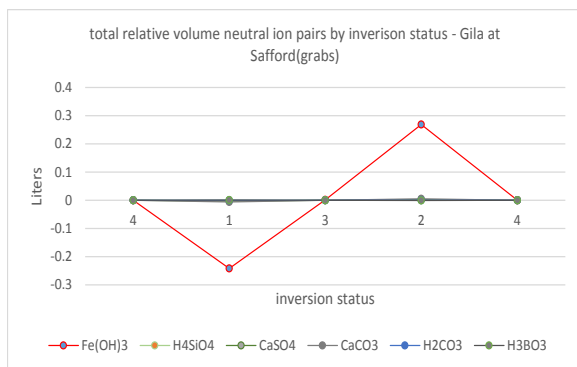


Figure 340 ([back](#))

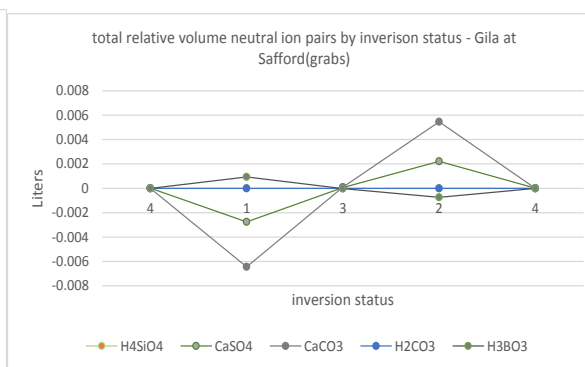


Figure 341

What this result means is that iron and the calcium ion pairs have not only to some extent dissolved in inversion status 1, as surmised elsewhere, but also, however much remains as ion pairs, are causing contraction of the system at a time when overall volumes and amounts are increasing. It is entirely possible that it is largely iron and calcium ion pairs that cause the lowering of sum solution total relative volume of the dissolved solids seen in [Figure 317](#).

But there is something else going on here as well. The percent differences ((scen1-scen 2)/scen2) for the individual ions volumes are in the 1-3 range but the percent difference of the sum of the ions drops considerably to the 0.5 range. The summing of the ions leads to a more proportional scen1/scen2 picture than any of the individual ions would suggest.

Even more interesting is that this situation continues across the board for entropy except % total entropy in the reaction in the aqueous phase view where the summation percent difference rises to the level of the ions at 2.6. Could the neutral ion pairs be working together as a group to make up a slight imbalance in entropy at another level? The difference (abs(scen1) – abs(scen2)) of all functions of water are 0 (perfectly proportional)., The sum solutions (total dissolved solids) differences with standard values of formation are also 0 but the values jump to 0.17 for volume, 0.15 for entropy in the reaction to the aqueous phase view.

The total entropy of Fe(OH)3 (below, aq phas) change in pattern, opposite to Fe(OH)3 volume change but following solution volume change, is unusual. Fe(OH)3 entropy has a noticeably higher scen1-scen2 difference than the other ion pairs while the summations percent difference remains lower than the individual ion pairs in both standard views. And there is a bit of an anomaly in that the Fe(OH)3 line does not go through zero at inversion status 3. There is no corresponding anomaly in total relative volume which suggests that the anomaly, if not just coincidental, is related to heat gain/loss rather than volume effects. As will be seen shortly, Fe(OH)3 has a much higher molar enthalpy of reaction in the aqueous phase than any other neutral ion pair. At the lower level, H2CO3 entropy follows the direction of iron and the calcium ion pairs, without any anomalies, while silica takes the opposite direction (right).

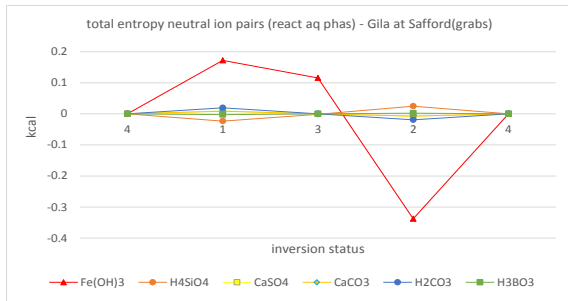


Figure 342

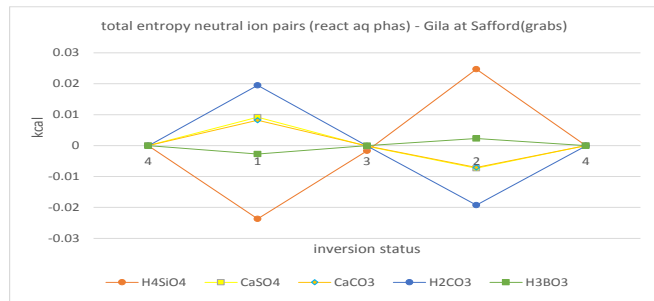


Figure 343

When standard values of formation are used, Fe(OH)3 and H4SiO4 flip patterns and H4SiO4 more closely balances Fe(OH)3. Now Fe(OH)3 entropy follows Fe(OH)3 volume but works opposite solution volume/entropy change. The anomaly at inversion status 3 remains for Fe(OH)3 and a slight one is picked up by H4SiO4. This is the full inversion process picture (below graphs), above is the at-this-moment, end-state inversion status picture. The unusual inverse relation to volume change for Fe(OH)3 is not the historical norm, it is only true during a limited time.

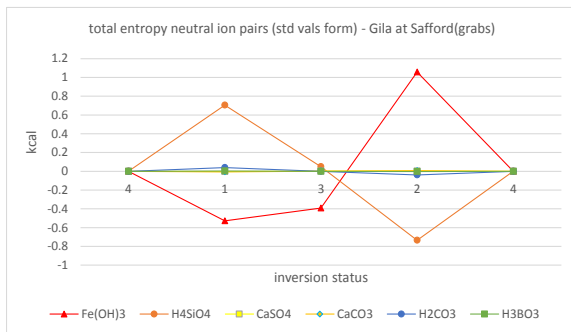


Figure 344

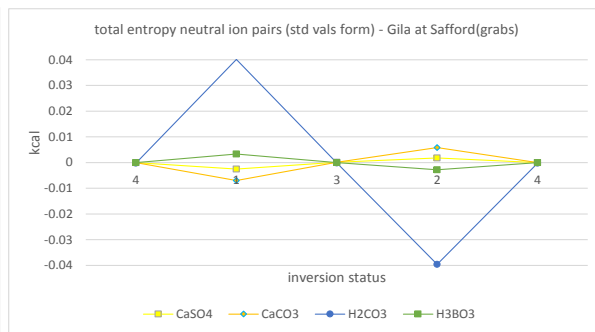


Figure 345

Switching to the percent entropy function view gives more information on the relative roles of the neutral ion pairs. The pattern of the entropy percents flip from primary to secondary (as those of the solution do) with the standard formation values (left below), remains in primary with the aqueous phase (right below). The anomaly in inversion status 3 remains though its meaning as a percent is not obvious.

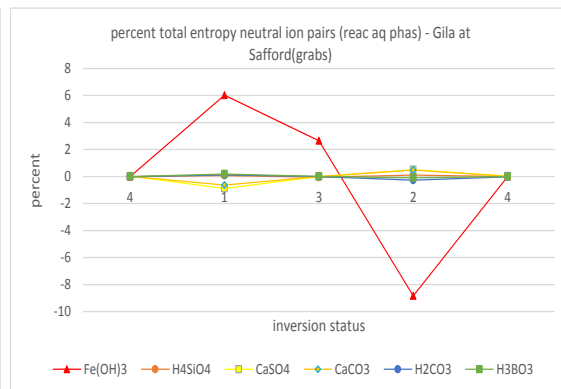
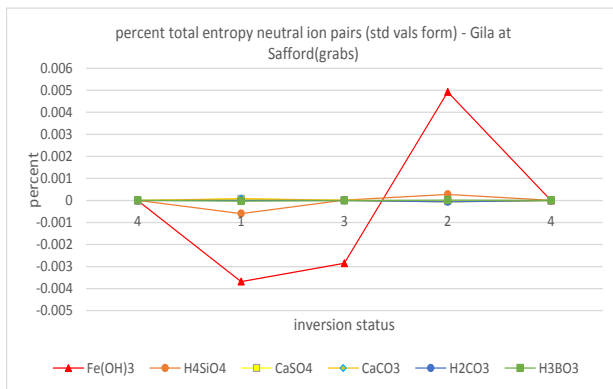


Figure 346

Figure 347

CaSO<sub>4</sub> is a minor player in the graphs above but offers an opportunity to tie together the various analyzes. First, CaSO<sub>4</sub> activity was seen to generally drop during inversion, rise during non-inversion ([Figures 266-7](#)). In accord with that, CaSO<sub>4</sub> is seen to be adding charge to the solution in inversion status 1 (dissolving), removing charge in inversion status 2 (forming) ([Figure 280](#)). These two results are ‘concentration’ effects, the latter due to mass action, much smaller and in opposite direction to the former. Now, viewed from the perspective of amount, moles CaSO<sub>4</sub> rise in scenario 1 and 3, fall in scenario 2 & 4, consistent with the direction of flow change. Since amount changes with flow, CaSO<sub>4</sub> is seen to have rising entropy in scenario 1, lowering entropy in scenario 2 when aqueous phase values are used, the opposite when standard values of formation are used because of a change in sign of the standard values. The tiny effect of mass action, which works opposite concentration change, works directly with entropy change in the case of CaSO<sub>4</sub> at the end states but inversely over the larger historical time frame. This situation presumably applies to CaCO<sub>3</sub> and Fe(OH)<sub>3</sub>. The only question is that of magnitudes – can a small change at one level have a large impact at another? Usually the assumption is ‘no’ unless the situation is a critical tipping point.

Similarly, the change in direction of Fe(OH)<sub>3</sub> entropy peaks and valleys between the two sets of standard values may mean that Fe(OH)<sub>3</sub> has different roles at different times in any given inversion context. Looking at the standard values may provide a partial explanation. Many of the neutral ion pairs’ standard entropies change sign when going from the standard values of formation to the reaction in the aqueous phase values. That is to say, their long-term function (which includes formation/dissociation) is different than their function just prior to inversion. The important exceptions are H<sub>4</sub>SiO<sub>4</sub> and H<sub>2</sub>CO<sub>3</sub>.

standard entropy values		
	std form	aq phas
Fe(OH) <sub>3</sub>	-0.083	0.026
MgCO <sub>3</sub>	-0.047	0.023
CaCO <sub>3</sub>	-0.026	0.027
CaSO <sub>4</sub>	-0.008	0.016
NaHCO <sub>3</sub>	0.036	-0.001
H <sub>3</sub> BO <sub>3</sub>	0.039	0.031
H <sub>4</sub> SiO <sub>4</sub>	0.043	0.001
H <sub>2</sub> CO <sub>3</sub>	0.045	0.022

Table 161

But this doubtlessly correct, if rather simple minded, explanation is made somewhat irrelevant when the anomaly at inversion status 3 entropy is investigated further. There are only 6 Fe(OH)<sub>3</sub> values out of a possible 28 and one of them is off-the-graphs high (1.94 entropy, 1851

enthalpy). Removing just this one, high value flips the direction of Fe(OH)<sub>3</sub> at inversion status 3 in both the standard value of formation and the aqueous phase views (not shown). Once again, it appears there are serious data reliability issues with Fe(OH)<sub>3</sub>. ‘Something’ appears to be ‘going on’ here but it is not possible to say with any certainty even what direction it is ‘going on’ in!

What is really outstanding about iron, however, is the high enthalpy of reaction in the aqueous phase for Fe(OH)<sub>3</sub> in contrast to a fairly in-the-middle standard value of formation. This fact is another aspect of why iron plays such a pivotal role, its influence is heavily weighted by timing.

neutral ion pair thermodynamic functions - reaction in aqueous phase			
	dHo	dGo	dSo
H3BO3	3.2	13	-0.031
H4SiO4	3.3	4	-0.001
NaHCO3	0	0	-0.001
CaSO4	1.7	-3	0.016
H2CO3	-2.2	-9	0.022
MgCO3	2.7	-4	0.023
Fe(OH)3	24.8	17	0.026
MgSO4	4.6	-3	0.026
CaCO3	3.5	-4	0.027

Table 162

Enthalpy of the neutral ion pairs are all in secondary action mode when standard values of formation are used (below left) and has the interesting switch to H<sub>4</sub>SiO<sub>4</sub> as the dominant player. When reaction in the aqueous phase values are used (below right), Fe(OH)<sub>3</sub> regains its leading role while both switch to primary action. It is a little puzzling, in the reaction in the aqueous phase view, that both deliver their higher enthalpy at a time when solution and HCO<sub>3</sub> entropy is going up, solution enthalpy going down, but those relations apply only to the limited, here-and-now end state context. The noticeably different values of Fe(OH)<sub>3</sub> relative to the other ions seen in entropy is also true in enthalpy except in % enthalpy in the standard values of formation view.

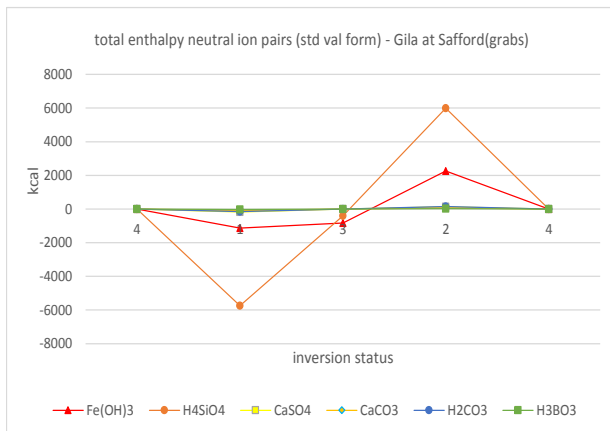


Figure 348

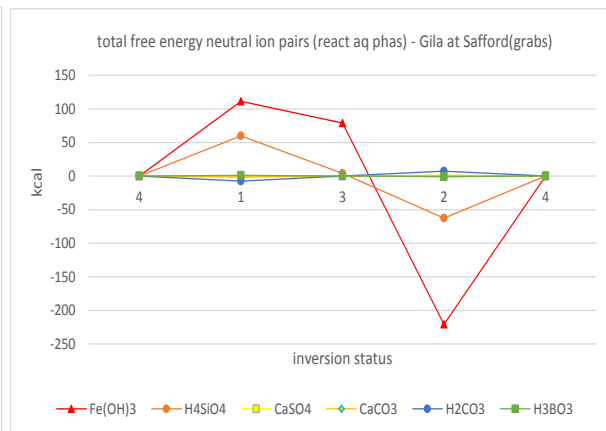


Figure 349

The percent enthalpies of the neutral ion pairs follow secondary action with the exception of  $\text{Fe}(\text{OH})_3$  which is the dominant player on a percentage basis. With the reaction in the aqueous phase,  $\text{Fe}(\text{OH})_3$ 's role reduces to a high percentage performance at inversion status 3.

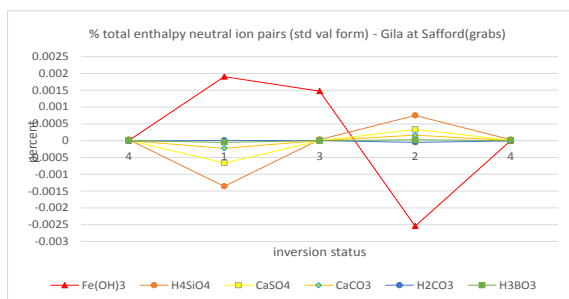


Figure 350

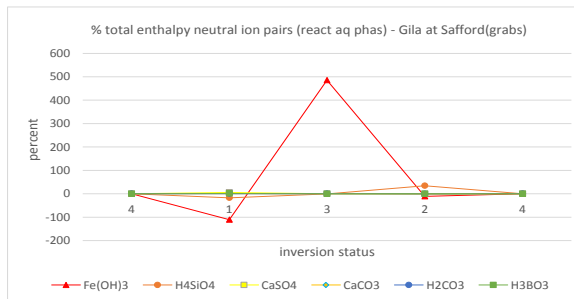


Figure 351

The free energy of the neutral ion pairs in standards of formation and reaction in the aqueous phase views follow their enthalpy patterns with very little variation and are therefore not shown.  $\text{Fe}(\text{OH})_3$  scen1-scen2 difference, however, drops to that of the other ions, opposite what was seen in entropy and enthalpy.

The charged ion pairs, though unimportant or at least unpredictable in their role in the ionic strength of the major ions, may have a role to play here and are included for completeness. The total relative volumes of most of the charged ion pairs (not shown) follow the direction of primary action. The only exception is  $\text{MgOH}$  which follows secondary action pattern.

The charged ion pairs show little of interest in terms of entropy, most following primary action while their percents, unusual for entropy, also follow primary action. The main players are  $\text{Fe}(\text{OH})_2^+$  with  $\text{Fe}(\text{OH})_4^-$  following the same pattern but at different levels. Both have anomalies at inversion status 3 though that of  $\text{Fe}(\text{OH})_2^+$  is much larger, the value even exceeding that of inversion status 1.

The enthalpy of the charged ion pairs (not shown) also have little interesting to show. The main players are again  $\text{Fe}(\text{OH})_2^+$  and  $\text{Fe}(\text{OH})_4^-$  which follow the same pattern, have higher anomaly at inversion status 3 than 1, and have high peaks/valleys at inversion status 2, markedly (relatively) higher than their entropy peaks/valleys.  $\text{H}_3\text{SiO}_4$  % enthalpy, like that of Na & Cl, stays on one side with a deflated look at inversion status 2. The percents of the other ion pairs, however, un-enthalpy-like, flip pattern from values.

The charged ion pair's total free energies have a familiar look, closely following the enthalpy patterns. As in enthalpy, patterns shift from primary to secondary action when the view is changed from reaction in the aqueous phase to standard values of formation.

In general, the standard formation view of entropy and enthalpy/free energy straight values produces pictures in which all the ions move in either primary or secondary action pattern following the solution pattern. The reaction in the aqueous phase views are usually a combination of primary and secondary patterns with one or more parameters at a much higher level and a number of others at a lower level with a balanced look to them.

It is hard to see in the blur of graphs for the various types of ion pairs but there is a curious rearrangement of function patterns between reaction in the aqueous phase and standard value of formation views. To begin and for reference, the total thermodynamic function of  $\text{HCO}_3^-$  in both views are plotted together on one graph with aqueous phase in red/orange and standard formation values in blues (below left). It is easy to see that the solution patterns for entropy (primary action) and enthalpy/free energy (secondary action) apply to both groups, at least one blue and one red in each group. The same graph for  $\text{Fe}(\text{OH})_3$  however, shows the differences in pattern between entropy and enthalpy beginning to blur.

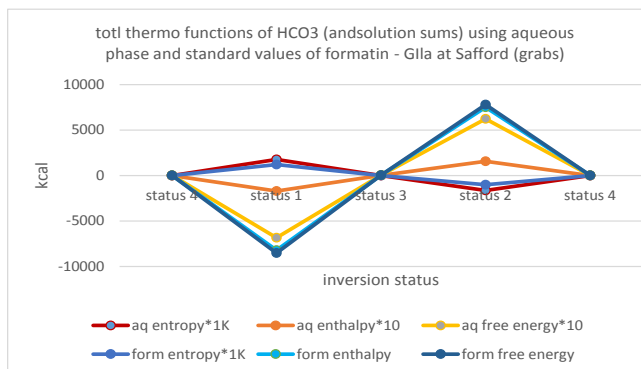


Figure 352

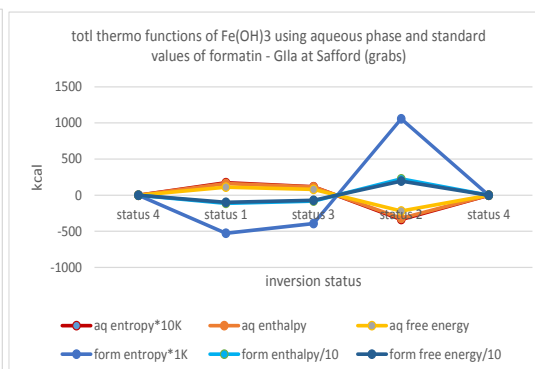


Figure 353

The shift is even more pronounced in the progression from  $\text{Fe}(\text{OH})_4^-$  (left) to  $\text{Fe}(\text{OH})_2^+$  (right). Here the reds and blues (aq phase and std. values) have migrated to above and below scenario 3 respectively, disrupting the combined primary and secondary patterns of both with  $\text{HCO}_3^-$  (figure 353)

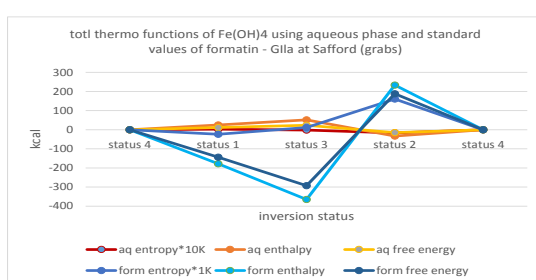


Figure 354

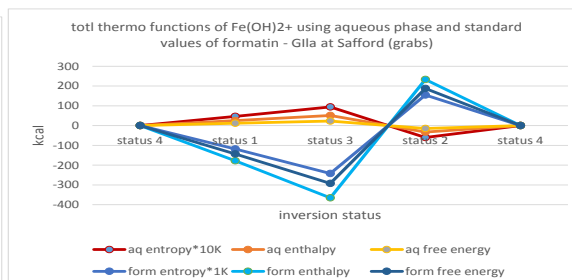


Figure 355

These shifts in pattern point to iron as one of those factors that opposes solution direction in both the full historical and current, end-state contexts. In the case of  $\text{Fe}(\text{OH})_2^+$ , at least one, either entropy or enthalpy, is going in the opposite of solution direction in each of the aqueous phase or formation view groups. The anomaly at inversion status 3, not visible in the  $\text{HCO}_3^-$ /solution graph above, widens as the trend develops.

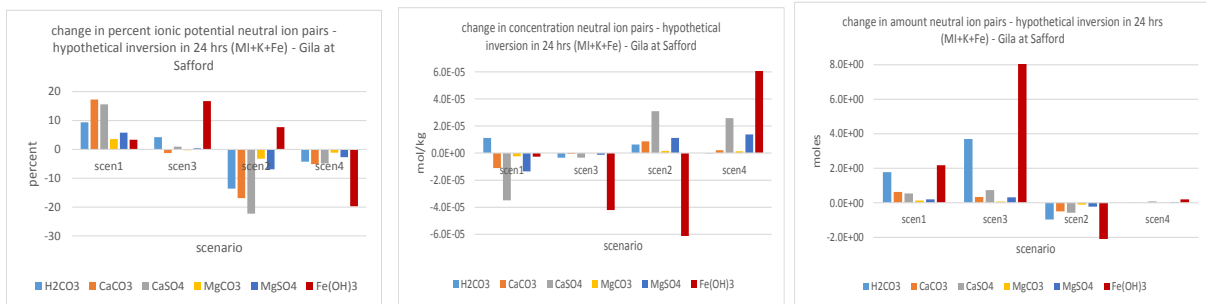
This survey of the total thermodynamic functions of the grabs has led to the general conclusion that parameters can have different roles in different contexts. But the further one delves into the structure, the less symmetrical things look. And it has not provided any clues as to when or why the switch from ion pair dissociation to formation occurs. That has been shown to be dependent not entirely on energy considerations but rather on amount. Amounts are, however, included in the total thermodynamic functions so there should be some evidence there.

It is time to turn from grab sample results to hypothetical analysis once again. Operationally, the procedure is simply an extension of the ionic potential analysis. It uses the same wateq4f output of the same grab sample input data. But instead of calculating ionic potential from concentration change, the total thermodynamic functions are calculated from change in amount. While using the same dataset, the two analyzes are worlds apart in what they are attempting to do. The ionic potential analysis calculates a hypothetical value, the neutral ion pair ionic strength potential, and makes transitory use of something that must have existed between the two dates – namely the extra free ions available for increased ion pair concentrations on day 2.



The total molar functions analysis uses the difference in **amount** of ion pairs to add or remove free ions from the solution. The question being asked is simply ‘what would the inversion look like if there was no change in ion pair amounts?’ To be more specific, the ion pairs are returned to their values before the inversion transition (at 00:00) by subtracting the 12:00 – 00:00 difference. The free ions that would have formed ion pairs are added to free ion values at **inversion (12:00)**. But while the concept is simple and straightforward enough, the consequences are not: the analysis as described here begins by violating the law of mass action – the operation could not possibly occur in nature. It raises the suspicion – if the first law is violated, what other ‘laws of nature’ may also be violated? Can such a picture possibly stand up on its own? Let’s see.

As a help in orientation, an attempt will be made to relate the results of the ionic potential analysis to the new thermodynamic function analysis. In the graphs below, the ionic potential of the neutral ion pairs is converted into the new thermodynamic function formatting. Below left is a rerun of the percent ionic potential of the neutral ion pairs up to Fe ([figure 280](#), left-most below) followed by the concentration changes they come from (middle graph) and, next, by the changes in amount (right-most). If Fe (large red column) is focused on, it is possible to see the general trend of inversion to the previous graph from left to right . . . with some exceptions.



Figures 356-58

Due to the relative smallness of some of the differences and the fact that percents/values and amounts/concentrations do not always change in the same direction, all the relations do not come out quite as nicely inverse as they should. In fact, concentration effects (ionic potential) and effects of differing amounts (thermodynamic functions) cannot be easily directly linked since the relations of flow with amounts and concentrations, while generally direct (amt) and inverse(conc), are more complex than that. Nevertheless, the differences in amount of the last graph to the right above can be converted into the neutral ion pair total relative volumes which come out as follows with the right hand being a close up of the lower level of the left hand view:

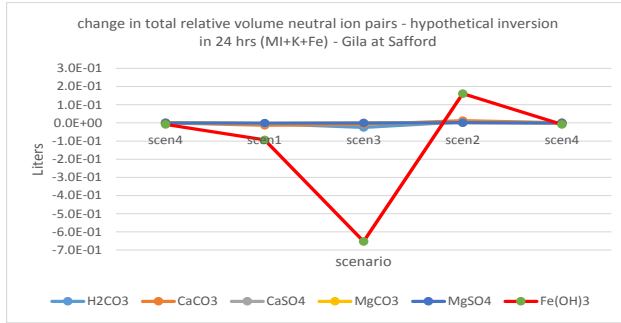


Figure 359

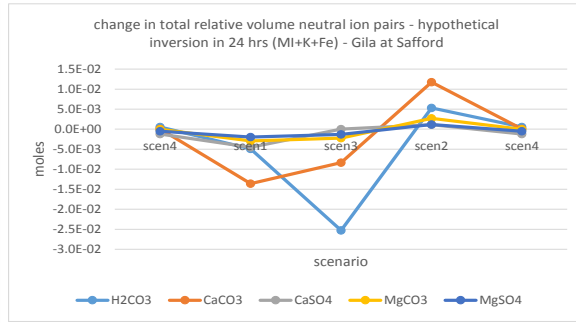


Figure 360

The charts above can be compared to the grab samples above (Figures 340-341). In evaluating the results, it is necessary to keep in mind that these graphs come from a hypothetical analysis in which the temperature may have gone from 6C at 00:00 to 33C at 12:00 – that is, the conditions are quite different from any of the grabs. With these qualifications in mind, it is probably sufficient that Fe(OH)<sub>3</sub> is identified as the dominant species and goes from contraction in inversion status 1 to expansion in inversion status 2 in secondary action pattern as do CaCO<sub>3</sub> and CaSO<sub>4</sub> similarly to the grabs. The big differences from the grabs are in inversion status 3. This result does not validate the hypothetical analysis but does show a continuity with the grab results that is encouraging.

To perform the hypothetical total thermodynamic functions analysis a new reconciliation area was created on the process spreadsheet. At first, the analysis is run with only the major ions and their ion pairs. Values are percents of total change with reaction in the aqueous phase standards used to calculate the total thermodynamic values used in the percentage calculation. The following example shows how the area serves as a check on the analysis. Here, besides MI for major ions, the abbreviations, NIP and CIP, are used for neutral ion and charged ion pairs respectively.

percent contribution to change in total relative volume at inversion scen1(nuMI,Tup,pHup)				
	expansion w ΔIP (actual)	contraction w ΔIP (actual)	expansion w/o ΔIP (hypotl)	contraction w/o ΔIP (hypothetical)
NaKCl	25	-4	26	-2
other MI	74	-86	74	-38
NIP as IP	0.2	-10.0	0.1	0.0
CIP as IP	0.3	-0.3	0.0	-59.7
	100	-100		
NIP as free ion			0.046	-0.015
CIP as free ion			0.007	-0.013
			100	-100

Table 163

The first two columns add up the percent free ions (NaKCL and ‘other MI’) with the ion pairs as ion pairs as in the original data– this is the ‘actual’ side of the picture. The third and fourth columns add up the percents of free ion groups after the ions from the ion pairs have been

redistributed back to or from them – this is the ‘hypothetical’ side. (Note that the ‘actual’ values come from a hypothetical analysis because it uses only the major ions. The ‘actual’ are therefore actually ‘hypothetical’ and the new ‘hypothetical’ values being generated are ‘super-hypothetical’ -- but the original terms will be used for ease of understanding.)

Also shown are the contribution in free ions by the ion pairs which are usually quite small but necessary for everything to sum up to +/-100%. The reconciliation center merely ensures that everything has been added or subtracted correctly on the two sides (+/-) of both analyzes (actual/hypothetical). It is used as a check on the mechanics of the analysis but has nothing to say, of course, about the appropriateness or correctness of the analysis.

In the example above, the big differences are on the contraction side where the major ions change from contributing 86 to 38% to the drop in relative volume. The percents are so high because water is now out of the picture (react aq phas). The neutral ion pairs change from 10 to 0 by design, and the charged ion pairs from 0.3 to 59%. The charged ion pairs, therefore, at their pre-inversion amounts, are taking over the role of neutral ion pairs in total relative volume change and the role of the major ions are also modified. A small drop of 10% in neutral ion pair formation, which however removes them entirely, leads to large percentage changes in the roles of major ions and charged ions.

For the hypothetical analysis that follows, all values will be in percent contribution to total inversion difference of the total thermodynamic function. This is different from percent of the straight values with relation to the sum solution straight values. There is little to no meaning in the straight values (kcal) themselves in such hypothetical scenarios as where, for example, only the major ions are present.

As can be seen in the reconciliation worksheet above, positive and negative percent values are tallied separately. The percent of negative change multiplied by the sum of the negatives, with a straight percent calculation, would be positive. But here, negative change in amount is handled in two ways. In the free ions, the percent is made negative to preserve the sign of change as either addition or removal. For the ion pair contribution to the free ions, if the change in amount is positive, the sign of the result is determined by the sign of the molar function. If negative, the molar function is still analyzed with the formula for the constituent ion (which may yield either a positive or a negative result) but it is multiplied by the absolute value of the amount difference. This method keeps removal of free ions negative, addition positive, while maintaining the inverse relation between amount change and function value. The sign changing is merely a book-keeping method intended to keep the direction of change consistent.

The actual and hypothetical results, like the signed results, are kept apart for two reasons – it makes a difference when differences are taken, i.e. the results have different error (actual/hypothetical), and they may lead to loss of information (averaging + and – percents). Below are the typical view of scenario 2 change in total relative volume (left) with the arrows showing the 12:00 to 00:00 difference being taken and (on the right) a column graph of the differences. The black line gives the reference base for calculation and the bicarbonate and chloride difference arrows are on top of one another.

Looking at the differences columns for chloride and bicarbonate (graph to right below) it is hard to see the inversion relation. Only a look at the values at 12:00 show that the scenario 2 relation,  $Cl > HCO_3$ , is in place but just barely –  $Cl = 0.4027$  L and  $HCO_3 = 0.3496$  at 12:00. Cl and  $HCO_3$  lines do cross at 12:00, but the scaling makes it impossible to see. The differences, however, do not convey anything about the values at 12:00 which makes it hard to ‘see’ the inversion when analyzing differences.

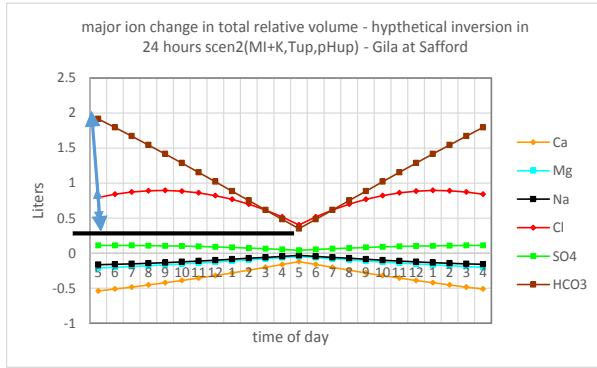


Figure 361

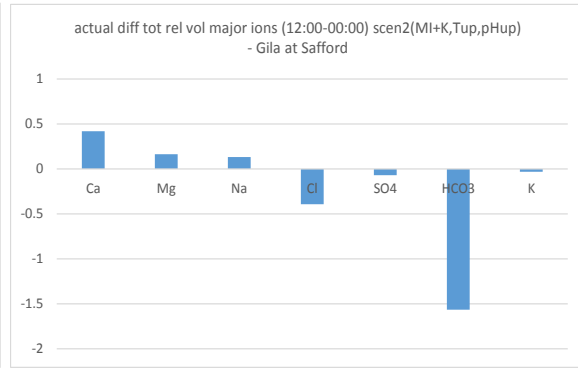


Figure 362

Because the hypothetical analysis is outside the sphere of the real, it is best to separate actual and hypothetical results as well. Shown below are the actual (left) and hypothetical (right) results, separated by a long blue line, for percent contribution to free energy change of the major ions in the MI +K system in the grabs analysis formatting.

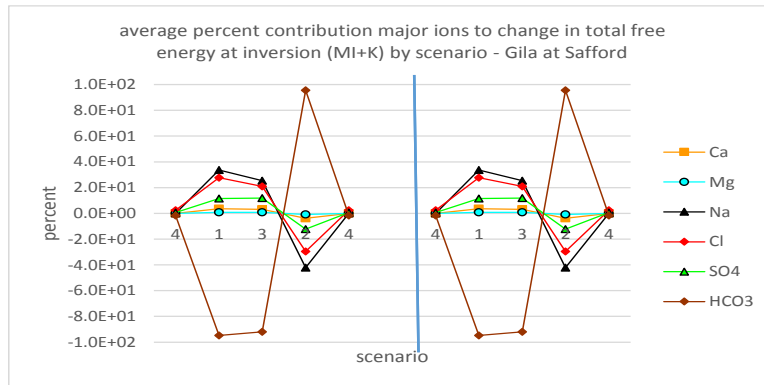


Figure 363

These patterns don't look anything like the grabs % free energy differences (aq phas) (Figure 338-39). The magnitudes are higher, more percent-like due to the fact that the grabs are differences of percents that are very small, being not only differences but also over solution sums, while the hypotheticals are percents of a total difference. In addition the grabs are a difference of averages while the hypotheticals are averages of differences; the two should, however, be the same so that is not the problem.

The reason the graphs look so different is that the grabs analysis uses the major ions at their percent values with all the other parameters present. Here they are alone and forced to balance

HCO<sub>3</sub>. The thermodynamic functions here are calculated with reaction in the aqueous phase standard values – they have little or no prior ‘history’ .What needs two graphs there to show upper and lower levels is included in one graph here. Na & Cl go from balancing each other at a lower level to being forced to be the main offset for HCO<sub>3</sub>.

Significantly, neither actuals nor hypotheticals pass through scenario 3. If not going through zero at scenario 3 is anomalous behavior, then Na, Cl and HCO<sub>3</sub> are all anomalous. Put another way, the major ions on their own do not have the capability of resolving the situation that scenario 3 presents. Before this point, scenario 3 anomaly has only been seen in the % thermodynamic functions and the straight functions of Fe(OH)<sub>3</sub>. ‘Balance’ changes with level and view.

Also, and most importantly at this point, actual and hypothetical results are the same. This is the ‘starting’ point for the analysis and it says that the inversion goes on with or without the (major ion) ion pairs with any problems in balance relegated to inversion status 3. The calcium and magnesium ion pairs may have the clearest ionic strength pattern of the ion pairs but their dissociation has little effect on the inversion response.

A closer look at the major ion enthalpy and entropy of this system, however, reveals that, while the enthalpies (left) are perfectly balanced, actual and hypothetical like free energy, actual and hypothetical entropies (right) are quite different. Na and Cl, the harbingers of the new (old) order of scenario 4, are not able to balance the entropy effect of HCO<sub>3</sub> without the ion pairs.

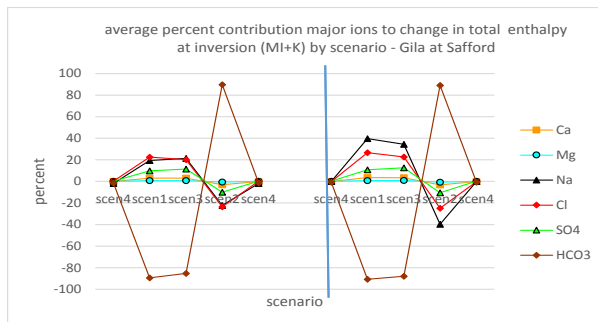


Figure 364 [\(back\)](#)

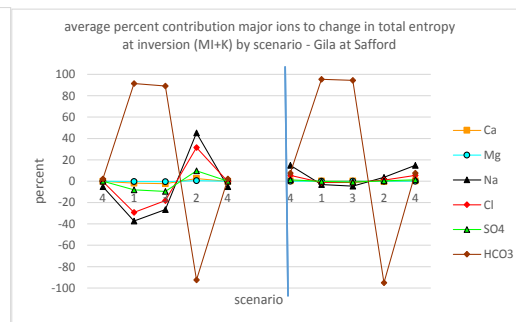


Figure 365

How is the entropy situation compensated for by the ion pairs when only those of the major ions are present? On the actual sides, the neutral ion pairs show a large anomaly for H<sub>2</sub>CO<sub>3</sub> at scenario 3 while the charged ion pairs have no role. On the hypothetical sides, the effect of the neutral ion pairs is non-existent (by design) while the charged ion pairs, at their lower pre-inversion amounts, have a new role in entropy response (below right) to fill the void left by the removal of the neutral ion pairs and the failure of Na & Cl to balance HCO<sub>3</sub>. Recall that the charged ion pairs were also seen above to take on a new role in contraction of total relative volume, emphasizing once more the strong entropy/volume relationship.

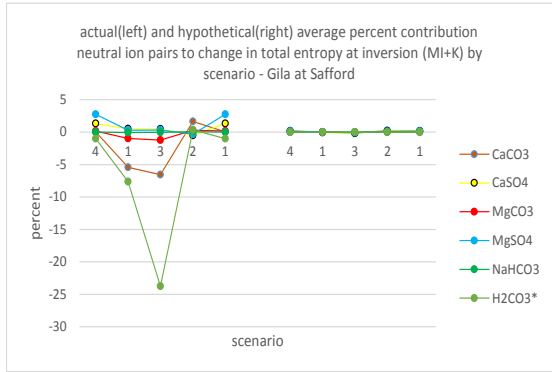


Figure 366

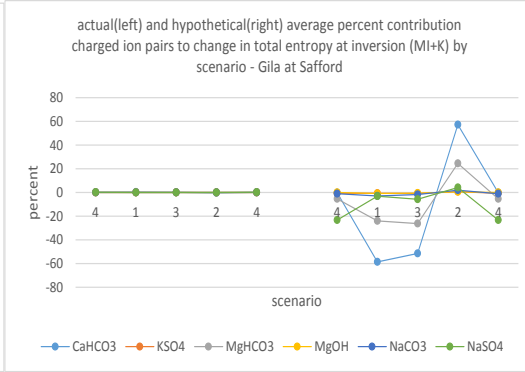


Figure 367

The situation for enthalpy (below) is that all the ion pairs flip direction between scenario 1 and 2 in primary action, as they did in ionic potential when  $\text{Fe}(\text{OH})_3$  and  $\text{H}_4\text{SiO}_4$  were not present.  $\text{CaCO}_3$  is the major actor, as it was in ionic potential for this system.  $\text{H}_2\text{CO}_3$  is almost nothing but an anomaly at scenario 3. With the charged ions pairs, there is little difference between actual and hypothetical,  $\text{CaHCO}_3$  keeping a low magnitude primary action pattern with a scenario 3 anomaly.

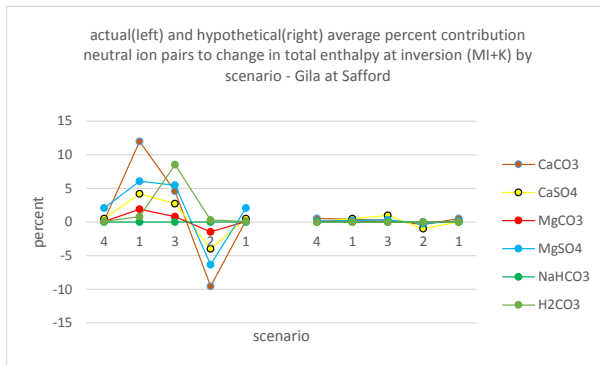


Figure 368

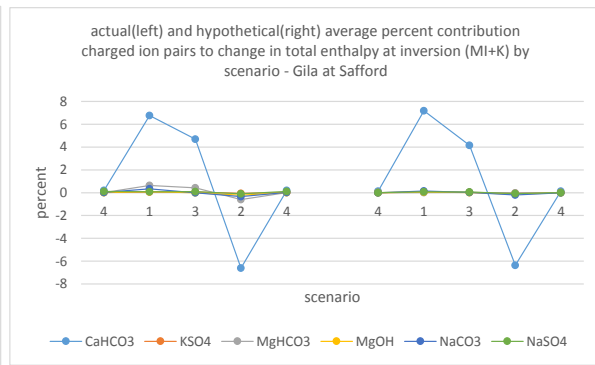


Figure 369

The neutral ion pairs total free energy percent changes (below left) show a really big anomaly for  $\text{H}_2\text{CO}_3$  on both actual and hypothetical sides as if playing the role of  $\text{Fe}(\text{OH})_3$  when that species is not present.  $\text{H}_2\text{CO}_3$  is selected to balance things out, regardless, it seems, of how much of it there is available. The charged ion pair response (below right) is lower, balanced and with only small anomalies at scenario 3 and the dominant role is that of  $\text{MgOH}$ . The free energy picture for the ion pairs is again hypotheticals pretty closely following the pattern of the actuals. Free energy balances out the imbalances of entropy and enthalpy that develop with or without major-ion ion pairs but cannot achieve a balance at scenario 3 with only the major ions.

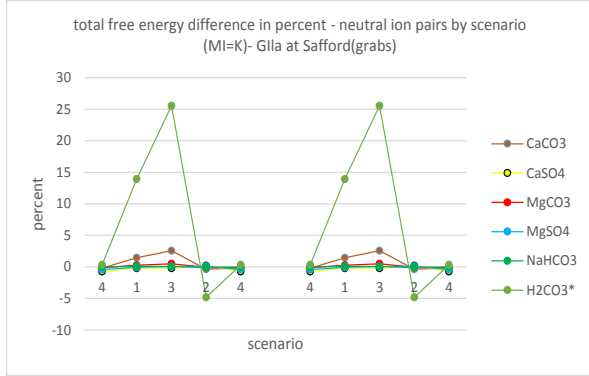


Figure 370

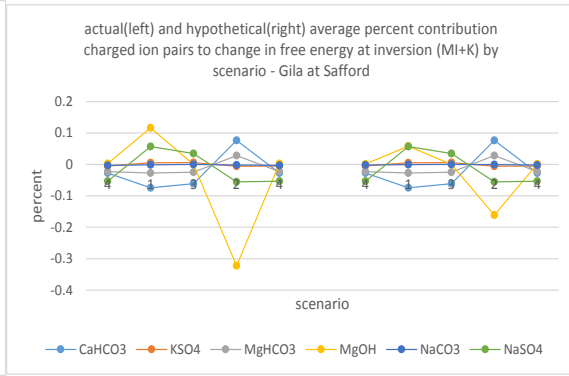


Figure 371

Summarizing the MI+K hypothetical system results: The inversion takes place with or without ion pair formation. In terms of free energy, it doesn't make any difference whether the ion pairs are held constant or not. Free energy balances the lopsided entropy situation no matter what parameters are available with little apparent regard for amounts. It appears, from this perspective, that the major actors in inversion free energy balancing are the unlikely pair of H2CO3 and MgOH! (the latter of which makes only transitory appearances in the grabs). But the free energy balancing of actual and hypothetical comes at the 'expense' of anomaly at scenario 3, in itself the sign of an unresolved imbalance.

Adding a little iron and silicon changes things immediately. The significant thing here is that % total free energy looks quite different on the hypothetical side than it does on the actual side. On the actual side, with Fe & Si ion pairs present, the Na & Cl anomalies at scenario 3 are much lower and Na seems to hang around the negative side more than Cl which flips between scenario 1&2. All these changes bring the actual side picture of the (overall) hypothetical analysis closer to the grab sample picture for % total free energy using reaction in the aqueous phase values ([Figure 338-9](#)). On the hypothetical side, lowering of Fe and Si ion pair amounts forces the major ions back into taking larger roles and increases the anomaly at 3 which makes this picture similar to the MI+K picture above but with more splitting of Na and Cl. Below is the blown up view (minus HCO3 which only changes slightly) of total free energy percent change in the MI+K+Fe+Si system.

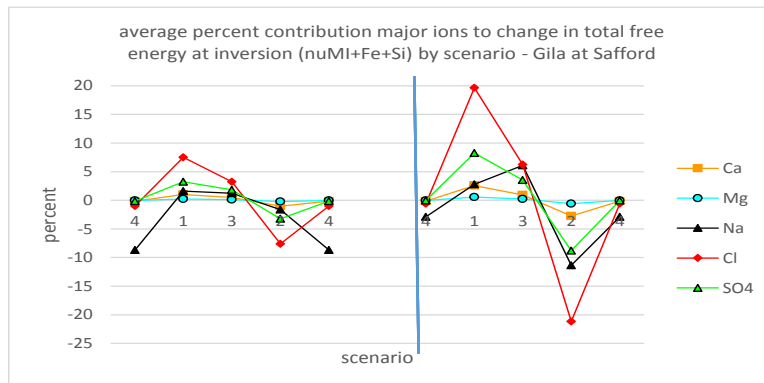


Figure 372

The picture for entropy and enthalpy of the nuMI+Fe+Si system (below) is, however, quite different from that seen in the MI+K system (Figures 364-365) With Fe and Si present (left graph below, actual side), Na and Cl entropy change is opposite that of HCO<sub>3</sub> and water (solution), in secondary action mode. Without the ion pairs, Na and Cl just collapse again in the role of maintaining entropy balance (left graph, hypothetical side). With enthalpy (right graph, actual side) there is very little contribution by Na & CL when Fe & Si are present, a higher contribution when ion pairs are held constant (right graph, hypothetical side). What seems to be happening here is one way in which an entropy problem can be ‘flipped’ to an enthalpy problem.

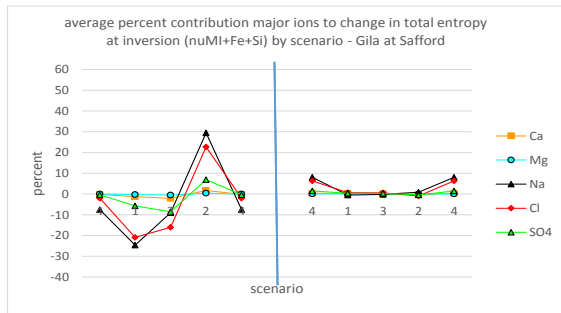


Figure 373

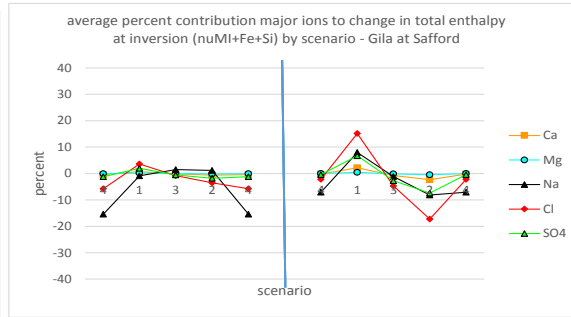


Figure 374

The percent entropy contribution of the neutral ion pairs (below left) shows a quite reduced, somewhat ambiguous, role for Fe(OH)<sub>3</sub> and a more prominent role for H<sub>4</sub>SiO<sub>4</sub> following secondary action with no anomaly at 3. The role of the charged ions (below right) is heightened on the hypothetical side into a fuller secondary action pattern with small anomaly at 3.

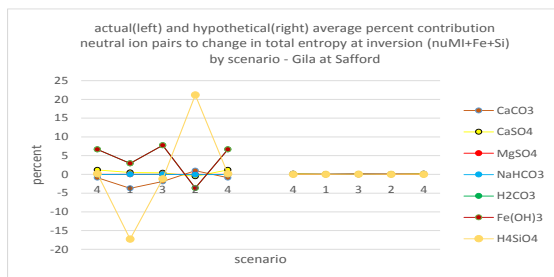


Figure 375

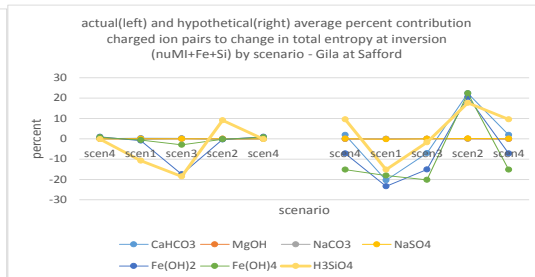


Figure 376

By contrast, in the % enthalpy contribution of the neutral ion pairs (below left), the role of Fe(OH)<sub>3</sub> is quite clear with the anomaly at 3 higher than 1. It is puzzling that Fe(OH)<sub>3</sub> is apparently playing a large role in providing its higher than normal molar enthalpy at a time when solution entropy is positive. Could it rather actually be making up for the deficiency of Na & Cl in balancing HCO<sub>3</sub> negative %entropy at scenario 1? H<sub>4</sub>SiO<sub>4</sub> is balanced, as in entropy, but follows primary action rather than secondary. The charged ions show increased values, with anomaly at 3, for Fe(OH)<sub>2</sub> and Fe(OH)<sub>4</sub>, also following primary action.



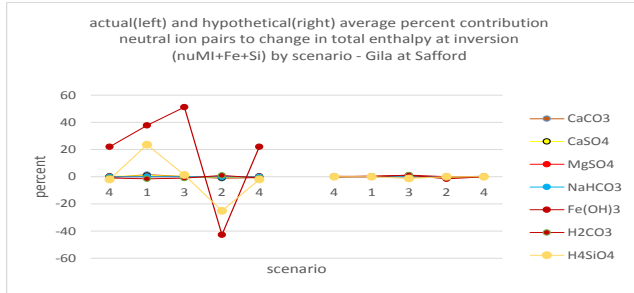


Figure 377

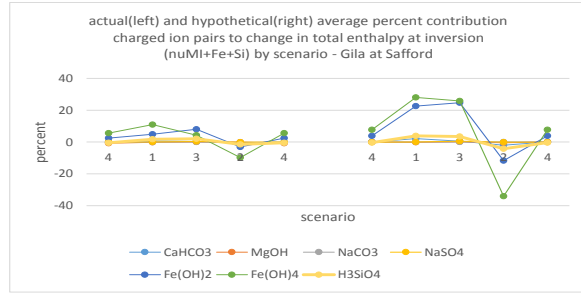


Figure 378

In the percent free energy change of the neutral ion pairs (below), iron shows its by now familiar anomaly at scenario 3, which now is actually higher than scenario 1, while H4SiO4 takes the pattern of primary action with no anomaly at 3. The other neutral ion pairs, as in ionic potential, are reduced to very minor roles. Actual and hypothetical sides are now no longer identical – the pre-inversion amounts of Fe(OH)3 and H4SiO4 are not up to the challenge for free energy balancing as H2CO3 and MgOH were. The charged ion pair response (right) does not change much from actual to hypothetical and NaSO4 and MgOH (on the hypothetical side only) show high scenario 3 values.

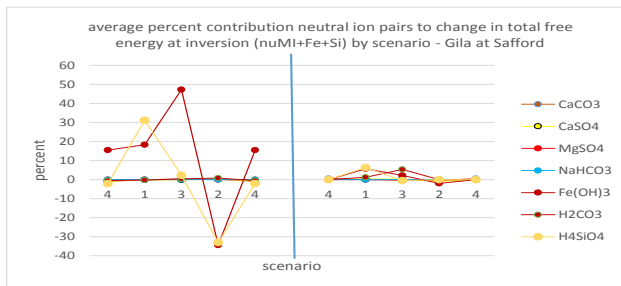


Figure 379

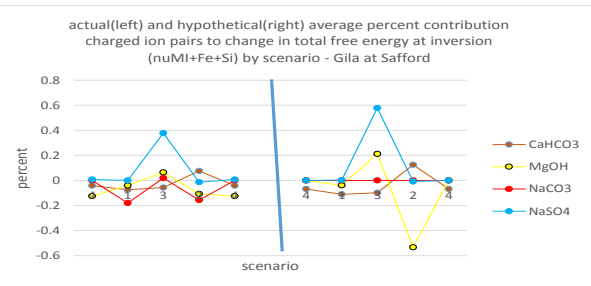


Figure 380

The thermodynamic analysis was continued to include the +NBP and the +allavgs systems. The results will be shown in summary fashion alongside those of the systems already examined in the order MI+k, +Fe&Si, +NBP, + allavgs, from left to right. The graphs below show the ‘actual’ side of each system for % enthalpy. The biggest change comes with the addition of Fe(OH)3 and H4SiO4 (second group from left), very little change after that. Free energy looks very similar and it is apparently the addition of iron and silicon that changes the roles of Na & Cl to that seen in the grabs. The role of HCO3 (right) changes very little across systems, with only a diminishment in scale starting with the third group (+NBP), just as it dominates in the grabs picture.

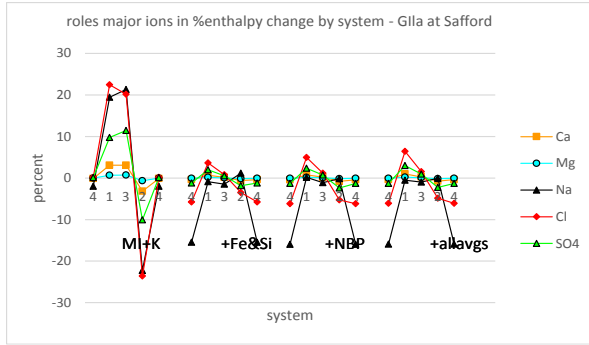


Figure 381

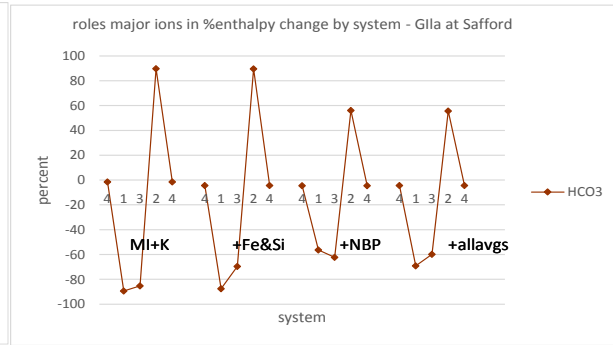


Figure 382

The story for %entropy is quite different. Here there is a gradual change in scale but not in pattern up to the allavgs system. ‘Something’ (or ‘some things’) in the allavg system changes the %entropy entirely, to the point that there is a qualitative (pattern changing) difference from the MI+K system. %Entropy change, although strongly influenced by which parameters are present (i.e. HCO<sub>3</sub>), is also greatly influenced by the number and types of other parameters present. The chloride and sodium peaks at inversion status 2 disappear completely which is in line with what was seen in the grabs. Note that the effect is so great that it changes the role of HCO<sub>3</sub> in inversion status 2 as well. In other words, the negative entropy of scenario 2 is resolved in this view at the dissolved solids level.

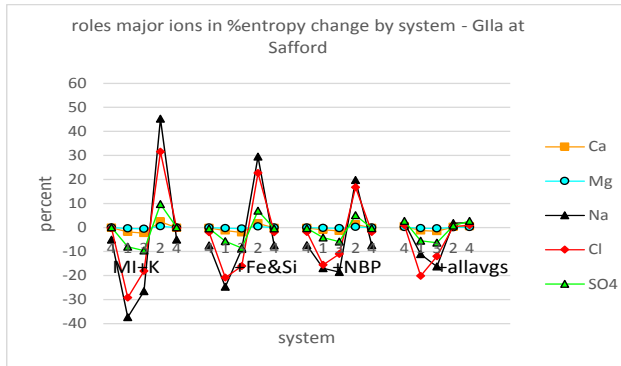


Figure 383

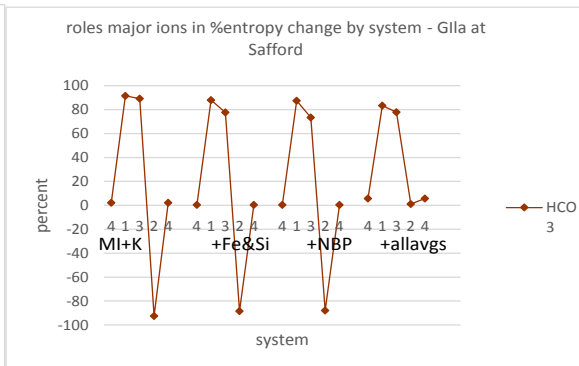


Figure 384

What role do the neutral and charged ion pairs play in these transformations? The % entropy of both groups (below) show that iron and silicon create new roles in entropy control for the ion pairs as well but then the relation with presence (increasing number of parameters present) leading to decreasing % entropy comes into play. Note that both groups are, like the major ions, in secondary action vs bicarbonate in primary action. The negative entropy of scenario 2 is therefore resolved at this level (and this level only), in a relative way, by the spreading out of entropy control to a large number of minor players.

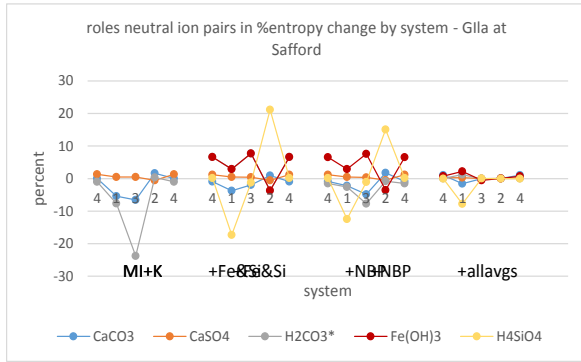


Figure 385

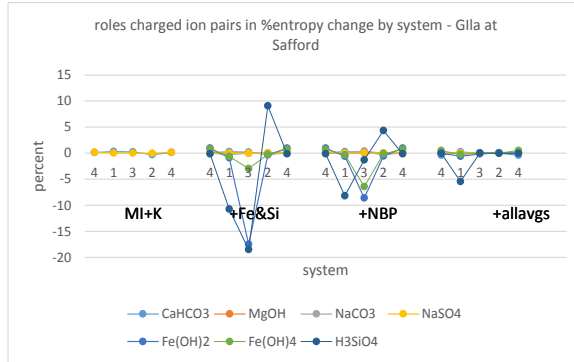


Figure 386

The hypothetical side results of the thermodynamic functions were, on the whole, rather disappointing, particularly after the MI+K system, and are not shown. They do, however, make a couple of things clear. First, in the all-averages system, % free energy and %enthalpy actual and hypothetical sides are almost identical. Only in % contribution to entropy are actual and hypothetical different. Second, new parameters (increased ‘presence’) diminish the magnitude of involvement for all parameters. This result is just the expected drop in percentage values as the number of parameters increases. More significantly, the hypotheticals also show that parameters can take on completely new roles in different contexts – i.e. as the need arises.

The final picture of major ion contribution to entropy control shows that they all take lesser roles (lower percent contribution) when all possible parameters are present. The all-avgs situation is a completely new system, even if it is only an artificial one.

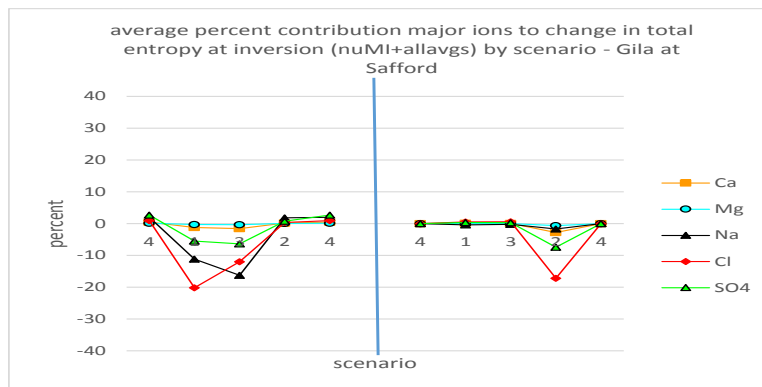


Figure 387

Being able to bring a hypothetical analysis to resemble grab results is very gratifying, particularly when they started out so far apart. The lopsided look of many of the final graphs, however, are not encouraging. But it is this very imbalance that points to the significance of inversion – it is the signal of a shift in the solution from a more concentrated, high ionic strength matrix (inversion status 4) to a more dilute, lower ionic strength matrix (inversion status 3).

The first indication of such a change is in the activity of water. The activity of water at around 55.5 is often considered a constant and used as such in various equations. But, in the dataset

here, it does change. From one grab sample to the next it differs by  $6.9 \times 10^{-5}$  which is 0.00013% of total activity (55.495). Amounts, back-calculated from activity, however, change by, on average, 3391 moles which, while only 0.38% of the average number of moles (857111), is still a sizeable number by any reckoning. Below are the activity (left) and difference in activity (right) of water by inversion status.

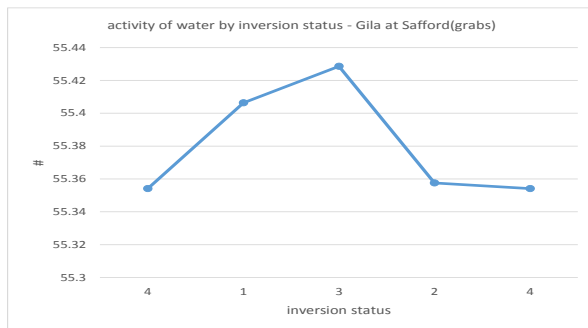


Figure 388

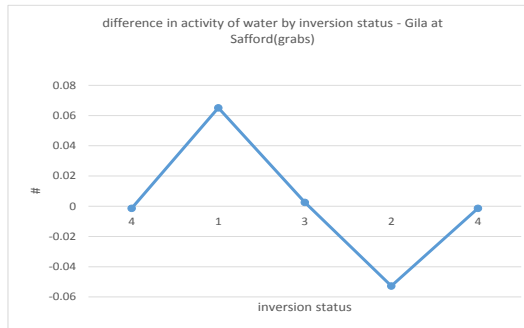


Figure 389

The ‘water’ being discussed here is not pure water, it is water as solvent in this particular solution which is relative to the rest of the solution. The average inversion difference of the activity of water (Figure 389 above) is quite small but can lead to a large change in the apparent amount (and volume) of water. It is this transformation of a very small to a very large number that allows the change to be easily seen in the thermodynamic functions.

The ‘motivational’ scenarios, 1 & 2, represent the energy barriers (2) or wells (1) to be hurdled as the system shifts from one matrix to the other. It is hard to imagine that such a radical transformation as inversion status 1 could occur in any context other than the turbulence of a high flow season -- but that would be relating external to internal energy, something it was promised would not be done. ‘Wells’, however, need to be hurdled as well as ‘hills’ climbed otherwise the system would not change, it would simply remain in its energetically favorable position.

The shift in matrix can clearly be seen in Piper Plots using the major ion concentrations in mg/L converted to meq and formatted as percents (100% anions, 100% cations). Below is the ‘all data’ view with scenario 4 (red), 1 (green), 3 (blue), 2 (yellow-green). The process plays out most clearly on the anion triangle (lower right) and is from right to left and back again.

The biggest jump (top arrow) is from scenario 4 to scenario 1 (red to green). Chloride goes from a max of around 80 to a max of about 60% while  $\text{HCO}_3$  goes from 20 to around 60%. Scenario 3 remains in the same area as 1 but the spread of values for chloride and bicarbonate increases and new possibilities, specifically higher sulfate percents, are explored. Higher sulfate values indicate that the dissolution of ion pairs started in scenario 1 are continuing into scenario 3. Two steps in the opposite direction, scenario 3 to scenario 2 (blue to yellow-green) and scenario 2 to 4 (yellow-green to red), complete the process (lower arrows). Formation of ion pairs in scenarios 2 & 4 keep free sulfate percentages low.

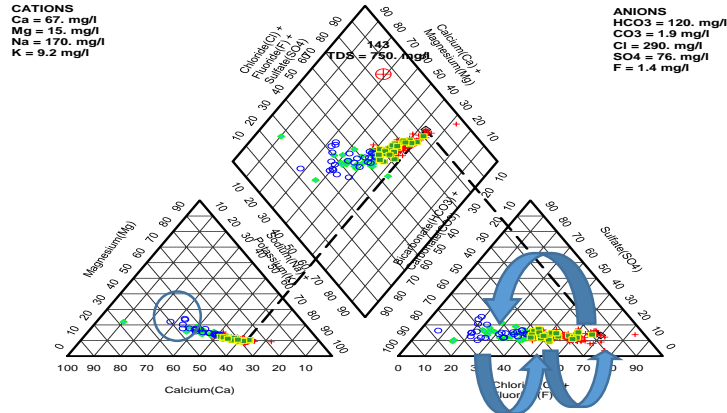


Figure 390 [\(back\)](#)

The cations start out in the lower right corner of the cation triangle with high sodium in scenario 4 but veer off the sodium axis and curl up in scenarios 1 & 3 to accommodate higher magnesium and calcium (in circle).

Does any change in water quality mean that a shift in the matrix has occurred? Aren't the activities of all parameters, including that of water, involved in any such change? The answers to these questions are 'no' and 'yes' respectively. Yes, any change in water quality is reflected in a change in solution activity. But no, any change in water quality does not warrant being called a matrix shift. A more precise definition of what a matrix shift consists of, however, is necessary here.

As a matter of fact, the claim being made here is, at this point, far too sweeping. The whole argument depends entirely on the thermodynamic properties of water. There must be, it seems, linkages between the activity of water and the thermodynamic properties of all the other parameters at all solution levels before a change in water quality can be called a 'matrix' shift. What a matrix shift means is a change in the solvent (here its activity) that changes the relations of all the other parameters at all levels of the solution in such a way that the new system is able to maintain itself in a new way for an indefinite period of time. It is in this context that the fact that inversion is a disproportionate (change in percents not equal to change in values) change becomes significant. A disproportionate change is most likely not a small, incremental change in system status but rather a 'sea change' in relationships.

To find corresponding states at various levels of the solution it is necessary to look more closely at the inversion end states. To be visible, a matrix shift has to be from one defined point to another and back again, i.e. it becomes visible by difference. The new matrix of inversion status 1 maintains itself somewhat precariously in an entirely different manner (inversion status 3) than the reference 'maintenance' matrix of scenario 4.

The 'history' in the total thermodynamic functions using the different standard values datasets, viewed on separate graphs earlier, may also be viewed as being along an axis perpendicular to

the action – reaction axis of a single graph. Sliding the time axis in and out of the graph produces changes not only in the y-scale but also reveals different relations between the ions.

The graphs below show the picture with (left) and without HCO<sub>3</sub> (right) for % entropy change of the major ions. Each graph has the aqueous phase picture to the left with the standard values of formation picture to the right. In the lower level entropy instantaneous situation just before the inversion (left side of right graph), Na is the primary balancer. In the fuller historical view of the inversion process (right side right graph), Ca and Mg are the primary balancers. The shift of the latter is highlighted with cones going from instantaneous (react aq phas) to fuller (std val form) view. For all this to happen, Na and Ca/Mg have to flip directions between the two end states.

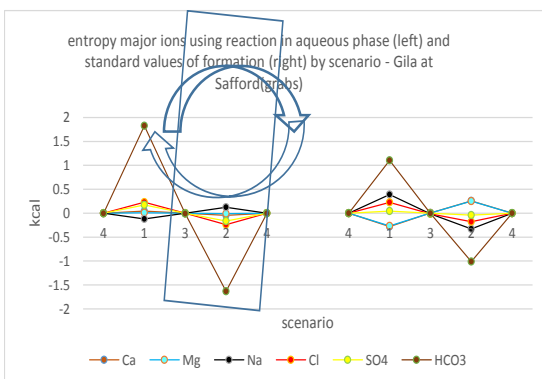


Figure 391 [\(back\)](#)

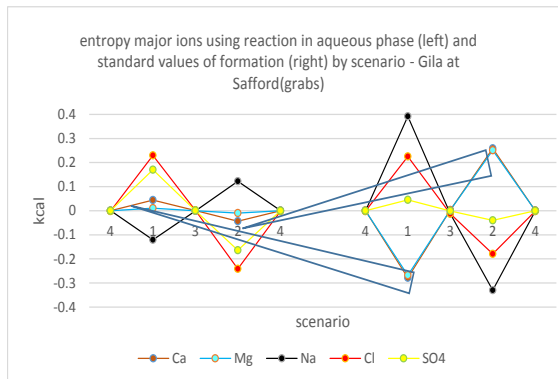


Figure 392

There may also be a fourth dimension needed. The inversion occurs with aqueous species but some of these, the ion pairs, need to go back to the un-aqueous or solid form ©, then dissociate, then become re-‘aqueated’. Somewhere in between the two extreme states depicted above there is some reversion to earlier energy states. This dimension is shown as a ‘window’ between the two states on the left hand, full magnitude graph. The upper and lower arrows are the energy steps for the change in HCO<sub>3</sub> total entropy due to dissociation of HCO<sub>3</sub> ion pairs.

While it cannot be seen in the difference-from-inversion-status-4 picture used here, it is assumed that Na is the primary balancer in inversion status 4, while Ca & Mg fulfill that role in inversion status 3. Viewing the individual scenario 3 & 4 (intra-scenario) differences helps verify this assumption. The aqueous phase entropy relations of Na & Cl in scenario 4 (left) and the standard values of formation entropy relations of Ca, Mg, and HCO<sub>3</sub> in scenario 3 (right) seem like the two extremes, end-points of the inversion process, the ‘before’ and ‘after’ shots.

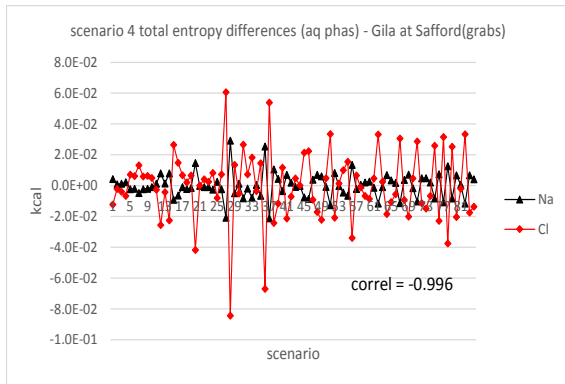


Figure 393

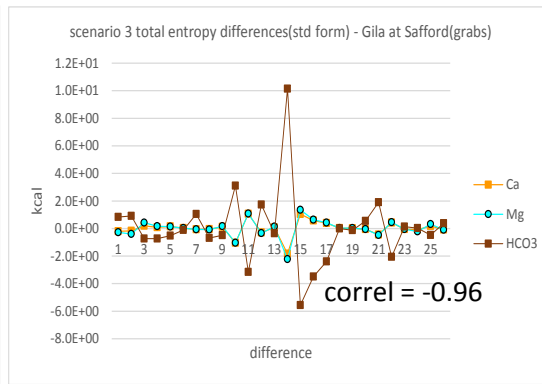


Figure 394

The matrix adjustment is not seen anywhere on these graphs, it occurs between them. As the system shifts from inversion state 4 to inversion state 3 via 1, the instantaneous inversion state 4 entropy balance of Na & Cl (Figure 393 above) drops down into the lower level summation energy relations of the std form inversion state 3 end state (Figure 394).

Below are the reaction in the standard formation value relations of Na & Cl in scenario 4 (left) and the aqueous phase relations of Ca, Mg, and HCO<sub>3</sub> in scenario 3 (right). These views are the transformed ‘remnants’ of the old system in the new. Notice that, in each case, an inverse is replaced by direct relationship. The end result is the conversion of Na-Cl being inversely related to HCO<sub>3</sub> to being directly related in the Ca/Mg-HCO<sub>3</sub> system.

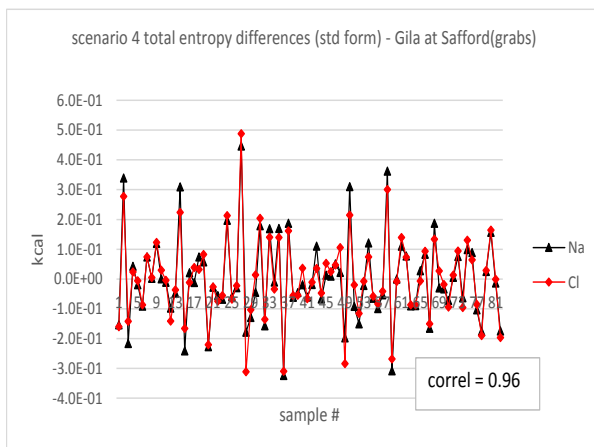


Figure 395

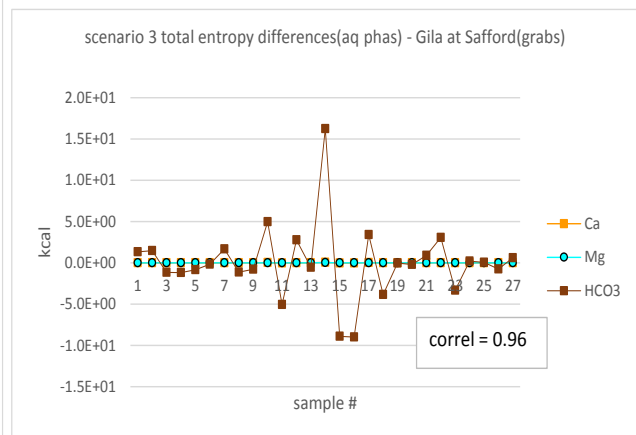


Figure 396

As the system shifts back from inversion state 3 to inversion state 4 via inversion state 2, the inversion state 3 instantaneous balance of HCO<sub>3</sub>, Ca, and Mg (Figure 396 above) drops down into the lower level summation energy relations of inversion state 4 (Figure 395 above). Since both are direct relations, all ions move in the same direction. These relations are just codifying and linking through time what the separate grab sample total thermodynamic function graphs show.

(It may be noted in passing that using  $(dH-dG)/T$  to calculate  $\Delta S$  in the Na, Cl, Ca, and HCO<sub>3</sub> entropy calculations for scenarios 3 & 4 completely changes the ion affinities picture developed to this point. In the new picture, Na and Cl entropy would be **directly** correlated in the

aqueous phase view of scenario 4 while Ca and HCO<sub>3</sub> entropy would be **inversely** correlated in the standard values view of scenario 3. If an inverse correlation shows entropy balance then Na and Cl would not be balancing one another in the aq phas view and only weakly balancing ( $r^2 = -0.67$ ) in the standard values view of scenario 4. The whole picture of parameters balancing one another entropy-wise would be down the tubes or would need a much more elaborate work up.)

The above relations are summarized in the table below as well as the relative magnitudes as expressed by the ratio of the sum of the absolute values of HCO<sub>3</sub> by the sum of the absolute values of Cl.

relations and magntides of entropy control major ions - Gila at Safford(grabs)			
correlations			
		std form	aq phas
scen 3	Ca&HCO <sub>3</sub>	-0.97	0.96
scen 4	Na&Cl	0.96	-1.00
magnitudeHCO <sub>3</sub> /Cl sum abs vals			
		std form	aq phas
scen 3		7.9	93.0
scen 4		1.5	15.0

Table 164

Up to the comparison of the two standard value views (Figures 391-2), the inversion diagrams used have been a mix of inter- and intra-scenario views. Inter-scenario differences are generally much larger and more unidirectional than intra-scenario differences. This bias toward larger, less evenly distributed differences gives the impression that intra-scenario differences are zero. But a closer look at the individual intra-scenario differences of Na & Cl in scenario 4 (Figure 393) shows that this is not the case. Na positive change in entropy over scenario 4 intra-differences calculate close to but are not equal to negative change and the same goes for Cl. The total sum positive for both Na and Cl is also close to, but not equal to the negative contribution. So neither ion completely balances its own entropy contribution nor does one ion cancel the other.

The original data total entropy values from std form sumpositive - sumnegative difference is 3.6 +/- 6.7 kcal/K which goes down slightly for the (chronological) differences to 2.9 +/- 4.7. The reaction in the aqueous phase values and differences are closer together at 1.5 +/- 3 and 1.4 +/- 2.3 respectively. Entropy is, therefore, not resolved for these lists but there is no reason that it should be since these 'systems' are not in any complete cycle.

To put them into a complete cycle, the total entropy values can be sorted by inversion status and intra-scenario differences taken. Now all inversion status groups are analyzed the same way. The sum positive, sum negative, and the difference of the two are calculated for each scenario and the average difference drops a little from the above to 0.87 +/- 0.67 for std form and -0.52 +/- 0.33 for aq phase. While the intra-scenario difference averages are generally lower than the chronological differences, there are still some high differences. These high values indicate an imbalance in total entropy contribution and they do not appear randomly in the different inversion status states.



Below are tables of the sum positive – sum negative total entropy intra scenario difference averages by scenario for std form (top) and aq phas (bottom) values. Because this calculation is the subtraction of a negative number, all results are positive regardless of the direction of entropy change. The top portion of the top table is a cut off version of the entire list with each set of 2 columns sorted separately from largest to smallest. The bottom list of the top table gathers together all the values of the major players. This list shows that the highest imbalance is coming from the major players in scenario 1, a host of minor players in the other scenarios. The std form view has identified scenario 1 as the major entropy change scenario in the long term view.

sum positive - sum negative total entropy intrascenario difference averages				
-- std values of formation -- Gila at Safford (grabs)				
	scen1	scen3	scen2	scen4
Fe(OH)3	2.7 Ni(CO3)2	1.0 SrCO3	0.9 CdCl2	0.9
CO2(g)	2.5 CuSO4	0.6 Fe(OH)4-	0.8 PbCl	0.8
HCO3	1.8 Fe(OH)4-	0.5 Fe(OH)2+	0.7 PbSO4	0.7
H4SiO4	0.6 MnF	0.3 Cd(CO3)2	0.7 MnO4	0.7
Ca	0.6 Sr	0.3 Fe(OH)3	0.7 BaHCO3	0.6
Mg	0.6 ZnF	0.3 Cd(SO4)2	0.7 Pb	0.6
Na	0.5 MgF	0.3 Zn(CO3)2	0.6 CdHCO3	0.5
N2(g)	0.5 HPO4	0.2 CdOH	0.5 PbHCO3	0.5
Fe(OH)2+	0.5 Na	0.2 Zn(OH)2	0.5 Cd(CO3)2	0.4
Cl	0.4 SrSO4	0.2 H4SiO4	0.4 Ba	0.4
Fe(OH)3	2.7 Fe(OH)3	-0.2 Fe(OH)3	0.7 Fe(OH)3	-0.1
CO2(g)	2.5 CO2(g)	0.0 CO2(g)	-0.1 CO2(g)	0.0
HCO3	1.8 HCO3	0.2 HCO3	-0.1 HCO3	0.1
H4SiO4	0.6 H4SiO4	-0.2 H4SiO4	0.4 H4SiO4	0.2
Ca	0.6 Ca	-0.1 Ca	-0.1 Ca	-0.2
Mg	0.6 Mg	-0.1 Mg	0.1 Mg	-0.1
Na	0.5 Na	0.2 Na	0.0 Na	0.1
Cl	0.4 Cl	-0.1 Cl	0.1 Cl	0.1

Table 168.1

sum positive - sum negative total entropy intrascenario difference averages				
-- aqueous phase -- Gila at Safford (grabs)				
	1	3	2	4
HCO3	2.963 HCO3	5.256 HCO3	0.605 HCO3	0.498
Fe(OH)3	0.853 Fe(OH)3	1.069 HPO4	0.034 Fe(OH)3	0.065
HPO4	0.385 Fe(OH)2+	0.561 Cl	0.032 Cl	0.033
Fe(OH)2+	0.193 HPO4	0.456 Fe(OH)3	0.026 Na	0.012
Cl	0.074 H2CO3	0.116 Na	0.012 SO4	0.009
H2PO4	0.072 H2PO4	0.080 SO4	0.011 H2CO3	0.007
CaHPO4	0.062 SO4	0.067 H4SiO4	0.010 Fe(OH)2+	0.006
H2CO3	0.047 Cl	0.053 CaSO4	0.005 HPO4	0.005
SO4	0.045 Na	0.037 H2CO3	0.005 CaCO3	0.005
CaPO4	0.039 CaHPO4	0.033 CaHPO4	0.004 H4SiO4	0.004
Na	0.036 H4SiO4	0.029 CaCO3	0.004 CaSO4	0.004

Table 168.2

The aq phase table shows many major parameters high on the list in all scenarios. Entropy imbalance is higher across the board scenario wise, leading credence that the aq phas view is ‘closer’ to the initial inversion imbalance. But there is also a grab bag assortment of very minor players mixed in: some familiar ion pairs but also, quite notably, PO4 compounds (not usually very common) and even some very transient characters (NO2, H2CO3, Fe(OH)2+). The

presence of CO<sub>2</sub> and H<sub>2</sub>CO<sub>3</sub> in the lists is surprising since there is no indication of any strong pH dependence in major ion concentration inversion. The aq phas view shows more imbalance in 1 & 3 than 2 & 4.

It is usually not a bad idea to occasionally go back to the original data, plot it, and see how the results compare with more contrived views. This analysis starts with the original total entropy values and chronological differences (not inter or intra scenario differences). Both produce roughly the same patterns so only the differences are shown. The chronological differences have been sorted and averaged by inversion status to produce the following pictures with the standard values of formation (left) and aqueous phase (right). The standard values view uses only values > +/- 10 whereas the aqueous phase view goes down to +/- 1. A negative percentile indicates percent contribution to negative entropy.

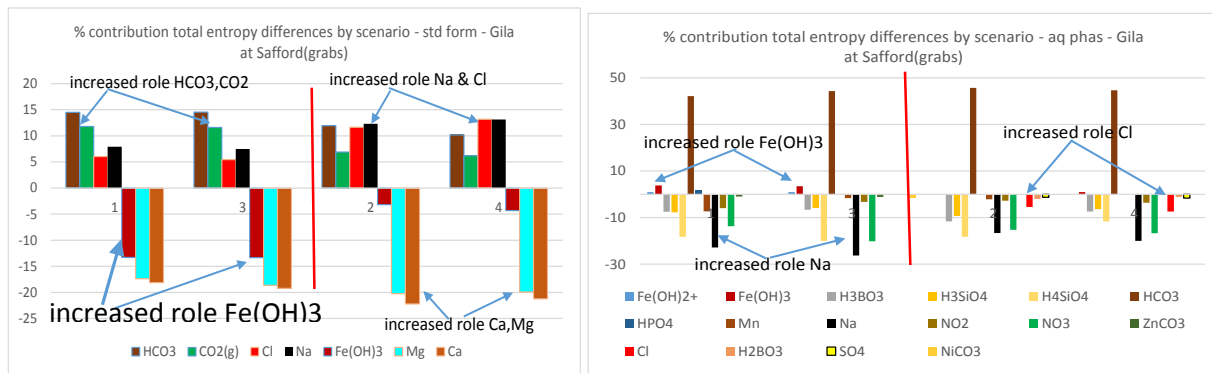


Figure 396.1 (for increase look 'across' mid line)

figure 396.2

The inversion and the matrix shift occur before scenario 1, off the chart to the far left of the graphs above. The return from inversion and back to the original matrix takes place at the vertical line across the middle of each. At first glance, all the states look surprisingly alike, particularly after the wild swings of the previous inversion diagrams. What most clearly separates the four states in the graphs above is whether the final state is an inversion (scen1&3, left two sets of columns) or a non-inversion (scen2&4, right two sets of columns). The 'increased' contribution of a parameter like Fe(OH)<sub>3</sub>, for example, is seen by comparing its column lengths in scen 1&3 with those in scen 2&4. (A much clearer picture of the differences between columns can be produced by taking residuals around the average but that creates confusion between "negative entropy" and "below average" and so is not used.)

The 'slight' changes are much 'slighter' in the aq phas view than the std form phase, undoubtedly a result of the shorter 'history' of the former. Over time, the smaller, changeable contribution of lesser actors at the moment of inversion are outweighed by larger contributions from major players. A new major player appears in std form view with CO<sub>2</sub> (H<sub>2</sub>CO<sub>3</sub> in aq phas) and Ca & Mg are not in the aq phase picture at all. This result supports the supposition that Ca & Mg replace Na as the major balancer of HCO<sub>3</sub> across the different std value time frame pictures. A host of minor players appear to balance HCO<sub>3</sub>, virtually the only significant positive entropy contributor, in the aq phas view.

Unfortunately the graph percents do not sum up to exactly 50% positive, 50% negative. The original difference percents over a single day do balance but dividing up the percents by scenario destroys the total. This is particularly true with the aqueous phase view. With  $\text{HCO}_3$  representing about 45% of the positive entropy contribution, the positives come close to balancing at 50% since all other parameters make only small additions. The negative entropies, with a large number of parameters making contributions, may have chance high values of lesser players appearing on certain dates and these can become scenario averages. The negatives quickly sum to around -80%. Initial entropy control is more random and involves many players. The picture could be a quantitative tool for any given day but, for inversion analysis, is only a qualitative assessment.

The very different look of the two pictures above are due to the fact that the matrix adjustment occurs, as with the intra-scenario differences of Figures 393-396, between the graphs. These pictures seem like two different systems responding to the same change – inversion and the associated matrix shift– in completely different ways. But they are really the same system viewed at two different times. The more closely one looks at entropy balance the more unbalanced it seems, over time things have a way of balancing out though over all time, we are told, they don't.

It is now possible to define the components of the matrix shift more precisely. It includes the change in activity of water, the dissociation of ion pairs, and the slight changes in ion entropy control contributions with the inversion. These are real physical changes in the system. The change of primary balancer from Na to Ca-Mg is not part of the matrix shift itself nor is it an 'inversion.' It is rather the system adjustment to the matrix shift and due, not to a physical change in the system, but to a change in the analytical view of the process. At its onset, increased  $\text{HCO}_3$  is responded to by Na and Cl and a host of minor players. Over the long run, the entropy imbalance caused by  $\text{HCO}_3$  is more fully responded to by Ca and Mg.

Note that the shift and the adjustment are tied together because the ion pair dissociation of Ca and Mg compounds, among others, fuels the long term response.  $\text{Fe}(\text{OH})_3$  response is a bridge with a part in both the short and the long term response, though it switches side. In the short term view it transiently opposes Na while in the long term it transiently defers to Ca & Mg depending on inversion status.

The alternating direct and inverse relations of Na&Cl and Ca, Mg &  $\text{HCO}_3$  on two different temporal levels changes the inter-relations of everything else in the solution. Below are correlation matrices showing the two extreme end-points of the inversion in terms of total entropy relations. Scenario 4 reaction in the aqueous phase view is to the left and the scenario 3 in the standard values of formation view to the right. (These matrices follow the pattern of Figures 393-6 above.)

total entropy correlations scen 4 intra-differences - reactaqphas							total entropy correlations scen 3 intra-differences - stdvalsform						
	Ca	Mg	Na	Cl	SO4	HCO3		Ca	Mg	Na	Cl	SO4	HCO3
Ca	1.00	0.99	-0.98	0.97	0.99	0.65	Ca	1.00	0.99	-0.91	-0.41	-0.98	-0.97
Mg	0.99	1.00	-0.98	0.97	0.99	0.65	Mg	0.99	1.00	-0.87	-0.35	-0.98	-0.97
Na	-0.98	-0.98	1.00	-1.00	-0.99	-0.60	Na	-0.91	-0.87	1.00	0.71	0.90	0.86
Cl	0.97	0.97	-1.00	1.00	0.98	0.60	Cl	-0.41	-0.35	0.71	1.00	0.38	0.34
SO4	0.99	0.99	-0.99	0.98	1.00	0.62	SO4	-0.98	-0.98	0.90	0.38	1.00	0.96
HCO3	0.65	0.65	-0.60	0.60	0.62	1.00	HCO3	-0.97	-0.97	0.86	0.34	0.96	1.00

Table 165

Table 166

In the scenario 4 instantaneous (react aq phase) picture to the left above, the correlation of Na & Cl is high and inverse and all the other ions, with the exception of HCO3, follow the leaders. Note that this matrix is very similar to the original major ion concentrations matrix – probably a reflection of the fact that scenario 4 has about 3 or 4 times as many samples as any other scenario. In the scenario 3 end-state picture with the full historical energy change (right above), Na & Cl lose their high inverse intra-correlation for a weaker direct correlation. Cl loses all its other high correlations while Na correlates inversely with the other cations, directly with the other anions.

The corresponding states are the scenario 4 standard values of formation views (below left) and the scenario 3 reaction in the aqueous phase view (below right), Scenario 3 retains low correlation for Cl but shows a higher Na-Cl correlation – another reason scenario 3 is unstable, there are two potentially competing systems. The long term historical energy summation of scenario 4 shows all the ions highly intra-correlated including, significantly, HCO3 (at a lower magnitude).

total entropy correlations scen 4 intra-differences - stdvalsform							total entropy correlations scen 3 intra-differences - reactaqphas						
	Ca	Mg	Na	Cl	SO4	HCO3		Ca	Mg	Na	Cl	SO4	HCO3
Ca	1.00	0.98	-0.93	-0.91	-0.84	-0.98	Ca	1.00	0.99	-0.93	0.58	0.99	0.96
Mg	0.98	1.00	-0.91	-0.88	-0.83	-0.98	Mg	0.99	1.00	-0.90	0.52	0.99	0.96
Na	-0.93	-0.91	1.00	0.96	0.75	0.91	Na	-0.93	-0.90	1.00	-0.83	-0.94	-0.85
Cl	-0.91	-0.88	0.96	1.00	0.78	0.89	Cl	0.58	0.52	-0.83	1.00	0.60	0.48
SO4	-0.84	-0.83	0.75	0.78	1.00	0.87	SO4	0.99	0.99	-0.94	0.60	1.00	0.95
HCO3	-0.98	-0.98	0.91	0.89	0.87	1.00	HCO3	0.96	0.96	-0.85	0.48	0.95	1.00

Table 167

Table 168

The contention is that the changing relations of the major actors, whether leading to balanced resolution of negative entropy or not, have a ripple effect across the whole system. It may be that entropy imbalance is what ultimately motivates change in relations. The view of major ion relations is expanded to include inter-relations with the ion pairs. Below are four super matrices that show the different intra and inter-relations of the major ions in the two ‘maintenance’ end-states, scenarios 3 & 4.

Since these matrices are rather large, a couple of preparatory steps will hopefully make them easier to evaluate. First, a diagram showing the content and positioning of the various sub-

matrices is given below. Along the diagonal (1-2-3 from left to right) are the intra-relations of the three groups (MI x MI, NIP x NIP, CIP x CIP) while off diagonal (4-6) are the inter-relations (MI x NIP, MI x CIP, NIP x CIP). The MI X MI (submatrix 1, upper left corner) are copies of those above but the rest are new.

relations major ions and ion pairs in maintenance inversion states -- Gila at Safford(grabs)

	Ca	Mg	Na	Cl	SO4	HCO3	Fe(OH)3	H4SiO4	CaSO4	CaCO3	H2CO3	H3BO3	Fe(OH)2+	Fe(OH)4-	CaHCO3	MgHCO3	NaSO4	MgOH
Ca																		
Mg																		
Na	1 MI X MI						4 MI X NIP						5 MI X CIP					
Cl																		
SO4																		
HCO3																		
Fe(OH)3	4 MI X NIP						2 NIP X NIP						6 NIP X CIP					
H4SiO4																		
CaSO4																		
CaCO3																		
H2CO3																		
H3BO3																		
Fe(OH)2+	5 MI X CIP						6 NIP X CIP						3 CIP X CIP					
Fe(OH)4-																		
CaHCO3																		
MgHCO3																		
NaSO4																		
MgOH																		

Table 169

It is also important to be aware of scenario 3 and 4 sample counts. There are no sample count issues for scenario 4 where the min (29) is higher than the scenario 3 max (26). Sample count issues do, however, exist in scenario 3, particularly in the case of Fe(OH)3 (6) and H4SiO4 (9) and, even more so, with the charged ion pairs of iron and MgOH which sometimes fall to 3 (highlighted in magenta). And, of course, a major charged ion, H3SiO4, is missing because no thermodynamic standard values of formation were found.

Scenario 3 total entropy correlation sample counts

	Ca	Mg	Na	Cl	SO4	HCO3	Fe(OH)3	H4SiO4	CaSO4	CaCO3	H2CO3	H3BO3	Fe(OH)2+	Fe(OH)4-	CaHCO3	MgHCO3	NaSO4	MgOH
Ca	26	26	26	26	26	26	6	9	26	26	26	24	6	6	26	26	26	26
Mg	26	26	26	26	26	26	6	9	26	26	26	24	6	6	26	26	26	26
Na	26	26	26	26	26	26	6	9	26	26	26	24	6	6	26	26	26	26
Cl	26	26	26	26	26	26	6	9	26	26	26	24	6	6	26	26	26	26
SO4	26	26	26	26	26	26	6	9	26	26	26	24	6	6	26	26	26	26
HCO3	26	26	26	26	26	26	6	9	26	26	26	24	6	6	26	26	26	26
Fe(OH)3	6	6	6	6	6	6	6	3	6	6	6	6	6	6	6	6	6	6
H4SiO4	9	9	9	9	9	9	3	9	9	9	9	9	3	3	9	9	9	9
CaSO4	26	26	26	26	26	26	6	9	26	26	26	24	6	6	26	26	26	26
CaCO3	26	26	26	26	26	26	6	9	26	26	26	24	6	6	26	26	26	26
H2CO3	26	26	26	26	26	26	6	9	26	26	26	24	6	6	26	26	26	26
H3BO3	24	24	24	24	24	24	6	9	24	24	24	24	6	6	24	24	24	24
Fe(OH)2+	6	6	6	6	6	6	6	3	6	6	6	6	6	6	6	6	6	6
Fe(OH)4-	6	6	6	6	6	6	6	3	6	6	6	6	6	6	6	6	6	6
CaHCO3	26	26	26	26	26	26	6	9	26	26	26	24	6	6	26	26	26	26
MgHCO3	26	26	26	26	26	26	6	9	26	26	26	24	6	6	26	26	26	26
NaSO4	26	26	26	26	26	26	6	9	26	26	26	24	6	6	26	26	26	26
MgOH	18	18	18	18	18	18	3	3	18	18	18	18	3	3	18	18	18	18

Table 170

Scenario 4 total entropy correlation sample counts

	Ca	Mg	Na	Cl	SO4	HCO3	Fe(OH)3	H4SiO4	CaSO4	CaCO3	H2CO3	H3BO3	Fe(OH)2+	Fe(OH)4-	CaHCO3	MgHCO3	NaSO4	MgOH
Ca	82	82	82	82	82	82	58	36	82	82	82	82	58	58	82	82	82	82
Mg	82	82	82	82	82	82	58	36	82	82	82	82	58	58	82	82	82	82
Na	82	82	82	82	82	82	58	36	82	82	82	82	58	58	82	82	82	82
Cl	82	82	82	82	82	82	58	36	82	82	82	82	58	58	82	82	82	82
SO4	82	82	82	82	82	82	58	36	82	82	82	82	58	58	82	82	82	82
HCO3	82	82	82	82	82	82	58	36	82	82	82	82	58	58	82	82	82	82
Fe(OH)3	58	58	58	58	58	58	58	36	58	58	58	58	58	58	58	58	58	58
H4SiO4	36	36	36	36	36	36	36	36	36	36	36	36	36	36	36	36	36	36
CaSO4	82	82	82	82	82	82	58	36	82	82	82	82	58	58	82	82	82	82
CaCO3	82	82	82	82	82	82	58	36	82	82	82	82	58	58	82	82	82	82
H2CO3	82	82	82	82	82	82	58	36	82	82	82	82	58	58	82	82	82	82
H3BO3	82	82	82	82	82	82	58	36	82	82	82	82	58	58	82	82	82	82
Fe(OH)2+	58	58	58	58	58	58	58	36	58	58	58	58	58	58	58	58	58	58
Fe(OH)4-	58	58	58	58	58	58	58	36	58	58	58	58	58	58	58	58	58	58
CaHCO3	82	82	82	82	82	82	58	36	82	82	82	82	58	58	82	82	82	82
MgHCO3	82	82	82	82	82	82	58	36	82	82	82	82	58	58	82	82	82	82
NaSO4	82	82	82	82	82	82	58	36	82	82	82	82	58	58	82	82	82	82
MgOH	75	75	75	75	75	75	53	29	75	75	75	75	53	53	75	75	75	75

Table 171

Despite these short-comings, the full picture of scenario 3 and 4 inversion instantaneous and summation end-states (below) does yield some interesting general patterns. The matrices follow the left to right top to bottom order of the graphs and tables above (top left – scen 4 aq phas, top right-scen3 std vals, bottom left – scen3 aq phas, bottom right – scen4 std vals)

The neutral ions as a group (#2 in diagram above) show few intra-relations. The exception is in scenario 4 instantaneous end-state (upper, left side matrix) where H4SiO4 and CaSO4 pick up a high inverse relation and both show increased correlation with the major ions, particularly HCO3. H3BO3 has few correlations to the major ions in this matrix, though it has many with



**Table 176**

These relations can be seen in action in the scenario 3 and scenario 4 intra-differences of total entropy (below). It appears to function both as an instantaneous and as long term end state control function since the high correlations hold in both standard views.

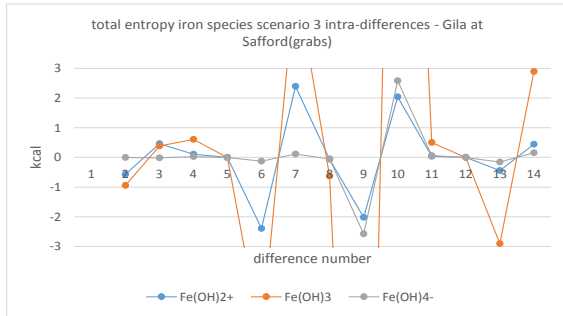


Figure 397

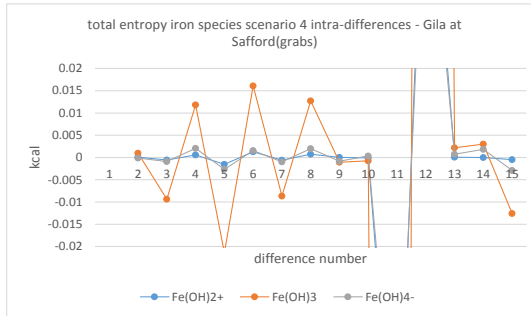


Figure 398

Note that the charged ion pair values in scenario 3 are about four or five orders of magnitude higher than in scenario 4. The difference may have something to do with the fact that scenario 1, high in  $\text{HCO}_3$ , is the state most sensitive to change in pH.

In fact, the relation of iron speciation and pH provides something of a ‘foundation’ to a picture plagued by low sample counts. The graph below shows the relationship of the mole fraction of the various species (relative to moles total Fe) vs pH and gives the correlation values with pH for each. Note that  $\text{Fe(OH)}_3$  is actually correlated to pH, but half the curve is directly related while half is inversely related so the result is little or no correlation.

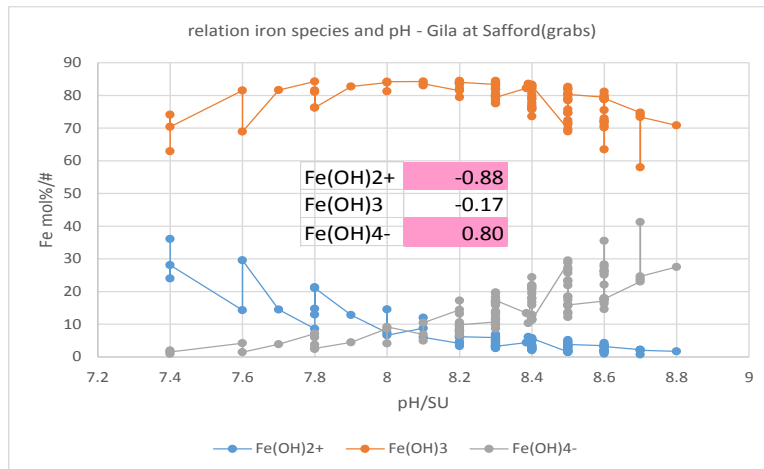


Figure 399

The dissociation of  $\text{Fe(OH)}_3$  will affect the mole fraction of  $\text{Fe(OH)}_2^+$  and  $\text{Fe(OH)}_4^-$  which will in turn have an effect on the pH. pH is the quintessential small factor with an instantaneous, big

effect, but it is also a long-term factor as seen in the interplay of  $\text{Fe}(\text{OH})_2^+$  and  $\text{Fe}(\text{OH})_4^-$  over time.

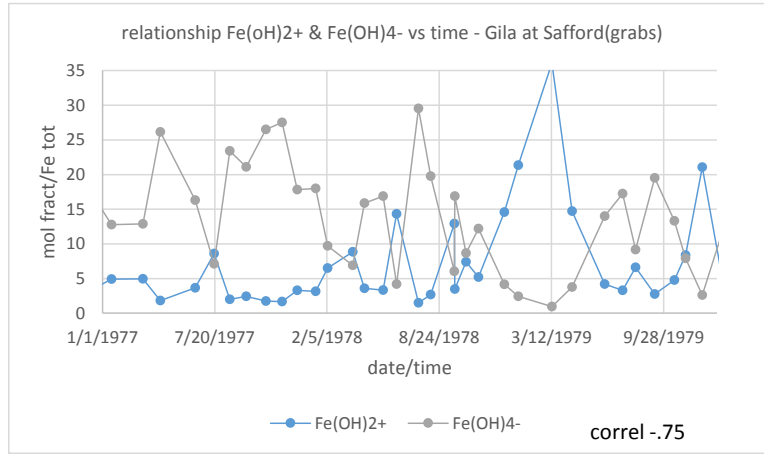


Figure 400

The above intra-correlations of iron species is, in some sense, trivial. Any species related by a common parameter, here Fe, will be correlated because speciation is a percent, when one species goes down another must go up. But here, the fact that speciation of Fe is highly dependent on pH raises the significance of speciation to another level, that of function. There is also a charge maintenance aspect with the two charged species having different signs.

There are other nexuses of inter-relations of ion pairs. These are the intra relations of the calcium carbonate, bicarbonate, and sulfate species. These probably also have a role in pH control, though possibly less significant than Fe, and so the relations are considered largely trivial.

But there is another relation that stands out because it is with an entirely different species. The total entropy of  $\text{H}_4\text{SiO}_4$  is, for some unknown reason, highly correlated to both that of  $\text{CaHCO}_3$  (0.91) and  $\text{MgHCO}_3$  (-.95). Taking inversion differences for scenario 3 and scenario 4 shows that the relation of  $\text{H}_4\text{SiO}_4$  applies only to scenario 4. The relation falls apart entirely in scenario 3, though to be fair there are data gap issues here. The result is the same regardless of which standard values set is used so the relation is not time dependent.

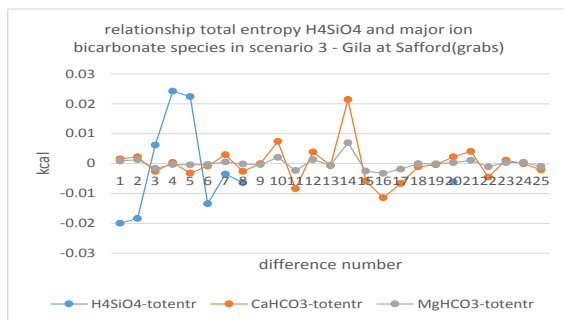


Figure 401

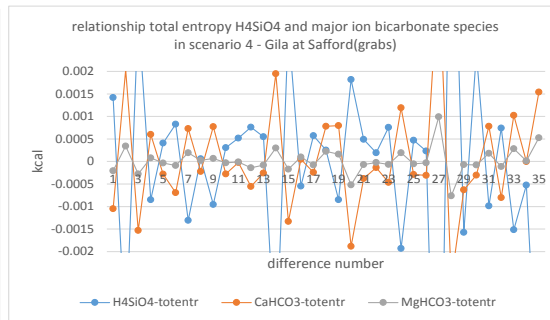


Figure 402



Here the lack of standard values of formation for H3SiO4 means that the relation cannot be examined fully. If reaction in the aqueous phase values for H3SiO4 are used instead, the above relations for H4SiO4, CaHCO3, MgHCO3 and HCO3 hold but H3SiO4 has no high correlations with any in either straight values or inversion differences. Unless the standard values of formation provide a completely different view, H3SiO4 does not appear to be involved.

correlations total entropy silicon species & bicarbonate species inversion differences scenario 4 - reaction in the aq phase - Gila at Safford(grabs)					
	H4SiO4	H3SiO4	CaHCO3	MgHCO3	HCO3
H4SiO4	1.00	0.14	-0.93	-0.95	-0.96
H3SiO4	0.14	1.00	-0.21	-0.13	-0.14
CaHCO3	-0.93	-0.21	1.00	0.96	0.97
MgHCO3	-0.95	-0.13	0.96	1.00	0.98
HCO3	-0.96	-0.14	0.97	0.98	1.00

Table 177

The total entropy of these species do not have any high correlations to pH so the next most likely function is to bolster Na & Cl in entropy control. The balancing of Na & Cl may provide a bed-rock for scenario 3 but Na & Cl follow solution total entropy patterns in the formation view showing that they are unable to resolve entropy at their own level.

Having seen some of the more interesting relations involved in the matrix shift, it remains only to say a few words about what may be the most crucial factor in entropy control, timing. The change in Na & Cl activity called 'the inversion' is a relatively rapid change and, continuing into scenario 3, occurs at a critical time for parameters that have appropriate magnitudes to fulfill crucial roles. Ion pair dissociation is small but is also a rapid change as can be seen in the mass action graphs for SO4 and HCO3 ([Figures 258 & 263](#)) where ion pair concentrations plunge as soon as reagent ion concentrations have peaked.

Ion pair formation in scenario 2 & 4 is, on the other hand, a gradual process which can be adjusted to over a period of time. As their neutral ion pairs gradually form, Fe & Si fall out of the ionic balance picture entirely and presumably take minor thermodynamic roles, as seen above, under the dominance of Na & Cl which largely balance each other.

In scenario 3, flow generally continues to rise and flow change becomes more variable, both of which make for wider swings. The concentrations of the free ions go up and down in direct relation to flow but the ion pairs remain slow to form, with variable lag time, though they remain quick to dissociate if local conditions permit. Their effect on the system is magnified in both ionic strength and the balance of entropy and enthalpy by free energy. Small changes in amount and/or activity can lead to large changes in ionic strength and free energy. Fe(OH)3 uses primarily its high reaction in the aqueous phase enthalpy but has an anomaly in 3 while H4SiO4 is able to balance both enthalpy and entropy without anomaly.

Following this line of reasoning, the shift to formation of ion pairs should, theoretically, really occur during inversion status 2 not inversion status 3. A shift during inversion status 3 is therefore a sign that the inversion may not last across the whole period. In other words, the system may actually be trying to shift to inversion status 2 ‘in between’ some inversion status 3 dates in an extended inversion period. But the flow distribution for inversion status 3 suggest that this reasoning is heavily reliant to the ‘average’ picture of scenario3. To find a more complete answer requires looking at system stability.

Thus far, there has only been speculation that the scenario 4 situation is more ‘stable’ than scenario 3. The most intuitive definition of stability is the mechanical – a ‘stable’ object is one that does not tip over under the influence of gravity. It has an intrinsic balance that allows it to keep its position in contrast to an unstable object which, unbalanced, will tip over. The definition needs to be expanded and generalized to cover systems rather than individual objects by reformulation to ‘the ability to resist change.’ The criteria of ‘balance’ remains but also needs to be modified to cover different types of ‘balance.’

The free energy function points to the possibility of spontaneous change (towards equilibrium) and is therefore an inverse indicator of stability: a large negative number indicates a high potential for change. If that applies to a solution as well as a reaction, then which inversion state is more stable should be clear from the free energy inversion state diagrams. But, according to these, both scenario 3 and 4 are states of zero change. The problem is that the diagrams are of free energy differences not values. To answer the question of stability, the values of total free energy are shown by inversion status below using standard values of formation (left) and reaction in the aqueous phase standards (right).

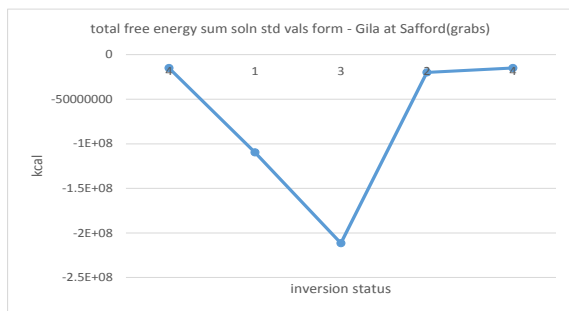


Figure 403

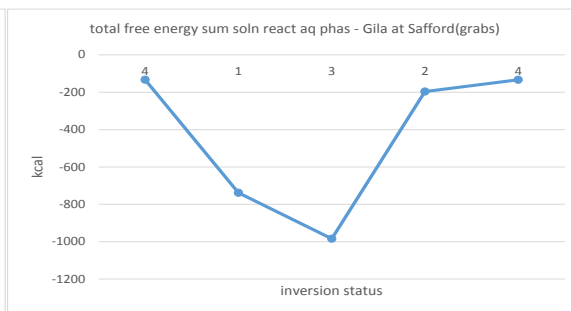


Figure 404

The only problem with using free energy as a measure of stability is that it gives no idea of how quickly or slowly the spontaneous change may be taking place. In some cases it may be so slowly that the system appears to be stable. That is not a problem here where, whether viewed from the long term or the short term energy change perspective, the potential for change of scenario 3 is much higher than 4 (i.e. scenario 3 has a more negative free energy than 4). Scenario 4 resists change, is more ‘stable’, than scenario 3.

There is also other evidence. If ‘stable’ systems occur more frequently or ‘last longer’ than less stable ones, then scenario 4 is more stable with almost four times more individual samples, covering longer consecutive time spans. Also to be considered is the fact that the flow values of

scenario 4 are normally distributed while those of 3 are in the non-normal portion of the flow distribution. Non-normal phenomena are usually sporadic and short lived.

Free energy points to the possibility of change but the motivation for change comes from entropy. To relate entropy change to any structural changes in the solution is difficult. The whole area of 'structure' in water is one fraught with danger. Recall the sad saga of 'polywater' in which various structures were claimed for water until they were found to be caused by an artifact of the analysis, sample contamination.<sup>19</sup>

Studies on structure in water continue, however, and can look at either the disruption of posited structures of water itself and or the influence on water of the building up of structure by things within it. These diametrically opposite approaches are presumably a result of the different interpretations given to entropy change. Negative entropy is commonly, if not always completely correctly, seen as the result of an increase in order. That would be the impetus for studies looking at the building up of discrete structures (solutes) within water that are able to impart their structure to water. The other common interpretation is that positive entropy is due to an increase in system degrees of freedom. That view would be the impetus for studies looking at the disruption of structure in water itself.

Even the stalwart Lewis and Randall, writing in 1923, are led to speculate a bit on structure to explain the contraction of solutions when some solutes are added. They assume that water is made up of regions with different structures, denser and more ice-like around 4C, less elsewhere. These solutes, acting like increasing temperature, disrupt the ice-like formations in water, causing the solution as a whole to contract<sup>20</sup>. They point out that this result is in accord with what is seen in the lab, the amount of solution contraction being proportional to solute concentration. Actually, Lewis had additional information, provided by Latimore around 1920, on hydrogen bonding in water.<sup>21</sup>

In fact, the contraction of many solutions when solutes are added is now well known.<sup>22</sup> Stumm, circa 1996, can be somewhat less speculative than Lewis and Randall in relating solution contraction caused by any solute to the disruption of the by-now-well-known and accepted hydrogen bond structure in water.<sup>23</sup> The motivation provided by entropy for this destruction of structure (order) is, presumably, an increase in the degrees of freedom of the system.

There is another example, however, that helps bring the two interpretations of what entropy is together. When water freezes to form ice there is an expansion in volume but the change in entropy is negative. The reasoning here is that ice is more 'ordered' than liquid water. The molecules are more 'constrained' and, as such, not all the rotational and vibrational modes of motion are possible, i.e. the degrees of freedom of the system are lowered. An input of heat causes the system to contract to the more disordered liquid form where all modes of motion are available.

The solution contraction seen here in the shift from scenario 1 to 2, is accompanied by negative entropy. Any contraction, no matter what the cause and what the temperature, brings molecules closer together. The molecules have to align themselves spatially in the most favorable position relative to all the other molecules, which is an entropy related change. The last energy step just

before the inversion, the formation of aqueous species, is also one with strong implications for entropy. The positioning of water molecules around metal species may be just a first step, a pre-disposition, when viewed from the inversion end-state perspective.

Could the increase in inversion status 2 of Na & Cl activity and their crystal-like ordered pairing behavior act like nucleation seeds aligning adjacent water molecules causing contraction of the solution as a whole? While the argument is consistent with the role of Na & Cl seen here, it does not follow logically. The negative entropy being considered is the summer time temperature dependent entropy of the solvent, water, and that has nothing to do with the make-up of the solution. These entropies exist on very different levels and are only related in being two aspects of the entropy of the solution, a solution that is in contraction mode.

The actual resulting 'closeness' of a solution in contraction is dependent on the initial solution concentration. Contraction leading to increased order via some sort of 'lattice' formation means that the molecules must be close enough together to begin bonding with each other. The dissolved solids concentrations seen here average around 0.028 M, with loflo and hiflo(s) samples around 0.029-0.033 and hiflo(w) samples around 0.0165. These numbers are considerably lower than those usually cited in studies on the subject as marking the beginnings of (foreign) structures in aqueous solutions. Hepler, in his analysis of 'structure-making' and 'structure-breaking' parameters, does not go any lower than 0.05 M.<sup>24</sup>

Arguments for structure in solution are primarily made on the basis of changes in volume. The 'control-volume' volume here is calculated from the change in the environment (flow). There is no other physical measurement to compare with that. The contraction of scenario 2 is proportional to the expansion of scenario 1, the reference volume is not zero but rather the volume of scenario 4. The accompanying negative entropy of scenario 2 is also proportional to the positive of scenario 1. If solution entropy valleys were greater or less than solution entropy peaks, then arguments based on entropy induced change in solution structure would have some ground to stand on.

The most reasonable explanation for the negative entropy of scenario 2 is simply that, going from the expansion of scenario 1 back to scenario 4 is a contraction that entails a net loss in degrees of freedom for the system. Scenario 1 is a bit of a saturnalia with an explosion of new species, inter-relating in new ways, and it is energetically 'hard' to go back to the old, limited but more stable situation of scenario 4. While not an equilibrium situation, scenario 3 is a 'balancing' act between high degrees of freedom and stability.

The above considerations lead to a reevaluation of the logical relation of volume and entropy. The relations seen here in the thermodynamic diagrams of water ([Figure 315-6](#)) are probably the most common because the other possibilities do not follow as logically from context. It is going to be more difficult for the structure of a part of the system to impart its structure to the whole system at a time when the system is expanding. It is going to be more difficult for the degrees of freedom of a system to be increasing when the system as a whole is contracting.

That is not to say that negative entropy in an expansion or positive entropy in a contraction are not possible. Specific examples are not difficult to find. The formation of ice is an expansion that occurs with negative entropy due to the increased order of ice as opposed to liquid water. The mixing of two gases with a contraction of total solution volume occurs because the entropy of mixing is always positive.

Most materials in the world around us expand upon heating and they do so because expansion is accompanied by positive entropy. Only a few materials (non thermal expansion materials or NTEs) contract upon heating, the process accompanied by positive entropy. These are, however, usually rare and unusual materials and/or situations. Water acts like an NTE but only between 0 and 4 C. What we commonly see in the world leads to certain 'prejudices.' In most cases, at the highest level of generality and without any further information, we assume expansion to be accompanied by positive entropy, contraction by negative entropy.

It is the unfavorable mechanics that help explain why the balancing posited for scenario 3 is so uneasy. It is part of an attempt to keep an entropy favored structure, with high degrees of freedom, from slipping back into a more stable configuration in a period of rapidly changing expansion and contraction. Neither expansion nor contraction of the system helps it quickly achieve and establish the stability it is seeking.

Whatever maintenance is achieved in scenario 3 is entirely fueled by the influx of new material. The new parameters spread entropy control out and, in scenario 2, lead to a flipping of an entropy into an enthalpy problem (which water alone can, presumably, handle). If these last speculations are correct, it seems that all parameters are equally important in the attempt. But the high positive free energy of certain parameters at scenario 3, often seen as an anomaly, signal an attempt to stabilize an unstable situation. Scenario 3 never achieves the stability of scenario 4 because the source of new material is too changeable and sporadic (non-normal).

With hopefully some ideas on what the inversion matrix shift means in terms of system stability, the burning question is 'do the total thermodynamic functions invert HCO<sub>3</sub> & Cl following the pattern of major ion concentration inversion?. That is to say, can the inversion matrix shift steps be fit into any larger energy pattern?

The table below shows averages under major ion concentration inversion/non-inversion using the standard values of formation. The total thermodynamic functions divide up nicely into hiflow (inversion) and loflow (non-inversion) groupings with a surprisingly consistent difference of one order of magnitude.

total thermodynamic sum solution averages with flow under major ion inversion/non-inversion - Gila at Safford(grabs)					
	flow-grab/	$\sum$ soln V/L	$\sum$ soln S/kcal	$\sum$ soln H/kcal	$\sum$ soln G/kcal
non-invers	141	3991	3608	-15124882	-16175759
inversion	1408	39887	35435	-151740228	-161728124

Table 178

This picture looks very promising. The one order of magnitude difference is surprisingly consistent but probably just coincidental. The difference between low and high flow is definitely seen in the total thermodynamic functions. But there is a major problem – negatives and positives divide by function following the thermodynamic relations not by inversion status, i.e. an artifact of the analysis rather than a change in the physical state of the system.

Amounts follow flow so the total thermodynamic functions, calculated using amount, should follow suit. If the inversion parameter (HCO<sub>3</sub>-Cl) is calculated for each grab total thermodynamic function and lined up with test parameter results for major ion concentration inversion, it is found that no thermodynamic total function has exactly 53 cases of HCO<sub>3</sub>>Cl as major ion concentration inversion does.

But recall that volume and mass follow the inversion pattern differently than the other analyzes looked at – they do invert on inversion days but they also invert on some non-inversion days as well. The test for inversion for these analysis is therefore, not simply ‘is HCO<sub>3</sub>>Cl?’, but ‘if this is a major ion concentration inversion day, is HCO<sub>3</sub>>Cl?’ (Begging the question, of course, of how an inversion date is determined in the first place). This statement is the ‘extended’ inversion test parameter test. And so the answer to the burning question is ‘yes’ for total relative volume and total entropy but ‘no’ for enthalpy and free energy. Recall that the **percent** total free energy and enthalpy did invert without any extended test being necessary but percent total volume and entropy did not.

The reason why enthalpy and free energy show no inversions of HCO<sub>3</sub> and Cl is easy to see. In the aqueous phase thermodynamic values, the ions of the elements have a standard state value of 0 while those considered compounds, like bicarbonate, are not. This situation has the result that, when Cl is subtracted from HCO<sub>3</sub>, Cl is only represented by its temperature compensation portion (CpdT), which is usually a small factor. But an even larger problem is that the standard state enthalpy and free energy of bicarbonate are negative. Given this fact the inversion test parameter, which should be positive for 1 & 3, negative for 2 & 4, is always going to be negative, so half the tests (1&3) fail.

The free energy of HCO<sub>3</sub> is simply too high and ensures the dominance of HCO<sub>3</sub> in the area of energy balance.

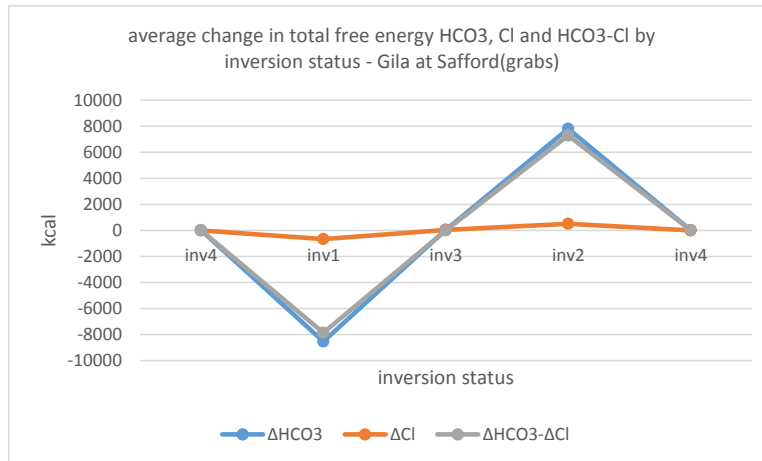


Figure 405

What this little exercise reveals is that following a certain pattern by inversion status is not the same thing as actually inverting. The observation may be patently obvious, after all flow difference follows a definite pattern when sorted by inversion status but does not, or rather cannot, invert. Total free energy has been shown, above, not to correlate with major ion inversion and yet, here it is, following the inversion function pattern. Apparently the technique designed to investigate inversion is so simple that it taps into general patterns that can be followed by a variety of phenomena.

It is interesting to note, in passing, that the average activity ratios  $HCO_3-Cl$  by inversion status form exactly the same pattern for inversion differences as those of the activity of water above while those for  $Na+Cl$  follow secondary action. It is to be further noted, however, that the scenario 1 & 2 peaks and valleys are not proportional: scenario 2 peaks and valleys being smaller than those of scenario 1.  $HCO_3/Cl$  and  $Cl/Na$  also follow primary and secondary action respectively but have scenario 2 proportional to scenario 1.

Major ion inversion is a process, the patterns formed by the analysis of the process reveal an inversion function which is of necessity operating at the same time as many other functions. Some functions are more central to certain processes than others – here the entropy function is seen as a major factor in the inversion process. Enthalpy and free energy functions as a whole, however, are ‘wider’ in significance than just inversion control, as important as that may be.

There is, however, a larger context for the matrix shift and it has already been seen and worked with extensively. It may have been noticed, above, that the inversion function matrix shift Piper Plot ([Figure 390](#)) has much the same look as the seasonal water quality plot shown earlier ([Figure 91](#)). That’s because it uses the same data, the individual grab samples are just labelled differently and sorted into different groups. The new grouping is functional, a subgroup of the seasonal grouping – inversion status 1 will have a higher proportion of winter and summer data than of fall or spring, etc.

It has already been seen that the relations between process and season change when viewed from different perspectives. In the analysis of density patterns, it was found that density values were

determined by season across all inversion types. Density differences, however, were determined by the inversion process more than by season. Similarly there are relations between seasons and functions that may change when viewed from different perspectives.

In the broadest sense, the seasons parallel the inversion function. In the graphs below the various inversion statuses are plotted along with the corresponding best-fit season. Summer is most closely associated with scenario 4, winter with 1, spring with 2 and fall has been shown here with scenario 3.

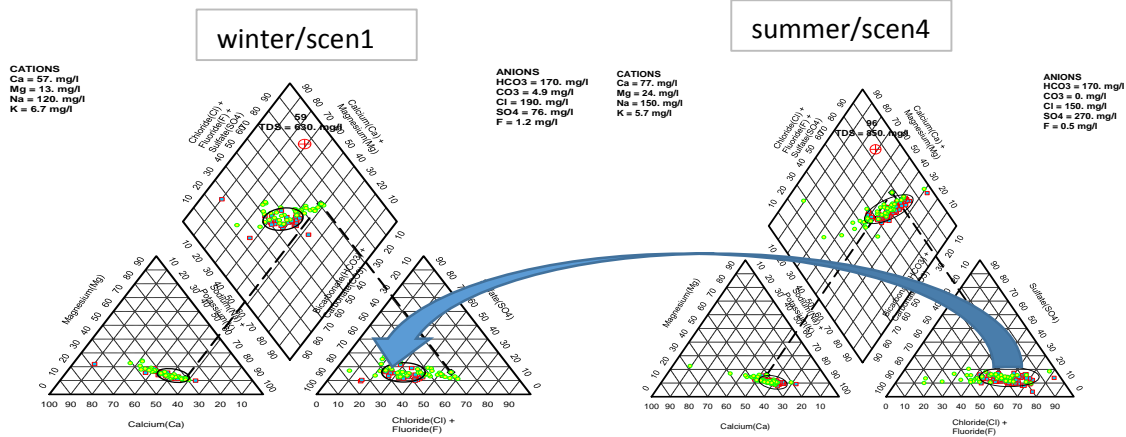


Figure 406 [\(back\)](#)

Figure 407

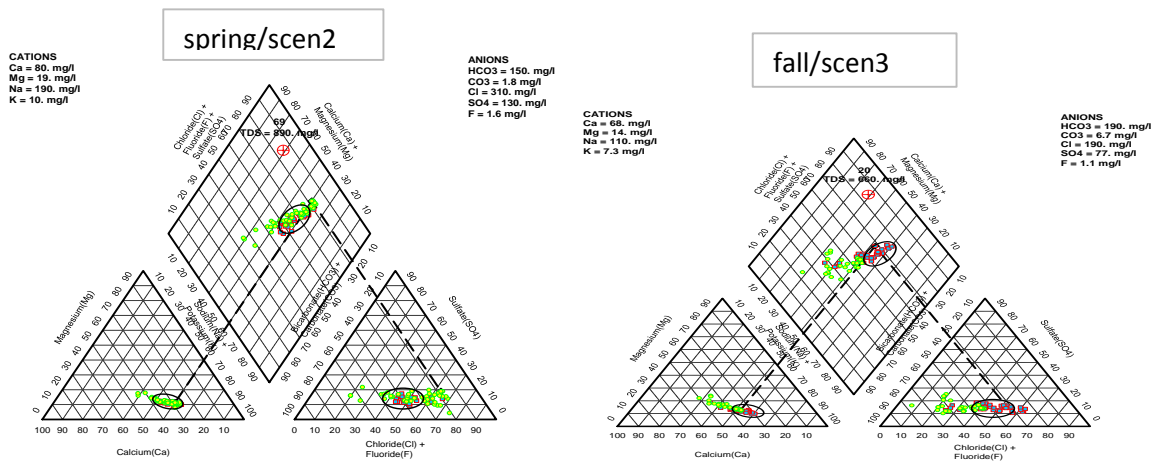


Figure 408

Figure 409

The intersection of season and the inversion function is shown by an oval in each subplot. In every case but one, the intersection is virtually the center of mass of the data in the central diamond with only a few outliers. Inversion status 3, however, has the inversion values scrunched to one side while seasonal values extend far in the opposite direction. The result is not unexpected since both the season and the function are highly variable and/or unstable.

The investigation of the inversion process has led to the formulation of an inversion status 'function' which is found to fit into the seasonal pattern. But if inversion, a non-normal



phenomenon that occurs randomly in several seasons, parallels seasonality it must be because seasonality is, itself, part of or a type of a larger function with which they both have points of contact.

The thermodynamic functions represent the system response to the totality of energy change in the environment. While there are points of intersection with inversion function and seasonality, the thermodynamic response as a whole must deal with all system processes both instantaneous and long term. It is a larger, more encompassing ‘function’ than either inversion or season.

The most intuitively graspable view of energy change is with the monthly averages of the total thermodynamic functions. Below are the sum solution total entropy (left) and total enthalpy (right) monthly averages.

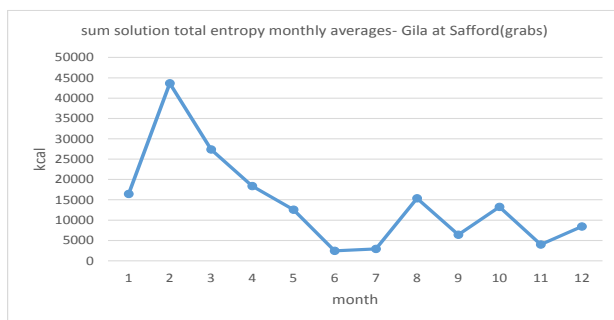


Figure 410 ([back](#))

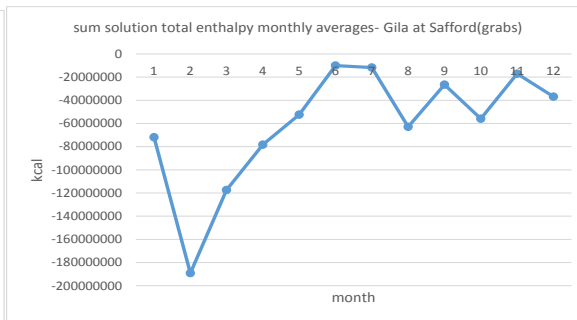


Figure 411

The picture for free energy is exactly that of enthalpy with only the scale changing. There is nothing new here: total entropy follows a flow curve pattern because set by amount which comes from flow and enthalpy/free energy are the exact reverse of entropy following the thermodynamic relations.

The temperature dependence of total entropy is, as it were, buried under the much larger scale dependence on amount. This temperature dependence should be seen in the molar function but is not all that clear in the sum solution monthly averages for molar entropy (left) and enthalpy (right). The reason sum solution entropies show no temperature dependence has already been covered ([Figures 166-167](#))

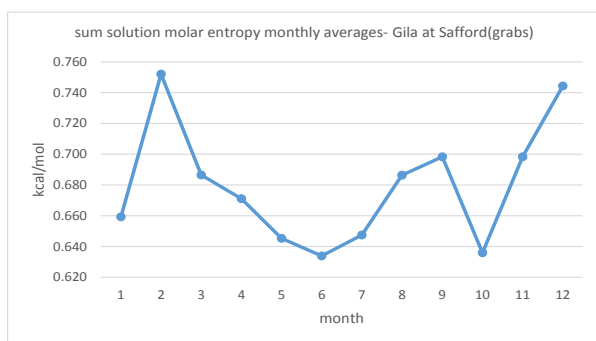


Figure 412

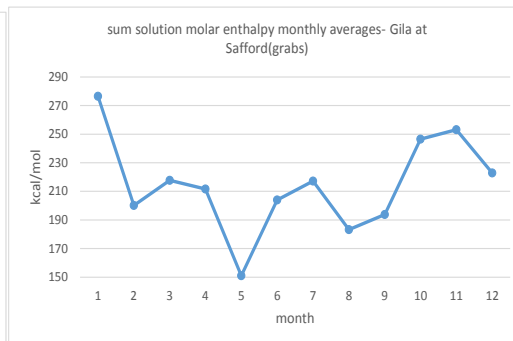


Figure 413

Both have the look of somewhat erratic annual density curves though the entropy curve has a somewhat flow-like look to it as well. (If the curves are simple enough, plenty of ‘almost’ coincident curves will be found.) Recall that percent molar entropies using sum MI to calculate percent have a definite relation to density while sum solution percents do not. That may be why looking for a ‘deeper’ temperature dependence in total entropy has had such limited success. But there must be ‘other’ patterns in the total thermodynamic functions that allow them to cover all situations. Whatever else these patterns are, they need to be normal and also to have a ‘normal’ way of handling non-normal behavior – that is, they must be able to operate on two levels. The search is on again for ‘underlying patterns.’

Actually, the tools to find these patterns have already been used earlier in this study. The frequency distributions of sum solution molar entropy (left) and total entropy (right) values can be used to illustrate how these tools work.

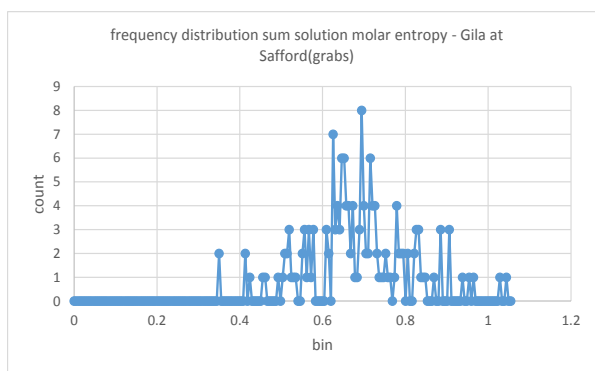


Figure 414

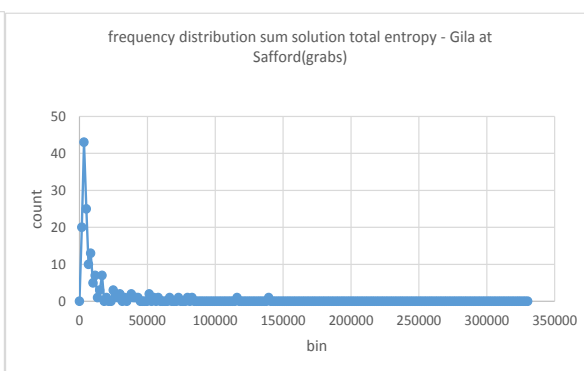


Figure 415

Taking a simple difference, for example, changes the distribution for sum solution total entropy quite a bit (left below). Taking a difference immediately moves the peak of values from the far left to the center. Following the other ‘views’ in order to the last,  $\text{difflnSSStotentr}$  (right below), shows that the logs ‘squeeze’ the distribution closer around the center.

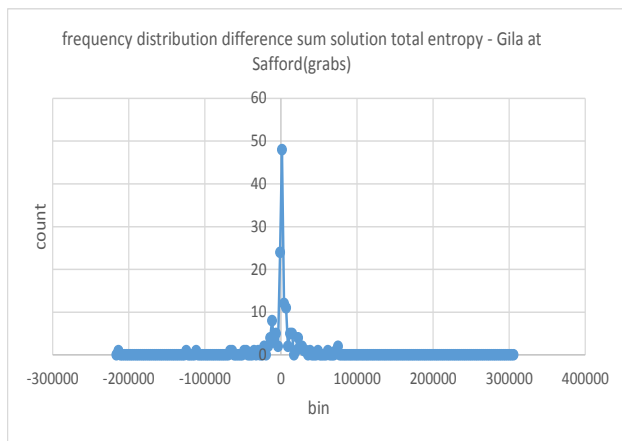


Figure 416

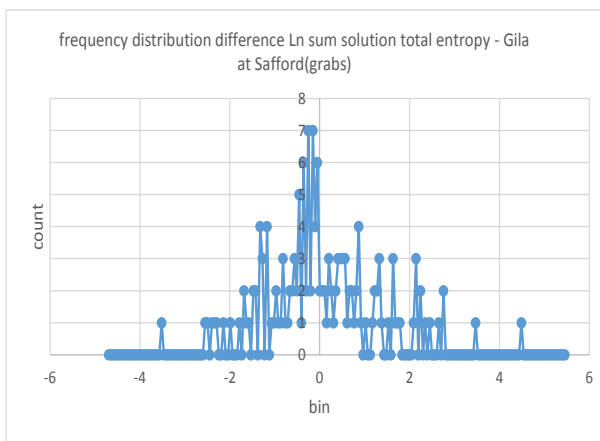


Figure 417

The different ‘views’ actually work to normalize the data. This effect is barely noticeable with the molar functions (table below) since the division by amount effectively has a ‘normalizing’ effect all by itself. But with the total functions, the various views bring the average closer to the center of the count (where the median always is by definition) and brings the sum of values above average closer to that below or a ratio of 1. That is, the average is being pushed closer to the center of the data in two senses, in position by count and by ‘weight’. The narrowing of both scales is possibly coincidental but does suggest a ‘parts to the whole’ relationship. Again the natural log seems to be bringing out an ‘underlying’ pattern which, in this case, is more normal than the original data.

frequency distribution statistics by view - Gila at Safford (grabs)						
	ratio(>/<)					
	max scale	bin(rng/200)	pos-avg	pos-med	sum-avg	sum-med
SSmolentr	1.06	0.0053	0.96	1.00	1.27	1.32
ΔSSmolentr	0.72	0.0035	0.95	1.00	-1.00	-1.00
lnSSmolentr]	0.06	0.0056	1.03	1.00	0.50	0.48
ΔlnSSmolentr	1.17	0.0098	0.95	1.00	-1.00	-1.00
signedlnΔSSmolentr	6.88	0.063	1.05	1.00	-1.16	-1.16
-----						
SStotentr	331973	-1660	0.29	1.00	3.19	10.26
ΔSStotentr	308283	-2623	0.76	1.00	-1.01	-1.01
lnSStotentr	12.7	0.054	0.69	1.00	0.87	1.25
ΔlnSStotentr	5.5	0.051	0.76	1.00	-1.02	-1.02
lnΔSStotentr	12.6	0.056	0.93	1.00	1.33	1.43
signedlnΔSStotentr	12.6	0.125	0.78	1.00	-0.82	-0.81

Table 179

The end result data is analogous to reducing flow values to the bell shaped portion. That procedure, however, would have the lamentable effect that ‘inversion’ values, which are in the non-normal part of the distribution, would be not be in the population at all.

The dilemma is that non-normal data points in a distribution, the so-called ‘outliers,’ can fall into two different groups – those that are just error and those that, as far as anyone can tell, are not. In a strictly controlled environment, such as a process control lab, charts with limits at +/- 2 and +/- 3 standard deviations of the average are used to spot error. Values greater than +/- 3 are the ‘outliers’ that indicate possible error and it is common practice that further analysis be stopped until they have been explained. But error may not always be found in which case the usual procedure is to place the ‘outliers’ on the process control chart and resume analysis.

It is said that there have been cases in process labs in which all outliers were left out of process control charts. This procedure was probably justified loosely on the grounds of ‘bad data’ but, more realistically, was probably done to make things ‘look good.’ The +/- 2 and 3 standard deviation control limits of process control charts are, however, constantly being recalculated. The result was that, in some cases, the throwing out of ‘bad data’ plus the continued narrowing of control limits led to a situation in which analyzes could no longer be run at all. Perfectly ‘normal’ data (under other circumstances) was being turned into ‘outliers’ because the control limits, consistently calculated with only normal data, became too tight. If it is permissible to extrapolate what happens in such a strictly controlled environment to the ‘real’ world, there may be a lesson here. Non-normal data points are a natural (one hesitates to say ‘normal’) and necessary part of a complete distribution.

To understand the world it is necessary to rely on normal behavior patterns but discarding the non-normal does not only not improve the picture, it may actually distort it. Normal and non-normal behaviors are, it seems, inextricably intertwined. It may very well be that the non-normal simply needs to be viewed in a longer or larger time and spatial framework for some pattern to emerge. But it could also just as well be true that normal and non-normal are qualitatively different . . . that there is a limit to our knowledge that no amount of fiddling with different views is going to change. Here the former, optimistic view is chosen as the mode of operation.

Changing the ‘view’ of the data is not the same thing as excluding non-normal data -- inversion values are included in the analysis but are normalized along with the rest of the data. This reformulation of the data redefines ‘normality’ with the result that the (old) non-normal portion can now be connected and integrated into the (new) normal behavior picture of the whole system. At least, that is the hope.

Casting the total thermodynamic functions into their most normal form finds fruition in autocorrelation where seasonality is found in the diffln and signedln diff views of all the thermodynamic functions.

autocorrelations			
sum soln thermodynamic functions			
	Gila at Safford(grabs)		
	entr	enth	free-e
SStot	0.34	0.37	0.37
$\Delta$ SStot	0.54	0.54	0.54
ln $\Delta$ SStot	0.06	0.11	0.11
lnSStot	0.43	0.40	0.40
$\Delta$ lnSStot	0.80	0.80	0.80
signedln $\Delta$ SStot	0.80	0.74	0.74

Table 180

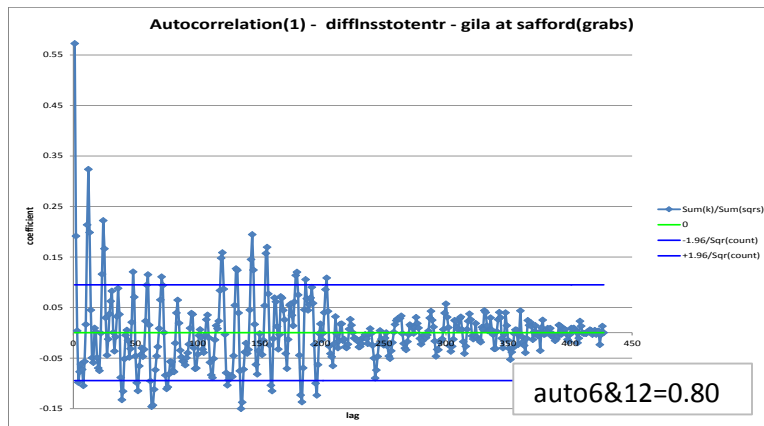


Figure 418

The inversion has been found to be a pattern that parallels the seasonal and now the total thermodynamic functions, including those which show no inversion, also have a seasonal aspect when viewed in a certain fashion. The three terms, inversion, seasonality, and the thermodynamic experiment, share a common factor – they are all complete analysis cycles. They exist at different time and spatial levels and their points of intersection vary with how they

are viewed. Here the fast and easy assumption that if any ‘view’ of a function is seasonal then the function as a whole is seasonal is used. The seasonality of total enthalpy and total free energy is an ‘underlying’ pattern, where the two are following volume and entropy, not visible at all levels. When the emphasis is put on normal behavior, however, all are found to have the same simple, functional pattern.

The graph below begins an attempt to pull together the relations between the main physical factors and system energy. This is all ‘real’ data numbers but normalized, i.e. from the low flow, low density regimes. The curves have been scaled to all fit together on one y-scale frame.

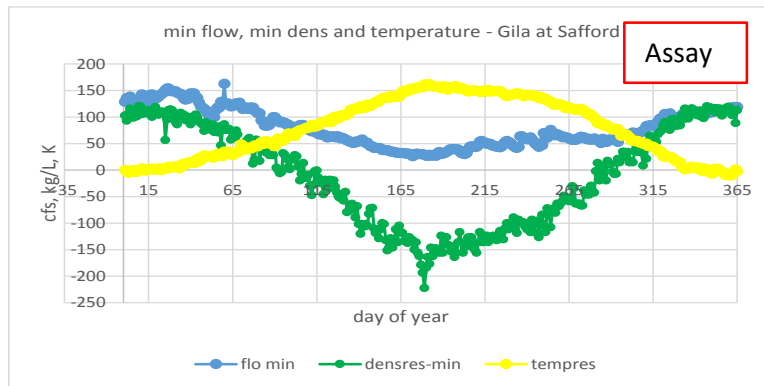


Figure 419

correlations major physical factors - Gila at Safford					
	alltemp	minflo	mindens	allflo	alldens
alltemp	1.00	-0.93	-0.99	-0.59	-0.99
minflo	-0.93	1.00	0.91	0.67	0.91
mindens	-0.99	0.91	1.00	0.59	0.99
allflo	-0.59	0.67	0.59	1.00	0.59
alldens	-0.99	0.91	0.99	0.59	1.00

Table 181

The matrix above shows the correlation coefficients among the major physical factors in both normalized (‘min’) and non-normalized (‘all’) forms. As expected, the day of year minimum flow is much more highly correlated to temperature than the non-normalized. There is not much difference for density because density is already normalized to volume which is highly correlated to temperature. So the more or less raw data shows similar patterns and high correlations when the data is normalized. But the picture is not functional – this is simply the way it is. A common pattern can be seen and linkages between the curves imagined but no clues are given as to what those links might be.

The graph below begins to move in that direction by working in the total thermodynamic functions and converting flow and density to the volume curves first found in the low flow analysis (Figure 70). The sum solution total entropy and enthalpy function curves were created by placing the monthly average values strategically on any day of the month to parallel the volume curves as much as possible. Thus, both volume and a surrogate for amount, total energy,

are shown to have similar patterns coincident at roughly the same points, for at least part of the year.

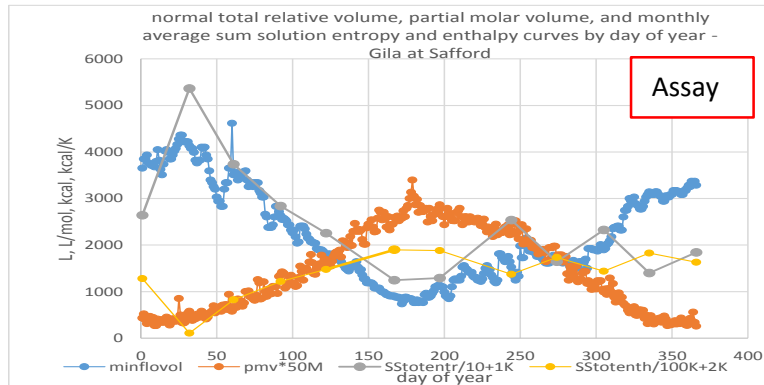


Figure 420

Changing the location of data points on the x-axis is not a recommended scaling technique because it changes the relation of the points to each other. It can be excused here on the grounds that a monthly average does not really ‘belong’ on one day any more than another. It is justified, in an ends-means sort of way, because it is helpful in fitting a dataset with gaps to one without. In this case, the overall shapes of the curves are not too affected as can be seen by comparing the above with the original monthly average curves. (Figures 410 & 411).

The energy curves, which have the same form as flow or inverse flow curves, follow the volume curves pretty well from Jan-Jun, not so well from Jul–Dec. The fact that they can be loosely fitted to the volume curve is not surprising since that is also derived from a flow curve of sorts. The relatively good fit is encouraging but the dimension of flow, despite its close relation to amount, is much too variably correlated and narrow in significance to adequately express the relations being sought here. And, in fact, the functional picture given by the flow-associated energy curves cannot possibly be correct.

The data just doesn’t ‘make sense’ in the late summer and fall period and the possible causes have already been covered. The summer monsoon is quite variable in start and end dates from year to year. The problems with designating the fall dry-down have also been discussed with the upshot that the October flow peak was dismissed as coincidental and probably due to low sample count. The thermodynamic data cannot be ‘wrong,’ if it is not simply erroneous, but it may not, for whatever reason, give the correct functional picture of the situation. The above picture is, for that reason, ‘incoherent.’

The conservation laws say that any expansion, any increase in mass or energy, in any part of the universe must be accompanied by an equal contraction, a decrease in mass or energy, in another part. If the system is complete enough to be considered a ‘universe’ of sorts and the dimension of time is substituted for the spatial distinction between system and environment then the relation becomes simply: any expansion at one time in the ‘universe’ (system) must be accompanied by an equal contraction. It is this equality that has never failed to be found which confirms that the two are cause and effect. In the temporal context, each is both -- a contraction is the effect of a

previous expansion and the cause of an expansion to follow. The full pattern is that of an ‘oscillator’ whose amplitude can increase, remain the same (equilibrium), decrease (dampening), or die depending on the magnitude of the original energy input and the amount of time involved.

The pairing of expansion and contraction appears to extend as far and as wide as one wishes to pursue it through time and spatial levels. But any symmetric pattern, any proportional reaction, is not necessarily a cause and effect relation. If the relation is understandable in terms of the thermodynamic laws, however, then it has a meaning it does not have otherwise.

The energy curves in Figure 420 above have basically zero average slope from Jul to Dec (day 200-365). The entropy valley for summer contraction, if it can be circumscribed at all without passing through a zero point reference, proceeds indefinitely to the right to produce an area quite out of proportion with the winter expansion peak. This result in turn means that the entropy curve must, at the beginning of the next year, precipitously and apparently spontaneously rise to produce an expansion peak that is no more proportional than the previous one was.

The picture below begins an attempt to use the patterns of inversion and season to show the true relations between the physical factors and the thermodynamic functions. In general, the solution (water) thermodynamic curves from the inversion difference by inversion status analysis (Figures 315-316) are superimposed on top of the physical volume curves found in the low flow analysis (Figure 70). The procedure is justified by the fact that these are two complete analysis cycles using the same data, the samples are just grouped and sorted differently. It is a two point fit using the best fit alignment of inversion status and season (Figures 406-409) with scenario 1 in winter and scenario 4 in summer. The functional is easily fitted to the chronological because, in the realm of normal behavior, they have the same pattern.

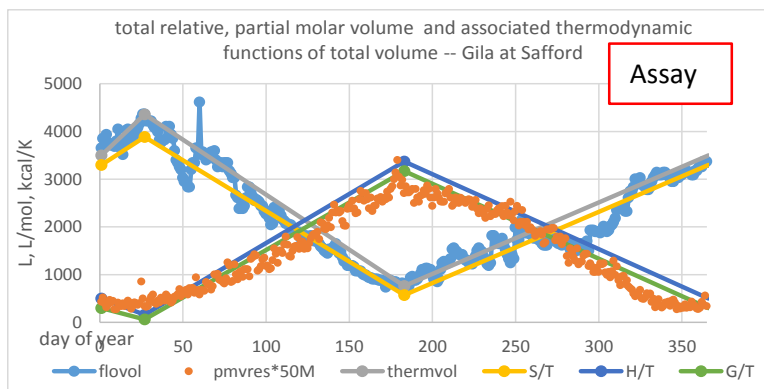


Figure 421

More specifically, the thermodynamic total volume curve is set equal to its corresponding physical volume curve. The thermodynamic volume curve is created with two points in Jan and Jun taken from the low flow derived physical volume curve. The slope of the line between the two points ( $r^2=-1$ ) is roughly equal to the trend line of the physical volume curve from Jan to Jun ( $r^2= -0.954$ ). For Jul to Dec, the thermodynamic slope changes sign to follow the associated physical curve. The thermodynamic volume curve associated with total volume is itself ‘normal’

because it is derived from the low flow doy curve which contains points from only the normal part of the flow distribution.

The question may be asked: ‘why just a two point fit? Why not equate the thermodynamic volume curve point for point with the physical volume curve?’ The thermodynamic volume is the volume with which all the relations of the other thermodynamic functions are in accord. It is only approximately related to the bulk physical volume which is determined by flow and physical barriers, etc. Not every specific instance of the physical volume is necessarily going to support the thermodynamic relations whereas every specific instance of the thermodynamic volume does by definition. If the thermodynamic volume followed the physical in every twist and turn the suggestion would be that the total volume was the only factor. The entropy would then also have to follow and the picture would be even more unrealistic because entropy has even more additional factors. The ‘artistic’ rendition makes it clear that these are two different curves with similar slopes at the full season level, not necessarily at any other level.

Entropy is determined from the proportional relationship of total volume and total entropy change as found in the inversion difference by inversion status analysis. The grouping by inversion status of grab sample entropies determined by temperature results in the creation of an entropy with respect to volume-amount change  $dS(dV)$ . Temperature, as it were, falls out of the equation or is subsumed in volume change. The rest of the thermodynamic functions follow by their proportional relations with entropy in the same analysis. They are converted to  $X(T)$  or  $X/T$  (where  $X = G$  or  $H$ ) by division by the characteristic temperature ( $T = (G-H)/S(T)$ ) for each scenario. Though scenario 1 ratios were used for winter, scenario 4 for summer, out of an excess of caution, the ratios are very similar for all scenarios. Scenario 3 is somewhat distinct from the others with higher entropy to volume proportion, lower enthalpy and free energy to entropy proportions and the highest characteristic temperature.

ratios with S/T				
sum solution total functions	V	H/T	G/T	char. T
scen 4	0.88	-15.1	-16.1	285
scen 1	0.89	-14.8	-15.8	288
scen 3	0.92	-13.7	-14.7	298
scen 2	0.89	-14.8	-15.8	288

Table 182

Let’s be clear about what is and what is not being done here. The trappings of a calculation makes the procedure appear to set up a relationship between volume and entropy for a liquid analogous to the ideal gas entropy equation --  $d(Vf/Vi)$ . In fact it is merely a rough correlation between volume and entropy. Its validity depends on there being a 1:1 relationship between a volume and an entropy, something that is not always true. While 30.1 L/mol of pure water at 1 atm has an entropy of 31.6 cal/mol\*K and no other, a 30.1L/mol solution at 1 atm can have any number of entropies depending on solution makeup. Here these differences are ridden over roughshod by using solution samples to derive the proportionality relationships. On the other hand, if a solution (not pure water) has an overall entropy of 31.6 then it cannot change in volume without changing total entropy. The thermodynamic volume codifies the relation



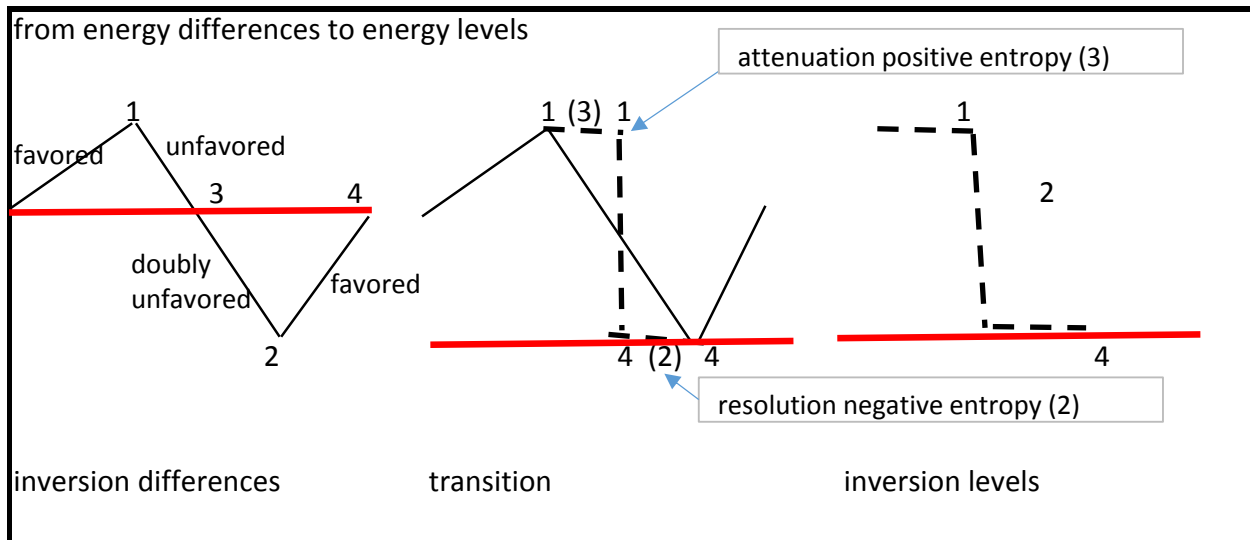
between volume and entropy that is really only one aspect of a complex relationship between temperature, amount, and pressure (for volume) and entropy via density. How simplified this picture is will be apparent shortly.

The first and last points of each curve are guesstimates based on where the curves need to end up to produce the same values in the next/previous year. Some of the point values have been changed slightly (100-200 kcal/K), without changing the slope, to keep the two parallel thermodynamic curves from overlapping each other. Enthalpy and free energy slopes are 'scaled' to match the associated entropy curve. Now the summer valley is proportional to the winter peak and the curve proceeds in a linear, incremental manner to produce another proportional peak in the following year. In a word, the data has been manipulated through the use of scaling and symmetry and forced to produce the 'correct' pattern.

All the major factors are included in Figure 421 – the partial molar volume curve is the same as the temperature curve and the inverse of density as well as a simplified version of non-solvent concentration while the total volume curve stands in for flow. More significantly, all the possible energy relations of a complete analysis cycle are also included here. The total volume/entropy expansion peak of winter leads to a proportional total volume/entropy contraction valley in the summer which is accompanied by an enthalpy/free energy peak with its own corresponding contraction the following winter.

Figure 421 above illustrates that both flow and density are linked to the energy implications of alternating system expansion and contraction. The underlying foundation is temperature change which not only sets the seasonal stage (x-axis) but also the bounds (y-axis). The partial molar volume and density are calculated from temperature and the thermodynamic functions are quite literally  $X(T)$ . The only factor not explicitly connected to temperature, flow, is connected by association with all the other factors. It is a 'web' of relations that can be examined for goodness of fit in terms of logical relations and/or quantitative links.

The observant reader will notice that Figure 421 above is not exactly as stated, the superposition of the inversion difference by inversion status thermodynamic curves for the solution (water). In the new picture, scenario 4 makes the valley in the summer rather than scenario 2. That's because the inversion pattern has changed from a 'differences' to a 'levels' picture. The rationale for the transformation is shown in the following schematic.



Schematic 10 ([back](#))

The transformation is brought about by dropping the zero reference line from ‘no change’ (3&4) to ‘scenario 4’. 3 and 2 are attenuations of 1 and 4 respectively in the differences picture and devolve to 1 & 4 in the levels picture. The dashed 1-4 line is constructed from the 1-2 line of the inversion differences and equal to it (something about congruent triangles here). The assignment of scenario 2 in the levels diagram goes back to its definition ‘from an inversion to a non-inversion sample.’ Scenario 3 (‘from an inversion to an inversion’) really should drop out of the picture but is devolved to 1 (non-inversion to inversion), to complete the seasons picture.

The large amount of extrapolation and use of symmetry and analogy needed to produce these pictures cannot be ignored. But neither should the final result be dismissed without looking at the inter-related patterns and what they may mean. But continued inspection is a two edged sword as the following considerations show.

The thermodynamic relations apply to the molar functions as well as to the total. So it should be possible to do the same association of the partial molar volume of water with the molar thermodynamic functions. The partial molar volume, however, presents some difficulties when the attempt is made to quantify its relations with the thermodynamic functions. To appear on the same graph with the total relative volume in Figure 421, the partial molar volume had to be turned into a residual and multiplied by 50 million. Here a residual is taken instead, subtracting the doy minimum from each value, and the result is a tiny value in the  $10^{-5}$  or  $10^{-6}$  range. (The sum solution of normalized partial molar volumes was also examined but the same problems referred to below were encountered)

Changing the visualization does not end the problems: the inversion difference by inversion status analysis, when run with the molar thermodynamic functions, looks rather strange. The characteristic temperature ( $T=(G-H)/S(T)$ ) found with the inversion difference analysis of the molar functions are in the 100K range, probably an indication that something is out of whack with the analysis. The slopes derived from the tiny residuals are huge and all plot on top of one

another, the fit to the thermodynamic partial molar volume is perfect, the relation to the physical data seemingly so small is completely ignored. The following table shows the results obtained and the ratios used.

ratios with dSm(T)					
	pmvres&dVm	dSm/T	dHm/T	dGm/T	
2/24	1.7E-05	1.7E-05	1.7E-05	1.6E-05	
6/30	7.2E-05	7.2E-05	7.2E-05	7.1E-05	
slope	2.3E+06	2.3E+06	2.3E+06	2.3E+06	
invstat	Sm/Vm	Hm/Sm	Gm/Sm	charTinvΔ	
4	1.01	3.0	2.0	100	
1	1.01	2.9	1.9	100	
3	1.02	3.0	2.0	96	
2	1.03	3.0	2.0	96	

Table 183

While it was possible to come up with some numbers, it is not possible to visualize them because the y-scale for the partial molar volume residual is incredibly tight. The ‘thermodynamic’ curves in the graph below are merely represented by the partial molar volume at those points and adjusted to follow the thermodynamic relations. In short, the ‘known’ thermodynamic function relations have been allowed to dominate and deviations from the actual physical data ignored. The values that ‘fit’ the thermodynamic functions to the pmv curve all plot on top of one another and are therefore only depicted as points. The only good thing about this picture is that it follows what might be expected from the daily analysis – the partial molar volume, entropy and enthalpy directly related to one another and free energy inversely related, also increasing but in the negative direction. It looks similar because it was constructed entirely from the daily analysis (also a hypothetical structure).

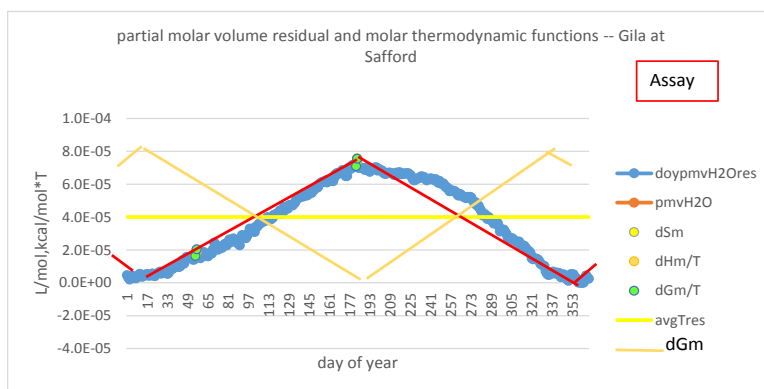


Figure 422

Almost anything can be scaled to anything else. The question is how ‘brutal’ is the procedure and when has it gone too far. In this particular case, the thermodynamic function residuals were converted to numbers with scenario 1-4 differences between -5.5 and -5.6E-5 which essentially strips their curves of any independent standing. That is not comparing one curve to another, it is

simply fitting a minuscule portion of one curve to another. A small enough segment can match any other curve.

The table below shows the original and final scaled numbers for the total relative (top) and partial molar (bottom) related thermodynamic functions. Because of all the ‘scaling’ involved here, about the only test of ‘fit’ is that between volume and entropy and even that is not totally independent. Note that the original partial molar volume and associated entropy slopes are very small and differ by about half an order of magnitude and that is about as much as needs be said for the ‘fit’.

the 'evils' of scaling				
original	totrelvol	totS	totH	totG
scen1	4361	3883	-57328	-61211
scen4	765	675	-10185	-10860
slopes	-23	-21	306	327
scen1-4dif	3596	3208	-47143	-50351
final	totrelvol	totS/T	totH/T	totG/T
scen1	4361	3883	163	163
scen4	765	675	3371	3371
slopes	-23	-21	21	21
scen1-4dif	3596	3208	-3208	-3208
original	pmv	Sm/T	Hm/T	Gm/T
scen1	0.01803	0.01821	0.01785	0.01767
scen4	0.01808	0.01830	0.01800	0.01785
slopes	0.59412	1.00000	1.67659	2.01489
scen1-4dif	-5.5E-05	-9.3E-05	-1.6E-04	-1.9E-04
final	pmv	Sm/T	Hm/T	Gm/T
scen1	0.000017	0.000017	1.7E-05	1.6E-05
scen4	0.000072	0.000073	7.2E-05	7.1E-05
slopes	2.3E+06	2.3E+06	2.3E+06	2.3E+06
scen1-4dif	-5.5E-05	-5.6E-05	-5.5E-05	-5.5E-05

Table 184

Returning to the picture of Figure 421 for a moment brings out a fine example of ‘pushing’ relationships too far. The fact that the enthalpy/free energy curve associated with total volume parallels the partial molar volume curve is coincidental, a result of having scaled the partial molar to the total relative volume curve. The association seems like it might be significant because the volume/entropy functions relate more to the bulk volume while the enthalpy/free energy seem more relevant to the ‘inner packing,’ whose representative is the partial molar volume. The association is, however, ‘reaching’ and the enthalpy/free energy curve of the total volume curve has no quantitative tie at all to the partial molar curve.

Having reached the edge of the precipice, there is really no reason not to look over the edge. The following graph is the same as Figure 421 with one sleight of hand difference. The picture has changed to include only the physical total and partial molar volume curves and their associated total and partial molar entropy curves respectively.

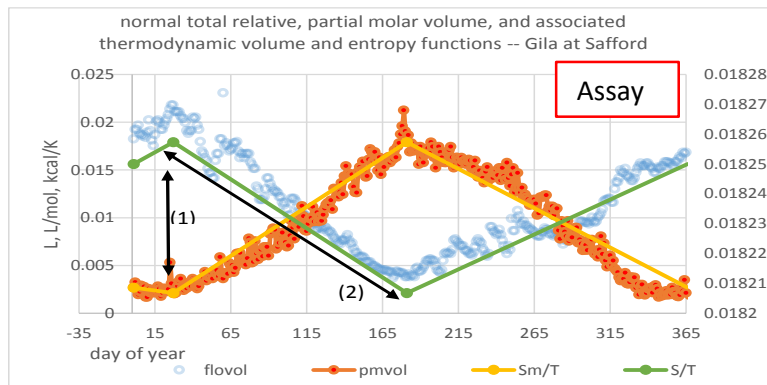


Figure 423

From their similar positions on the graph, a relation is suggested between the winter total volume/entropy peak and the winter partial molar volume/entropy valley (1). The relation looks just as convincing as that between winter total volume/entropy peak and the summer total volume/entropy valley (2). In fact, the relation was suggested as so important that it is one of two that 'prove' the basic two season structure posited here (Figure 70). But while physical volume curves become 'coherent' through their similarity to thermodynamic function curves, different physical curves have no such relation.

Being able to visualize a relation does not make it real. Besides having quantitative links to physical factors, the relation must fit in with other relations, i.e. they must corroborate each other. Sometimes the only way one can realize that one is on the wrong path is when a graph generates a relation that cannot possibly be correct (Figure 423). Here it is the difference in magnitudes that makes one hesitate. On the other hand, just because a relation cannot easier be visualized (partial molar volume and molar functions) does not mean it does not exist.

The immediate consequence here is, at the very least, that not all the curves of Figure 421 are related to each other in the same way. The normal total volume and partial molar volume are both affected by temperature at very different levels but have presumably little or no cause and effect relation with each other. The result is disappointing but not, maybe, unexpected and means that the 'pulses' of [Figure 70](#) will have to be re-formulated.

Attempts to perform even a limited analysis on 'real' world, un-normalized data also leads quickly to difficulties. With a low flow year, such as 1977, and extrapolating out the summer monsoon, the analysis seems to work fairly well. The graph below left shows only the crucial two point fits for the total volume associated curves in 1977. With a high flow year such as 1993, below right, there are obvious problems at the outset. The Jan to Jun average slope is anyone's guess. Either an average would have to be devised and the slope would depend entirely on that value or the max flow period ignored entirely to rely completely on the spring dry down slope. Neither 'solution' seems acceptable.

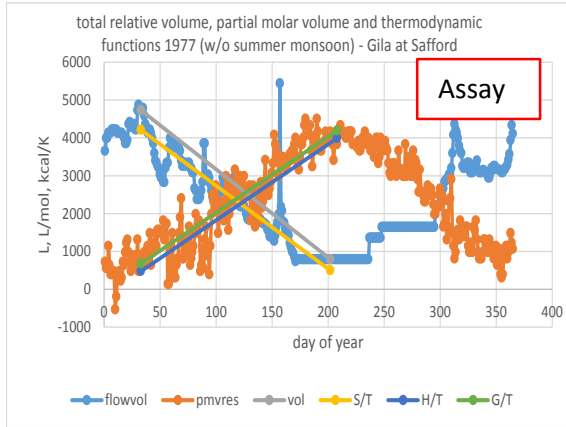


Figure 424

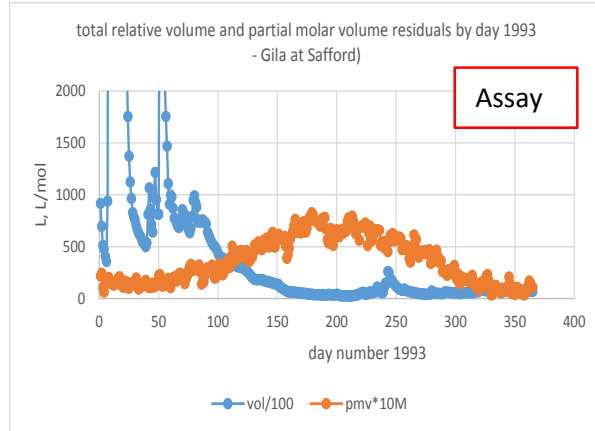


Figure 425 [\(back\)](#)

Trying to put ‘everything’ into one picture, as desirable as that may be, seems to be a hopeless task. The final picture will instead be divided into two graphs. In the first, temperature is shown directly, not represented by anything else, and is, in addition, divided into two curves – the seasonal and the daily temperature fluctuation, the latter shown in a cut-out. Density re-enters the picture and the total relative volume and associated total thermodynamic curves are removed. The partial molar volume of water takes its rightful, central role.

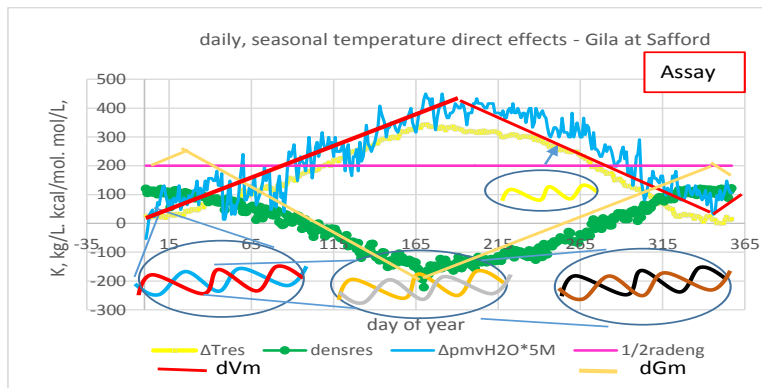


Figure 426

Aside from looking a little cluttered, the above figure neatly sums up the patterns of direct temperature induced expansion and contraction. Density follows inversely the pattern of the annual temperature curve. The partial molar volume of water and the thermodynamic functions with free energy in functional form, are inversely related to density,

The thermodynamic molar function daily fluctuations are shown in three cut-outs of the partial molar volume curve. The first shows the daily molar volume group (blue) and the undifferentiated heat content group (red) inversions. The second presents the heat content group daily inversion of entropy/enthalpy (grey) and free energy (gold). The third shows Na (black) balancing the other major ions for entropy/enthalpy and Ca & Mg (brown) balancing for free energy. The magenta line across the center of the graph is the sum  $\frac{1}{2}$  radiant energy input

differences as well as the average absolute temperature. It will vary only slightly in position from year to year. The influence of temperature is so immediate, apparent, and predictable that the patterns of direct temperature dependence are a large part of what we conceive to be 'normal' behavior.

The splitting of the temperature curve into a daily and a seasonal fluctuation suggests that these are two distinct levels of energy change. They are the same pattern of alternating radiant energy input and the lack (or lessening) thereof but manifesting in different time and spatial frames. The daily energy input pulse is caused by the rotation of the earth on its axis, the seasonal modulation by the earth's rotation around the sun. The response pattern elicited may or may not coalesce into a coincident pattern. The seasonal density response, for example, is clearly the inverse of the input. The daily energy input for density, however, is dissipated into a number of different curves based on a variety of factors and more sophisticated methods would be required to delineate these and find an acceptable average curve.

The tiny molar thermodynamic function daily differences are entirely a function of the daily temperature range. The effect of dividing by volume (density) is quite different from that of dividing by amount (partial molar volume) because the former is sensitive to temperature change while the latter is not. The sameness of areas for day/night or winter/summer is an artifact of the analysis which makes the energy cycle seem a complete one. But the response to temperature of the partial molar volume is to differences of temperature not absolute temperature. While the daily temperature curve represents a more or less complete energy cycle, a temperature range is not a cycle.

The second 'final' picture (below) also has the seasonal temperature at center stage with a cut out for the daily temperature curve. The total relative volume and associated total thermodynamic functions as developed above return to the picture. The slight daily fluctuations in the total functions caused by small changes in the molar entropy/enthalpy (yellow) and free energy (green) (Table 139) are shown in a cut-out. These last are probably only measurable in the months of May and June when variation in amount is at a minimum.

The green line running across the center of the graph is the seasonal  $\frac{1}{2}$  volume line. It will vary in position only slightly from year to year in the normal mode picture. It ensures that the winter volume/entropy peak and the summer volume/entropy valley are proportional to each other. The line is a definite physical value but it has 'magical' properties because it casts the spell of 'coherence', a term which will be defined shortly.

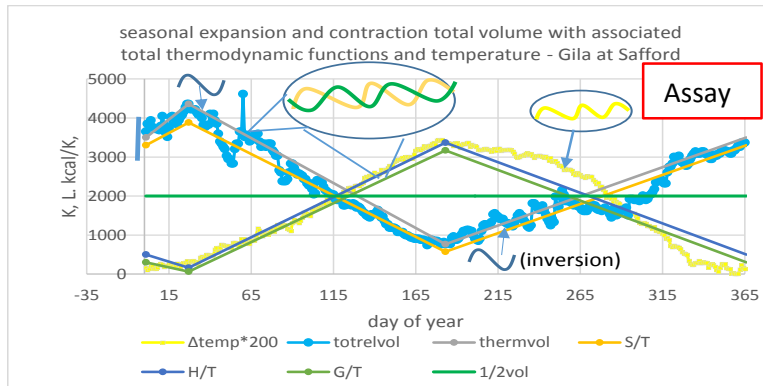


Figure 427

This picture sums up the flow (amount) induced expansion and contraction of volume in the normal, low flow mode. It is an on-going process, the negative entropy change of summer resolved by the positive enthalpy change of summer as well as the positive entropy change of the following winter in seemingly unending succession. It is caused by the seasonal precipitation pattern which is ultimately a result of temperature change, though as ‘climate.’ So, somewhat ironically, the nebulous ‘clouds somewhere over the Pacific or the Gulf of Mexico’ are back!

This innocent looking graph stretches the norms of graphing far more than any of the previous graphs that merely use residuals. Here, the temperature shown on the graph, the temperature at Safford, is only a surrogate for the temperature that actually causes the change in amount. The entire mechanism proposed, cloud formation and subsequent condensation and precipitation, starts not only outside but also ‘above’ what is depicted on the graph. The graph shows only the effect and not the cause or any clue as to the mechanism.

The increase in the total volume of water of the early part of the year is not caused by the drop in temperature at that time. Rather, it is the effect of a previous temperature / volume increase in (an)other place(s). The winter total volume expansion at Safford is a result of a summer volume partial molar volume expansion occurring in a different place or places, not in the same spatial framework of the picture. That is to say, the increase in amount here is a lagged result of another temperature/volume change and not related to the current temperature. So while the increase in total volume appears to be inversely related to temperature it is actually the time-lapsed effect of a direct relationship with the partial molar volume. The bottom line is that the mechanism would not have been discovered with correlational analysis alone and is imposed on the data with information from entirely outside the dataset.

Temperature is the most important factor in the picture of amount transport here but not the only one. At Safford in the early part of the year a large amount of material (largely water) is transported from another area (over the oceans) via temperature and pressure induced change in volume. The amount of water that falls on Safford is exactly the same as the sum of all the water that formed the clouds over the oceans minus the amount that fell elsewhere (not being able to easily calculate, we take this on faith). As the water vapor condenses over Safford, forms rain, and falls to earth, it begins to flow from higher to lower elevation and ‘picks up’ new amounts of material (the ‘things’ in water) to transport. There are a host of factors such as location, geology



(hard and soft terrain, deposits) and current speeds which determine exactly which parameter amounts will increase and by how much. This type of post-precipitation change in amount has nothing to do with change in temperature but is loosely related to the quantity of water so is indirectly and weakly related to the initial cloud forming temperature change (see schematics 3 & 4).

The big picture here is that an expansion and contraction cycle at one level (in the atmosphere) is translated or transformed into an expansion and contraction cycle at another level (increased amount/flow of the river). The only common factor between the cycles is the amount of material transferred in its entirety from one to the next. In terms of energy, each cycle is assumed to be complete and negative entropy completely resolved at each level.

Here the water cycle has been broken up into two complete sub-cycles. If the water cycle is considered as a whole, the following would apply. In winter, increasing amount of material from the environment causes the system to expand, working on the environment. The environment responds by gaining an amount of heat equivalent to the increased amount of the system. In summer, the environment works on the system, forcing part of the new material amount back to the environment. The system gains heat equivalent to the amount of material returned to the environment.

In both the daily and the seasonal view, the enthalpy change is in the same direction as ambient temperature change but in relation to expansion/contraction the role of enthalpy is different. Heat gain fuels daily volume expansion, heat loss accompanies seasonal amount expansion. What remains the same across the two scenarios is that volume expansion is accompanied by positive entropy and increasing functional free energy, the last being made possible by the flip in the role of enthalpy. These remarks merely tabulate graph results but 'slice' the system and the environment for a different view.

One final remark may be made comparing and contrasting daily and seasonal enthalpy. In the daily volume expansion, a huge amount of heat is available but only a tiny fraction used to make a slight increase in system volume. The corresponding work of the environment in night-time contraction is therefore quite small. In the case of seasonal amount expansion, the environment is comparatively speaking 'moving mountains,' making large scale changes to the system over a longer time period. The daily is an 'instantaneous' phenomenon involving a tiny uptake of heat from the environment, the seasonal is an 'incremental' phenomenon involving a larger change in the system and a much larger work effort by the environment.

The data in Figure 427 shows that the fit of the seasonal temperature curve and total volume-related enthalpy/free energy is very tight from Jan to Jul, not so much from Jul to Dec. The lack of fit suggests that the problems associated with scenario 3/fall season may not be entirely a matter of difficulties in delineating the chronological boundaries. It may be symptomatic of a deeper discontinuity in the system. Fortunately, the most predictable portion of the year, the May-Jun dry-down, clearly separates hiflo and loflo, making the anomalous nature of summer storms, which occur during the loflo period, apparent.

Some seasons are commonly thought of as being seasons of ‘expansion’ and so equating their pattern with the inversion pattern seems natural. But how closely do the details of the seasonal flow induced expansion at Safford follow the details of the inversion pattern? What would be predicted would be that winter be a season of 1) relatively higher activity of water, 2) lower Cl and higher HCO<sub>3</sub> activity, 3) higher solution entropy 4) higher solution ionicity, 5) high percent speciation of ion pair forming free ions, and 6) lower neutral ion pair activity. The graphs below plot loflo, hiflo-summer, and hiflo-winter results from left to right of the above six analyses.

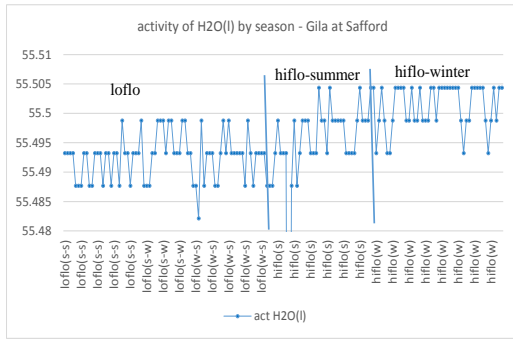


Figure 428

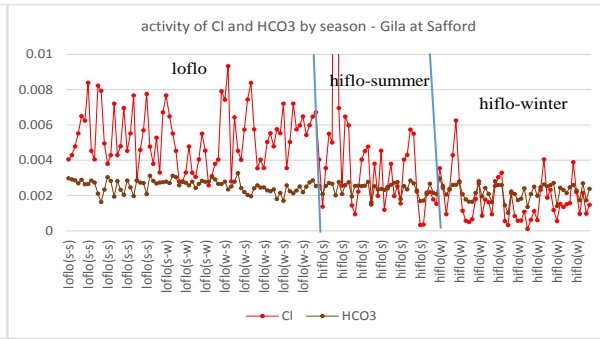


Figure 429

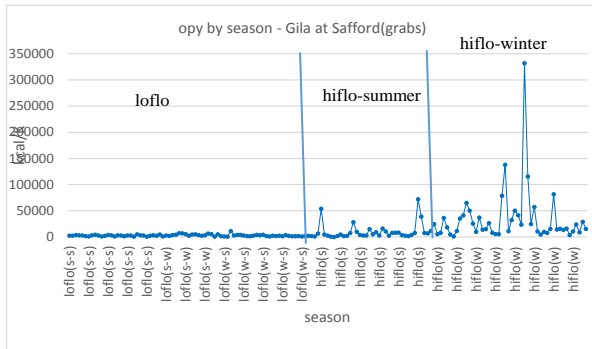


Figure 430

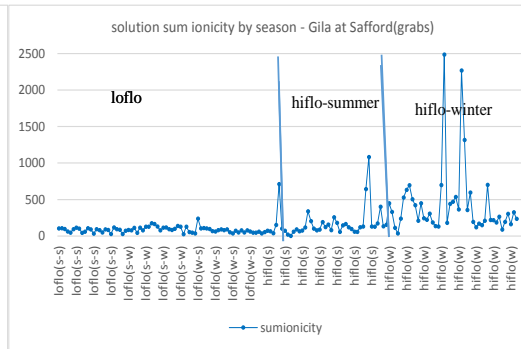


Figure 431

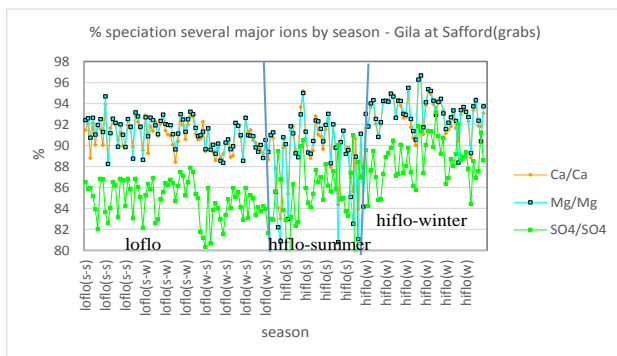


Figure 432

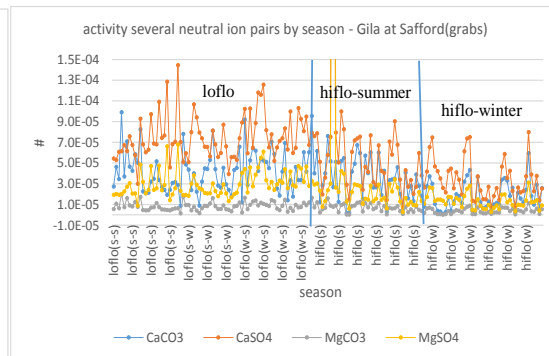


figure 433

The first three graphs show that the hiflo context is the same, the last three suggest that the matrix shift of inversion may manifest itself on a seasonal basis. Note how, in several of the graphs above, the summer season has a bit of a slope that connects loflo to winter hiflo even though these are random, non-sorted, non-chronological values. The summer season is, in many ways, a transitional state. It is therefore not surprising at all to find Fe(OH)<sub>3</sub>, the ‘transitional’ parameter, with high activity in summer.

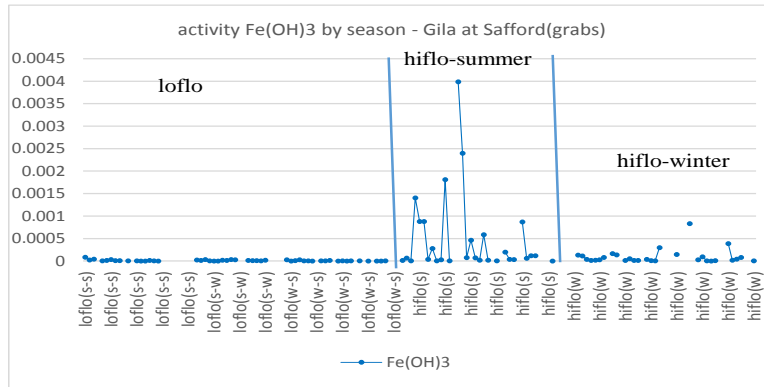
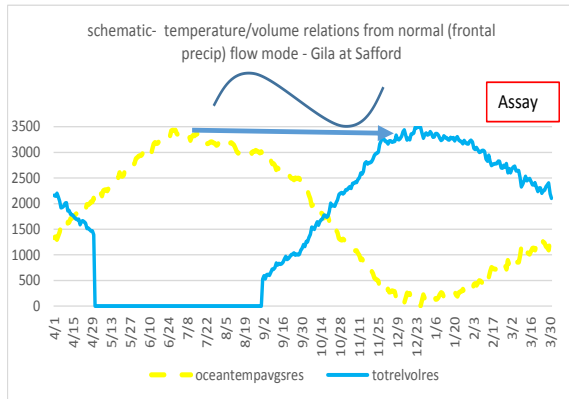


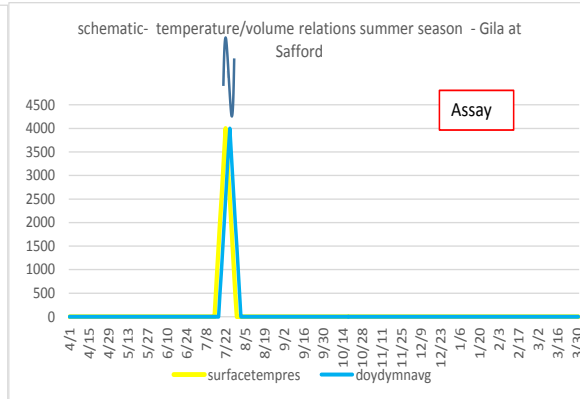
Figure 434

Altering the perspective may or may not help visualize relations but finding a normal (i.e. reproducible) pattern is usually the end of the story. The above normalized picture of system seasonal expansion and contraction at Safford (Figure 427) is made possible by the fact the frontal rain precipitation pattern dominates the normal flow mode over the time span of the study. It is not, however, the only picture possible here and, in fact, the most reproducible part of the season is the summer monsoon. In the convective storms of summer, temperature induced cloud formation occurs near Safford, not somewhere far away. The ‘temperature’ change that causes the storms is not what is commonly called the ‘ambient’ temperature but rather localized pockets of warm air rising from the surface of the heated earth.

The following schematics, which change the time frame to 4/1 of one year to 4/1 of the next, illustrate the two regimes (recalling the earlier reference to the probable importance of April and November). The arrow in the frontal precipitation mode picture to the left below depicts the spatial/temporal distance as well as the true, directly correlated cause and effect. Only one storm is shown for the summer monsoon to the right and the temperature is an earth surface temp not an average ocean temp. The two regimes are separated in the schematics but cannot be separated in the normal mode picture. The summer monsoon registers on the normal mode picture (Fig 427) as a slightly steeper slope from 163 (7/1) to 268 (9/24) than might be expected for the normal curve and there is a compensatory ‘step down’ after day 268.



Schematic 11



Schematic 12

So while the summer season is in many ways ‘transitional,’ it may also, in certain views, represent a discontinuity in the normal mode picture. The anomalous dips that occur in July, August, or September in many analyzes are the result of a collision between the two different entropy situations that the system finds itself in. It may be wondered why the entropy situation of the river is different in summer than winter. After all, the ‘explosive’ summer entropy situation is in the clouds above the river not in the river water itself. But while the entropy situation above is presumably completely resolved above, the material transferred is placed in a similar situation. Flows are lower in summer, so a local downpour represents a sudden, large percentage increase in volume. More importantly, not followed by more precipitation, the initial surge subsides rapidly and the system contracts rapidly.

The schematics above are two versions of the same underlying physical phenomenon – the water cycle – in different spatial and temporal frameworks. The frontal volume expansion is the gradual attenuation of the positive entropy of an expansion that occurs far away: the tendency toward a negative entropy slope with contraction is put off as long as possible. The summer monsoon may be seen as an attempt to quickly resolve the entropy consequences of a rapid local expansion and contraction. The normal mode picture is ‘squeezed’ in both time and space and the result is explosive. The differences between the two water cycle regimes, winter/frontal and summer/convective, suggest that over time mechanisms come into play that mitigate the ‘explosive’ aspects of entropy control in rapid, local expansion and contraction.

Bringing the ‘clouds somewhere over the Pacific or the Gulf of Mexico’ back into the picture, treated as an ironic development before, actually does two things for the analysis. It reveals the connection between what is going on at Safford and the ‘water cycle’ which is a well-known and established physical phenomenon. But it also provides a needed sense of proportion, if only in a relative way, back into the picture. It was stated earlier that the partial molar volume of water is at the heart of the analysis here but only a slight temperature dependence was found and the relation to the total relative volume labeled as ‘misleading.’ Now, however, it is possible to see that there is, in fact, a huge change in the partial molar volume involved here – namely that associated with the phase change from water to water vapor – from 0.017 L/mol to (ideally) 24 L/mol about 1400 times (1600-1700 times is often cited). An expansion of this magnitude is accompanied by a huge change in entropy.

These considerations shed light on the failed attempt to create a rapprochement between flow and density. The relationship was translated to that between the total relative and partial molar volumes. But the crucial relationship is between the partial molar volume and density as the following considerations make clear. Liquid water at 273.16 has a volume of 0.018 L/mol and an entropy of 2.9E-5 cal/mol\*K whereas water vapor at 373.15 has a volume of 30.1 L/mol and an entropy of 31.7 cal/mol\*K (webbook.nist calculations both at 1 atm). But while a pressure change of 1 atm causes only a small change in volume at 273.16, an additional 0.0009 change in atm at 373.15 causes a huge change in volume because it causes a huge change in density (0.033 to 53.2 mol/L). The attempted rapprochement was being made not only with the wrong 'view' (analyzes) but also in the wrong place and at the wrong time!


The proposed mechanism will, unfortunately, have to remain largely 'up in the air' for a number of reasons. The first is that atmospheric physics is outside the scope of the methodology used here. The second, and more important, is that our database gives no clues as to what is going on in the atmosphere above Safford. The ambient pressure of the grab samples is completely uninteresting, presents no patterns and does not correlate with any other parameter. Any conjectures on the details of the water cycle mechanism, beyond the general volume/entropy relations, would be even more speculative so only a few general remarks will be made.

What can and what cannot be said about the system as portrayed in figure 427? What cannot be said is that solution entropy is negative in summer, positive in winter. The solution entropy as a single value at any particular point is not known. For the above picture to make any sense at all, it is necessary to postulate that entropy can exist at any number of levels. The most that can be gathered from the above picture is that the volume component of solution entropy is lower in summer than in winter because the system as a whole is in a period of contraction. Lower or lessening entropy is analogous to 'negative' entropy and must be resolved. That the volume component is one of major significance can be deduced from the fact that system enthalpy, heat gain in the summer loss in the winter, follows in line with the natural process.

But there are other components and/or levels of entropy control not included in the picture that may be involved in the summer/winter response difference. It was suggested earlier that winter samples may better represent the entire watershed than summer. One might therefore expect to see more parameters present in winter samples than summer but that does not seem to be the case. Of the 157 parameters analyzed, summer storms average 53% while winter and loflo about 49% each: too close for such a crude analysis to be significant.

Where a more significant difference may be found is in the percent non-H<sub>2</sub>O contribution to total entropy but it does not divide winter from summer samples. Instead, hiflo samples (i.e. both winter and summer at 0.018 and 0.024% respectively) are quite distinct from loflo samples at 0.030%. This finding has several implications. It suggests another reason why scenario 4 (loflo) is more stable than 1 or 3 in spite of lower volume/entropy. But it also underlines why summer storms are such a discontinuity in the normal mode picture – there are less not more parameters involved in entropy control than in the loflo regime in which they occur.

The two regimes are seemingly two extremes of a situation that plays itself out in numerous different fashions, depending on local conditions, all over the globe. The phase expansion of the partial molar volume of water is undoubtedly larger in the tropics than in more northerly regions where, for aught we know, there may be different and unique mechanisms at work in the stratosphere. Different weather patterns existing on top of local factors like mountain ranges, wind speeds and directions, and humidity will result in the same basic response being expressed in different ways.

Figure 434 and schematics 11 & 12 are the last pictures of data, either real or hypothetical, and the study proceeds with verbal argument only and at a more general level. Analysis divides up phenomena on different graphs, synthesis requires not only creating 'summaries' but, as has already been seen, occasionally even looking 'between' or 'outside' the graphs. There is another way in which what is not in Figure 427 above is as important as what is. The max flow regime is largely left out of the picture. The inversion is the only representative shown (  ) because it can be located in time, at least in a very loose way, whereas max flows are random across most of the year. The inversion is depicted as points of non-normal behavior randomly dotting the larger, normal behavior curve. The icon represents only a single point or, at most, a number of consecutive points, along the larger curve. It is emblematic of a much larger, similar curve that parallels the normal curve point for point which cannot easily be visualized due to its variability from year to year.

Consider the inversion icon and the normal seasonal total relative volume curve of Figure 427. There is a happy coincidence of curve form which suggests that non-normal and normal behavior are also coincident. That is, the response to higher than normal flow in an inversion period is exactly the same as that to normal flow over the course of the year. It is just different in magnitude and condensed into a smaller time frame.

'Normal' and 'non-normal' behavior have been separated in Figure 427 but the full picture, including non-normal behavior, would be largely the same in any given year with only steeper total volume curves. The total thermodynamic functions adapt to each new situation seamlessly, adopting steeper slopes, perfectly able to adjust to the expanded y-scale. The 1/2 volume line moves magically up and down the y-scale, ensuring the proportionality of volume/entropy peaks and valleys. The 'problems' of [Figure 425](#), the non-linear total volume curves of Jan-Jun, are just problems in the analysis.

The normal flow curve is an average of single year minimum flow curves. If all the yearly day of year minimum curves are shown together, as in [Figure 60](#), they have the same tight relationship between curves and average as seen with the density curves. A more explicit and extended definition of seasonality for flow/amount has, with some manipulation, been achieved. The low flow, normal curve can be reformulated without much loss of information into a mathematical curve, roughly a sine wave.

Reducing everything to normal conditions is only important because it suggests that the thermodynamic functions fit to the physical data is a general relation, not one that applies only under certain conditions. The patterns are the same but the slopes are either always a part of the (early, normal) response or only applicable to very particular cases (non-normal). It was said earlier, in the comparison of min and max flows, that the maximums are not simply multiples of the minimum flow. That, however, is only because multiplying by a constant changes the slope of the entire curve not just a portion of the curve. It is more useful to think of the 'normal' as an 'underlying' pattern, an integral part of the non-normal 'multiples' of the real world.

The various visualizations of the relation between normal and non-normal behavior shown or suggested all grow out of how time is used or depicted. The only invariant dimension of the

control volume, time, becomes the essential factor in separating control volumes under normal conditions from those under non-normal conditions. With the same imaginary time axis into and out of the figure as used in [Figures 391-392](#), it is possible to ‘squeeze’ the seasons into an inversion period or ‘expand’ the inversion out to the thermodynamic curves of the universe. The more time and space is allowed for a process to work out, the more normal the resulting pattern. So much for sameness of pattern which is a property of all complete analysis cycles.

The meaning and scope of the three patterns, however, range from extremely particular to highly general. The inversion is limited to very particular conditions in time and space while the seasonal applies only to the full year frame. In either case, even a slight change of the temporal and/or spatial framework disrupts the pattern entirely. The thermodynamic functions apply over any and all periods of time and from the most particular to the most general conditions but are only seen at work in complete cycles of complete systems.

The crucial thermodynamic relation linking inversion and season is the relation of entropy to time. It is the superposition of the chronological physical data onto the analytical entropy end states that makes the picture ‘coherent’ by revealing (physical) form and (thermodynamic) function to be the same, as they are in nature. Not only are the patterns the same, but the chronological physical data is also seen to fit the same energy-in-proportional-to-energy-out requirement of the thermodynamic functions of a complete cycle. It is the differing ‘history’ of the thermodynamic function standard values that allows the inversion entropy end states to be isolated. It is the timing of dissociation and formation of ion pairs that allows the inversion to maintain the new high entropy inversion matrix. The connection between entropy and volume is most apparent at first glance, the connection between entropy and time (and ‘timing’) takes on more significance upon further consideration.

Time is the essential factor in finding the ‘pulses’ so long sought. Previous attempts had the level (flow) and time frame (high flow periods) too narrow. Pulses exist at many levels but are usually clear and unambiguous only at the most general level and the longest time frames. They are expressions of alternating expansion and contraction but their scope and significance comes from the fact that they are embodiments of ‘time’s arrow:’ i.e. entropy. It is entropy that makes the ‘direction’ of (simple) functions like expansion and contraction meaningful. Only when the energy implications are fully expressed do the pulses begin to clearly stand out from the ‘noise’ of lesser, not fully expressed, pulses. Note that the pulses shown in [Figure 427](#) are not, as in [Figure 70](#), of internal and external volume (mechanical), but those of the total thermodynamic functions that follow total relative volume. They are energy pulses growing out of earlier volume pulses which in turn grow out of earlier energy pulses.

There is really nothing new or unexpected here. The ultimate dependence of system energy on the alternating presence/absence or lessening of radiant energy input from the sun is obvious. The alternation of expansion and contraction, the high flow context of major ion concentration inversion, is intuitively understood to apply to the seasons as a whole as well. The only thing here that is possibly ‘new,’ though hardly unexpected, is to show how much ‘reduction’ of the data to its most normal form had to be done to make the parallels in pattern apparent.

The problem with such a highly generalized picture using such unassailable factors as the thermodynamic laws is that it may lead to the belief that what has been found here can easily be seen in all waters. It is undoubtedly true that alternating expansion and contraction and the energy relationships they entail are universal functions. But linking these to the seasons may have a very different look in other cases. And major ion concentration inversion is not a very common phenomenon, as far as is known, in other waters. Even if it were, without the link to the seasons the parallels to the total thermodynamic functions could not be made.

But maybe a less sweeping finding may point to the general relevance being sought here. That entropy control is spread out to as many players as possible, which is in line with the view of entropy as a maximizing of probabilities, is probably universally true. Nature, it seems, solves problems of balance by seeking out alternative parameters to solve common functions. Resilience is not merely the presence of many parameters or how many are taking part in entropy control (cf p. 330) but rather the average 'replace-ability' of those parameters.

A simple example of resilience is found in the roles of iron and silicon. Both have important roles to play in the entropy difference between inversion status 1 and 4, inversion and non-inversion states. They seem to provide largely the same functions and act independently of one another. Though the data is a bit sketchy, it seems reasonable to suppose that if iron is in short supply, silicon may be able to take its place and vice versa.

Resilience is, in its most fundamental definition, a mechanical property of materials to want to maintain their most stable form. It is built-in to the molecular makeup of material objects (i.e. exists at a level unknown to classical thermodynamics). Highly elastic or compressible materials that quickly regain their original shapes after they have been stretched or compressed are called 'resilient.' All materials have some resilience though it may not be great in magnitude or a particularly rapid response. It is difficult to define the resilience of (bulk) water because it alters its most stable form depending on conditions: it is either infinitely resilient or not resilient at all at a bulk level.

To apply the term beyond the simple mechanical response of a material object to heterogeneous, complex systems there must be more than one option available to the system. Both types of inversion, molar function and major ion concentration inversion, have options built in but at different times and levels. In the first, it is the existence of two different responses to the change in sign of the temperature difference slope that is the sign of inversion. The second has no options at its onset, beyond the differential response to increasing flow of bicarbonate and chloride (both directly related to flow), but develops them as it proceeds.

(It must be admitted that the molecular level picture of resilience being developed here is probably not at all what most people have in mind as the 'resilience' of a river. The factors affecting larger scale resilience have more to do with water quantity than quality and geological and human factors are more important than simple temperature dependence. It is not reasonable to assume that molecular level resilience can have any effect when a river is faced with continual drainage that exceeds inputs. Resilience here is a property of 'living', or at least pulsating, systems capable of 'growth,' or at least expansion, and cannot overcome death)



The daily on/off pulsing of radiant energy from the sun as seen from behind the collinear earth is like a 'Morse' code sent out to the rest of the universe. For the earth, modulated by the near/far seasonal relation of the earth, the energy pulsing 'teaches' organized systems the meaning of entropy. Too much expansion (positive entropy) leads to disintegration of organized systems which can be stretched only so far before 'flying' or 'falling apart' – the signature of entropy. Too much contraction leads to annihilation because forcing together the 'inner workings' too much leads to repulsion. Daily and seasonal thermal expansion and contraction elicit a relatively mild 'resilience' response that allows each system to 'test' the feel of change in entropy.

Resilience is a type of 'stability' – the ability of a system to resist change. It is, however, not only a property but also a function with two inputs – entropy and system organization – that works on form. While the preferred direction of entropy is clear, the meaning of direction in entropy with respect to an organized system is essentially ambiguous. Too much expansion leads to disintegration but some expansion is necessary for growth and development of the system. Too much contraction leads to inner repulsions but some contraction promotes the development of 'inner' structures that strengthen the system. Resilience is the finding of optimal options in the opposing tendencies that both positive and negative entropy present, neither explosion nor implosion but rather continued, modulated growth.

This basic a function with a relation to entropy control cannot involve only random sets of parameters like iron and silicon in the above example. It has to involve the structural relations of all the parameters that make up the entire organization of a system in the process of a major expansion. Scenario 3 represents the attempt, at the cost of a certain amount of heat loss, to maintain a newly re-organized system in a period of maximum expansion without flying apart and without incurring the cost of negative entropy. Only two 'scenario 3' samples occur in summer, the other twenty five occur in winter, the period of greatest system total volume expansion.

The matrix shift is accompanied by a host of new players which the system must incorporate. The roles and relations of old players must change to accommodate the new: the major balancing factor in entropy control goes from Na and Cl balancing each other to their both balancing HCO<sub>3</sub>. These are the options the system is presented with and fluctuates between as the inversion process plays itself out. The change causes a 'ripple' effect throughout the system with the inter-relations of all parameters changing to adjust. All of the inversion diagrams of the thermodynamic functions, since they are all involved one way or another with entropy control, are therefore 'patterns of resilience' at different levels.

While still adjusting to 'what is there,' the system in the matrix shift has more options to choose from. The same lining up of affinities depending on what happens to be available works itself out all down the hierarchy of values. The configurations with the most parameters involved in entropy control are more stable because each player is responsible for only a small portion of total entropy and is more easily replaced by a like parameter, also with a small portion. Ease of replacement becomes a major factor in stability in high entropy situations. In high enthalpy situations, the effect of changing the enthalpy contribution of one minor player for another is usually negligible and the major players dominate.

The movement of rivers has fascinated men for centuries. It is the extreme plasticity of water, the acme of fluidity and power, which makes a river the embodiment of resilience. The shift in matrix seen in the inversion process is in the non-normal, high flow domain but it is also present in the normal flow, seasonal picture. In either case, the response can be seen as part of an attempt to attenuate the positive entropy of a state of expansion, flying in the face of the fact that, over time, all oscillations eventually dampen and die. It is for that reason that the matrix needs an influx of new material (an entropy boost) to maintain itself. But the mass action response of the ion pairs is 'normal' behavior, in the loose sense of 'not limited to the particular case of inversion', occurring within what, at another level (flow), is a non-normal phenomenon. The response, it seems, always starts out as normal of course, is pushed by particular circumstance into the non-normal, but retains the same characteristic pattern.

What makes the Gila distinct from other rivers is that, because of the extreme environment in which it exists, the response is accentuated, the different forms isolated from each other over time. The patterns that evolve in both the individual inversion event and the normal mode can be categorized by the relationship options that emerge to resolve negative entropy and / or attenuate positive entropy. But is a matrix shift, the attempt to attenuate the positive entropy of an inherently unstable system expansion, found in any river in a period of expansion or is it unique to that most resilient of rivers – the Gila?

.....

## Afterword

The dream of classical thermodynamics is that everything is related to everything else, an idea that has resonance in the religious thinking of many different faiths. But the hard reality of thermodynamics is that the basic ideas that give rise to this ‘dream’ were built up with a series of experiments of very limited scope performed under conditions of excruciatingly tight control. Infinitesimal change in closed systems under isobaric, isothermal, and/or isenthalpic conditions for the most part.

Attempting to bridge the gap between dream and reality using classical thermodynamics means extending the sphere of relevance to times and places in which, in some cases, it may not be easy to show that the laws of thermodynamics apply. In practical terms, it means looking for moments of ‘balance’ in ‘complete’ systems. The latter are only approximated in the real world and the former is generally temporary. Arguments built on such shaky foundations are bound to lead to a lot of hand-waving, qualitative arguments, and speculation. Speculation is ‘fun and easy’, costs little, but often disappears like smoke in open air when faced with facts. There is no substitute for quantification to quickly and thoroughly dispel false speculation.

But if the interest is in analyzing entire systems by comparing patterns and relations, qualitative arguments allow a certain freedom of inquiry not possible with strictly quantitative work. And qualitative arguments are not always necessarily speculative. When speculation does occur here it has been labelled as such and tested against fact as thoroughly and rigorously as possible with the given dataset and available outside information.

The fact that qualitative arguments lend themselves to speculation is only part of the problem, other aspects of the methodology here do also. Rather than formulating a hypothesis and then gathering the data to prove or disprove it, this study looks at available data using descriptive statistics and correlational analysis. It asks ‘what conclusions can we draw from this body of information?’ ‘Do the patterns that emerge from the raw data correlate with one another in a meaningful way?’ The raw data is treated as ‘experimental’ and manipulated to produce many interesting and unusual views of the system. This method of ‘survey and correlation’ has all the promise and the excitement of discovery of a first look at the world.

It does, however, have its drawbacks. It is usually only the first step in the scientific process and for good reason. It doesn’t have the built in sense of direction of the hypothetical method and can easily spin off into irrelevance and analytical dead-ends. More importantly, it also lacks the safeguards, the associated statistical tools that have grown up around the hypothetical method.

Correlational analysis invites speculation because it has no mechanism for differentiating true cause and effect from coincidence. When two parameters have a high correlation, it could be because one is effecting the other, or something outside the correlation is effecting both, or it could be entirely coincidental. Nonetheless, correlations of real world data are almost always the cornerstone on which the hypothesis edifice is constructed. Sometimes, as in the applied science surveys of data such as this one, it may be the only part of the scientific process used. Seeking to eliminate correlational analysis in order to eliminate speculation is not possible and like throwing the baby out with the bath water. The only reasonable solution is to deal with speculation in an

intelligent manner. A preponderance of evidence approach (multivariate correlation), reliance on logical relations, and relation to known patterns are ways of dealing with speculation. 'Dealing with speculation' helps guard against but does not guarantee that one is not, in spite of best efforts, merely being speculative.

This study uses the survey method almost exclusively as a sort of challenge to see what can be accomplished with it alone. Less ambitiously and more realistically, it seeks to improve the method to, in turn, improve the hypothesis method. A couple of simple guidelines at the initial 'survey' stage, maintaining a wide scope, keeping a fluid approach, a reliance on linked multivariate correlation, and keeping a close eye on logical relations, increase the probability that, when hypotheses are developed, they will hit the mark.

It must be admitted, however, that while individual examples of speculation are labelled, the entire enterprise as laid out above as the 'dream' is highly speculative in nature. The challenge of this study is to see if an inherently speculative endeavor using methods that lend themselves easily to speculation can nonetheless yield results that are not, themselves, speculative. Here preponderance of evidence and the logical links between relations are used to ground results in facts but these do not 'add up' to a 'yes' or a 'no' as in the hypothesis method. The curves of Figure 427 were analyzed for the longest time before it was realized that they represent the 'water cycle,' a relation that exists quite outside the correlations seen on the graph (but illustrated in schematic 11).

If style is any indication, the (self) prognosis is not good: the last few pages of text are rather chaotic and repetitive because so many relations had been generated and new connections were popping up so fast it was hard to get them all down in an organized manner. Reworking only caused more connections to pop up. This is not a good sign because speculation is well known to be a hydra-like monster that sprouts new heads whenever one is chopped off. On the other hand, one of the last relations to emerge, as mentioned above, was the 'water cycle' which, it is claimed, is the logical underpinning of the final picture. That's a good sign. Like reaching bedrock.

One way of dealing with speculation is to differentiate it from something that seems very close: an 'intuitive' approach. After a while, in a number-crunching exercise such as this one, the numbers start talking to each other. Answers pop up before the question is even consciously asked. The danger here is that the 'chatter' of numbers can lead to conclusions that have nothing to do with physical realities. But it is also possible to have worked the material to such an extent that it is possible to proceed intuitively.

It was said, early on in that part of the analysis, that the inversion state difference diagrams are comparing everything to scenario 4. If that is the case, why are scenario 2 samples subtracted from scenario 1 rather than scenario 4? The decision was made very quickly, without conscious thought. One alternative to the calculation would have been to stick to the chronological order of scenarios. The flow distributions for scenario 2 minus scenario 3, however, is a valley twice the area of the scenario 1 peak. If chronological order is not significant then the flow distributions

for scenario 2 minus scenario 4 would have led to a small peak. That translates to a small positive entropy peak for water at scenario 2.

The idea of the thermodynamic experiment was, however, in the background, guiding the analysis, and so the correct decision was made. The scenario 2 from scenario 1 difference valley is, in most cases, proportional to the peak of scenario 1; energy out is proportional to energy in, which is what the conservation laws predict for a complete cycle in a complete system. An intuitive approach saves itself from being merely speculative when the basic 'intuition' can be traced back to solid relationships and known laws.

Only later, when trying to rationalize the procedure, was it realized that a transition had quite unconsciously been made from an inversion differences to an inversion (energy) level approach. The inversion difference 2 minus 1 is equal to the inversion level 1 minus 4 difference. ([schematic 10](#)). The 'unconscious' transition here is a relic of the quite conscious transition that occurred when the focus shifted from the crossing lines of the inversion test parameter view to areas of the inversion end state view.

The analysis has involved a number of words, examining them from various points of view. Words, like numbers, start 'talking to one another' after a while, with the same potentially dangerous consequences. Terms like a 'complete' or closed or isolated system, expansion and contraction, pulse, 'proportional' and 'balanced', normal and non-normal, general and particular, form and function, and 'coherent' are all related. They have been bandied about in a rather loose manner to describe situations at a variety of different 'levels' and 'views.'

Some of the more important terms that have been used can be brought together and defined a little more specifically. A complete analytical cycle involves the energy implications of a complete temperature change cycle ( $T_1-T_2-T_1$ ). A complete system (i.e. a 'universe of sorts') is one that can, by itself, undergo a complete energy cycle. That is, negative entropy can be resolved during the course of the cycle by the system without outside assistance. It can be balanced by positive entropy or positive enthalpy or free energy. (It should be noted that the term 'universe of sorts' has not been found in the thermodynamic literature. It is a consequence of the assumption here that what the thermodynamic laws are really about is 'functional completeness'). A regular system (not a 'universe of sorts'), needs an input of entropy or enthalpy from the environment.

But a complete system has to have the appropriate balance of amount-volume for the thermodynamic functions to work. That is why, in this analysis, water ties the system and the functions together. Amount and volume, while so intimately tied to one another that it is almost impossible to think of the one without thinking of the other, simply have a different response to temperature change. This is the analytical distinction that makes directly linking the two responses difficult.

This study began as a sort of unravelling of the dataset. Since 'everything' is related to 'everything else', it should be possible to investigate the entire system by pulling on any strand. Here, the 'inversion' was the stray loose end that, when pulled, began the unravelling process.

The need to see what would develop next and where it would lead became somewhat obsessive; more than ten years were spent continually pulling on the thread of ‘inversion.’

The unraveled threads, however, very nearly remained just that and might never have been put back together into a coherent pattern. In fact, this study could easily have met an early demise. To explain why is complicated but probably worthwhile as a further note on the practical problems often involved in research.

The ADEQ database from which the chemistry data was taken uses a ‘filing’ system called the ‘STORET’ system. STORETs are five or six digit numbers that code an analysis result. For example, 00440 is the ‘total bicarbonate ion reported as HCO<sub>3</sub> in mg/L’. This is the STORET for the analytical bicarbonate values used in the calculation of bicarbonate activities at the heart of this study.

Having a number that sums up a variety of different aspects of an analysis result is extremely handy when data is being processed. The drawbacks to STORETs sometimes complained of are usually a result of careless use. In one dataset contributed by an outside organization, for example, trace metals suddenly dropped about a thousand fold half way through. As it turned out, the dimensions used in reporting had changed from mg/L to ug/L but the STORET had not been changed to cover that. What seemed like it might lead to a momentous discovery in process control turned out to be simply a processing error.

Often there are several STORETs that cover the same or similar results. The bicarbonate number in this study could have been 00453 which is “BICARBONATE, WATER, DISS, INCR TIT, FIELD, AS HCO<sub>3</sub>, MG/L” though the fact that this is a titration done in the ‘field’ raises higher reliability concerns than those of lab results. It could also have been derived by calculation from any one of several total alkalinity storets 00410, 39086, 39038. Often, in an organization’s dataset, some storets will be used more frequently than others just by habit or convention. Laboratory results are in the format dictated by the lab analyzes used. While dissolved values (meaning from a filtered sample) were used by preference here, those were available only for the cations. The anion values used were ‘total’ (even for Cl where that is not a very meaningful distinction) because these analyzes are most commonly run on ‘whole’ (non-filtered) samples, and may be pH modified. The choice often comes down to which types seem the closest to and most reliable for what is being looked at and which of these has the most data points. That is the case for the selection of the bicarbonate storet used here.

After a while, double checking numbers becomes almost a reflex, like that of a chemist in a ‘water’ lab unconsciously shaking a sample bottle he has just been handed. The comparison of the 00440 bicarbonate values with numbers derived from alkalinity turned up some facts that were pretty gut-wrenching at the time. Surveying the results with both dissolved and total bicarbonate showed many samples with bicarbonate values considerably higher than their corresponding total alkalinity. Now the dissolved and total numbers are from different analyzes and so cannot be expected to be exactly the same. But having the bicarbonate alkalinity considerably higher than the corresponding total alkalinity in a single sample makes no sense at

all. It appears there is something wrong with some of these numbers but without the original data workup it's impossible to know what happened and how many of the numbers are affected.

In the legal or semi-legal, say 'regulatory', environment in which a lot of practical research is done, the data becomes 'tainted' by error and all or part of it needs to be thrown out. In one instance, known to the author by word of mouth, sample blanks were contaminated, making all the associated analysis numbers questionable. While that in itself is not an unusual occurrence, the reason it occurred in an organization collecting scientific data is almost unbelievable: lab DI water was being kept in 55 gallon drums and transferred by manual siphon. In another dataset submitted by an outside organization, the data collectors apparently did not understand that 'dissolved' values considerably higher than 'total' values of a single sample do not make sense (and there were other data issues as well). These are only two in a host of 'horror stories' that could be told. In such cases whole datasets can be tossed if the data shows such a fundamental lack of understanding and/or competence that the analyst loses faith in the ability of the submitter to provide credible information. These types of errors need to be caught, preferably by the 'owners' of the data, or an organization will quickly lose its credibility in the scientific community.

In less constricted environments, however, error can be strictly circumscribed and isolated by analysis and only the bad numbers ejected. Information is too valuable to be tossing all numbers out because some are bad. And, after all, all analysis values are questionable to one extent or another. The most convincing proof of validity is usually just that they 'fit' together well, which is 'circumstantial' evidence at best.

Without knowing how the 00440 bicarbonate values were obtained, it is not possible to know whether the 'tainted' alkalinity values are in any way related. The 00440 bicarbonate values did, however, pass all the mass and charge balance tests so do not, on their own, seem to present any problems.

But the consequences of picking the 00440 STORET for the study are immeasurable. Had one of the alkalinity STORETS been chosen to calculate bicarbonate, there would have been no 'inversion,' only 'dips' as seen in Figure 3. It would have had to be referred to as 'major ion dipping,' a significantly less dramatic and rather silly sounding term. More importantly, it would have required a complicated and arbitrary procedure to determine 'how close' to each other  $\text{HCO}_3$  and Cl needed to be in order to be classified as a 'dip.' Dealing with the complications of 'dip' analysis would probably have fairly quickly ended the study dead in its tracks. The nice, clean crossing of lines, while just as arbitrary and simplistic to boot, allowed attention to be directed to more interesting subjects.

The analysis mode of operation here is simple enough -- to find 'complete' systems, look for 'balance', to find 'balance' look for 'complete' systems. But 'balance' does not always have the same significance -- the balanced flow distributions of scenario 3, as an example, are probably just coincidental. The picture of entropy for the whole universe over all time would presumably be a larger area peak at scenario 1 than the valley area of scenario 2. That is to say, in the largest spatial and temporal frame, entropy is not, as far as we know, 'balanced.' And 'completeness' is

not an invariant attribute of a system, it varies with level and view. The total dissolved solids, for example, form a complete system when it comes to charge balancing but are not complete at the total thermodynamic function level because entropy is not resolved at that level. It is neither proportional to volume change nor, more importantly, inversely proportional to enthalpy change ([Figures 317-318](#)).

So the actual execution of the simple analysis plan could become a blind search through a bewildering number of parameters at different levels and in different views with no simple guide as to which are likely to lead to a meaningful and coherent final picture. The more complete and all-encompassing in scope one tries to be, the more confused one is likely to become. Or one can just wait for nature to present the whole picture at a fortuitous time and place such as Safford.

‘Complete,’ if not closed, subsystems do exist in open systems, and they can often be spotted by checking for ‘balance.’ Revealing the major players involves cutting a ‘slice’ at exactly the right place and time in a ‘complete’ system and changing the actors until the ‘balanced’ picture of a complete cycle is found. At least, that is the fervent hope when one attempts to study large scale, irreversible, non-equilibrium change in open systems with methods of equilibrium theory developed through the study of infinitesimal, reversible change in strictly controlled closed systems.

It is very gratifying to have found what was being looked for, the matrix shift, and to have at least some things ‘fit together’ so well. Not being able to finish it off and link ‘everything’ to ‘everything else’ is disappointing. Still, who would have thought that starting out with a small event in the water quality, one would end up linking that to the thermodynamic functions of the universe? For now, satisfaction will have to be taken in having produced a fairly comprehensive, coherent, functional picture of how a particular river responds to its specific environment. While not connecting ‘everything’ to ‘everything else’, the new picture does have a ‘complete’ feel about it, thanks largely to the presence of the thermodynamic laws.

There was a lot of luck involved here, both in noting the phenomenon at just the perfect spot, Safford, and the choice of analysis methods and data. The amount of preparation, maintaining a wide scope, and keeping a fluid approach undoubtedly helped but wouldn’t amount to much without a little luck. Hopefully that luck has extended to correcting all the error that creeps into any heavily processed analysis, especially one with such wide scope and such simple methods.



## Footnotes

1. Hem, John D., "Quality of Water of the Gila River Basin above Coolidge Dam, Arizona" USGS Water Supply Paper 1104. Washington, D. C., U.S. Government Printing Office, 1950 pp. 34, 83. [back to p.6](#) [back to p. 93](#)
2. See [page 151](#)
3. Wateq4f version 2.63, 5/26/2004, USGS [back to p. 8](#)
4. Standard Methods for the Examination of Water and Wastewater 15<sup>th</sup> edition, Washington, American Public Health Association, 1981 pp. 30-33. [back to p. 30](#)
5. Burkham, D. E., "Channel Changes of the Gila River in Safford Valley, Arizona, 1846-1970" USGS Professional Paper 655G, p. G3 [back to p.31](#)
6. Lewis, Gilbert, Merle Randall, Thermodynamics and the Free Energy of Chemical Substances, New York, McGraw-Hill, 1923. p.8 [back to p.34](#)
7. Baldys, Stanley, John Bayles, "Flow Characteristics of Streams that Drain the Fort Apache and San Carlos Indian Reservations, East-Central Arizona, 1930-1986" Water Resources Investigations Report 90-4053, p. 4. [back to p.35](#)
8. Baldys, Stanley, Lisa K. Ham, Kenneth D. Fossum, Summary Statistics and Trend Analysis of Water Quality Data at Sites in the Gila River Basin, New Mexico and Arizona, USGS Report 95 – 4083 [back to p. 82](#)
9. Halford, Keith J., Piper Plot QW (Excel program), USGS, created 7/31/199X. [back to p. 104](#)
10. Millero, Frank J. "Partial Molar Volumes of Electrolytes in Aqueous Solution", in R. A. Horne, Water and Aqueous Solutions, New York, Wiley Interscience, pp. 518-563 [back to p. 107](#)
11. McCutcheon, S.C., Martin, J.L, Barnwell, T.O. Jr. 1993. Water Quality in Maidment, D.R. (Editor). Handbook of Hydrology, McGraw-Hill, New York, NY (p. 11.3 ) [back to p. 117](#)
12. Uchida, Hiroshi, Yohei Kayukawa, Yosaku Maeda, Ultrahigh Resolution Seawater Density Sensor based on a Refractive Index Measurement using Spectroscopic Interference Method, scientific reports, Nature, 2019, [back to page 117](#)
13. [www.princeton.edu glossary](http://www.princeton.edu/glossary) [back to p147](#)
14. Atkins, Physical Chemistry, San Francisco, W.H. Freeman, 1982 pp 154,107 [back to p. 153](#)
15. Vemulapalli, G. K Physical Chemistry, Englewood Cliffs, NJ, Prentice Hall, 1988. p. 219 [back to p. 163](#)
16. [www.weatherspark.com](http://www.weatherspark.com) [back to p. 180](#)
17. Nordstrom, D.K., J. Ball "User's Manual for WATEQ4F ....", Menlo Park, CA USGS, 1991 Open file Report 91-183 p. 75 [back to p. 209](#)
18. Rheinfelder, John class notes for Chemical Principles Environmental Science, Rutgers, 11:375:202 "Chemical Composition of Natural Waters 3: Redox Chemistry" pp. 413-430 [back to p. 209](#)
19. Ramirez, Ainissa, "The Rise and Fall of Polywater" Feb. 2020 [back to p. 304](#)
20. Lewis and Randall, p. 85 [back to p. 304](#)
21. Smith, Douglas "A Brief History of the Hydrogen Bond," ACS, 1994 [back to p. 304](#)

22. "Salt's Effect on Density of Water" University of Illinois, Urbana, Dept. of Physics, 2007 [back to p. 304](#)
23. Stumm, Warner, James J. Morgen Aquatic Chemistry, New York, John Wiley and Sons, 1996. p. 7 [back to p. 304](#)
24. Hepler, Loren G., "Thermal Expansion and Structure in Water and Aqueous Solution", Canadian Journal of Chemistry, 1969 [back to p. 304](#)

Title page photograph: wifl\_habitat\_upper\_Gila\_box\_hatten (Oct\_2012).jpeg

Questions or Comments? Contact [pcbaz1239@gmail.com](mailto:pcbaz1239@gmail.com) using subject title 'gila river study'////